ORGANIC TRANSFORMATIONS USING NOVEL CATALYTIC SYSTEM

A Thesis submitted to the University of North Bengal

For the Award of

Doctor of Phiiosophy

in

Chemistry

Submitted by

Puja Basak

Under the supervision of

Prof. Pranab Ghosh

Department of Chemistry

University of North Bengal

March, 2022

Dedicated to.....

My beloved parents, brother and my husband

Declaration

I declare that the thesis entitled "**ORGANIC TRANSFORMATIONS USING NOVEL CATALYTIC SYSTEM**" has been prepared by me under the guidance of Dr. Pranab Ghosh, Professor of Chemistry, University of North Bengal. No part of this thesis has formed the basis for the award of any degree or fellowship previously.

Puja Basak

.....

Puja Basak

Department of Chemistry

University of North Bengal

Darjeeling-734013

West Bengal

India

Date: 03.03.2022

UNIVERSITY OF NORTH BENGAL

Accredited by NAAC with grade 'A'

Prof. P. Ghosh
Department of Chemistry
University of North Bengal
Darjeeling – 734013, India

Ph: +91 3532776381 (off)
+91 9474441468 (M)
Fax: +91 3532699001
Email: pizy126@yahoo.com

CERTIFICATE

I certify that **Ms. Puja Basak** has prepared the thesis entitled "**ORGANIC TRANSFORMATIONS USING NOVEL CATALYTIC SYSTEM**" for the award of Ph.D. degree of the University of North Bengal, under my supervision. She has carried out the research work at the Department of Chemistry, University of North Bengal. No part of this thesis has formed the basis for the award of any degree or fellowship previously.

03/03/2022

Prof. Pranab Ghosh
Department of Chemistry
University of North Bengal
Darjeeling - 734013
West Bengal, India
Date.

Prof. Pranab Ghosh
Department of Chemistry
University of North Bengal
Darjeeling - 734013, India

Curigional

Document Information

Analyzed document	Puja Basak_Chemistry pdf (D128628648)
Submitted	2022-02-23T06:44:00.0000000
Submitted by	University of North Bengal
Submitter email	nbuplg@nbu.ac.in
Similarity	1%
Analysis address	nbuplg.nbu@analysis.urkund.com

Sources included in the report

W	URL: https://www.degruyter.com/document/doi/10.1515/znb-2017-0023/html Fetched: 2022-02-23T06:44:31.1830000	5
W	URL: http://www.scielo.cl/scielo.php?script=sci_arttext&pid=S0717-97072015000300021 Fetched: 2021-12-10T12:53:10.4030000	3
W	URL: https://pubs.rsc.org/en/content/articlehtml/2019/ra/c9ra05406d Fetched: 2021-07-20T13:30:02.9400000	1

Puja Basak
03.03.2022

03/03/2022

Prof. Pranab Ghosh
Department of Chemistry
University of North Bengal
Darjeeling - 734013, India

Acknowledgements

There are many people without whom the entire journey of my Ph.D would have been impossible. I would like to thank and express my deep gratitude for their contributions, both directly and indirectly. First of all, I would like to express my sincere gratitude to my honourable supervisor, Dr. Pranab Ghosh, Professor, Department of Chemistry, University of North Bengal, Darjeeling, for his constant guidance, supervision, advice, and motivation at all stages of my entire Ph.D work. His expertise, patience, continuous support in my research activities, and immense knowledge has made this thesis writing possible.

I am thankful to the Head, Dept. of Chemistry, University of North Bengal and all the faculty members and non-teaching staff of this department for their cooperation throughout this time. I am also grateful to the CSIR, in New Delhi for awarding me Junior and Senior Research Fellowships, as well as the University of North Bengal for providing the necessary infrastructure. I am thankful to University Science Instrumentation Centre (USIC), NBU for SEM-EDX analysis and Dr. Mayukh Deb for IR and NMR spectroscopic analysis of my synthesized compounds.

I would like to thank to my labmates Rabindranath, Bipota, Sourav, Sovodip, Gyan Da, Amirul, Tonuka, Bittu Da, Hridoydip da, Manashita, Kumaresh, Dinabandhu, and others for their active participation throughout my research period. I would like to thank, Sachandra, Prasun, Sudip, Prasanjit da, Pranesh da, Ananya di, Goutam and all the other scholars with whom I have worked or shared ideas during this time. I am also grateful to my close friends Rjarita, Urmi, Jayanti Di, Krishnendu, Rongkar, Anusua Di, Rhettika, Arindam, Tarif, and all of my relatives for their constant encouragement and support. I convey special thanks to all my colleagues from Kalyaganj, Milanmayee Girls' High School, Kalyaganj, Uttar Dinajpur, whose cooperation really helped me to complete my Ph. D.

I would like to remember my elder brother, Liton Basak, who has gone forever away from our loving eyes and left a void never to be filled in our lives. He always used to encourage me and help me a lot in my studies so that I could overcome all the difficulties.

I would also like to express my deep gratitude to my dearest husband Dr. Biswajit Kundu, for his endless help, and constant motivation throughout my Ph.D journey and Thesis work, without his constant support my journey would have been next to impossible.

Lastly, and obviously not the least, I offer my deepest gratitude to my parents, Mr. Swapan Kumar Basak and Mrs. Purnita Basak, for their love, sacrifice, encouragement, and support in pursuing my research. To achieve higher studies, they always stood by my side, showering me with their love and affection and constant support. Without them, I would never be able to be here today. I would also like to thank my in-laws for their affection and support, which motivated me to complete my thesis work.

Puja Basak
03.03.2022

NBU, Darjeeling.

March, 2022

(Puja Basak)

Abstract

The present thesis entitled "**ORGANIC TRANSFORMATIONS USING NOVEL CATALYTIC SYSTEM**" focused on the application of graphene oxide (GO) and its derivatives in organic synthesis. Graphene oxide and its derivatives are emerging as a new class of metal-free, inexpensive, environmentally friendly, heterogeneous carbocatalyst. GO can easily be derived from the abundant and inexpensive natural source graphite. The current active research area replaces environmentally hazardous Lewis solid acid catalyst and liquid Bronsted catalyst with heterogeneous solid catalyst. GO has been featured as a thin 2D layer with several oxygen-containing functional groups which attracted much attention in the field of the heterogeneous catalytic system. There is a huge application of GO in different fields of fuel cells, nanocomposite material, electronic devices, and catalytic support. In this thesis, we have focused on the applicability of graphene oxide and graphene-based materials in an organic reaction. The thesis is mainly divided into three chapters and each chapter is further divided as given below.

Chapter I is divided into three parts **Section A** shows a brief introduction on carbonaceous nanomaterial graphene and the development of its functionalized form graphene oxide. These carbonaceous nanomaterials are mainly heterogeneous and show activity like homogeneous one. Many research works have been published on these carbocatalysts owing to their affordability, sustainability, and high thermal and chemical stability. The use of graphene oxide (GO) and it's derivative as an outlook for green sustainable catalysis has been discussed in this chapter.

Section B represents the one-pot multicomponent synthesis of 3,5-disubstituted 1,2,4-oxadiazoles using robust solid acid catalyst graphene oxide (GO). GO plays a dual role of an oxidizing agent and solid acid catalyst for synthesizing 1,2,4-oxadiazole scaffolds with diverse functionality. The use of this carbocatalyst facilitates the synthesis of oxadiazoles under the benign condition without any undesired by-product. A plausible mechanism is proposed based on few controlled experiments and gives a clean strategy to synthesize a wide variety of oxadiazoles.

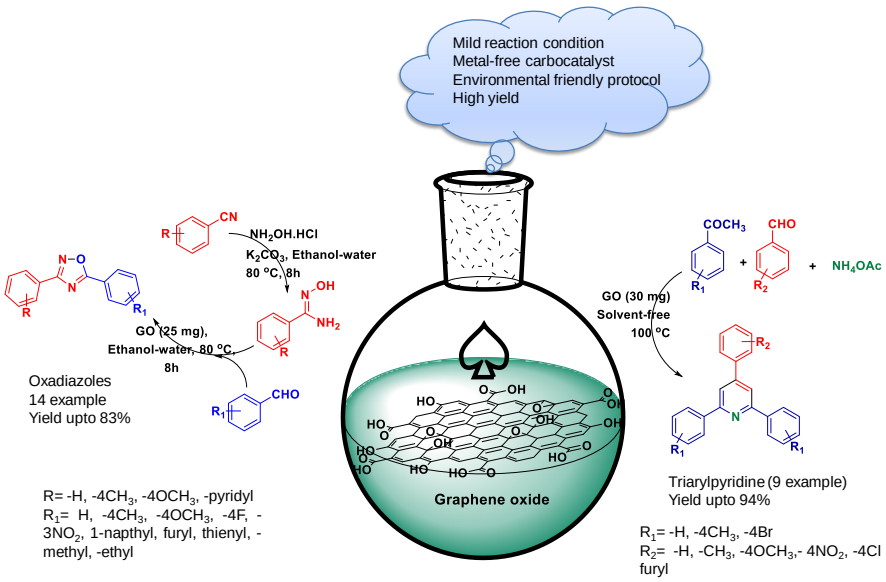

In **Section C** from the same chapter the synthesis of 2,4,6-triarypyridines from benzaldehydes, acetophenones, and ammonium acetate in presence of graphene oxide (GO) as a solid acid catalyst has been described. The oxygen-containing acidic groups in GO have a profound role in catalyzing the synthesis of 2,4,6-triarypyridine derivatives with good to excellent yield.

Chapter II is divided into two sections; **Section A** provides a generalized view of heterogeneous palladium (Pd) catalyzed C-C cross-coupling reaction in water. With growing interest in green chemistry, solid-supported ligand-free heterogeneous catalysts are in demand. The solid supports mostly include activated carbon, polymer, zeolites, mesoporous carbon, silica, alumina, titania. In recent years, graphene oxide (GO) has attracted much consideration as solid catalyst support for organic reaction owing to its large surface area and easy recovery after the reaction. The addition of polymer on GO significantly increases the mechanical and thermal stability of the composite. The necessity of new solid support automatically comes which allows high thermal stability, easy recovery and this led the chemists to find out the new one.

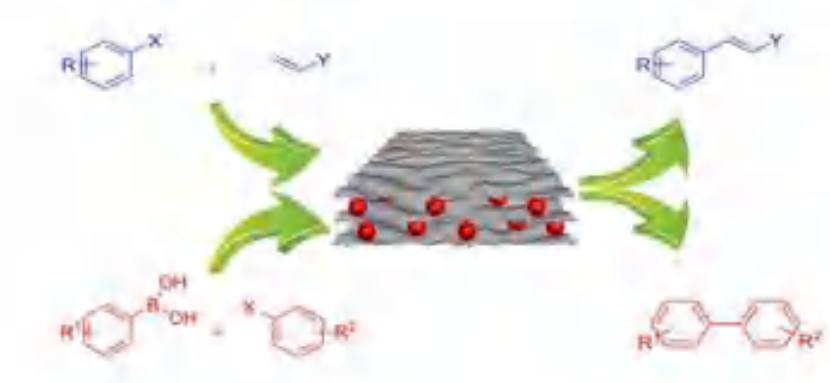

Section B from the same chapter deals with a ligand-free protocol for SuzukiMiyaura and Mizoroki-Heck C-C cross-coupling reaction using low palladium loaded graphene oxide-polymer (GO-PMMA-Pd) composite catalyst. Water has been selected as the medium instead of hazardous solvents like DMF, NMP, DMA,etc considering the environmental concern. GO-PMMA composite enhances the thermal stability of the support and Pd NPs are immobilized in between the layers of this solid composite. This solid supported Pd catalyst was characterized by HRTEM, ICP-AES, PXRD, TGA, XPS, and FT-IR .

In the end, **Chapter III** is divided into two sections. **Section A** describes sulfonated graphene oxide (SGO) catalyzed one-pot synthesis of 3-methyl-4-(hetero) arylmethylene isoxazole-5(4*H*)-ones. This novel methodology involves a greener, radiation, and metal-free approach for synthesizing isoxazoles with a broad range of substrate applicability. The prepared catalyst SGO was characterized by HR-TEM, FEG-SEM, FT-IR, powder XRD analysis, and recyclable upto 5th run without a remarkable drop in its catalytic activity.

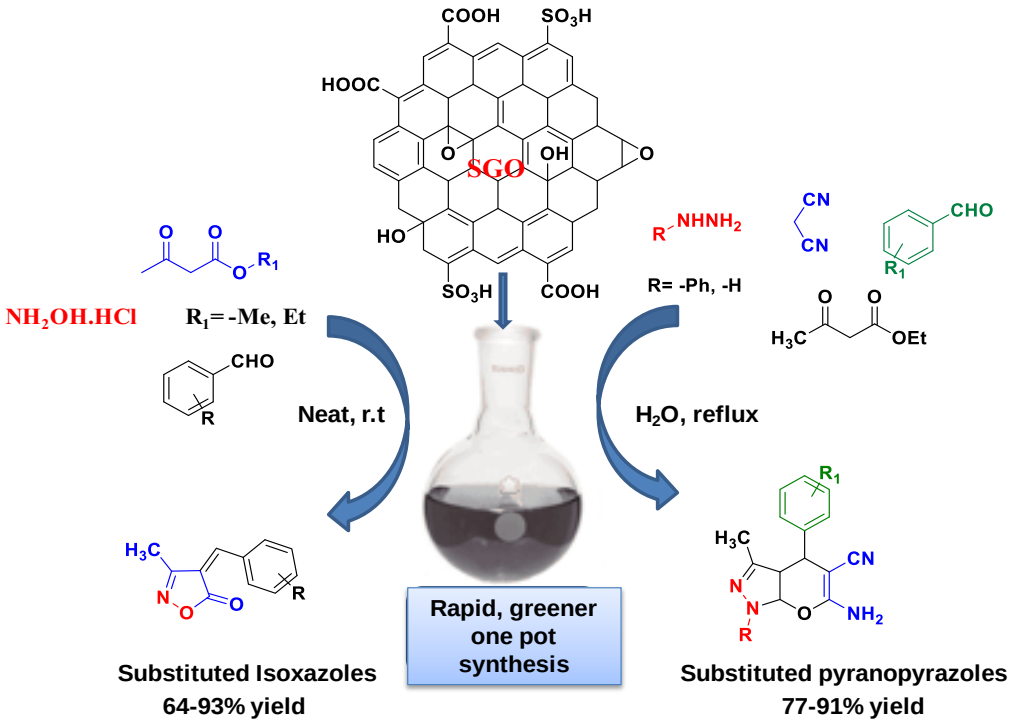

Section B represents the catalytic performance of SGO for the one-pot four-component synthesis of 1,4-dihydropyrano[2,3-c] pyrazoles with excellent yield. The use of SGO as a catalyst seems to be more fascinating due to its high surface area, easy recovery, higher reusability, excellent acidic property and holds great potential for an acid-catalyzed synthesis of pyranopyrazoles.

Preface

Scientific interest on graphene and its derivatives in heterogeneous catalysis has grown dramatically over the past several years. The role and the advantages of graphene and chemically derived graphene (CDG) as heterogeneous catalyst cannot be overlooked. Among the heterogeneous catalytic support graphene and its derivatives has been considered as the most promising area of research. Regarding heterogeneous catalyst, various polymeric supports like, zeolite, silica, polymers etc are similarly very important for immobilization of metals as well as other catalytic application. This research work mainly covers the metal-free heterogeneous catalysis, although reactions involving metal-composite catalysts are also described here.

Chapter I is divided into three sections; Section A gives a detailed discussion on graphene oxide (GO) and its application in organic synthesis. In the Section B graphene oxide (GO) used as efficient catalyst for the one-pot synthesis of 3,5-disubstituted 1,2,4-oxadiazoles using robust solid acid catalyst graphene oxide (GO). In Section C from the same chapter shows graphene oxide (GO) as a solid acid catalyst for the synthesis of 2,4,6-triarypyridines from benzaldehydes, acetophenones, and ammonium acetate.

Chapter II is divided into two sections; Section A deals with the aqueous mediated metal-composite catalyzed C–C cross coupling reaction. Section B depicts SuzukiMiyaura and Mizoroki-Heck C–C cross-coupling reaction using low palladium loaded graphene oxide-polymer (GO-PMMA-Pd) composite catalyst under ligand free condition.

Chapter III is divided into two sections. Section A shows the synthesis of substituted isoxazoles using graphene oxide (GO) as metal-free and

environmental friendly catalyst. Section B deals with the one-pot four-component synthesis of substituted pyrazoles in presence of efficient carbocatalyst GO.

Contents

List of Tables

List of Schemes

List of Figures

List of Publications

1) Convenient one-pot synthesis of 1,2,4-oxadiazoles and 2,4,6-triarylpyridines using graphene oxide (GO) as a metal-free catalyst: Importance of dual catalytic activity
   Puja Basak, Sourav Dey,and Pranab Ghosh
   RSC Advances, 2021, **11**, 32106.

2) Sulfonated Graphene-Oxide as Metal-Free Efficient Carbocatalyst for the Synthesis of 3-Methyl-4-(hetero)arylmethylene isoxazole-5(4H)-ones and Substituted pyrazole
   Puja Basak, Sourav Dey, and Pranab Ghosh
   ChemistrySelect, 2020, **5**, 626.

3) Poly (methyl methacrylate)-graphene oxide supported palladium catalyst: A ligand free protocol for Suzuki and Heck coupling reaction in water medium
   Puja Basak, and Pranab Ghosh
   Synthetic Communications, 2018, **48**, 2584.

4) A Green Synthetic Approach Towards One Pot Multicomponent Synthesis of Hexahydroquinoline and 9-Arylhexahydroacridine-1, 8-dione Derivatives Catalyzed by Sulphonated Rice Husk
   Sourav Dey, **Puja Basak**, and Pranab Ghosh
   ChemistrySelect, 2020, **5**, 15209*,*

5) Graphene Oxide Catalyzed One-pot Synthesis of Pyrimido [4, 5-b] quinolinone-2, 4-diones and their Biological Evaluation
Rabindra Nath Singha, **Puja Basak**, Malay Bhattacharya and Pranab Ghosh
   ChemistrySelect, 2020, **5**, 6514.

6) Green Organic Transformations: Novelty of Graphene Oxide (GO) and Sulfonated Graphene Oxide (SGO)
   Puja Basak, and Pranab Ghosh
   Current Green Chemistry, 2021, **8**, 28.

7) Green Organocatalysis
Puja Basak, and Pranab Ghosh
Green Organic Reactions,Springer,Chapter, 2021, **9**, 149.

8) A design for convenient and greener root towards one pot multi-component synthesis of 7-aryl/heteroaryl substituted pyrano[3,2-c:5,6-c']dichromene-6,8-dione and 7-aryl/heteroaryl substituted chromeno[4,3-d]pyrido[1,2-a]pyrimidinone derivatives using rice husk based heterogeneous catalyst
Sourav Dey, **Puja Basak**, and Pranab Ghosh
Asian Journal of Green Chemistry,
(*accepted*)

9) Catalytic applications of graphene oxide towards the synthesis of bioactive scaffolds through the formation of carbon-carbon and carbon-heteroatom bonds, Green bond forming reactions: carbon-carbon and carbon-heteroatom
Rabindra Nath Singha, **Puja Basak**, and Pranab Ghosh
(*communicated*).

10) Metal-composite catalyzed C-C coupling reactions in wateraqueous mediated heterogeneous catalysis
Puja Basak, and Pranab Ghosh
(*communicated*).

Poster presentation

1) An effective low Pd loading Graphene oxide–polymer supported catalyst for aqueous Suzuki and Heck C-C cross coupling reaction, **Puja Basak**, Pranab Ghosh, National Seminar on Frontiers in Chemistry 2017-2018 organized by Department of Chemistry, University of North Bengal and sponsored by UGC-NEW DELHI, held at University of North Bengal, Darjeeling, September 14, 2017.

2) Explorative studies on Graphene oxide (GO) as an efficient carbocatalyst: synthesis of 3,5 disubstituted 1,2,4 oxadiazole, **Puja Basak**, Pranab Ghosh, International Seminar on Frontiers in Chemistry 2018 organized by Department of Chemistry, University of North Bengal and CRSI North Bengal Local Chapter held at University of North Bengal, Darjeeling, August 27, 2018.

3) A novel graphene oxide (GO) catalysed one-pot synthesis of substituted pyridines, **Puja Basak**, Pranab Ghosh, National Seminar on Frontiers in Chemistry 2018 organized by Department of Chemistry, University of North Bengal and CRSI North Bengal Local Chapter held at University of North Bengal, Darjeeling, August 22, 2019.

Abbreviation

2D	Two dimensional
GO	Graphene oxide
AGO	Amide functionalized graphene oxide
rGO	Reduced graphene oxide
SGO	Sulfonated graphene oxide
tert-BuOK	Potassium tert-butoxide
H_2O_2	Hydrogen peroxide
CDC	Cross-dehydrogenative coupling
MCR	Multicomponent reaction
NPs	Nanoparticles
XPD	X-raydiffraction spectroscopy
XPS	X-ray photoelectron spectroscopy
IR	infrared spectroscopy
TEM	Transmission electron microscopy
TGA	Thermogravimetric analysis
HMF	5-hydroxymethylfurfural
DHPM	Dihydropyrimidone
SRGO	Sulfonated reduced graphene oxide
EDS	Energy dispersive spectroscopy
PTSA	p-Toluenesulfonic acid
DMF	*N,N*-Dimethyl formamide
DMSO	Dimethyl sulfoxide
NBS	N-Bromosuccinimide
DBU	1,8-diazabicyclo[5.4.0]undec-7-ene
HBTU	*N,N,N′,N′*-Tetramethyl-*O*-(1*H*-benzotriazol-1-yl)uronium hexafluorophosphate
DIEA	N,N-Diisopropylethylamine
PS	Polystyrene
BEMP	2-*tert*-Butylimino-2-diethylamino-1,3-dimethylperhydro-1,3,2-diazaphosphorine
MW	Microwave

TBTU	*N,N,N′,N′*-Tetramethyl-*O*-(benzotriazol-1-yl)uronium tetrafluoroborate
DCC	*N,N′*-Dicyclohexylcarbodiimide
EDC	*N*-(3-Dimethylaminopropyl)-*N′*-ethylcarbodiimide hydrochloride
HOBt	1-Hydroxybenzotriazole
TLC	Thin layer chromatography
TEA	Triethylamine
SEM	Scanning electron microscope
EDX	Energy-dispersive X-ray spectroscopy
ppm	Parts per milion
HRMS	High resolution mass spectroscopy
TMS	tetramethylsilane
PFPAT	Pentafluorophenylammonium triflate
IL	Ionic liquid
rt	Room temperature
n-TSA	Nano titania-supported sulfonic acid
MNP	Magnetic nanoparticles
FT-NMR	Fourier Transform- Nuclear magnetic resonance
CDG	Chemically derived graphene
Nf	Nafion
PCA	1-Pyrenecarboxylic acid
DMA	*N,N*-Dimethylacetamide
NMP	*N*-Methyl-2-Pyrrolidone
PMMA	Poly (methyl methacrylate)
BZP	Benzoyl peroxide
ICP-AES	Inductively Coupled Plasma-Atomic Emission Spectrometers
PPI	Potassium phthalimide
TCNE	Tetracyanoethylene
HPA	Heteropolyacid
DCM	Dichloromethane
THF	Tetrahydrofuran
br	broad
d	Doublet

Hz	Hertz
m	Multiplet
s	Singlet
t	Triplet
min	Minute
mg	Milligram
^{o}C	Degree Celsius
h	Hour
mL	milliliter
wt %	Weight percent
PPh3	Triphenylphosphine
TBAB	Tetrabutylammonium bromide
SDS	Sodium dodecyl sulfate
TPAOH	Tetrapropylammonium hydroxide
Pd@zeolite	Zeolite-supported Pd catalyst
CS	Chitosan
MPTA	Poly-triallylamine

Chapter I

Section A

A brief introduction on carbonaceous nanomaterial graphene and its derivative

I.A.1. Introduction to graphene

Graphene, single-layered 2D carbonaceous material mainly contains a honeycomb C (carbon) network and is prevalent in several carbon-based nanomaterials. Novoselov and his co-workers prepared single-layer graphene and few-layer graphene by peeling of graphite layer repeatedly (Scheme I.A.1). In general, single and few-layer graphene nanosheets are obtained by the mechanical exfoliation ("Scotch-tape" method) [1] and by epitaxial chemical vapour deposition of bulk graphite [2]. The exfoliation of graphene sheets from graphite has attracted much attention as it enhances the quality of graphene and enables large scale synthesis. Many researchers have been focusing on graphene owing to its unique electrical, optical, mechanical properties and its modified form CMG (chemically modified graphene) is used in catalysis and catalytic support [3]. There are two methods for the graphene functionalization covalent and non-covalent method, although the first one is mainly used by chemists for reaction purposes [4]. The covalent functionalization is achieved mainly through a few techniques, such as reaction with residual functional groups present on graphene during the production, atom doping, etc [4]. The non-covalent functionalization of graphene involves π-π interaction and van der waals forces of interaction with polymers and various organic molecules with hydrophobic properties. Due to non-covalent functionalization, the extended π system of graphene is not disturbed, which indicates that the mechanical strength and electrical conductivity of functionalized graphene remain unaffected [5]. In the covalent modification, graphene loses some of the conjugation systems, and thereby compromising some of its properties. Covalent functionalization produces some lattice defects in the nanosheets due to the interruption of π-π conjugation whereas the conjugation is not disturbed in non-covalent

functionalization. The covalent functionalization of graphene increases its dispersibility in organic solvents. Generally, the organic covalent functionalization reaction of graphene involves the covalent bond formation between dienophiles or free radicals and the C=C bonds of pristine graphene [6]. Graphene possesses a large surface area of up to 2600 m^2 g^{-1}, which is a significant factor that affects its use as support in a heterogeneous catalytic system [3]. The chemical modification and chemical production of graphene is a great challenge for synthetic chemists. Hydrogenated, fluorinated and oxygenated derivatives of graphene possesses interesting properties and are so called graphane, fluorographene and graphene oxide respectively [9]. Among them, graphene oxide (GO) has been regarded as the outcome of the oxidation and chemical exfoliation of natural graphite [10-12]. The application of metal-free carbon materials as heterogeneous catalysts replaces hazardous liquid BrØnsted and Lewis acid catalysts in organic synthesis [7, 8]. This accounts for the use of functionalized graphene in catalysis as a rich class of nonpolluting and reusable solid-state material.

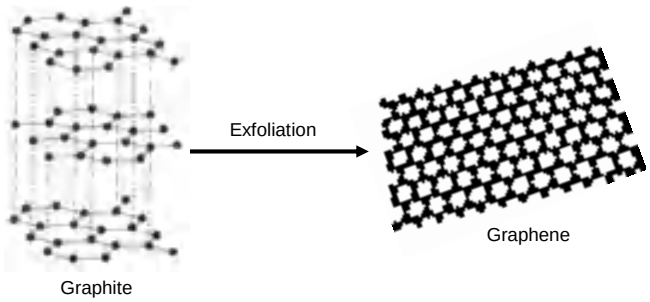

Scheme I.A.1. *Single-layer of graphene extraction by exfoliating graphite.*

I.A.2. Introduction to graphene oxide (GO)

GO is a single layer of graphite oxide and is obtained from the oxidation of graphite powder. The properties of GO are far from those of graphene, although both of them are two-dimentional carbon materials. In 1855, graphite oxide (a bulk form of GO) was first synthesized by Brodie from graphite powder using a strong oxidizing agent like $KMnO_4$, $NaNO_3$, $KClO_3$, and H_2SO_4 [13]. Graphite oxide can be readily exfoliated through ultrasonication in water and other organic solvents owing to its hydrophilic nature and greater interlayer distance than graphite. The single and multi-layer GO make a stable dispersion in these solvents [14]. GO behaves as an acid catalyst due to the presence of extrinsic oxygenated groups on its basal plane. Thus the structural difference between graphene (possesses only hexagonal sp^2 carbon network) and graphene oxide (GO) have a huge influence on their properties. In 1898, a modification of Brodie's method, was described by Staudenmeir [15]. This method eliminates the demerits of Brodie's method and concentrated H_2SO_4 was added to graphite powder along with $KClO_3$ and fuming HNO_3 and resulted in highly oxidized GO in a single step. However, the most widely used method for the synthesis of GO was developed by Hummers in the year 1958. This method involves the addition of $NaNO_3$, conc. H_2SO_4 and $KMnO_4$ for the oxidation of graphite to GO. However, $NaNO_3$ evolves some toxic gases like NO_2/N_2O_4 during GO synthesis and dissolves Na^+ and NO^{3-} ions in the water waste. Later, a few modifications are made to the modified Hummers method. After that, Tour *et al.* (2010) refurnished the Hummers method by eliminating $NaNO_3$, increasing the amount of $KMnO_4$, and introducing the reaction mixture of H_2SO_4/H_3PO_4 in a 9:1 volume ratio for a prolonged time. The environmental issues of the

Hummers method was addressed by Tour and reported a better method to synthesize heavily oxidized GO (Scheme I.A.2) [16].

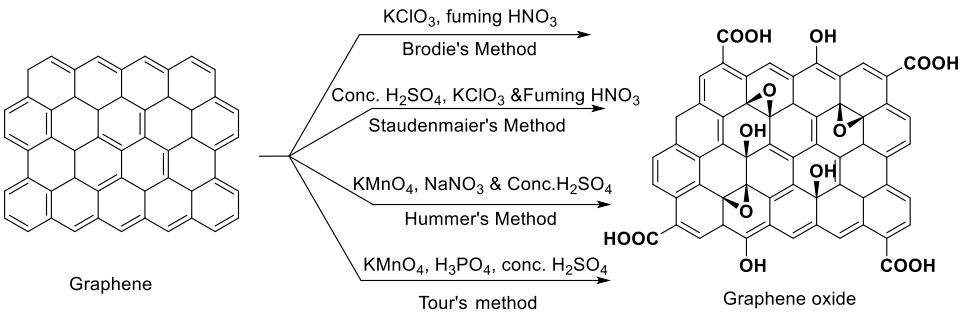

Scheme I.A.2. *Different methods for graphene oxide (GO) synthesis.*

Dimiev *et al.* proposed the structural formula of GO which clearly describes its acidic property in an aqueous solution [17]. Although the exact structure of GO is uncertain, Klinowski *et al.* proposed the structural model of GO which has been widely accepted, shows only the chemical connectivity (Figure I.A.3). Some other proposed structural models of GO are shown in the following figure I.A.1.

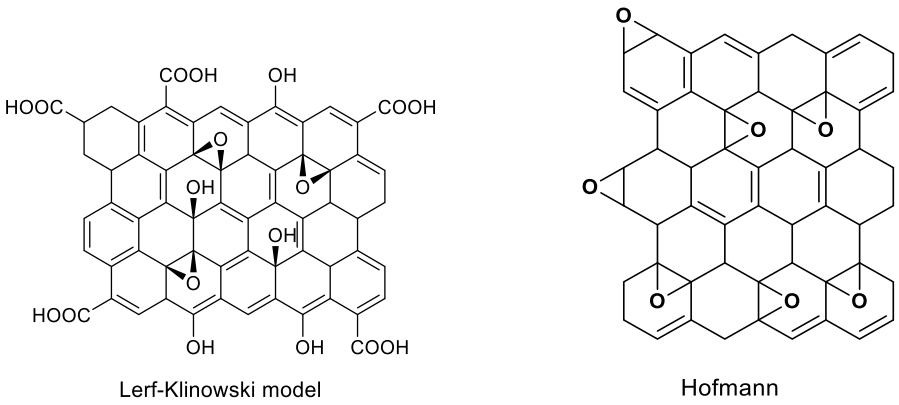

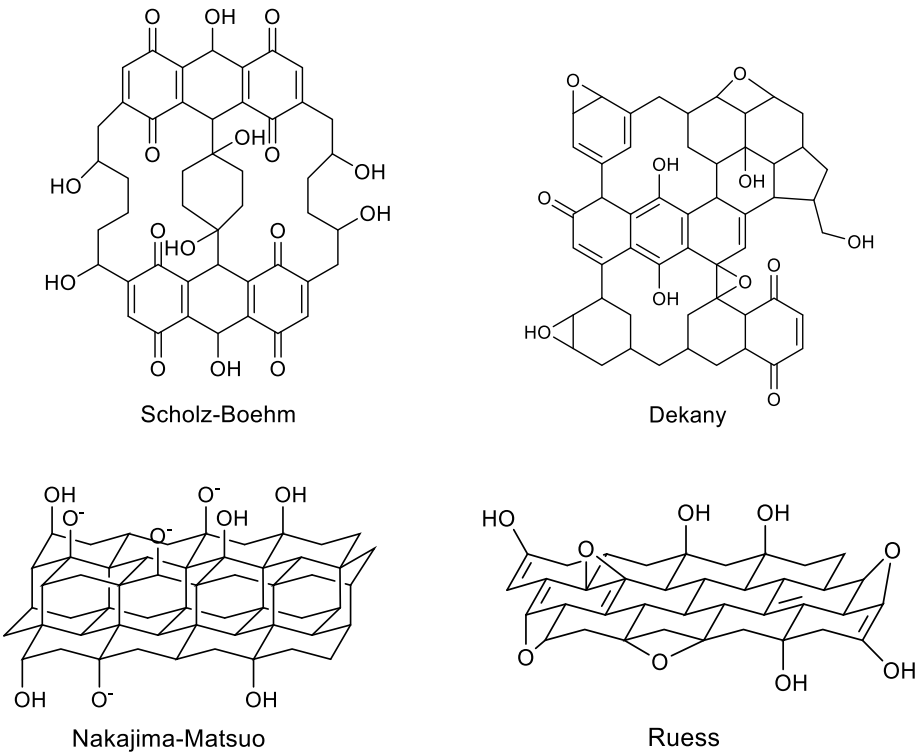

Figure I.A.1. *Proposed structural models of GO.*

Since GO is an oxidized form of natural graphite, it is an inexpensive and abundant source of carbocatalyst. GO is built on a C grid forming a graphite plane, and the layers are terminated with -OH and -COOH groups. The acidic property of GO is due to the presence of extrinsic oxygen functionalities on the GO basal plane. Due to the presence of a large number of oxygen-containing functional groups in GO, such as carbonyl (C=O), carboxyl (–COOH), epoxy (–O–), and hydroxyl (–OH), GO has been considered as an acid catalyst as well as an oxidant (pH 4.5 at 0.1 mg mL^{-1}) [18].

I.A.2.1. Preparation of graphene oxide derivatives

Since GO has epoxide rings, they can participate in epoxide ring opening reaction by amine. Therefore, a new acid-base bifunctional solid catalyst is formed where the amino group is covalently bonded to the acidic GO surface (Scheme I.A.3) [19]. The modification in GO through amination enhances the material stability and is widely used in the chemical industry and in organic transformations. Similarly, the incorporation of imidazolium [20], dopamine [21], and *p*-nitrophenyl [22] on the GO surface by covalent attachment increases the physicochemical properties. For example, isocyanate functionalized GO makes a stable dispersion in a polar protic solvent and has been used for organic field effect transistors [23]. Sing *et al.* developed another interesting graphene-based materials, where amines are grafted with carboxyl group to form amide functionality onto the surface of GO [24]. Amide functionalized GO (AGO) achieved enhanced thermal stability as compared to GO and its dispersibility in polar solvents is stable more than two months. Another GO derivative reduced graphene oxide (rGO) is obtained by the reduction of the oxygen content of GO chemically, thermally or electrochemically [25]. GO is highly dispersible in water and other solvents whereas rGO is less. As the property of rGO is similar to that of graphene, it is used in the production of batteries, printable graphene electronics and in biomedical applications. Due to the presence of oxygen functionality on the surface of graphene oxide, surface modification through covalent attachment can be achieved for the synthesis of various graphene oxide derivatives (Scheme I.A.3). Kumar *et al.* performed covalent functionalization of GO using esterification reaction by m-Toluic acid. GO modified via esterification was soluble in polar organic solvents and have various application in gas sensors [26]. The mineral-acid catalyzed reaction using H_2SO_4, HNO_3,

HCl used in industry and laboratory has several drawbacks severe reaction condition, catalyst reusability problem and corrosion problem. Thereby, solid acid catalysts effectively erase the problems regarding corrosion and reusability and securing environmental sustainability. Bazarganipour *et al.* synthesized sulfonated graphene oxide (SGO) using chlorosulfonic acid and investigated its catalytic activity for the hydrolysis of cellulosic substrates [27].

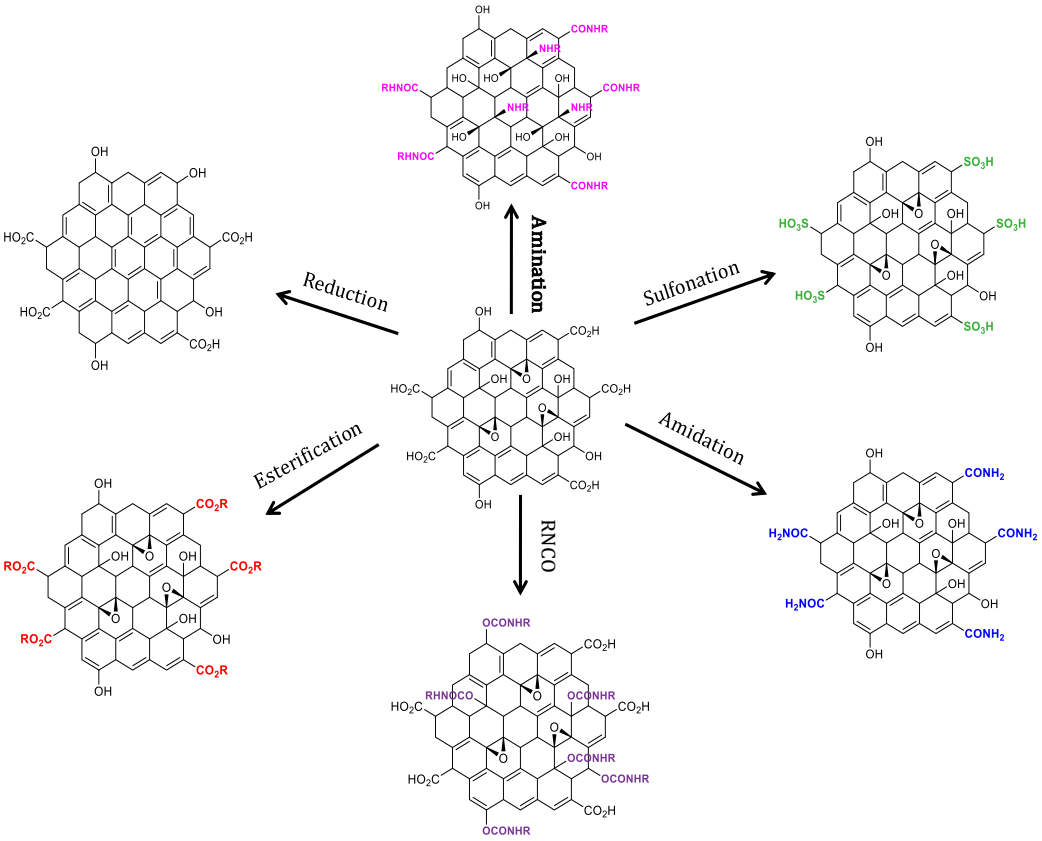

Scheme I.A.3. *Functionalization of graphene oxide (GO) using different approaches.*

I.A.2.2. Graphene oxide (GO)- catalyzed organic reactions

GO has been emerging as a solid heterogeneous carbocatalyst that shows activity and selectivity like a homogeneous one [28]. Some organic transformations using GO as carbocatalyst are shown below which depicts the versatility of this carbonaceous nanomaterial. In 2010, Dreyer *et al.* demonstrated GO as a metal-free inexpensive carbocatalyst to facilitate the oxidation of various alcohols, alkenes, and alkynes (Scheme I.A.4). These organic transformations afforded the desired product (aldehyde or ketone) in excellent yield and proceeded under mild reaction conditions [29].

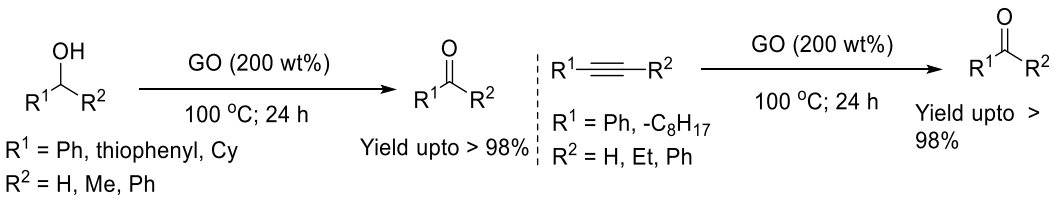

Scheme I.A.4. *GO catalyzed oxidation of various alcohols and hydration of alkynes.*

In 2011, the same group described graphene oxide catalyzed selective oxidation of thiols and sulfides to disulfides and sulfoxides (Scheme I.A.5) [30]. They observed that this oxidative transformation efficiently produced thiols and sulfoxides with good to excellent yield (51- 100 %) in a short reaction time (within 10 min in most cases). However, there was no case of over-oxidation of the substrate and the heterogeneous nature of GO has a profound effect to facilitate the above transformation and isolation of the target product.

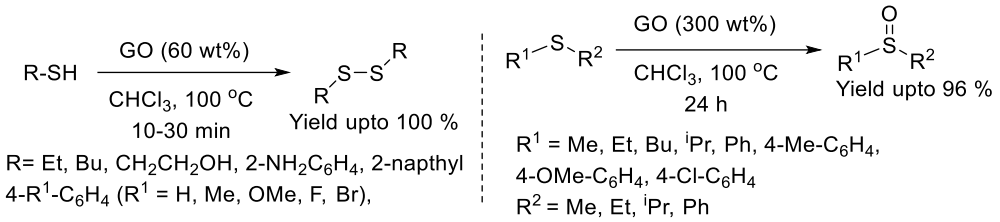

Scheme I.A.5. *Selective oxidation of thiols and sulfides to disulfides and sulfoxides using GO as heterogeneous catalyst.*

Huang *et al.* described GO as a durable and efficient catalyst for the transformation of various amines to their corresponding imines via a metal-free route (Scheme I.A.6) [31]. This method proceeds under neat reaction conditions with molecular O_2. GO was found to be highly efficient to produce symmetrical, asymmetrical, and cyclic imines through an eco-friendly reaction protocol. Here, GO was prepared by the Hummers method and characterized by a range of spectroscopic tools.

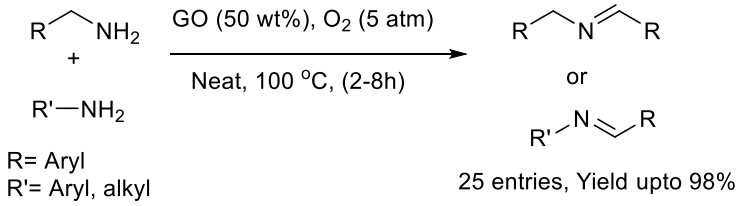

Scheme I.A.6. *Aerobic oxidative coupling of various amines to imines catalyzed by GO.*

Gao *et al.* observed C-C bond formation reaction via C-H bond activation using graphene oxide (GO) as a reusable and inexpensive heterogeneous catalyst (Scheme I.A.7) [32]. Herein, the target product biaryls were obtained in presence of *tert*-BuOK at 120 °C using GO as a metal-free catalyst. Aryl iodides with electron-donating groups are more reactive in this

reaction than electron-neutral aryl iodides. Aryl chlorides and bromides are also employed in this reaction but resulted low yield.

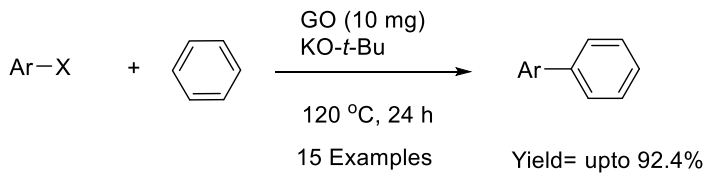

Ar= C_6H_5, 4-MeO-C_6H_4, 4-Me-C_6H_4, 4-Et-C_6H_4, 1-napthyl, 4-Cl-C_6H_4 etc
X= I, Br, Cl

Scheme I.A.7. *Graphene oxide catalyzed C-C bond formation reaction.*

Dhopte *et al.* investigated the catalytic activity of graphene oxide (GO) for the synthesis of benzimidazoles/benzothiazoles from the mixture of *o*-phenylenediamine/*o*-aminothiophenol, aromatic and aliphatic aldehydes in methanol solvent at 60 °C/35 °C under heating as well as microwave irradiation (Scheme I.A.8) [33]. The excellent yield of desired product benzimidazoles/benzothiazoles was observed under microwave irradiation at a short reaction time (within 1 hour) at room temperature. Here, GO plays a dual role as an oxidizing agent and solid acid catalyst. The yield of the target product is higher in the polar solvent than in the non-polar solvent and the reason may be owing to the better dispersibility of GO in polar solvents. The heterogenous catalyst GO produced the target product with diverse functionality via an eco-benign process.

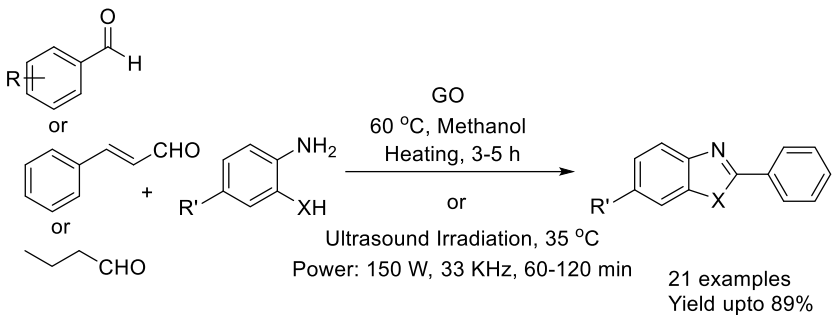

Scheme I.A.8. *The synthesis of benzimidazoles/benzothiazoles from o-phenylenediamine/o-aminothiophenol using GO as solid heterogeneous catalyst.*

Bhattacharya *et al.* reported GO catalyzed transamidation of aliphatic amides (Scheme I.A.9) [34]. Generally, transamidation involves the interconversion of the amide with amines which is a common alternative to the amide formation from amines and carboxylic acids. A wide variety of functional groups ranging from electron-donating to withdrawing exerted the target product with good to excellent yield. However, aliphatic amines and aromatic amides did not produce any kind of target product.

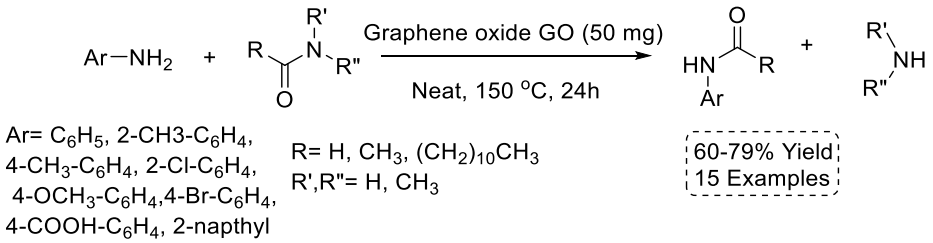

Scheme I.A.9. *GO catalyzedtransamidation reaction of aliphatic amides.*

In 2019, Ebajo Jr. *et al.* demonstrated GO catalyzed eco-friendly pathway for the synthesis of bioactive heterocyclic compound

tetrazoloquinazolinone starting from 3-amino-1,2,4-triazole, benzaldehyde, and dimidone (Scheme I.A.10) [35]. This GO catalyzed reaction is not influenced by the nature of substituents present in the aromatic aldehyde. It was assumed that this reaction was accelerated by the BrØnsted acid edges and lewis acidic sites of GO.

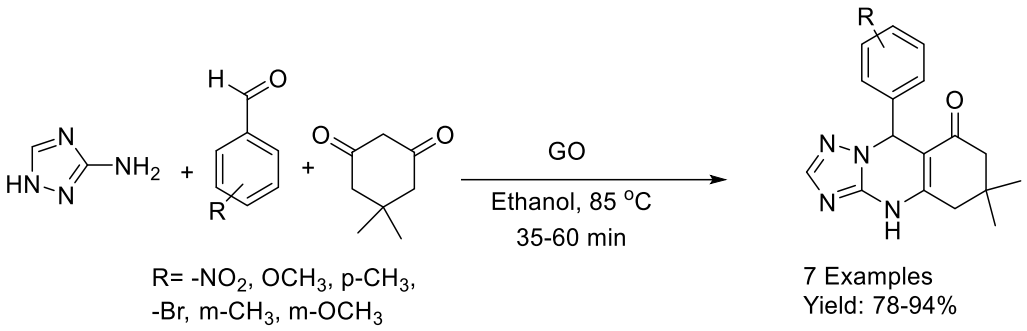

Scheme I.A.10. *The multicomponent reaction of tetrazoloquinazolinone derivatives using GO.*

In 2019, the synthesis of phenols through ipso-Hydroxylation of arylboronic acids using GO as sustainable carbocatalyst was demonstrated by Karthik *et al.* (Scheme I.A.11) [36]. The outstanding catalytic activity of GO was observed in water and this may be due to the better dispersibility of GO in a polar solvent. GO mediated oxidation redaction generally requires high catalyst loading but in presence of H_2O_2, this reaction is completed with a minimum GO loading. The oxygen functionalities mainly carboxylic acid groups of GO played a vital role inipso-Hydroxylation of arylboronic acids.

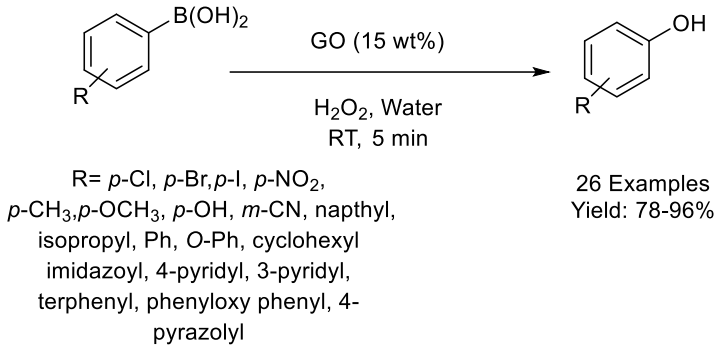

Scheme I.A.11. *Graphene oxide catalyzedipso-Hydroxylation of boronic acids.*

CDC (Cross-dehydrogenative coupling) is a class of reaction that results in the direct formation of C-C and C-N bonds from two unmodified C-H bonds or C-H and N-H bonds. Wu *et al.* demonstrated the metal-free synthesis of 3-aryloxindoles and 3-sulfenylated oxindoles via CDC (cross dehydrogenative coupling) reaction of oxindoles with arenes and thiophenols using commercially available robust catalyst GO (Scheme I.A.12) [37]. In absence of GO catalyst the reaction did not take place and the best result was obtained with 50 wt % of GO. This reaction is highly regioselective and produced only one regioisomer. A wide variety of substituted oxindoles produced the target coupling product with excellent yield.

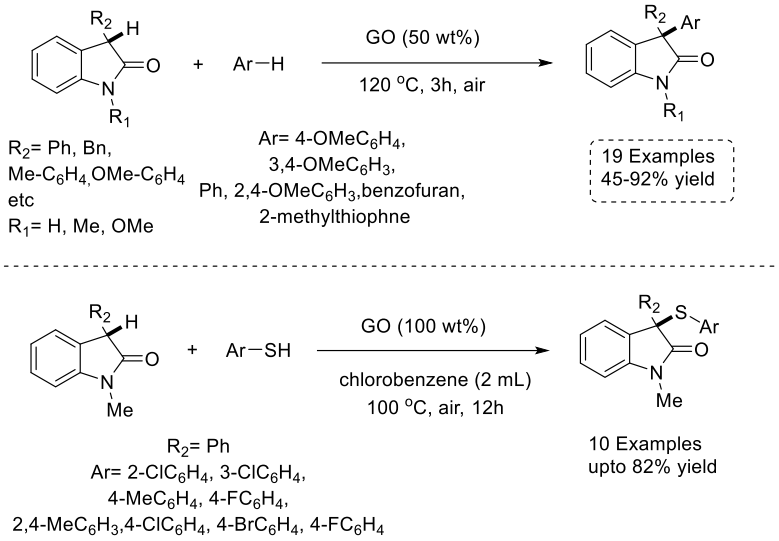

Scheme I.A.12. *GO catalyzed cross dehydrogenative coupling of oxindoles with arenes and thiophenols to yield 3-aryloxindoles and 3-sulfenylated oxindoles.*

The emergence of GO as a heterogeneous catalyst has also found application in Fridel craft alkylation [38], selective hydrogen transfer [39], oxidation of glutaraldehyde to glutaric acid [40], Fisher esterification [41], oxidation of 5-hydroxymethylfurfural into 2, 5-diformylfuran [42] and many more have also been reported [43-46]. With growing interest in green chemistry, multicomponent reaction (MCR) has been considered an important tool of green chemistry. Concerning the environmental factors, the carbocatalyst graphene oxide has been exclusively utilized in MCR for the expedient synthesis of a different heterocyclic motif. Apart from the numerous application in diverse organic transformation GO can be employed as solid support for different NPs via the simple synthetic procedure. From the sustainable perspective, high chemical and thermal stability, high surface area, high recyclability, and easy separation are the most desirable attributes of a heterogeneous solid supported metal catalyst [47, 48].

I.A.3. Graphene oxide as catalyst support: Formation of various metal composites

The activity of the supported catalysts mainly depends on the interaction between the catalyst and the support. GO has been proved to be more advantageous as support of catalyst than pristine graphene owing to the presence of functional groups and inherent structural defects which enables catalysts to bond easily through surface functionalization [49]. GO is cheap and easily available, along with this its amphiphilic nature and better dispersibility in aqueous as well as in organic solvents make the supported catalyst accessible to different reactants in the reaction. GO has a high range of binding energy with different metals, which leads to higher stability with a lower reaction barrier [50-51]. Metal nanoparticles (NPs) can be assumed as the intermediate of homogeneous and heterogeneous catalysts [52]. The main difficulty in NPs application is their agglomeration, that deactivates the catalyst after reaction and causes trouble in the regeneration process. Due to the small size of the NPs, they are not easily removed from the reaction mixture. Therefore, there is a need for heterogeneous catalysts via immobilization of metal NPs on solid supports to achieve high catalytic activity, high mechanical and thermal stability, easy regeneration, and separation procedure [53-62]. Among the other metals, palladium (Pd) has attracted special attention [63-64] as it catalyzes a wide variety of organic reactions. Among the reactions, oxidative cyclization [65], cross-coupling reactions, especially Suzuki coupling [66], Negishi coupling [67], Stille coupling [68], Stille-Kelly coupling [69], Kumada coupling [70], Hiyama coupling [71], and Sonogashira coupling [72] are noteworthy to mention. Usually, these cross-coupling reactions involve mostly soluble Pd organic complex under homogeneous conditions [73]. However, the high cost and low

efficiency in the separation of homogeneous catalysts at successive runs always remains a challenge. To overcome this more attention has been given to the development of heterogeneous catalysts where palladium ions or palladium nanoparticles are immobilized on the solid support. The novel graphene-based materials are promising candidates for catalyst support due to the large specificsurface area and delocalized π-electron system. Over the recent years, PdNPs supported on GO has been successfully employed as a catalyst for different organic transformation reaction [74-76]. Generally, it is a very difficult process to remove Pd metal (poisoned) from the convenient inorganic supports such as silicates, alumina, and zeolites, but GO can be burned simply to evolve CO, pure Pd, and ash. GO covers its surface with a nearly monoatomic layer of Pd atoms through binding with oxygen functionalities via a coordinate-covalent bonding mechanism [77]. Another advantage of using GO as catalyst support is the recycling experiment of the used catalyst.

Gómez-Martínez *et al.* demonstrated an efficient pathway for the Suzuki-Miyaura coupling reaction between aryl bromides and potassium aryltrifluoroborates using PdNPs supported on graphene oxide (GO) and reduced graphene oxide (rGO) (Scheme I.A.13) [78]. Both catalysts disperse properly in a mixture of MeOH/H_2O (3:1) and proved to be very active at 80 ^oC under conventional heating and microwave irradiation technique. The catalyst can be reused upto 8 cycles under microwave irradiation due to the lower aggregation of PdNPs. However, the higher agglomeration of metal nanoparticles under heating conditions may be the reason for the deactivation of the catalyst. A dissolution/re-deposition mechanism has been proposed based on Pd leaching during the reaction and again re-deposited after the reaction.

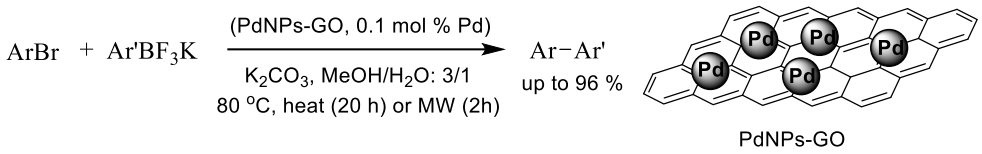

Scheme I.A.13. *PdNPs-GO catalyzed Suzuki–Miyaura reaction of potassium aryltrifluoroborates.*

In 2013, N. Shang *et al.* reported the synthesis of palladium supported on polyamine modified graphene oxide (GO-NH_2-Pd^{2+}) and investigated its catalytic activity in the Suzuki-Miyaura reaction (Scheme I.A.14) [79]. The catalyst was characterized by TEM, X-raydiffraction spectroscopy (XRD), X-ray photoelectron spectroscopy (XPS), and infrared spectroscopy (IR). It was found that the prepared catalyst retains the reactivity characteristics of a homogeneous catalyst, but at the same time, it can be easily recovered and reused up to 10 successive runs without significant loss of its catalytic activity.

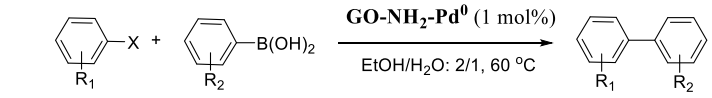

R_1 = Ph, 4-$OMeC_6H_4$, 4-$CO_2EtC_6H_4$, 4-$NO_2C_6H_4$, 4-MeC_6H_4
R_2 = Ph, 3-$NO_2C_6H_4$, 4-FC_6H_4

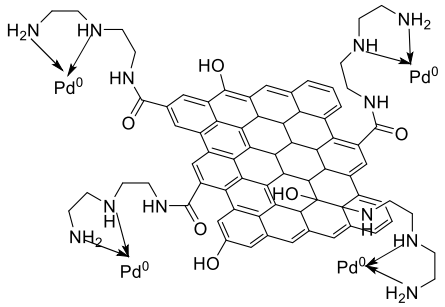

Scheme I.A.14. *The Suzuki–Miyaura coupling of aryl halides and arylboronic acids catalyzed by GO-NH_2-Pd^{2+}.*

Al-Marri *et al.* described a single pot, environmental friendly, and facile synthesis of palladium (Pd)@graphene nanocomposites (SP-HRG-Pd) by the in situ reductions of graphene oxide (GO) and $PdCl_2$ using miswak (Salvadora persica L.) root extract as bioreductant (Scheme I.A.15) [80]. The flavonoids (polyphenolic) and terpenoids moieties of the miswak root extract facilitated the reduction of GO and $PdCl_2$ as well as confirmed the homogeneous binding of PdNPs on the graphene layer. Due to the high dispersibility of SP-HRG-Pd nanocomposite by the stabilization of phytomolecules, the synthesized nanocomposite catalyst showed excellent catalytic activity towards the selective oxidation of aromatic alcohols.

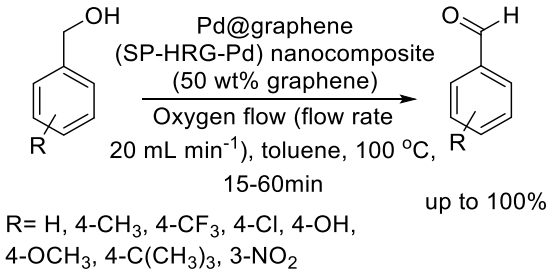

Scheme I.A.15. *Pd@graphene nanocomposite catalyst mediated selective oxidation of alcohols.*

The application of Cu-based nanoparticles has generated great attention in recent years because Cu is inexpensive and earth-abundant. The possible modification of these nanoparticles using different synthetic methods, post-synthetic chemical treatments and the development of novel supports has also been largely responsible for the growing interest in this field. Cu-based materials undergo a wide variety of organic reactions due to Cu's variable oxidation states (Cu0, CuI, CuII, and CuIII) [81-84]. The most economical way to create

advance Cu-based nanomaterials is to anchor CuNPs on carbon-based catalytic support.

Zhang *et al.* described the synthesis of graphene oxide (GO) supported by CuO nanoparticles (CuO-GO) by a facile hydrothermal self-assembly process, (Scheme I.A.16) [85]. The synergetic coupling effect of copper oxide nanoparticles with GO in this hybrid nanocomposite presented an excellent performance in aqueous $NaBH_4$ for the reduction of a variety of nitroaromatics. Although CuONPs and GO separately displayed negligible catalytic activity for the above reduction at room temperature. The CuO-GO can be easily recovered from the reaction mixture and reused up to the 6th consecutive cycle.

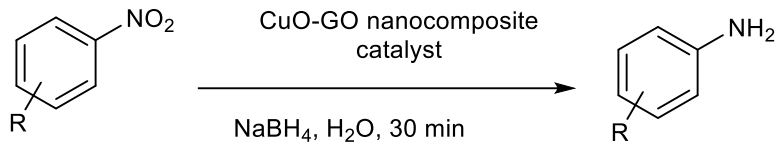

R= H, 4-NH_2, 2- NH_2, Br, Cl, Me, OH Yield: 92-98 %

Scheme I.A.16. *CuO–GO nanocomposite catalyzed heterogeneous reduction of substituted nitroaromatics in aqueous solution.*

The Chan-Lam coupling is the most powerful synthetic route for carbon-heteroatom bond formation through the oxidative coupling of aryl boronic acids, organostannanes or siloxanes with N-H or O-H containing compounds in the air [86]. In 2019, Mittal *et al.* synthesized graphene oxide (GO) supported Cu (II) Schiff's base complex (GO@AP/L-Cu) and examined its catalytic activity in the cases of Chan-Lam coupling and C-H activation reaction (Scheme I.A.17) [87]. Both the reaction was found to be simple, efficient and a higher yield of the product was obtained (~90%). (GO@AP/L-Cu) was characterized by Raman,

FT-IR, UV–Visible, PXRD, FESEM, TEM, EDAX, TGA, XPS, Elemental mapping, BET, CHNS, and AAS analysis.

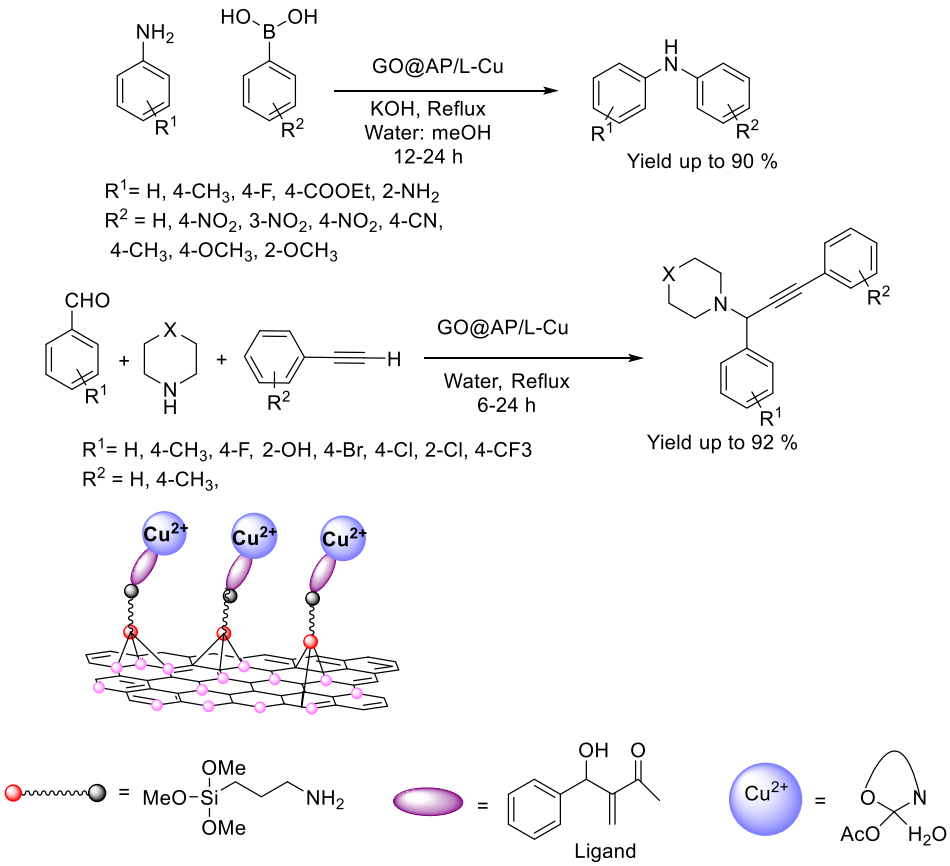

Scheme I.A.17. *Graphene oxide supported Cu (II) ligand complex (GO@AP/L-Cu) catalyst for N-arylation and C-H activation reactions.*

Transition metal-catalyzed C-H activation, especially cyanation of tertiary amines at α-position is a powerful synthetic tool due to the importance of α-aminonitriles as very useful synthetic intermidiates [88-90]. These compounds can be easily converted into a wide variety of biologically active compounds such as α-amino acids and 1,2-diamino compounds, among others (Scheme I.A.18) [91]. Verma *et al.* developed a cheap, simple, and highly efficient

composite of iron (Fe) nanoparticles supported on graphene oxide (GO) for the oxidative cyanation of tertiary amines to biologically important α-aminonitriles in high yields. Moreover, they reported a magnetically separable graphene oxide (GO) supported catalyst for the first time and it was recycled successfully several times without significant loss of its catalytic activity [91].

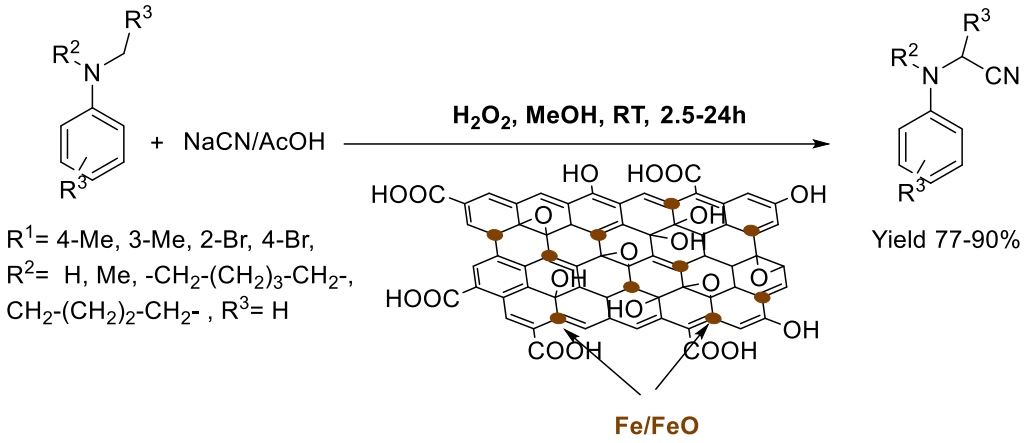

Scheme I.A.18. *Oxidative cyanation of tertiary amines catalyzed by magnetically separable iron nanoparticles supported on graphene oxide.*

I.A.4. Sulphonated graphene oxide synthesis and its application

Solid acid has attracted much attention as an environmentally safe catalyst due to its great potential to replace homogeneous liquid acid [92-94]. Among solid acids, sulfonated-based materials of carbon are noteworthy for mention [95-99]. A large series of sulfonated catalysts of carbon were synthesized by the carbonization of sugar, cellulose [100-101] followed by direct sulfonation of the resulting carbon. However, these sulfonated based carbon materials have a low surface area (approx 2 m^2 g^{-1}), do not swell up, and exhibited higher thermal stability [93]. During the last two decades, GO has been employed as a catalyst as well as catalyst support due to its outstanding

properties like appropriate chemical and thermal stability, high surface area, easy synthesis, low cost, and surface functionalization possibility. Due to the interesting properties of GO as catalyst support for heterogeneous catalytic systems, many synthetic routes have been discovered for the attachment of sulfonated groups on the surface of GO nanosheets. Sulfonated graphene oxide (SGO) can be synthesized by various sulfonating agents such as H_2SO_4 [102], chlorosulfonic acid [103], 2-chlorosulfonic acids [104], sulfanilic acids [105]. In 2014, Naeimi and Golestanzadeh prepared sulphonated reduced graphene oxide, sulfonated graphene oxide, and sulfonated propylsilane graphene oxide nanosheets and used them for the eco-friendly synthesis of bisphenolic antioxidants [105]. Some previous work showed that the catalytic efficiency of sulphonated graphene oxide (SGO) is higher than GO owing to the presence of sulphonic acid groups on the surface [106-108]. So far, some organic reactions have been conducted using sulfonic acid functionalized reduced graphene oxide (rGO-$PhSO_3H$) [109-111]. These procedures however involve the reduction of graphene oxide (GO) to reduced graphene oxide (rGO) using $NaBH_4$ as a reducing agent (Scheme I.A.19).

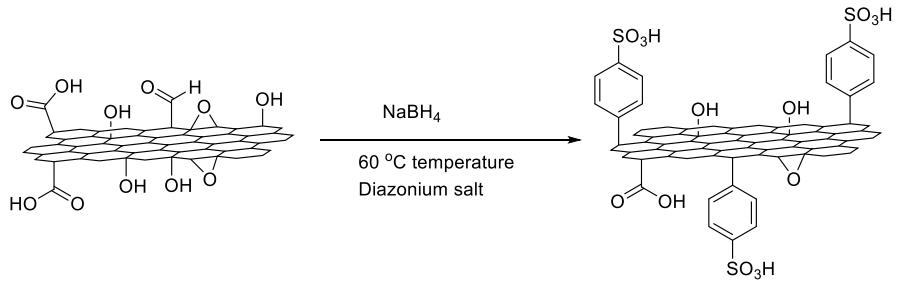

Scheme I.A.19. *Preparation of sulfonated reduced graphene oxide (SRGO) from GO.*

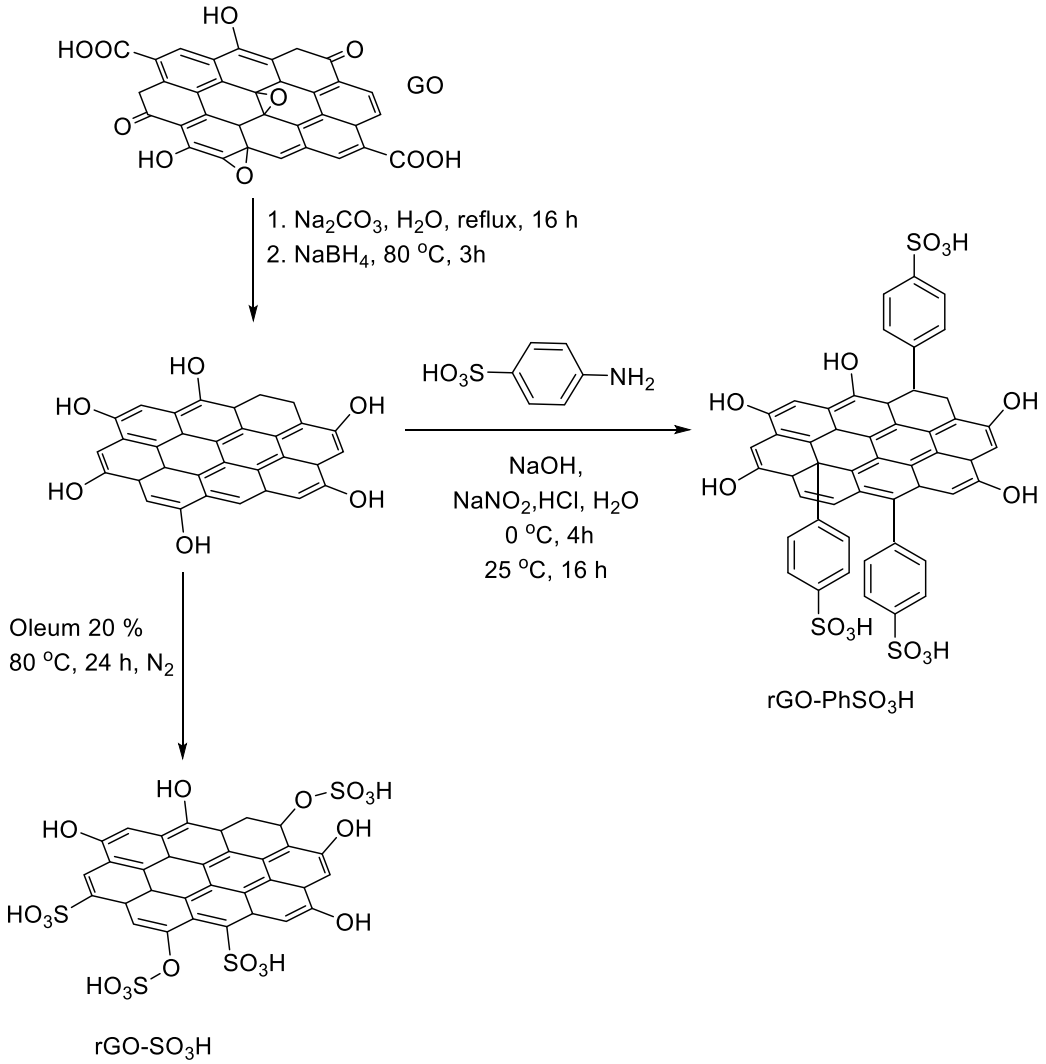

Scheme I.A.20. *Schematic diagram for the synthesis of rGO-PhSO₃H and rGO-SO₃H from graphene oxide.*

After that, there are two chemical methods for the immobilization of sulfonic acid groups on the surface of rGO. Chemical modification of reduced graphene oxide (rGO) involved the grafting of diazonium salt of sulfanilic acid on the rGO surface to produce rGO-PhSO$_3$H [112]. Another sulfonation process

involves simple stirring and heating with oleum containing free SO_3 (20 %) species to produce rGO-SO_3H (Scheme I.A.20) [102]. A covalent bond is formed between carbon and sulfur atoms that are further confirmed by FT-IR and Raman spectroscopic analysis. This covalent functionalization allows stability to the material against leaching when they are employed in liquid phase catalytic reaction.

In 2016, Hou *et al.* reported the one-pot synthesis of sulfonated graphene oxide (SGO) and used it for the efficient conversion of fructose to 5-hydroxymethylfurfural (HMF) [113]. Their synthesized SGO catalysts were named as SGO-1, SGO-2 and SGO-3, however, SGO-1, SGO-2, SGO-3 were synthesized by Tours method and Modified Tours method respectively (Scheme I.A.21).

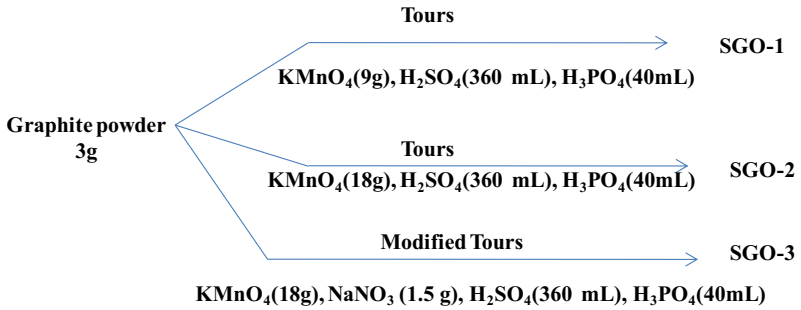

Scheme I.A.21. *Sulfonated graphene oxide synthesis by Hou et al.*

SGO-3 showed the maximum yield (85 %) for the conversion of fructose to HMF whereas SGO-1 and SGO-2 exerted relatively low yield of HMF. The catalytic activity of sulfonated graphene oxide (SGO) depends on the density of the active sites and on its accessibility (Scheme I.A.22) [114]. They showed SGO catalyst for fructose degradation can be recycled upto 5th run with slightly loss of its catalytic activity.

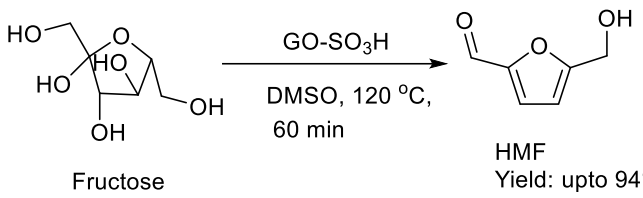

Scheme I.A.22. *SGO catalyzed one-pot conversion of fructose to HMF.*

Vessally *et al.* demonstrated an efficient synthesis of 3,4-dihydropyrimidine-2(1H)-ones/thiones from ethyl acetoacetate, urea or thiourea and aldehydes in presence of sulfonated graphene oxide/graphene oxide in aqueous solvent at room temperature (Scheme I.A.23) [115]. The dihydropyrimidones (DHPMs) can be easily separated from the reaction mixture without workup. The reactants with diverse functionalities successfully reacted and exerted the corresponding DHPMs with high purity. In this reaction SGO has been found to be more suitable than GO.

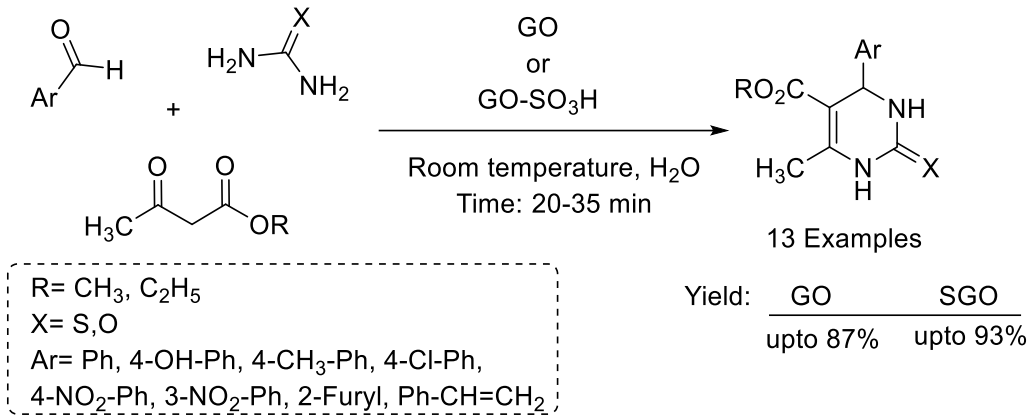

Scheme I.A.23. *SGO catalyzed synthesis of 3,4-dihydropyrimidine.*

The SGO catalyst was recycled upto 6th run and characterized by XRD, Raman, FT-IR. After 6th run no structural change in SGO catalyst was observed

but slight decrease in the yield of the reaction may be due to the reduction of oxygen functionalities and covering the SGO surface with some impurity.

Brahmayya *et al.* described the cyclization of hydrazides to 1,3,4-oxadiazole synthesis using sulfonated reduced graphene oxide ($rGOPhSO_3H$) shown in scheme I.A.24 [116]. They observed the direct cyclization of 4-methyl benzoyl hydrazide with carbon dioxide (CO_2) under room temperature as well as ultrasonic irradiation. Although, the percentage of conversion under ultrasonic irradiation was 84 % using 5 wt % of $rGOPhSO_3H$ in just 50 min and the best yield was obtained with 200 wt% of this nanocatalyst. The product yield was found to be same upto 4th run and the yield decreases from 5-7th run and the reason may be due to the leaching of some SO_3H group from the catalyst surface.

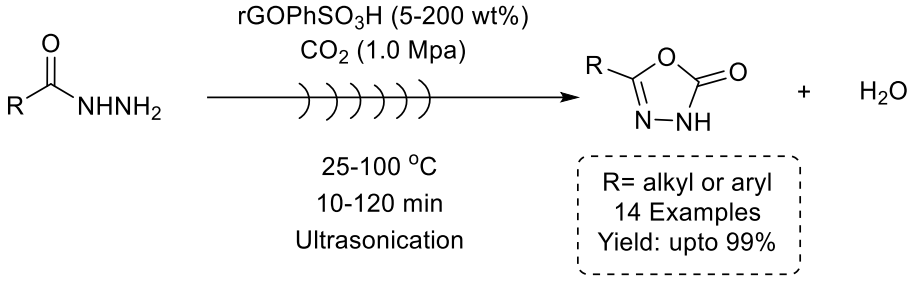

Scheme I.A.24. *The synthesis of 5-susbstituted-1,3,4-oxadiazole-2-ones using sulfonated reduced graphene oxide ($rGOPhSO_3H$).*

In 2017 Brahmayya *et al.* synthesized amides through N-acetylation of amines with acetonitrile using sulfonated reduced graphene oxide (SRGO) as catalyst under sonication (Scheme I.A.25) [117]. SRGO was found to be more favourable than GO in this catalytic reaction. The highest yield was observed in presence of 60 mg of SRGO within 40 min at 60 °C temperature. Electron withdrawing group containing aromatic amines afforded the corresponding

amide with slightly lower yield than electron donating group containing aromatic amines (96-99 %). Interestingly, some sensitive substrates like phenol and thiophenol produced the corresponding *N*-acetylation product in good to excellent yield without protecting –OH, -SH groups. The catalytic activity of sulfonated reduced graphene oxide (SRGO) was nearly constant upto 4th cycle and reused easily without inactiveness.

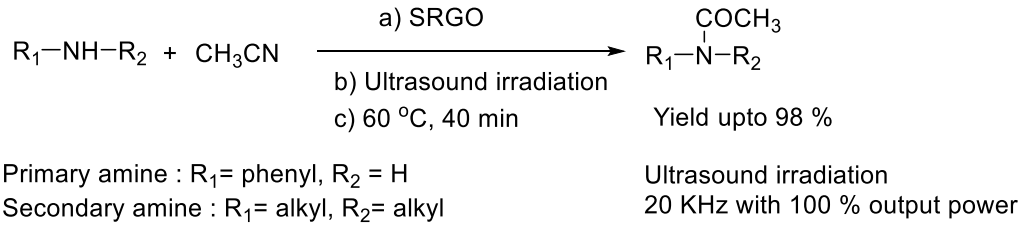

Scheme I.A.25. *Sonochemical N-acetylation with various amine compounds.*

In 2020 Ghosh *et al.* employed sulfonated graphene oxide (SGO) as metal-free catalyst for the synthesis of 3-methyl-4-(hetero)arylmethylene isoxazole-5(4H)-ones and 6-Amino-3-methyl-4-phenyl-1,4-dihydropyrano[2,3-c]pyrazole-5-carbonitriles (Scheme I.A.26) [118]. Substituted isoxazoles were prepared from aldehyde, ethyl acetoacetate and hydroxylamine hydrochloride at room temperature under solvent free condition using of SGO. The catalytic potential of SGO was investigated for another important heterocyclic moiety substituted pyranopyrazole using reactants such as phenyl hydrazine, ethyl acetoacetate, malononitrile and aromatic aldehyde in H_2O medium at refluxed condition. The catalyst can be reused upto five consecutive cycles without lose of its catalytic activity.

In the year 2014, Antunes *et al.* reported the synthesis of biofuels or fuel additives in the carbohydrate platform from 5-(hydroxymethyl)-2-furfural and ethanol using sulfonated graphene oxide as effective catalyst (Scheme I.A.27)

[119]. They synthesized rGO from GO by the treatment of benzyl alcohol at 190 ^{o}C for 20 min under microwave irradiation. To collect the solid the solution was centrifuged and washed with ethanol repeatedly and then dried at 65 ^{o}C. After that rGO was heated in presence of H_2SO_4 (30 mL, 97 wt%) at 160 ^{o}C for 5 h under N_2 atmosphere to obtain sulfonated, partially reduced graphene oxide (S-rGO). The incorporation of the sulfur on H_2SO_4 treatment was confirmed by energy dispersive spectroscopy (EDS).

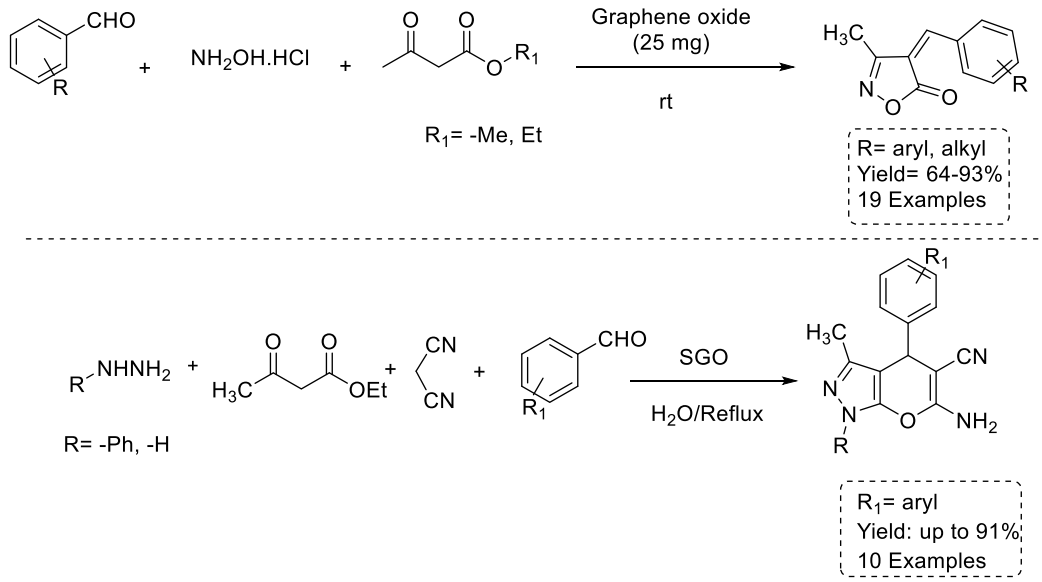

Scheme I.A.26. *SGO catalyzed benign synthesis of isoxazoles and pyranopyrazoles.*

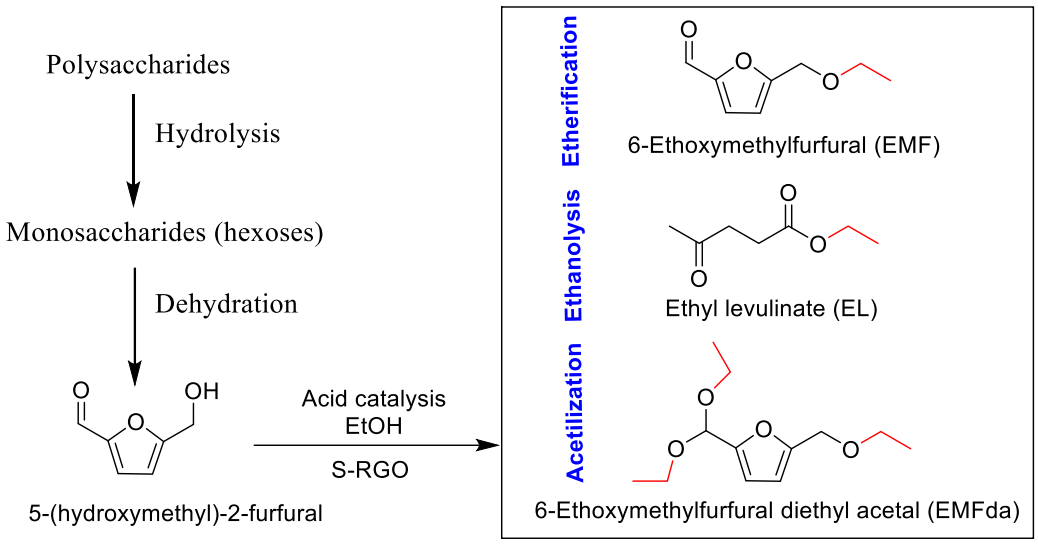

Scheme I.A.27. *Conversion of HMF to the products for biofuel application using S-rGO.*

I.A.5. References

References are given in Bibliography under Chapter I, Section A

Chapter I

Section B

Graphene oxide (GO) catalyzed one-pot synthesis of 3,5-disubstituted 1,2,4-oxadiazoles

I.B.1. Introduction

Nitrogen-containing heterocyclic compounds are valuable due to their potential application as a key intermediate in the synthesis of numerous drugs [1]. 3,5-disubstituted 1,2,4-oxadiazoles are remarkably an important class of nitrogen-containing heterocyclic scaffold as it is widely used as pharmacophores, bioactive molecules, and functional materials [1-2]. Among the oxadiazole derivatives, the 1,2,4-oxadiazole motif has received interest due to its application as a stable bioisostere in place of an amide, ester, or urea functionality [3]. The 1,2,4-oxadiazole moiety is generally found in many drugs including potent S1P1 agonist I [4] and the metabotropic glutamate subtype 5 (mGlu5) receptor antagonist II for the treatment of Alzheimer's disease [5]. In previous literature, 1,2,4-oxadiazoles have shown good affinities for serotonin and norepinephrine transporters [6]. These compounds when selectively functionalized, have performed as various muscarinic agonists [7], benzodiazepine receptor partial agonists [8], serotonergic (5-HT_3) antagonists [9], dopamine transporters [10], antischistosomal drug [11], G-quadruplex ligands for probing DNA superstructure in antitumor research (Figure I.B.1) [12-13].

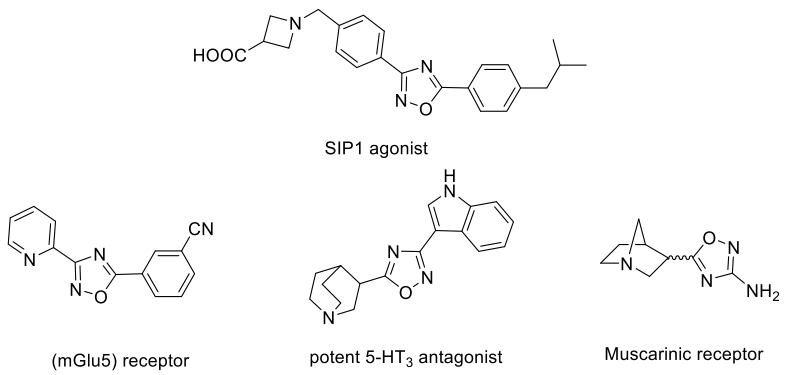

Figure I.B.1. *Some biologically active 1,2,4-oxadiazoles.*

I.B.2. Background and objectives

In the past decade, Multicomponent reactions (MCRs) have been accounted as very elegant and efficient methods to form complex structures in a single synthetic pathway from three or more reactants. The great synthetic efficiency, High atom economy, and procedural convenience in the construction of new multiple bonds in a one-pot procedure are the advantages of multicomponent reactions (MCRs) [14, 15]. The development of new MCRs and the improvement of known MCRs are popular research areas in current synthetic organic chemistry.

It is noteworthy that, in the last decade many efficient protocols have been developed to synthesize significant heterocyclic moieties 1,2,4-oxadiazoles. Among the known synthetic strategies of 1,2,4-oxadiazoles, the most conventional approach involves the use of amidoximes as starting materials or intermediates. Other common approaches involve i) *O*-Acylation of amidoximes by an activated carboxylic acid derivative, followed by cyclodehydration [16], ii) the 1,3-dipolar cycloaddition of nitrile oxide to nitriles [17], iii) intermolecular cyclodehydration reaction of amidoximes (as starting material) with aldehydes to give 4,5-dihydro 1,2,4-oxadiazoles followed by oxidative dehydrogenation [18], iv) formation of amidoxime intermediate through the reaction of nitrile with hydroxylamine which further reacts with aldehyde to provide 4,5-dihydro 1,2,4-oxadiazoles and oxidative dehydrogenation give 3,5-disubstituted 1,2,4-oxadiazoles [19]. Besides this, base-mediated one-pot synthesis and microwave-assisted efficient synthesis of oxadiazoles using PTSA and $ZnCl_2$ have also been reported [17, 19-20]. However, all the methods mentioned above are efficient enough but most of the methods suffer from the use of harsh conditions (microwave irradiation, the

addition of strong acid/ strong base or strong dehydrate, high reaction temperature) and unavailable starting materials.

I.B.2.1. Synthesis 3,5-disubstituted 1,2,4-oxadiazoles from amidoxime

Augustine *et al*. developed p-toluenesulfonic acid (PTSA) mediated zinc chloride ($ZnCl_2$) catalyzed synthesis of 3,5-disubstituted 1,2,4-oxadiazoles (Scheme I.B.1) using amidoximes and organic nitriles [17]. They examined the reaction of various amidoximes with acetonitrile and interestingly all the reactions were complete within 1-2 h to provide 3-substituted 5-methyl-1,2,4-oxadiazoles. The strained cycloalkyl amidoximes were successfully reacted with different aromatic and aliphatic nitriles in DMF solvent and resulted in the corresponding product with a good yield. The mechanism of the reaction was explained through the initial activation of amidoxime by PTSA-$ZnCl_2$ resulting in the formation of nitrile oxide and 1,3-Dipolar cycloaddition of nitrile oxide to nitriles resulted in the formation of 1,2,4-oxadiazoles.

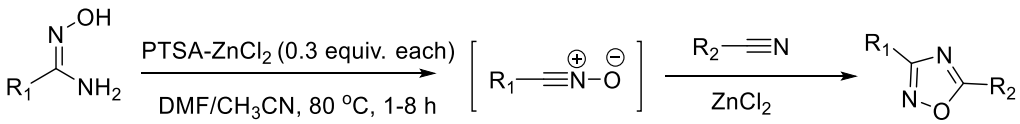

R_1= alkyl, aryl
R_2= alkyl aryl

Yield 77-95 %

Scheme I.B.1. (PTSA) mediated zinc chloride ($ZnCl_2$) catalyzed synthesis of 3,5-disubstituted 1,2,4-oxadiazoles.

The formation of *O*-acyl amidoxime from the reaction of an amidoxime with an acyl chloride is the most difficult and time-consuming step and generally requires a long reaction time and sealed tube condition. Kaboudin *et al.* reported a new efficient method for the synthesis of 1,2,4-oxadiazoles via the reaction of amidoximes with anhydrides under mild, catalyst-free conditions (Scheme I.B.2) in aqueous media [16]. They observed that under the reaction conditions benzoyl

chloride (PhCOCl) is not much effective as benzoic anhydride and provides a very low yield of the product. Substituted benzamidoximes and aliphatic amidoximes afforded 1,2,4-oxadiazoles in presence of benzoic anhydride in good yields. However, the reaction of aliphatic anhydride, with various amidoximes gave the corresponding products in lower yields which may be due to the electronic effect.

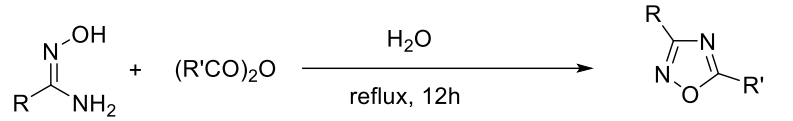

R= C_6H_5, *p*-Cl-C_6H_4, *p*-Br-C_6H_4, 2,4-$Cl_2C_6H_3$
m-ClC_6H_4, *p*-$MeOC_6H_5$, Cyclohexyl
R'= C_6H_5, *p*-$CH_3C_6H_5$, n-C_5H_{11}

Scheme I.B.2. The synthesis of 1,2,4-oxadiazoles via the reaction of amidoximes with anhydrides under mild and catalyst-free conditions.

Kandre *et al*. evaluated microwave-assisted one-pot synthesis of 1,2,4-oxadiazoles from amidoximes and commercially available benzoyl cyanides (Scheme I.B.3). Generally, microwave heating reduced the reaction time as well as improved the yield over conventional heating [20]. It was assumed that the higher temperature in microwave irradiation, aids in the cyclization of *O*-carboxyaryl amidoxime intermediate. Among the solvents, DMF was found to be suitable for conducting the reaction at 95 °C for 1h. However, the yield was reduced at elevated temperatures due to the formation of side products. Here, the reactivity of the electron donating group containing phenyl amidoxime is higher than that of the phenyl amidoxime bearing electron-withdrawing groups.

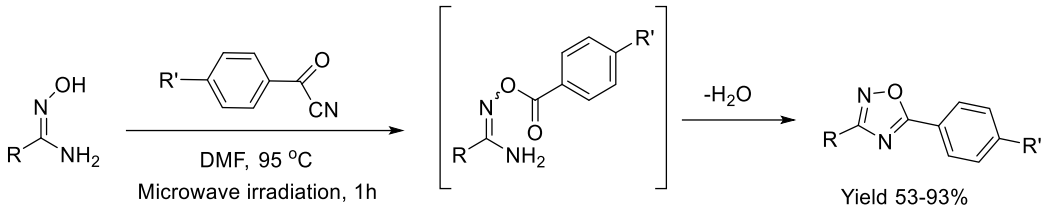

R= Phenyl, 2-Methoxyphenyl, 3-Methoxyphenyl,
4-Methoxyphenyl, 2-Nitrophenyl, 3-Nitrophenyl,
4-Nitrophenyl, Cyclohexyl, Adamantyl
R'= H,-F,-CH_3

Scheme I.B.3. The one-pot synthesis of 1,2,4-oxadiazoles from amidoximes and commercially available benzoyl cyanides.

Lade *et al.* reported the synthesis of 1,2,4-oxadiazoles from *N*-benzyl amidoximes using oxidizers such as *N*-bromosuccinimide (NBS)-1,8-diazabicyclo[5.4.0]undec-7-ene (DBU) and I_2-K_2CO_3 at room temperature (Scheme I.B.4) [21]. The use of 1 equiv. of NBS oxidant and 1 equiv. of DBU base was found to be the best-optimized condition of the product conversion at room temperature in 1h. In absence of both oxidant and base, the reaction could not occur, indicating the vital role of oxidant and base during the reaction. Oxidative cyclization of amidoxime with electron-donating substituents offered a moderate yield of the product whereas, amidoximes with electron-withdrawing substituents underwent this oxidative pathway with high reactivity. The higher yield may be due to the formation of a more stable imine bond.

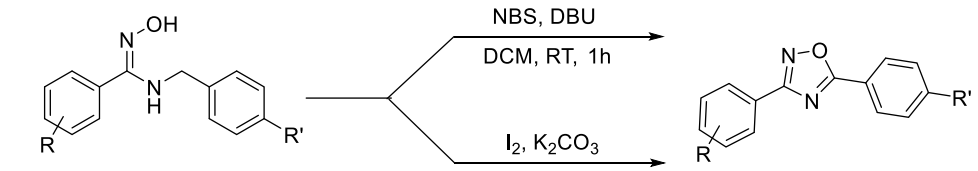

R= H, Cl, F, Br, OMe, OPh, Me, NO_2, CN
R'= H, OMe, F

Scheme I.B.4. The synthesis of 1,2,4-oxadiazoles from *N*-benzyl amidoximes.

Wang *et al*. developed a polymer-assisted solution-phase synthesis of 1,2,4-oxadiazoles using amidoxime and carboxylic acids in presence of a coupling reagent. They began their investigation to synthesize 1,2,4-oxadiazoles in presence of HBTU and *N,N*-diisopropylethylamine (DIEA) [22]. But the conversion was low under microwave irradiation at a higher temperature. The use of polymer-supported bases MP-carbonate and PS-BEMP showed much higher reactivity than DIEA. The use of HBTU/PS-BEMP in this protocol worked well for a wide range of amidoximes and afforded the corresponding oxadiazoles in good to excellent yield (Scheme I.B.5). Among many reported procedures, the use of PS-PPh_3/CCl_3CN is attractive, because it converts carboxylic acids to the corresponding carboxylic acid chloride in situ. After the generation of carboxylic acid chloride DIEA was added and heated in MW at 150 ^oC for 15 min.

The most common method for the synthesis of 1,2,4-oxadiazoles through cyclization of *O*-acyl amidoximes obtained from the acylation of amidoximes and carboxylic acids or acid chlorides have some drawbacks. The acid chlorides are very hard to handle and store, on the other hand, carboxylic acids require a long reaction time along with a coupling reagent such as TBTU, DCC, EDC, HOBt to react with amidoxime [23, 24].

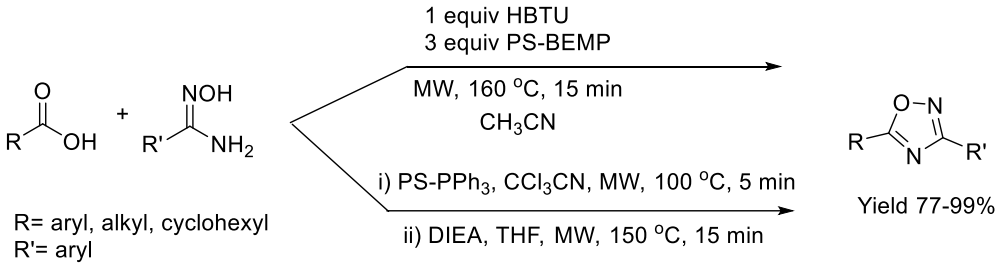

Scheme I.B.5. Polymer-assisted solution-phase synthesis of 1,2,4-oxadiazoles.

I.B.2.2. Synthesis of 3,5-disubstituted 1,2,4-oxadiazoles from nitriles

Kaboudin *et al*. reported the one-pot synthesis of 1,2,4-oxadiazoles through the solvent-free reaction of nitriles with hydroxylamine hydrochloride ($NH_2OH.HCl$) in the presence of magnesia-supported sodium carbonate (Scheme I.B.6) followed by reaction with acyl halides under microwave irradiation [25]. Other bases were also employed in this reaction but they were not much effective as Na_2CO_3. Different substituted benzonitriles reacted with hydroxylamine hydrochloride under the same reaction condition followed by the addition of acyl halide and afforded the product with a good yield.

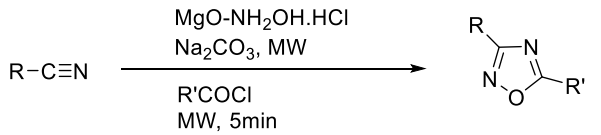

R= C_6H_5, *p*-$ClC_6H_4CH_2$,*p*-ClC_6H_4, 2,4-$Cl_2C_6H_3$, m-ClC_6H_4, Cyclohexyl
R'= C_6H_5, *p*-$CH_3OC_6H_4$, *p*-$NO_2C_6H_4$

Yield 40-70 %

Scheme I.B.6. Magnesia-supported sodium carbonate catalyzed synthesis of oxadiazole.

Adib *et al.* reported a facile one-pot three-component synthesis of 3,5-disubstituted 1,2,4-oxadiazoles from nitriles, hydroxylamine, and aldehydes under solvent-free conditions and microwave irradiation (Scheme I.B.7) [19]. This reaction was carried out in presence of a catalytic amount of acetic acid. After a minute of MW irradiation nearly full conversion of the amidoxime intermediate was observed, then aldehyde was added to the reaction mixture and irradiated for a further 3 min. The formation of the 1,2,4-oxadiazoles in excellent yields was indicated by TLC analysis. Different substituted nitriles and aldehydes were successfully implemented in this protocol to synthesize the corresponding oxadiazoles in excellent yield.

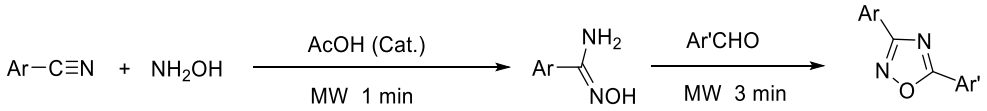

Yield 92-97%

Ar= C_6H_5, 4-$CH_3C_6H_4$, 3-ClC_6H_4
Ar'= C_6H_5, 4-$CH_3C_6H_4$, 4-$OCH_3C_6H_4$, 3-ClC_6H_4, 4-ClC_6H_4

Scheme I.B.7. 3,5-disubstituted 1,2,4-oxadiazoles synthesis from nitriles, hydroxylamine, and aldehydes under solvent-free conditions and microwave irradiation.

Wang *et al.* developed an efficient base-mediated synthesis of 3,5-disubstituted 1,2,4-oxadiazoles using nitrile, hydroxylamine hydrochloride, and aldehyde (Scheme I.B.8) [26]. Aldehydes are weak oxidants as they take part in self-redox reactions using a concentrated strong alkaline solution. They observed that the formation of oxadiazole was carried out by three sequential steps a) nucleophilic addition of hydroxylamine to produce amidoxime intermediate in the presence of triethylamine (TEA) for 18 h without exclusion of air at 80 °C, b) base mediated cascade coupling and cyclization reaction, c) oxidative dehydrogenation to form the target compound. Two different solvents were used in this reaction, *t*-BuOH was used as the solvent in the 1st step at 80 ºC and DMSO was the best solvent in the 2nd step of the reaction at 100 °C. The electron-donating and electron-withdrawing groups in aromatic nitriles, heterocyclic nitriles, and aromatic aldehydes were successfully capable to afford the corresponding oxadiazoles in moderate to excellent yield. However, the presence of larger steric hindrance in the substituents lowers the yield of the product.

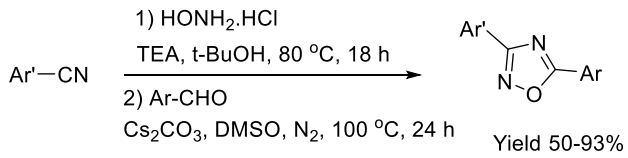

Ar'= C_6H_5, 4-$CH_3C_6H_4$, 3-$CH_3C_6H_4$, 2-$CH_3C_6H_4$, 4-$OCH_3C_6H_4$, 4-$CF_3C_6H_4$, 4-BrC_6H_4
Ar= C_6H_5, 4-$CH_3C_6H_4$, 3-$CH_3C_6H_4$, 2-$CH_3C_6H_4$, 4-$OCH_3C_6H_4$, 4-ClC_6H_4, napthyl, furyl, thinyl, pyridyl

Scheme I.B.8. An efficient base-mediated synthesis of 3,5-disubstituted 1,2,4-oxadiazoles.

Kuram *et al*. reported a Cu-catalyzed one-step protocol for the synthesis of 1,2,4-oxadiazoles from stable, readily available, and less toxic amides and organic nitriles by an oxidative rare N–O bond formation using oxygen as the sole oxidant (Scheme I.B.9) [27]. The optimized condition was obtained when CuI (10 mol%), bathophenanthroline ligand (10 mol%), K_2CO_3 base (2.0 equiv.), ZnI_2 (10 mol%), were used in 1,2-dichlorobenzene (1,2-DCB) at 130 °C temperature for 24 h. The substrates bearing electron-donating and withdrawing groups at the para position of the benzonitrile afford the corresponding product in good yields. This method showed good tolerance for diverse functional groups and broad substrate scope.

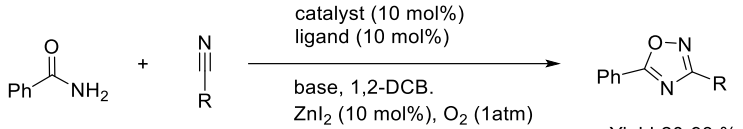

R= (hetero)aryl or alkyl

Scheme I.B.9. Cu-catalyzed one-step protocol for the synthesis of 1,2,4-oxadiazole.

I.B.3. Present work: Result and discussion

Herein we have developed a convenient and efficient process for the synthesis of 3,5-disubstituted 1,2,4-oxadiazoles (Scheme I.B.10) using an inexpensive, environmentally benign, metal-free heterogeneous carbocatalyst, graphene oxide (GO). GO plays a dual role of an oxidizing agent and solid acid catalyst for synthesizing 1,2,4-oxadiazoles. This dual catalytic activity of GO is due to the presence of oxygenated functional groups which are distributed on the nanosheets of graphene oxide. A broad scope of substrate applicability and good sustainability is offered in this developed protocol.

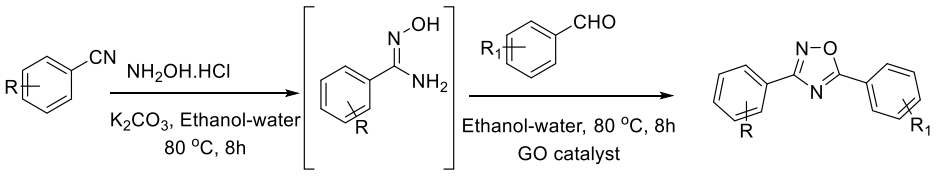

R= H, 4-CH_3, 4-OCH_3, 4-pyridinecarbonitrile
R_1= H, 4-CH_3, 4-OCH_3, 4-F, 3-NO_2, 4-$N(CH_3)_2$
1-Napthaldehyde, Furan-2-carbaldehyde,
Thiophene-2-carbaldehyde, Acetaldehyde

Scheme I.B.10. Synthesis of 1,2,4-oxadiazole using GO as catalyst.

I.B.3.1. Optimization of the reaction condition

For screening the reaction parameter benzonitrile (1.5 mmol), hydroxylamine hydrochloride (1.5 mmol), and base (1.5 mmol) were taken as model substrates to find out suitable conditions for the synthesis of amidoxime (intermediate). To satisfy our curiosity, the reaction was performed in different solvents e.g. polar protic, polar aprotic, and nonpolar. However, in absence of a base, a low yield was obtained (Table 1.B.1, entry 6). Gratifyingly, the reaction results showed (Table 1.B.1) the formation of amidoxime is highly favored in mixed solvent ethanol-water (1:3) using K_2CO_3 as a base. To control the reaction conditions, after completion of the reaction,the solvent was removed by a rotary

evaporator to separate the intermediate. While monitoring the TLC, only one spot was observed other than the reactant. After workup and purification by column chromatography, 91% yield of the intermediate (amidoxime) was obtained (Table I.B.1, entry 7). Although other bases were also employed (Table 1.B.1, entry 2, 5, 9), K_2CO_3 exerted the best result in an ethanol-water solvent. The synthesized amidoxime was characterized by NMR (300 MHz) spectroscopy.

Table I.B.1. Optimization of reaction condition for the synthesis of amidoxime (intermediate)[a]

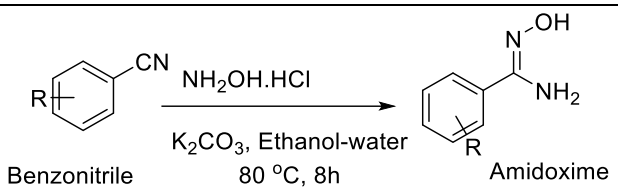

Benzonitrile — Amidoxime

Entry	Solvent	Temp. (°C)	Base	Yield(%)[b]
1	Water	100	K_2CO_3	68
2	Water	100	Cs_2CO_3	72
3	Ethanol	80	K_2CO_3	66
4	Ethanol	80	TEA	70
5	Ethanol-water	80	TEA	80
6	Ethanol-water	80	-	<50[c]
7	**Ethanol-water**	**80**	**K_2CO_3**	**91**
8	Ethanol-water	80	K_2CO_3	94[d]
9	Ethanol-water	80	Cs_2CO_3	93
10	THF	120	K_2CO_3	54
11	Toluene	110	K_2CO_3	<50
12	CH_3CN	82	K_2CO_3	68
13	DMF	120	K_2CO_3	76

[a]Reaction condition: Benzonitrile (1.5 mmol), hydroxylamine hydrochloride (1.5 mmol), base (1.5 mmol) and solvent (5 mL).
[b]Isolated yield.
[c]No base was added.
[d]The reaction was carried out for 24 hrs.

In the second step of the reaction, benzaldehyde (1 mmol) and the catalyst were added to the synthesized amidoxime in ethanol-water solvent to prioritize the synthesis of 3,5-disubstituted 1,2,4-oxadiazole. In presence of a small amount of GO, 73% yield of the product was obtained at 80 ^{o}C temperature (Table I.B.2, entry 2). Further increase in the amount of GO, proved to be favorable in the formation of 1,2,4-oxadiazole. No product was obtained when the reaction was carried out in absence of GO (Table I.B.2, entry 1). High yield of the product was observed in aqueous ethanolic solution with a ratio ethanol-water (1:3). The outstanding catalytic activity of GO in ethanol-water (1:3) is revealed due to its better dispersibility. To establish the catalytic activity of GO, few controlled experiments were carried out using various catalysts. Other carbonaceous nanomaterials e.g. powdered graphite, reduced graphene oxide (rGO) showed less catalytic activity than GO because they do not contain as many hydroxyl and carboxylic groups, indicating oxygen-containing functional groups in graphene oxide have a profound effect in catalyzing the synthesis of 3,5-disubstituted 1,2,4-oxadiazole. The reaction was also carried out in presence of GO and an oxidant H_2O_2, the reason for the low yield may be due to the oxidation of benzaldehyde to benzoic acid in presence of H_2O_2 (Table I.B.2, entry 12). The yield was not improved when only an H_2O_2 oxidant was used (Table I.B.2, entry 13). These control experiments infer the significant catalytic role of GO in the reaction.

Table I.B.2. Optimization of reaction condition for the synthesis of 3,5-disubstituted 1,2,4-oxadiazole from amidoxime[a]

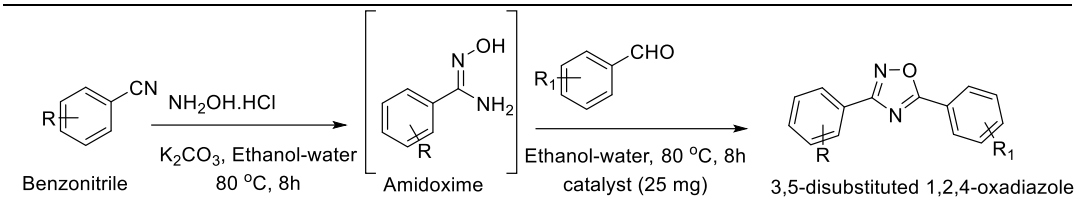

Entry	Catalyst (mg)	Solvent	Temp. (°C)	Time (h)	Yield%
1	-	Ethanol	80	12	Trace
2	15 (GO)	Ethanol	80	12	73
3	15 (GO)	Water	100	12	77
4	15 (GO)	DMF	100	12	60
5	15 (GO)	Ethanol-water	80	12	79
6	15 (GO)	Ethanol-water	80	24	83
7	25 (GO)	Ethanol-water	80	12	89
8	**25 (GO)**	**Ethanol-water**	**80**	**8**	**88**
9	25 (GO)	Ethanol-water	rt	12	52
10	25 (Graphite)	Ethanol-water	80	8	40[b]
11	25 (rGO)	Ethanol-water	80	8	45[c]
12	25 (GO)/Oxidant	Ethanol-water	80	8	67[d]
13	Oxidant	Ethanol-water	80	8	<40[e]
14	25 (GO)	Neat	80	8	69
15	25 (GO)	Ethanol-water	80	8	85[f]
16	-	Ethanol-water	80	8	Nil[f]

[a]Reaction condition: Benzaldehyde (1 mmol), amidoxime (1 mmol) and Ethanol-water (5 mL), pristine GO (25 mg).
[b]Graphite powder was used.
[c]Reduced graphene oxide (rGO).
[d]GO and extra oxidant 30 % H_2O_2 (1 mmol) were used.
[e]Only H_2O_2 was used.
[f]Under inert atmospheric condition.

The scope and the substrate applicability of the reaction were also examined and results were summarized in Table I.B.3. With the optimized condition in hand, we have extended the substrate scope in organic

transformations and a series of diversely substituted aldehydes and benzonitriles are subjected to the synthesis of 3,5-disubstituted 1,2,4-oxadiazole (Table I.B.3). Both the electron-donating (Table I.B.3, entries 2-3, 10-11) and electron-withdrawing groups (entries 4-5) in the substituents afforded the corresponding product in good to excellent yield which indicates that the electronic nature of the substituents is not much influential to determine the yield of the reaction. 1-Napthaldehyde offered the product with low yield and the reason may be due to steric hindrance (Table I.B.3, entry 7).

Table 1.B.3. Synthesis of diversely functionalised 3,5-disubstituted 1,2,4-oxadiazole[a]

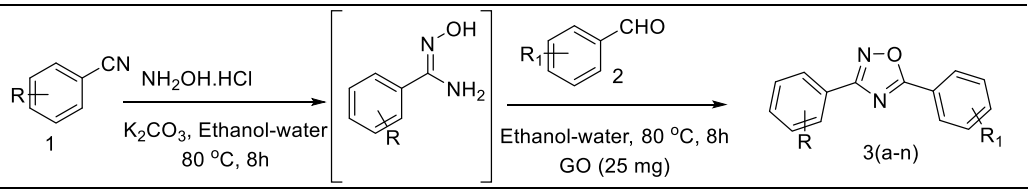

Entry	R	R_1	Product	Yield (%)[b]
1	4-H	4-H	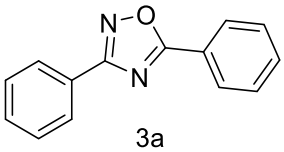 3a	83
2	4-H	4-CH_3	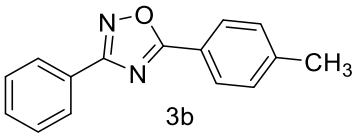 3b	81
3	4-H	4-OCH_3	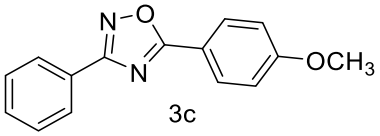 3c	80
4	4-H	4-F	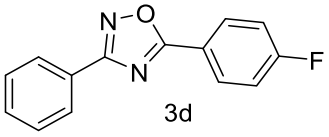 3d	78

5	4-H	3-NO_2	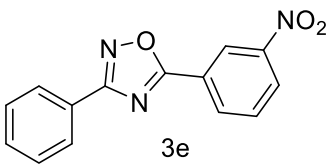 3e	75
6[c]	4-H	4-$N(CH_3)_2$	No 1,2,4-oxadiazole, only imine formation	-
7	4-H	1-Napthaldehyde	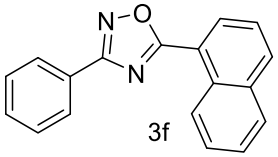 3f	62
8	4-H	Furan-2-carbaldehyde	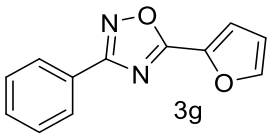 3g	72
9	4-H	Thiophene-2-carbaldehyde	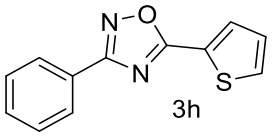 3h	70
10	4-CH_3	4-H	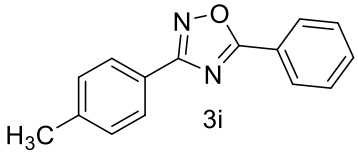 3i	80
11	4-OCH_3	4-H	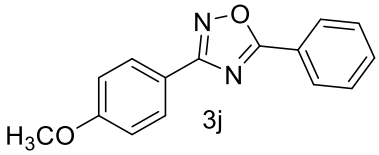 3j	78
12	4-OCH_3	4Cl	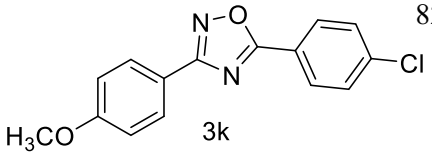 3k	82
13	4-Pyridinecarbonitrile	4-H	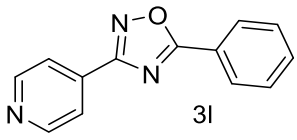 3l	68

14	4-H	CH_3CHO	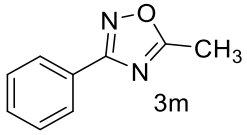 3m	75
15[d]	4-H	Heptaldehyde	NR	-
16[e]	CH_3CN	4-H	NR	-

[a] In the first step, Benzonitrile (1 mmol), hydroxylamine hydrochloride (1.5 mmol), K_2CO_3 (1.5 mmol), and Ethanol-water (5 mL) were stirred for 8 hr and in the 2nd step benzaldehyde (1 mmol) and GO (25 mg) were added in same reaction vessel and stirred for another 8 hr.
[b] Isolated yield after purification through column chromatography.
[c] 4-(dimethylamino)benzaldehyde (1 mmol) was used.
[d] Heptaldehyde was used.
[e] Acetonitrile (1 mmol) was used.

In the case of 4-*N,N*-(dimethylamino)benzaldehyde, the reaction was stopped at amidoxime, no desired oxadiazole is obtained (Table I.B.3, entry 6). The present catalytic condition showed a wide tolerance to heterocyclic aldehydes (Table I.B.3, entries 8, 9) and they were found to be highly effective to afford the corresponding product. The generality of the reaction was examined in the case of aliphatic aldehydes also. Interestingly, acetaldehyde was equally effective to yield the product with excellent quantity (Table I.B.3, entry 14). However, no product was found with increasing the side chain of aliphatic aldehydes (Table I.B.3, entry 15). It was disappointing that acetonitrile did not exert the corresponding product (Table I.B.3, entry 16). Due to the heterogeneous nature of GO, it can be easily isolated from the reaction mixture and reused. The catalytic activity of GO was examined for five consecutive cycles for the synthesis of 3,5-disubstituted 1,2,4-oxadiazole from benzaldehyde and amidoxime under reflux conditions for 8h to ascertain the recyclability potential of graphene oxide. The catalyst was separated after each recycles and washed thoroughly with ethanol and reused. A marginal decrease in the yield of oxadiazole is observed after each cycle which indicates a slight loss of catalytic activity of GO with recycling (Figure I.B.2).

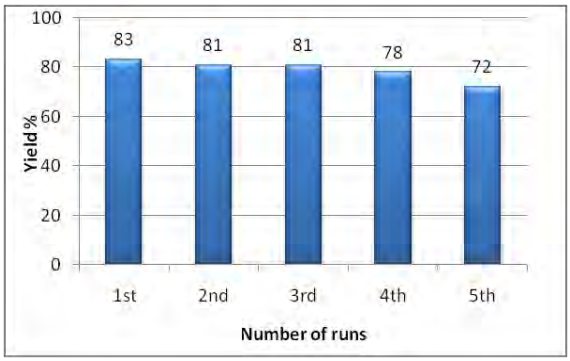

Figure I.B.2. Recyclability study of GO for the synthesis of 3,5-disubstituted 1,2,4-oxadiazole.

The catalytic activity arises some structural changes in GO which were analyzed by FTIR, XRD, SEM, HR-TEM, and EDX analysis. The XRD spectra of fresh GO and recycled catalyst (GO after 3rd run and 5th run) are shown in Figure I.B.3.

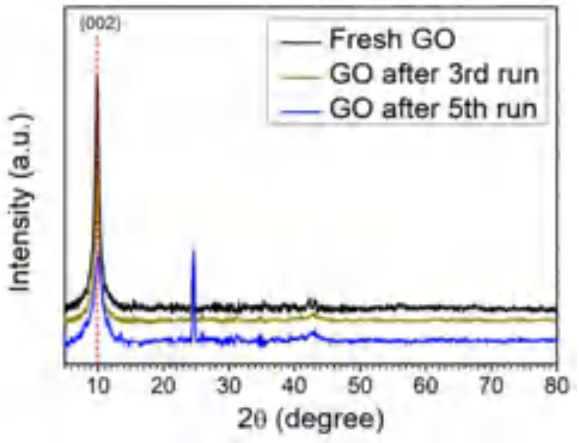

Figure I.B.3. *XRD spectra of fresh GO, after 3rd run and 5th run.*

A comparison of spectra indicates the reduction in the intensity of the first characteristic peak of GO (2Θ = 10.01) and the appearance of a new peak at (2Θ

= 24.62) due to the formation of partially reduced GO/ reduced graphene oxide upon reuse. These results confirm the reduction of the functional groups of GO during the reaction.

The comparison of the FTIR spectra revealed that the peak at 1720 cm^{-1} in fresh GO has completely disappeared after reuse. In addition to this, the peak intensity of the hydroxyl group at 3400 cm^{-1} decreases after reuse. FTIR data strongly support the reduction of GO to rGO in this oxidative cyclization reaction (Figure I.B.4).

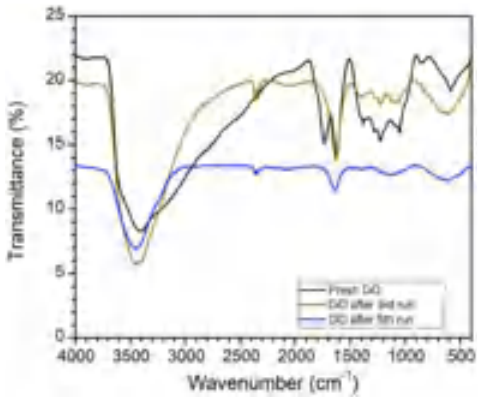

Figure I.B.4. *Comparative FTIR of fresh GO, after 3rd run and 5th run.*

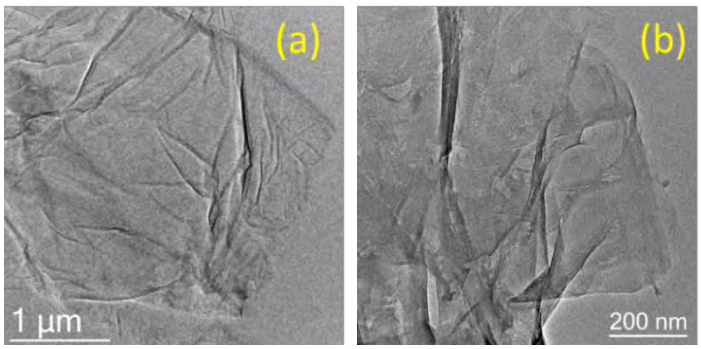

Figure I.B.5. *HR-TEM images of (a) GO and (b) GO after the 5th run.*

A morphological study of GO and GO after the 5th run was carried out using SEM and HR-TEM to investigate the disintegration of graphene oxide sheets after the reaction. In HR-TEM, the graphene oxide sheets are disintegrated into smaller sheets with slight aggregation after recycle (Figure I.B.5).

Moreover, the SEM images (Figure I.B.6) also reveal the formation of multiple small GO sheets after reuse. As GO catalyzes the reaction,its reduction to reduced graphene oxide possibly leads to its disintegration into smaller sheets.

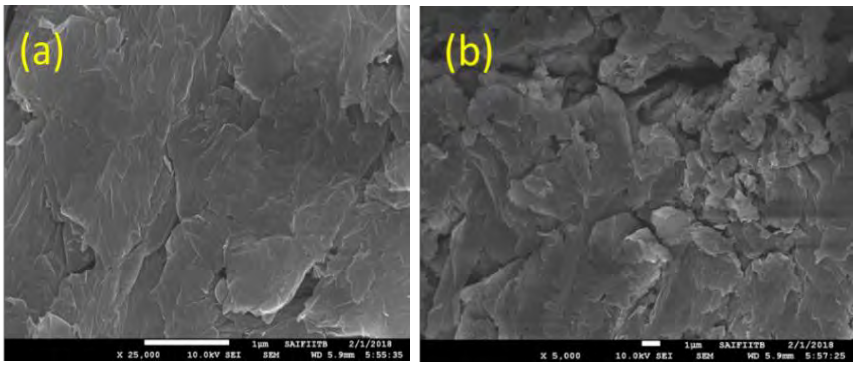

Figure I.B.6. *SEM images of (a) GO and (b) GO after the 5th run.*

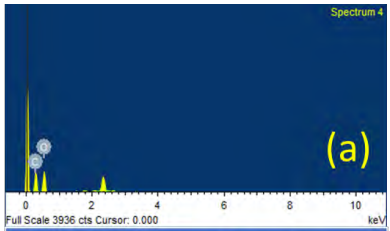

Weight percent of constituent elements	
C	52.65
O	47.35

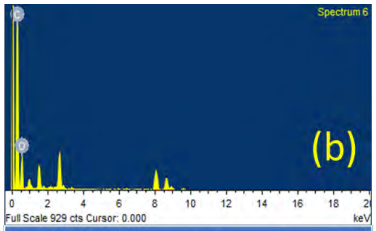

Weight percent of constituent elements	
C	71.79
O	28.21

Figure I.B.7. *EDX spectra of (a) GO and (b) GO after the 5th run.*

The contribution of oxygen-containing functionalities during the reaction was further confirmed by the EDX analysis (Figure I.B.7). The carbon content was increased from 52.65% (fresh GO) to 71.79% (GO after 5th run) and the oxygen content was decreased from 47.35% (fresh GO) to 28.21% (GO after 5th run). The decrease in the oxygen content, therefore, indicates the role of GO in this cyclization reaction as an oxidizing agent. The universality and the dual catalytic activity of GO were established by a plausible mechanism (Scheme I.B.11).

I.B.3.2. Mechanism

A plausible mechanism of GO catalyzed synthesis of 3,5-disubstituted 1,2,4-oxadiazole has been proposed (Scheme I.B.11) based on literature reports [28] and our controlled experiments (Table I.B.2). Now, we propose the formation of amidoxime intermediate (I) from benzonitrile and hydroxylamine hydrochloride. However, in the first step, a base is required to neutralize hydroxylamine hydrochloride. In the 2nd step, protonation of aldehyde, oxygen occurs and subsequently, a nucleophilic attack by amidoxime occurs at the electrophilic center of aldehyde. After that, the intermediate (II) undergoes an oxidative cyclization in presence of GO to produce 1,2,4-oxadiazoles. This mechanism is in good agreement with the control experiments as described in table I.B.2. However, in presence of only H_2O_2 oxidant the yield of the reaction was diminished (Table I.B.2, entry 13). The role of GO as an acid catalyst and an oxidant was confirmed as its absence did not lead to the oxadiazole product (Table I.B.2, entry 1). The oxygen containing functional groups of GO are consumed during the reaction and the activity of GO gradually decreases. The activity of recycled GO is lower than that of the pristine GO. Good yield of the

product was obtained even under an inert atmosphere which strongly establish (Table I.B.2, entry 15), the prime role of GO in absence of atmospheric oxygen.

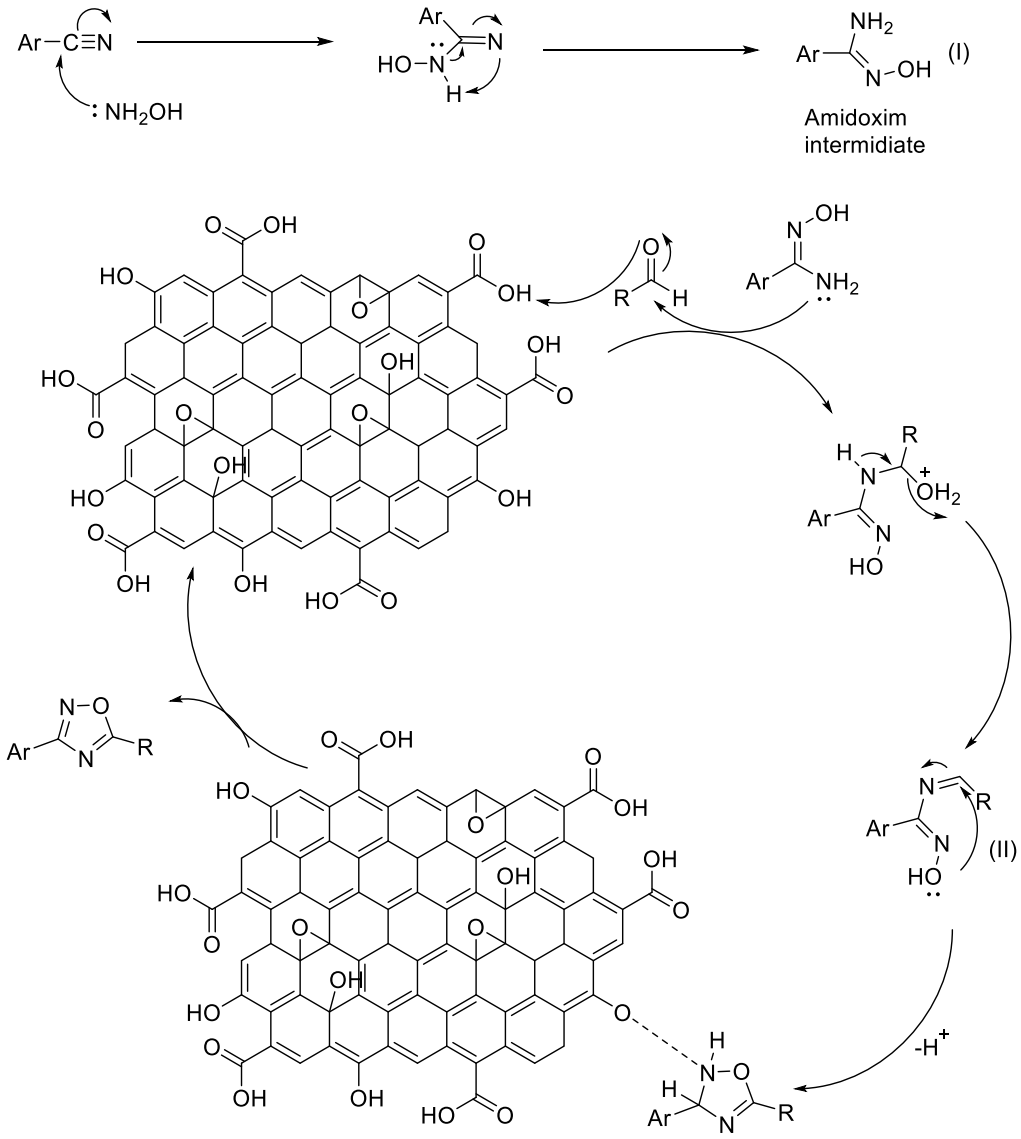

Scheme I.B.11. *A plausible route to the synthesis of 3,5-disubstituted 1,2,4-oxadiazole.*

I.B.4. Conclusion

In conclusion, carbocatalyst based metal-free catalytic pathway for the synthesis of 3,5-disubstituted 1,2,4-oxadiazoles has been established. The solid acid catalyst, GO facilitates the synthesis of oxadiazoles with good yield, easy recovery, and under mild reaction conditions. The dual catalytic activity of GO has been demonstrated without any undesired by-product under benign conditions. The present protocol gives a clean strategy to provide a wide variety of substituted oxadiazoles .

I.B.5. Experimental section

I.B.5.1. General experimental procedure

All the chemicals and reagents were purchased from Sigma–Aldrich, Spectrochem, TCI and were used without further purification. The solvents were purchased from commercial suppliers and were used after proper distillation. The progress of the reaction was monitored by Merck TLC plates which are coated with silica gel (60 F_{254}) and UV light was used as visualizing agent. NMR spectra of all the synthesized compounds were carried out in $CDCl_3$/DMSO-d_6 solvent and TMS was used as an internal standard. All the NMR spectroscopic data are recorded in BrukerAvance FT-NMR operating for 1H at 300/400 MHz. The ^{1}H NMR data are represented by chemical shift δ (ppm), multiplicity (s = singlet, d= doublet, t = triplet, m = multiplet), integration, coupling constants (Jvalues) in Hertz (Hz). The ^{13}C NMR spectroscopic data are also reported in ppm as ^{1}H NMR spectra.

I.B.5.2. General procedure for the preparation of (GO) catalyst

There are several methods for the preparation of graphene oxide (GO). Herein, Graphene oxide (GO) was synthesized by the Tours method using

graphite powder as starting material [29]. At first, 9:1 volume ratio of (180 mL) sulfuric acid (H_2SO_4) and (20 mL) phosphoric acid (H_3PO_4) were taken in a 500 ml conical flask, and then 1.5 g of graphite powder was added to it under stirring condition. The temperature of the whole mixture was kept below 10 ^oC using an ice bath and 9g of potassium permanganate ($KMnO_4$) was added very slowly into it as the addition of $KMnO_4$ evolves heat. Then the reaction mixture was stirred for 12 hrs and after that hydrogen peroxide (H_2O_2) was added drops wise to eliminate excess $KMnO_4$. After that, 30-40 mL hydrochloric acid (HCl) (strength 30%) was added to this mixture followed by the addition of 200 mL of deionized water. Then the mixture was centrifuged at 5000 rpm for 20 minutes. After that, the supernatant liquid was decanted away and the residual was dried at 90 ^oC rotary evaporator to get dry graphene oxide (GO) with pH (4.2 at 0.1 mg/mL).

I.B.5.3. General procedure for the synthesis of 3,5-disubstituted 1,2,4 oxadiazoles

50-mL of RB was charged with benzonitrile (1.5 mmol), hydroxylamine hydrochloride (1.5 mmol), K_2CO_3 (1.5 mmol), and Ethanol-water (5 mL), and then the reaction mixture was stirred at 80 ^oC for 8 hrs. After 8 hrs, benzaldehyde (1 mmol) and 25 mg of GO were added to it and the reaction was carried out for another 8 hrs. The progress of the reaction was governed by thin-layer chromatography (TLC). After completion of the reaction, the solvent was evaporated by a rotary evaporator. The reaction mixture was extracted by ethyl acetate and the catalyst was separated by a simple filtration procedure. After workup, ethyl acetate extract was concentrated in a water bath and further purified by column chromatography using silica gel 60-120 mesh.

I.B.5.4. ^{1}H and ^{13}C NMR data of various 3,5-disubstituted 1,2,4 oxadiazoles

***N'*-Hydroxybenzenecarboximidamide (Table I.B.1, entry 7) [26]**

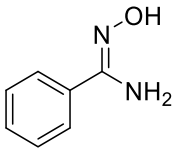

White solid;

MP: 72-74 ^{o}C

^{1}H NMR (300 MHz, $CDCl_3$) δ (ppm) 5.07 (bs, 2H), 7.32-7.42 (m, 3H), 7.55-7.59 (m, 2H), 8.79 (bs, 1H);

^{13}C NMR (75 MHz, $CDCl_3$) δ (ppm) 126.00, 128.67, 130.01, 132.38, 158.88 .

3,5-diphenyl-1,2,4-oxadiazole (Table I.B.3, entry 1) [28]

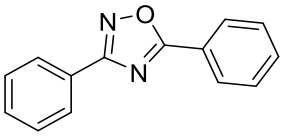

White solid;

MP: 103-104 ^{o}C;

^{1}H NMR (300 MHz, $CDCl_3$)δ (ppm) 7.42-7.51 (m, 6H), 8.15-8.20 (m, 4H);

^{13}C NMR (75 MHz, $CDCl_3$) δ (ppm) 126.96, 127.52, 128.16, 128.84, 129.09, 131.17, 132.72, 133.90, 168.04, 173.96.

3-phenyl-5-(p-tolyl)-1,2,4-oxadiazole (Table I.B.3, entry 2) [28]

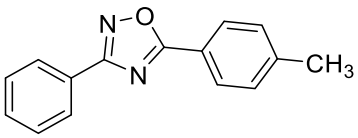

White solid;

MP: 110-112 ºC;

^{1}H NMR (300 MHz, $CDCl_3$) δ (ppm) 3.89 (s, 3H), 7.06-7.20 (m, 2H). 7.49-7.54 (m, 3H), 7.80-7.90 (m, 4H);

^{13}C NMR (75 MHz, $CDCl_3$) δ (ppm) 54.76, 126.98, 127.55, 128.19, 128.88, 129.13, 131.22, 132.77, 150.49, 168.76, 174.91.

5-(4-methoxyphenyl)-3-phenyl-1,2,4-oxadiazole (Table I.B.3, entry 3) [28]

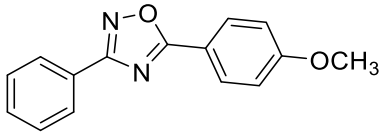

White solid;

MP: 100-101 ºC;

^{1}H NMR (300 MHz, $CDCl_3$) δ ppm: 3.89 (s, 3H), 7.04 (d, 2H, *J*= 8.7Hz), 7.50-7.52 (t, 3H), 8.15-8.18 (m, 4H);

^{13}C NMR (75 MHz, $CDCl_3$) δ (ppm) 55.07, 122.80, 126.71, 127.41, 128.09, 129.63, 130.62, 131.90, 133.93, 168.09, 174.91.

5-(4-fluorophenyl)-3-phenyl-1,2,4-oxadiazole (Table I.B.3, entry 4) [28]

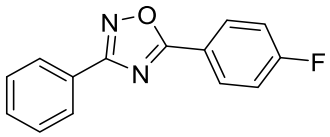

White solid;

MP: 118-119 ºC;

^{1}H NMR (300 MHz, $CDCl_3$) δ (ppm) 7.25 (d, 2H, *J*= 8.1 Hz), 7.52-7.57 (m, 3H), 8.21-8.47 (m, 4H);

^{13}C NMR (75 MHz, $CDCl_3$) δ (ppm) 120.80, 126.21, 127.10, 127.98, 128.77, 130.58, 130.74, 133.80, 169.05, 175.57.

5-(3-nitrophenyl)-3-phenyl-1,2,4-oxadiazole (Table I.B.3, entry 5) [29]

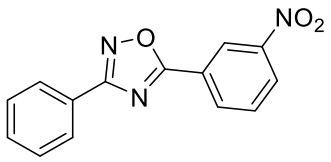

White solid;

MP: 140-142 °C;

^{1}H NMR (300 MHz, $CDCl_3$) δ (ppm) 7.75-7.89 (m, 3H), 8.14-8.31 (m, 5H), 8.62 (s, 1H);

^{13}C NMR (75 MHz, $CDCl_3$) δ (ppm) 123.57, 126.25, 126.71, 127.41, 127.93, 129.34, 130.83, 131.93, 133.90, 149.04, 169.67, 173.91.

5-(naphthalen-1-yl)-3-phenyl-1,2,4-oxadiazole (Table I.B.3, entry 7) [28]

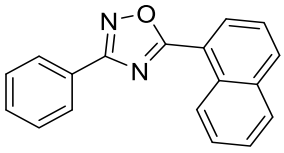

White solid;

MP: 99-101 °C;

^{1}H NMR (400 MHz, $CDCl_3$) δ (ppm) 7.63-7.73 (m, 5H), 8.02-8.14 (m, 5H), 8.60 (d, 1H, *J* = 8.4 Hz), 8.93 (d, 1H, *J* =8.4 Hz);

^{13}C NMR (100 MHz, $CDCl_3$) δ (ppm) 122.77, 126.77, 127.27, 127.53, 128.89, 129.15, 129.46, 129.53, 129.74, 130.89, 131.31, 131.79, 139.20, 169.06, 174.81.

5-(furan-2-yl)-3-phenyl-1,2,4-oxadiazole (Table I.B.3, entry 8) [28]

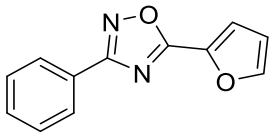

Yellow solid;

MP: 100-101 °C;

^{1}H NMR (300 MHz, $CDCl_3$) δ (ppm) 7.25-7.33 (t, 1H), 7.52-8.03 (m, 4H), 8.09 (d, 2H, J = 7.2 Hz), 8.18 (d, 2H, J = 6.9 Hz);

^{13}C NMR (75 MHz, $CDCl_3$) δ (ppm) 112.85, 116.69, 126.76, 127.91, 129.42, 131.68, 140.43, 147.05, 167.91, 168.99.

3-phenyl-5-(thiophen-2-yl)-1,2,4-oxadiazole (Table I.B.3, entry 9) [28]

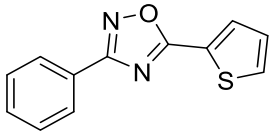

White solid;

MP: 107-108 °C;

^{1}H NMR (400 MHz, $CDCl_3$) δ (ppm) 7.23-7.29 (m, 1H), 7.54-7.68 (m, 4H), 7.98 (s, 1H), 8.17-8.24 (m, 2H);

^{13}C NMR (100 MHz, $CDCl_3$) δ (ppm) 127.58, 128.17, 128.51, 129.11, 131.26, 131.74, 132.88, 168.85, 171.36.

5-phenyl-3-(p-tolyl)-1,2,4-oxadiazole (Table I.B.3, entry 10) [28]

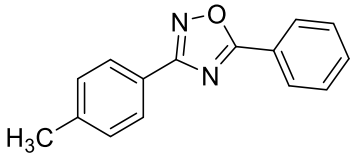

White solid;

MP: 100-102 ^{o}C;

^{1}H NMR (300 MHz, $CDCl_3$) δ (ppm) 2.43 (s, 3H), 7.53-7.61 (m, 3H), 8.00 (d, 2H, *J* = 6.9 Hz), 8.12 (d, 2H, *J* = 8.1 Hz), 8.59-8.78 (m, 2H);

^{13}C NMR (75 MHz, $CDCl_3$) δ (ppm) 21.61, 124.10, 127.95, 128.57, 128.92, 129.07, 129.39, 132.67, 141.50, 168.95, 174.10.

3-(4-methoxyphenyl)-5-phenyl-1,2,4-oxadiazole (Table I.B.3, entry 11) [28]

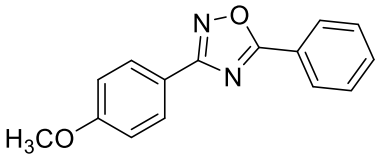

White solid;

MP: 101-102 ^{o}C;

^{1}H NMR (300 MHz, $CDCl_3$)δ (ppm) 3.88 (s, 3H), 7.02 (d, 2H, *J* = 8.7 Hz), 7.52-7.63 (m, 3H), 8.10-8.23 (m, 4H);

^{13}C NMR (75 MHz, $CDCl_3$) δ (ppm) 54.87, 113.759, 118.99, 123.97, 127.64, 128.54, 128.63, 132.09, 161.46, 168.18, 174.94.

5-(4-chlorophenyl)-3-(p-tolyl)-1,2,4-oxadiazole (Table I.B.3, entry 12) [28]

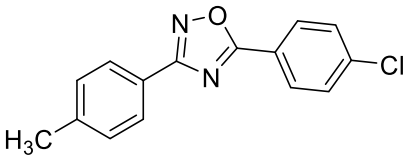

White solid;

MP: 132-134 ºC;

^{1}H NMR (300 MHz, $CDCl_3$) δ (ppm) 2.43 (s, 3H), 7.31 (d, 2H, *J* = 7.8 Hz), 7.51-7.54 (t, 2H), 8.04 (d, 2H, *J* = 8.1 Hz), 8.15 (d, 2H, *J* = 8.7 Hz);

^{13}C NMR (75 MHz, $CDCl_3$) δ (ppm) 21.124, 122.329, 123.418, 126.418, 126.943, 128.945, 129.002, 129.105, 138.612, 141.162, 168.552, 174.135.

5-phenyl-3-(pyridin-4-yl)-1,2,4-oxadiazole (Table I.B.3, entry 13) [28]

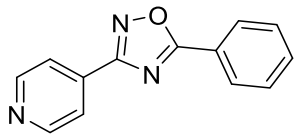

White solid;

MP: 145-146 ºC;

^{1}H NMR (300 MHz, $CDCl_3$) δ (ppm) 7.47-7.64 (m, 3H), 8.07-8.08 (t, 1H), 8.13-8.20 (m, 2H). 8.21-8.85 (m, 3H);

^{13}C NMR (75 MHz, $CDCl_3$) δ (ppm) 121.044, 123.294, 127.744, 129.460, 132.399, 134.321, 149.758, 166.834, 176.054.

5-methyl-3-phenyl-1,2,4-oxadiazole (Table I.B.3, entry 14) [28,30]

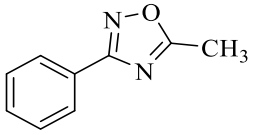

Colourless liquid;

BP>200 ºC;

^{1}H NMR (300 MHz, $CDCl_3$)δ (ppm) 2.57 (s, 3H), 7.36-7.38 (m, 3H), 7.95-7.98 (m, 2H);

^{13}C NMR (300 MHz, $CDCl_3$) δ (ppm) 12.36, 126.82, 127.33, 128.84, 131.11, 168.35, 177.28; LCMS (ESI-APCI) $C_9H_8N_2O$ for: 161$[M+H]^+$, Anal. Calcd for $C_9H_8N_2O$: C= 67.39, H= 5.09, N= 17.49.

I.B.5.5. Scanned copies of ^{1}H and ^{13}C NMR spectra of synthesized compounds

Figure I.B.8. *Scanned copy of ^{1}H and ^{13}C NMR spectra of N'-Hydroxybenzenecarboximidamide*

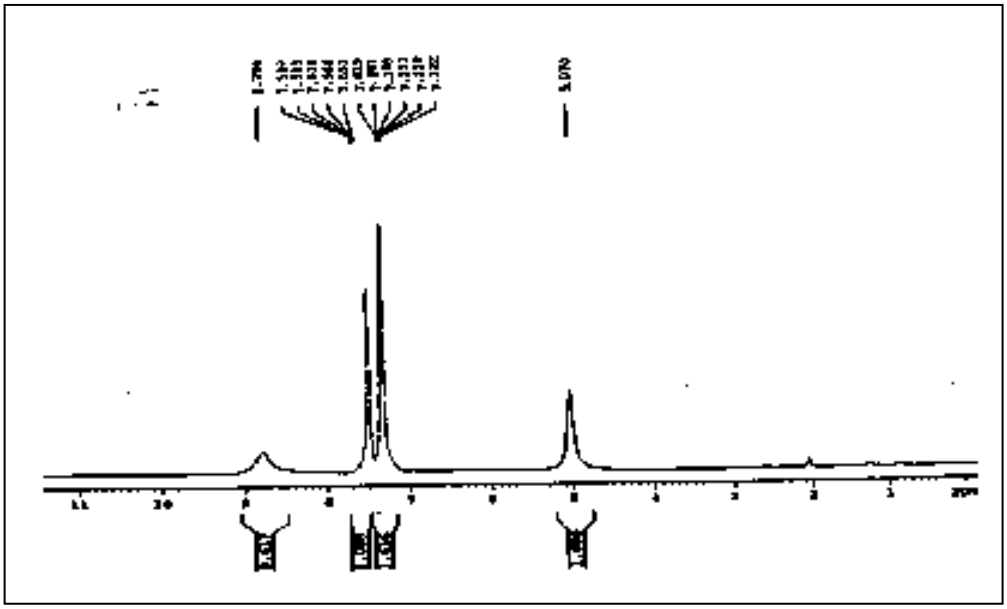

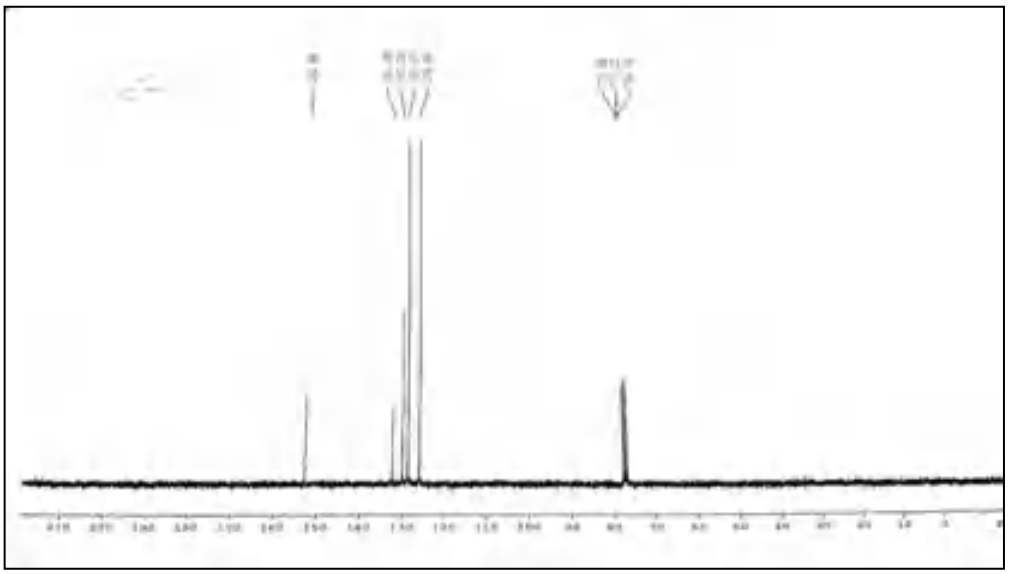

Figure I.B.9. *Scanned copy of ^{1}H and ^{13}C NMR spectra of 3,5-diphenyl-1,2,4-oxadiazole*

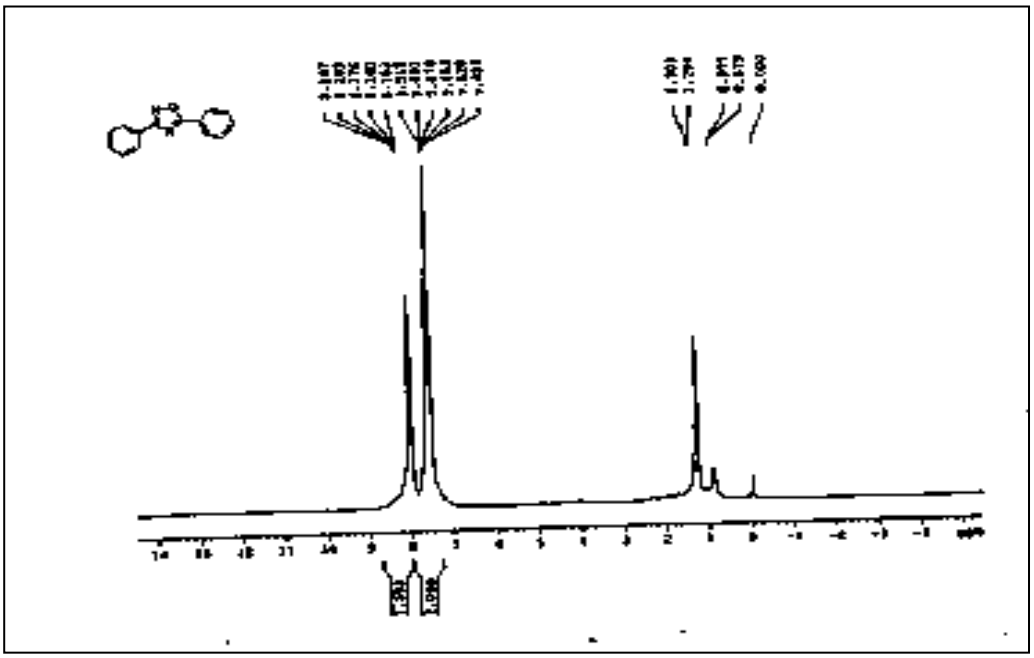

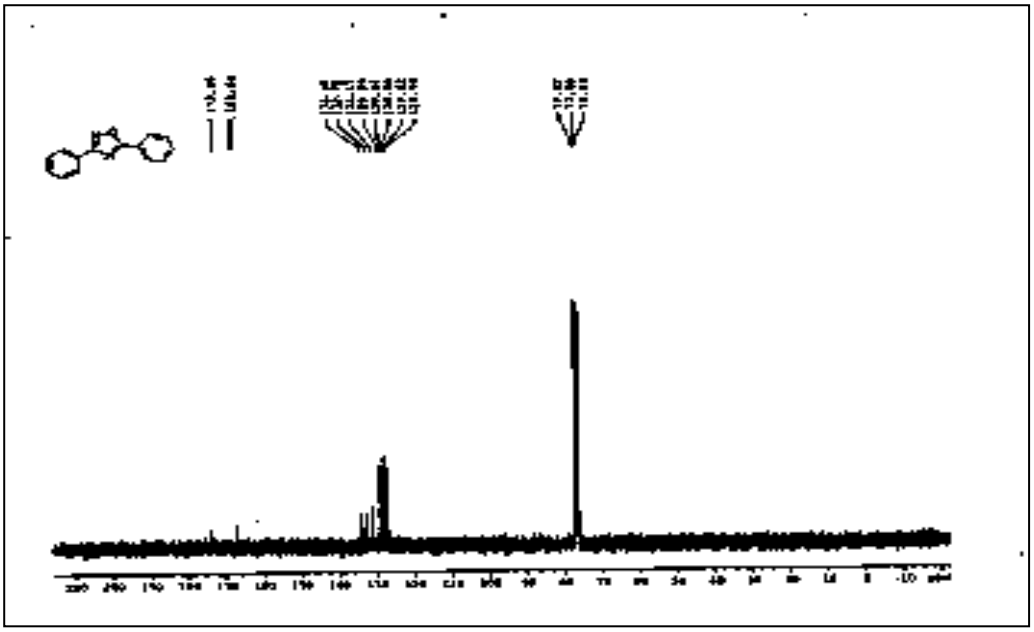

Figure I.B.10. *Scanned copy of ^{1}H and ^{13}C NMR spectra of 3-phenyl-5-(p-tolyl)-1,2,4-oxadiazole*

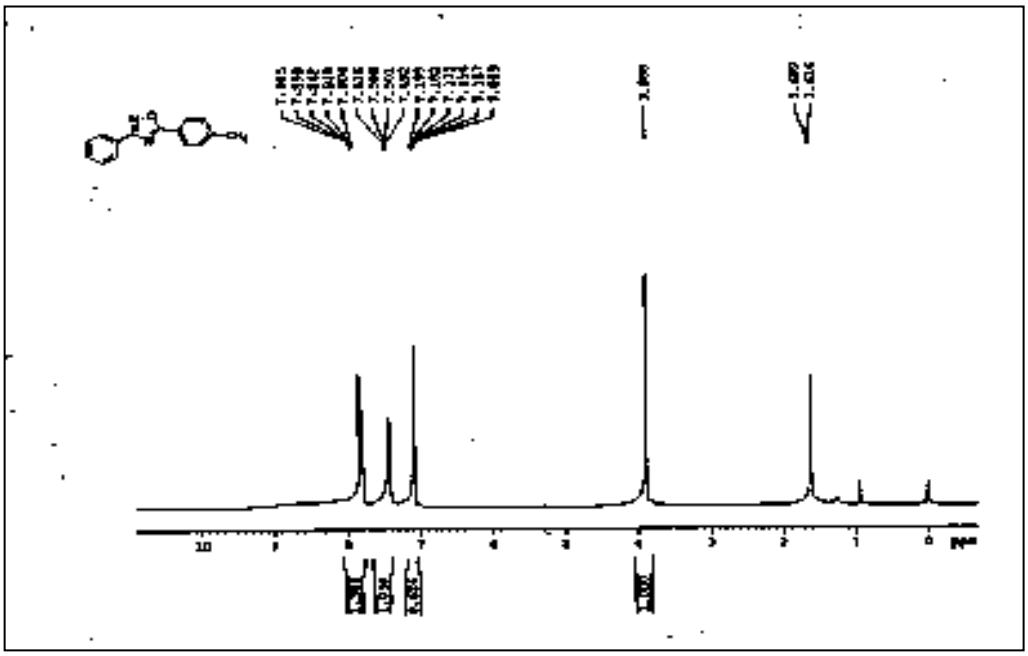

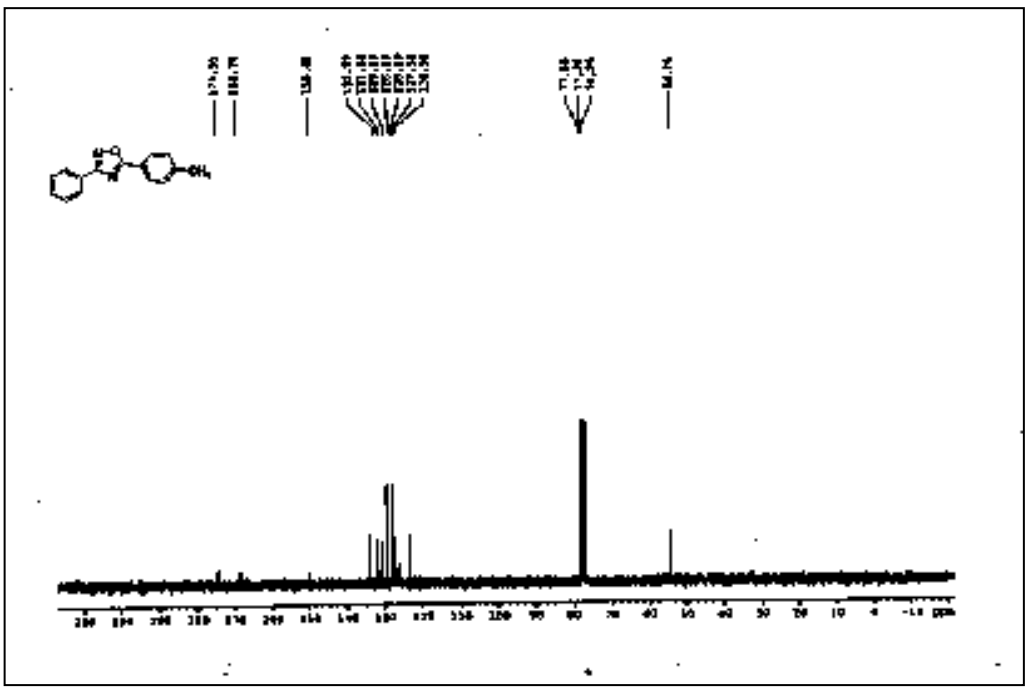

Figure I.B.11. *Scanned copy of ^{1}H and ^{13}C NMR spectra of 5-(4-methoxyphenyl)-3-phenyl-1,2,4-oxadiazole*

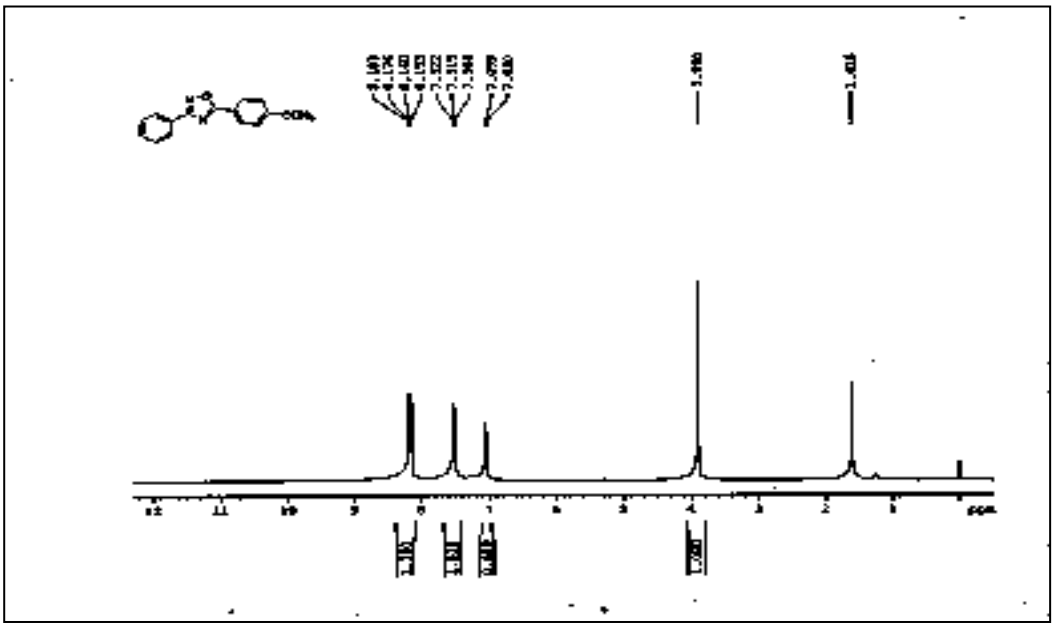

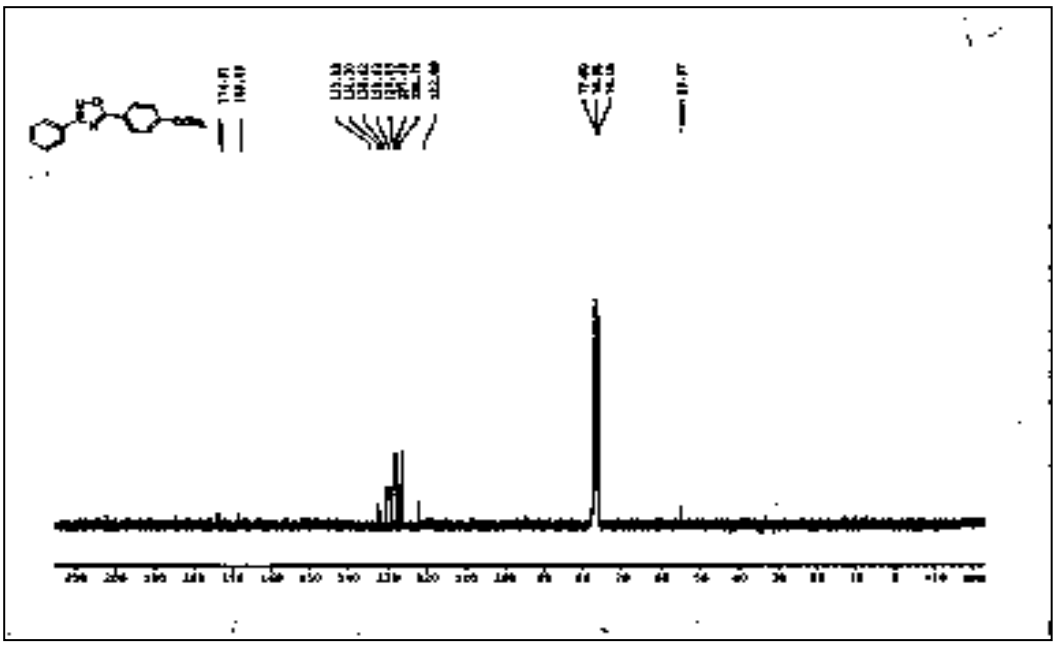

Figure I.B.12. *Scanned copy of ^{1}H and ^{13}C NMR spectra of 5-(4-fluorophenyl)-3-phenyl-1,2,4-oxadiazole*

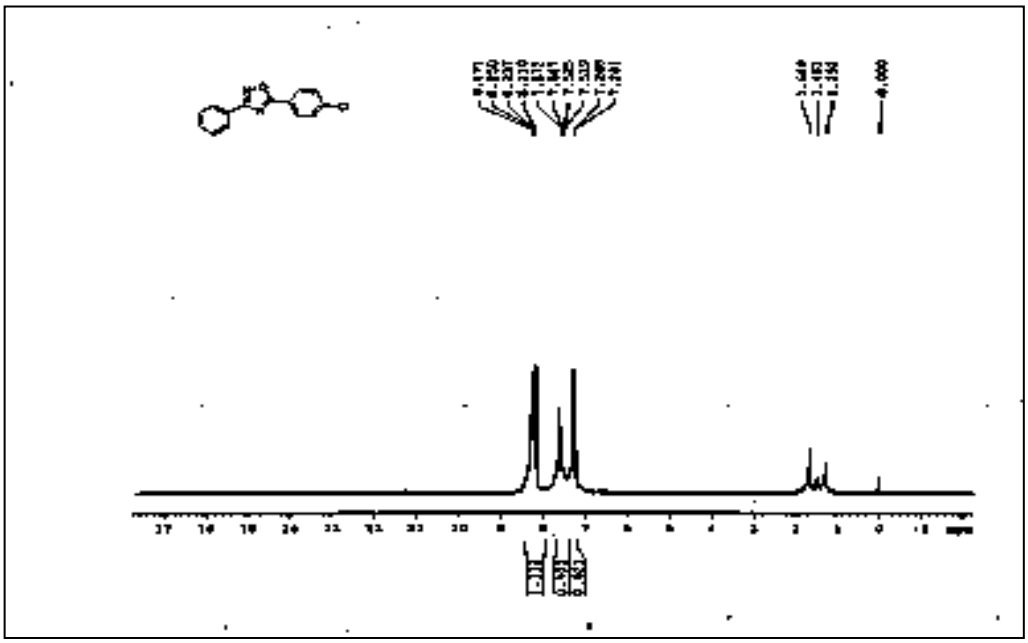

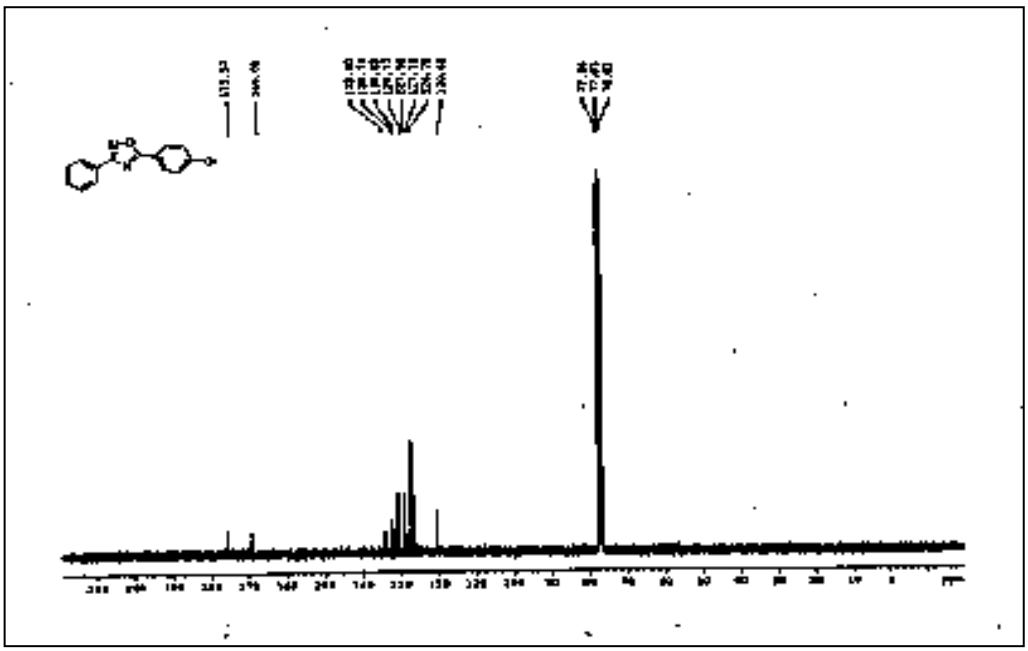

Figure I.B.13. *Scanned copy of ^{1}H and ^{13}C NMR spectra of 5-(3-nitrophenyl)-3-phenyl-1,2,4-oxadiazole*

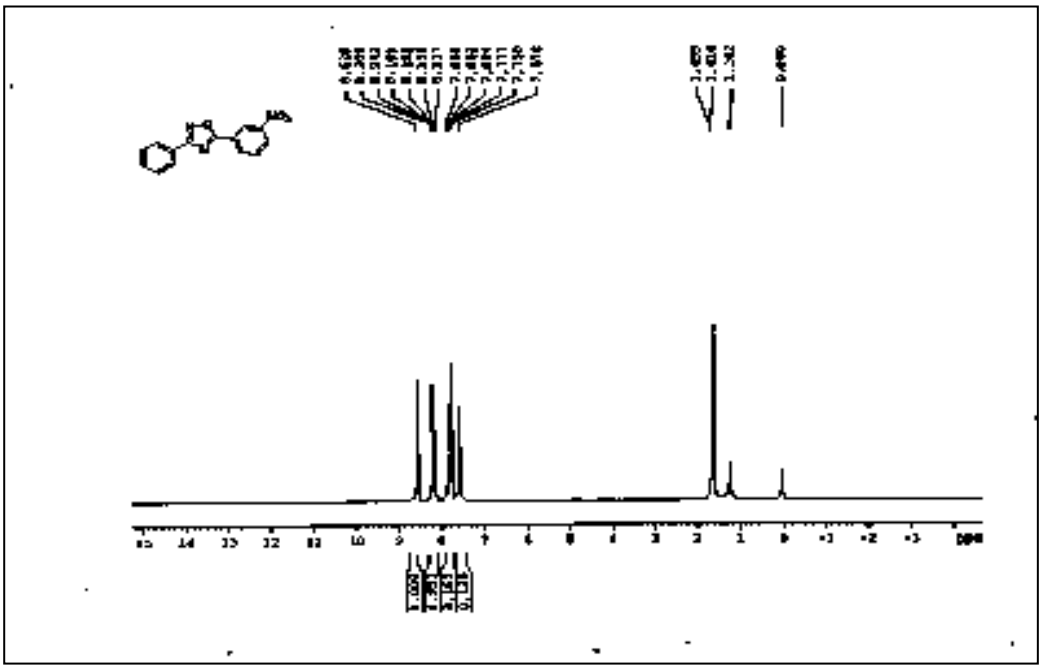

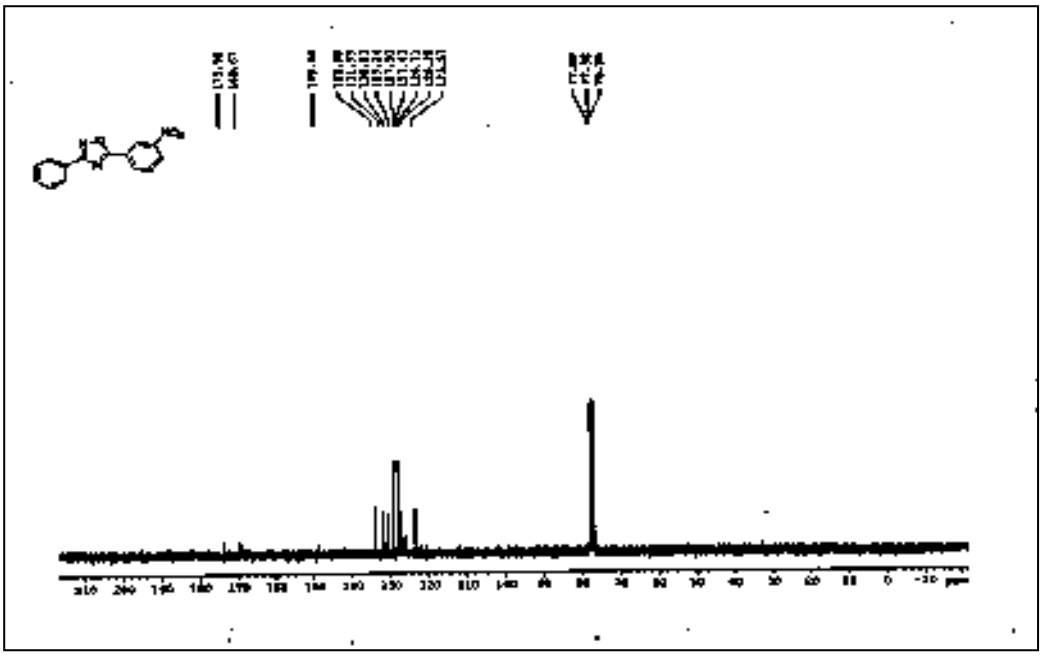

Figure I.B.14. *Scanned copy of ^{1}H and ^{13}C NMR spectra of 5-(naphthalen-1-yl)-3-phenyl-1,2,4-oxadiazole*

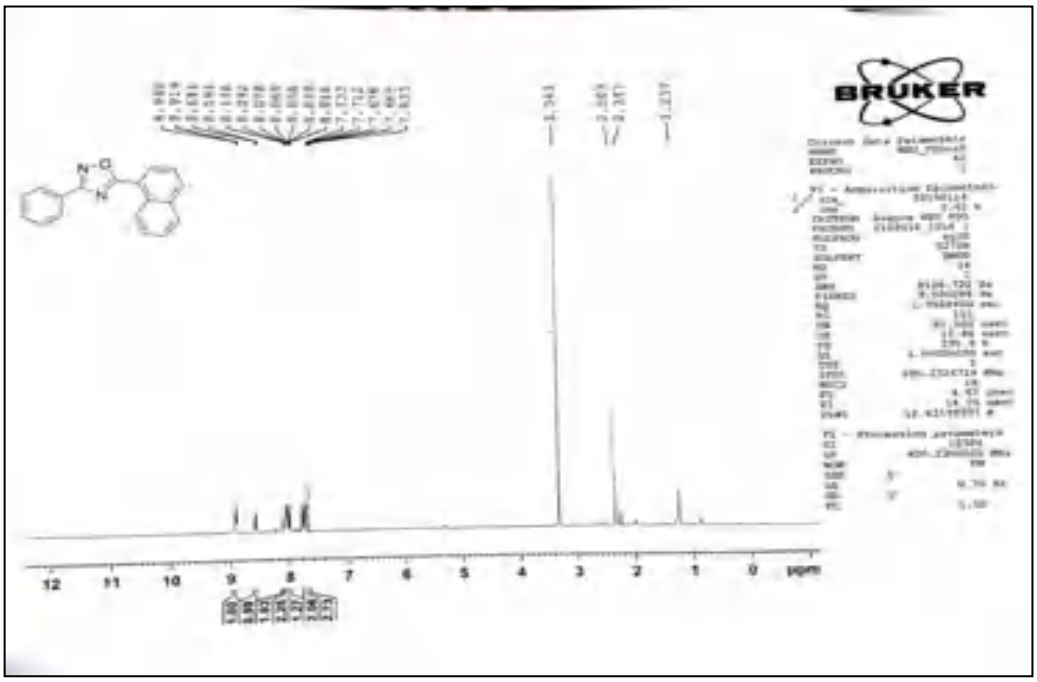

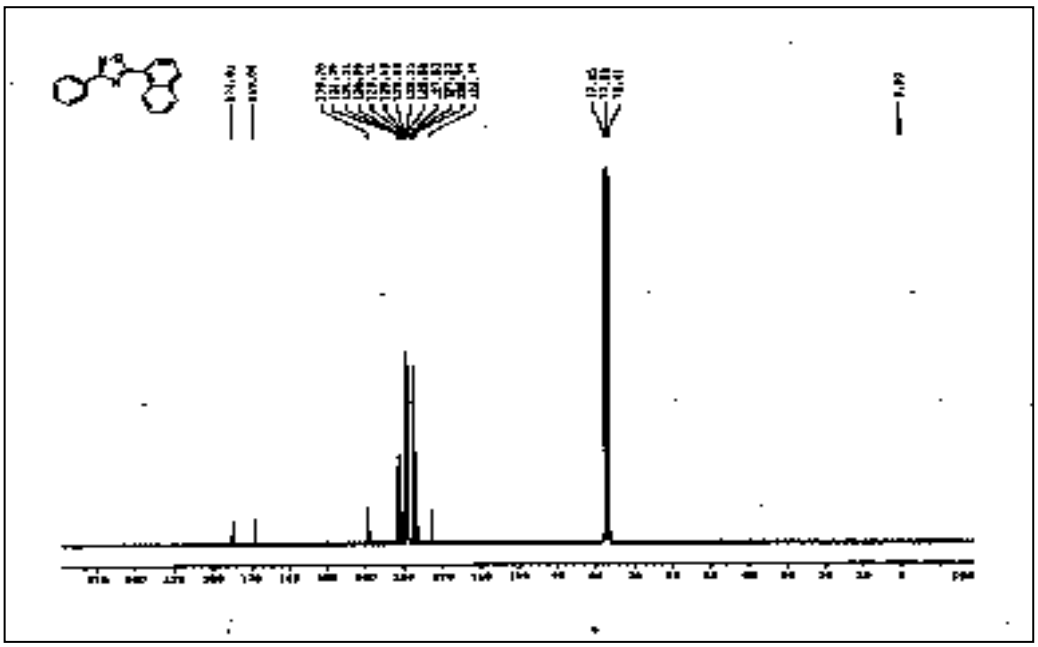

Figure I.B.15. *Scanned copy of ^{1}H and ^{13}C NMR spectra of 5-(furan-2-yl)-3-phenyl-1,2,4-oxadiazole*

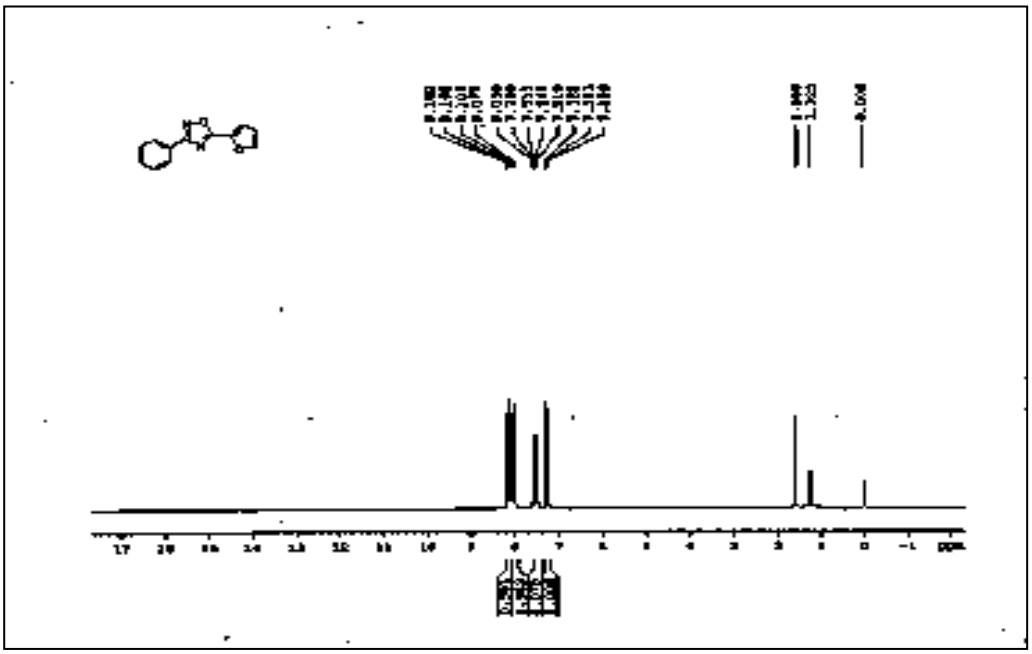

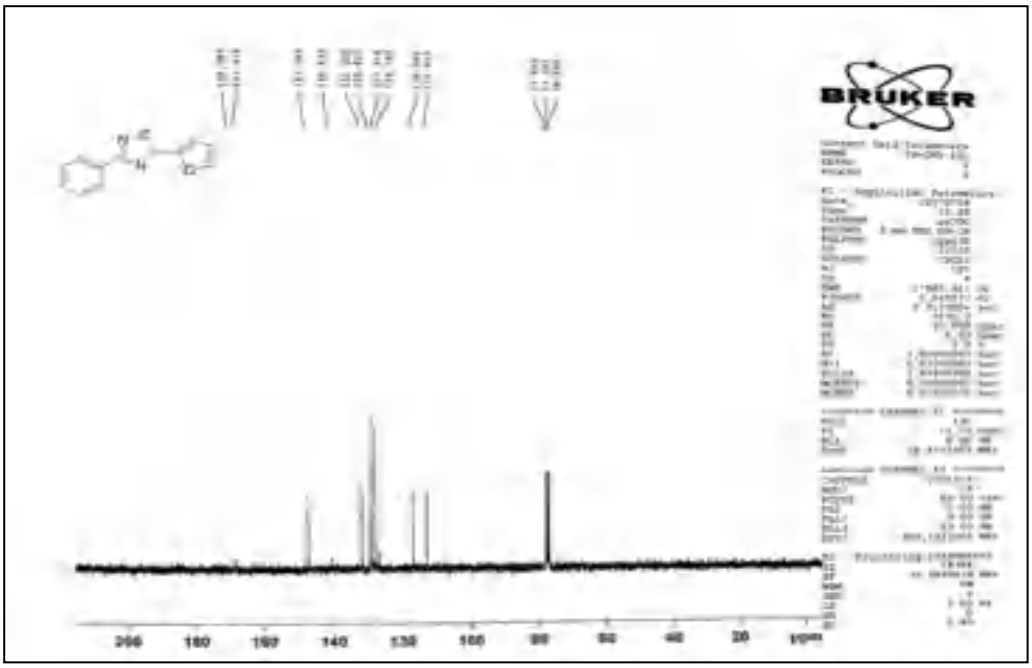

Figure I.B.16. *Scanned copy of ^{1}H and ^{13}C NMR spectra of 3-phenyl-5-(thiophen-2-yl)-1,2,4-oxadiazole*

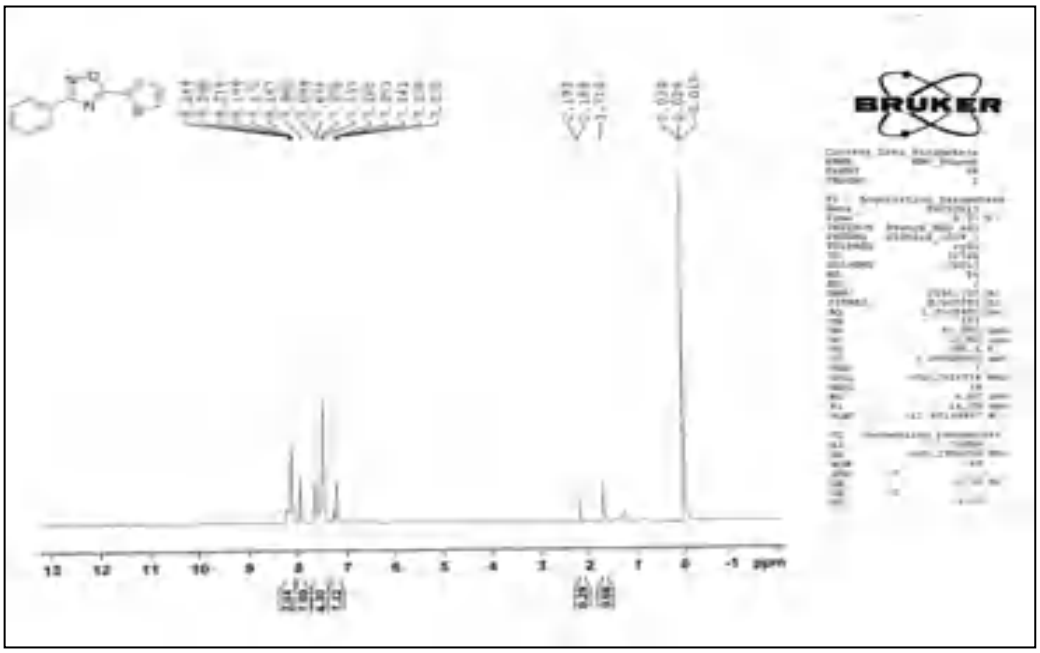

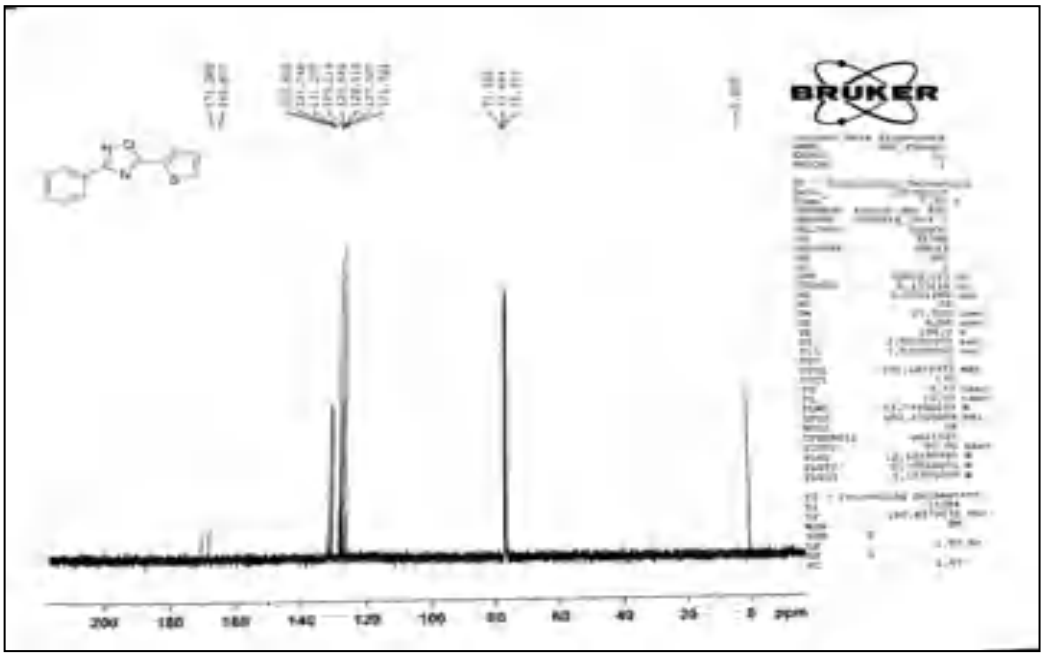

Figure I.B.17. *Scanned copy of ^{1}H and ^{13}C NMR spectra of 5-phenyl-3-(p-tolyl)-1,2,4-oxadiazole*

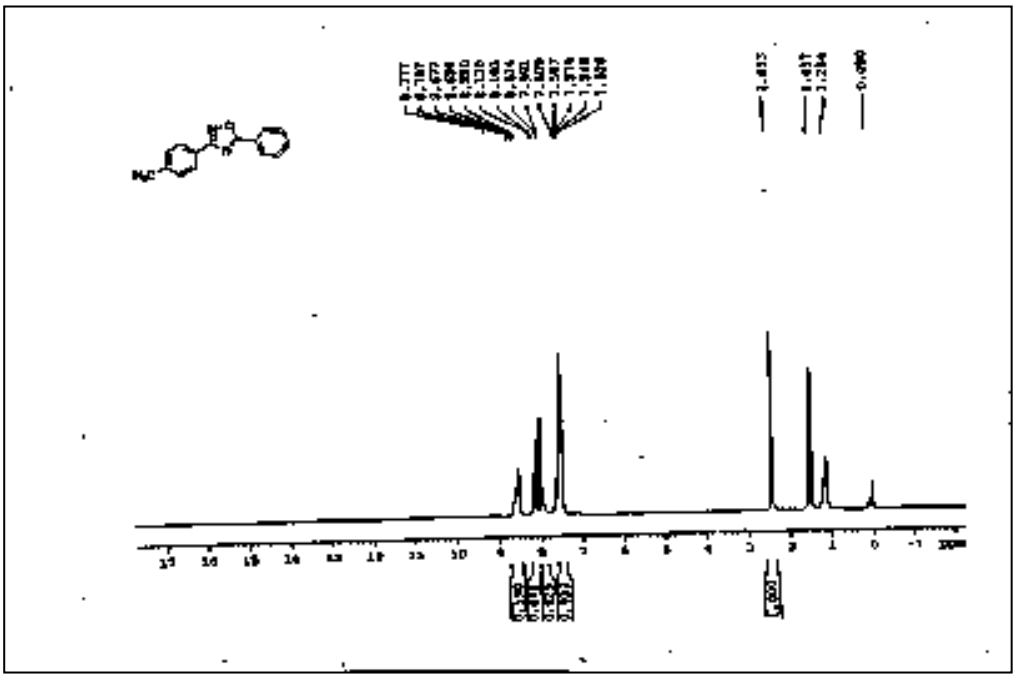

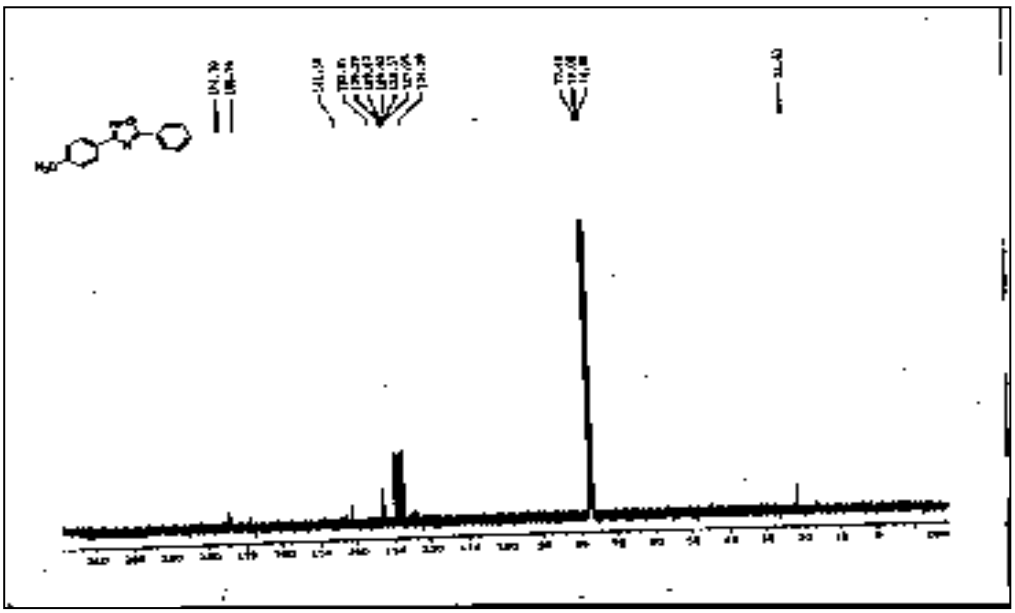

Figure I.B.18. *Scanned copy of ^{1}H and ^{13}C NMR spectra of 3-(4-methoxyphenyl)-5-phenyl-1,2,4-oxadiazole*

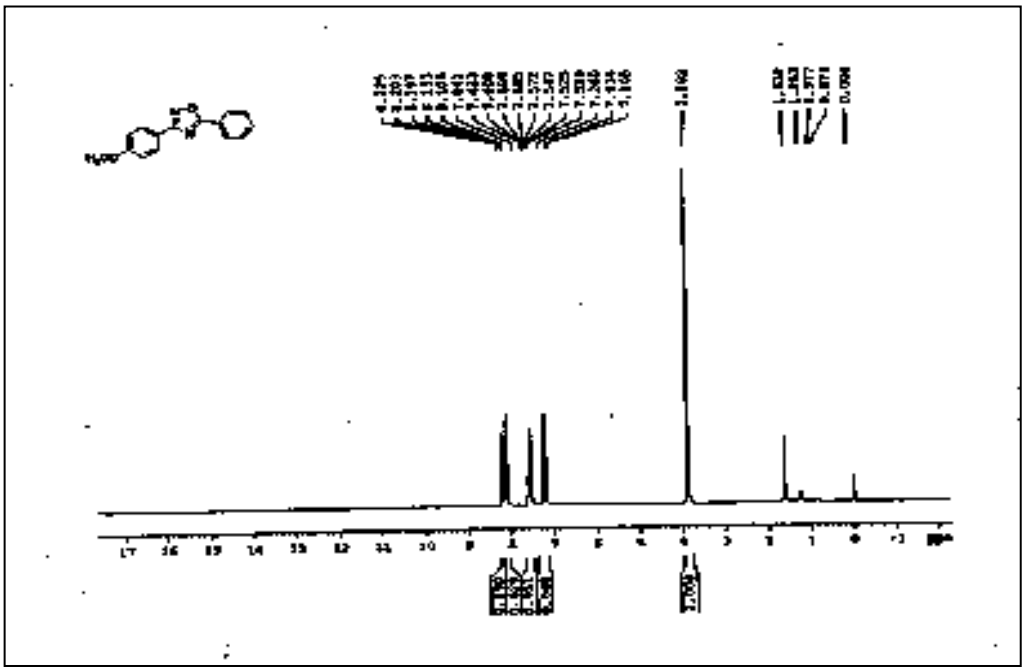

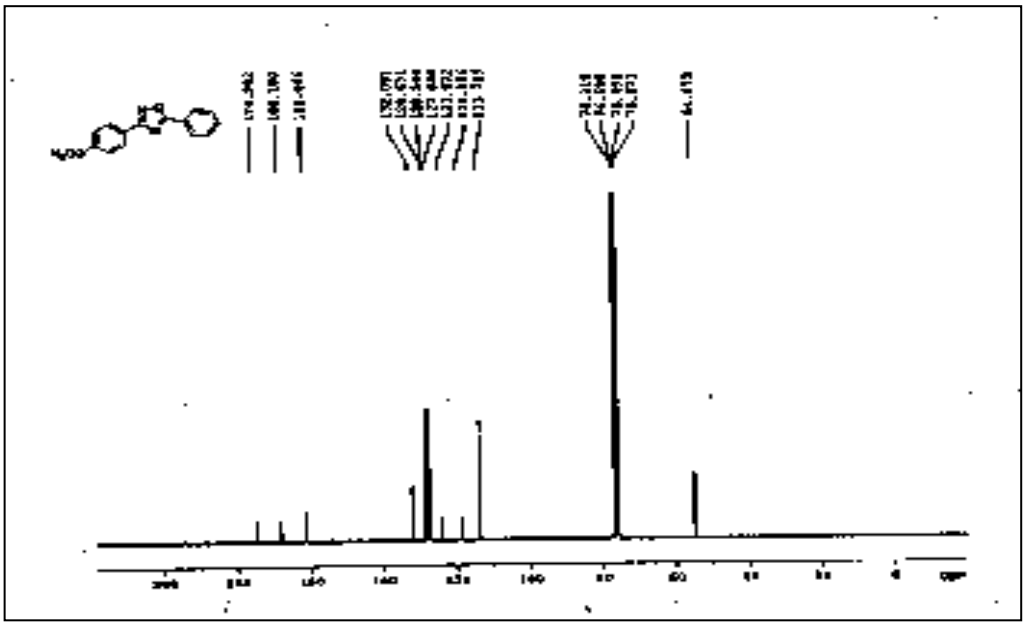

Figure I.B.19. *Scanned copy of ^{1}H and ^{13}C NMR spectra of 5-phenyl-3-(pyridin-4-yl)-1,2,4-oxadiazole*

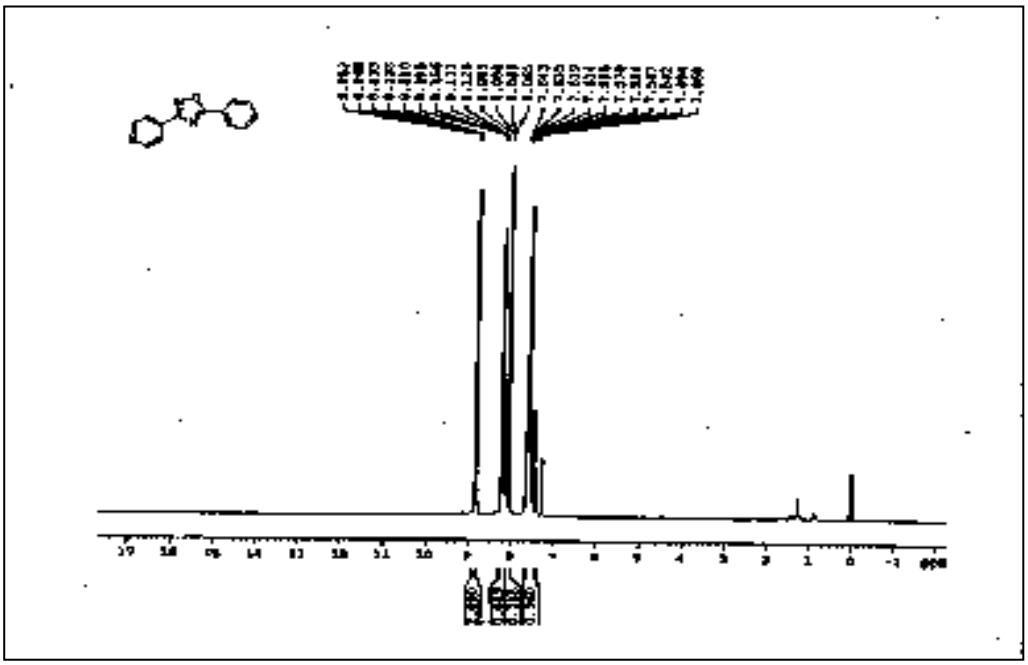

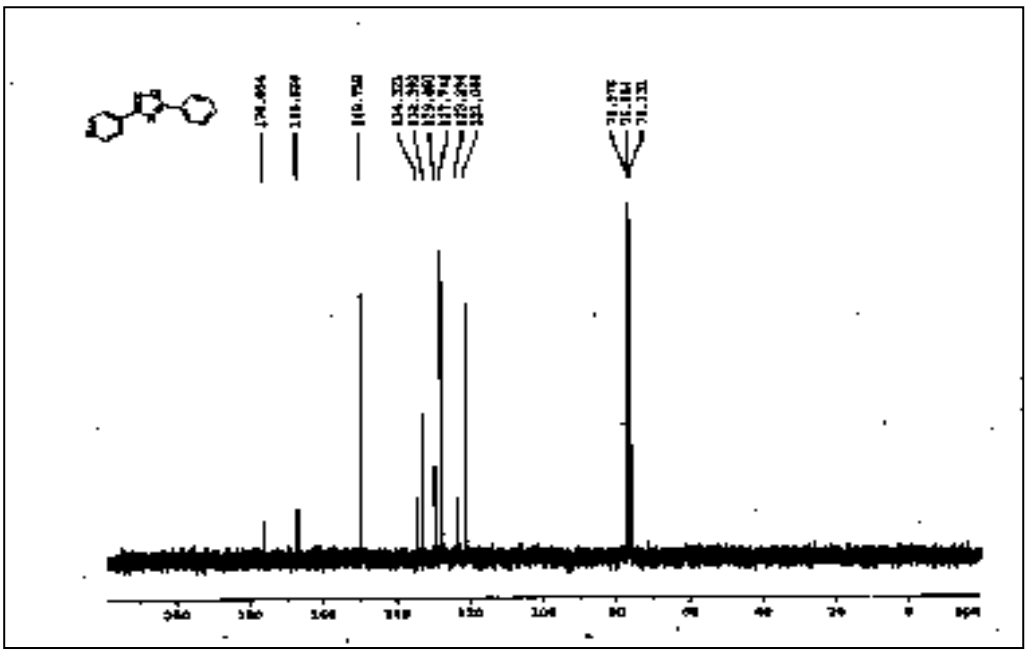

Figure I.B.20. *Scanned copy of ^{1}H and ^{13}C NMR spectra of 5-phenyl-3-(pyridin-4-yl)-1,2,4-oxadiazole*

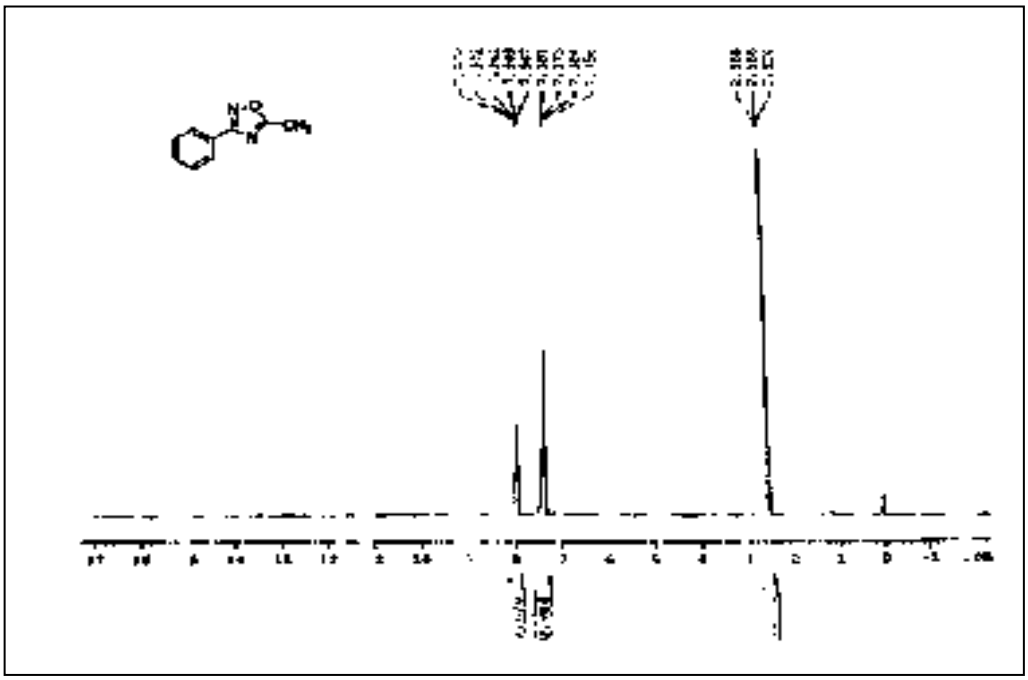

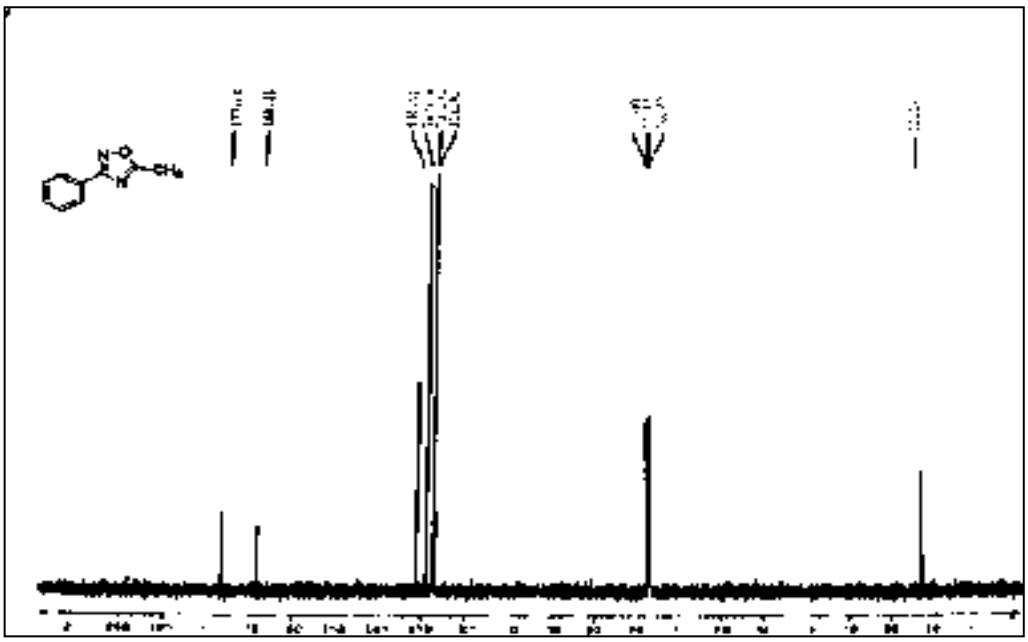

I.B.6. References

References are given in Bibliography under Chapter I, Section B

Chapter I

Section C

Graphene oxide (GO): a metal-free catalyst for one-pot three-component synthesis of triarylpyridines

I.C.1. Introduction

Pyridine ring systems are of great interest because of the occurrence of their derivatives in natural products and biologically active compounds such as pyridoxal (vitamin B_6), NAD nucleotides, and pyridine alkaloids [1]. These compounds have a unique position in synthetic organic chemistry because of their wide range of activities in pharmaceuticals such as antimalarial, anesthetics, vasodilators, anticonvulsants, antiepileptics, and agrochemicals such as pesticides and herbicides [2-4]. In addition, pyridines have received a growing interest as monomeric building blocks in thin films and organometallic polymers [5]. Among the pyridine derivatives, 2,4,6-triarylpyridines are frequently used as a synthon in supramolecular chemistry owing to their π-stacking ability along with directional hydrogen-bonding capacity [6].

I.C.2. Background and objectives

During the last two decades, multicomponent reactions (MCRs) have been widely used as an attractive strategy in organic synthesis due to their efficiency to generate heterocyclic compounds in a single synthetic step [7]. In MCRs, complex organic molecules are formed after a cascade of bond-forming individual steps without the isolation of intermediates using three or more reactants. MCRs are an environmentally friendly process that reduces the number of synthetic steps, waste production, and energy consumption. Thus, the improvement of known MCRs and the discovery of new MCRs are of significant interest. In view of the different chemical and biological applications of substituted pyridines, the evolution of suitable synthetic pathways for their preparation has been a great topic of interest. The general method for 2,4,6-triarylpyridine (Kr hnke pyridine) synthesis involves the reaction between α,β-unsaturated ketones, and N-phenacylpyridinium salts using ammonium acetate

[8]. In recent years, many efforts have been given to develop 2,4,6-triarylpyridines using benzaldehydes, acetophenones, and ammonium acetate in presence of different acid catalysts such as pentafluorophenylammonium triflate [9], heteropolyacid [10], $HClO_4$–SiO_2 [11], Brønsted-acidic ionic liquid [12], and nano-metal catalyst [13, 14]. Synthesis of 2,4,6-triarylpyridines using various synthons is given below.

Kr hnke *et al*. synthesized 2,4,6-triphenylpyridines using *N*-phenacylpyridinium bromide and benzalacetophenone in a mixture of glacial acetic acid and ammonium acetate (Scheme I.C.1) in one step in about 90 % yield [8]. This mixture promotes Michael's addition and does not cause any acid cleavage of the adduct formed using phenacylpyridinium bromide and unsaturated ketone.

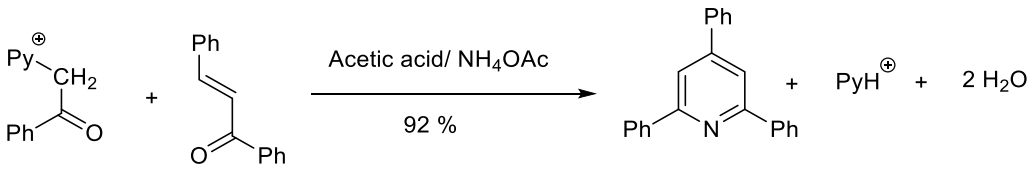

Scheme I.C.1. Kr hnke pyridine synthesis.

Adib *et al.* focused their study to introduce a new facile and efficient method for pyridine synthesis. Therefore, a certain range of symmetrical 2,4,6-triarylpyridines was synthesized using 1,3-diaryl-2-propen-1-ones with NH_4OAc [15] in presence of a catalytic amount of AcOH at 100 °C under solvent-free condition for 4 h with 93-98 % yield (Scheme I.C.2). Here, the formation of the pyridine ring system involves the formation of three bonds from [3+2+1] atom fragments. The structures of the isolated products were analyzed with element analysis and spectral data (mass, IR, ^1H, and ^{13}C NMR).

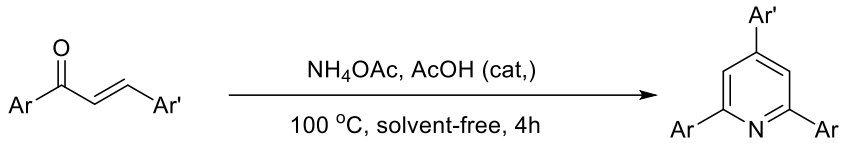

Yield 93-98 %

Ar= C_6H_5, *p*-$CH_3C_6H_5$, *p*-$OCH_3C_6H_5$, 2,4-$Cl_2C_6H_3$
Ar'= C_6H_5, *p*-$CH_3C_6H_5$, *o*-$CH_3C_6H_5$, *p*-$OCH_3C_6H_5$
p-$N(CH_3)_2C_6H_5$, *p*-ClC_6H_5, *o*-$CH_3C_6H_5$, 4-$NO_2C_6H_5$
pyridyl, furyl, thienyl

Scheme I.C.2. *The synthesis of triarylpyridine from* 1,3-diaryl-2-propen-1-ones.

Nagarapu *et al*. reported the synthesis of 2,4,6-triarylpyridines by a one-pot reaction of substituted acetophenones, aldehydes, and NH_4OAc at 120 °C temperature using $HClO_4$–SiO_2 as a powerful heterogeneous catalyst (Scheme I.C.3) [11]. This solid-supported perchloric acid ($HClO_4$–SiO_2) offers excellent yield, shorter reaction time (4-8 h), simple reaction procedure and the catalyst showed remarkable reusability. The effect of the nature of substituents present on the aromatic ring of the aldehyde and acetophenone showed no obvious effect on the yield of the reaction.

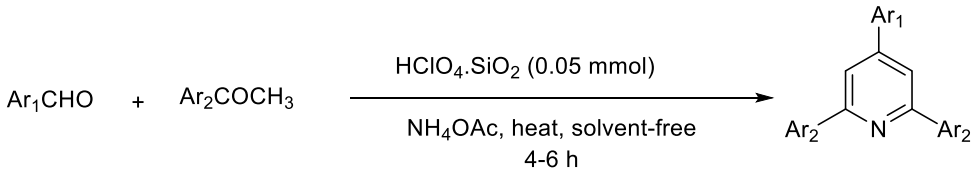

Yield 68-88 %

Ar_1= C_6H_5, *p*-ClC_6H_4, *p*-BrC_6H_4,
p-$CH_3C_6H_4$, *p*-OHC_6H_4
Ar_2= *p*-ClC_6H_4, 2,4-$Cl_2ClC_6H_4$, *p*-BrC_6H_4, *p*-OHC_6H_4
p-$OCH_3C_6H_4$, *p*-$N(CH_3)_2C_6H_4$, furyl, napthyl

Scheme I.C.3. *Synthesis of* 2,4,6-triarylpyridines using $HClO_4$–SiO_2.

Pentafluorophenylammonium triflate (PFPAT) was found to be a novel organocatalyst in organic transformations such as Mukaiyama aldol and Mannich reactions [16], esterification of carboxylic acids with alcohols [17],

synthesis of coumarins via von pechmann condensation [18]. Montazeri *et al.* developed a one-pot three-component synthesis of 2,4,6-triarylpyridines using aryl aldehydes, acetophenone, and ammonium acetate at 120 ^{o}C temperature under neat reaction conditions (Scheme I.C.4). The presence of electron-withdrawing groups at aromatic aldehyde favored the product formation; however, the electron-donating group containing aldehydes lowered the yield of the reaction. Moreover, reactions with substituted acetophenones proceeded very well and no undesirable side product was observed.

Ionic liquids (ILs) are generally salt-type compounds that exist as a liquid at room temperature (rt) and have a very low vapor pressure. Due to the lack of evaporation, they are considered promising green solvents for replacing harmful conventional solvents. Davoodnia *et al*. described the synthesis of 2,4,6-triarylpyridines in presence of a Brønsted acidic ionic liquid, 3-methyl-1-(4-sulfonylbutyl)imidazolium hydrogen sulfate [$HO_3S(CH_2)_4MIM][HSO_4$], as an effective and reusable catalyst (Scheme I.C.5) [12]. The catalyst was recycled upto three times with a slight reduction in its catalytic activity.

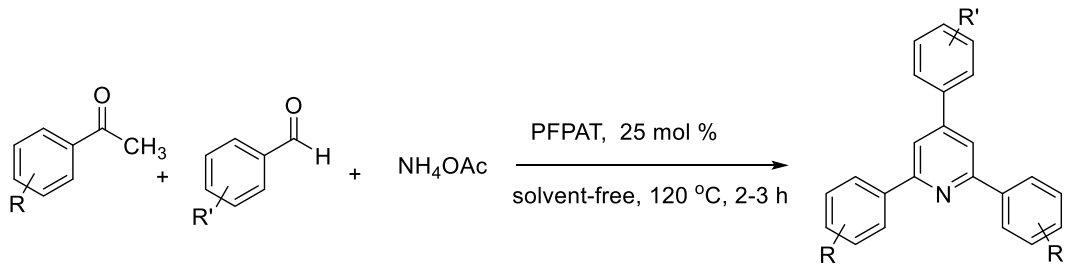

R= H, 4-Br, 4-Me, 4-NO_2, 4-OMe
R'= H, 4-NO_2, 4-Me, 2-Me, 4-OH, 4-OMe, 4-Cl, 2-Cl

Yield 86-94 %

Scheme I.C.4. (PFPAT) catalyzed pyridine synthesis.

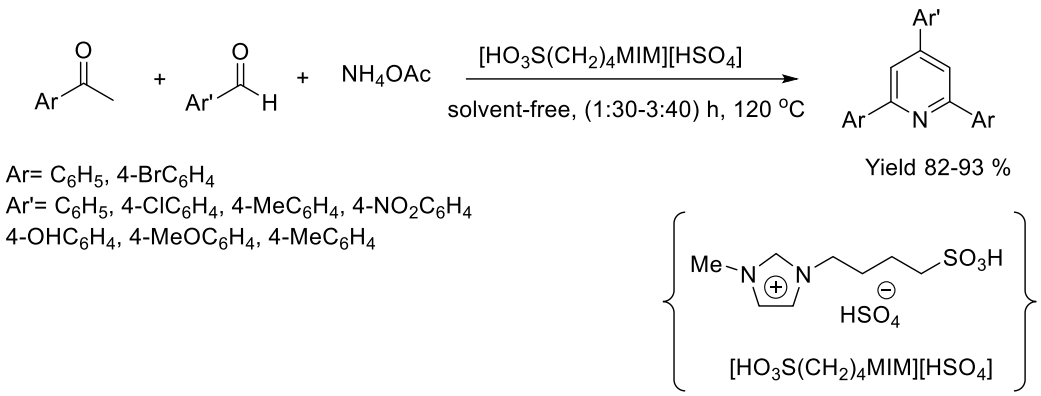

Scheme I.C.5. *Ionic liquid catalyzed synthesis of triarylpyridines.*

The nanosized spinel particles have found much application as catalyst support [19], humidity sensors [20], ceramic pigments [21] because of their good physical and chemical properties [22]. Magnesium aluminate ($MgAl_2O_4$) is one of the widely used and best-known spinel materials. Safari *et al.* designed nanocrystalline $MgAl_2O_4$ as a powerful heterogeneous catalyst for the synthesis of 2,4,6-triarylpyridines under microwave irradiation (Scheme I.C.6) [14]. The catalyst can be recycled upto 5 successive runs without a significant decrease in its catalytic activity.

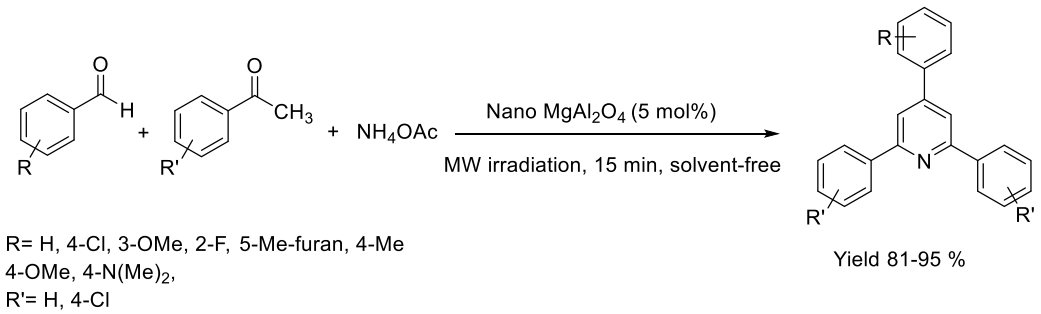

Scheme I.C.6. *Synthesis of triarylpyridine catalyzed by magnesium aluminate.*

Tabrizian *et al*. reported a highly efficient, eco-friendly, and recyclable heterogeneous catalyst nano titania-supported sulfonic acid (n-TSA) for the one-

pot solvent-free synthesis of 2,4,6-triarylpyridines through the reaction of acetophenones, aryl aldehydes, and ammonium acetate at 110 °C temperature (Scheme I.C.7) [23]. Aromatic aldehydes with electron-donating and electron-withdrawing substituents reacted successfully and afforded the product in good yield. The simple work-up process without tedious column chromatographic purification, operational simplicity, short reaction time, and solvent-free condition are the main advantages of the reported protocol.

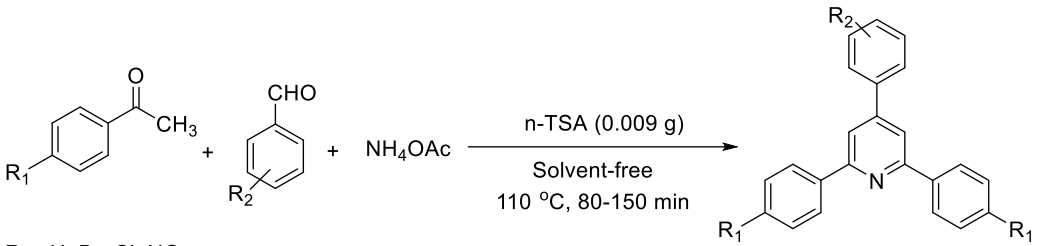

R_1= H, Br, Cl, NO_2
R_2= 4-H, 4-Cl, 4-Br, 4-CH_3, 4-OCH_3, 4-$N(CH_3)_2$, 4-NO_2

Scheme I.C.7. Nano titania-supported sulfonic acid as efficient catalyst for the synthesis of triarylpyridines.

Maleki *et al.* synthesized nanomagnetic catalyst Fe_3O_4\SiO_2\propyltriethoxysilane\L-proline (LPSF) (Scheme I.C.8) and applied for the one-pot synthesis of 2,4,6-triarylpyridines under solvent-free mild reaction condition (Scheme I.C.9) [13]. Recently, magnetic nanoparticles (MNPs) have been considered as a new type of catalytic support for organocatalysts owing to their price, good stability, high dispersion, easy synthesis and functionalization method, high surface area, and easy separation with the help of an external magnetic field [24-27]. The structure of the prepared nanoparticles was characterized by FT-IR, FE-SEM, TGA, EDX analysis.

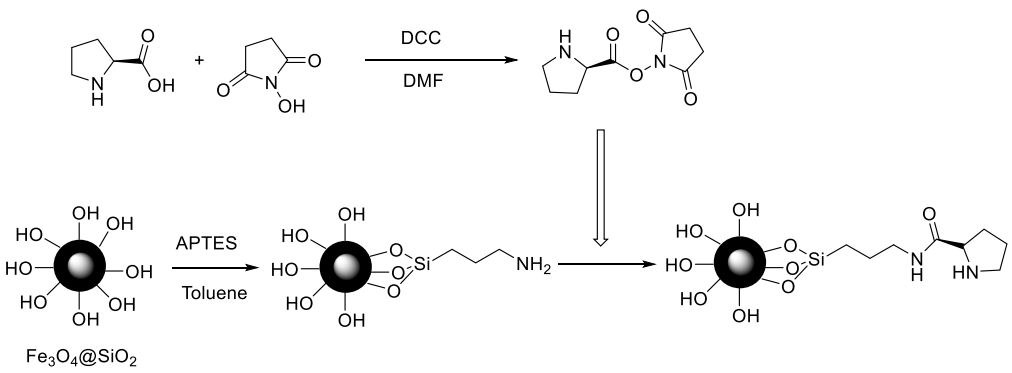

Scheme I.C.8. *Preparation of LPSF magnetic nanocatalyst.*

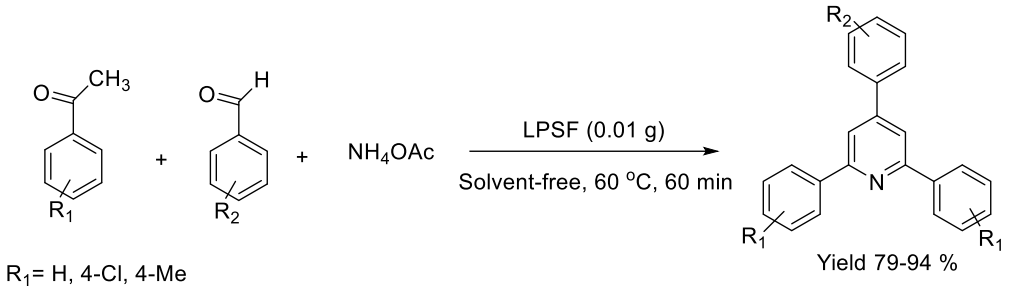

Scheme I.C.9. *LPSF nanocatalyst used for the synthesis of triarylpyridine.*

I.C.3. Present work

Nevertheless, most of the traditional synthetic method requires harsh reaction condition, prolonged heating, and use of toxic transition metal catalyst as well as only a few protocols have shown greener context and high atom economy. Recently, GO has been emerged as an efficient carbocatalyst for various organic transformations. Our present study (Scheme I.C.10) explores the role of GO as an acid catalyst using the surface-bound oxygen-containing functional groups. The versatility and sustainability of GO as a catalyst leads us to employ GO as a metal-free catalyst for the synthesis of 2,4,6-triarylpyridines

to overcome the drawbacks of the reported protocols and reduce environmental hazards

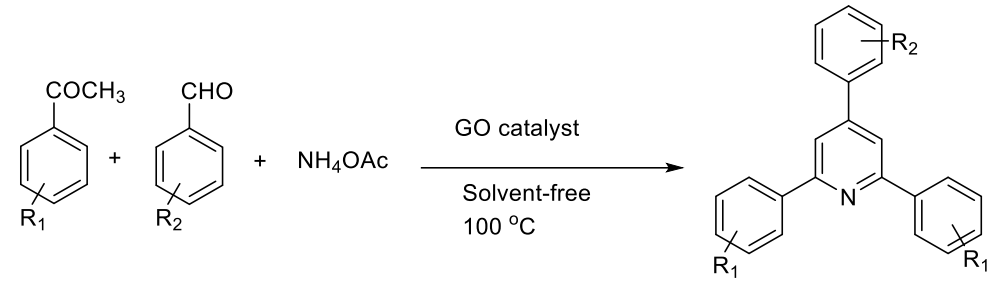

R_1= 4-H, 4-Me,4-Br
R_2= 4-H, 4-Me, 4-Cl, 4-NO_2, 4-OMe, Furan-2-carbaldehyde, 4-Cl

Yield 78-93 %

Scheme I.C.10. *Graphene oxide (GO) catalyzed one-pot synthesis of triarylpyridines.*

I.C.3.1. Result and disscussion

In connection to our previous work, the catalytic activity of synthesized GO was investigated in the case of 2,4,6-triarylpyridine synthesis. To find out the optimized condition of the reaction, acetophenone (2 mmol), benzaldehyde (1 mmol), and ammonium acetate (2 mmol) were selected as model substrates and the results were summarized in Table I.C.1. As can be seen from Table I.C.1 that neither polar nor non-polar solvents were found suitable for the reaction. The best result was obtained under neat or solvent-free conditions (Table I.C.1, entry11). The effect of temperature and the amount of catalyst was also examined to find out the optimized condition. Studies reveal that the yield increases with increasing temperature. Room-temperature reaction afforded only 20% of the product which strongly indicates the vital role of temperature in governing the reaction (Table I.C.1, entry 16). However, after 120 ^oC the yield decreases with a further increase in temperature (Table I.C.1, entry 10). To

ascertain the catalytic function of GO, the reaction was performed in absence of catalyst and only a trace amount of product was obtained. The amount of the catalyst was also altered and optimum condition offered a neat reaction with 30 mg of GO at 100 ^{o}C temperature (Table I.C.1, entry 11). Ammonia sources other than ammonium acetate produced the corresponding product with a low yield (Table I.C.1, entries 14-15).

Table I.C.1. Optimization of reaction condition for the reaction of 2,4,6-triarylpyridine[a]

Entry	Temp (^{o}C)	Solvent	Catalyst (mg)	Ammonia source	Yield (%)[b]
1	100	H_2O	15	NH_4OAc	65
2	80	Ethanol	15	NH_4OAc	55
3	100	DMF	15	NH_4OAc	53
4	100	DMSO	15	NH_4OAc	45
5	100	Toluene	15	NH_4OAc	50
6	80	CH_3CN	15	NH_4OAc	30
7	100	Ethylene glycol	15	NH_4OAc	60
8	100	Neat	15	NH_4OAc	83
9	120	Neat	30	NH_4OAc	90
10	150	Neat	30	NH_4OAc	86
11	**100**	**Neat**	**30**	**NH_4OAc**	**92**
12	80	Neat	30	NH_4OAc	80
13	100	Neat	-	NH_4OAc	Trace
14	100	Neat	30	$(NH_4)_2CO_3$	48
15	100	Neat	30	$(NH_4)_2SO_4$	Trace
16	rt	Neat	30	NH_4OAc	<20[c]

[a]Reaction condition: Acetophenone (2 mmol), benzaldehyde (1 mmol), ammonium acetate (2 mmol), reaction time: 2h.
[b]Isolated yields.
[c]Room temperature reaction.

To explore the catalytic activity of GO, a wide variety of aromatic aldehydes and substituted acetophenones were subjected to synthesize 2,4,6-triarylpyridines. Based on the above-optimized results, GO catalyzed reaction was carried out at 100 ^{o}C temperature under solvent-free condition and the

results are summarized in Table I.C.2. First, the compatibility of the substituents in the phenyl ring of acetophenone and benzaldehyde was examined. All the electron-donating and electron-withdrawing substituents on the aromatic ring are equally capable of producing the corresponding product with a good yield. However, aldehydes with electron-withdrawing groups (Table I.C.2, entries 3-4, 8-9) exerted excellent yield and reacted faster than the aromatic aldehydes with electron-donating groups (Table I.C.2, entries 2, 5, 7). In the case of heterocyclic aldehydes, the reaction has smoothly proceeded as can be seen from Table I.C.2, entry 6.

Table I.C.2. Synthesis of 2,4,6-triarylpyridine derivatives in presence of GO[a]

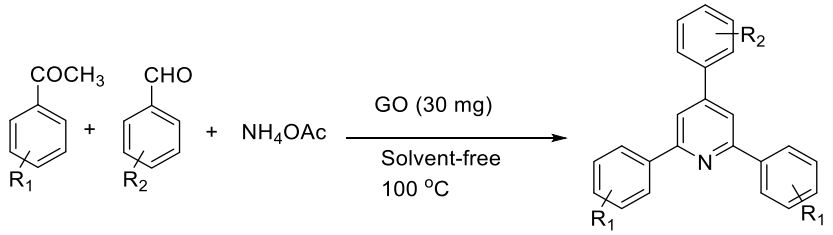

Entry	R_1	R_2	Product	Time (h)	Yield (%)[b]
1	4-H	4-H	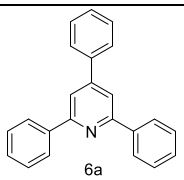 6a	2h	92
2	4-H	4-Me	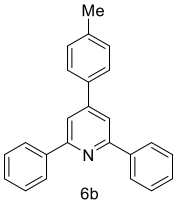 6b	2h	86

3	4-H	4-Cl	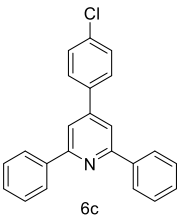 6c	1h	93
4	4-H	4-NO_2	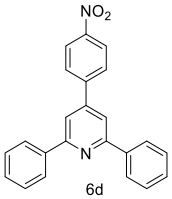 6d	1h	88
5	4-H	4-OMe	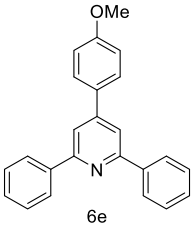 6e	2h	83
6	4-H	Furan-2-carbaldehyde	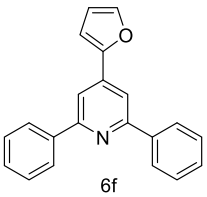 6f	2h	78
7	4-Me	4-H	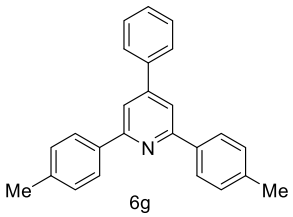 6g	2h	87
8	4-Br	4-H	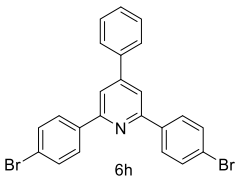 6h	1h	90

9	4-Br	4-Cl	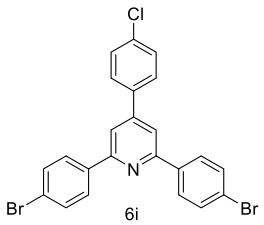 6i	1h	94

[a]Reaction condition: Acetophenone (2 mmol), benzaldehyde (1 mmol), ammonium acetate (2 mmol) and GO (30 mg).
[b]Isolated yields after purification through column chromatography on silica gel.

I.C.3.2. Mechanism

The probable mechanism for the synthesis of 2,4,6-triarypyridines using GO is described in Scheme I.C.11. At the very first step, aldol condensation occurs between acetophenone and aromatic aldehyde. Acetophenone is activated by the acidic group of GO and the nucleophilic attack occurs at the carbonyl carbon of aromatic aldehyde. After that, an acetophenone molecule is reacted with an ammonia source to form enamine (II). In the third stage, Michael's addition between enamine (II) and the aldol condensation product (I) occurs. GO protonates the condensation product (I), thereby facilitating the Michael addition by enamine (II). The intermediate (III) is formed by Michael's addition and undergoes cyclization to form dihydropyridine (V). At the last step, oxidation to dihydropyridine occurs and gives the ultimate product 2,4,6-triarylpyridine (VI).

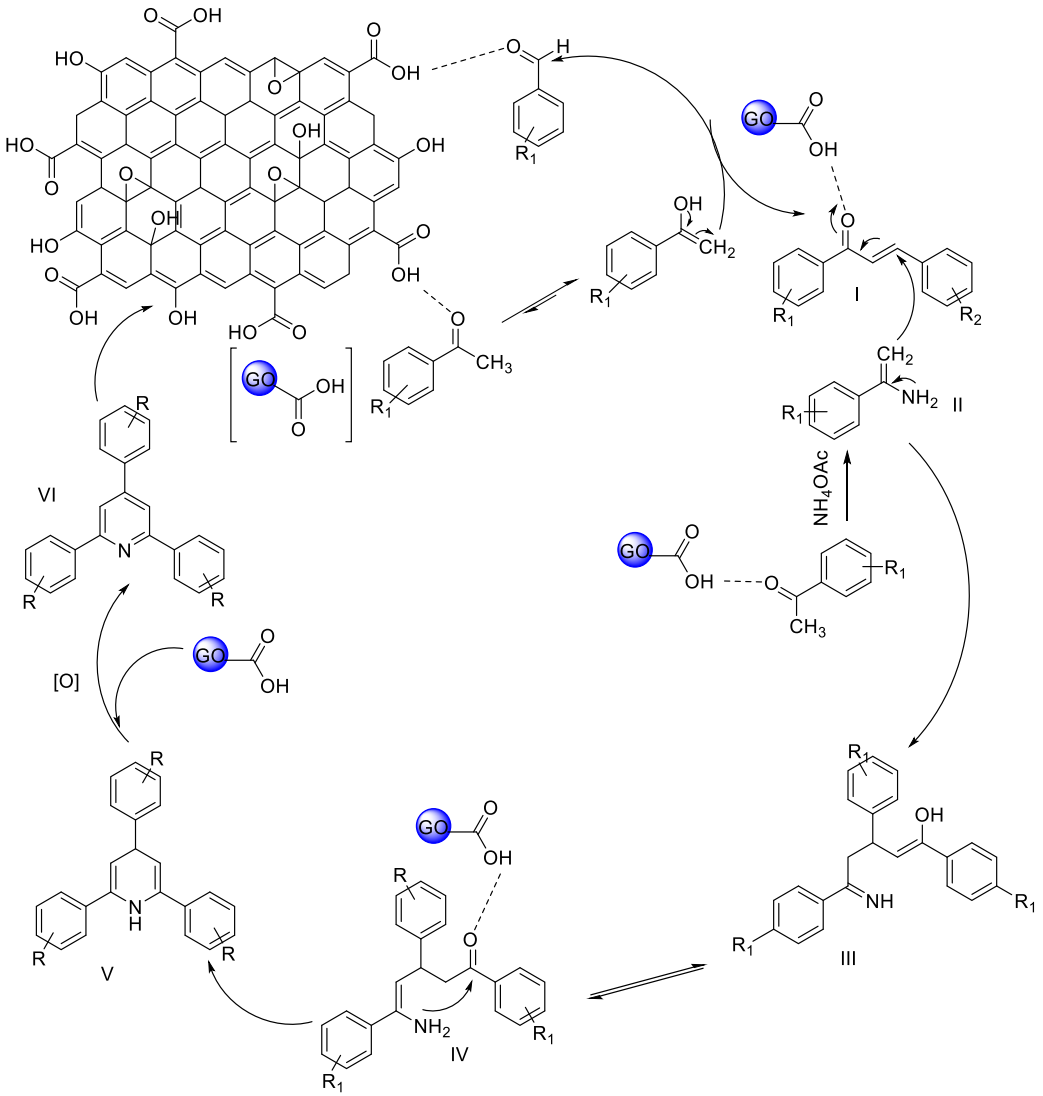

Scheme I.C.11. *A possible route of GO catalyzed synthesis of 2,4,6-triarylpyridine.*

The main advantage of heterogeneous catalysts is their reusability in organic transformation. For this purpose, acetophenone, benzaldehyde, and ammonium acetate were taken in a reaction vial in presence of 120 mg of GO.

The model reaction was carried out for an adequate time and after completion of the reaction, ethyl acetate (30 mL) was added into the reaction vial and centrifuged for four times. The supernatant liquid after centrifugation was decanted off and the residual catalyst was washed repeatedly with water and acetone. The dry GO was then collected and reused for the 2nd run. It was observed that GO could easily retain its acidic property without significant loss in its catalytic activity even after 5 successive runs (Figure I.C.1). Although there may be loss of some oxygenated groups due to subsequent runs, the recovered catalyst shows almost equal efficiency with the fresh GO.

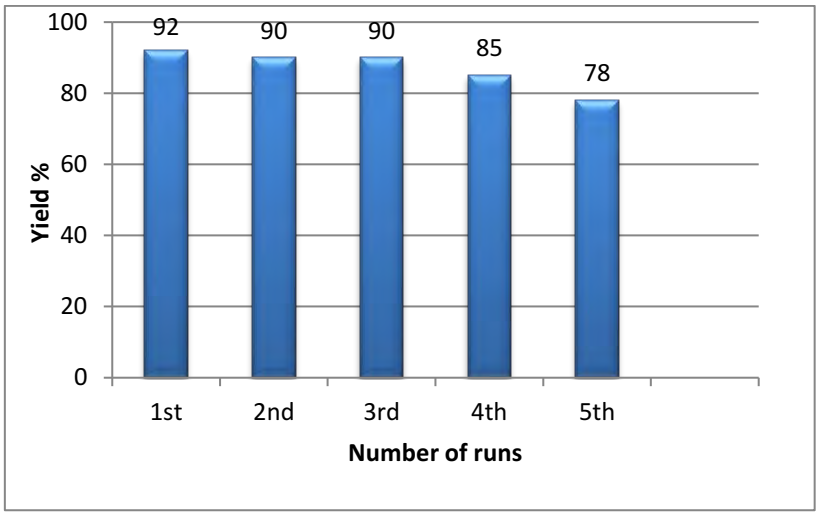

Figure I.C.1. *Recyclability experiment of catalyst GO for the synthesis of 2,4,6-triarylpyridines.*

I.C.4. Conclusion

In conclusion, GO has been proved to be efficient carbocatalyst for the synthesis of 2,4,6-triarylpyridines. Replacement of metal-free and toxic catalysts by inexpensive carbocatalyst is the main advantage of this protocol. The solid

acid catalyst, GO exerts the the desired triarylpyridines with good yield under neat reaction. Easy recovery and reusability of the catalyst provides a clean strategy to form a wide variety of trisubstituted pyridines.

I.C.5. Experimental section

I.C.5.1. General experimental procedure

All the chemicals and reagents were purchased from Sigma–Aldrich, Spectrochem, TCI and were used without further purification. The solvents were purchased from commercial suppliers and were used after proper distillation.The progress of the reaction was monitored by Merck TLC plates which are coated with silica gel (60 F_{254}) and UV light was used as visualizing agent. NMR spectra of all the synthesized compounds were carried out in $CDCl_3$/DMSO-d_6 solvent and TMS was used as an internal standard. All the NMR spectroscopic data are recorded in BrukerAvance FT-NMR operating for ^1H at 300/400 MHz. The ^1H NMR data are represented by chemical shift δ (ppm), multiplicity (s = singlet, d= doublet, t = triplet, m = multiplet), integration, coupling constants (J values) in Hertz (Hz). The ^{13}C NMR spectroscopic data are also reported in ppm as ^1H NMR spectra.

I.C.5.2. General procedure for the preparation of (GO) catalyst

There are several methods for the preparation of graphene oxide (GO). Herein, Graphene oxide (GO) was synthesized by the Tours method using graphite powder as starting material. At first, 9:1 volume ratio of (180 mL) sulfuric acid (H_2SO_4) and (20 mL) phosphoric acid (H_3PO_4) were taken in a 500 ml conical flask, and then 1.5 g of graphite powder was added to it under stirring condition. The temperature of the whole mixture was kept below 10 ^oC using an ice bath and 9g of potassium permanganate ($KMnO_4$) was added very slowly

into it as the addition of $KMnO_4$ evolves heat. Then the reaction mixture was stirred for 12 hrs and after that hydrogen peroxide (H_2O_2) was added drops wise to eliminate excess $KMnO_4$. After that, 30-40 mL hydrochloric acid (HCl) (strength 30%) was added to this mixture followed by the addition of 200 mL of deionized water. Then the mixture was centrifuged at 5000 rpm for 20 minutes. After that, the supernatant liquid was decanted away and the residual was dried at 90 ^oC rotary evaporator to get dry graphene oxide (GO) with pH (4.2 at 0.1 mg/mL).

I.C.5.3. General procedure for the synthesis of 2,4,6-triarylpyridines

A mixture of acetophenone (1 mmol), aromatic aldehyde (1 mmol), ammonium acetate (1.5 mmol), and 30 mg of GO was stirred for 2h at 100 ^oC temperature. The reaction was monitored by TLC and after completion of the reaction; the reaction mixture was extracted with ethyl acetate. The catalyst was recovered by centrifugation and washed with acetone and water and then dried. The ethyl acetate extractswere further purified by column chromatography using silica gel of 60-120 mesh and the desired product is obtained.

I.C.5.4. ^1H and ^{13}C NMR of various synthesized compounds

2,4,6-triphenylpyridine (Table I.C.2, entry 1) [26]

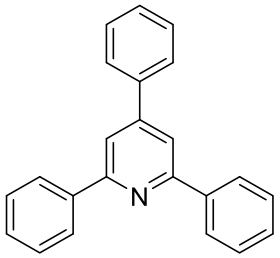

White solid;

MP 132-133 ^oC;

^{1}H NMR (300 MHz, $CDCl_3$) δ (ppm) 7.42-7.48 (m, 9H), 7.77 (d, 2H, *J* = 7.2 Hz), 8.14 (s, 2H), 8.28 (d, 4H, *J* =7.8Hz);

^{13}C NMR (75 MHz, $CDCl_3$) δ (ppm) 117.16, 127.20, 127.23, 128.08, 128.76, 129.02, 129.10, 129.16, 139.11, 139.65, 150.23, 157.55.

2,6-diphenyl-4-(*p*-tolyl)pyridine (Table I.C.2, entry 2) [27]

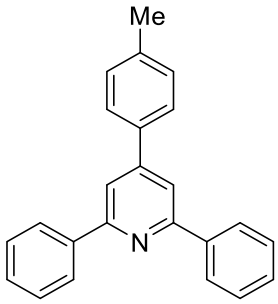

Light yellow solid;

MP 118-119 ^{o}C;

^{1}H NMR (300 MHz, $CDCl_3$) δ (ppm) 2.49 (s, 3H), 7.45-7.56 (m, 8H), 7.90 (d, 2H, *J* = 7.2Hz), 8.11 (s, 2H), 8.23 (d, 4H, *J* = 7.8Hz);

^{13}C NMR (75 MHz, $CDCl_3$) δ (ppm) 21.01, 116.36, 126.65, 127.98, 128.08, 128.47, 129.21, 137.92, 139.22, 140.56, 150.42, 157.37.

4-(4-chlorophenyl)-2,6-diphenylpyridine (Table I.C.2, entry 3) [26]

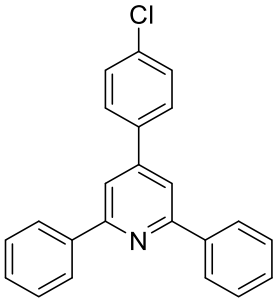

White solid;

MP 121-123 ^{o}C;

^{1}H NMR (300 MHz, CDCl^{3}) δ (ppm) 7.39-7.48 (m, 8H), 7.80 (d, 2H, *J* = 7.2 Hz), 8.13 (s, 2H), 8.30 (d, 4H, *J* = 7.8Hz);

^{13}C NMR (75 MHz, $CDCl_3$) δ (ppm) 116.59, 127.15, 128.07, 128.41, 128.67, 129.04, 129.42, 138.91, 139.77, 148.77, 157.45.

4-(4-nitrophenyl)-2,6-diphenylpyridine (Table I.C.2, entry 4) [26]

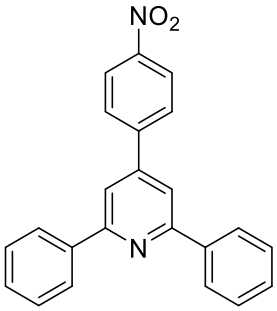

Off white solid;

MP 192-193 ^{o}C;

^{1}H NMR (300 MHz, $CDCl_3$)δ (ppm) 7.46-7.56 (m, 8H), 7.89 (d, 2H, *J* =8.1Hz), 8.21 (s, 2H), 8.40 (d, 4H, *J* = 7.8Hz);

^{13}C NMR (75 MHz, $CDCl_3$) δ (ppm) 116.42, 123.85, 126.64, 127.67, 128.31, 128.93, 133.11, 133.65, 143.53, 147.37, 157.52.

4-(4-methoxyphenyl)-2,6-diphenylpyridine (Table I.C.2, entry 5) [26]

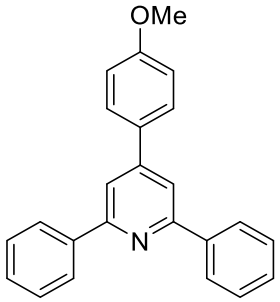

White solid;

MP 100-102 ^{o}C;

^{1}H NMR (300 MHz, $CDCl_3$) δ (ppm) 3.74 (s, 3H), 7.10 (d, 2H, J = 7.8 Hz), 7.29-7.51 (m, 8H), 7.72 (s,2H), 7.92 (d, 4H, J = 6.9 Hz);

^{13}C NMR (75 MHz, $CDCl_3$) δ (ppm) 54.90, 119.35, 127.16, 127.92, 128.06, 129.73, 132.04, 138.05, 140.37, 144.18, 151.72, 161.22.

4-(furan-2-yl)-2,6-diphenylpyridine (Table I.C.2, entry 6) [26]

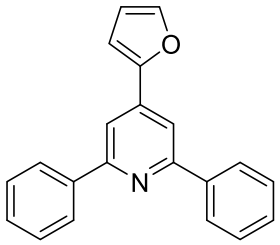

Light brown solid;

MP 112-13 ^{o}C;

^{1}H NMR (300 MHz, $CDCl_3$) δ (ppm) 6.56 (d, 1H, *J* =1.5Hz), 6.96 (d, 1H, *J* = 3Hz), 7.44-7.58 (m, 7H), 7.92 (s, 2H), 8.19 (d, 4H, *J* = 8.1 Hz);

^{13}C NMR (75 MHz, $CDCl_3$) δ (ppm) 107.96, 111.61, 112.51, 126.58, 128.18, 128.59, 138.57, 138.99, 143.12, 151.51, 157.03.

4-phenyl-2,6-di-p-tolylpyridine (Table I.C.2, entry 7)

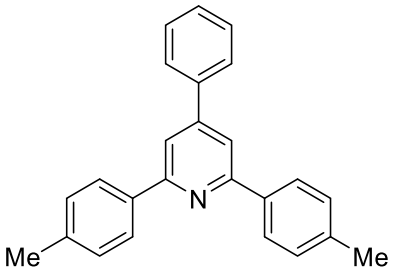

White solid;

MP 152-154 ^{o}C;

^{1}H NMR (300 MHz, $CDCl_3$) δ (ppm) 2.37 (s, 6H), 7.21 (d, 4H, *J* =7.2Hz), 7.38-7.43 (m, 3H), 7.61-7.72 (m, 2H), 7.74 (s, 2H), 7.99 (d, 4H, *J* =8.1Hz);

^{13}C NMR (75 MHz, $CDCl_3$) δ (ppm) 21.40, 116.56, 127.05, 127.23, 128.54, 128.92, 129.12, 136.94, 139.00, 139.30, 150.04, 157.43.

2,6-bis(4-bromophenyl)-4-phenylpyridine (Table I.C.2, entry 8) [27]

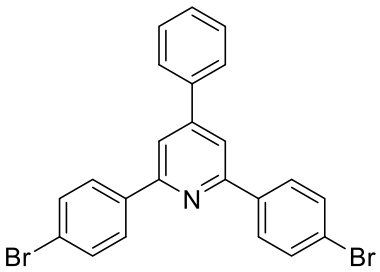

White solid;

MP 105-106 ºC;

^{1}H NMR (300 MHz, $CDCl_3$)δ (ppm) 7.09-7.36 (m, 5H), 7.49 (s, 2H), 7.76 (d, 4H, *J* = 7.8 Hz), 8.10 (d, 4H, *J* =8.1 Hz);

^{13}C NMR (75 MHz, $CDCl_3$) δ (ppm) 116.46, 123.05, 127.05, 128.40, 128.94, 129.49, 132.94, 135.19, 139.60, 149.07, 154.16.

2,6-bis(4-bromophenyl)-4-(4-chlorophenyl)pyridine (Table I.C.2, entry 9) [28]

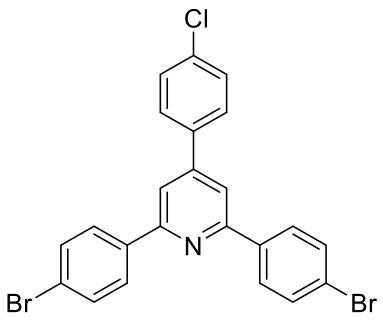

White solid;

MP> 250 ºC;

^{1}H NMR (300 MHz, $CDCl_3$) δ (ppm) 7.02-7.06 (m, 4H), 7.34 (d, 2H. *J* = 7.2 Hz), 7.73 (d, 2H, *J* = 7.5 Hz), 7.87 (s, 2H), 8.13 (d, 4H, *J* = 8.4 Hz);

^{13}C NMR (75 MHz, $CDCl_3$) δ (ppm) 116.32, 122.89, 128.68, 128.87, 129.10, 130.59, 137.58, 138.07, 149.38, 156.62.

I.C.5.5. Scanned copies of ^{1}H and ^{13}C NMR spectra of synthesized compounds

Figure I.C.2. *Scanned copy of ^{1}H and ^{13}C NMR spectra of 2,4,6-triphenylpyridine*

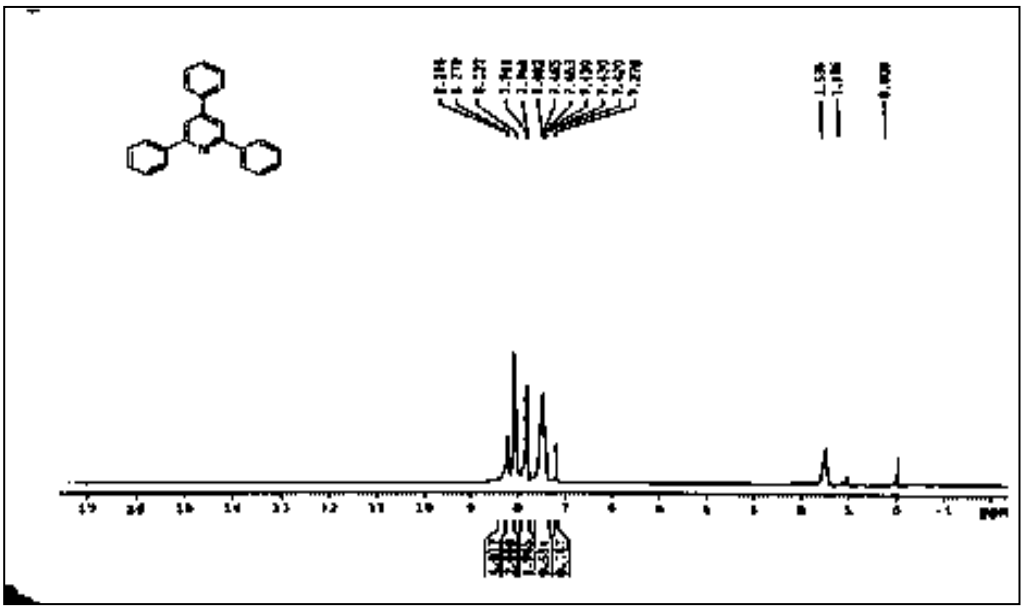

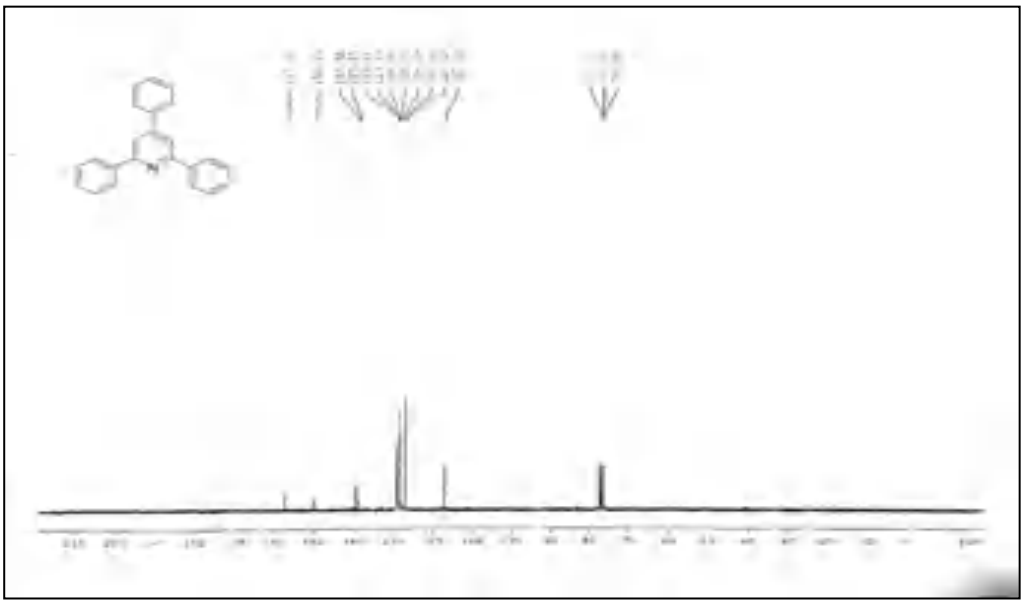

Figure I.C.3. *Scanned copy of ^{1}H and ^{13}C NMR spectra of 2,6-diphenyl-4-(p-tolyl)pyridine*

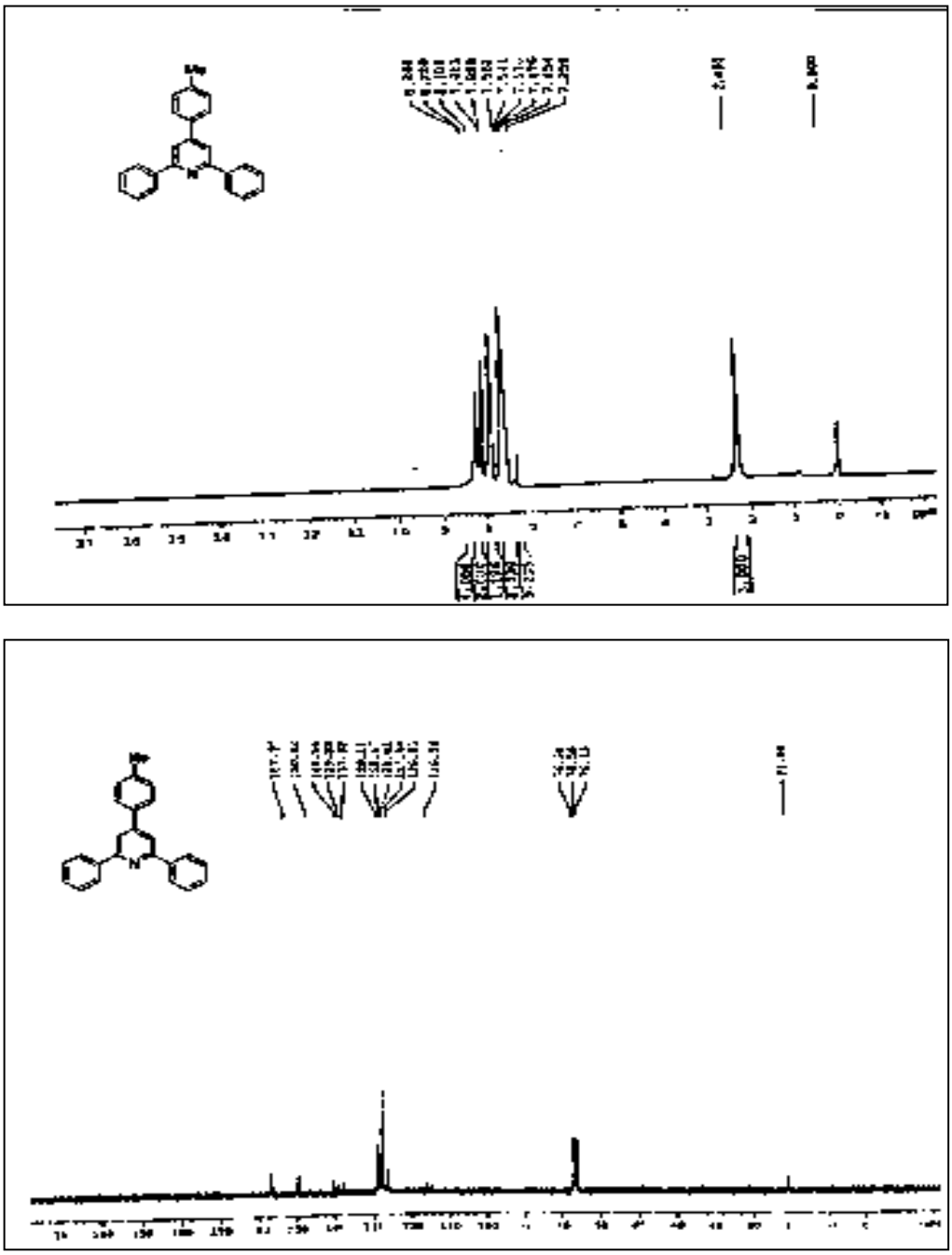

Figure I.C.4. *Scanned copy of ^{1}H and ^{13}C NMR spectra of 4-(4-chlorophenyl)-2,6-diphenylpyridine*

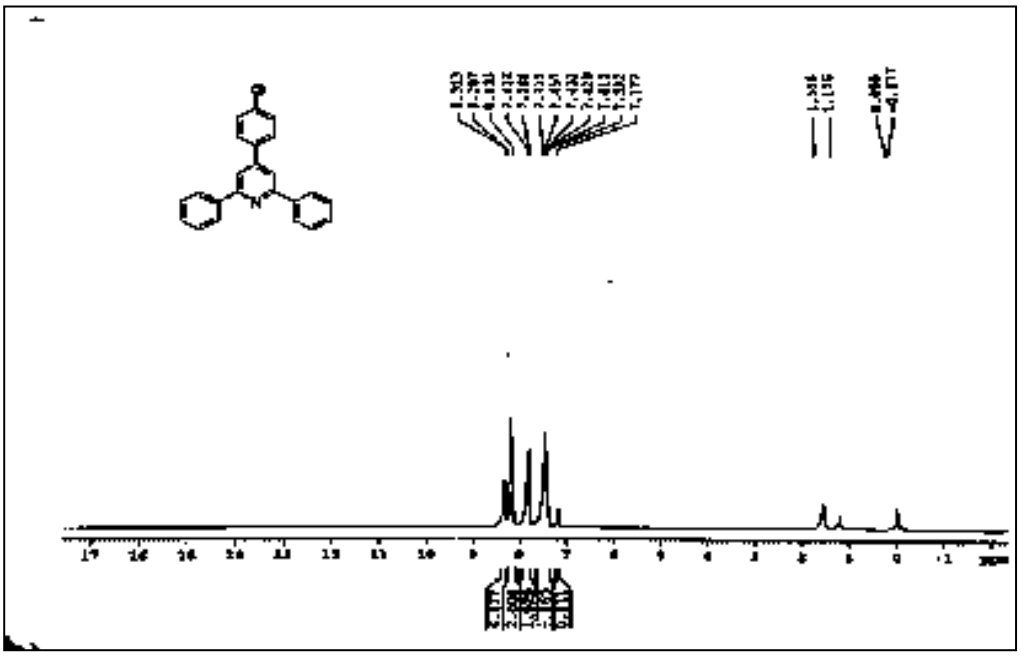

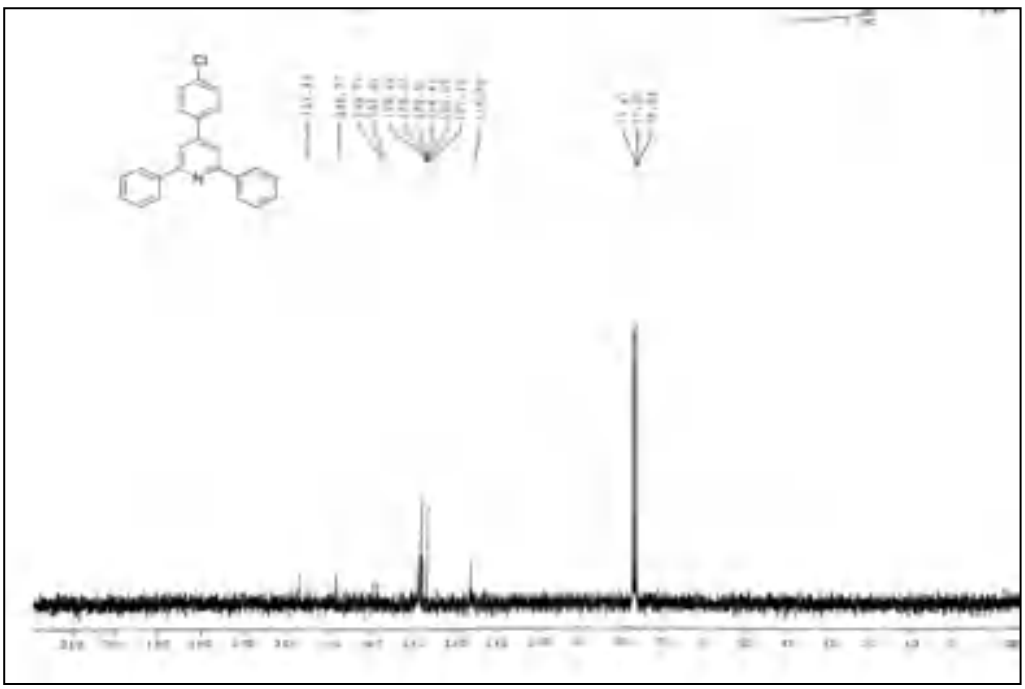

Figure I.C.5. *Scanned copy of ^{1}H and ^{13}C NMR spectra of 4-(4-nitrophenyl)-2,6-diphenylpyridine*

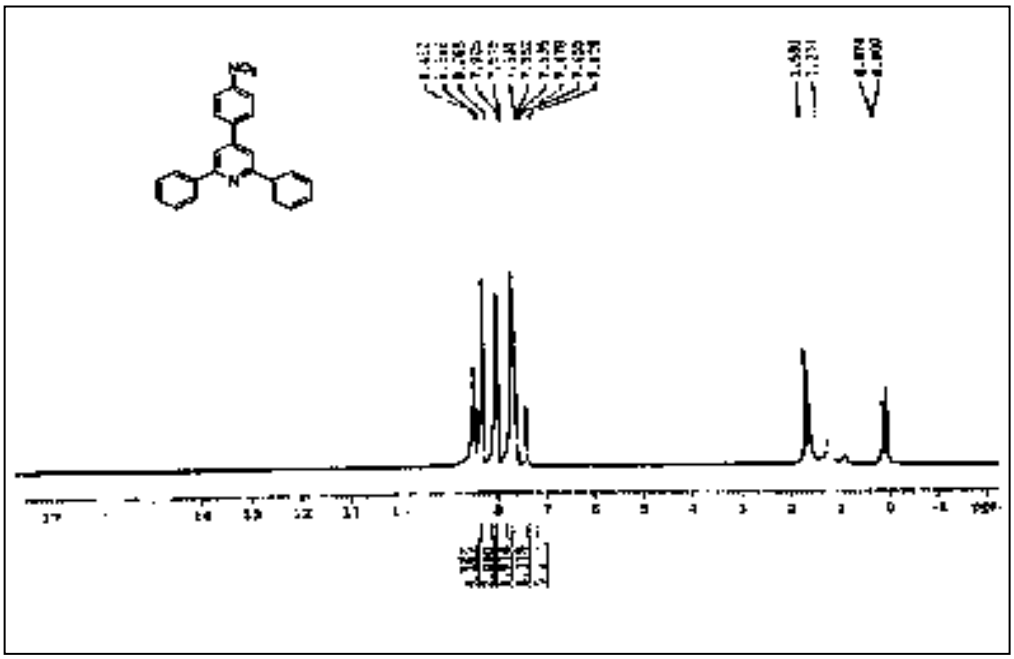

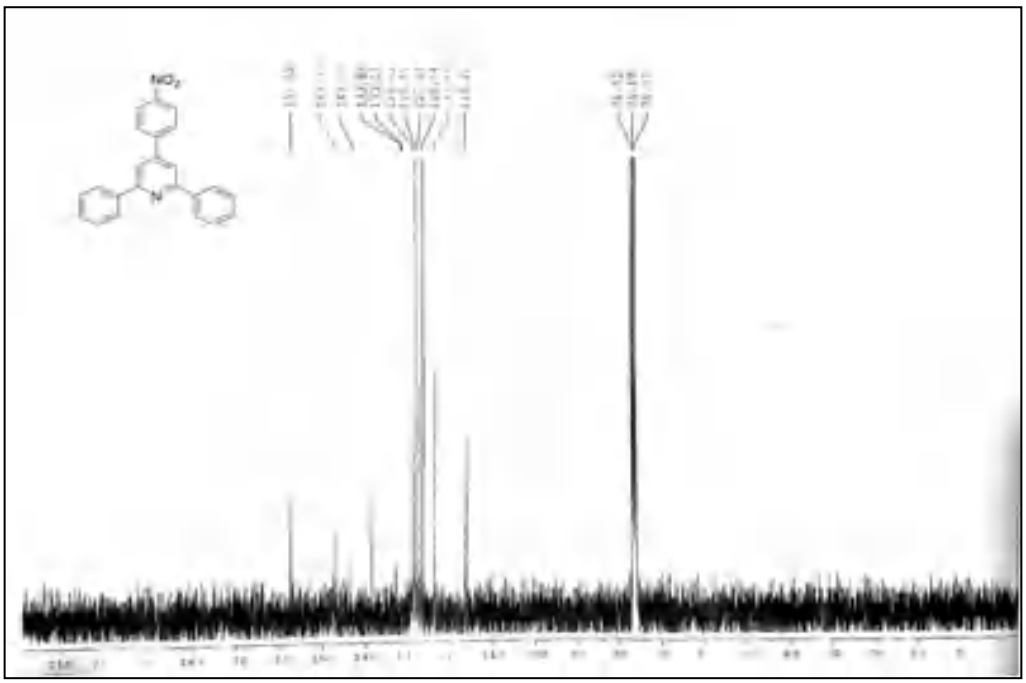

Figure I.C.6. *Scanned copy of ^{1}H and ^{13}C NMR spectra of 4-(4-methoxyphenyl)-2,6-diphenylpyridine*

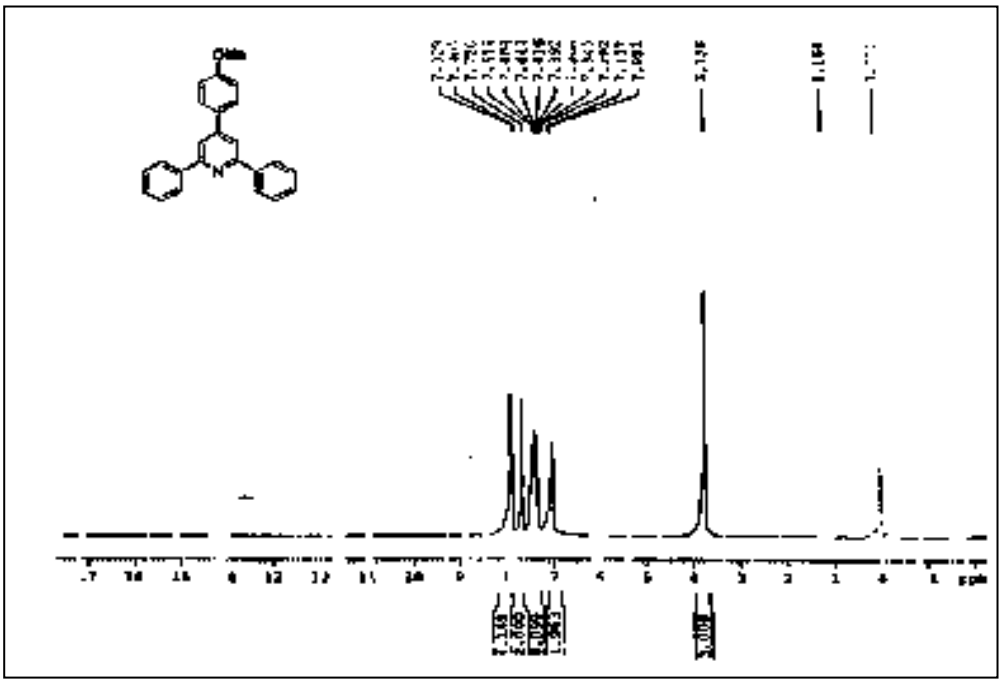

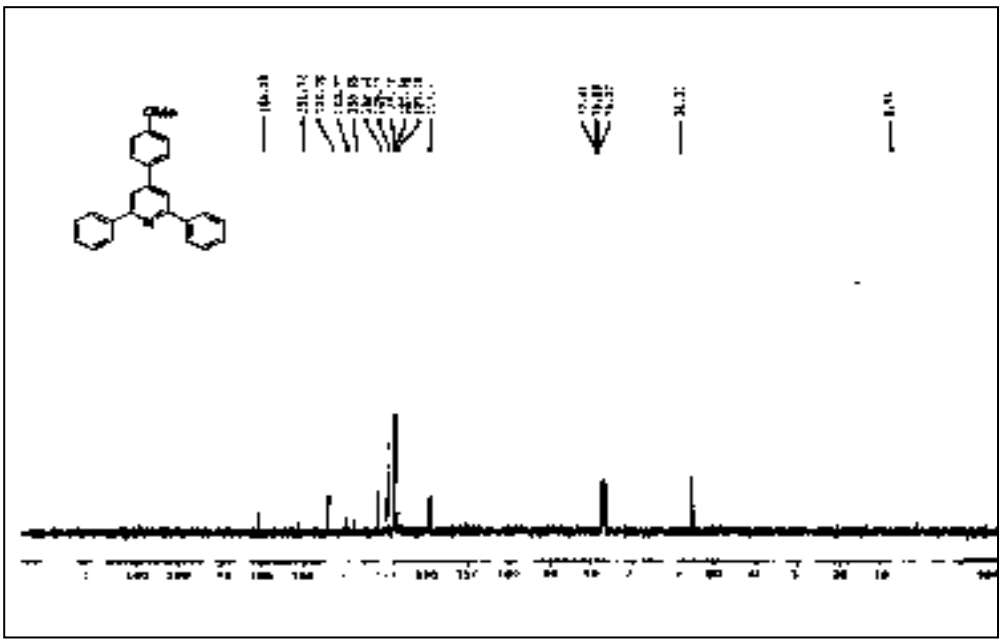

Figure I.C.7. *Scanned copy of ^{1}H and ^{13}C NMR spectra of 4-(furan-2-yl)-2,6-diphenylpyridine*

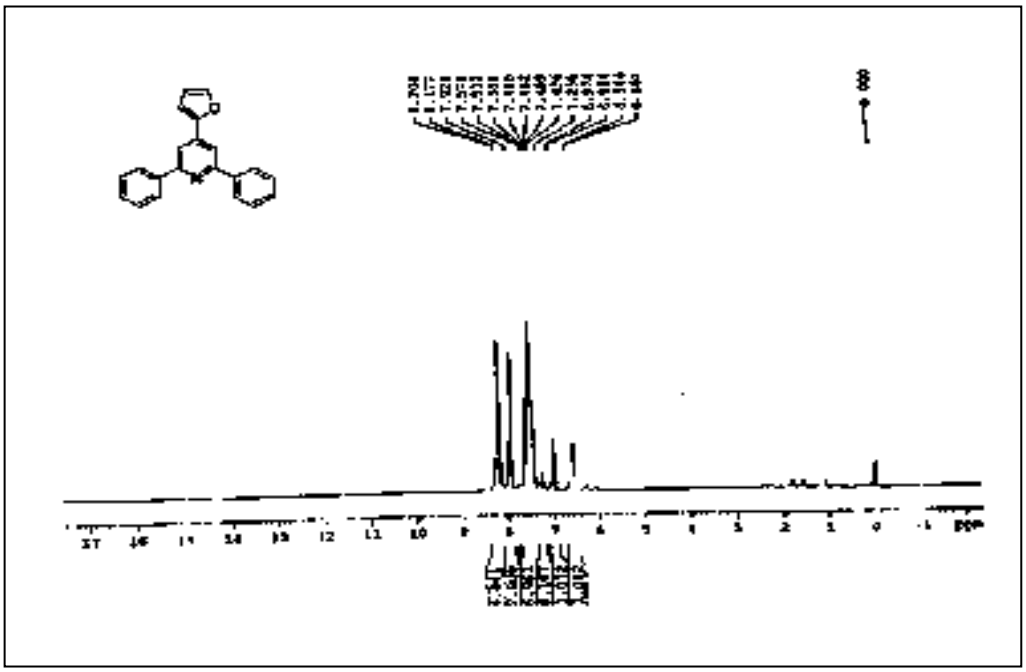

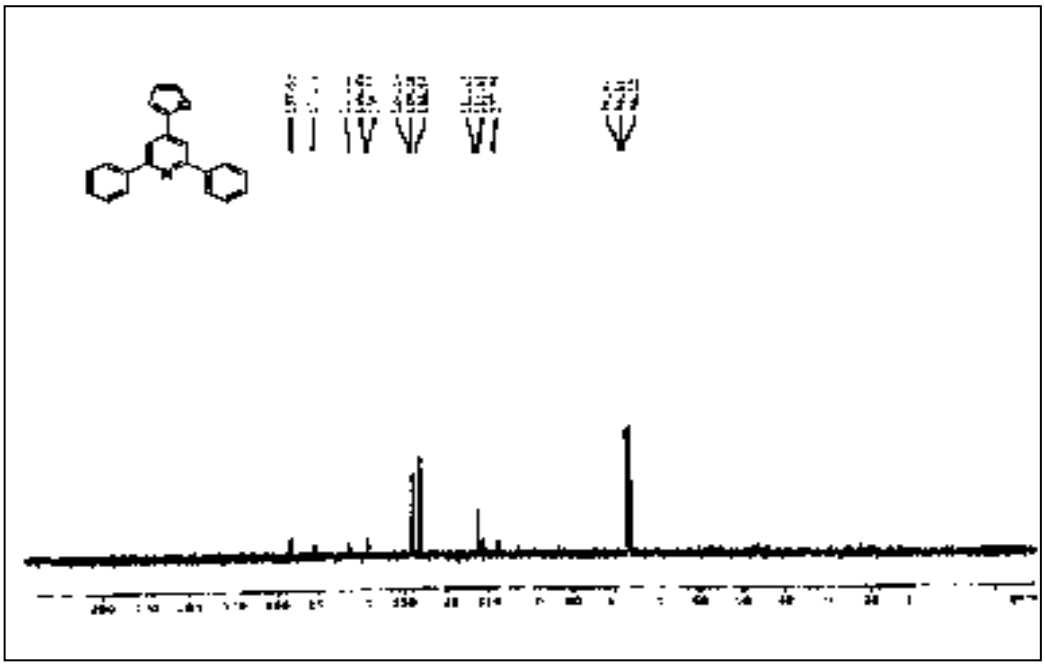

Figure I.C.8. *Scanned copy of ^{1}H and ^{13}C NMR spectra of 4-phenyl-2,6-di-p-tolylpyridine*

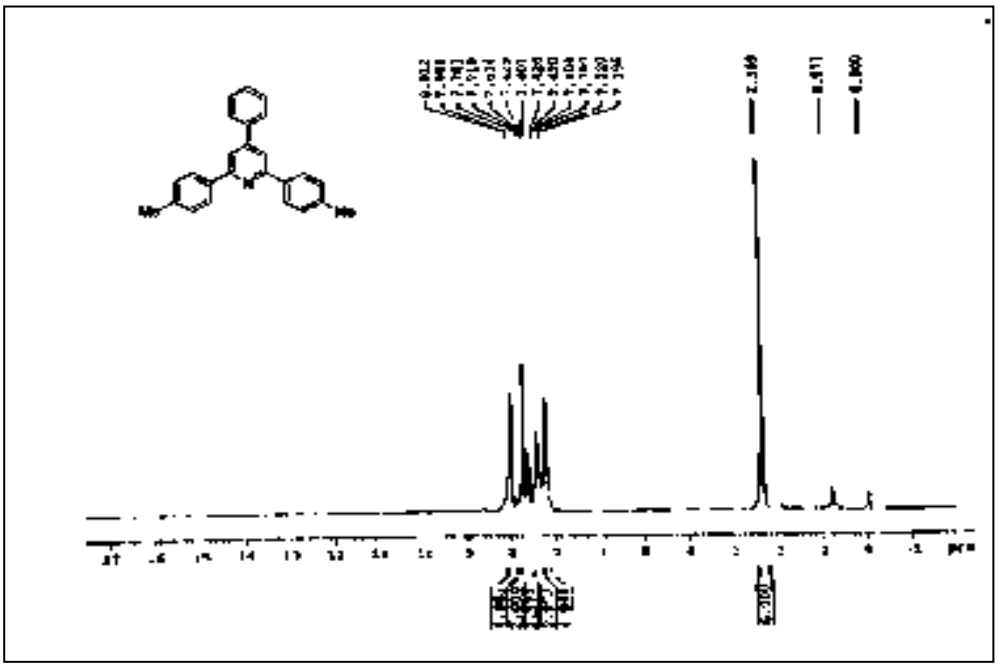

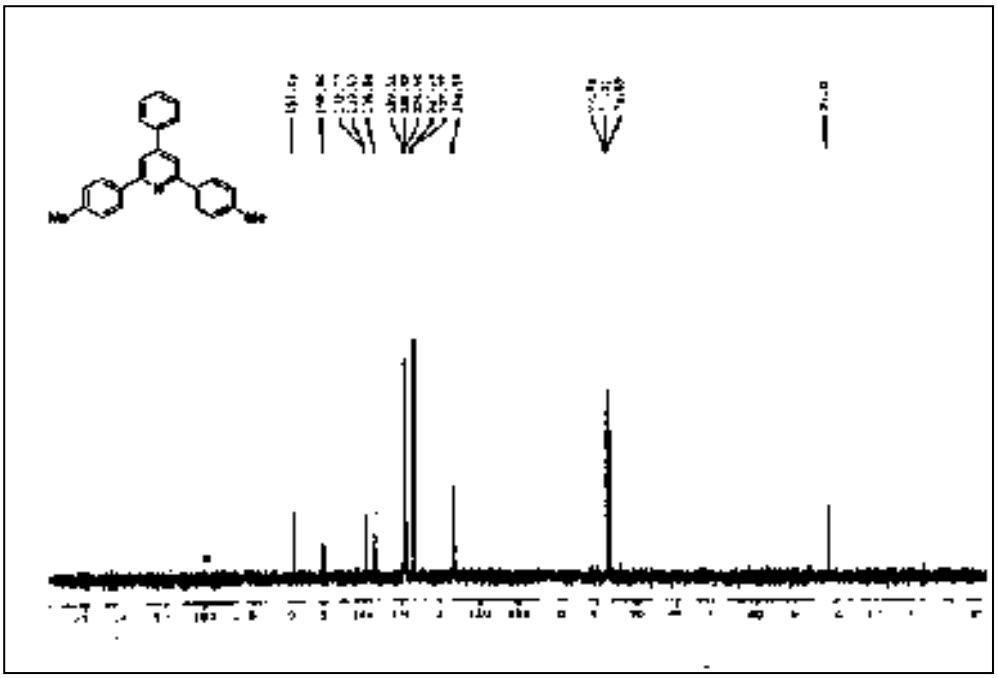

Figure I.C.9. *Scanned copy of ^{1}H and ^{13}C NMR spectra of 2,6-bis(4-bromophenyl)-4-phenylpyridine*

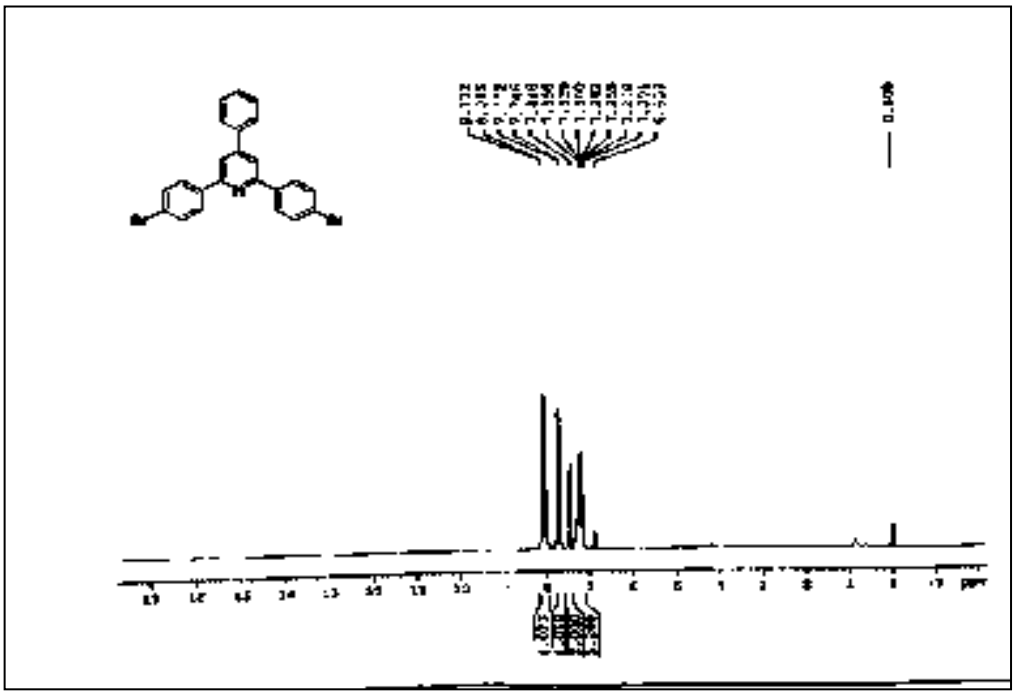

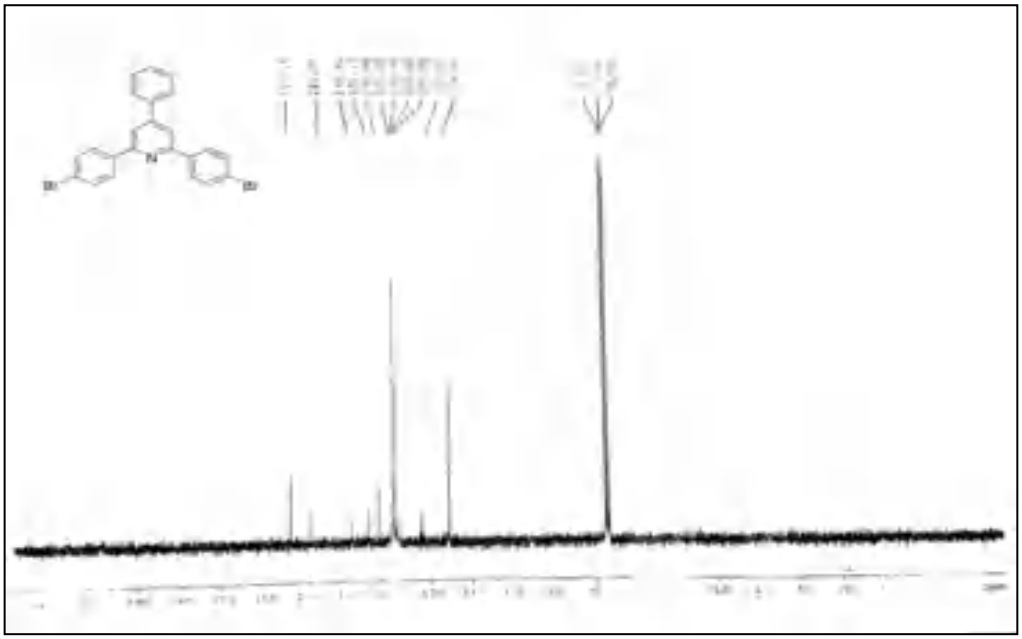

Figure I.C.10. *Scanned copy of ^{1}H and ^{13}C NMR spectra of 2,6-bis(4-bromophenyl)-4-(4-chlorophenyl)pyridine*

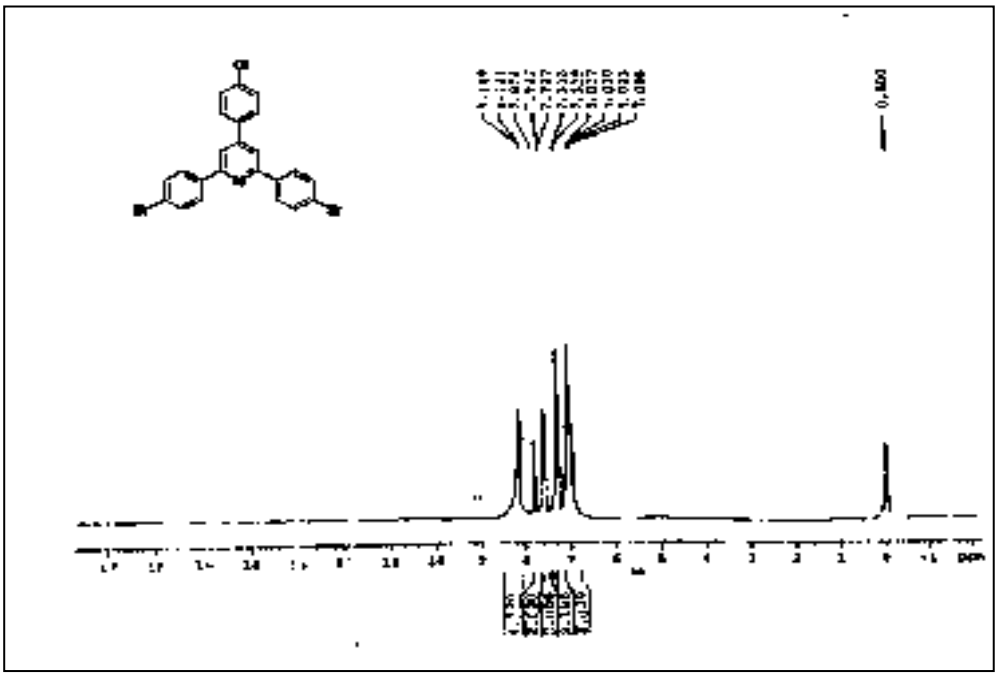

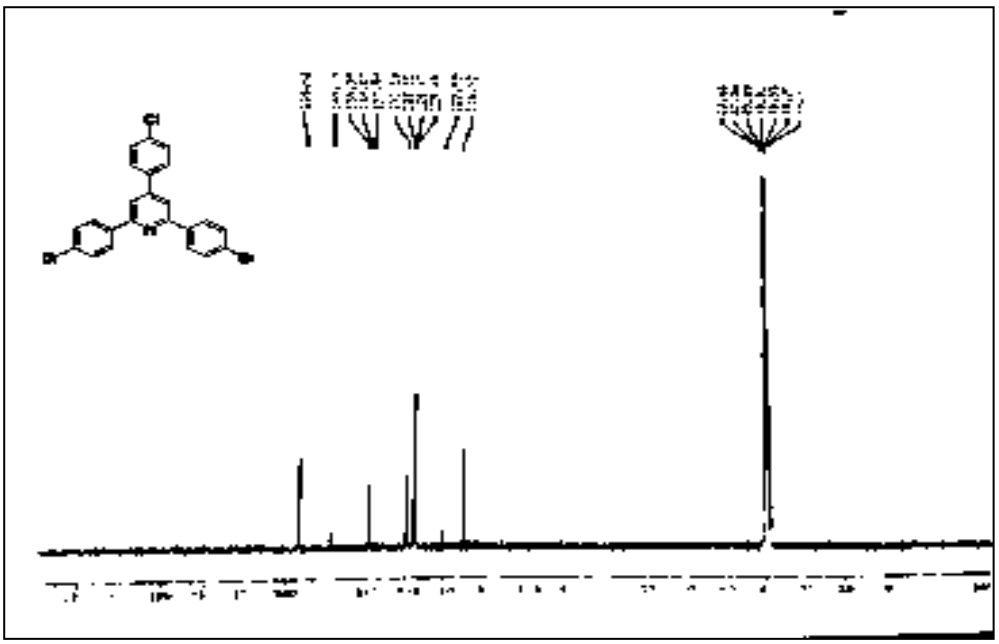

I.C.6. References

References are given in Bibliography under Chapter I, Section C

Chapter II

Section A

Heterogeneous Pd composite catalyzed Suzuki and Heck coupling reaction in water

II.A.1. Introduction

Carbon-carbon bond formation reaction is the essence of the synthesis in organic chemistry. Kolbe's fundamental laboratory-based C-C bond formation in 1845 for his well-known acetic acid synthesis played an important role in shaping chemical synthesis [1]. The enzymatic processes must take place in an aqueous environment in nature, but water has been avoided as a reaction medium in common organic synthesis. Since the historic study of Breslow for Diels-Alder reactions [2], the recognition of water as a solvent in C-C coupling reactions has been increased and proved to be advantageous over organic solvents [3]. Generally, protection and deprotection processes under aqueous solvent in organic synthesis can be simplified and there has already been great advance to understand the organic reaction in water at high temperatures and its broad scopes are varying from the source of life to energy and fuels to chemical synthesis [4]. In the 20th century, carbon-carbon bond formation reactions have shown a new paradigm that has amplified the effectiveness of organic chemists appreciably in synthesizing complex molecular frameworks, which has substituted our thinking completely about organic synthesis. Based on transition metal catalysis, the C-C bond formation reactions joining functionalized and sensitive substrates are fundamental for organic molecule synthesis and provide new opportunities in medicinal as well as nanotechnology. In organic chemistry, the C-C coupling reaction is a general term for a wide variety of organic reactions where, in the presence of metal catalysts, two fragments are combined together. Generally, two types of coupling reactions have been identified. Homo-coupling reaction occurs when two identical chemical species are joined together to afford a single product and Hetero-coupling reaction (also known as cross-coupling) occurs when two dissimilar chemical species are combined to form a

single product. Among the homo-coupling reactions, the Wurtz reaction [5], the Pinacol coupling reaction [6], Glaser coupling [7], and the Ullmann reaction [8] are important. On the other hand, the C-C cross-coupling reaction includes Cadiot-Chodkiewicz coupling [9], Castro-Stephens coupling [10], Corey-House synthesis [11], Kumada coupling [12], Heck reaction [13], Sonogashira coupling [14], Negishi coupling [15], Stille cross-coupling [16], Suzuki reaction [17], Murahashi coupling [18], Hiyama coupling [19], Fukuyama coupling [20], and Liebeskind-Srogl coupling [21]. Over the past 30 years, the development of C-C cross-coupling reactions catalyzed by transition metals has profoundly revolutionized the protocols for the synthesis of natural products, organic materials, and polymers, building blocks for supramolecular chemistry, and medicinal chemistry from simpler moieties. In 2010 E. Negishi, R. Heck, and A. Suzuki were awarded the Nobel Prize in chemistry for developing direct bond formation between carbon atoms (palladium-catalyzed C-C cross-coupling reaction). However, the growth of highly active catalysts has drawn much consideration for the development of efficient, green, and cost-effective synthesis in organic chemistry. Metal-nanoparticle (NP)-based catalysts can be assumed as an intermediate between homogeneous and heterogeneous catalysts, and they are considered half-heterogeneous catalysts [22]. Due to the small size of metal-NPs, they are not easily removed from the reaction mixture and this problem is usually solved by binding the NPs with structural support. Therefore, there is a need for heterogeneous catalysts via immobilization of metal NPs on solid supports to achieve high catalytic activity, high mechanical and thermal stability, easy regeneration, and separation procedures [23-26]. Metal NPs on structural support or metal-composite catalysts (composite materials are combinations of two or more materials having different phases) are being investigated as a new dimension of catalysis [27-29]. Normally, composites are

composed of two types of different materials, One is called a binder or matrix, which binds the fragments together and is termed reinforcement. If one of the combining elements of the composite is in the nanometer dimension, then it is called a nanocomposite [30]. In addition, as the subject is so broad in this chapter, we have shown the application of different nanostructured materials as host elements for the heterogeneous PdNPs-catalyzed Suzuki and Heck coupling reactions.

II.A.2. General outline of C-C cross-coupling reaction mechanism

The mechanism of the C-C cross-coupling reaction generally comprises three important steps

1. Oxidative addition
2. Transmetalation
3. Reductive elimination

The oxidative addition and reductive elimination are generally multistep processes as they involve ligand association and dissociation processes respectively. On the other hand, the transmetalation process involves ligand exchange between two metal centers.

II.A.2.1. Suzuki coupling

The Suzuki coupling is categorized as a C-C cross-coupling reaction, where two dissimilar fragments boronic acid and organohalide or triflate are combined to yield substituted biphenyls in presence of palladium (0) complex catalyst [31]. The relative reactivity order of halides and triflate is R-I > R-OTf> R-Br >> R-Cl. Since its discovery in 1979, this reaction becomes utmost acceptable process for the carbon framework expansion in organic molecules. Suzuki-Miyaura

coupling reaction is extremely helpful for the assembly of a conjugated diene, polyene systems, and biaryl systems with high stereoisomeric purity.

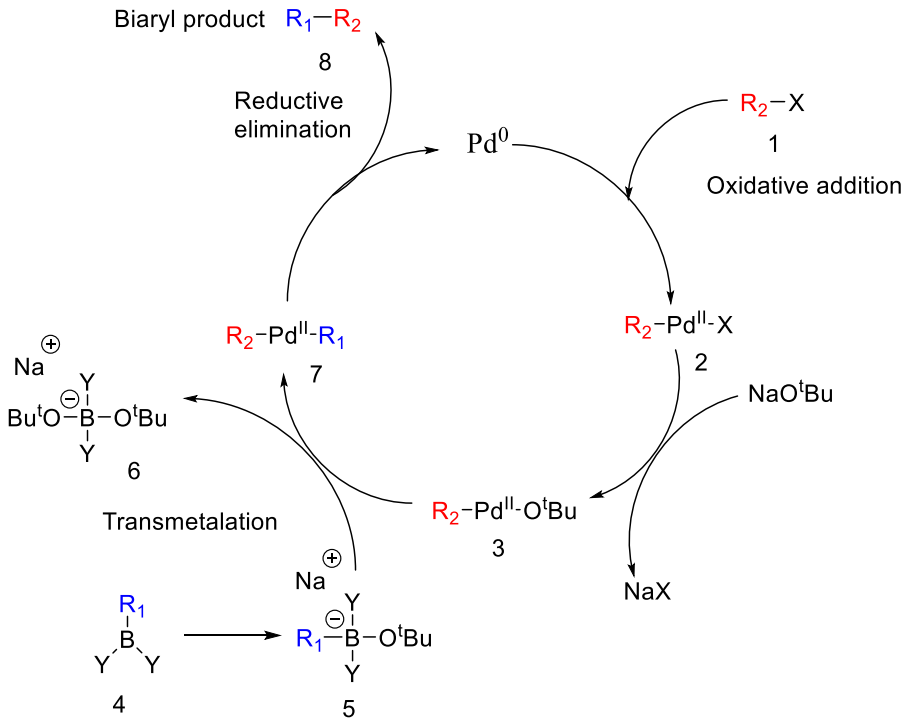

Scheme II.A.1. *Suzuki coupling reaction mechanism.*

Suzuki Miyaura coupling using inactivated alkyl halides to form C (sp^2)–C (sp^3) and even C (sp^3)–C (sp^3) bonds, has made incredible progress in the field of coupling reaction [32, 33]. The first step of the Suzuki coupling mechanism (Scheme II.A.1) is the oxidative addition of Pd (0) to the aryl halide (1) to form the organopalladium species (2). Afterthat, intermediate (3) is formed by the reaction with a base, which again forms the organopalladium species via transmetalation (4) with the complex (boronate complex) formed by the reaction of the boronic acid (5) with base. The last step is reductive elimination which yields the biaryl product (8) and brings back the original Pd (0) catalyst. The

Suzuki coupling reaction occurs in presence of the base and the base has three roles in this coupling reaction: formation of the palladium complex, formation of trialkyl borate and accelerates the reductive elimination by the reaction of alkoxide with Pd complex.

II.A.2.2. Heck reaction

The Heck reaction is the cross-coupling reaction (also known as Mizoroki-Heck reaction) where halides or triflates with unsaturation are joined with an alkene to form substituted alkene in the presence of a base and a palladium Pd(0) catalyst (or palladium nanomaterial-based catalyst) [34]. Tsutomu Mizoroki (1971) describes the synthesis of stilbene from iodobenzene and styrene in presence of potassium acetate base and $PdCl_2$ catalyst at 120 ^oC temperature (Scheme II.A.2.).

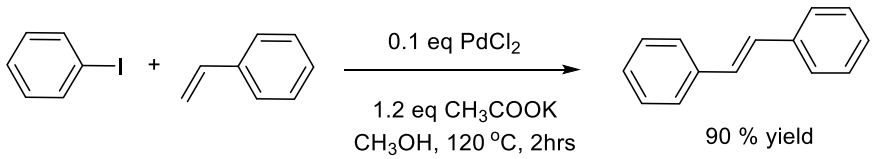

SchemeII.A.2. *Mizoroki-Heck C-C cross-coupling reaction*

In 1972, Heck appreciated the Mizoroki publication and independently discover the same reaction with different conditions (palladium acetate catalyst, catalyst loading 0.01 equivalent, a hindered amine base, and in absence of solvent) [34]. The mechanism of the Heck reaction involves several steps. At first, palladium (II) acetate [$Pd(OAc)_2$] is reduced by triphenylphosphine (PPh_3) to bis(triphenylphosphine)palladium (0). Step 1 of the coupling reaction involves the insertion of Pd (0) into the aryl bromide bond (Scheme II.A.3). In step 2 alkene and Pd forms a C-Pd bond in a syn-addition step. In the third step, a Pd-alkene π complex is generated through *β*-hydride elimination. The Pd (0)

compound is then regenerated by the reductive elimination of the Pd (II) complex with the help of a base in the final step of the coupling reaction.

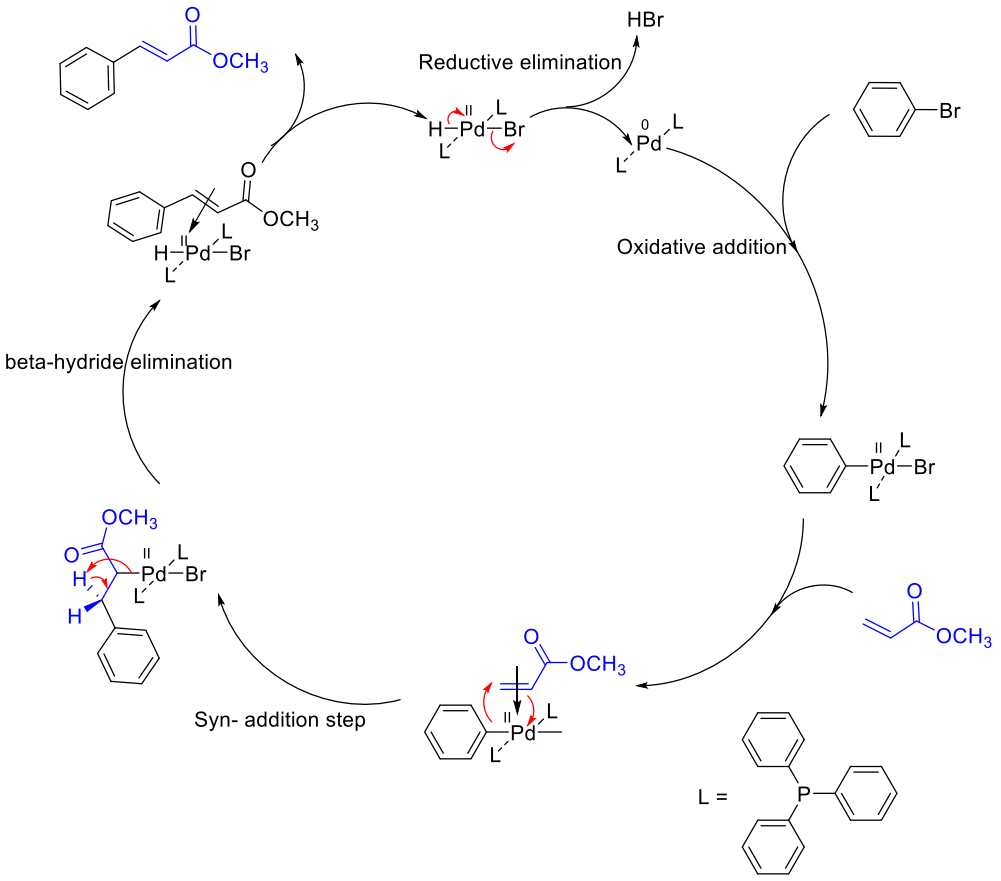

Scheme II.A.3. *Pd catalyzed Heck coupling reaction mechanism.*

II.B.3. Background of heterogeneous metal-composite catalyst for cross-coupling

Heck and Suzuki cross-coupling reactions are typically catalyzed by Pd-based homogenous systems that require the use of ligands (phosphine or *N*-heterocyclic) to design active catalytic systems. As a consequence, the separation of the homogeneous catalyst after reaction has been appeared as

biggest problem in the field of catalyst. Accordingly, the catalyst may incorporate in the final product, thus results the loss of catalyst in the reaction, and a devalued product is formed from a pharmaceutical point of view. The main challenge is to develop heterogeneous catalytic systems for C-C cross-coupling reactions and establish the nature of the active catalyst species. The literature of coupling reaction with homogeneous catalytic systems is well developed, but the contrary is observed for heterogeneous systems [37]. Some researchers claim to develop solid pre-catalyst of soluble catalytically active Pd species [38-40], while others recognize absolutely heterogeneous systems, where catalysis takes place on the surface of Pd-based solid heterogeneous catalyst [41, 42]. The effectiveness of a good catalytic system is generally decided by the activity, selectivity, and lifetime of the prepared catalyst [43]. The activity of the catalyst is measured by the percentage of the reactants converted into a product, however, the selectivity is measured by the percentage of the reactants that are transformed into desired final products and the lifetime of the catalyst is that time when the catalyst attain its activity and selectivity to the expected level.

Pd NPs have become attractive forms of heterogeneous catalyst due to their size and shape dependence and efficient catalytic activity in C-C cross-coupling reaction [37, 44]. Nevertheless, their use as a catalyst has been restricted because of scantiness of efficient separation procedures and techniques like centrifugation and filtration are not much effective to recover the NPs completely. Moreover, the agglomeration and sintering property of NPs upon heating, they are leached to form the insoluble non-catalytic Pd black [37]. Supported Pd catalyst has drawn profound interest due to their easy reusability in the C-C cross-coupling reaction. Most often, PdNPs immobilized on solid support become less catalytically active and better understanding of the activity

of PdNPs leads to design more effective heterogeneous catalysts in the cross-coupling reaction. Supported metal catalyst or metal-composite catalyst can be categorized as: inorganic, organic, and inorganic-organic materials.

II.B.3.1. Inorganic support

II.B.3.1.1. PdNPs in carbonaceous supports

In C-C cross coupling reaction, the use of carbonaceous nanomaterial supported PdNPs opened up a new paradigm in the field of heterogeneous catalysis [45-47]. Amongst them, due to the commercial availability of activated charcoal, often (Pd/C) where Pd is immobilized on charcoal is used as heterogeneous catalyst. In addition, different solid supports like alumina and silica possess lower surface area than charcoal support [47]. From literature, it is reported that Pd/C is stable in air, water, acid, and bases and it does not require any inert atmospheric condition to be performed [47, 48]. Xu *et al.* developed a pathway for the reaction between water-soluble bromo arenes with sodium tetraphenylborate to synthesize substituted biphenyl (Scheme II.A.4) in presence of 0.0025 mol% of Pd/C under a refluxed condition in water (reaction time was varied from 1-7 h) [49]. The Comparison between inorganic bases showed that sodium bases are more effective than potassium bases in this reaction. The catalyst was recycled upto five cycles with a gradual loss of reactivity.

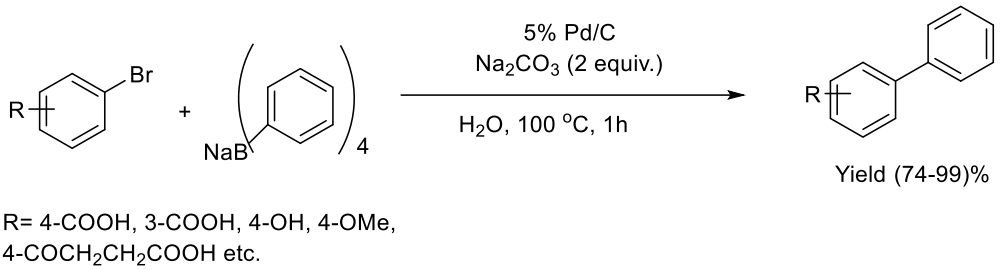

Scheme II.A.4. *Suzuki-Miyaura reaction by Xu et al.*

Previous reports showed that surfactants are used as additive to increase the solubility of the reactants aryl halides. Kohler *et al.* performed the coupling reaction of aryl chlorides with aryl boronic acids (Scheme II.A.5) in presence of ligand less Pd/C catalyst in water [50]. All reactions were carried out under an ambient condition to minimize the chance of homocoupling. Although a lower Pd concentration (0.2–0.5 mol%) is required for activated aryl chlorides and higher Pd concentration (2 mol%) is needed for deactivated chloroarenes. The addition of surfactant TBAB as an additive and application of NaOH amongst the inorganic bases have profound role in this reaction. Not only the aryl boronic acids but the boronated esters and potassium trifluoroborates are equally effective under this optimized reaction condition. The reactivation of the catalyst [Pd (0) to Pd (II)] using iodine as an oxidizing agent was carried out to recycle the catalyst in successive runs.

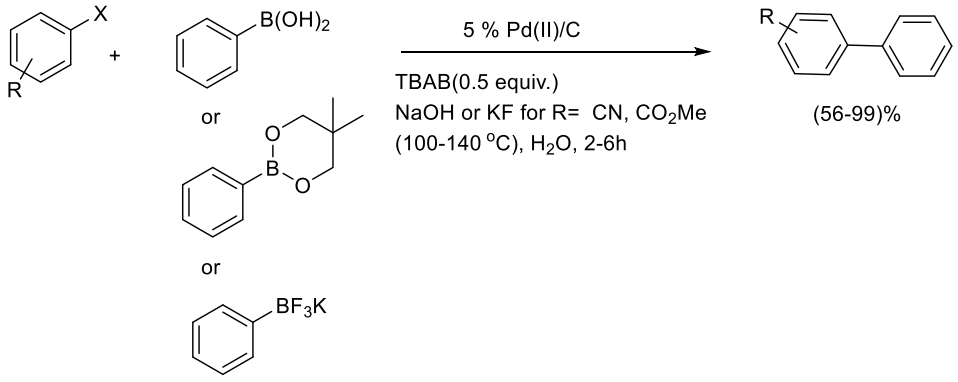

X= I, Br, Cl
R= 4-COMe, 4-CN, 2-CN, 4-COOMe, 2-COOMe
4-F, H, 4-Me, 2-Me, 4-OMe, 4-OH, 4-NH_2

Scheme II.A.5. *Suzuki coupling reaction by Kohler et al.*

Among the nanomaterials, graphene is solely able to stand out far ahead of all other nanomaterials because of its unique structure and exclusive

characteristics [51]. Graphene and its derivative have widely been used as catalytic support due to their high flexibility and strength like solid substrates. They exhibit a high surface area and are homogeneously embedded into metal matrices which make graphene and its derivative a viable candidate to be used as catalyst support. Due to the immobilization of metal NPs on the surface of graphene and its derivatives, the surface area of the composite material increases, thereby increasing the distance between the sheets. The catalytic activity of these metal composite materials successfully enhance the productivity of the most studied C-C cross-coupling reactions [52-57]. Zhang *et al.* reported graphene-modified PdNPs by reducing $Pd(OAc)_2$ (Scheme II.A.6) using a surfactant sodium dodecyl sulfate (SDS) [58].

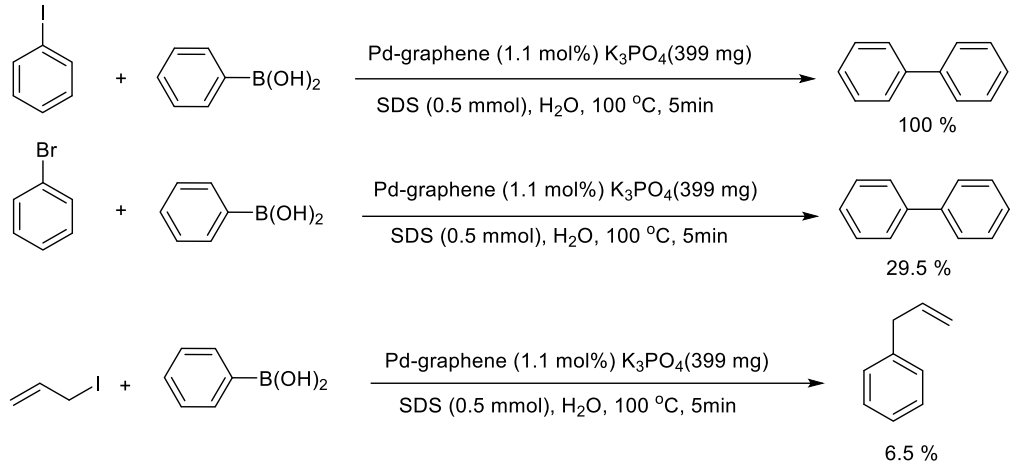

Scheme II.A.6. *Pd-graphene composite catalyzed synthetic approach by Zhang et al.*

The use of SDS can be showed as surfactant as well as a reducing agent. The prepared catalyst was highly efficient under aqueous as well as in aerobic conditions and exerted the product within 5 min. The recovery of the catalyst was done by filtration process and reused upto ten consecutive cycles. Allyl

iodides and bromobenzene were also employed in this coupling reaction but resulted in a lower yield of allylbenzene and biphenyl.

Shendage *et al.* electrochemically deposited PdNPs on nafion-graphene support (Pd/Nf-G) which showed eminent catalytic activity for the Suzuki coupling reaction to produce substituted biphenyls from substituted aryl boronic acids (Scheme II.A.7) under ethanol/water mixture at 80 ^{o}C [59]. Under the reaction temperature, Nafion is chemically and thermally stable. It is used to disperse and stabilize graphene on the electrode surface. The electrochemical process is generally heterogeneous in nature and allows easy recovery of the desired product. Besides this, no side product formation, short time of reaction, simple operation, and percentage of purity of side product make this process advantageous than conventional processes.

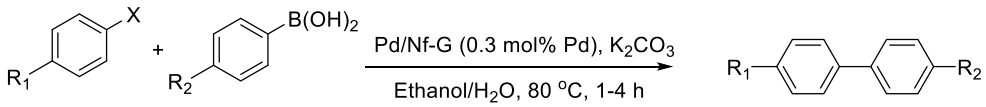

R_1= CH_3, OCH_3, NO_2, $COCH_3$, OH, H
R_2= CH_3, OCH_3, Cl, H
X= I, Br

Yield (88-94%)

SchemeII.A.7. *The Suzuki coupling reaction using Pd/Nf-G catalyst.*

The formation of PdNPs on Nf-G support was confirmed by SEM-EDAX, XRD, TEM, thermogravimetric analysis (TGA). The reaction between different aryl iodides and arylboronic acid was studied using a Pd/Nf–G catalyst. The electron-donating and electron-withdrawing aryl iodides afforded the product with excellent yield; however, aryl bromides require longer reaction time.

Gómez-Martínez *et al.* used boron-derived nucleophiles like potassium aryltrifluoroborates or boronic acid esters and aryl halide as reactants to afford biaryls for Suzuki coupling reaction using PdNPs (6 % Pd w/w) supported on

graphene (PdNPs–G) and reduced graphene oxide (PdNPs–rGO). They prepared three types of catalysts (Figure II.A.1), catalyst 1 is PdNPs immobilized on rGO sheets functionalized with octadecylamine (PdNPs–rGO/ODA), where 13 nm average size Pd (0) NPs have been immobilized. Catalyst 1 disperses better in organic solvents due to the presence of amino-functional groups.

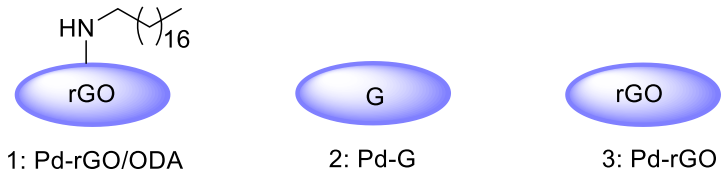

Figure II.A.1. *Pd(0) NPs supported catalyst employed in Suzuki coupling.*

Catalyst 2 is (PdNPs–G) where 5 nm average size Pd (0) NPs are distributed on the sheets of graphene oxide, while, catalyst 3, (PdNPs–rGO) contains Pd (0) NPs with an average size of 6.9 nm. Catalyst 2 and catalyst 3 are well dispersed in an aqueous medium. Due to the better dispersibility in water, both the catalysts, 2 (PdNPs–G) and 3 (PdNPs–rGO) are highly active in this process with a solvent ratio (MeOH/H2O:3/1) (Scheme II.A.8). Under the microwave irradiation, the catalyst 2 was reused upto eight consecutive cycles without the loss of its catalytic activity. Moreover, the catalytic activity dropped significantly under the conventional heating reaction conditions after five consecutive cycles.

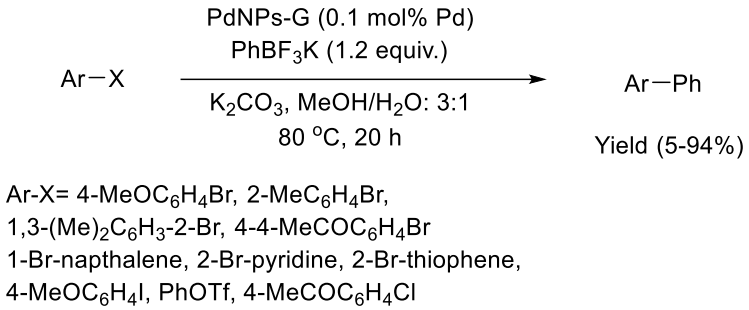

Scheme II.A.8. *Suzuki coupling catalyzed by Pd (0) NPs supported GO and rGO.*

II.A.3.1.2. Zeolite support (Inorganic support)

Among the catalyst support, zeolites having an anionic framework provides high surface area and it is conducive to the high dispersion and adsorption of metal species [60, 61]. As crystalline nanoporous materials, zeolite can trap or recover heavy metals including Pd from industrial water waste due to its well-distributed microporous space [62]. Wang *et al.* prepared the zeolite-supported Pd (II) catalysts by placing Pd (II) species on the solid surface of zeolite with an anion framework based on the charge balance principle (Figure II.A.2). They developed a highly efficient zeolite-supported Pd catalyst (0.84% Pd@zeolite USY) for in water C-C cross-coupling reaction using tetrapropylammonium hydroxide (TPAOH) base (Scheme II.A.9) [63]. This catalyst was successfully employed to produce substituted alkynes and biaryl from terminal alkynes and aryl boronic acids. The interaction between metal and support may be varied due to the interaction between metal-reactant and the form of the metal [64].

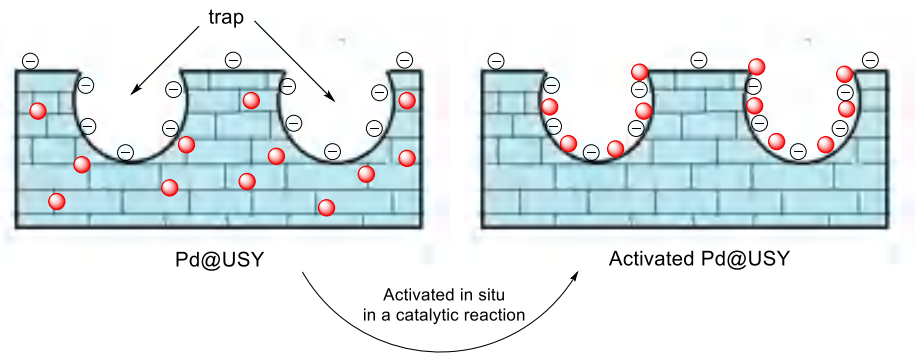

Figure II.A.2. *The migration of Pd during the activation in catalysis.*

In an aqueous system, the Pd species migrate in the catalytic process and the Pd (II) intermediate undergoes ion exchange with cations (Na^+, K^+ etc.) present in an aqueous medium and easily escapes from the zeolite support. Therefore, it is quite necessary for the metal species to get stabilized on the catalytic support during the reaction. They observed that in some alkaline aqueous systems, Pd (II) intermediate species uses zeolites (with an anionic framework) as a sink for coupling reaction, therefore, the position of Pd on the surface of zeolites can be controlled by release/capture capability of metal ions [65].

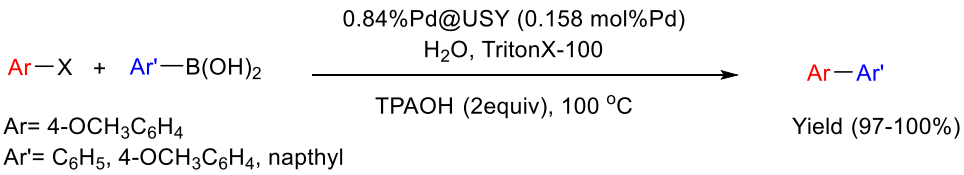

Scheme II.A.9. *Pd@zeolite USY catalyzed Suzuki coupling reaction.*

II.B.3.2. PdNPs on organic-inorganic support

Corma *et al.* reported the use of oxime palladacycle anchored to amorphous silica-based inorganic supports [66]. They synthesized oxime palladacycle

anchored with silica (Pd/SiO_2) or with MCM-41 (Pd/MCM-41). The schematic diagram for the preparation of this catalyst is shown in (Scheme II.A.11).

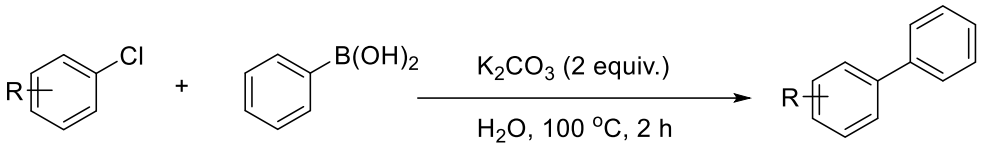

R= 4-Ac
5 mol % Pd/SiO_2: >99%
5 mol % Pd/MCM-41: 94%

R= 2-NO_2
5 mol % Pd/SiO_2: 89%
5 mol % Pd/MCM-41: 40%

Scheme II.A.10. *Suzuki coupling reaction described by Corma et al.*

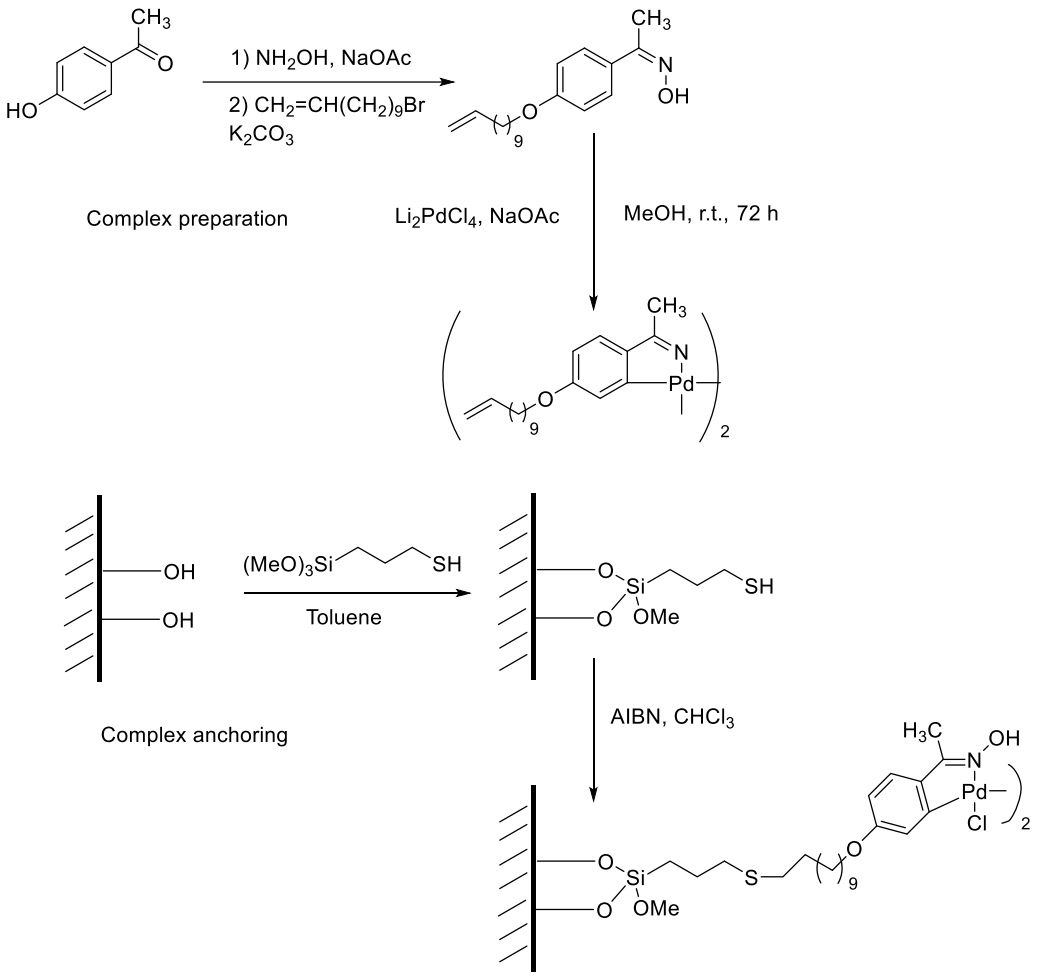

Scheme II.B.11. *The procedure of anchoring of oxime carbapalladacycle with marcaptipropyl modified high silica surface*

However, Pd/SiO_2 showed the best result using bromoarens and activated chloroarens with 5 mol% Pd in presence of K_2CO_3 base. The same oxime palladacycle anchored to polystyrene and polyethylene glycol afforded lower yield of the coupling product (Scheme II.A.10). The Pd/SiO_2 catalyst can also be recycled without significant drop in its catalytic activity upto eight consecutive runs. They also carried out the leaching study of the catalyst through three-phase

test and observed no detectable Pd species was observed in the medium which confirms the true heterogeneous nature of the process.

II.B.3.3. Organic support

Among various polymeric supports, the natural polysaccharide of chitosan (CS) is cheap, non-toxic, and has excellent complexation capability with transition metal due to the presence of polar functional groups. Moreover, chitosan is very easy to process into different forms, such as microspheres, films, fibers, and so on. Cotugno *et al.* developed an efficient protocol for Suzuki cross-coupling reaction using Pd (0) Chitosan composite catalyst [68]. The excellent yield and selectivity were achieved using this catalyst at a relatively short reaction time (5 h). They carried out the reaction between different aryl halides and aryl boronic acids using K_2CO_3 as a base, PdNPs@Chitosan (0.1 mol%) catalyst, molten TBAB at 70-90 ^oC under aqueous solvent (Scheme II.A.12). To obtain the catalyst, in presence of TBAB, $Pd(OAc)_2$ was reduced electrochemically on the surface of chitosan. Subsequently, the PdNPs metallic core is stabilized by tetrabutylammonium cations mixed with Br- and $[PdBr_4]^-$ and the core-shell nanostructured catalyst is further chemically absorbed on chitosan surface (Figure II.A.3).

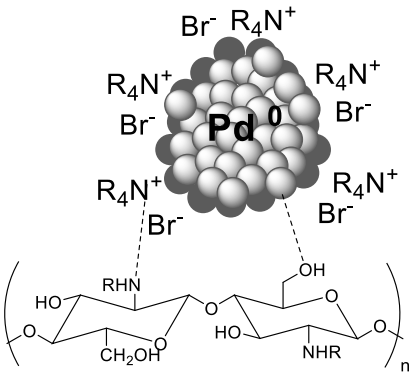

Figure II.A.3. *The core-shell structure of Pd nanoparticles is chemisorbed on chitosan in tetraalkylammonium-based ionic liquids (ILs).*

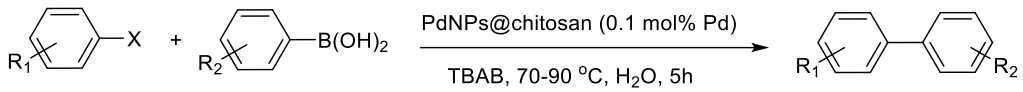

Scheme II.A.12. *Suzuki cross-coupling reaction catalyzed by PdNPs@Chitosan.*

Mondal *et al.* synthesized PdNPs grafted mesoporous organic polymer catalyst by reacting (Scheme II.A.13) $Pd(OAc)_2$ and poly-triallylamine (MPTA-1) in presence of methanol [69]. The mesoporous materials generally exhibits high surface area and the active metal centrers are distributed on this large surface, thereby capable to run organic transformation effectively [70]. These materials act as an ideal tethering agent to bind the active metals strongly at their surface. Cross-linking polymers minimize the chance of metal leaching from its surface and extensively stabilizes the metal in long-term. are extensively used as long-term stabilization of the metals, which minimizes the possibility of leaching of metals under reaction conditions [71]. They observed the Heck coupling reaction between different aryl and heteroaryl halides and substituted alkenes using this heterogeneous Pd–MPTA-1 catalyst in a water medium. However, substituted chlorobenzenes underwent this C-C coupling reaction and took a longer reaction time along with a lower yield of the product compared to the corresponding bromobenzene and iodobenzene.

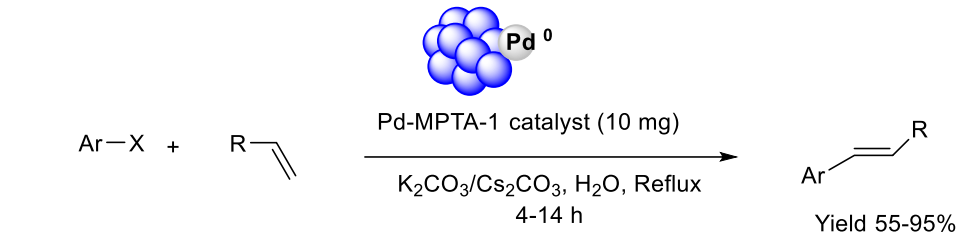

Ar=C_6H_5, 4-$OCH_3C_6H_4$, 4-$CH_3C_6H_4$, 4-$NO_2C_6H_4$,
3-FC_6H_4,4-$CHOC_6H_4$, 3-pyridyl, Thienyl
R= Ph, COOH, COOnBu,

Scheme II.A.13. *Heck reaction catalyzed by Pd-MPTA-1 catalyst in water media.*

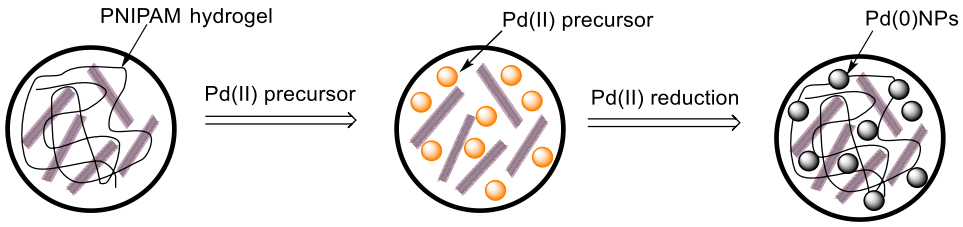

Figure II.A.4. *Pd(0) gtrafted on Poly(N-isopropylacrylamide-co-4-vinylpyridine) [poly(NIPAM-co-4-VP)] copolymer hydrogel.*

Lee *et al.* synthesized PdNPs immobilized on Poly(*N*-isopropylacrylamide-co-4-vinylpyridine) [poly(NIPAM-co-4-VP)] copolymer hydrogel for Suzuki and Heck cross-coupling reaction in water (Scheme II.A.14) [72]. Poly(*N*-isopropylacrylamide) (PNIPAM) is an example of temperature-responsive polymer which shows a phase transition from coil-to-globule in an aqueous solution at 32 ^oC which is the lower critical solution temperature (LCST) [73]. The swelling of PNIPAM polymer hydrogels is due to changes in the H-bonding of the PNIPAM polymer with water molecules [74]. Above LCST of PNIPAM, some H-bonds are dissociated and hydrophobic interactions are dominant among the PNIPAM network. Therefore, it is possible to carry out Suzuki coupling

reaction with hydrophobic substrates in absence of surfactants and organic solvents. Moreover, PNIPAM can be easily recovered from an aqueous medium by simple filtration above its LCST. Due to the versatile properties of PNIPAM, PdNPs immobilized on it have been utilized as recyclable heterogeneous catalysts [75, 76]. They observed that the PNIPAM matrix could not be restored after recycle and the leaching of Pd occurred.

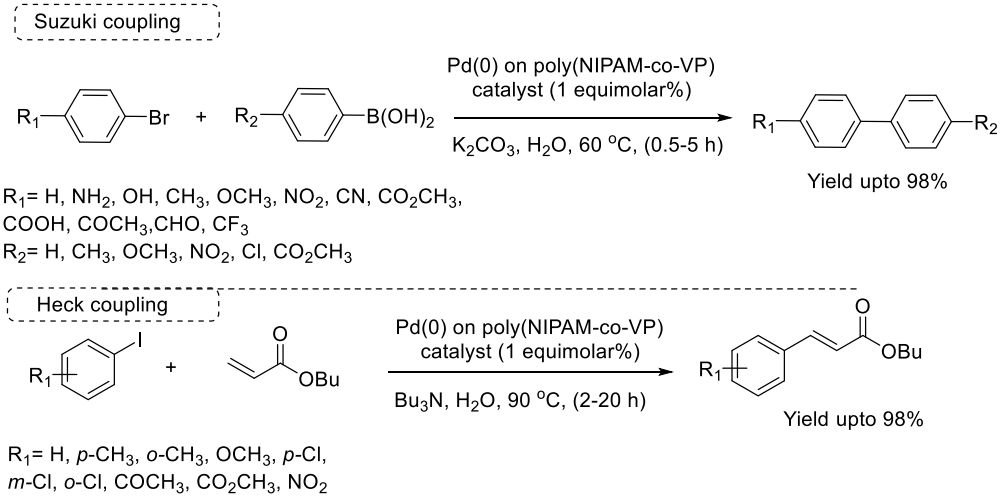

Scheme II.A.14. *Suzuki, Heck coupling reaction catalyzed by Pd(0) [poly(NIPAM-co-4-VP)] catalyst.*

To resolve this difficulty they have utilized temperature-responsive poly(*N*-isopropylacrylamide-co-4-vinylpyridine) [poly(NIPAM-co-4-VP)] co-polymers [77] as the PdNPs support (Figure II.A.4). The poly(NIPAM-co-4-VP) copolymer stabilized PdNPs were prepared by reducing the Pd(II) precursor on the copolymer surface using $NaBH_4$ as reducing agent in MeOH solvent.

II.B.4. Conclusion

The Suzuki and Heck, cross-coupling reactions have been widely exploited for decades for the expeditious C-C, C=C, C≡C bond formation which is used for

the development of organic compounds, polymers and natural products in drug discovery. From the industrial point of view, Pd catalyzed coupling reactions in greener way using alternative reaction media are the current area of interest. Among green solvents, the utmost choice is water due to its environmental benefits, safeties, and cost. The use of homogeneous Pd catalyst is not appropriate in industrial purposes due to their lower stability, higher cost of synthesis, problem in their separation procedure and difficulty in reusability. To overcome the drawbacks of a homogeneous catalyst, the concept of PdNPs immobilized on a solid support has attracted much interest to merge all the advantages of homogeneous and heterogeneous catalysts. PdNPs immobilized nanostructured catalysts having high surface to volume ratio, low cost of processibility, good mechanical and thermal stability, and high reusability, that's why they have been used in long-lasting, cost-effective cross-coupling reaction.

II.A.5. References

References are given in Bibliography under Chapter II, Section A

Chapter II

Section B

Poly (methyl methacrylate)-graphene oxide supported palladium catalyst: A ligand free protocol for Suzuki and Heck coupling reaction in water medium

II.B.1. Introduction

Heterogeneous palladium catalyzed C-C cross coupling reactions have attracted much attention over past two decades. As a representative of this class of reaction, Suzuki and Heck coupling are most significant because biaryl moieties and substituted olefins are present in pharmaceuticals [1-4], wide range of natural products such as alkaloids and many agrochemicals and biologically active compounds [5,6]. Although homogeneous catalyst offers excellent result but they have some drawbacks because of difficult separation procedure often contaminates the products. However, most of them employ different types of ligands such as sterically hindered trialkyl phosphines, triarylphosphines [7], *N*-heterocyclic carbenes [8], based Pd (II) complexes. Use of these ligands is unenviable because they are toxic and moisture sensitive. However, with growing interest towards greener reactions, ligand free solid supported heterogeneous catalysts are in demand. They have the advantage of enhanced synthetic efficiency and operational simplicity [9-12]. Previous reports include the immobilization of Pd on activated carbon [13], polymers [14,15], zeolites [16], mesoporous carbon [17], silica, alumina or titania [18,19].

II.B.2. Background and objectives

In the recent years, graphene oxide (GO) has attracted much attention owing to its wide range of application in different fields such as fuel cells [20], nanocomposite materials [21-24], and electronic devices [25]. GO has two dimensional layered sheets with several oxygen containing functional groups like epoxy, hydroxy, carbonyl, carboxyl, etc. Palladium nanoparticles supported on graphene and graphene derivatives enlarge the surface area of the composite [26], increasing the distance between the sheets.

Scheuermann *et al.* employed PdNPs supported on chemically derived graphene (CDG) for Suzuki coupling reaction (Scheme II.B.1) [27]. The CDG-Pd catalyst was prepared by the immobilization of Pd^{2+} ions through cation exchange on graphite oxide followed by chemical reduction. In comparison to the Pd/C catalyst, garphene-based and graphite oxide based Pd catalyst showed higher catalytic activity due to low Pd leaching. The prepared catalyst was characterized by different spectroscopic techniques such as FTIR, AAS, XPS, solid state ^{13}C NMR.

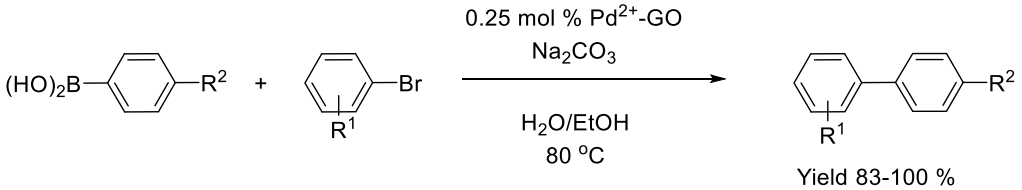

R^1= 4-OH, 3-OH, 4-OMe, 3-OMe, 4-CN, 4-CO_2H,4-CO_2Et, 4-NO_2, 3-CHO, heterocycle
R^2= OMe, H

Scheme II.B.1. *Chemically derived graphene (CDG)-Pd catalyzed Suzuki coupling reaction.*

Nagarkar *et al.* synthesized electrochemically deposited reduced graphene oxide and Pd catalyst (ERGO-Pd) for the efficient Suzuki and Heck C-C cross coupling reaction (Scheme II.B.2) [25]. The use of homogeneous palladium complexes has been restricted due to the problem of separation and their instability at elevated temperature. To overcome these major drawbacks, they developed a new GO-based heterogeneous catalyst and employed it in Suzuki and Heck reaction. They optimized the Suzuki coupling between aryl iodides/bromides and aryl boronic acids using K_2CO_3 base in ethanol solvent under refluxed condition. Whereas the optimized condition for the Heck reaction was achieved in DMF solvent in presence of Et_3N base at 120 ^oC temperature.

The high catalytic activity of ERGO-Pd in Suzuki and Heck reaction, attributed to the high dispersion of palladium NPs (PdNPs) on the ERGO support.

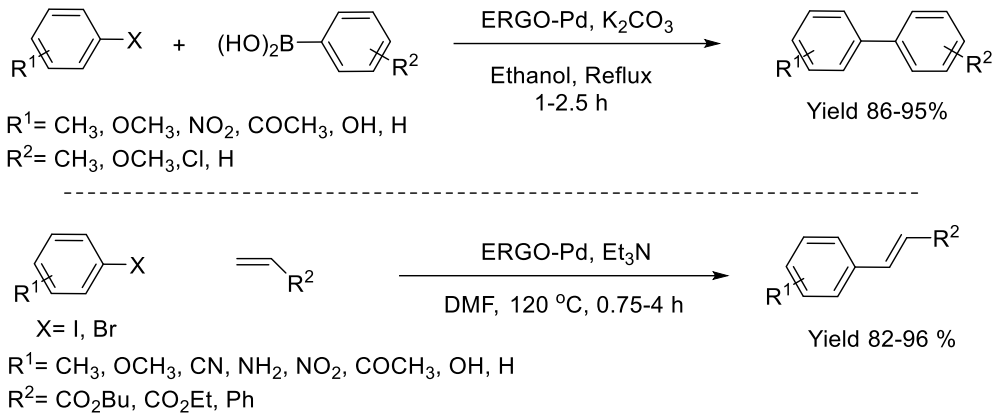

Scheme II.B.2. *Suzuki and Heck cross coupling reaction catalyzed by ERGO-Pd catalyst.*

In 2013, Kim *et al.* described the synthesis of the noble metal-graphene nanocomposites by reducing both noble metal and GO in hot water using ascorbic acid as reductant under hydrazine-free and surfactant free condition (Scheme II.B.3) [28]. During the synthesis of noble metal-graphene composite containing Pd, Pt, Ag and Au metal nanoparticles, complete reduction of metal salts and graphene oxide has been carried out by this procedure. Amongst them, Pd-graphene nanocomposite was utilized to catalyze the Suzuki-Miyaura coupling reaction with excellent product yield using K_2CO_3 as base at 90 ^oC temperature in presence of DMF solvent. This catalyst was recycled for many times without significant loss of the catalytic activity.

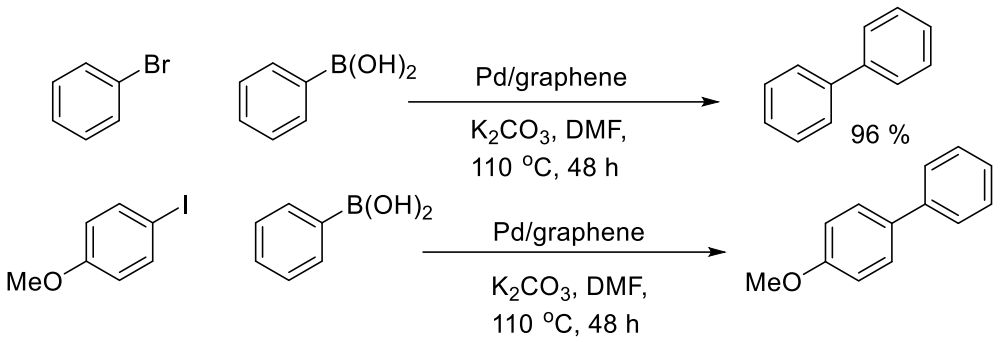

Scheme II.B.3. *Surfactant free Suzuki coupling reaction using Pd/graphene.*

In 2013, Nagarkar *et al.* synthesized Pd/nafion-graphene (Pd/Nf-G) catalyst from aqueous solution of Pd^{2+} ions by the electrochemical reduction followed by deposition on Nf-G support (Scheme II.B.4) [29]. The prepared catalyst was characterized by different spectroscopic techniques SEM, TEM, EDAX, XRD, TGA. The average size of the nanoparticle was maintained in the range of 4-12 nm. The high catalytic activity of this catalyst was observed for Suzuki coupling reaction using K_2CO_3 base, ethanol-water solvent at 80 °C temperature. This prepared catalyst was reused upto 5th cycle without loss of catalytic activity.

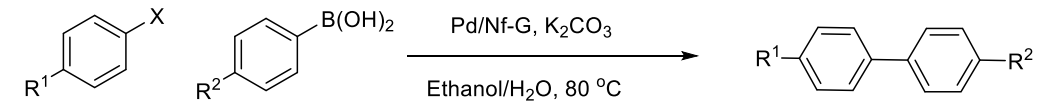

R^1= CH_3, OCH_3, NO_2, $COCH_3$, OH, H
R^2= CH_3, OCH_3, Cl, H
X= Cl, Br

Yield 88-95 %

Scheme II.B.4. *Synthesis of substituted biaryls using Pd/Nf-G catalyst.*

In 2014, Ghosh *et al.* described an efficient method for the synthesis of PdNPs supported on noncovalently functionalized graphene using 1-pyrene carboxylic acid (PCA-GNS-Pd). The catalytic activity of this novel PCA-GNS-Pd catalyst was observed in case of Suzuki and Heck cross coupling reaction in

water medium (Scheme II.B.5) [30]. The catalyst is highly stable in water due to its amphiphilic nature and it can be easily recovered and recycled up to five consecutive cycles. The electron rich and electron poor bromoarenes and chloroarenes are more challenging substrates but they exerted good yield of the desire alkenes and biphenyls using this catalyst.

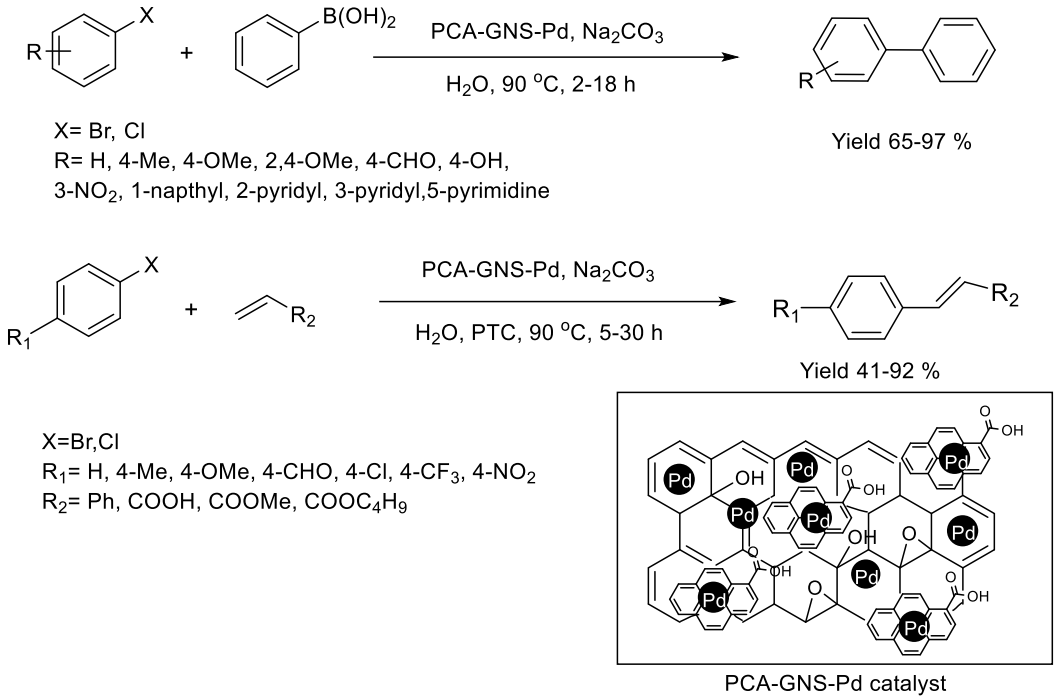

Scheme II.B.5. *Use of PCA-GNS-Pd catalyst in Suzuki and Heck coupling reaction.*

In 2016, Jain *et al.* designed a nanocomposite catalyst where PdNPs are dispersed on GO which is chemically modified with bidentate ligand containing N and S atoms (Scheme II.B.6) [31]. This synthesized graphene-ligand Pd complex (GL-Pd) with low weight % of Pd displayed excellent catalytic activity in Heck reaction between acrylates and arylhalides in presence of DMF/water solvent at 120 ^{o}C temperature. The structural analysis of GL-Pd hybrid was carried out using different spectroscopic techniques such as PXRD, FTIR,

Raman, XPS, SEM, TEM. The important feature of this prepared catalyst is its dispersibility in organic solvents which enables it to work effectively with a wide substrate scope.

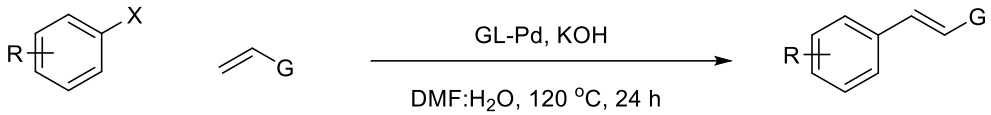

X= I, Br
R= H, 4-OMe, 2-OMe, 2-Me, 3-Me, 4-OAc, 4-CN
G= C_6H_5, 4-FC_6H_4, 4-*t*BuC_6H_4, 1-napthyl, 2-napthyl, CN, CO_2Me, CO_2Bu

Yield 73-97 %

Scheme II.B.6. *Suzuki coupling reaction catalyzed by GL-Pd hybrid catalyst.*

In 2018, Chen *et al.* discovered a biogenic method for the synthesis of PdNP modified reduced graphene oxide by using Ficus carica fruit juice as the efficient reducing agent. The catalyst PdNP/rGO has been applied as effective catalyst for Suzuki coupling reaction under both aerobic and aqueous condition (Scheme II.B.7) [32]. The catalyst was characterized by UV-Vis spectroscopy, Raman spectroscopy, XRD, TEM and FT-IR spectroscopy. The experimental results supported the spherical shape of PdNP/rGO and the dimension was estimated nearly 0.16 nm.

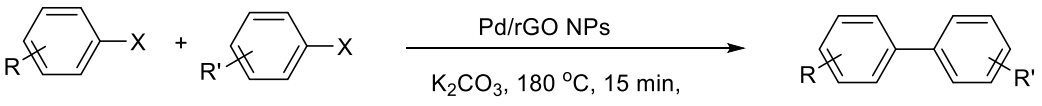

X- I, Br
R= H, 4-NO_2,4-CN, 4-OCH_3
R'= 2-CN, 3-Cl, 2,6-OCH_3, 3,4,5-OCH_3, 2,4-Cl

Yield 90-97 %

Scheme II.B.7. *PdNP/rGO for the synthesis of substituted biaryls.*

In 2020, Elhamifar *et al.* designed chemically modified graphene oxide supported Pd catalyst, through the coordination between $PdCl_2$ and 1,2-bis(4-aminophenylthio) ethane ligand (N_2S_2) which was grafted on the surface of GO

covalently (Scheme II.B.8). The catalytic activity of this prepared catalyst was observed in Suzuki coupling reaction between aryl halides and phenylboronic acids in presence of base K_2CO_3 in ethanol solvent [33]. This heterogeneous catalyst was characterized using different techniques XRD, FTIR, Raman, TEM, TGA. The catalyst was highly stable under reaction condition, recovered easily and reused upto several cycle without leaching of the active metal species.

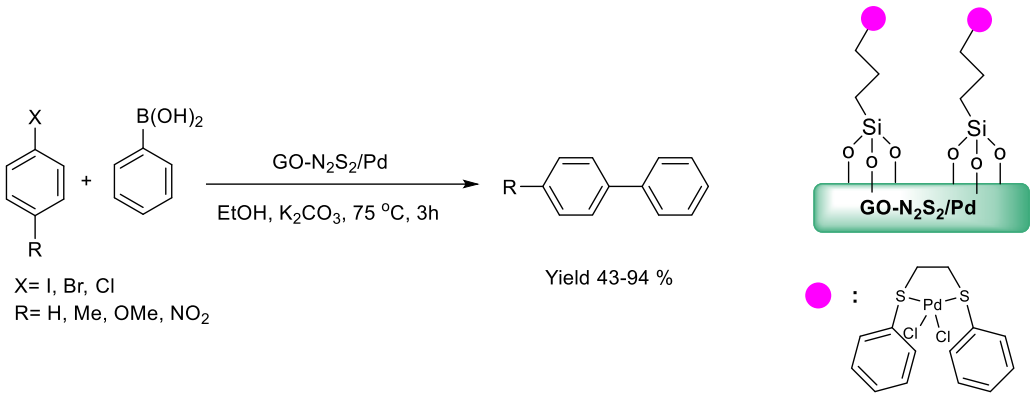

Scheme II.B.8. *GO-N_2S_2/Pd catalyzed Suzuki cross coupling reaction.*

II.B.3. Present Work: Result and Discussion

Preliminary studies on polymer supported GO has revealed significant increase in mechanical and thermal properties of the composite [34-37]. Driven by this fact, the idea of a new solid support automatically comes which allows better stability, easy recovery of products and simple separation procedure. Poly (methyl methacrylate) [PMMA] is a nonconductive polymer and its composite with GO enhances the thermal stability of the material. Based on the above perspective, our present explorative work involves the deposition of Pd NPs on GO-PMMA composite via in situ polymerization of MMA. Wielded by the environmental concern, water is selected as solvent instead of hazardous solvents such as DMF, DMA, NMP, etc. Utility of GO enhances the thermal

stability of poly (methyl methacrylate) [38, 39] and Pd NPs are strongly immobilized in between the layers of graphene oxide–PMMA composite [25, 29]. To the best of our knowledge, GO-PMMA supported Pd catalyst has not been employed in Suzuki and Heck coupling reactions (Scheme II.B.9). Simpler reaction conditions, ligand free protocol, low Pd content and tolerance to wide range of functional groups are the salient features of our work.

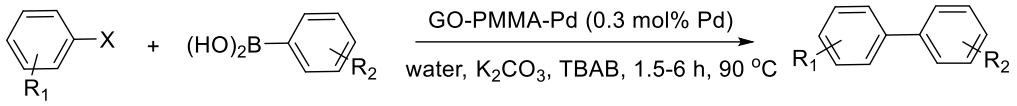

Yield (58-93 %)

R_1= 4-OMe, 3-OMe, 3-NO_2, 4-Me, 3-Me, 4-COMe, 4-OMe, Thienyl
R_2=H, 4-Me, 4-OMe, 3-NO_2
X= I, Br

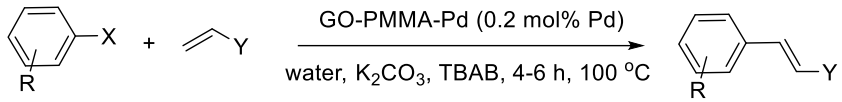

R= 4-OMe, 3-NO_2, 4-COMe
X= I, Br, Y= COOMe, COOEt, COOBu, Ph

Yield (79-90%)

Scheme II.B.9. *GO-PMMA-Pd(0) composite catalyzed Suzuki and Heck reaction.*

II.B.3.1. General procedure for preparation of GO-PMMA-supported Pd catalyst

Initially for the preparation of catalyst 20 mg of GO was suspended in 20 mL of toluene. The slurry was then dispersed through ultrasonication for 60 min. After ultrasonication methyl methacrylate was injected to well dispersed solution of GO. Benzoyl peroxide (BZP, 0.1 mol%) was added to initiate the polymerization of methyl methacrylate (MMA). The resulting mixture was then

stirred well at 90 ºC for 4 h. The temp of the solution was maintained at 90 ºC. Stirring was continued for another 3 h followed by the addition of 40 mg $Pd(OAc)_2$ and 100 mg of HCOOH as shown in Scheme II.B.10. The dark brown precipitate instantly turned into black after the addition of HCOOH. The obtained residue was washed several times with water and residual solvent was shuffled off by rotary evaporator, and dried at 60 ºC.

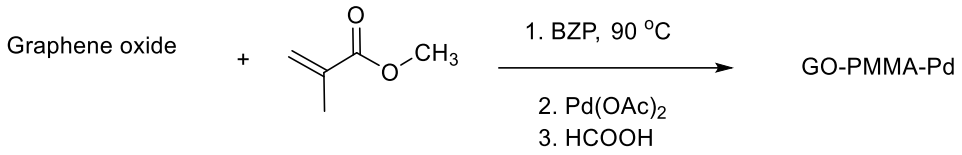

Scheme.II.B.10. *GO-PMM Preparation of GO-PMMA-Pd catalyst.*

II.B.3.2. Characterisation of GO-PMMA-Pd catalyst

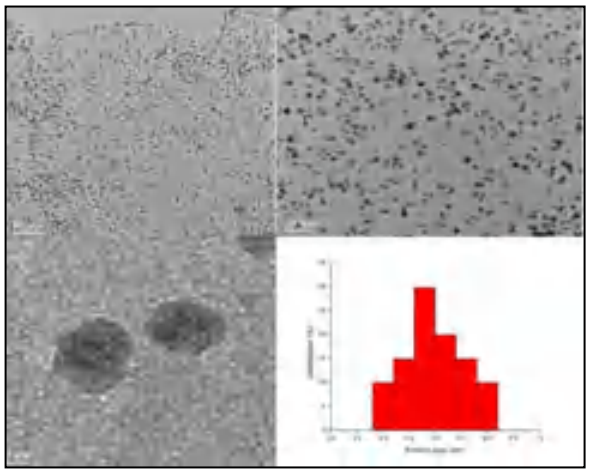

Figure II.B.1. *TEM image of GO-PMMA-Pd composite catalyst (a) at 50 nm (b) at 20 nm (c) at 2 nm (d) Particle size distribution curve of GO-PMMA-Pd catalyst.*

The morphology of the catalyst (GO-PMMA-Pd) was analyzed by Transmission Electron Microscope. The micrograph and particle size distribution curve of in situ prepared GO-PMMA-Pd catalyst is represented in Figure II.B.1. The TEM images show the mono dispersed palladium without agglomeration on the GO-PMMA-sheet during in situ polymerisation of MMA. The average size of the Pd NPs has been determined from the TEM images and was found to be around 4.8 nm.

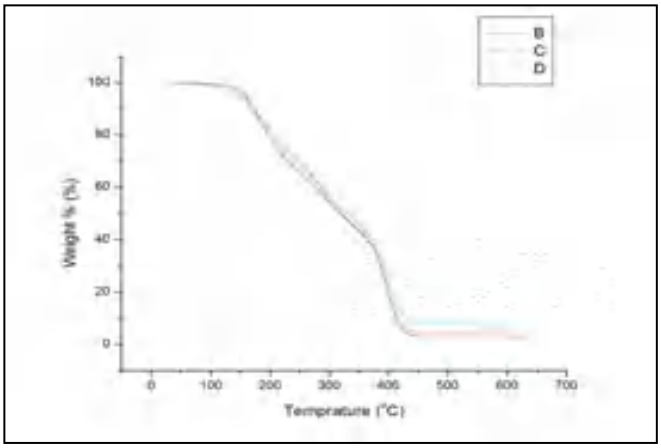

Figure II.B.2. *TGA results of (B) 2wt% (C) 5wt% (D) 10wt% GO in PMMA.*

The catalyst life is a factor that can control the economic viability of industrial processes and as a consequence high thermal resistance of a catalyst support is found to be suitable for different kinds of thermal reaction [40]. In view of the above, thermogravimetric Analysis (TGA) of the solid support has been analyzed for several samples with different wt % of GO loading as shown in Figure II.B.2. It is very interesting to observe that composite with the lowest wt % of GO exhibited maximum thermal stability (Figure II.B.2.).

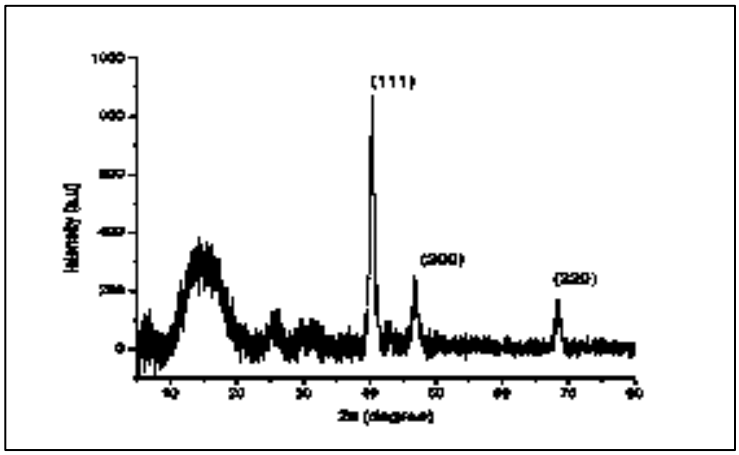

Figure II.B.3. *XRD pattern of GO-PMMA-Pd composite catalyst.*

The catalyst was subjected to powder X-ray diffraction (XRD) for composition analysis (Figure II.B.3). Three sharp peaks at around 2Θ 40.1°, 46.6° and 68.9° represents the crystalline planes (111), (200) and (220) respectively in fcc structure of Pd [38]. However the intensity of (111) plane is higher than (200) and (220) plane. The absence of strong GO peak at 2Θ= 10.63° [41] and the appearance of characteristic broad PMMA peak at 2Θ= 14.8° indicated the formation of GO-polymer composite. The FTIR spectrum of GO has a peak at 1735 cm^{-1} which is assigned to the carbonyl stretching frequency. The FT-IR peak of PMMA at 1148 cm^{-1} is associated with the stretching vibration of the C-O bond in the C-O-C moiety whereas the peak at 1731 cm^{-1} is due to the acrylate carbonyl groups. FT-IR spectrum (Figure II.B.4) revealed that the resultant GO-PMMA-Pd composite catalyst contained several functional groups like –OH (3454 cm^{-1}) and C=O (1731 cm^{-1}). Therefore, it has a strong tendency to readily interact with metal ions by hydroxyl and carboxyl group.

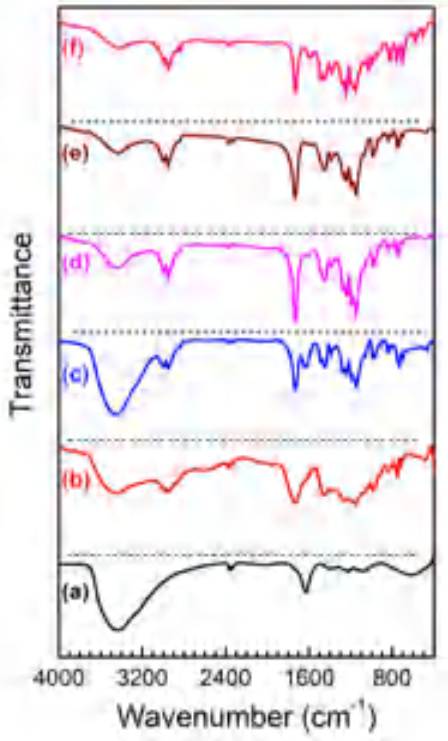

Figure II.B.4. *Comparison of FT-IR spectra of (a) GO (b) GO-PMMA (c) GO-PMMA-Pd (d) PMMA-Pd (e) PMMA and (f) recycled catalyst after fifth run.*

It is considered that the bond between Pd and GO-PMMA can be formed through some physical / chemical interactions such as Vander Waals force, H-bonding and other bonds [42]. The shift of other stretching frequencies also points towards the association of PMMA with GO (Figure II.B.4). Furthermore, a hump obtained at around $2\Theta = 23^{o}$ suggests the presence of reduced graphene oxide (rGO) (Figure II. B.3) [43]. Hence, it can be concluded that a small amount of GO has been converted into rGO when HCOOH was employed. GO-PMMA-Pd catalyst was further characterized by XPS, as shown in Figure II.B.5. High-resolution XPS spectrum was corrected with reference to the carbon 1s peak at 284.8 eV shown in figure 5 (b). The binding energies of Pd 3d at 335.87

and 341.2 eV for GO-PMMA-Pd corresponded to the Pd^0 Pd $3d_{5/2}$ and Pd $3d_{3/2}$, respectively. Thus the presence of metallic Pd in the composite is confirmed [Figure II.B.5 (c)].

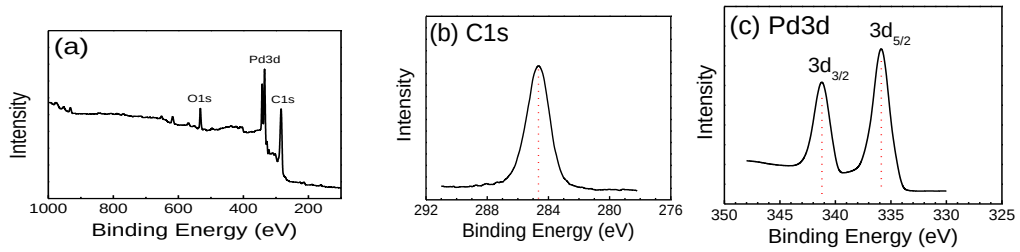

Figure II.B.5. *(a) Full-range XPS spectrum of GO-PMMA-Pd catalyst. C 1s peak at 284.8 eV shown in (b). In (c) the binding energies of Pd 3d at 335.87 and 341.2 eV for GO-PMMA-Pd corresponded to the Pd^0 Pd $3d_{5/2}$ and Pd $3d_{3/2}$, respectively.*

II.B.3.3. Catalytic activity of GO-PMMA-Pd catalyst in Suzuki and Heck cross coupling reaction

The development of recoverable catalyst is one of the indispensable principles of the green synthetic organic chemistry and the key purpose of this study was to place a recyclable catalyst for Suzuki and Heck reaction in aqueous medium. Initially, for screening the reaction, phenylboronic acid and 4-iodo anisole has been chosen as the model substrates in presence of GO-PMMA-Pd catalyst. The favorable condition of the reaction was achieved by varying the parameters such as catalyst loading, solvent, time, base and temperature. Finally the protocol was optimized by using water as solvent, K_2CO_3 as base and catalyst loading (0.3 mol % Pd) in 6 mg of GO-PMMA-Pd catalyst at 90 ^oC (Table II.B.1). In order to enhance the yield of 4-methoxy-1,1′ biphenyl in water,

different surfactants were employed in the study (Table II.B.1). It is established that the yield of the product can be improved by increasing the reaction time. We started increasing the reaction time by keeping all parameters similar and found that the best yield is achieved in 4 hrs of reaction (Table II.B.1, entry 6). However, ortho-substituted compounds require longer reaction time.

Table II.B.1. Optimization of reaction parameters for Suzuki reaction based on the result of the following combination in the protocol[a]

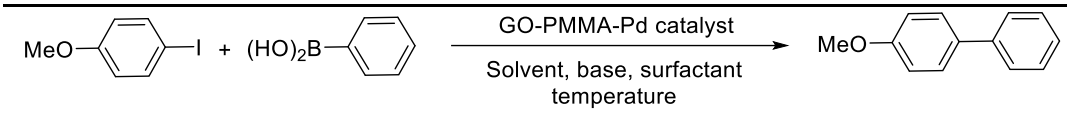

Entry	Solvent	Base	Pd loading (mol%)	Additive	Time (h)	Yield (%)[b]
1	DMF	K_2CO_3	0.1	Bu_4NBr	1	42
2	DMSO	K_2CO_3	0.1	Bu_4NBr	2	29
3	Water	K_2CO_3	0.2	Bu_4NBr	3	63
4	Ethanol	K_2CO_3	0.2	Bu_4NBr	3	58
5	Water	K_2CO_3	0.3	SDS	4	72
6	**Water**	**K_2CO_3**	**0.3**	**Bu_4NBr**	**4**	**90**
7	Water	Na_2CO_3	0.3	Bu_4NBr	6	76
8	Water	Cs_2CO_3	0.3	Bu_4NBr	6	75
9	Water	Et_3N	0.3	Bu_4NBr	6	78
10	Water	KOH	0.3	Bu_4NBr	4	62
11	Water	K_2CO_3	0.3	CTAB	6	72

12	Water	K_2CO_3	0.3	TMAI	4	52
13	Water	K_2CO_3	0.3	Bu_4NBr	24	25[c]
14	Water	K_2CO_3	0.5	Bu_4NBr	12	86[d]

[a]Reaction of 4-Iodo anisole (1 mmol), Phenyl boronic acid (1.5 mmol), Pd loading (0.3 mol%), K_2CO_3 (1 mmol), TBAB (10 mol%), water (2 mL) at 90 ^oC.

[b]Isolated yields.

[c] Room temperature reaction.

[d]Temp of the reaction 100 ^oC.

The synthetic efficacy of this catalyst in water mediated Suzuki coupling reaction was conducted with a number of different aryl halides and arylboronic acids under optimized condition. The electron withdrawing aryl iodides and bromides gave excellent yields of corresponding products. Although relatively longer reaction time was required for electron donating aryl iodides and bromides but each of them offered an excellent yield of products (Table II.B.2). The aryl chlorides gave only trace amount of the corresponding product even after 24 h of exertion of reaction (Table II.B.2, entry 14). The arylboronic acids with methoxy, methyl, nitro groups were rapidly converted to their corresponding products at high to moderate yield at 90 ^oC.

Table II.B.2. GO-PMMA-Pd catalyzed Suzuki reaction of different aryl halides with phenyl boronic acid[a]

Entry	Aryl halide	Boronic acid	Product	Time (h)	Yield (%)[b]

1	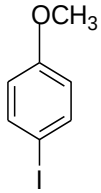	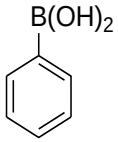	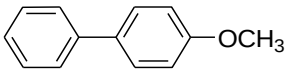	4	90
2	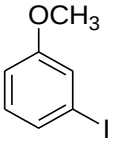	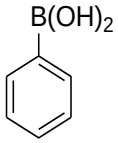	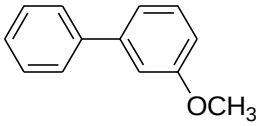	4	88
3	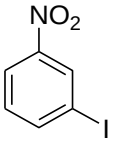	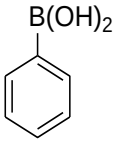	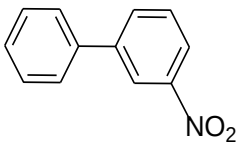	2	92
4	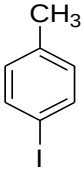	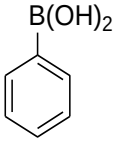	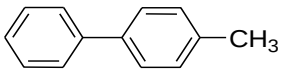	6	86
5	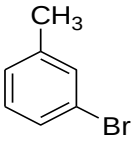	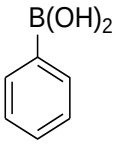	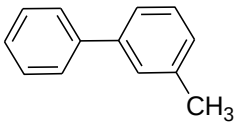	6	84
6	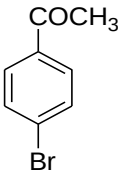	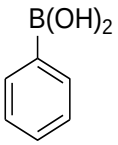	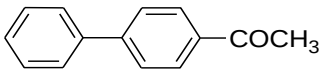	1.5	93

7	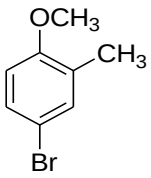	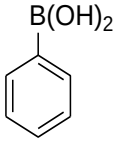	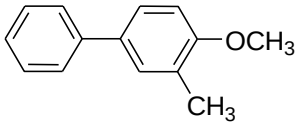	4	85
8	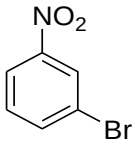	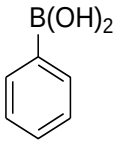	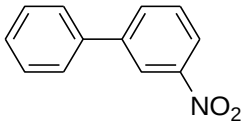	3	89
9	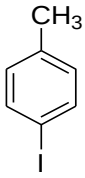	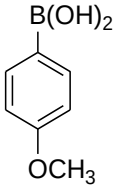	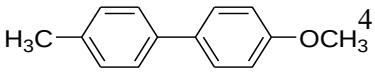	4	86
10	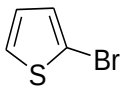	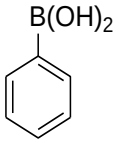	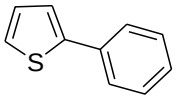	6	58
11	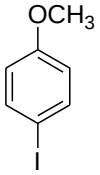	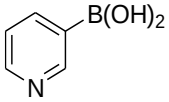	No reaction	-	Nil
12	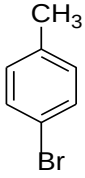	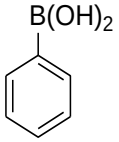	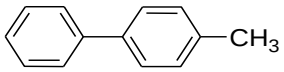	6	79

13	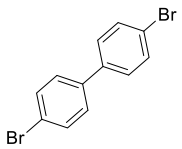		No reaction	-	Nil
14	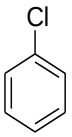	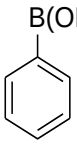	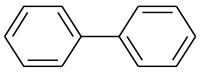	24	35[c]
15	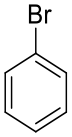	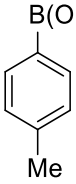	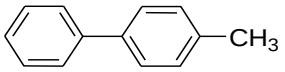	4	88
16	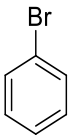	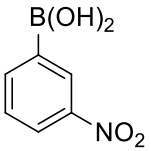	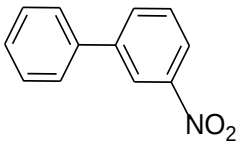	4	71

[a]Reaction of Aryl halide (1 mmol), Phenyl boronic acid (1.5 mmol), palladium loading (0.3 mol%), K_2CO_3 (1 mmol), TBAB (10 mol%), water (2 mL) at 90 °C.

[b]Isolated yields.

[c]Reaction temperature 120 °C

The above success in Suzuki coupling reaction prompted us to look for such expectancy in Heck coupling reaction too. The Heck reaction was optimized by varying the reaction parameters temperature, solvent, base, catalyst loading (Table II.B.3). In that instance, 4-iodo anisole was successfully coupled with methyl acrylate in presence of TBAB and 0.2 mol% Pd in GO-PMMA-Pd catalyst at 100 °C (Table II.B.3, entry 4). All types of aryl halides gave good to excellent yield which indicates the high efficiency of this heterogeneous catalyst (Table II.B.4) in Heck coupling too.

Table II.B.3. Optimization of reaction parameters of Heck reaction[a]

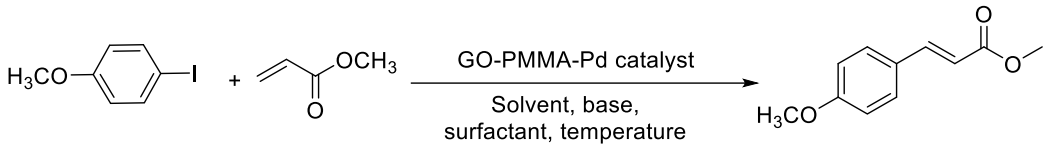

Entry	Solvent	Base	Temp (°C)	Pd-loading (mol%)	Time (h)	Yield(%)[b]
1	DMF	K_2CO_3	120	0.1	4	75[c]
2	Water	K_2CO_3	100	0.1	5	72
3	Water	Et_3N[d]	100	0.2	5	80
4	**Water**	**K_2CO_3**	**100**	**0.2**	**4**	**85**
5	Water	K_2CO_3	80	0.3	5	78
6	Water	K_2CO_3	rt	0.3	24	25[e]

[a]Reaction of 4-Iodo anisole(1 mmol), methyl acrylate (2 mmol), Pd loading (0.2 mol%), K_2CO_3 (1 mmol), TBAB (10 mol%), water 3 mL.

[b]Isolated yields.

[c]Solvent was DMF.

[d]Triethyl amine was used as base.

[e]Room temperature.

Table II.B.4. Reaction of aryl halides with different vinyl compounds[a]

Entry	Aryl halides	Olefins	Product	Time (h)	Yield (%)[b]

1	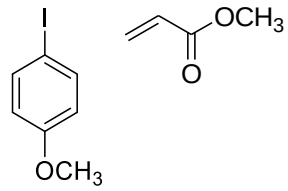		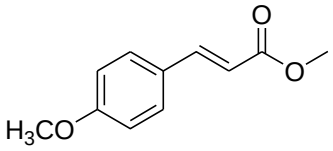	4	85
2	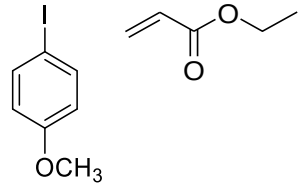		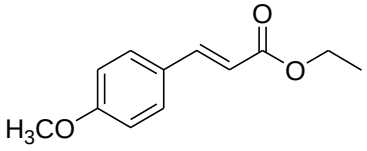	4	83
3	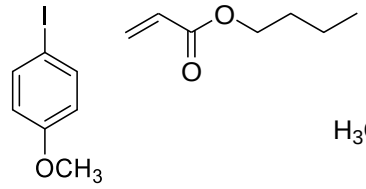		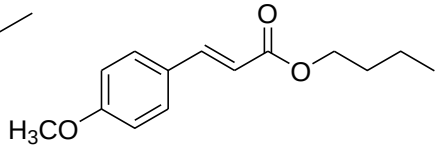	6	84
4	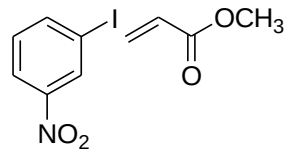		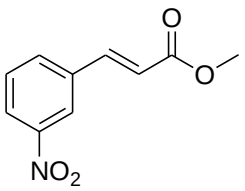	4	88
5	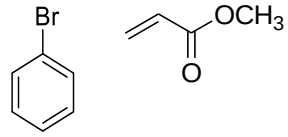		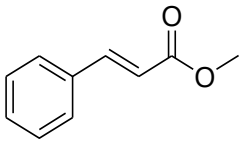	5	90
6	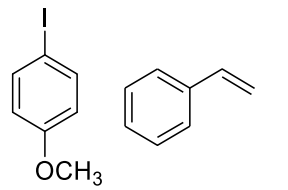		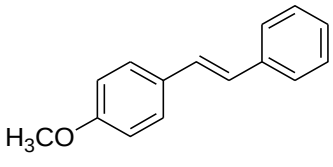	5	79

7	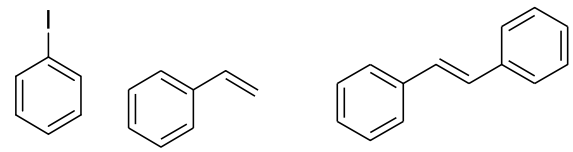		4	80
8	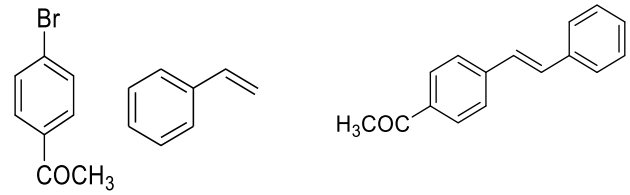		4	84

[a]Reaction of aryl halide (1 mmol), vinyl compound (2 mmol), GO-PMMA-Pd catalyst (0.2 mol%), K_2CO3 (1 mmol), TBAB (10 mol%), water 3 mL.

[b]Isolated yields.

The reduction of yield after 5th run of Suzuki coupling reaction (Figure II.B.6) could be due to the leaching of Pd NPs from GO-PMMA surface. The palladium content after 5th run was confirmed by ICP-AES and it was found to be 1.357 wt%. However, when the reaction was performed with only PMMA-Pd^0, a drastic change in yield was observed from 88% to 56% in 2nd run. This observation clearly indicated that presence of GO in the composite plays a vital role to improve the catalytic ability of GO-PMMA-Pd system.

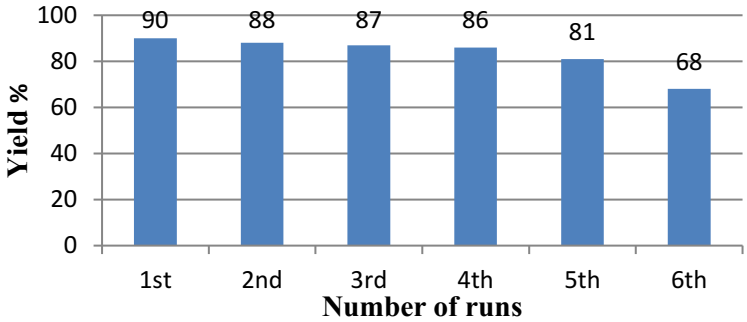

Figure II.B.6. *Recycling efficiencies of GO-PMMA-Pd catalyst for Suzuki coupling reaction.*

Leaching of metal from the heterogeneous GO-PMMA support was examined by hot filtration test as described in the literature [44]. After 1 h completion of reaction, the reaction mixture was filtered to separate out the catalyst and HPLC was carried out with the obtained filtrate (38 % conversion). The ICP-AES analysis of the filtrate showed the absence of any palladium. The filtrate was then heated for another 4 hrs at 90 ^{o}C without the addition of catalyst and the corresponding HPLC pattern did not show any noticeable conversion which implied that metals are not getting leached from the solid GO-PMMA support during 1st 1 h of the reaction (Figure II.B.7).

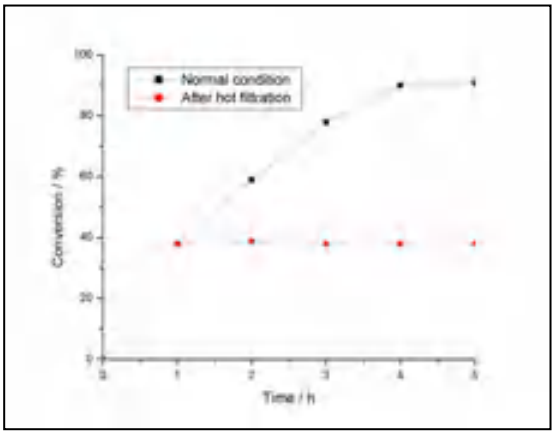

Figure II.B.7. *Comparison of normal time profile with hot filtration test. Conversions (±2%) at different time intervals for each plot were measured by HPLC.*

The Pd content was found to be 5.559 wt% in this heterogeneous catalyst. The recyclability of the catalyst was tested for Suzuki coupling reaction and the catalyst was recyclable for five consecutive runs without significant drop in activity. The sudden drop in yield (Figure II.B.6.) after the fifth run may be attributed to the leaching of Pd from the catalyst.

II.B.4. Conclusion

A greener protocol using ligand free GO-PMMA-Pd catalyst is proposed. The prepared catalyst was characterized by different spectroscopic and microscopic techniques. The newly made catalyst effectively generates different C-C cross coupled product even at a very low Pd content in high yields at optimal condition. The simple operational procedure, easy removal of catalyst, reusability of the catalyst and environmentally benign process are the most significant and outwit factors of our proposed scheme in comparison to the existing protocols.

II.B.5. Experimental Section

II.B.5.1. General Information

Palladium (II) acetate 99.98% was purchased from Sigma Aldrich. Graphite powder, H_2O_2 (solution 30%), 98.5% pure methyl methacrylate were purchased from commercial supplier. The morphology of the catalyst (GO-PMMA-Pd) was analyzed by Transmission Electron Microscope (TEM, Model: JEM-2100, accelerating voltages 60-200 KV in 50 V steps; resolution: 1.9Å to 1.4Å). Inductively coupled plasma spectroscopy (ICP) was analysed on ARCOS, Simultaneous ICP spectrometer (SPECTRO analytical instruments GmbH, Germany). Powder XRD data and X-ray photoelectron spectroscopy (XPS) was obtained from Bruker D8 Advanced X-ray Powder Diffractometer (Cu Kα radiation, λ = 1.54 Å) and an XPS instrument (Omicron: Serial no. 0571). NMR spectra were taken in $CDCl_3$ using a Bruker AV–300 spectrometer operating for ^1H at 300 MHz and for ^{13}C at 75 MHz. Splitting patterns of protons were described as s (singlet), d (doublet), t (triplet), br (broad) and m (multiplet).

Chemical shifts were reported in parts per million (ppm) relative to TMS as internal standard.

II.B.5.2. Procedure for cross coupling of 4-iodo anisole and phenyl boronic acid using GO-PMMA-Pd catalyst

A 25 mL RB was charged with 4-iodo anisole (1.0 mmol), phenylboronic acid (1.5 mmol), GO-PMMA-Pd catalyst (0.3 mol % Pd), K_2CO_3 (1 mmol), TBAB (10 mol %) and 2 mL water. The mixture was allowed to stir at 90 oC for an appropriate time (Table II.B.1) and the extent of the reaction was monitored by thin layer chromatography (TLC). After the completion of the reaction, the reaction mixture was extracted by ethyl acetate (2×25 ml) and washed with water repeatedly. The catalyst was filtered off and washed several times with ether and water (1:1) until no significant product was obtained in the wash. The recovered catalyst was reused for the next coupling experiment. The reaction mixture was dried over anhydrous Na_2SO_4, concentrated in vacuum and purified by column chromatography on silica gel 60-120 mesh using petroleum ether as eluent to obtain pure product. The catalyst recovered after 5th run was subjected to ICP-AES for Pd content analysis. The isolated products were analysed by ^1H NMR and ^{13}C NMR spectroscopy.

II.B.5.3. General procedures for the Heck coupling reactions

A mixture of 4-iodo anisole (1 mmol), methyl acrylate (2 mmol), GO-PMMA-Pd catalyst (0.2 mol % Pd), K_2CO_3 (1 mmol), TBAB (10 mol %) and 3ml water was stirred under 100 ^oC. The reaction took significant time for completion (Table II.B.3) and the progress of the reaction was monitored by TLC. After completion, the reaction mixture was extracted with ethyl acetate and washed with water repeatedly. The combined organic mixture was dried over anhydrous

Na_2SO_4 and purified by column chromatography using petroleum ether/ethyl acetate as eluent to afford pure product. The catalyst was separated and washed for several times with ether and water. The recovered catalyst was used in next cycles and the isolated products were characterized by ^1H and ^{13}C NMR spectroscopy.

II.B.5.4. Spectroscopic data of the products

4-methoxy-1,1′ biphenyl (Table II.B.2, entry 1) [45, 46]

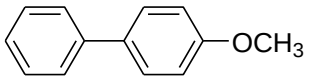

^1H NMR (300 MHz, $CDCl_3$) δ (ppm) 3.85 (s, 3H), 6.98 (d, 2H, *J* = 6.9 Hz), 7.24-7.32 (1H, m), 7.39 (d, 2H, *J* = 7.8Hz), 7.51-7.56 (m, 4H, *J* = 8.7 Hz);

^{13}C NMR (75 MHz, $CDCl_3$) δ (ppm) 55.37, 114.22, 126.68, 126.76, 128.18, 128.75, 133.80, 140.85,159.16.

3-methoxy-1,1′-biphenyl (Table II.B.2, entry 2) [45, 46]

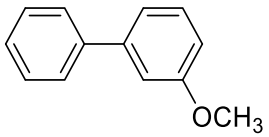

^1H NMR (300 MHz, $CDCl_3$) δ (ppm) 3.84 (s, 3H), 6.89 (d, *J* = 8.1 Hz, 1H), 7.12-7.18 (m, 2H), 7.31-7.36 (m, 2H), 7.39-7.44 (m, 2H), 7.58 (d, *J* = 8.1 Hz, 2H);

^{13}C NMR (75 MHz, $CDCl_3$) δ (ppm) 55.33, 112.72, 112.95, 119.74, 127.25, 127.47, 128.79, 129.81, 141.15, 142.82, 159.89.

3-nitro-1,1'-biphenyl (Table II.B.2, entry 3) [45, 46]

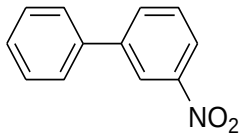

^{1}H NMR ($CDCl_3$, 300MHz) δ 8.41 (s, 1H), 8.15 (s,1H), 7.87 (s,1H), 7.41-7.59 (m, 7H, *J* = 8.4Hz);

^{13}C NMR (75 MHz, $CDCl_3$) δ (ppm) 121.93, 122.04, 127.17, 128.58, 129.20, 129.70, 133.06, 138.65, 142.86, 148.74.

4-methyl-1,1′-biphenyl (Table II.B.2, entry 4) [45, 46]

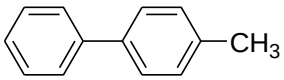

^{1}H NMR (300 MHz, $CDCl_3$) δ (ppm) 2.174 (s, 3H), 6.95-6.99 (d, 2H, *J* = 6.9Hz), 7.23-7.31(m, 1H), 7.38-7.51 (m, 2H), 7.52-7.56 (q, 4H);

^{13}C NMR (75 MHz, $CDCl_3$) δ (ppm) 21.12, 122.00, 127.01, 128.74, 129.20, 129.50, 133.07.

3-methyl 1,1'-biphenyl (Table II.B.2, entry 5) [52]

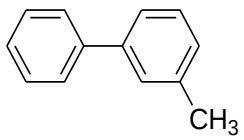

^{1}H NMR (300 MHz, $CDCl_3$) δ (ppm) 2.39 (s, 3H), 6.88 (d, *J* = 8.1Hz, 1H), 7.13-7.19(m, 2H), 7.31-7.36 (m, 2H), 7.42-7.44 (m, 2H), 7.59 (d, *J* = 8.1Hz, 2H);

^{13}C NMR (75 MHz, $CDCl_3$) δ (ppm) 26.68, 124.30, 127.20, 127.28, 128.02, 128.69, 128.78, 138.35, 141.26, 141.37.

4-acetyl 1,1'-biphenyl (Table II.B.2, entry 6) [47]

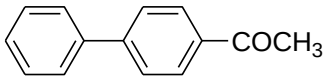

^{1}H NMR (300 MHz, $CDCl_3$) δ (ppm) 2.68 (s, 3H), 7.39-7.49 (m, 3H, *J* = 7.5Hz), 7.61-7.68 (m, 4H, *J* = 7.2Hz), 8.00 (d, 2H, *J* = 8.1Hz);

^{13}C NMR (75 MHz, $CDCl_3$) δ (ppm) 26.68, 127.24, 127.29, 128.26, 128.94, 128.98, 135.86, 139.87, 145.79, 197.80.

4-methoxy-3-methyl-1,1'-biphenyl (Table II.B.2, entry 7) [47]

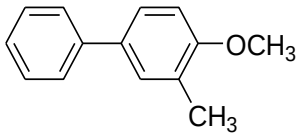

^{1}H NMR (300 MHz, $CDCl_3$) δ (ppm) 2.28 (s, 3H), 3.86 (s, 3H), 7.17 (s, 1H), 6.81(s, 1H), 7.39 (t, 4H), 7.55 (t, 2H);

^{13}C NMR (75 MHz, $CDCl_3$) δ (ppm) 16.43, 55.45, 110.17, 126.40, 126.55, 126.78, 126.91, 128.69, 129.52, 133.36, 141.07, 157.39.

4-methyl-4'-methoxy-1,1'-biphenyl (Table II.B.2, entry 9) [45, 47]

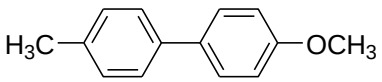

^{1}H NMR (300 MHz, $CDCl_3$) δ (ppm) 2.39 (s,3H), 3.84 (s, 3H), 6.97 (d, 2H, *J* =7.5Hz), 7.23 (d, 2H, *J* = 8.4Hz), 7.44-7.55 (m, 4H);

^{13}C NMR (75 MHz, $CDCl_3$) δ (ppm) 24.25, 58.52, 117.34, 129.77, 131.14, 132.64, 136.92, 139.55, 141.14, 162.10.

2-phenylthiophene (Table II.B.2, entry 10) [46, 47]

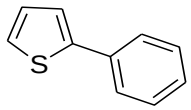

^{13}C NMR (75 MHz, $CDCl_3$) δ (ppm) 118.98, 126.24, 127.97, 129.06, 130.63, 131.21, 132.06, 137.51.

(*E*)-methyl 3-(3-nitrophenyl) acrylate (Table II.B.4, entry 4) [50]

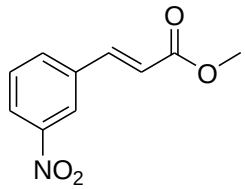

^{1}H NMR (300 MHz, $CDCl_3$) δ (ppm) 3.84 (s, 3H), 6.57 (d, *J* = 15.9 Hz), 7.57-7.84 (m, 3H), 8.24 (d, 1H, *J* = 8.1 Hz), 8.38 (s, 1H);

^{13}C NMR (75 MHz, $CDCl_3$) δ (ppm) 55.18, 124.10, 125.58, 127.70, 133.12, 136.78, 139.24, 145.12, 151.81, 169.73.

(*E*)-methyl 3-(4-methoxyphenyl) acrylate (Table II.B.4, entry 1) [49]

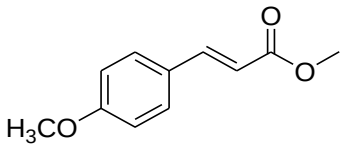

^{1}H NMR (300 MHz, $CDCl_3$) δ (ppm) 3.68 (s, 1H), 3.77 (s, 1H), 6.47 (d, 1H, *J* = 15.9Hz), 6.95 (d, 2H, *J* = 8.7Hz), 7.65 (d, 3H, *J* = 8.8Hz);

^{13}C NMR (75 MHz, $CDCl_3$) δ (ppm) 51.27, 55.29, 114.33, 115.03, 126.57, 130.13, 144.31, 161.11, 166.91.

(*E*)-ethyl 3-(4-methoxyphenyl) acrylate (Table II.B.4, entry 2) [47, 49]

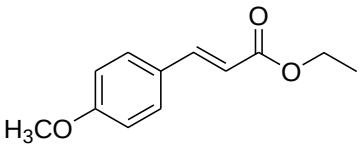

^{1}H NMR ($CDCl_3$, 300 MHz) δ 0.98-1.02 (t, 3H), 3.47 (s, 1H), 4.13-4.17 (q, 2H), 6.43 (d, 1H, *J* =16.2 Hz), 6.92-6.95 (d, 2H, *J* = 8.4Hz), 7.58-7.62 (m,3H);

^{13}C NMR (75 MHz, $CDCl_3$) δ (ppm) 14.06, 55.08, 59.71, 114.21, 115.30, 116.53, 126.58, 129.92, 137.84, 144.00, 161.04, 166.39.

(*E*)-butyl 3-(4-methoxyphenyl) acrylate (Table II.B.4, entry 3) [51]

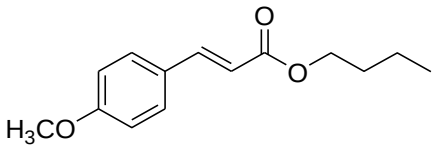

^{1}H NMR (300 MHz, $CDCl_3$) δ (ppm) 1.00 (t, 3H, *J* = 6.6Hz), 1.44 (m, 2H), 1.69 (m, 2H), 3.80 (s, 3H), 4.16-4.23 (t, 2H, *J* = 6.6Hz), 6.89 (2H, d, *J* = 8.7Hz), 7.63 (d, 1H, *J* = 16.2Hz), 7.47 (t, 3H);

^{13}C NMR (75 MHz, $CDCl_3$) δ (ppm) 16.90, 22.35, 33.96, 58.43, 67.37, 117.42, 118.85, 130.30, 132.81, 147.34, 164.46, 170.54.

1-(4-styrylphenyl)ethanone (Table II.B.4, entry 8) [47]

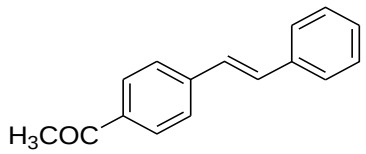

^{1}H NMR (300 MHz, $CDCl_3$) δ (ppm) 2.55 (s, 3H), 7.08-7.19 (m, 2H), 7.21 (d, 1H, *J* = 16.8Hz), 7.29-7.58 (m, 5H), 7.97 (d, 2H, *J* = 8.4Hz);

^{13}C NMR (75 MHz, $CDCl_3$) δ (ppm) 29.79, 129.70, 130.02, 130.62, 131.52, 132.00, 132.08, 134.65, 139.12, 139.87, 145.19, 200.71.

II.B.5.5. Scanned copies of ^{1}H and ^{13}C NMR spectra of synthesised compounds.

Figure II.B.8. *Scanned copy of ^{1}H and ^{13}C NMR spectra of 4-methoxy-1,1′ biphenyl.l*

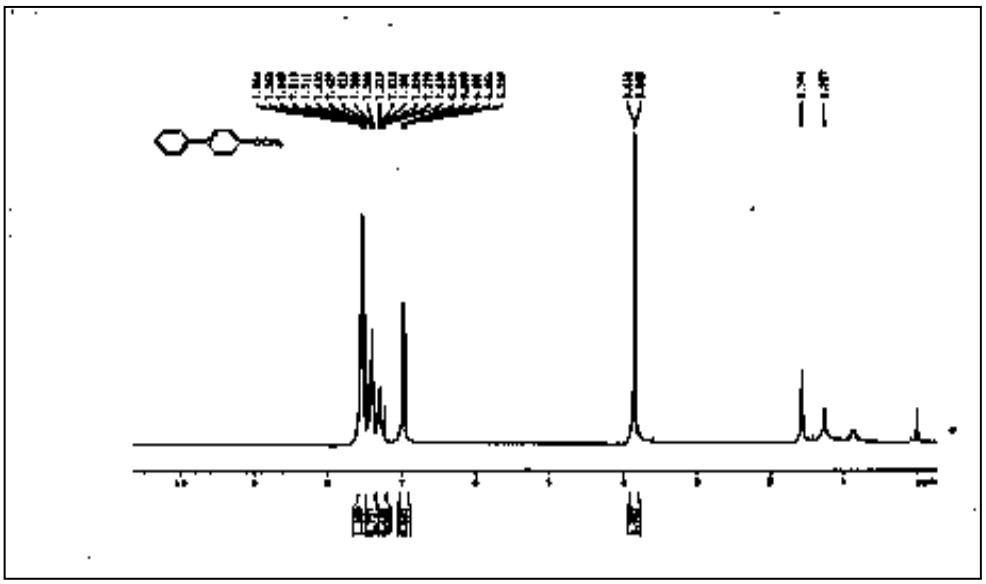

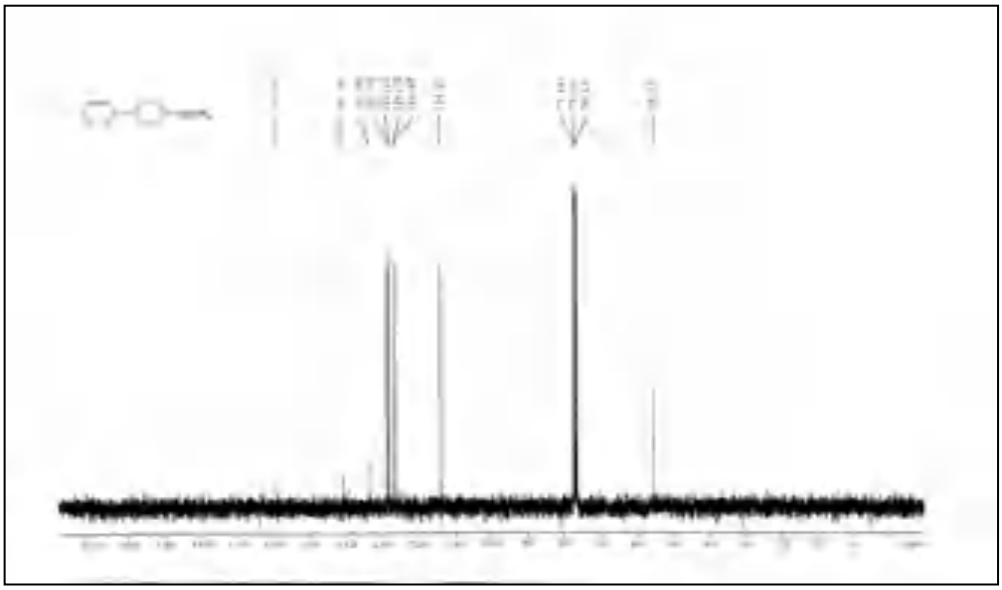

Figure II.B.9. *Scanned copy of ^{1}H and ^{13}C NMR spectra of 3-methoxy-1,1′-biphenyl.*

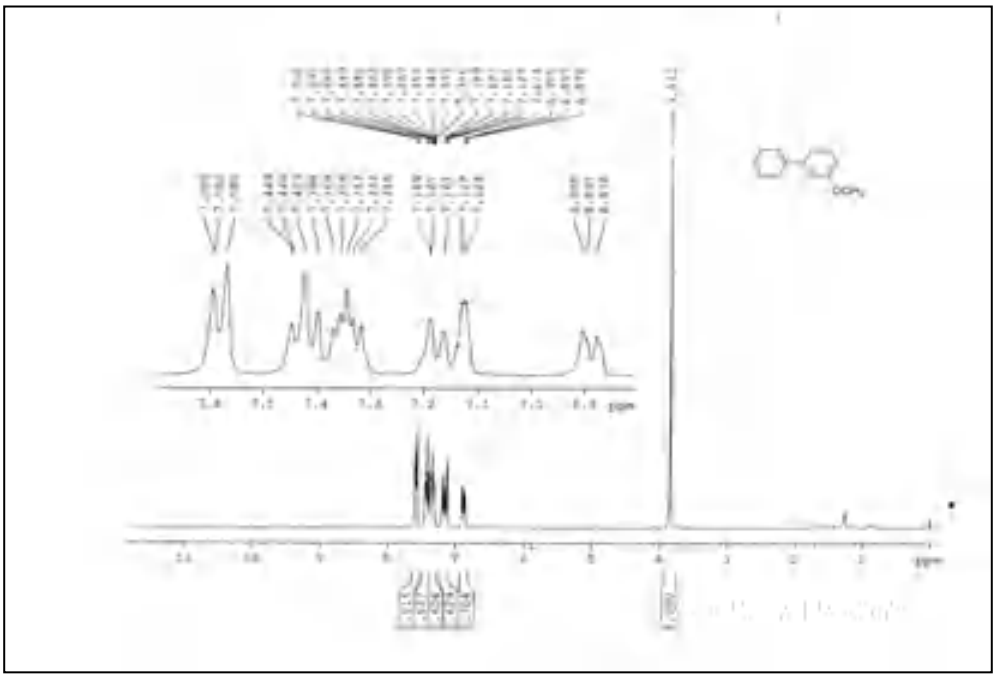

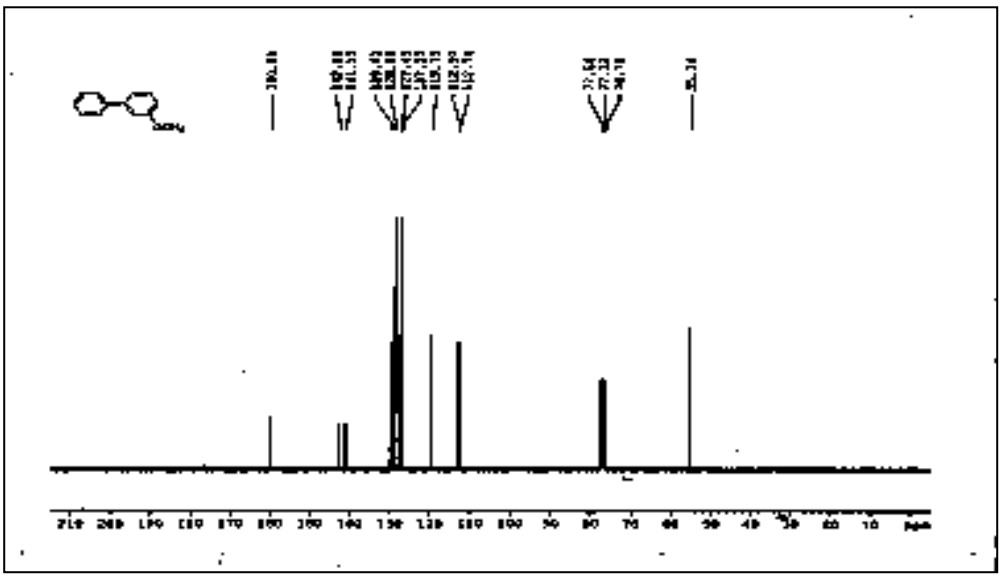

Figure II.B.10. *Scanned copy of ^{1}H and ^{13}C NMR spectra of 3-nitro-1,1'-biphenyl.*

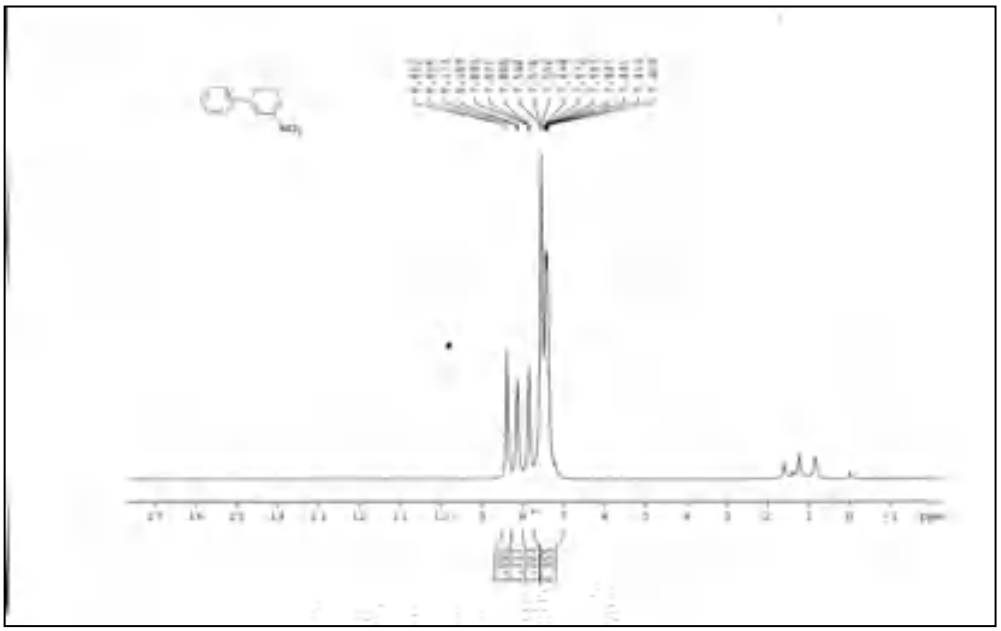

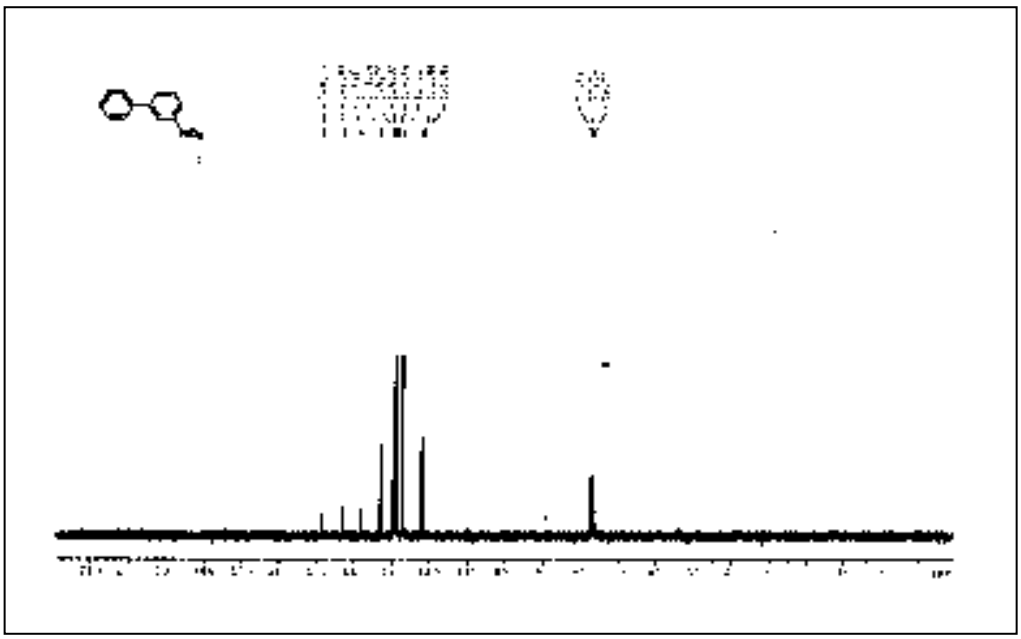

Figure II.B.11. *Scanned copy of ^{1}H and ^{13}C NMR spectra of 4-methyl-1,1′-biphenyl.*

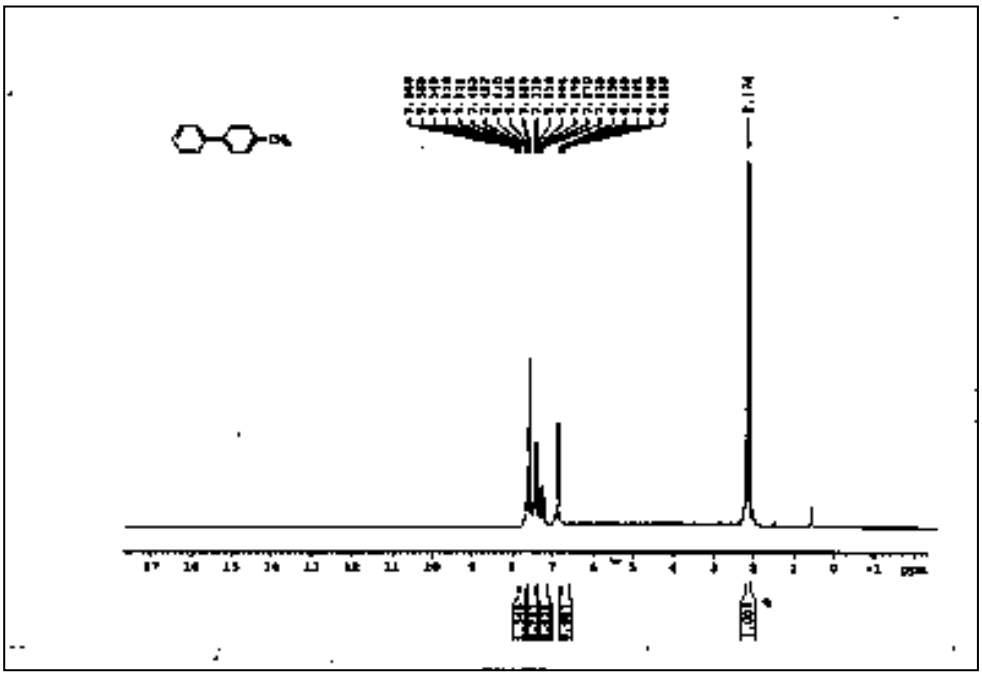

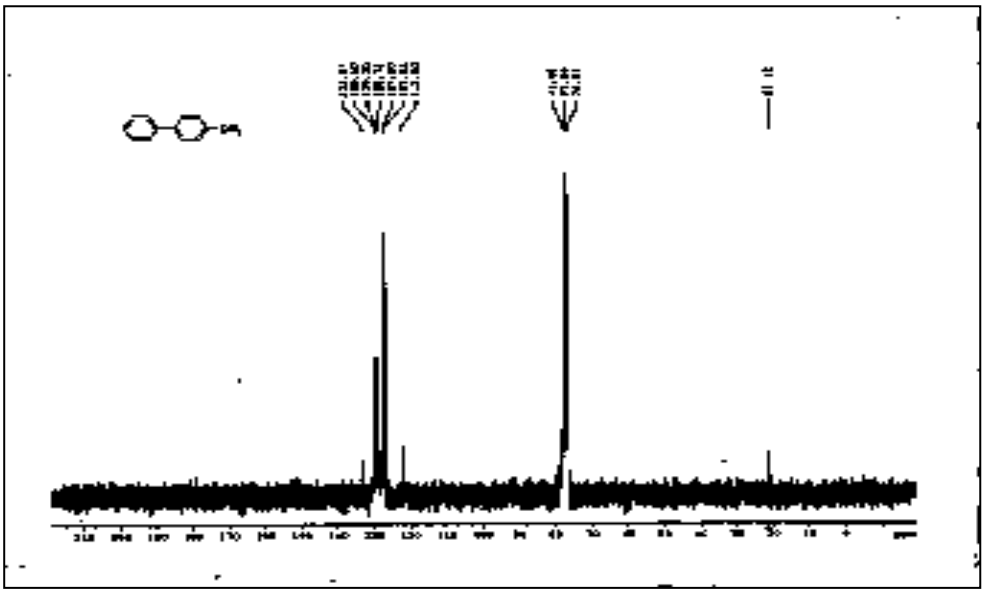

Figure II.B.12. *Scanned copy of ^{1}H and ^{13}C NMR spectra of 4-acetyl 1,1'-biphenyl.*

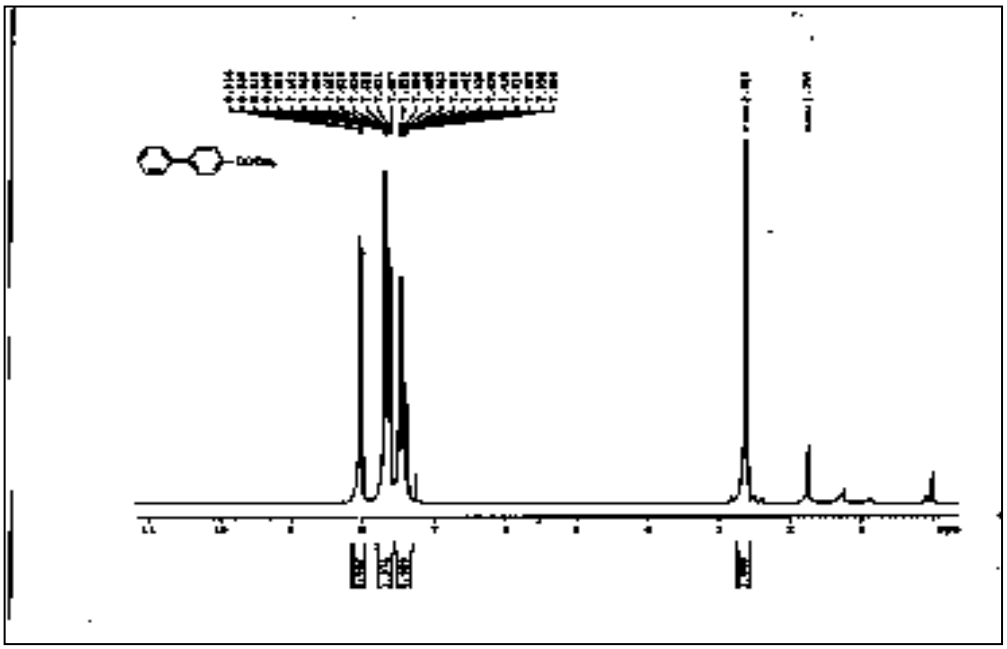

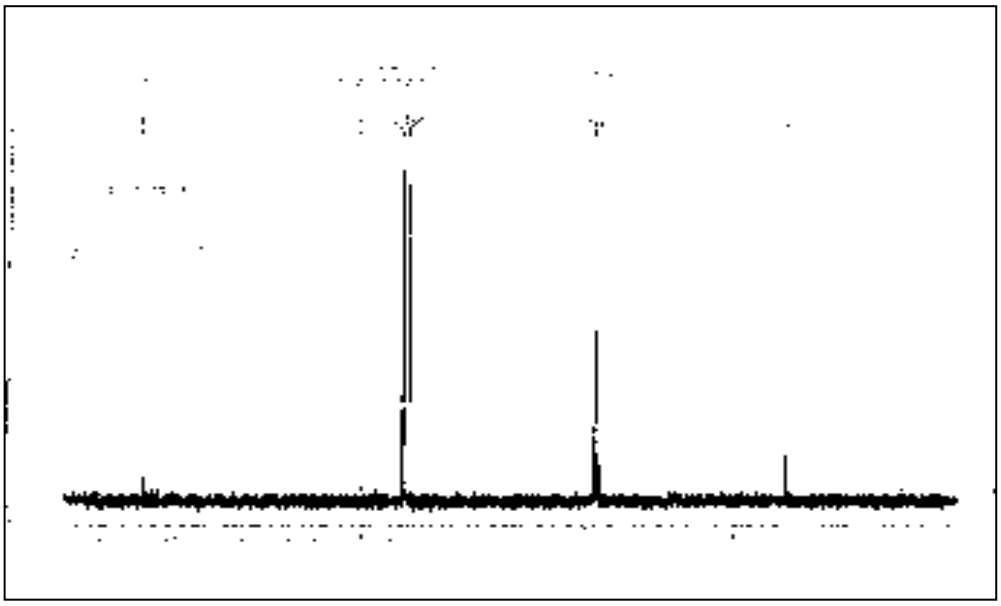

Figure II.B.13. *Scanned copy of ^{1}H and ^{13}C NMR spectra of 4-methoxy-3-methyl-1,1'-biphenyl.*

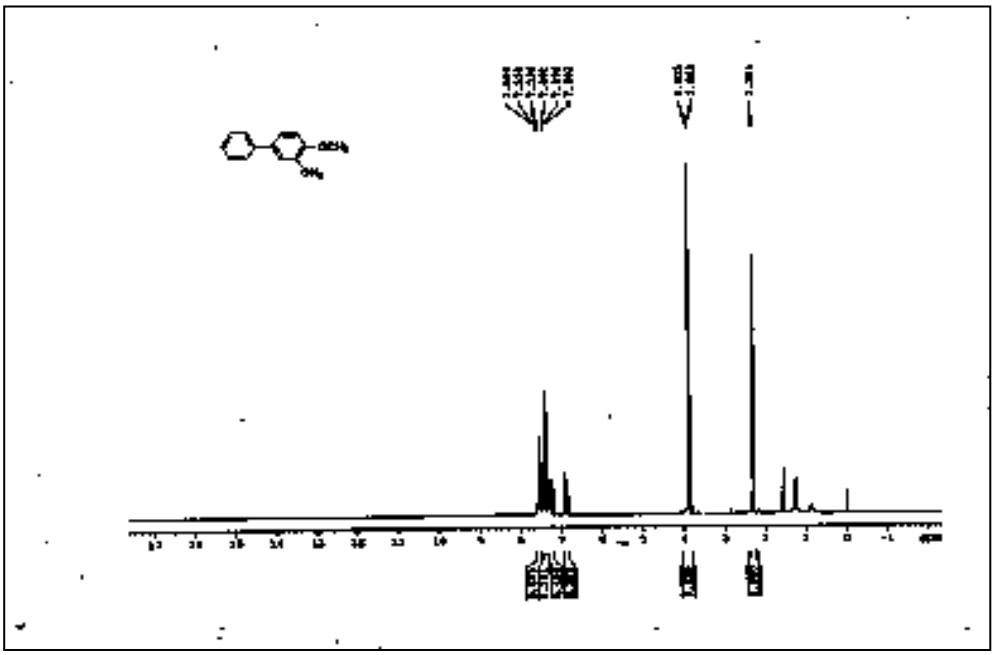

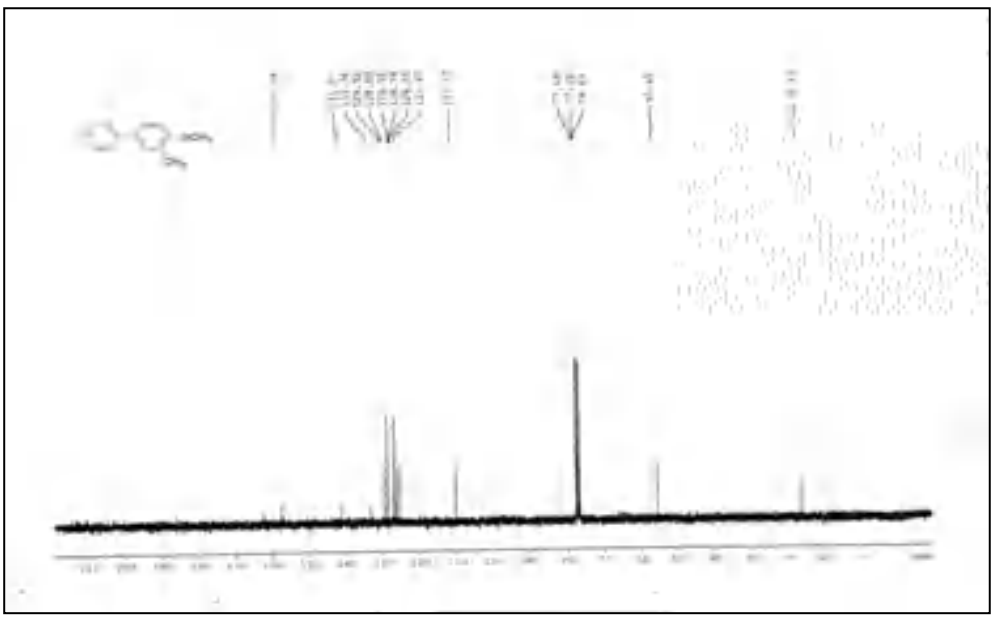

Figure II.B.14. *Scanned copy of ^{1}H and ^{13}C NMR spectra of 4-methyl-4'-methoxy-1,1'-biphenyl.*

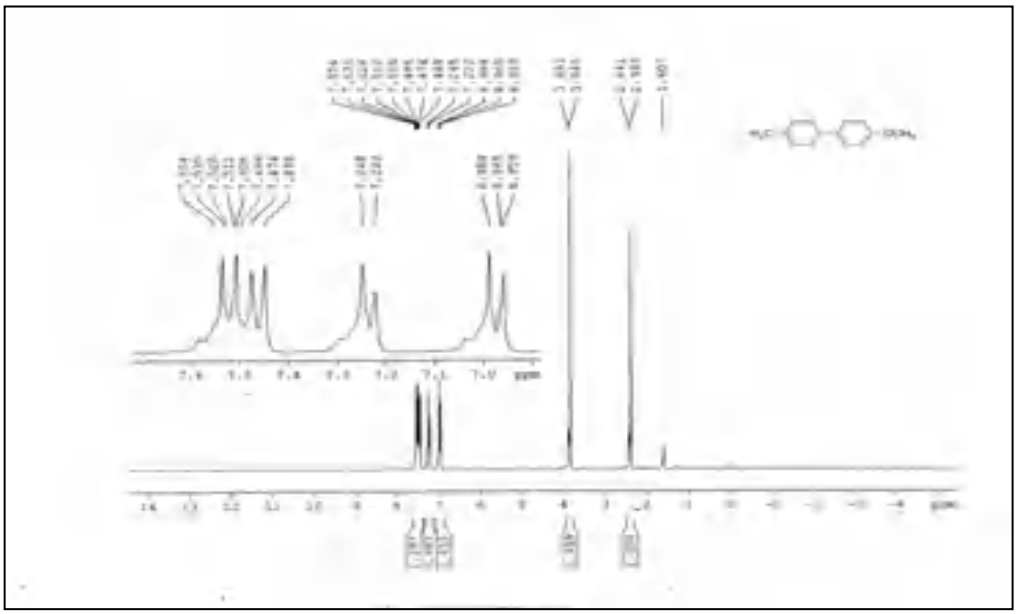

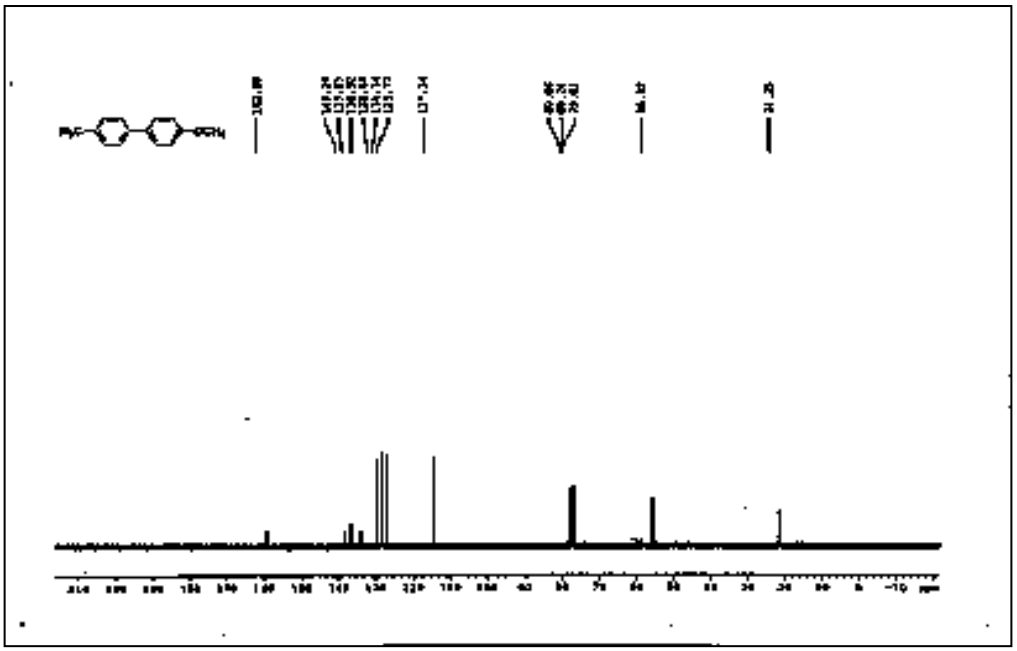

Figure II.B.15. *Scanned copy of ^{1}H and ^{13}C NMR spectra of (E)-methyl 3-(3-nitrophenyl)acrylate.*

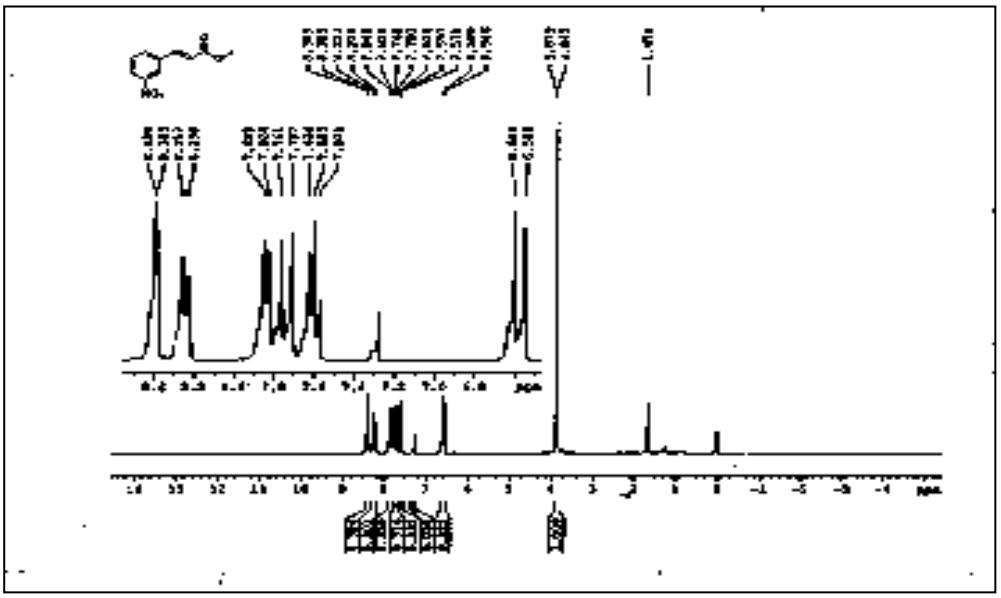

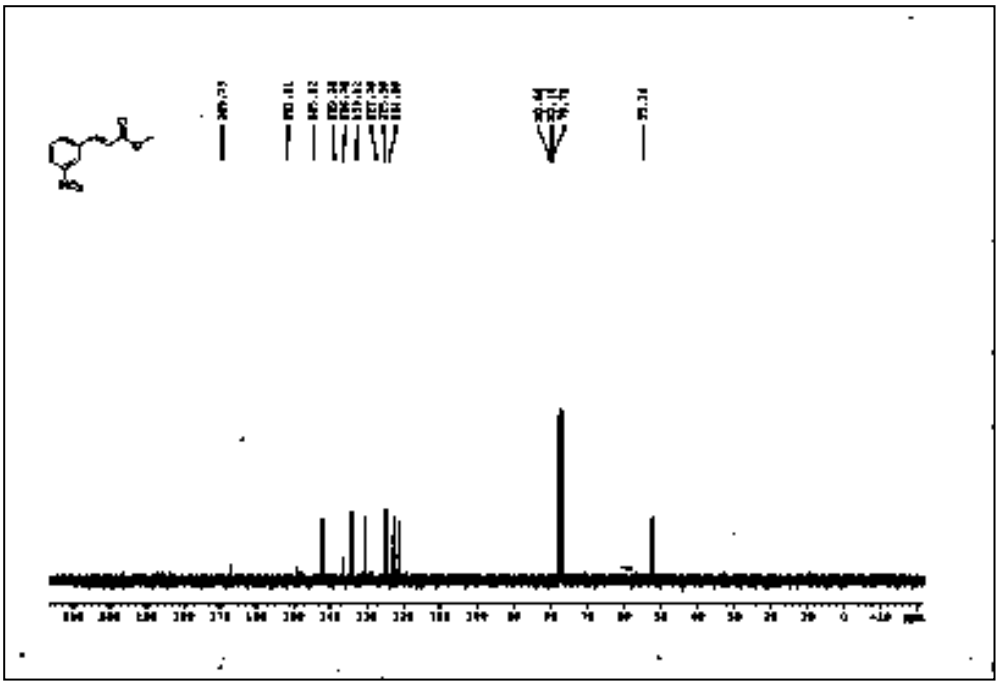

Figure II.B.16. *Scanned copy of ^{1}H and ^{13}C NMR spectra of (E)-methyl 3-(4-methoxyphenyl) acrylate.*

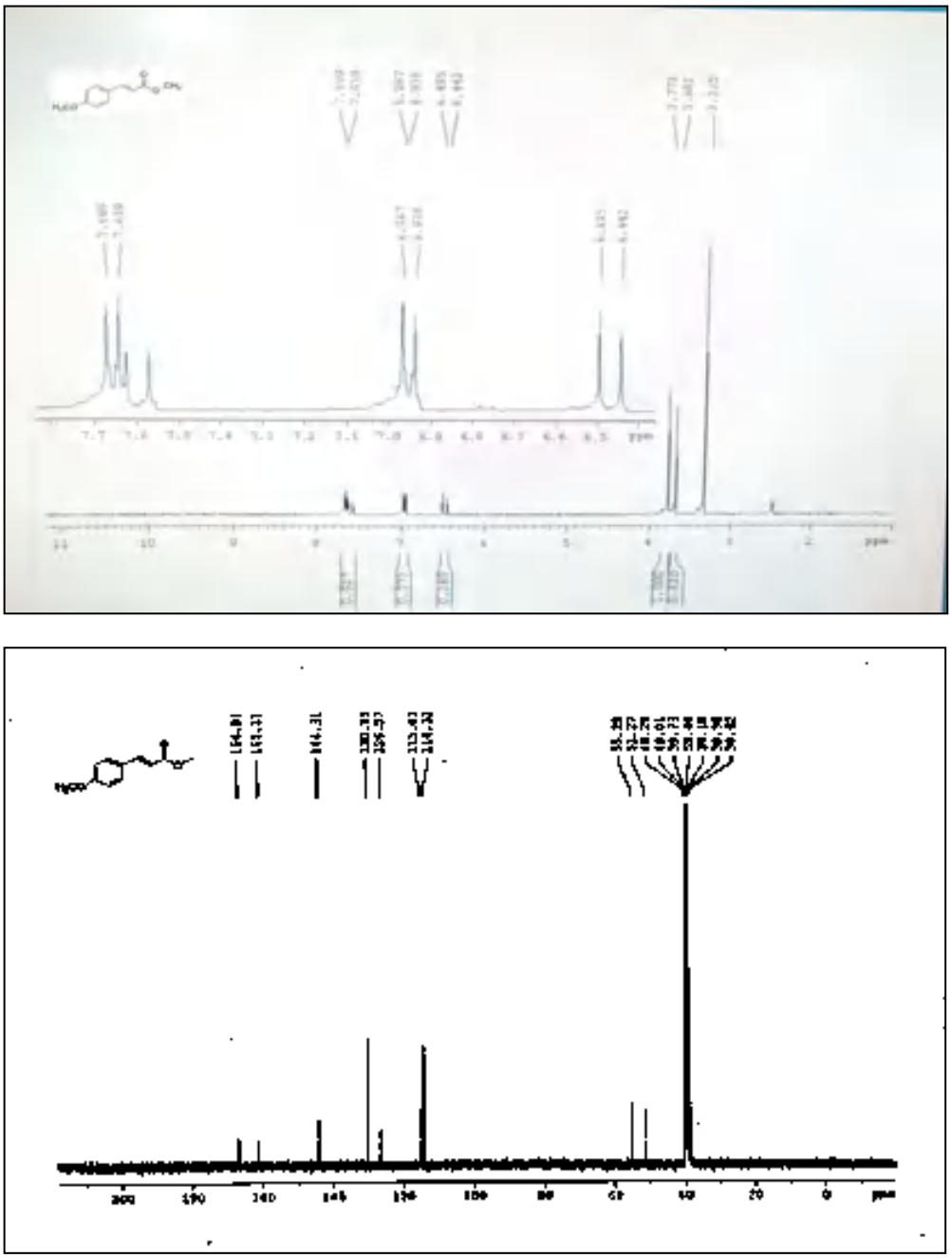

Figure II.B.17. *Scanned copy of ^{1}H and ^{13}C NMR spectra of (E)-ethyl 3-(4-methoxyphenyl) acrylate.*

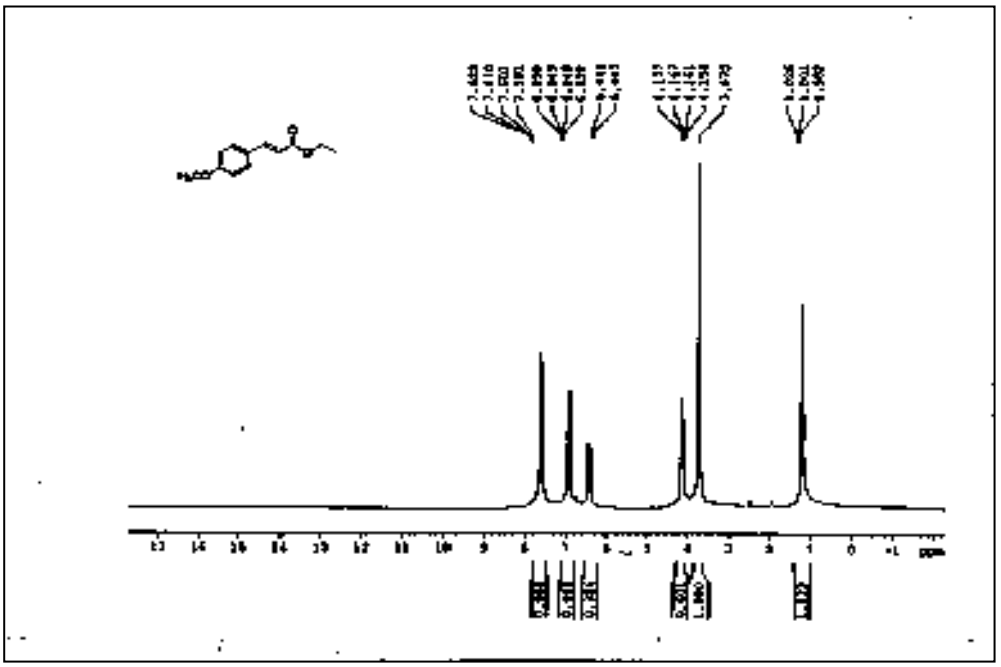

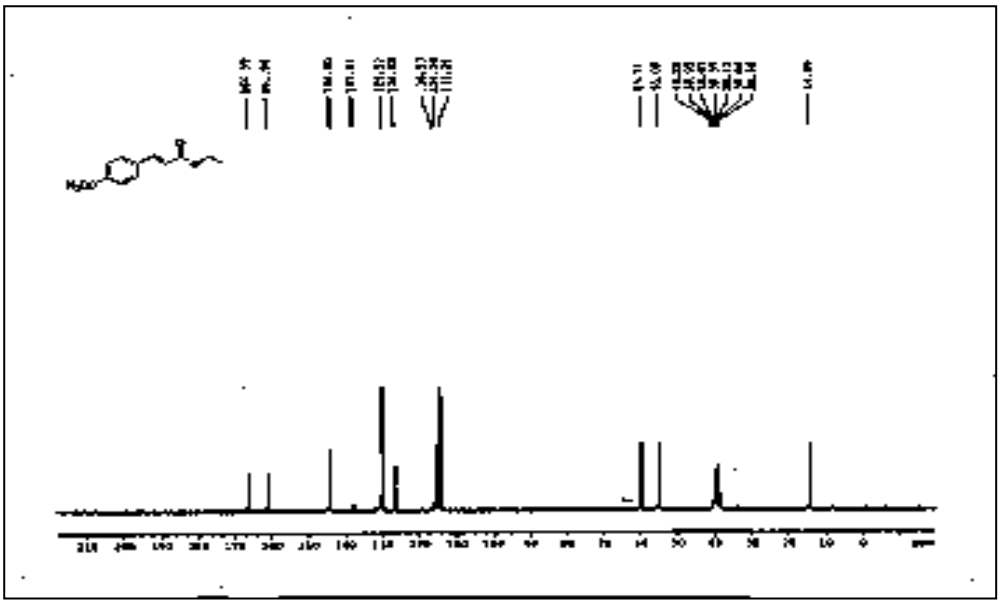

Figure II.B.18. *Scanned copy of ^{1}H and ^{13}C NMR spectra of (E)-butyl 3-(4-methoxyphenyl) acrylate.*

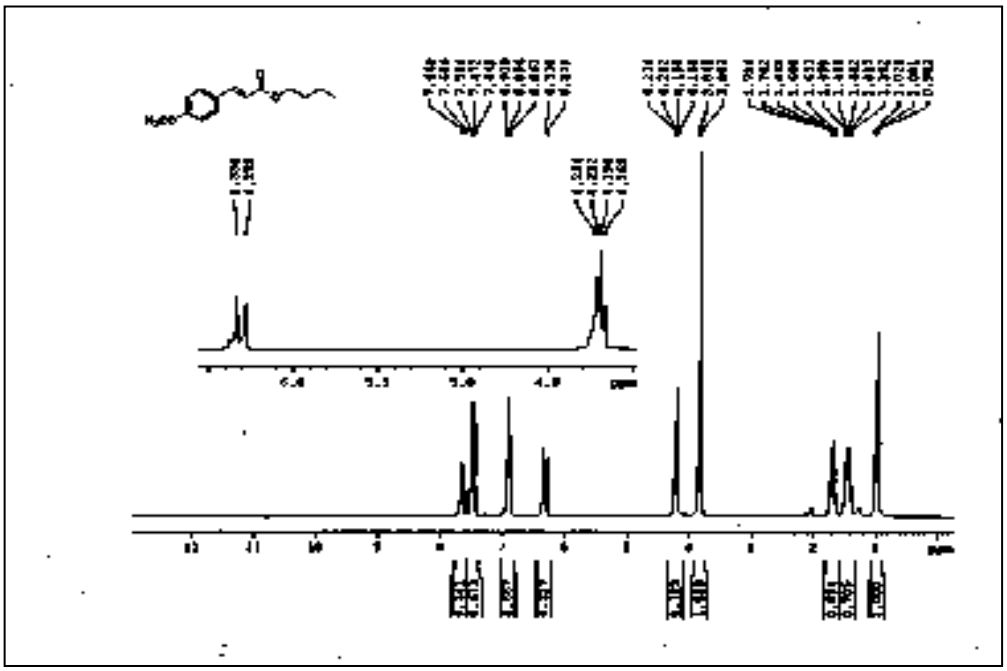

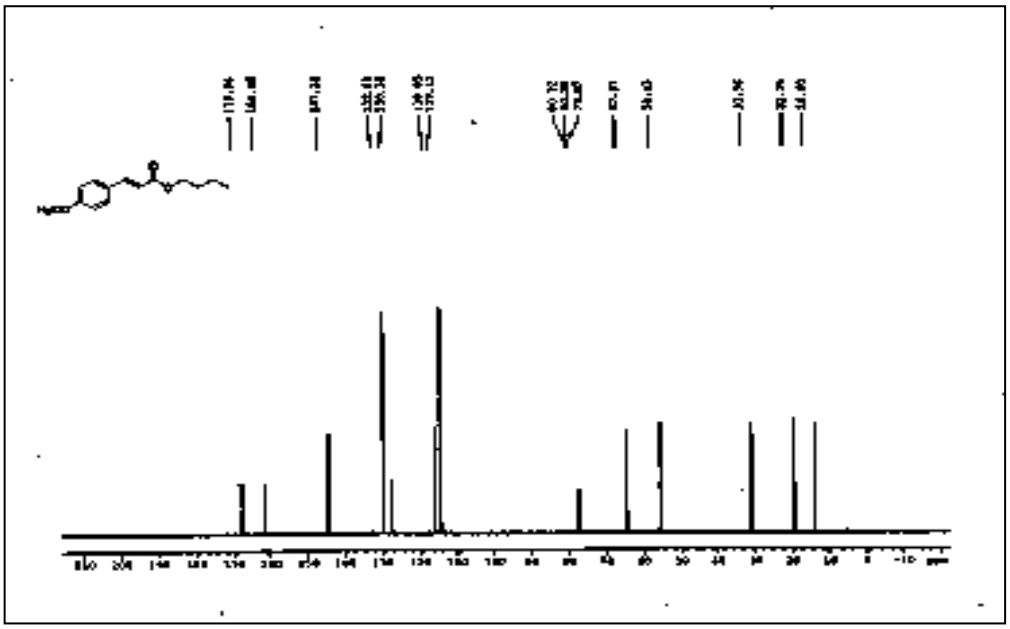

Figure II.B.19. *Scanned copy of ^{1}H and ^{13}C NMR spectra of 1-(4-styrylphenyl)ethanone.*

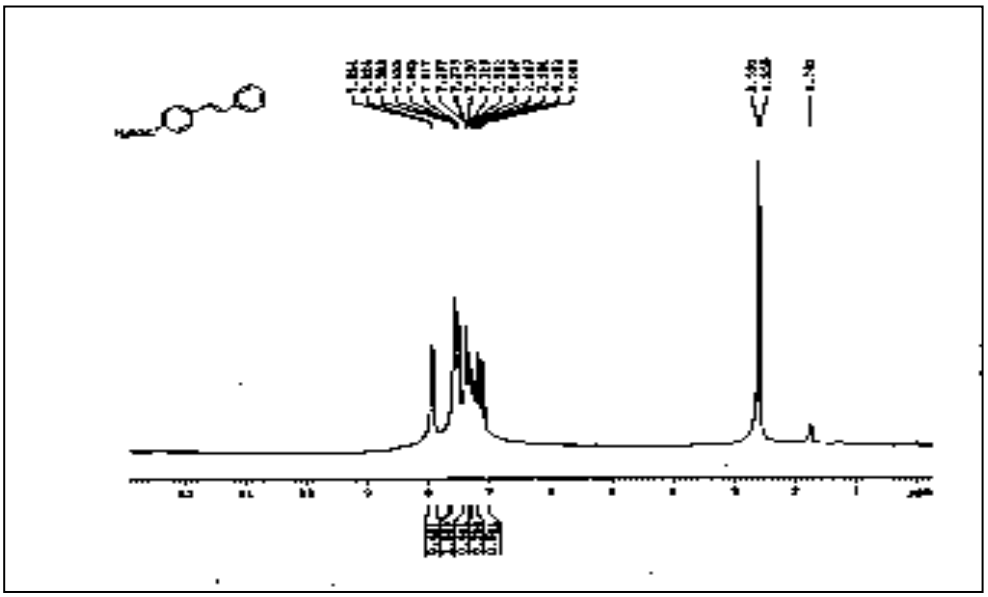

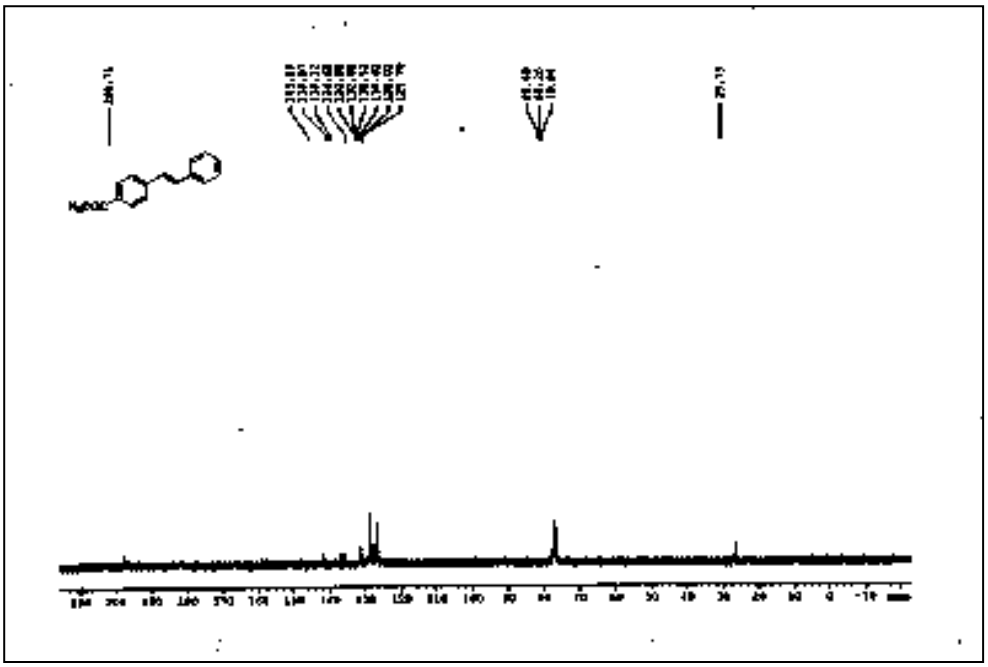

II.B.6. References

References are given in Bibliography under Chapter II, Section B

Chapter III

Section A

Sulfonated graphene oxide (SGO) as metal-free efficient carbocatalyst for the synthesis of 3-methyl-4-(hetero) arylmethylene isoxazole-5(4H)-ones

III.A.1. Introduction

Isoxazoles and isoxasolone derivatives are an important class of heterocyclic compounds that display beneficial biological properties such as antitumor [1], antifungal [2], cytotoxic, anti-inflammatory [3], antibacterial, and anti-HIV activities [4-6]. Isoxazole scaffold is considered as a major compound in the combinatorial synthesis and protein kinase inhibitors as well as playing a crucial role in the development of chemotherapeutic agents [7-8]. Moreover, many compounds belonging to this class have also been employed as versatile building blocks of synthetic drug molecules [9], a variety of natural products [10], fungicides, and insecticides [9]. Isoxazoles are beneficial starting materials in various organic synthesis [11] and found application in liquid crystalline material [12], optical storage and nonlinear optical research [13], filter dyes in photographic films [14]. A series of androgen antagonists with isoxazole scaffold are found to have medicinal utility [15] and some of them also exhibit full antagonistic activity towards human metastatic breast cancer cells and human prostate tumor cells [16]. Panathur *et al.* also studied biological activities (in vitro) of some isoxazolone derivatives showing their I12, I17 compounds (Figure III.A.1) with cytotoxicity against cancer cells viz. Human metastatic breast cancer cells (MDA-MB-231), Human breast cancer cells (MCF-7), Human colon adenocarcinoma cells (HT-29) remarkably without affecting the noncancerous cells (HEK-239) [16].

In recent times, one-pot multicomponent reactions (MCR) are emerging as ecologically sustainable processes in pharmaceutical chemistry, drug designing, and have been considered as a powerful tool for the synthesis of biologically active heterocyclic compounds. With increasing demand in green

chemistry, much attention has been paid to MCRs to achieve high yield, high selectivity, and synthetic simplicity in various research fields.

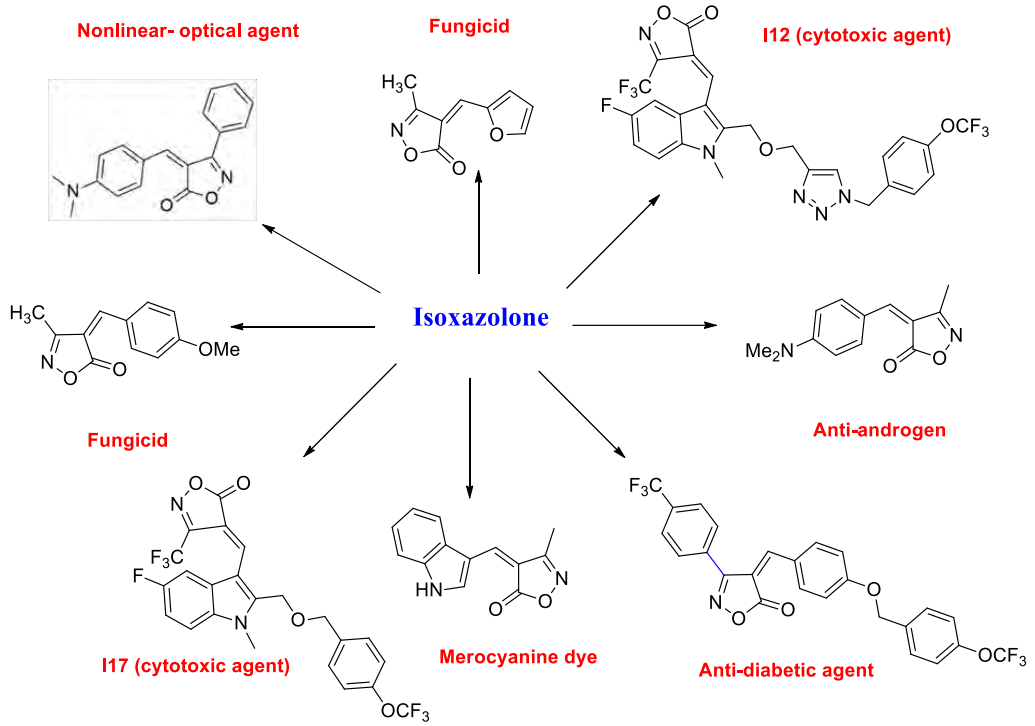

Figure III.A.1. *Some examples of biologically active compounds containing isoxazole moiety.*

III.A.2. Background and objectives

There are several methods for synthesis of isoxazole-5(4*H*)-one derivative, a) cyclization of *O*-propionyl oximes [17], b) condensation between substituted benzaldoximes and 1,3-dicarbonyl compounds [18], c) the reaction of *β*-ketoesters with hydroxylamine and sodium hydroxide followed by the subsequent addition of aqueous HCl under heating condition [19]. The traditional procedure to synthesize 3-methyl-4-(hetero)arylmethylene isoxazole-5(4*H*)-ones involve two consecutive steps viz. a) formation of an oxime from the condensation of ethyl acetoacetate with hydroxylamine hydrochloride followed

by b) Knoevenagel type reaction with aromatic aldehydes [20]. The convenient methodologies demand solid state grinding, solid state heating [21], microwave heating [22], ultrasonic irradiation [23], application of sodium acetate in presence of visible light in ethanol solvent [24]. It is worth mentioning that different moisture-sensitive reagents like sodium sulphide [25], phthalimide-*N*-oxyl salts [26], sulphated polyborate [27], boric acid [28], sodium azide [29], SnII-montmorillonite [30], potassium sorbate [31] etc [32-35]. However, most of the conditions, suffer from drawbacks such as high temperature, harsh reaction conditions, prolonged reaction time, strongly acidic/basic condition, low yield, use of homogeneous catalyst and suffer from rapid loss of catalytic activity. Although in most of the reported protocols acceptable yield of isoxazolone has been reported using toxic metal catalysts, costly reagents [27, 29] as well as people suffered tedious reaction conditions and work up process [24, 29, 30]. To avoid these drawbacks it is imperative to develop a high-yielding greener, radiation, and metal-free efficient method for its synthesis with a broad range of substrate applicability.

In 1928-1929 Minunni *et al.* investigated the reaction between acetoacetic ester oxime with various aromatic aldehydes in presence of acid (Scheme III.A.1) [36]. The striking similarity of the product obtained by this procedure to those obtained by R. Schiff and M. Betti [37] may lead to an assumption that the products were isoxazolones. The probable mechanism of this reaction was discussed and it was found that the reactions are feasible in presence of strong acids.

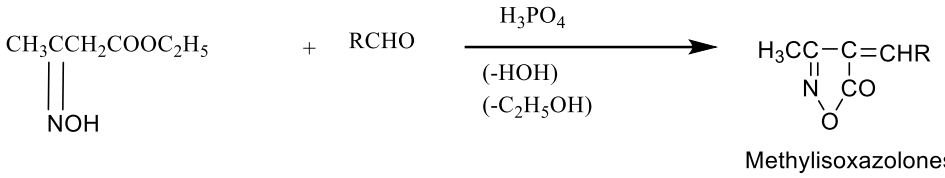

Scheme III.A.1. *The reaction of acetoacetic ester oxime with an aromatic aldehyde.*

Nakamura *et al.* demonstrated gold-catalyzed cyclizations of *O*-propioloyl oximes to 4-arylideneisoxazol-5(4*H*)-ones in good to excellent yields via C-N bond formation followed by arylidene group transfer (Scheme III.A.2) [17]. As a representative reaction, (*E*)-benzaldehyde *O*-3-phenylpropioloyl oxime was reacted in acetonitrile in the presence of $Au(PPh_3)NTf_2$ (5 mol %) at 25 °C temperature to give 4-benzylidene-3-phenylisoxazol-5(4*H*)-one with excellent yield (90%). Crossover experiments showed the arylidene "migration" proceeded through an intermolecular manner.

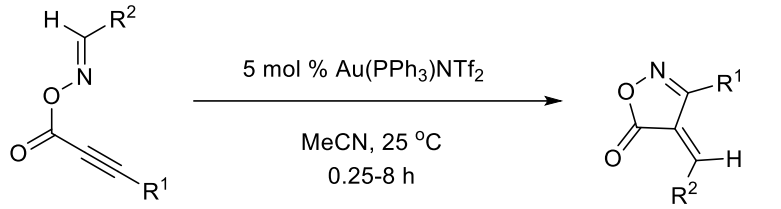

R^1 = Ph, *p*-tolyl, *p*-anisyl, *p*-$CF_3C_6H_4$, *n*-Pr, Cy, *t*-Bu
R^2 = Ph, *p*-tolyl, *p*-anisyl, *p*-$CF_3C_6H_4$, *p*-ClC_6H_4, *p*-$iPrC_6H_4$

Scheme III.A.2. *Au-catalyzed synthesis of 4-arylideneisoxazol-5(4H)-ones.*

Maddila *et al.* described the one-pot synthesis of 3-methyl-4-(phenyl)methylene-isoxazole-5(4*H*)-ones in a water medium using Ag/SiO_2 as heterogeneous catalyst (Scheme III.A.3) [34]. Interestingly, different aromatic aldehydes with several electron-withdrawing and electron-donating substrates in

ortho, meta, and para positions have also contributed positively to produce the desired substituted isoxazoles in good to excellent yield. All the synthesized products were characterized by FTIR, ^{1}H NMR, ^{13}C NMR, and HRMS spectra.

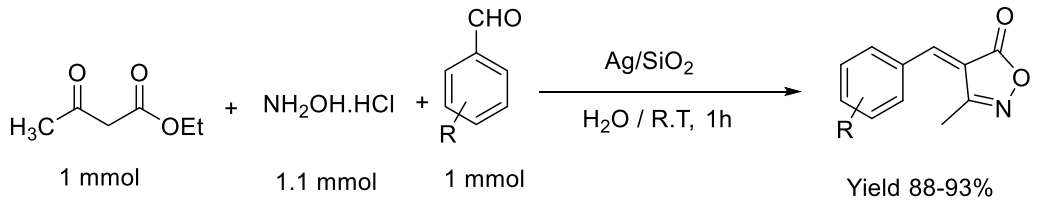

R = H, 4-OH, 4-OMe, 4-$N(Me)_2$, 2,5-$(OH)_2$, 3,4-$(OH)_2$,
3-OH, 2,3-$(OMe)_2$, 2,5-$(OMe)_2$, 2,4,6-$(OMe)_3$, 2,4-$(Me)_2$, 4-Et

Scheme III.A.3. *Ag/SiO_2 catalyzed green synthesis of 3-methyl-4-(phenyl)methylene-isoxazole5(4H)-ones.*

Patil *et al.* developed a mild and rapid synthesis of 3-methyl-4-(hetero)arylmethylene isoxazole-5(4*H*)-ones via an eco-benign protocol involving a new heterogeneous catalyst sulfated polyborate (Scheme III.A.4). The boric acid was dehydrated at 200 ^{o}C and converted into polymeric Lewis acid form and then sulfonated to induce the Bronsted acid character into the polymerized form [38]. Several electron-withdrawing and donating groups on the aromatic nucleus showed no significant change in the yield of the product. The main advantage of this method was a solvent-free approach, easy work-up, recyclable catalyst, and short reaction time.

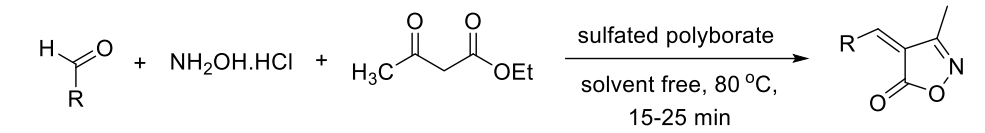

R = C_6H_5, 2-OH-C_6H_4, 2-NO_2-C_6H_4, 3-Cl-C_6H_4,3-Br-C_6H_4
4-Cl-C_6H_4, 4-Br-C_6H_4, 4-CH_3-C_6H_4, 4-OCH_3-C_6H_4, 4-OH-C_6H_4
4-NO_2-C_6H_4, 2-Thienyl, 5-Methyl furan-2-yl, Indol-3-yl

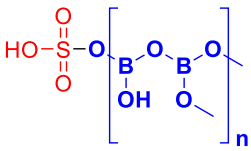

Sulfated ployeborate

Scheme III.A.4. *Sulfated polyborate catalyzed synthesis of 3-methyl-4-(hetero)arylmethylene isoxazole-5(4H)-ones.*

Liu *et al.* described the one-pot three component synthesis of isoxazolones using ethyl acetoacetate, hydroxylamine hydrochloride, and aromatic aldehydes in presence of sodium sulfide as catalyst (Scheme III.A.5) [39]. Probably, sodium sulfide is one of the oldest and widely used industrial chemicals that has been used as an effective catalyst in some reactions [40]. The electron-donating group containing aromatic aldehydes afforded the target products in high yield in a short time while aromatic aldehydes with electron-withdrawing groups were failed to convert to the target products. Although, the heterocyclic aldehydes and *α,β*- unsaturated aldehydes exerted the corresponding isoxazolones with moderate to high yield.

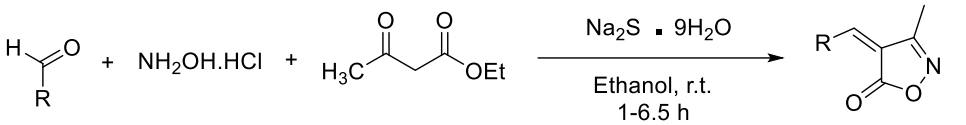

R = C_6H_5, 2-Furyl, 4-$CH_3OC_6H_4$, 2-OHC_6H_4,
Vaniline, C_6H_5CH=CH, 2-ClC_6H_4, 2,4-$Cl_2C_6H_3$

Scheme III.A.5. *The one-pot synthesis of 3-methyl-4-(hetero)arylmethylene isoxazole-5(4H)-ones catalyzed by sodium sulfide.*

Photochemical reactions in presence of visible light in eco-friendly solvents are particularly useful and are considered an extremely green and clean procedure. The photo activation of the substrates minimizes the chance of the byproduct formation and requires much less time than the thermal procedure (Scheme III.A.6) [41]. Saikh *et al.* reported an eco-friendly synthesis of 3-methyl-4-arylmethylene-isoxazole-5(4*H*)-ones induced by visible light in the aqueous-ethanol solvent [42]. However, it was observed from the reaction that the electron-donating group containing aromatic aldehydes smoothly participate whereas, the electron-withdrawing group containing aromatic aldehydes (nitro or chloro) failed to produce the target product.

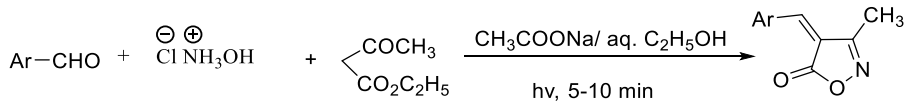

Ar = C_6H_5, 4-OHC_6H_4, 4-$OCH_3C_6H_4$, 2,4-$(OCH_3)_2C_6H_3$
3,4-$(OCH_3)_2C_6H_3$, benzodioxole, 2-Thiophenyl, Indole

Yield 56-89 %

Scheme III.A.6. *Synthesis of 3-methyl-4-arylmethylene-isoxazole5(4H)-ones induced by visible light in an aqueous-ethanol solvent.*

Kiyani *et al.* developed an environmentally benign protocol for the synthesis of 3,4-disubstituted isoxazol-5(4*H*)-ones at room temperature using Potassium phthalimide (PPI) as an efficient and effective basic organocatalyst (Scheme III.A.7) [43]. Potassium phthalimide (PPI) is a mild, inexpensive, commercially available basic recyclable catalyst, and also a stable reagent.

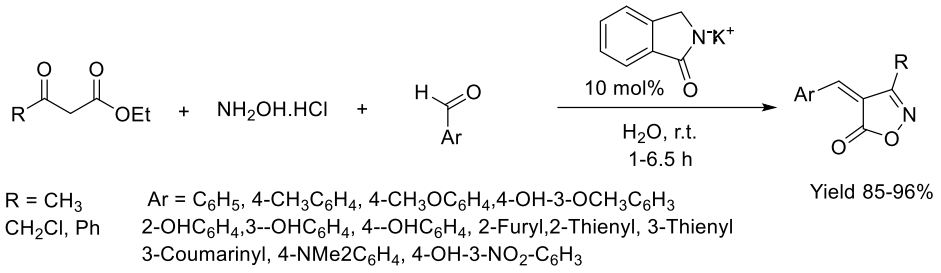

Scheme III.A.7. *Synthesis of 3,4-disubstituted isoxazol-5(4H)-ones catalyzed by Potassium phthalimide (PPI) in water at room temperature.*

This reagent (PPI) has been widely used in the synthesis of primary amines by the Gabriel method [44], particularly used for the synthesis of phthalimide derivatives [45, 46] and the preparation of cyanohydrin trimethylsilyl ethers [47].

As an alternative to non-metal for organic synthesis, carbonaceous nanomaterials have been received considerable attention due to their sustainability and affordability [48]. Graphene oxide (GO), a 2D unique nanomaterial, contains a variety of oxygen-containing functional groups (e.g. alcohols, carboxylates, epoxides, sulphate groups), the presence of these extrinsic functionalities provides moderate acidic properties (pH = 4.2) to GO and its high surface area males it an efficient catalyst for several organic transformation reactions. In addition to this, its derivative sulfonated graphene oxide (SGO) possesses BrØnsted acid properties in organic reactions. The use of GO and SGO as heterogeneous catalysts has been attracted consideration owing to their acidic property, thermal stability in reaction, high surface area, and easy recovery of the catalyst [49-52].

III.A.3. Present work: Result and discussion

Over the past decades, as an alternative of nonmetal carbonaceous nanomaterials have received considerable attention owing to their sustainability and affordability in organic transformation [53-55]. Herein, we report a simple and unprecedented transformative protocol to furnish a wide variety of biologically active substituted 3-methyl-4-(hetero)arylmethylene isoxazole-5(4*H*)-ones using aldehyde, ethyl acetoacetate, and hydroxylamine hydrochloride in presence of sulfonated graphene oxide (SGO) at room temperature (Scheme II.A.8). The catalyst SGO was characterized by different spectroscopic techniques and reused up to the 5th run without a significant drop in its catalytic activity.

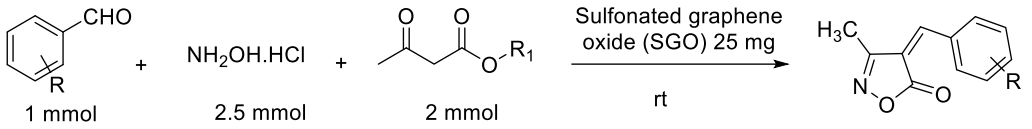

R = H, 4-OMe, 4-NO_2, 4-Me, 4-Cl, 3-NO_2, 2-Furyl, 2-Thienyl, 2-Napthyl, 4-OH, 4-Br, 4-NMe_2, 2-OH, 3-Me, Indole-3-carbaldehyde, Cinnamaldehyde

R_1= -Me, Et

Yield 64-93 %

Scheme III.A.8. *One-pot three-component synthesis of 3-methyl-4-(hetero)arylmethylene isoxazole-5(4H)-ones using SGO as a catalyst.*

III.A.3.1.Synthesis of the catalyst

We have assessed the catalytic activity of SGO as an acid catalyst in the promotion of isoxazole synthesis. SGO was synthesized by the Tours method shown in scheme III.A.9 and was extensively purified to remove any metal impurity.

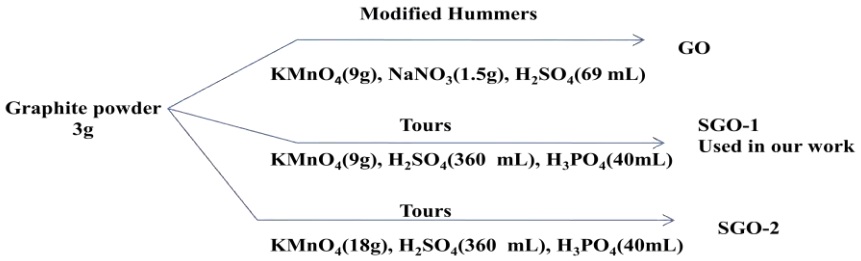

Scheme III.A.9. *Synthesis of SGO using different method.*

III.A.3.2. Optimization of the reaction conditions

For screening the reaction condition, benzaldehyde, ethyl acetoacetate, and hydroxylamine hydrochloride were selected for the model reaction. The effects of the reaction parameters such as solvent, temperature, amount of the catalyst are discussed briefly in Table III.A.1. It was noticed that except toluene other solvents produced the desired product in moderate to good yield. Further investigation revealed that solvent-free stirring yielded the corresponding products with an excellent yield at room temperature (Table III.A.1). Inspired by this expectancy, we altered the amount of the catalyst SGO under solvent-free conditions to achieve the optimal condition of the reaction. Depending upon the time, yield and temperature, 25 mg SGO-1 displayed the best result (Table III.A.1, entry 8) and was opted as the optimum quantity for the promotion of the reaction (Table III.A.1). To show catalytic efficiency, SGO-1 was also compared with GO and SGO-2 (Table III.A.1, entry 9 and10) and results revealed that SGO-1 exerted the desired product with a high yield.

Table III.A.1. Optimization of reaction parameters for the synthesis of 3-methyl-4-(hetero)arylmethylene isoxazole-5(4*H*)-ones based on the result of the following combination intheprotocol[a]

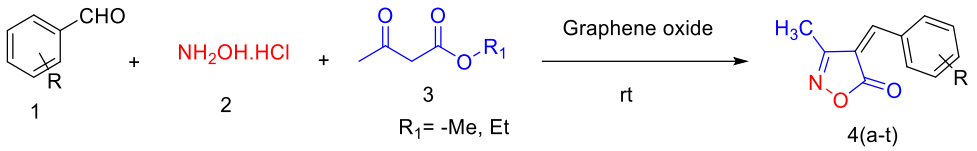

Entry	Catalyst (SGO-1) mg	Solvent	Temperature ° C	Time(h)	Yield (%)[b]
1.	None	Water	Rt	8	Trace
2.	50	Water	Rt	2	82%
3.	50[d]	Water	100	1	84%
4.	50	Ethanol	rt	2	74%
5.	50	MeCN	rt	2	52%
6.	50	Neat	rt	2	91%
7.	50	Toluene	rt	2	NR
8.	**25**	**Neat**	**rt**	**1**	**90%**
9.	25 (GO)	Neat	rt	1	84%[e]
10	25 (SGO-2)	Neat	rt	1	87%[f]
11.	25	Neat	rt	12	86%
12.	15	Neat	rt	4	60%
13.	10	Neat	rt	12	49%
14.	100[g]	Neat	rt	4	81%

[a]Reaction of benzaldehyde (1 mmol), ethyl acetoacetate (2 mmol), hydroxylamine hydrochloride (2.5 mmol) at room temperature (rt).
[b]Isolated yield after purification through column chromatography on silica gel.
[c]No sulfonated graphene oxide (SGO) was added.
[d]Temperature of the reaction 100 °C.
[e]GO was used as catalyst,
[f]SGO-2 was used as a catalyst.
[g]The reactants are used 5 mmol each.

To test the water tolerance of the catalyst, we have also carried out the reaction in an aqueous medium (Table III.A.1, entry 2). Upto 82% yield of the entry suggested that there is no chance of poisoning the catalyst by water. To

reconfirm the anticipation, after the 1st run the recovered catalyst was dried in a rotary evaporator at 50 °C and reused under the identical condition and in each case, we observed almost identical yield up to the 3rd run.

After achieving the optimized condition, we used some substituted aromatic aldehydes to get different substituted 3-methyl-4-(hetero)arylmethylene isoxazole-5(4*H*)-ones. The study also indicated that various aromatic aldehydes afforded the corresponding products with high yields (except 2-nitro and 4-nitrobenzaldehyde). Aldehydes with electron-donating groups considerably increase the nucleophilicity on carbonyl oxygen, thereby efficiently yielding the desired product with excellent yield (Table III.A.2, entries 2, 4, 8, 13, 18, and 22), whereas, the aldehydes with electron-withdrawing groups affording relatively poor yield of the product. 2-Napthaldehyde (Table III.A.2, entry 9) gave moderate yield whereas 1-Naphthaldehyde (Table III.A.2, entry 10) did not respond to reaction and the reason may be due to the hindrance offered by steric factor. Again, we examined the reaction in the case of aliphatic aldehyde also (Table III.A.2, entry 20) which gave a trace amount of product. The generality of the reaction was further extended in the case of heterocyclic and α,β-unsaturated aldehydes which also afforded the corresponding product with good yield (Table III.A.2, entries 7, 11, and 17, 19). The versatility of the reaction was further tested by using methyl acetoacetate instead of ethyl acetoacetate. As expected we get the same product and with an almost identical yield (Table III.A.2, entry 21, 22, 23).

Table III.A.2. SGO catalyzed synthesis of different substituted 3-methyl-4-(hetero)arylmethylene isoxazole-5(4*H*)-ones[a]

Entry	Aldehyde	R	Product	Time	Yield (%)[b]	Mp (°C)	
						Found	Reported
1.	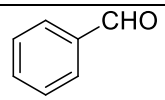	Et	4a	1	90	141-142	141-143
2.	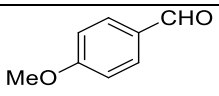	Et	4b	1.5	89	176-178	174-176
3.	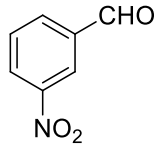	Et	4c	1.5	80	141-143	142-144
4.	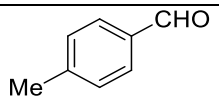	Et	4d	1.5	87	135-136	135-136
5.	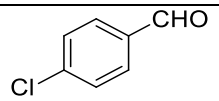	Et	4e	2	84	119-121	118-120
6.	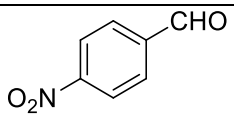	Et	4f	4	Trace	-	-
7.	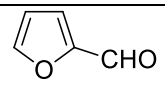	Et	4g	1.5	91	237-239	238-241

8.	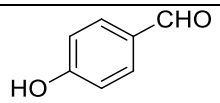	Et	4h	1.5	84	215-216	214-216
9.	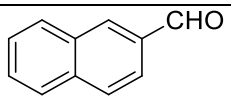	Et	4i	3	64	165-166	-
10.	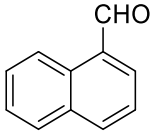	Et	4j	8	NR	-	-
11.	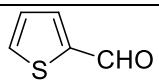	Et	4k	1.5	90	144-146	146-147
12.	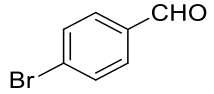	Et	4l	2.5	82	122-125	120-122
13.	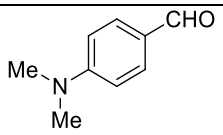	Et	4m	1	93	225-227	227-228
14.	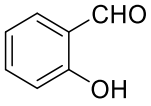	Et	4n	2	82	200-202	198-201
15.	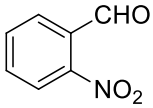	Et	4o	8	Trace	-	-

16.	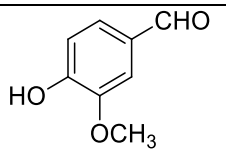	Et	4p	2.5	90	214-216	211-214
17.	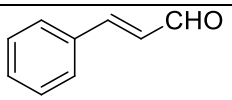	Et	4q	2	84	172-174	171-173
18.	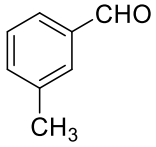	Et	4r	2.5	87	108-110	-
19.	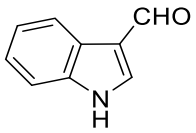	Et	4s	2.5	86	239-240	240-242
20.	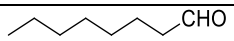	Et	4t	8	Trace	-	-
21.	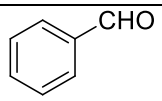	Me	4a	2	84	141-142	141-143
22.	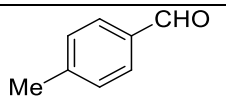	Me	4d	2	86	135-136	135-136
23.	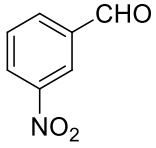	Me	4c	2	78	141-143	142-144

[a]Reaction of aldehyde (1 mmol), ethyl acetoacetate (2 mmol), hydroxylamine hydrochloride (2.5 mmol), SGO (25mg) at room temperature.

[b]Isolated yield after purification through column chromatography on silica gel.

III.A.3.3. Mechanism

A probable mechanism for the synthesis of 3-methyl-4-arylmethylene isoxazole-5(4*H*)-ones by SGO is depicted below (Scheme III.A.10). It is suggested that acid-catalyzed oxime (I) formation initiated the reaction. The oxime so formed subsequently guided the Knoevenegal condensation between aromatic aldehyde and intermediate (I). This will be followed by successive cyclization along with the elimination of ethanol to yield the desired product.

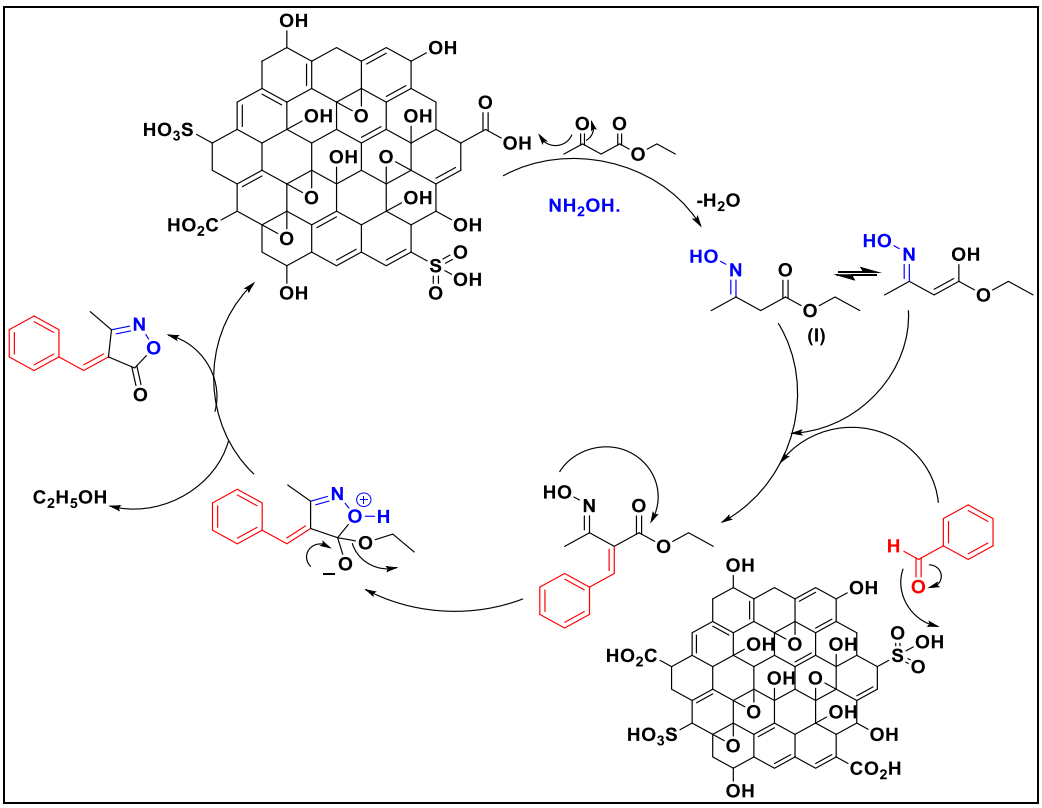

Scheme III.A.10. *Possible route for SGO catalyzed synthesis of 3-methyl-4-(hetero) arylmethylene isoxazole-5(4H)-ones.*

III.A.3.4. HR-TEM and SEM analysis

A morphological study of graphene oxide (SGO) and SGO after the 5th run was carried out by HR-TEM microscopy to investigate the disintegration of SGO sheets due to the reactions (Figure III.A.2). After reuse SGO sheets appear to have disintegrated along with slight aggregation. The possible explanation may be put forward that, after catalysis, its reduction to rGO leads to disintegration into smaller sheets. Furthermore, the morphological study (SEM images) confirms the formation of multiple SGO sheets (Figure III.A.3). Thus, from the above, it may be included that SGO has taken part in the reaction.

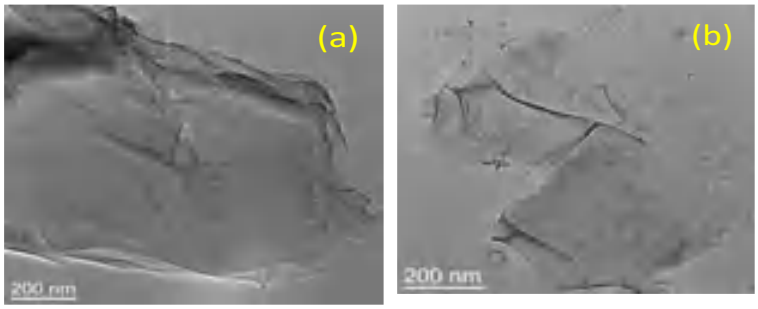

Figure III.A.2. *HR-TEM images of (a) SGO and (b) SGO after 5th run.*

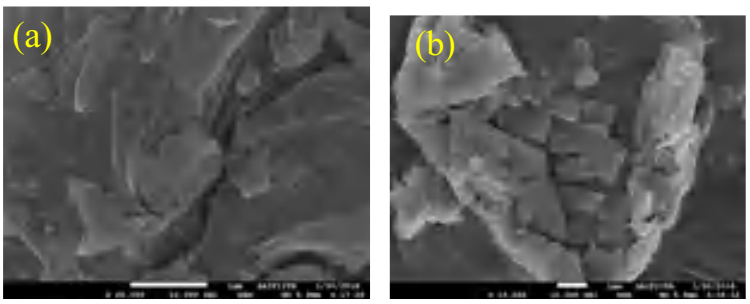

Figure III.A.3. *SEM images of (a)SGO and (b) SGO after the 5th run.*

The S content in fresh SGO and the residue left after the 5th run was 3.12 and 0.68 wt% respectively (Figure III.A.4). The decreased percentage of S in

SGO after the 5th run reveals that the functional groups containing sulfur have had participated in the reaction.

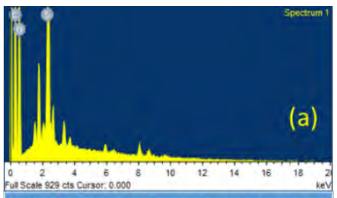

Weight percent of constituent elements	
C	50.41
O	46.47
S	3.12

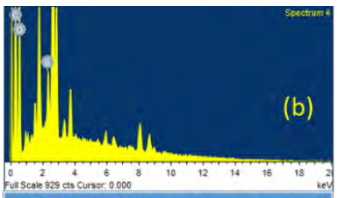

Weight percent of constituent elements	
C	53.7
O	45.62
S	0.68

Figure III.A.4. *EDX spectra of (a) SGO and (b) SGO after 5th run.*

III.A.3.5. XRD and Raman spectra analysis

For structural studies, XRD spectra of the synthesized catalyst SGO, and that of it after the 5th run are shown in Figure III.A.5.

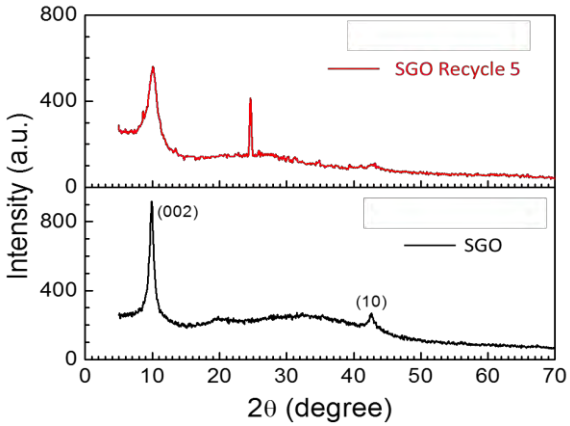

Figure III.A.5. *XRD spectra of synthesized SGO and SGO catalyst after 5th recycle.*

A comparison indicates a reduction in the intensity of the first peak (2Θ=9.98) which is a characteristic peak of sulfonated graphene oxide. After the 5th cycle, a new peak appears at 2Θ=24.64, which indicates the partial formation of rGO. These results show a proportional reduction of the content of functional groups on SGO during the reaction.

The Raman spectra of both SGO and used SGO after the 5th run showed a characteristic D peak at 1346 cm^{-1} and G peak at 1582cm^{-1} (Figure III.A.6). The ratio of intensities of D and G band (I_D/I_G) of SGO and used SGO after 5th run displayed 0.91 and 0.93 respectively. However, the slight increased (I_D/I_G) ratio suggested that during successive runs partial formation of rGO has occurred through the restoration of some C=C bonds.

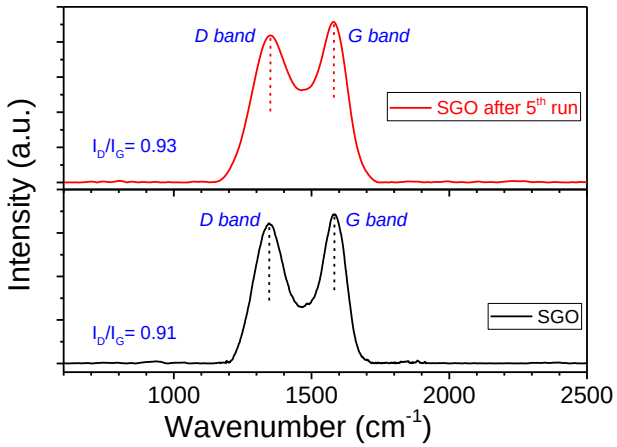

Figure III.A.6. *Raman spectra of SGO and SGO after 5th run.*

III.A.3.6. Recyclability experiment

To check the recyclability of the catalyst SGO, a model reaction between benzaldehyde, ethylacetoacetate, and hydroxylamine hydrochloride in presence of 100 mg of SGO was carried out. After the completion of the reaction, ethyl

acetate (20 ml) was added into the reaction mixture and centrifuged at 4000 rpm for 5 minutes. The supernatant liquid containing the product was decanted off and the process was repeated thrice.The recovered catalyst was then washed with water and acetone repeatedly to obtain dry SGO.

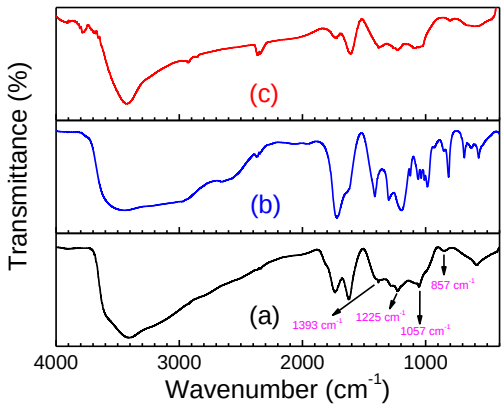

Figure III.A.7. *FTIR spectra of SGO (a) fresh (b) after 2nd run (c) after 5th run.*

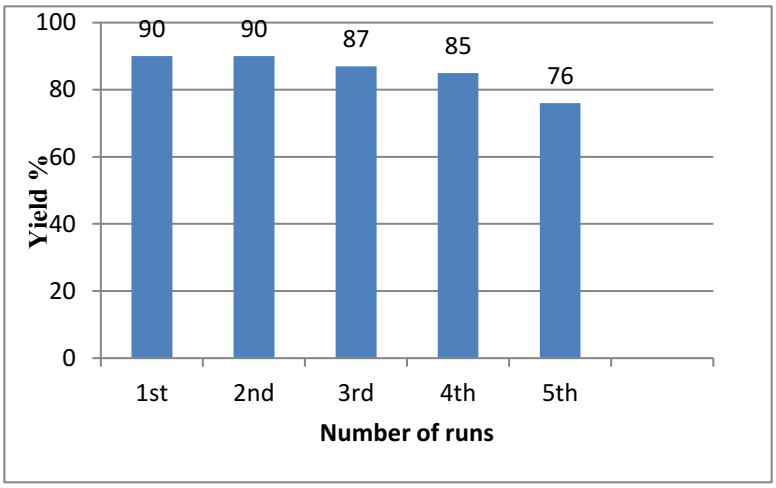

Figure III.A.8. *Recyclability experiment of catalyst SGO.*

The SGO catalyst could easily be separated from the reaction mixture by simple centrifugation and was found to retain its acidic property, even after 5 runs (Figure III.A.8). This was further supported by comparing the FTIR data of fresh SGO and recovered catalyst (Figure III.A.7). This may be attributed that the involvement of the nucleophilic oxo groups in SGO during the reaction may reduce the catalytic activity of SGO after the 5th run.

III.A.4. Conclusion

In conclusion, a green and efficient methodology for the synthesis of a variety of isoxazoles from commercially available aldehydes has been established. We have unfolded a new role of sulfonated graphene oxide as an efficient and heterogeneous carbocatalyst. SGO, itself is capable of furnishing the desired 3-methyl-4-(hetero)arylmethylene isoxazole-5(4*H*)-ones with excellent yield. It can be envisioned that such a cheap and robust solid acid catalyst SGO holds great potential for a wide range of acid-catalysed reactions.

III.A.5. Experimental section

III.A.5.1. General information

The reactions were monitored by TLC [carried out on Merck silica gel (60 F_{254}) by using UV light as the visualizing agent]. The HR-TEM characterization was performed on a JEM 2100F Jeol TEM. The PXRD data and Raman spectra were obtained from Bruker D8 Advanced X-ray Powder Diffractometer (Cu Kα radiation, λ = 1.54 Å) and Enspectr R532 (laser used 532 nm). NMR spectra of all the products were taken in $CDCl_3$/DMSO-d_6 (TMS as an internal standard) using a Bruker AV-300 spectrometer operating for ^1H at 300 MHz and ^{13}C at 75 MHz. ^1H NMR spectroscopic data are represented as follows: chemical shift (ppm), multiplicity (s = singlet, d= doublet, t = triplet, dd

= doublet of doublets, m = multiplet, brs = broad), integration, coupling constants in Hertz (Hz). ^{13}C NMR spectroscopic data are reported in ppm. Coupling constants were reported as J values in Hertz (Hz). The chemicals and reagents were purchased from Merck, Spectrochem, and Sigma-Aldrich.

III.A.5.2. General procedure for the preparation of the catalyst

SGO-1 and SGO-2 were prepared by the Tours method according to the literature [55]. In brief, a 9:1 mixture of concentrated H_2SO_4/ H_3PO_4 (360:40 ml) was taken in a beaker, after that graphite powder (3.0 g) was added slowly to it taking the whole system in an ice bath to keep the temperature below 20°C. $KMnO_4$ (9.0 g) was then added slowly in portions to the solutions. Afterward, the reaction mixture was heated to 50 °C and stirred for 12 h. After the reaction, the mixture was centrifuged (5000 rpm for 30 min), and the supernatant was decanted away. The remaining solid material was then washed with water successively, 30% HCl and ethanol to remove the remaining salt. The solid obtained was then dried to obtain the powdered graphene oxide [55] In SGO-2 9.0 g $KMnO_4$ is only replace by 18 g.

III.A.5.3. General procedure for the synthesis of 3-methyl-4 arylmethylene isoxazole-5(4*H*)-ones

25-ml RB was charged with benzaldehyde (1.0 mmol), ethyl acetoacetate (2.0 mmol), hydroxylamine hydrochloride (2.5 mmol), and 25mg of SGO. The mixture was allowed to stir at room temperature for adequate time (Table III.A.1) and the extent of the reaction was governed by thin-layer chromatography (TLC). The reaction mixture was extracted by ethyl acetate after completion of the reaction and further purified by Column Chromatography using silica gel 60-120 mesh to get the desired product.

III.A.5.4. Spectral data of compounds mentioned in Table III.A.2

4a. 4-benzylidene-3-methylisoxazol-5(4*H*)-one (Table III.A.2, entry 1) [28]

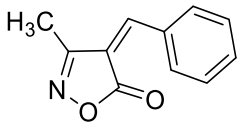

^{1}H NMR (300 MHz, $CDCl_3$) δ (ppm) 2.21 (s, 3H), 7.36 (s, 1H), 7.39-7.52 (m, 3H), 8.25-8.27 (d, 2H, *J*=7.5Hz);

^{13}C NMR (75 MHz, $CDCl_3$) δ (ppm) 11.67, 119.54, 128.95, 129.05, 130.55, 132.28, 133.86, 134.08, 150.23, 161.31, 167.96;

IR (KBr, cm^{-1}) bands 3431, 1741, 1590, 1347, 1218, 1107, 681.

4b. 4-(4-methoxybenzylidene)-3- methylisoxazol-5(4*H*)-one (Table III.A.2, entry 2) [28]

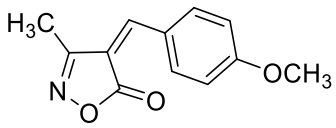

^{1}H NMR (300 MHz, $CDCl_3$) δ (ppm) 2.212 (s, 3H), 3.84 (s, 3H), 6.92-6.95 (d, 2H, *J*=8.1Hz), 7.27 (s, 1H), 8.35-8.38 (d, 2H, *J*= 8.4Hz);

^{13}C NMR (75 MHz, $CDCl_3$) δ (ppm) 11.75, 56.02, 114.11, 116.30, 117.14, 125.50, 132.08, 147.96, 152.33, 154.38, 162.74, 169.48.

4c. 4-(3-nitrobenzylidene)-3-methylisoxazol-5(4*H*)-one (Table III.A.2, entry 3) [36]

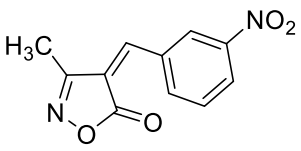

^{1}H NMR (300 MHz, DMSO-d_6) δ (ppm) 2.24 (s, 3H), 8.20-8.26 (t, 1H, *J*=8.1Hz), 2.57-2.59 (d, 1H, *J*=7.5Hz), 8.73-8.76 (d, 1H, *J*=7.8Hz), 8.86 (s, 1H), 8.95 (s, 1H);

^{13}C NMR (75 MHz, DMSO-d_6) δ (ppm) 11.53, 121.79, 124.65, 125.04, 125,65, 130.24, 131.06, 133.31, 135.92, 149.12, 162.21.

4d. 3-methyl-4-(4-methylbenzylidene)isoxazol-5(4*H*)-one (Table III.A.2, entry 4) [28]

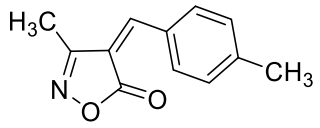

^{1}H NMR (300 MHz, DMSO-d_6) δ (ppm) 2.34 (s, 3H), 2.50 (s, 3H), 7.35-7.37 (d, 2H, *J*=9.2Hz), 7.80 (s, 1H), 8.27-8.29 (d, 2H, *J*= 8.4 Hz);

^{13}C NMR (75 MHz, DMSO-d_6) δ (ppm) 11.82, 21.62, 116.12, 119.25, 128.79, 130.05, 135.92, 152.01, 162.78, 168.47;

IR (KBr, cm^{-1}) bands 3415, 1730, 1585, 1356, 1203, 1109, 685.

4e. 4-(4-chlorobenzylidene)-3-methylisoxazol-5(4*H*)-one (Table III.A.2, entry 5) [36]

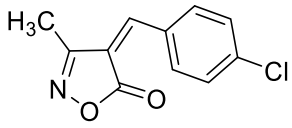

^{1}H NMR (300 MHz, DMSO-d_6) δ (ppm) 2.50 (s, 3H), 6.93-6.96 (d, 2H, *J*=7.5Hz), 7.57 (s, 1H), 8.20-8.23 (d, 2H, *J*=8.1Hz);

^{13}C NMR (75 MHz, DMSO-d_6) δ (ppm) 11.71, 116.27, 116.91, 119.57, 119.94, 125.19, 132.42, 137.21, 145.52, 160.08, 162.62.

4g. 3-methyl-4-(furan-3-ylmethylene)isoxazol-5(4*H*)-one (Table III.A.2, entry 7) [4]

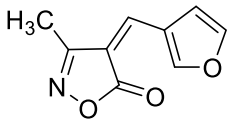

^{1}H NMR (300 MHz, DMSO-d_6) δ (ppm) 2.23 (s, 3H), 6.90-6.93 (d, 2H, *J*=8.4Hz), 7.07 (s, 1H), 8.39-8.41 (d, 2H, *J*=8.4Hz);

^{13}C NMR (75 MHz, DMSO-d_6) δ (ppm) 11.70, 114.31, 116.59, 125.02, 137.99, 151.84, 162.64, 164.28, 169.25;

IR (KBr, cm^{-1}) bands 3402, 1730, 1553, 1388, 1295, 1177

4h. 4-(4-hydroxybenzylidene)-3-methylisoxazol-5(4*H*)-one (Table III.A.2, entry 8) [36]

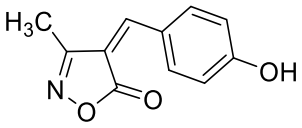

^{1}H NMR (300 MHz, DMSO-d_6) δ (ppm) 2.20 (s, 3H), 6.90-6.93 (d, 2H, *J*=8.4Hz), 7.70 (s, 1H), 8.31-8.41 (d, 2H, *J*=8.4Hz), 11.07 (s, 1H);

^{13}C NMR (75 MHz, DMSO-d_6) δ (ppm) 11.75, 114.11, 116.30, 125.50, 132.08, 147.96, 154.38, 162.74, 168.48.

4i. 3-methyl-4-(naphthalen-2-ylmethylene)isoxazol-5(4*H*)-one (Table III.A.2, entry 9) [56]

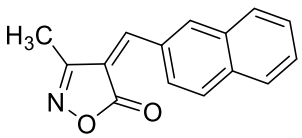

^{1}H NMR (300 MHz, DMSO-d_6) δ (ppm) 2.31 (s, 3H), 7.65-7.70 (m, 2H), 8.02-8.07 (t, 3H), 8.55-8.58 (d, 2H, *J*=8.1Hz), 8.90 (s, 1H);

^{13}C NMR (75 MHz, DMSO-d_6) δ (ppm) 11.80, 119.19, 127.73, 128.24, 128.55, 128.79, 130.09, 130.79, 132.65, 135.49, 137.06, 146.18 151.95, 162.75, 168.45;

IR (KBr, cm^{-1}) bands 3431, 1732, 1558, 1388, 1290, 1107; HRMS-ESI (m/z) calcd for $C_{15}H_{11}NO_2$ $[M+H]^+$ 238.0878 found 238.0856.

4k. 3-methyl-4-(thiophen-3-ylmethylene)isoxazol-5(4*H*)-one (Table III.A.2, entry 11) [36]

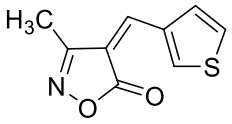

^{1}H NMR (300 MHz, DMSO-d_6) δ 2.26 (s, 3H), 7.38-7.40 (t, 1H, *J*=4.4 Hz), 8.22-8.23 (d, 1H, *J*=3.6 Hz), 8.27 (s, 1H), 8.31-8.33 (d, 1H, *J*=4.8 Hz);

^{13}C NMR (75 MHz, DMSO-d_6) δ (ppm) 11.59, 113.54, 129.50, 136.66, 141.69, 142.17, 143.57, 162.15, 169.01.

4m. 4-(4-(dimethylamino)benzylidene)-3-methylisoxazol-5(4*H*)-one (Table III.A.2, entry 13) [30]

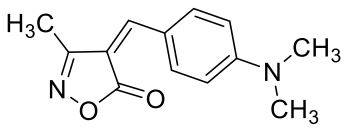

^{1}H NMR (300 MHz, DMSO-d_6) δ (ppm) 2.20 (s, 3H), 3.16 (s, 3H), 3.35 (s, 3H), 6.83-6.86 (d, 2H, *J*=8.7Hz), 7.60 (s, 1H), 8.43-8.46 (d, 2H, *J*=8.1Hz);

^{13}C NMR (75 MHz, DMSO-d_6) δ (ppm) 11.70, 52.41, 109.46, 112.09, 121.43, 135.04, 150.35, 154.51, 162.59, 170.29;

IR (KBr, cm^{-1}) bands 3444, 1715, 1558, 1382, 1203, 994, 668

4n. 4-(2-hydroxybenzylidene)-3-methylisoxazol-5(4*H*)-one (Table III.A.2, entry 14) [36]

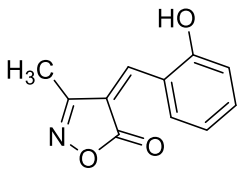

^{1}H NMR (300 MHz, DMSO-d_6) δ (ppm) 2.21 (s, 3H), 6.91-7.02 (m, 2H), 7.44-7.57 (m, 1H), 8.09 (s, 1H), 8.72-8.74 (d, 1H, *J*=8.1Hz), 9.96 (s, 1H);

^{13}C NMR (75 MHz, DMSO-d_6) δ (ppm) 11.68, 116.61, 116.91, 119.57, 119.94, 132.77, 137.22, 145.51, 160.10, 162.53, 168.45;

IR (KBr, cm-1) bands 3431, 1730, 1564, 1284, 1089, 776

4p. 4-(4-hydroxy-3-methoxybenzylidene)-3-methylisoxazol-5(4*H*)-one (Table III.A.2, entry 16) [24]

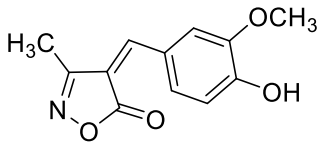

^{1}H NMR (300 MHz, DMSO-d_6) δ (ppm) 2.23 (s, 3H), 3.83 (s, 3H), 6.95 (s, 1H), 7.57-7.89 (m, 2H), 8.50 (s, 1H), 10.41 (s, 1H);

^{13}C NMR (75 MHz, DMSO-d_6) δ (ppm) 11.71, 56.02, 114.17, 116.27, 117.19, 125.51, 132.42, 147.95, 152.30, 154.31, 162.73, 169.41;

IR (KBr, cm^{-1}) bands 3416, 1730, 1557, 1284, 1023, 685

4q. 3-methyl-4-((E)-3-phenylallylidene)isoxazol-5(4*H*)-one (Table III.A.2, entry 17) [36]

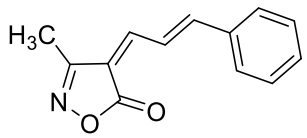

^{1}H NMR (300 MHz, DMSO-d_6) δ (ppm) 2.248 (s, 3H), 6.924-7.014 (m, 4H), 7.484-7.505 (d, 2H, *J*=6.3Hz), 8.079 (s, 1H), 8.706-8.733 (d, 1H, *J*=8.1Hz);

^{13}C NMR (75 MHz, DMSO-d_6) δ (ppm) 11.66, 116.61, 116.91, 119.57, 119.94, 125.19, 132.76, 137.21, 145.52, 160.04, 162.62, 168.73.

4r. 3-methyl-4-(3-methylbenzylidene)-3-methylisoxazol-5(4*H*)-one (Table III.A.2, entry 18)

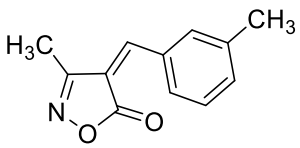

^{1}H NMR (400 MHz, DMSO-d_6) δ (ppm) 2.26 (s, 3H), 2.34-2.36 (s, 3H), 7.45-7.47 (m, 2H), 7.90 (s, 1H), 8.19 (s, 1H), 8.23-8.25 (m, 1H);

^{13}C NMR (100 MHz, DMSO-d_6) δ (ppm) 11.74, 21.31, 119.10, 128.84, 130.18, 132.94, 135.58, 135.13, 138.60, 152.29, 162.69, 168.30;

HRMS-ESI (m/z) calcd for $C_{12}H_{11}NO_2$ $[M+H]^+$ 202.0878 found 202.0825.

4s. 4-((1H-indol-3-yl)methylene)-3-methylisoxazol-5(4*H*)-one (Table III.A.2, entry 19) [36]

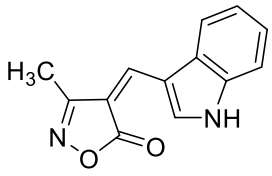

^{1}H NMR (400 MHz, DMSO-d_6) δ (ppm) 2.31 (s, 3H), 7.29-7.32 (m, 2H), 7.56-7-59 (m, 1H), 8.12-8.16 (m, 2H), 9.48-9.49 (d, 2H, *J*=3.2Hz), 12.77 (br, 1H);

^{13}C NMR (100 MHz, DMSO-d_6) δ (ppm) 11.66, 109.32, 113.13, 113.59, 119.30, 123.04, 124.42, 128.43, 136.84, 138.96, 140.93, 162.17, 170.86.

III.A.5.5. Scanned copies of ^{1}H, ^{13}C NMR and HRMS spectra of synthesized compounds

Figure III.A.9. *Scanned copy of ^{1}H and ^{13}C NMR spectra of 4-benzylidene-3-methylisoxazol-5(4H)-one.*

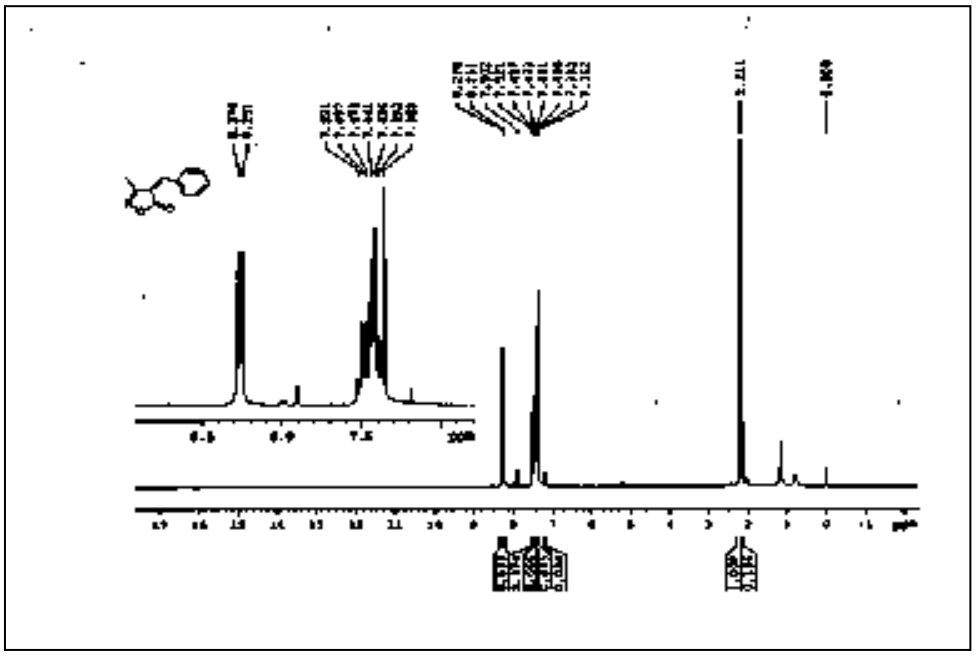

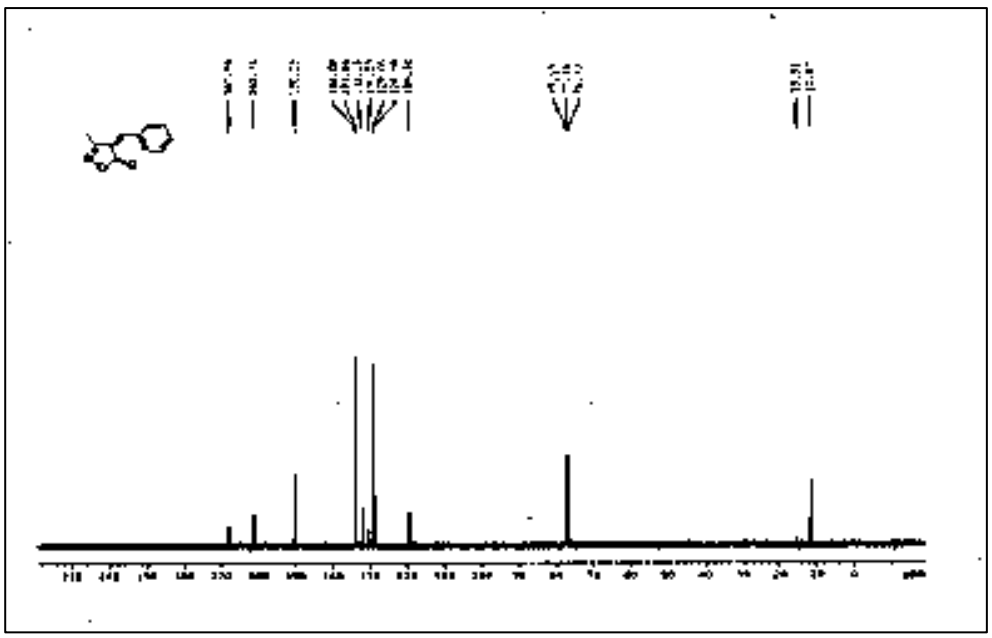

Figure III.A.10. *Scanned copy of ^{1}H and ^{13}C NMR spectra of 4-(4-methoxybenzylidene)-3- methylisoxazol-5(4H)-one.*

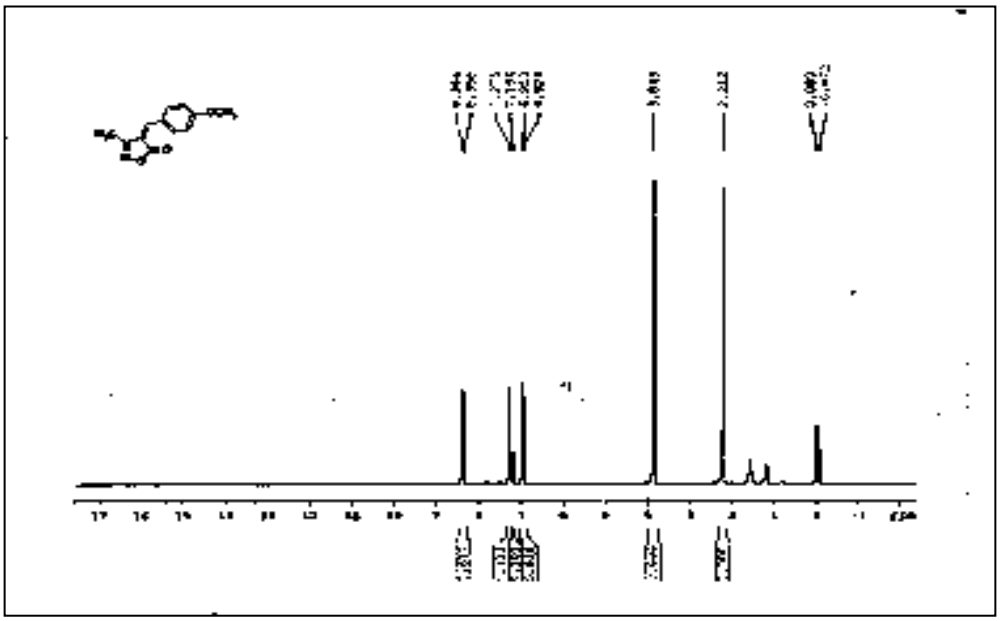

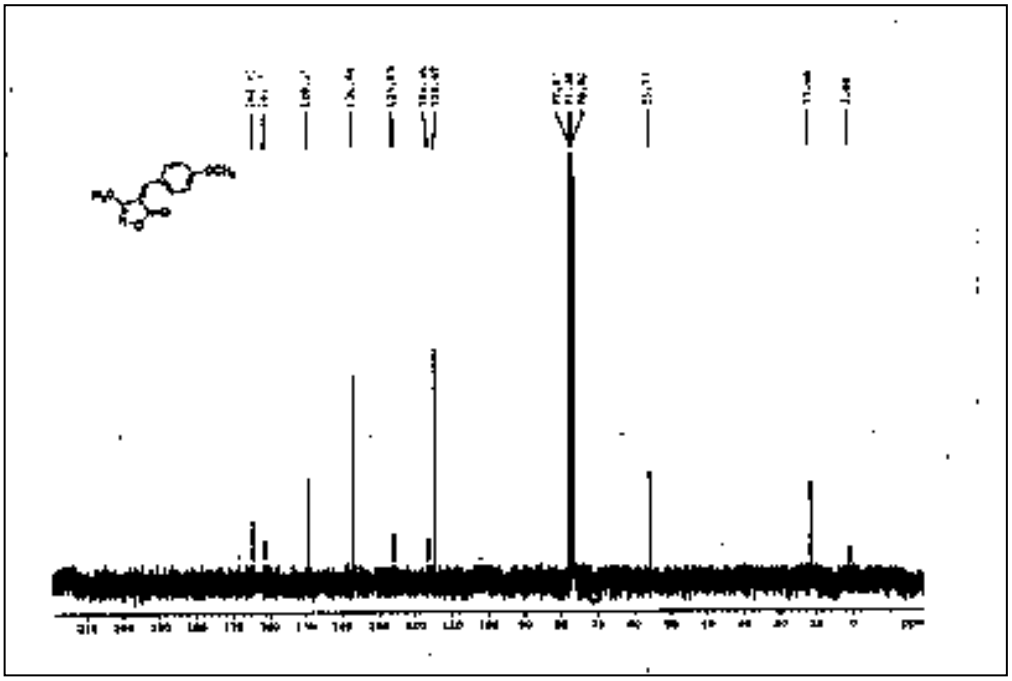

Figure III.A.11. *Scanned copy of ^{1}H and ^{13}C NMR spectra of 4-(3-nitrobenzylidene)-3-methylisoxazol-5(4H)-one.*

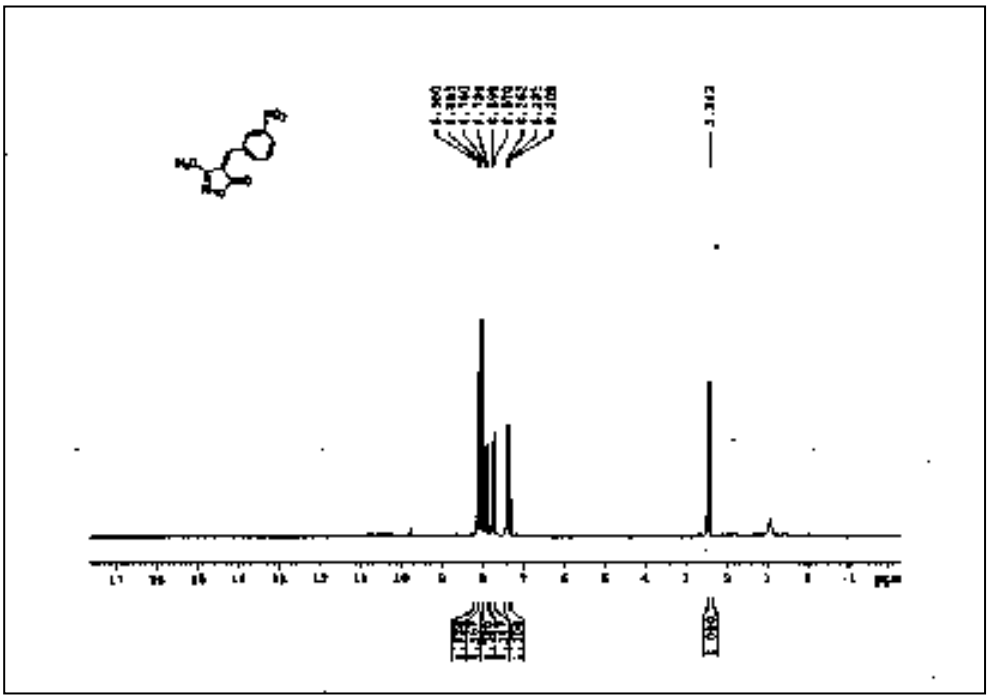

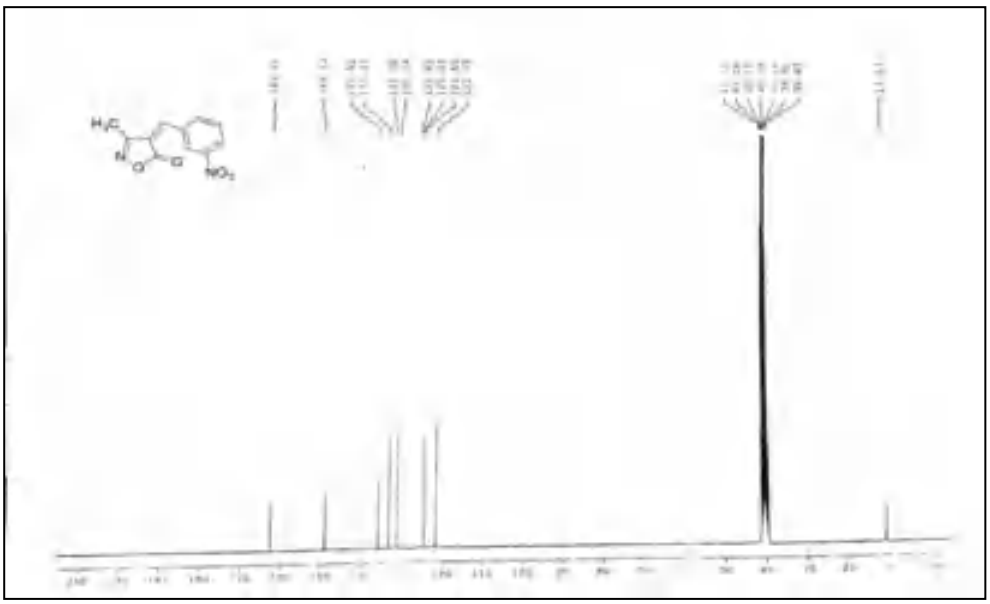

Figure III.A.12. *Scanned copy of ^{1}H and ^{13}C NMR spectra of . 4-(4-chlorobenzylidene)-3-methylisoxazol-5(4H)-one.*

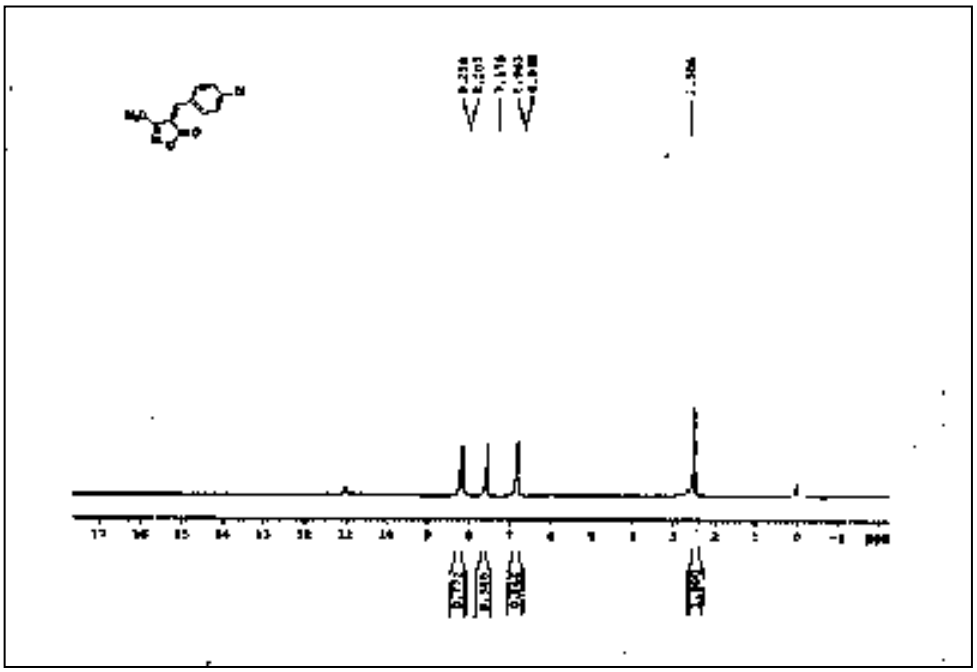

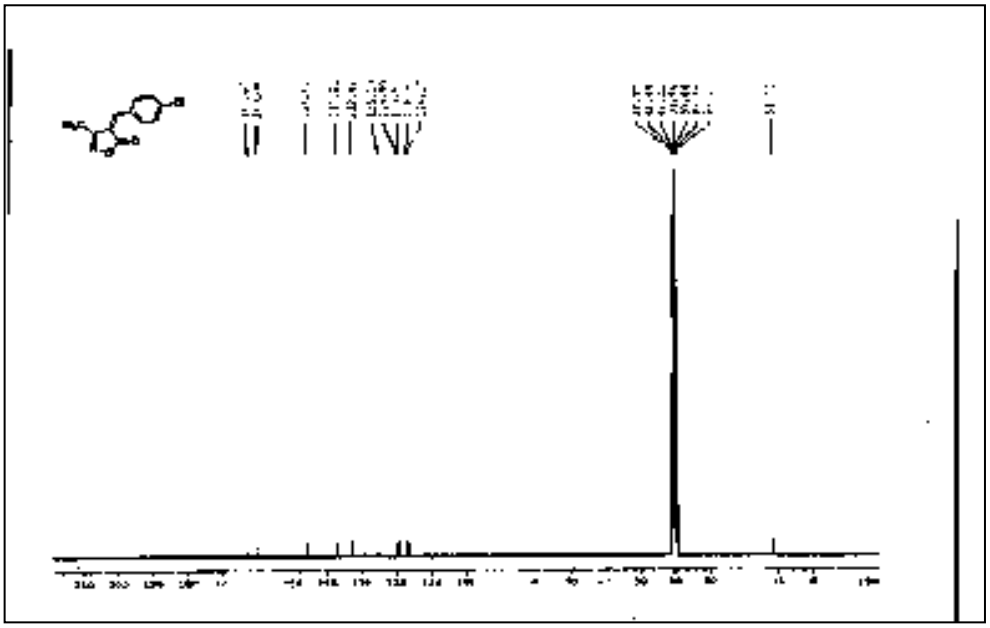

Figure III.A.13. *Scanned copy of ^{1}H and ^{13}C NMR spectra of 3-methyl-4-(furan-3-ylmethylene)isoxazol-5(4H)-one.*

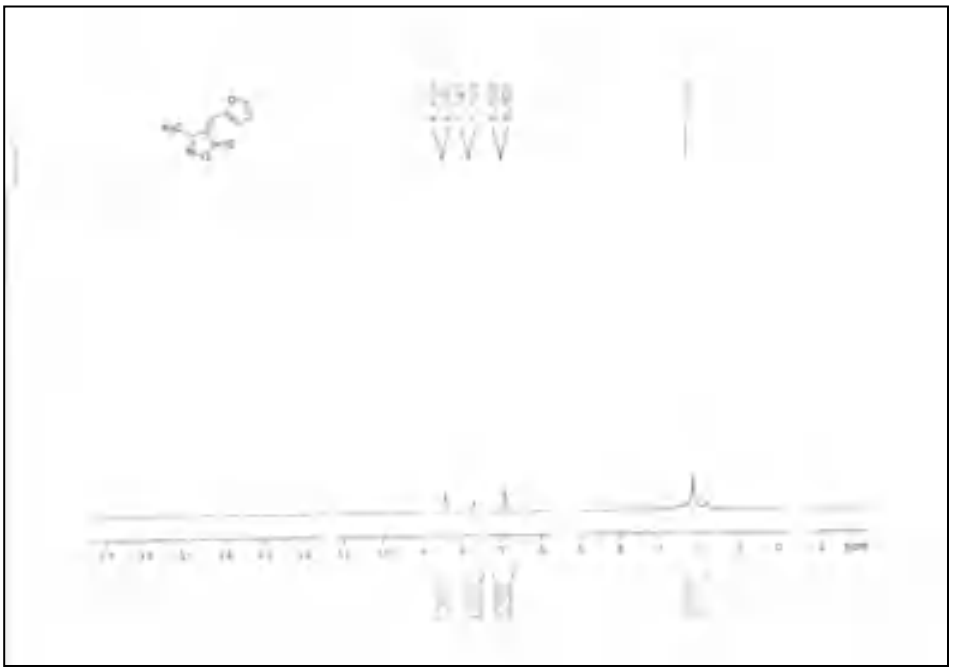

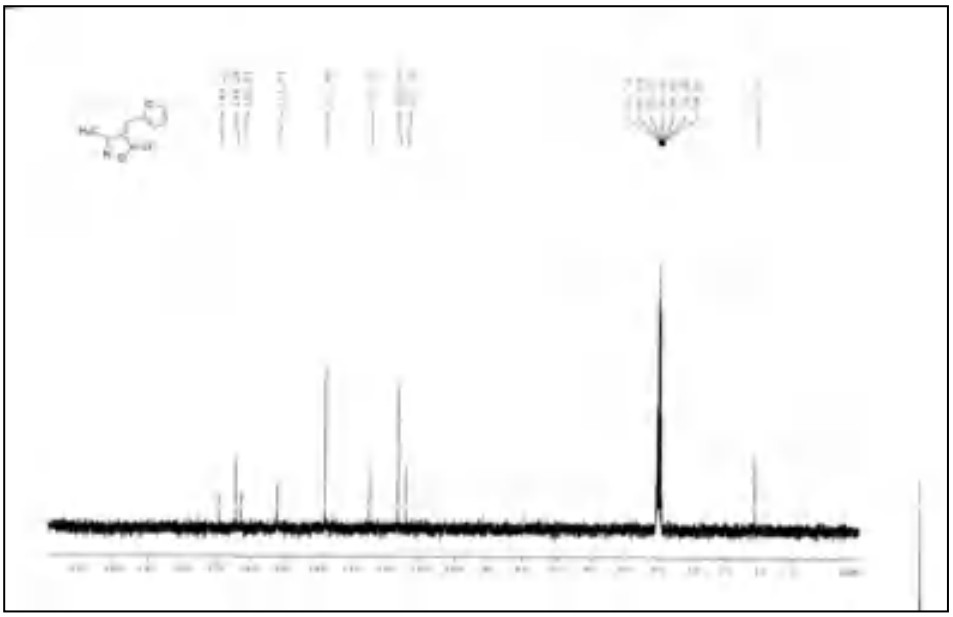

Figure III.A.14. *Scanned copy of ^{1}H and ^{13}C NMR spectra of 4-(4-hydroxybenzylidene)-3-methylisoxazol-5(4H)-one.*

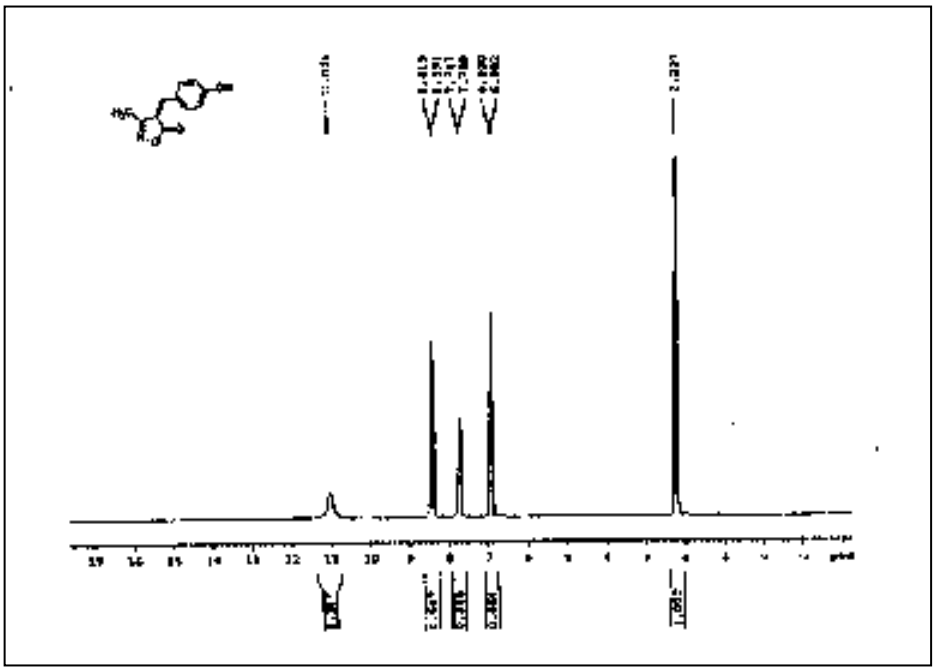

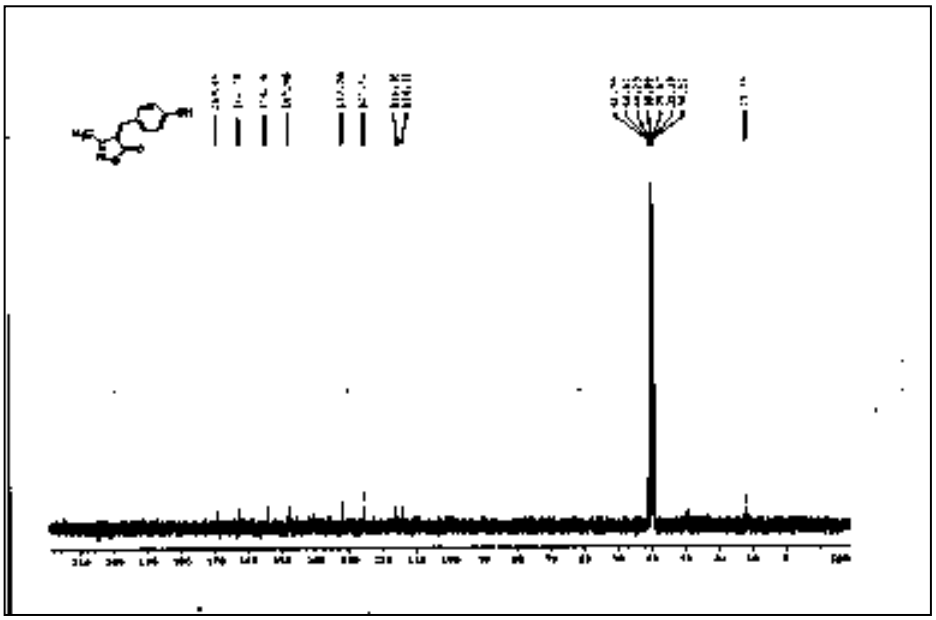

Figure III.A.15. *Scanned copy of ^{1}H and ^{13}C NMR spectra of 3-methyl-4-(naphthalen-2-ylmethylene)isoxazol-5(4H)-one.*

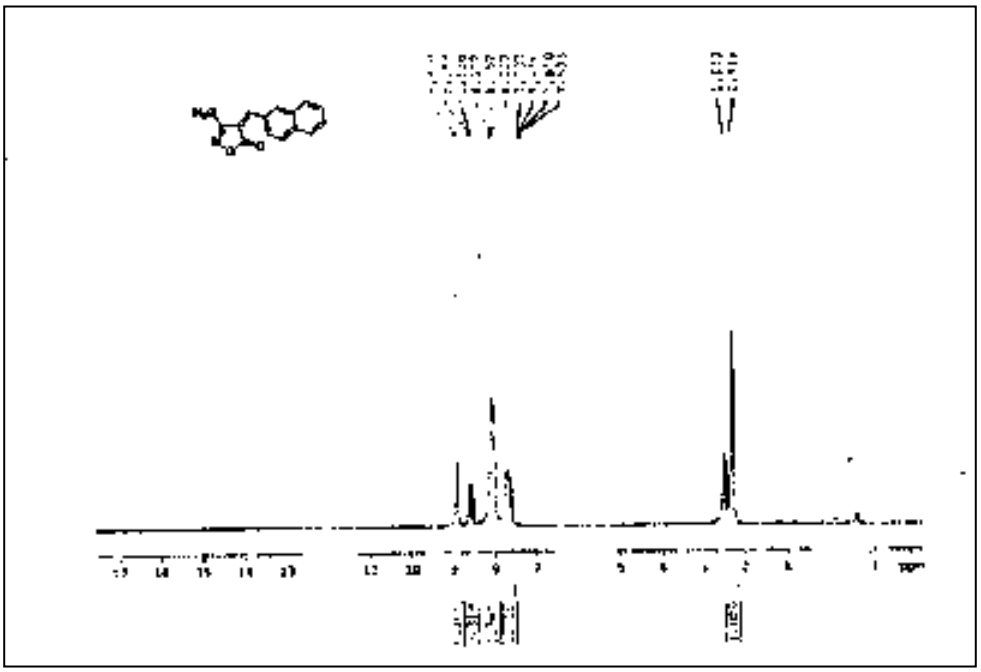

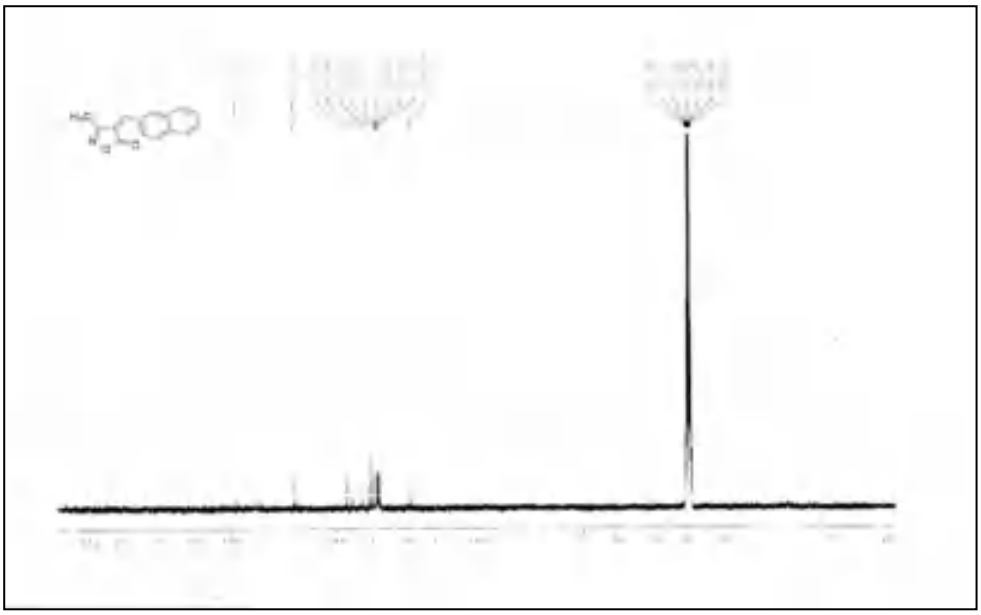

Figure III.A.16. *Scanned copy of ^{1}H and ^{13}C NMR spectra of 3-methyl-4-(naphthalen-2-ylmethylene)isoxazol-5(4H)-one.*

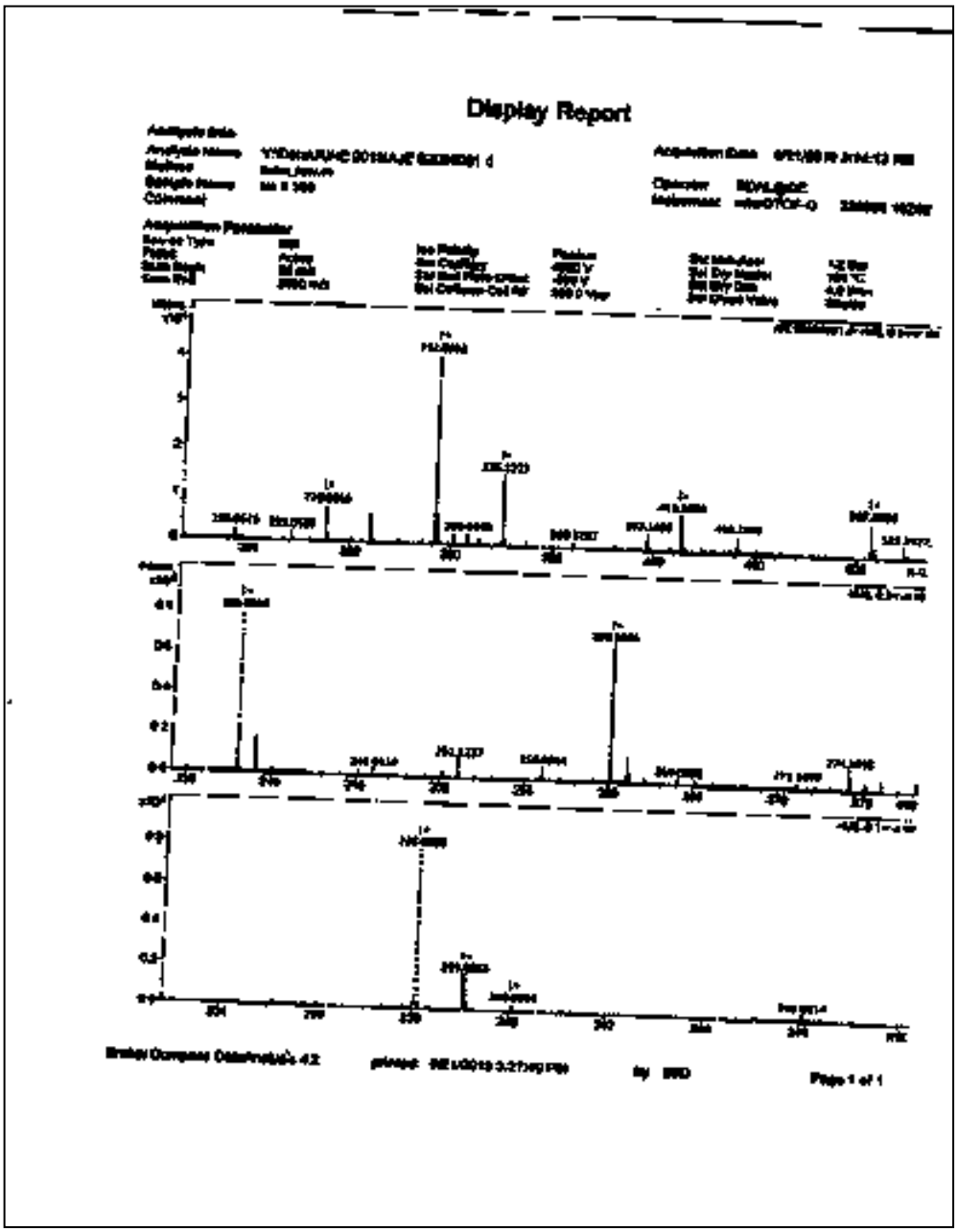

Figure III.A.17. *Scanned copy of ^{1}H and ^{13}C NMR spectra of 3-methyl-4-(thiophen-3-ylmethylene)isoxazol-5(4H)-one.*

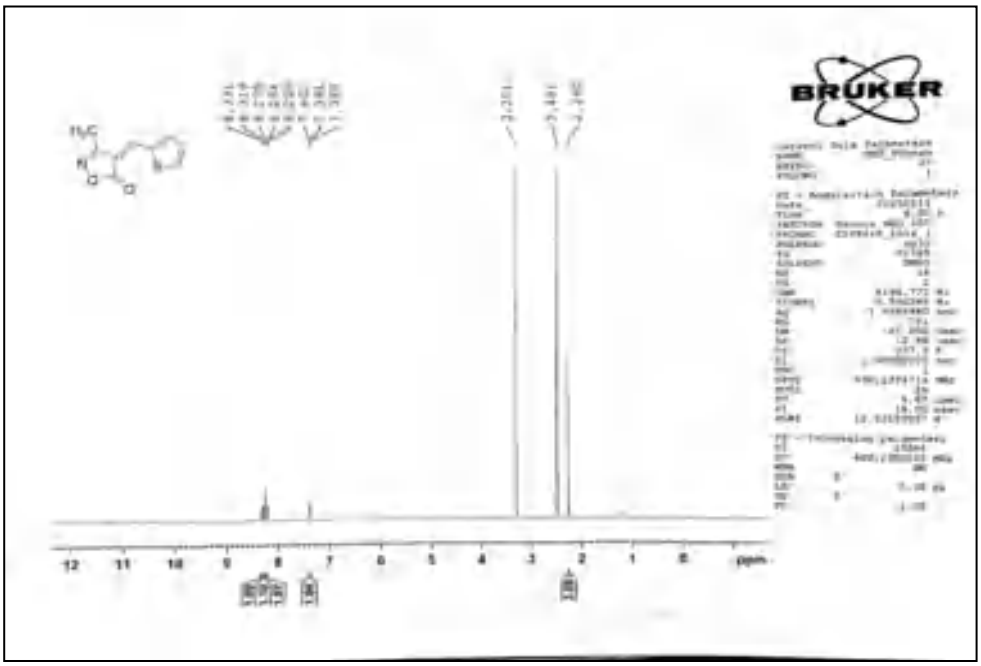

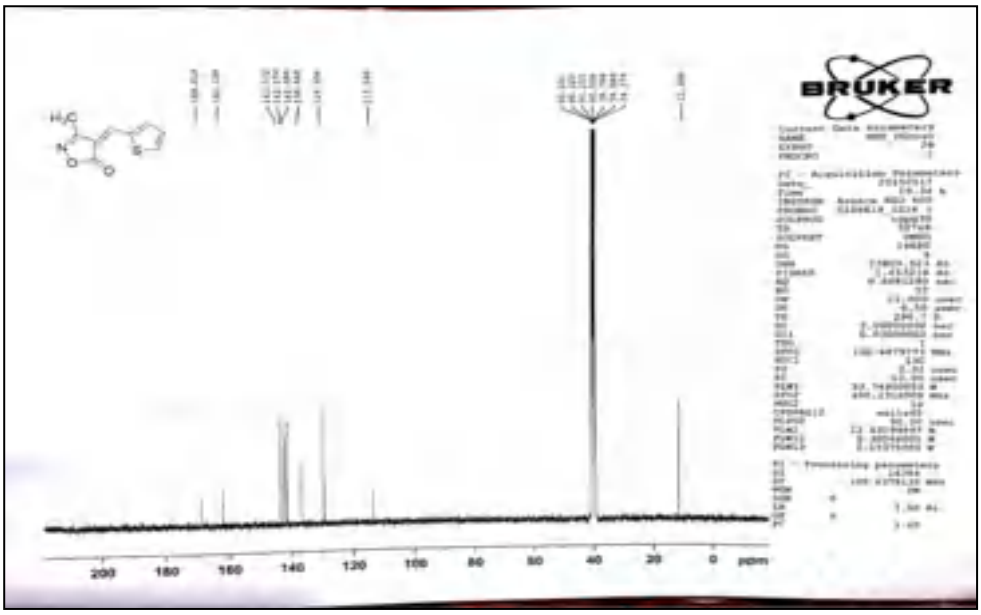

Figure III.A.18. *Scanned copy of ^{1}H and ^{13}C NMR spectra of 4-(4-(dimethylamino)benzylidene)-3-methylisoxazol-5(4H)-one.*

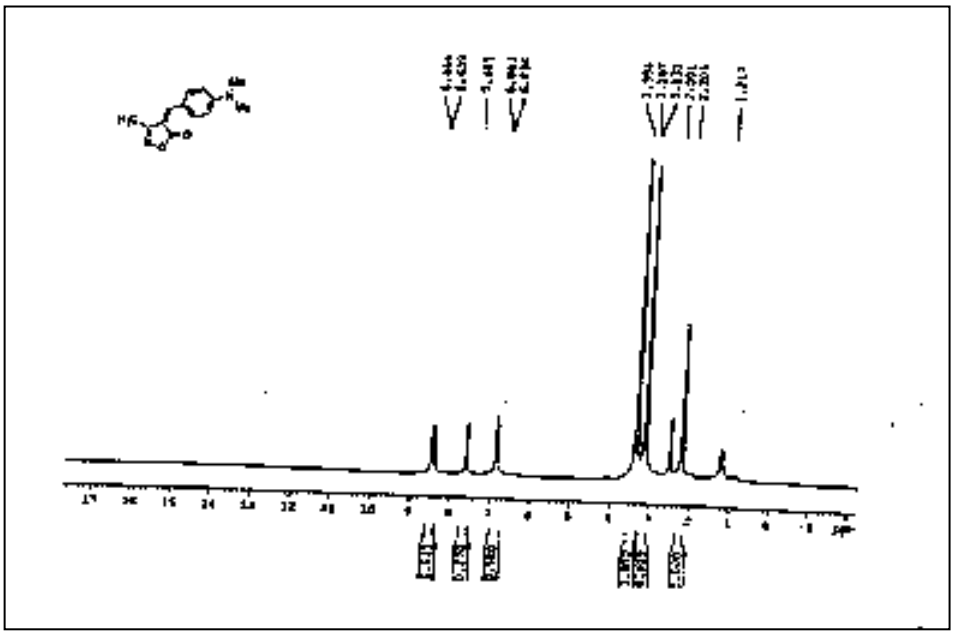

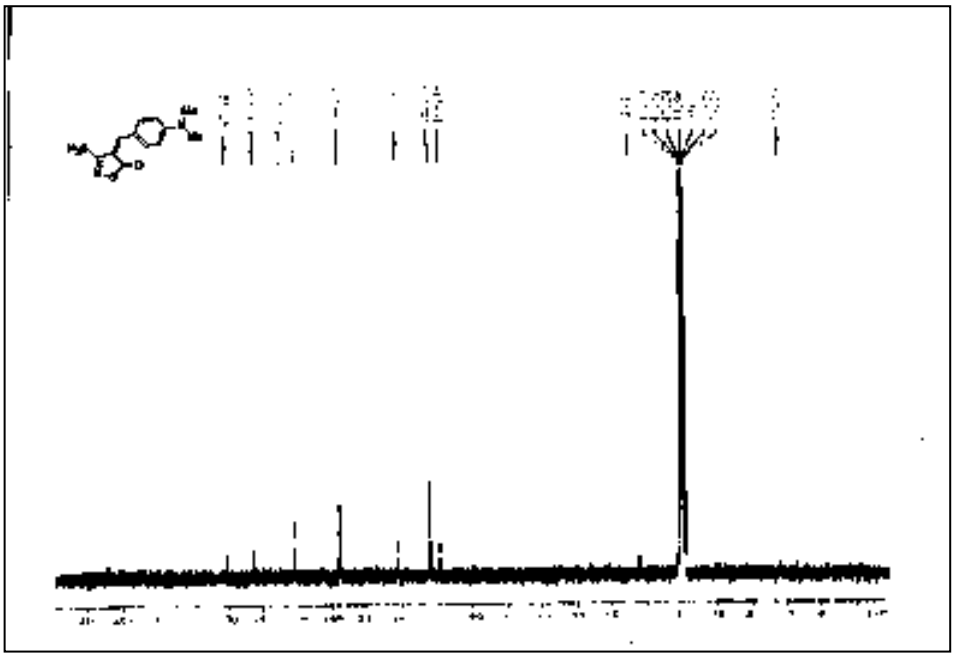

Figure III.A.19. *Scanned copy of ^{1}H and ^{13}C NMR spectra of 4-(2-hydroxybenzylidene)-3-methylisoxazol-5(4H)-one.*

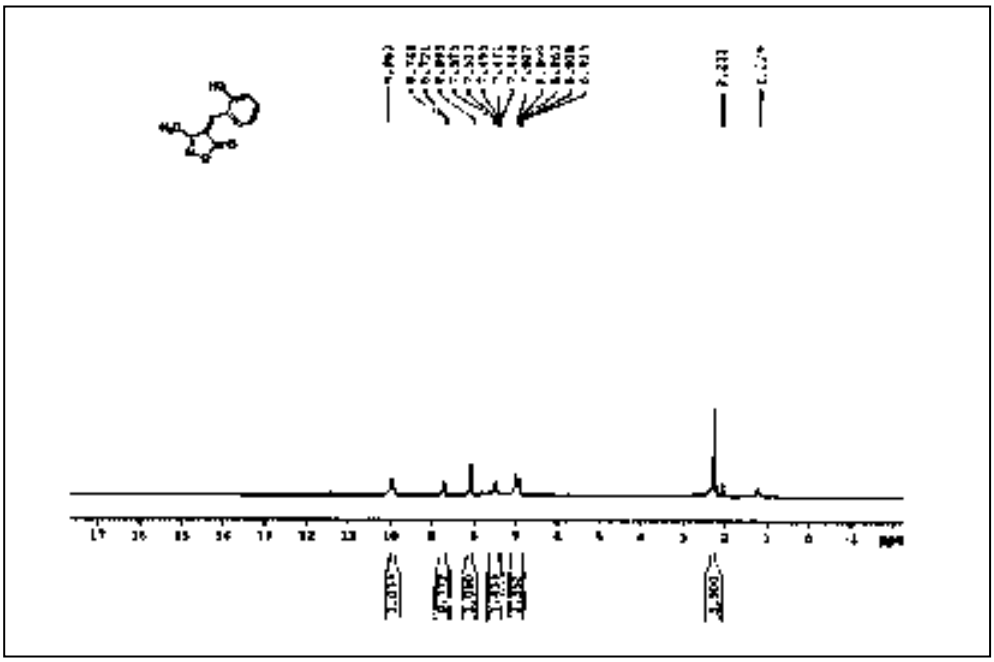

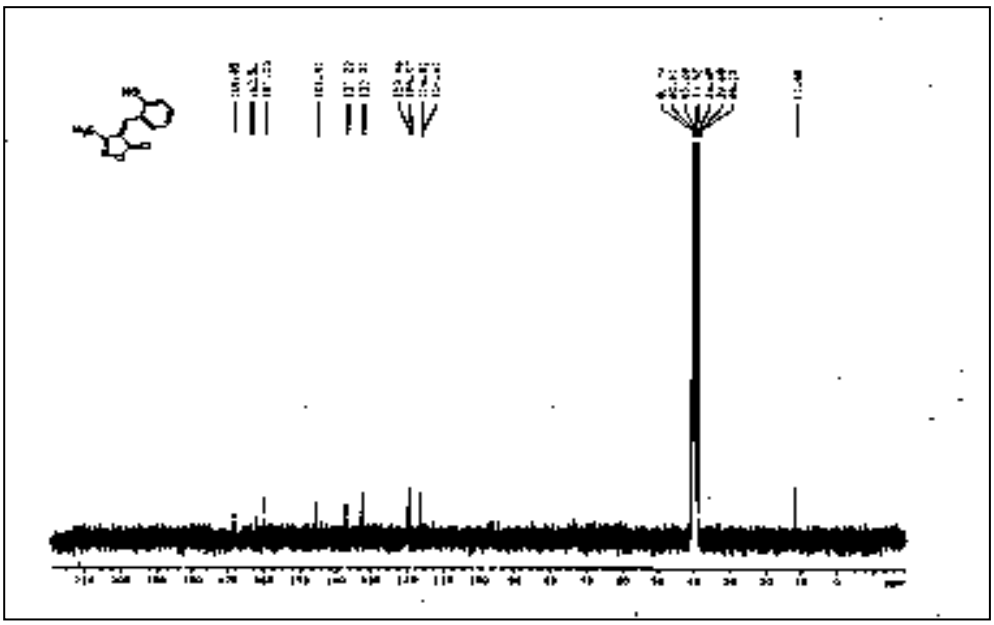

Figure III.A.20. *Scanned copy of ^{1}H and ^{13}C NMR spectra of 4-(4-hydroxy-3-methoxybenzylidene)-3-methylisoxazol-5(4H)-one.*

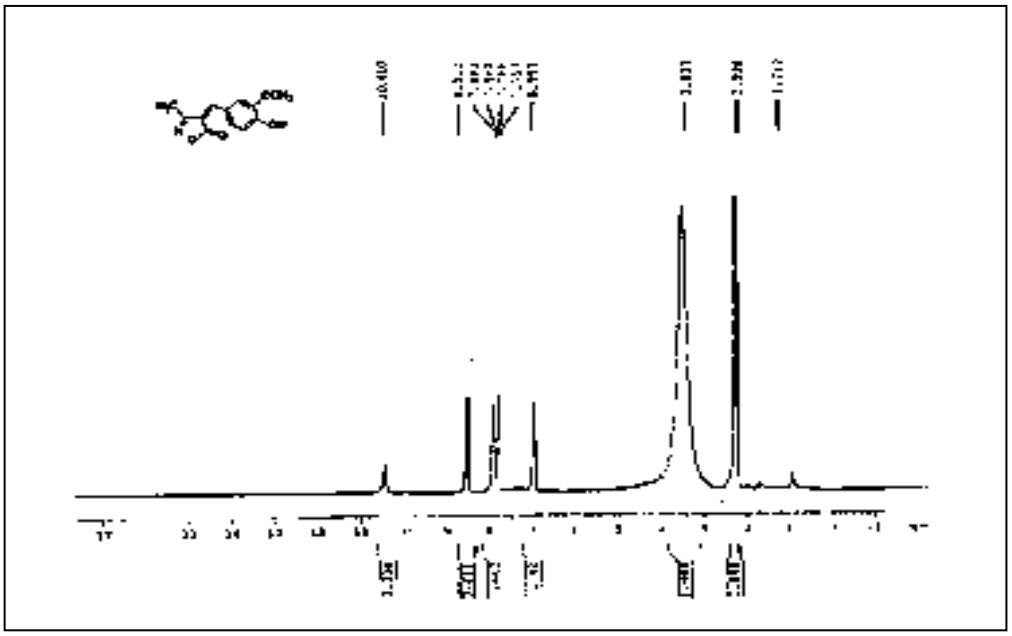

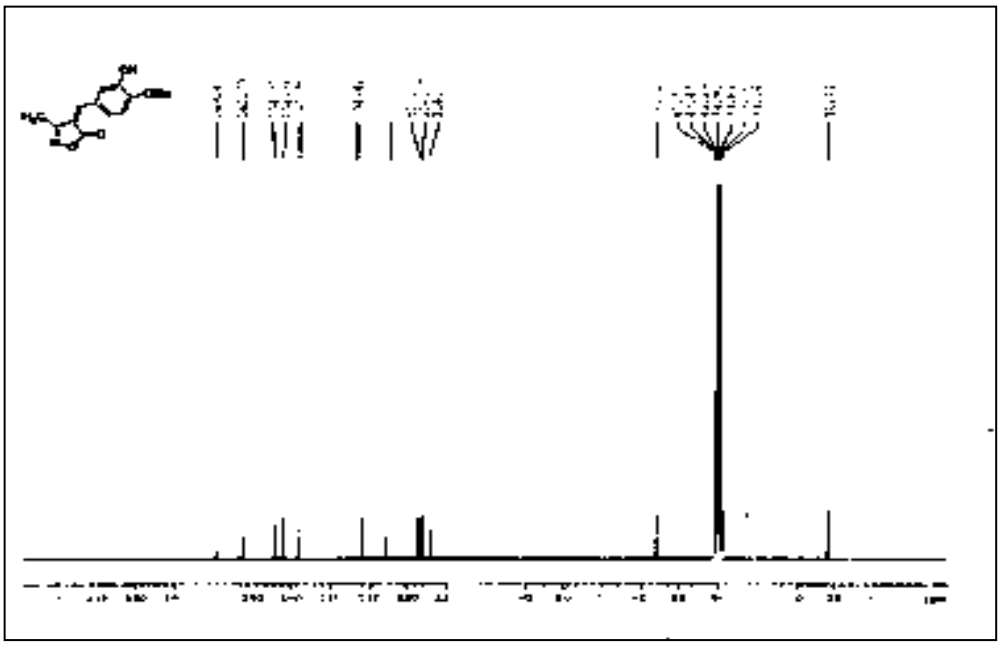

Figure III.A.21. *Scanned copy of ^{1}H and ^{13}C NMR spectra of 3-methyl-4-((E)-3-phenylallylidene)isoxazol-5(4H)-one.*

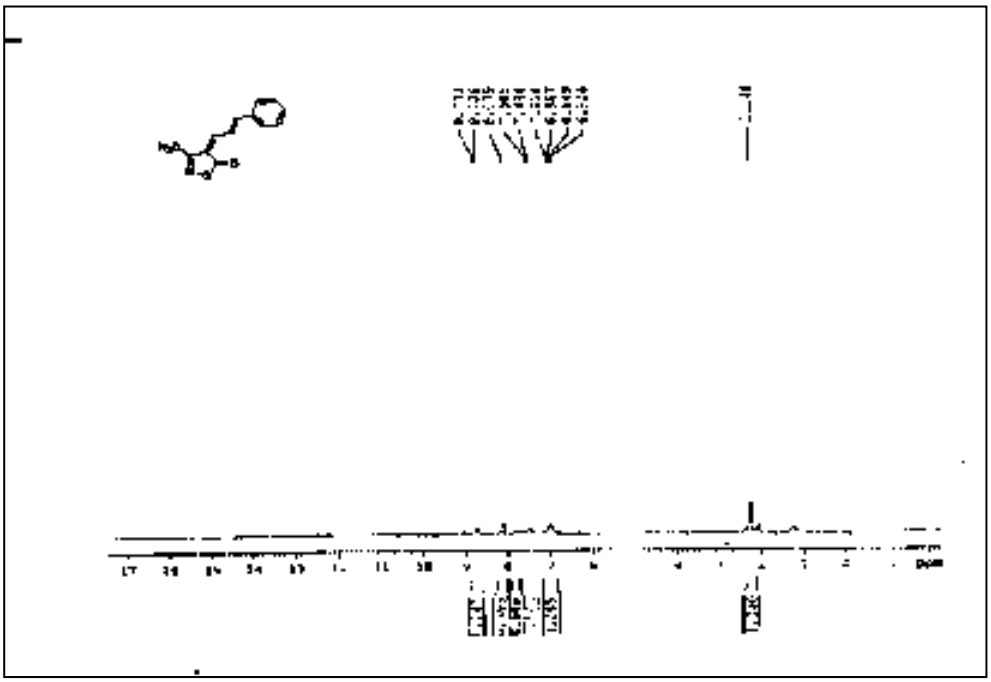

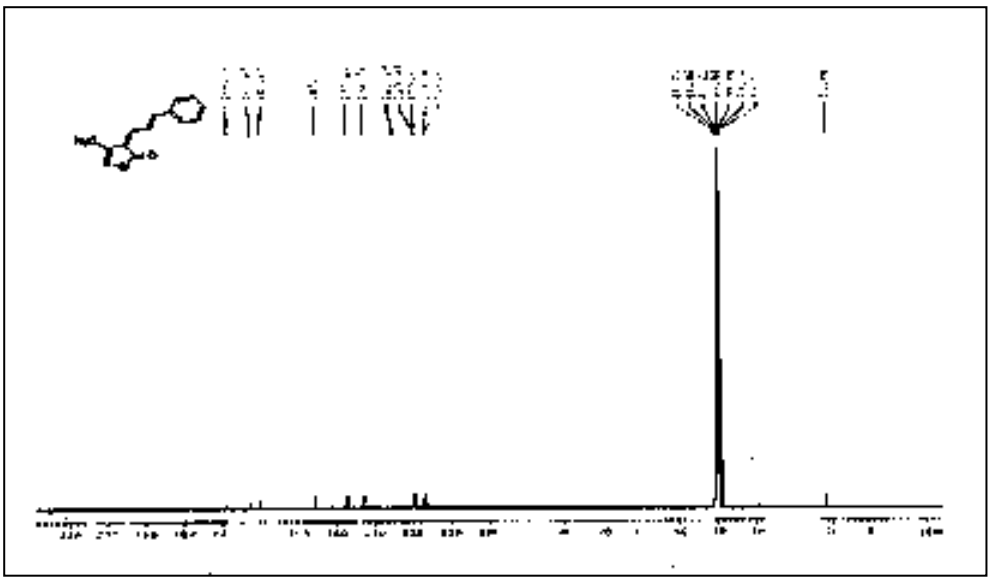

Figure III.A.22. *Scanned copy of ^{1}H and ^{13}C NMR spectra of 3-methyl-4-(3-methylbenzylidene)-3-methylisoxazol-5(4H)-one.*

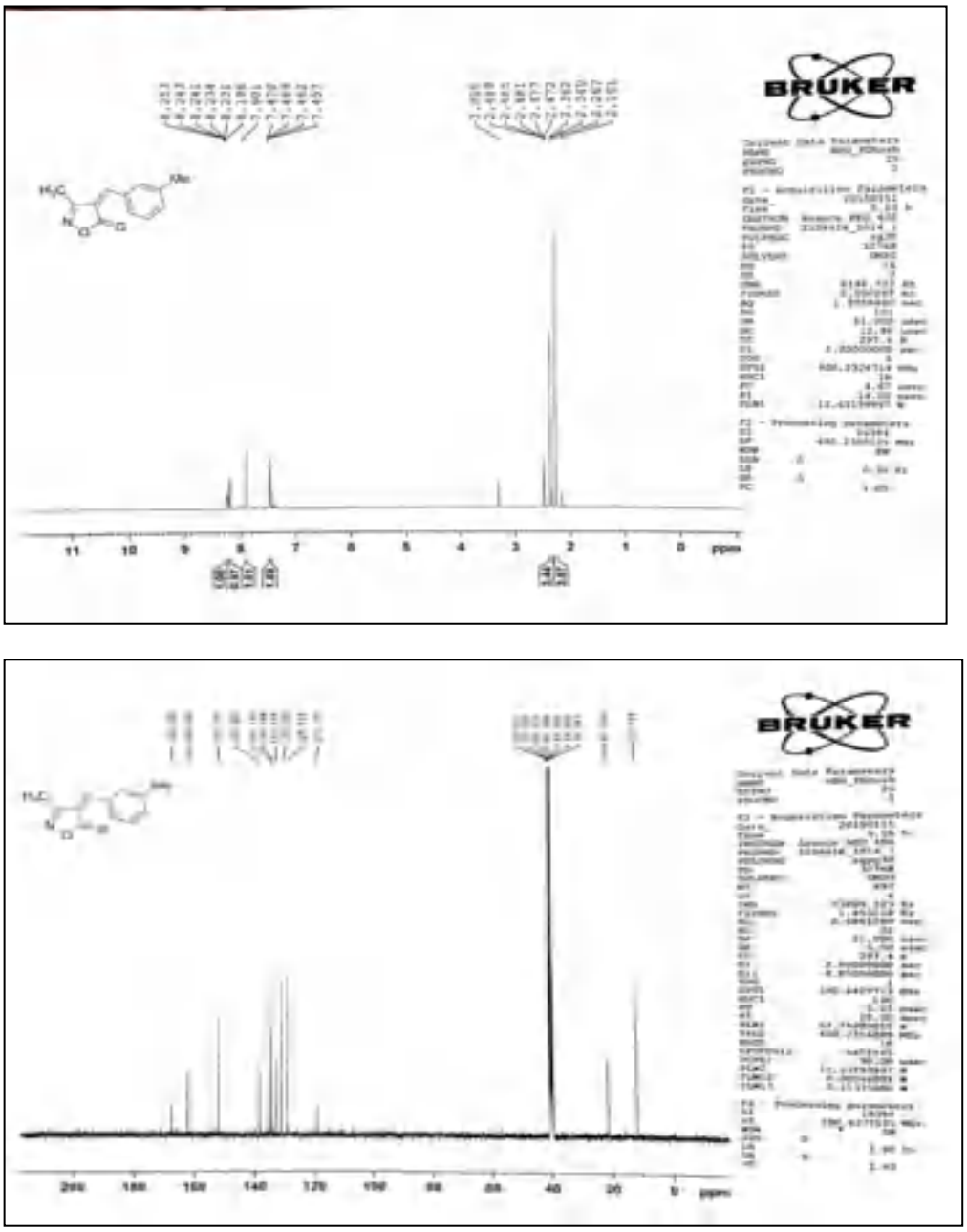

Figure III.A.23. *Scanned copy of [1]HRMS spectra of 3-methyl-4-(3-methylbenzylidene)-3-methylisoxazol-5(4H)-one.*

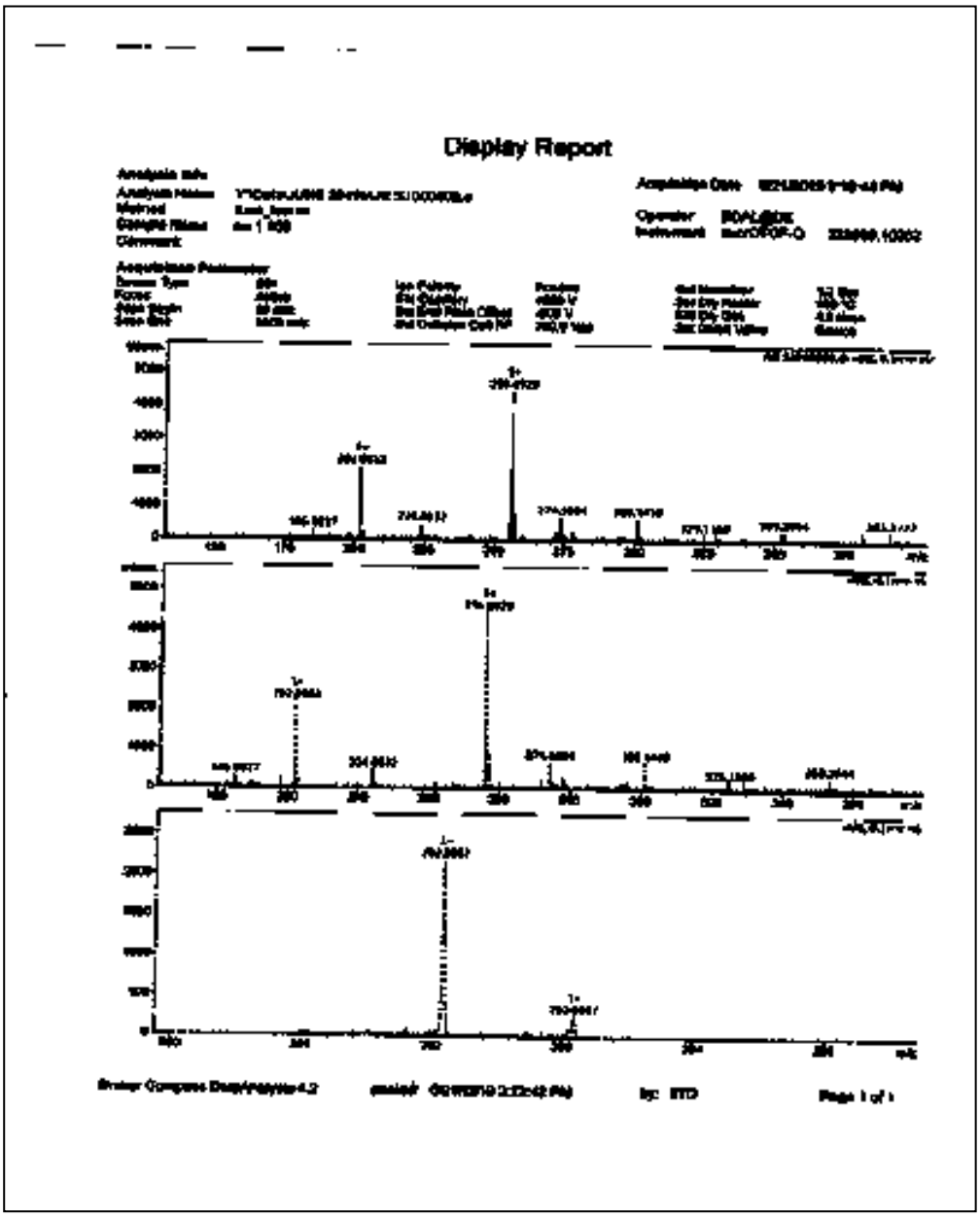

Figure III.A.24. *Scanned copy of ^{1}H and ^{13}C NMR spectra of 4-((1H-indol-3-yl)methylene)-3-methylisoxazol-5(4H)-one.*

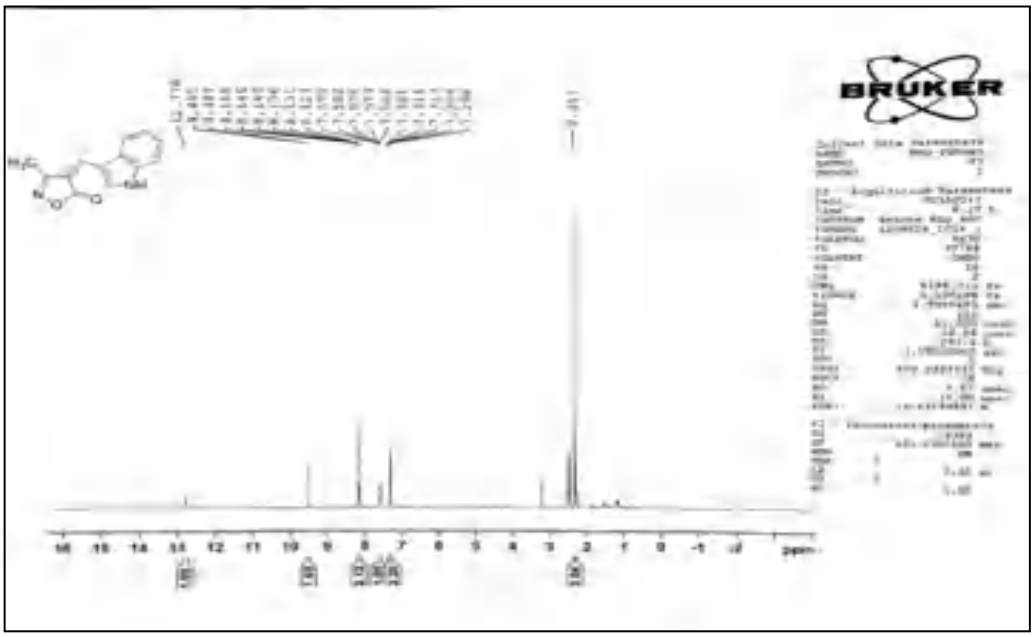

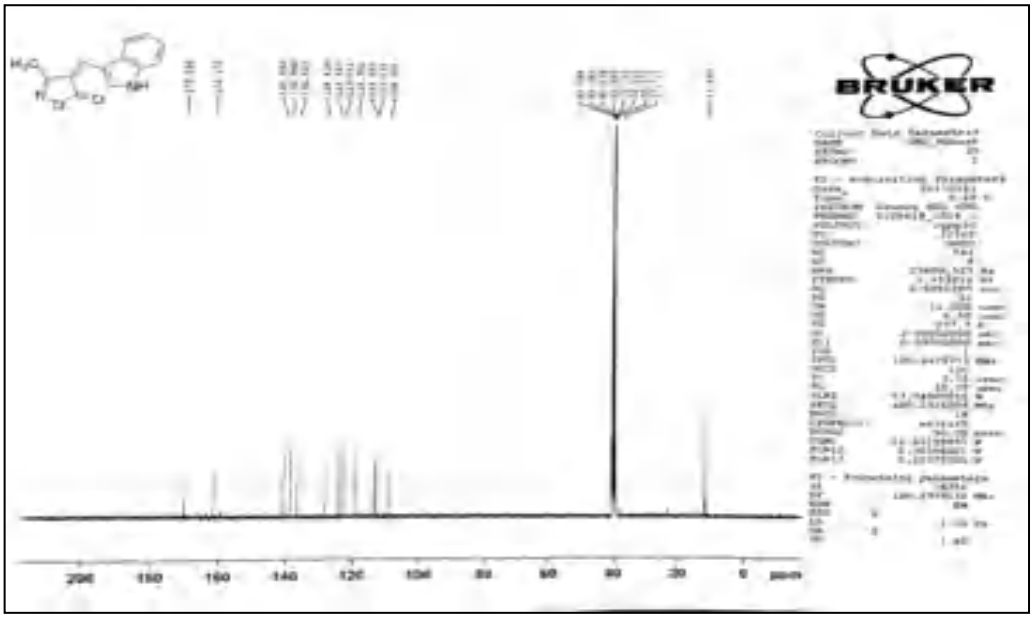

III.A.6. References

References are given in Bibliography under Chapter III, Section A

Chapter III

Section B

Sulfonated graphene oxide (GO) catalyzed one-pot synthesis of substituted pyrazole

III.B.1. Introduction

The dihydropyranopyrazole compounds are versatile building blocks and structural units of a wide variety of therapeutic agents. Pyranopyrazoles, are ubiquitous in many biologically active heterocyclic compounds and has attracted much consideration because of its wide range of activity like antimicrobial [1], antitumor [2], anticancer [3], anticoagulant [4], diuretic, anti-inflammatory [5,6], inhibition of human Chk1 kinase activities [7] antifungal, antidepressant and so on [8]. Some important Pharmaceutical agents and drug molecules containing dihydropyranopyrazole ring in their core structure were shown in (Figure III.B.1).

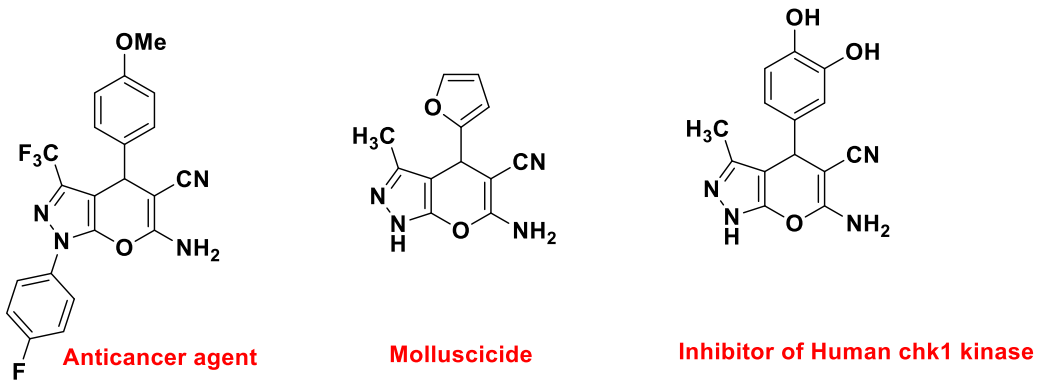

Figure III.B.1. *Some biologically active pyranopyrazoles.*

III.B.2. Background and objectives

In 1973 Junek *et al.* reported the first synthesis of pyranopyrazole from the reaction between 3-methyl-1-phenylpyrazolin-5-one and tetracyanoethylene (TCNE) (Scheme III.B.1) [9]. 5-Pyrazolones (5 mmol) reacted with TCNE in ethanol solution at refluxed conditions. 5-Pyrazolones were proved to be very reactive substrates towards TCNE. They observed that 3-phenyl-5-pyrazolone and 3-ethoxycarbonyl-1-phenyl-5-pyrazolone gave the cyclizing addition

product pyrano-pyrazoles whereas it was not possible to react 2,3-dimethyl-1-phenyl-5-pyrazolone (antipyrine) with TCNE.

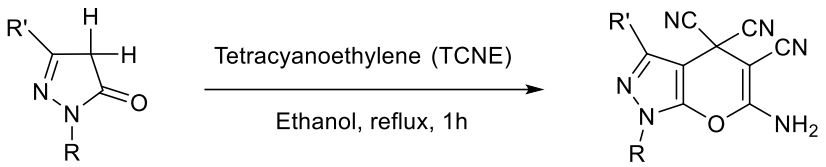

R= H, C_6H_5
R'= C_6H_5, $CO_2C_2H_5$

Scheme III.B.1. *Synthesis of pyranopyrazole from pyrazolone and tetracyanoethylene (TCNE).*

In 1980, Tacconi *et al.* reported a new route to the synthesis of pyranopyrazoles (Scheme III.B.2) [10]. Malononitrile is well-known to react with *α,β*-unsaturated carbonyls in the presence of different bases to form Knoevenagel or Michael adducts.

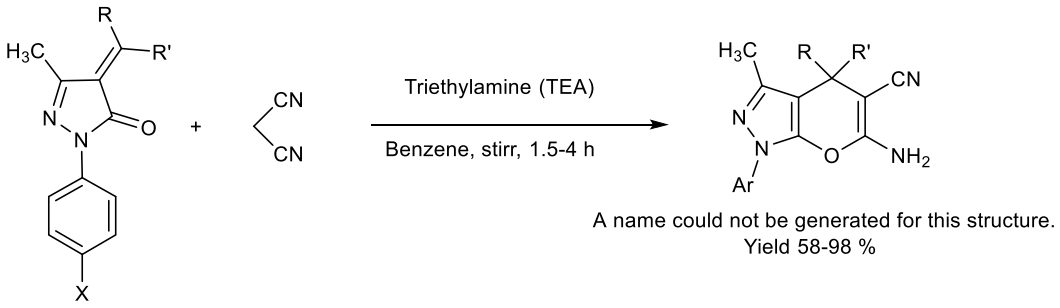

A name could not be generated for this structure.
Yield 58-98 %

X= H, NO_2, R= H, CH_3
R'= CH_3, Ph, *p*-CH_3-C_6H_4, *p*-NO_2-C_6H_4, *p*-Cl-C_6H_4, 3,4-$C_6H_3Cl_2$

Scheme III.B.2. *The synthesis of pyranopyrazole from pyrazolone and malononitrile*

They added malononitrile to the suspension of 4-arylidene (4-alkylidene)-5-pyrazolone in benzene solution in presence of triethylamine base

and then stirred for 1.5-4 hrs. Herein, benzene is proved to be far better than methanol or ethanol solvent and triethylamine must be used instead of sodium ethylate or piperidine.

In 1983, Sharanin Yu *et al.* have developed first one-pot three-component reaction of pyrazolone, aldehyde, and malononitrile to synthesize pyranopyrazole in presence of ethanol using triethylamine as the catalyst [11]. Recently, the use of the grinding method has found application in organic synthesis. This method is more efficient and selective compared with traditional methods [12-14]. In 2007, Guo *et al.* synthesized 1,4-dihydropyranopyrazoles by a grinding method using D,L-Proline under the solvent-free condition at room temperature (Scheme III.B.3) [15]. Proline is a bifunctional abundant molecule that is inexpensive and readily available in both enantiomeric forms. These two functional groups help it to act as both acid and base and also facilitates the chemical transformations in concert, similar to the enzymatic catalysis [16].

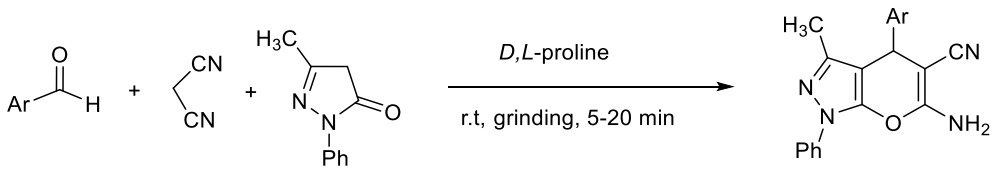

Ar= C_6H_5, 4-ClC_6H_4, 3-ClC_6H_4, 2-ClC_6H_4, 4-$NO_2C_6H_4$
3-$NO_2C_6H_4$, 4-BrC_6H_4, 2,4-ClC_6H_3, 4-$CH_3C_6H_4$, 4-OHC_6H_4
4-$CH_3OC_6H_4$

Yield 85-99 %

Scheme III.B.3. *Proline catalyzed synthesis of pyranopyrazole using the grinding method.*

In 2008, Vasuki *et al.* developed an environmentally benign four-component pathway for the synthesis of pyranopyrazoles using catalytic amounts of bases such as piperidine, pyrrolidine, morpholine, and triethylamine at room temperature (Scheme III.B.4) [17]. The maximum yield (94%) of the target product was obtained in presence of piperidine and water as the solvent

provided the best yield compared to common organic solvents. However, the reaction between benzaldehyde, hydrazine hydrate, ethyl acetoacetate, and malononitrile resulted in the corresponding pyranopyrazole without the need for a base.

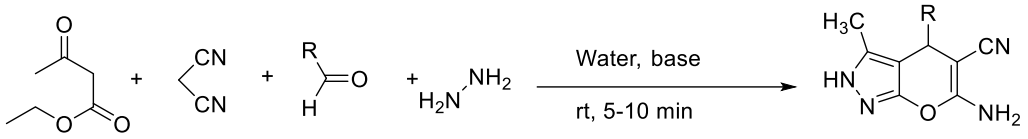

R= C_6H_5, 4-Me-C_6H_4, 4-MeO-C_6H_4, 4-NO_2-C_6H_4, 4-Cl-C_6H_4
4-OH-C_6H_4, 4-F-C_6H_4, 2-MeO-C_6H_4, 3-MeO-C_6H_4, 3-NO_2-C_6H_4,
3-Pyridinyl, 4-Pyridinyl, 2-Furanyl, 2-Thiophenyl, Isopropyl

Scheme III.B.4. *The base-mediated four-component protocol for the synthesis of pyranopyrazoles in an aqueous medium at room temperature.*

In 2011, Babaie *et al.* reported a four-component route for the generation of pyranopyrazoles from hydrazine hydrate or phenyl hydrazine, ethyl 3-alkyl3-oxo propanoate, aldehydes, and malononitrile in the presence of nanosized magnesium oxide (MgO) as a highly effective heterogeneous base catalyst (Scheme III.B.5) [18]. The same group in 2010 studied the Knoevenagel condensations of aldehydes with malononitrile in the presence of magnesium oxide (MgO) catalyst and found that the rate of the reactions was very fast. Mechanistically, the synthesis of pyranopyrazole initially involves the formation of arylidene malononitrile in quantitative yield by the Knoevenagel addition of malononitrile to the aldehyde and nanosized magnesium oxide (MgO) catalyzes all the steps as an efficient heterogeneous catalyst.

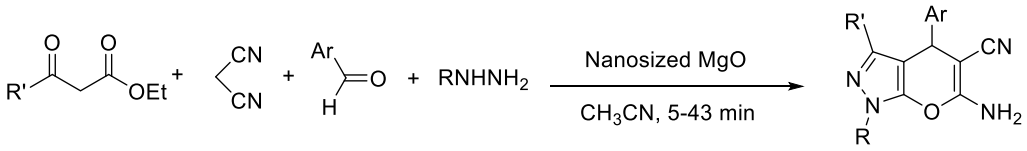

Scheme III.B.5. *Nanosized MgO catalyzed synthesis of pyranopyrazole.*

In 2013, Kangani *et al.* developed a simple and efficient one-pot four-component synthesis of 1,4-dihydropyranopyrazoles using maltose as an inexpensive and non-toxic catalyst (Scheme III.B.6) [19]. The reaction proceeds smoothly under solvent-free thermal conditions to produce the target product. Solvent-free reactions not only reduce the pollution but also the reaction handling cost by simplifying the experimental procedure and work-up [20]. This procedure has the advantages such as operational simplicity, non-hazardous catalyst, high yield, short reaction time, and minimum pollution of the environment.

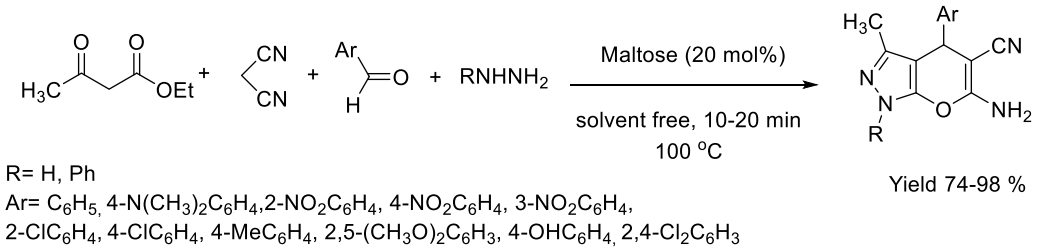

Scheme III.B.6. *Synthesis of 1,4-dihydropyrano[2,3-c]pyrazoles in the presence of maltose as a biodegradable catalyst.*

Among the solid acids, Heteropolyacid (HPA) has unique properties and its acidity is much higher than that of the mineral acids. Moreover, HPA is capable of activating substrates by protonation and sometimes is more effective

than traditional acid catalysts. The high solubility of HPA makes some difficulties to separate it from the reaction mixture. Thus immobilization of HPA on the supports having high surface area facilitates their separation and use as heterogeneous catalyst in organic transformation [21-23]. In 2015, Maleki *et al.* prepared chemical support of Keggin ($H_3PW_{12}O_{40}$) heteropolyacid (HPA) on silica-coated $NiFe_2O_4$ magnetic nanoparticles ($NiFe_2O_4@SiO_2$– $H_3PW_{12}O_{40}$ or NFS–PWA) and investigated its catalytic activity for the synthesis of pyranopyrazol (Scheme III.B.7) [24].

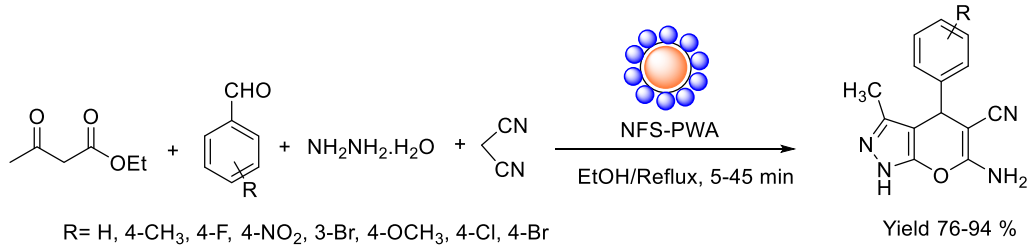

Scheme III.B.7. *$NiFe_2O_4@SiO_2$–$H_3PW_{12}O_{40}$ or NFS–PWA catalyzed synthesis of pyranopyrazole.*

In 2018, Konakanchi *et al*. employed sodium fluoride (NaF) as an efficient catalyst for the one-pot three-component synthesis of series of dihydropyrano [2,3-c]pyrazoles (Scheme III.B.8) [25]. The best yield of the target product was obtained using ultrasonic irradiation (50 kHz) in presence of water:methanol (1:1 v/v) at 25 ^oC bath temperature. The increase in the product yield under ultrasonication may be due to the cavitation effect [26]. They obtained a wide variety of substituted 1,4-dihydropyranopyrazoles in good to excellent yield (88–98%) in 5–10 min utilizing the optimized condition.

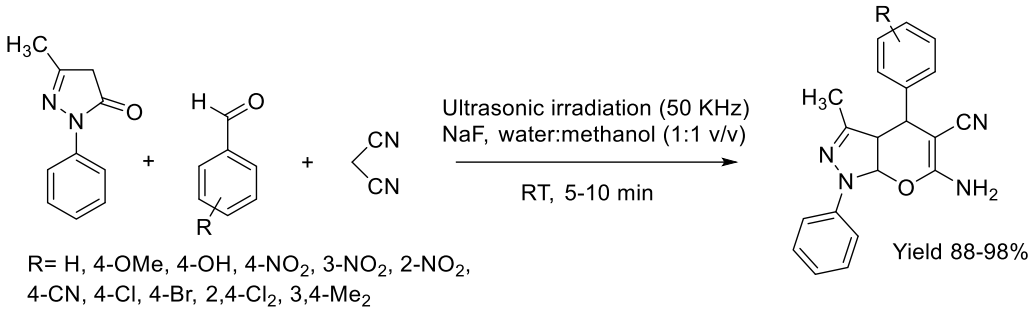

Scheme III.B.8. *NaFcatalyzed one-pot three-component synthesis of pyranopyrazole.*

III.B.3. Present work: Result and discussion

Previously, GO and its derivative sulfonated graphene oxide (SGO) has been used as an efficient carbocatalyst in hydration, oxidation, Aza-Michael addition, condensation, hydrolysis of cellulose and hydration of alkynes.[27-29] Among metal free catalysts, sulfonated graphene oxide (SGO) is a highly air-stable, environmentally friendly acid catalyst for use in various chemical reactions.

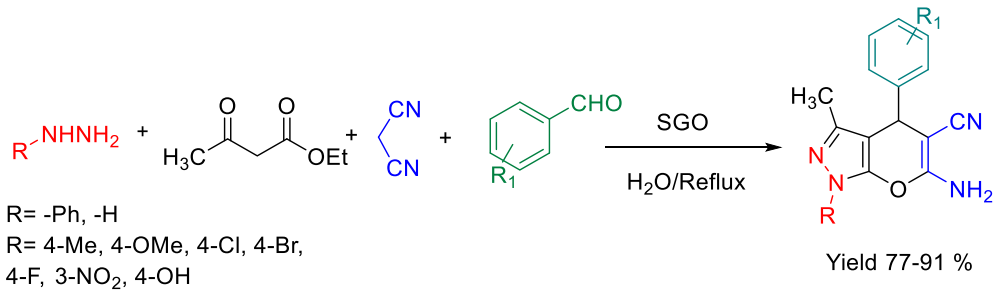

Scheme III.B.9. *SGO catalyzed one-pot four-component synthesis of pyranopyrazole.*

The versatility and the catalytic performance of the catalyst SGO were observed in one pot-four component synthesis of 1,4-dihydropyranopyrazoles (Scheme

III.B.9) using hydrazine hydrate/phenylhydrazine, aromatic aldehyde, malononitrile, ethyl acetoacetate, and the results are summarised below.

III.B.3.1. Result and discussion

Table III.B.1. Optimization of reaction condition for the synthesis of 1,4-dihydropyranopyrazoles[a]

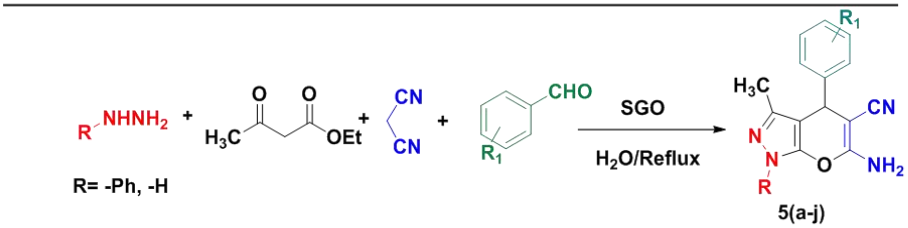

Entry	Time (min)	solvent	Catalyst amount(mg)	Yield(%)
1	120	No solvent	20	<50
2	60	EtOH /Reflux	20	55
3	60	DMF/Reflux	20	45
4	60	CH_3CN/Reflux	20	40
5	120	DCM/Reflux	20	<40
6	120	THF/Reflux	20	<30
7	60	H_2O/Reflux	20	65
8	**60**	**H_2O/Reflux**	**30**	**91**
9	60	H_2O/Reflux	50	94
10	60	H_2O/Reflux	10	<50
11	120	H_2O/r.t	40	<40[b]

[a]Reaction of phenylhydrazine (1.5 mmol), ethyl acetoacetate (1 mmol), malononitrile (1 mmol), 4-bromo benzaldehyde (1 mmol), and SGO-1 with a varying amount at refluxed conditions.

[b]Room temperature reaction

To examine the feasibility of the reaction and to optimize the reaction parameters, a model reaction was carried out using phenylhydrazine, ethyl acetoacetate, malononitrile, and 4-bromo benzaldehyde as the starting components. Different solvents EtOH, DMF, DCM, CH_3CN, THF (Table III.B.1, entry 2-6) were implemented to get the desired product in high yield, but H_2O, the green solvent was proved to be more appropriate for this reaction (Table III.B.1, entry 8). However, the temperature has a considerable effect on

the reaction, as can be seen from (Table III.B.1, entry 11) that room-temperature reaction exerted less than 40 % yield.

Investigating the catalytic efficiency of synthesized SGO-1, it was compared with GO and SGO-2, but SGO-1 afforded the desired product with a high yield. Other Lewis acids were also employed to get the desired product. The results indeed showed that high yield was only achieved in the presence of SGO-1 (Table III.B.2, entry 3)

Table III.B.2. Comparison of the efficiency of the present catalyst with a different catalytic system[a].

Entry	Condition	Catalyst	Yield(%)
1	No solvent	-	<30
2	H_2O/Reflux	GO	78[b]
3	H_2O**/Reflux**	**SGO-1**	**91[c]**
3	H_2O/Reflux	SGO-2	85
4	H_2O/Reflux	Al_2O_3	<40
5	H_2O/Reflux	$FeCl_3$	70
6	H_2O/Reflux	$ZnCl_2$	<50

[a]Reaction of phenylhydrazine (1.5 mmol), ethyl acetoacetate (1 mmol), malononitrile (1 mmol), 4-bromo benzaldehyde (1 mmol), catalyst 30 mg at the refluxed condition in water.
[b]GO was prepared by Modified hummers method,
[c]SGO-1 by Tours method.

After optimizing the reaction parameters, the versatility of the reaction was examined by varying different aromatic aldehydes and the results were summarized in Table III.B.3. Aldehydes with electron-withdrawing groups, however, exerted the desired product with a high yield and quicken the entire process (Table III.B.3, entry 5, 6, 7, 10). As an extension of our present work we have replaced phenylhydrazine with hydrazine hydrate and the results were satisfactory as shown in (Table III.B.3, entry 8-10).

Table III.B.3. Synthesis of different substituted 1,4-dihydropyranopyrazoles[a].

Entry	Product	R	Aldehyde	Time	Yield	Mp (°C)	
						Found	Reported
1	5a	-Ph	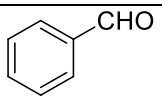	60	80	169-170	170-172
2	5b	-Ph	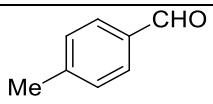	60	82	180-182	180-182
3	5c	-Ph	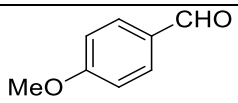	60	84	175-176	177-179
4	5d	-Ph	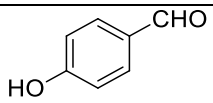	60	83	197-198	195-197
5	5e	-Ph	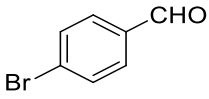	50	89	180-182	180-182
6	5f	-Ph	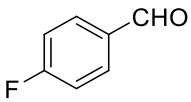	50	91	177-178	174-177
7	5g	-Ph	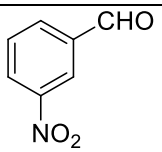	60	88	188-190	190-191
8	5h	-H	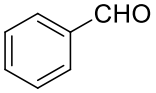	50	77	240-241	240-242
9	5i	-H	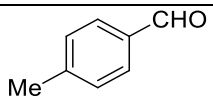	50	80	203-205	205-207
10	5j	-H	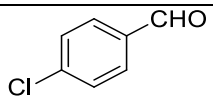	50	88	231-232	231-233

[a]Reaction of R-$NHNH_2$(1.5 mmol), ethyl acetoacetate (1 mmol), malononitrile (1 mmol), aromatic benzaldehyde (1 mmol), 30 mg of SGO atthere fluxed condition in H_2O.

III.B.3.2. Mechanism

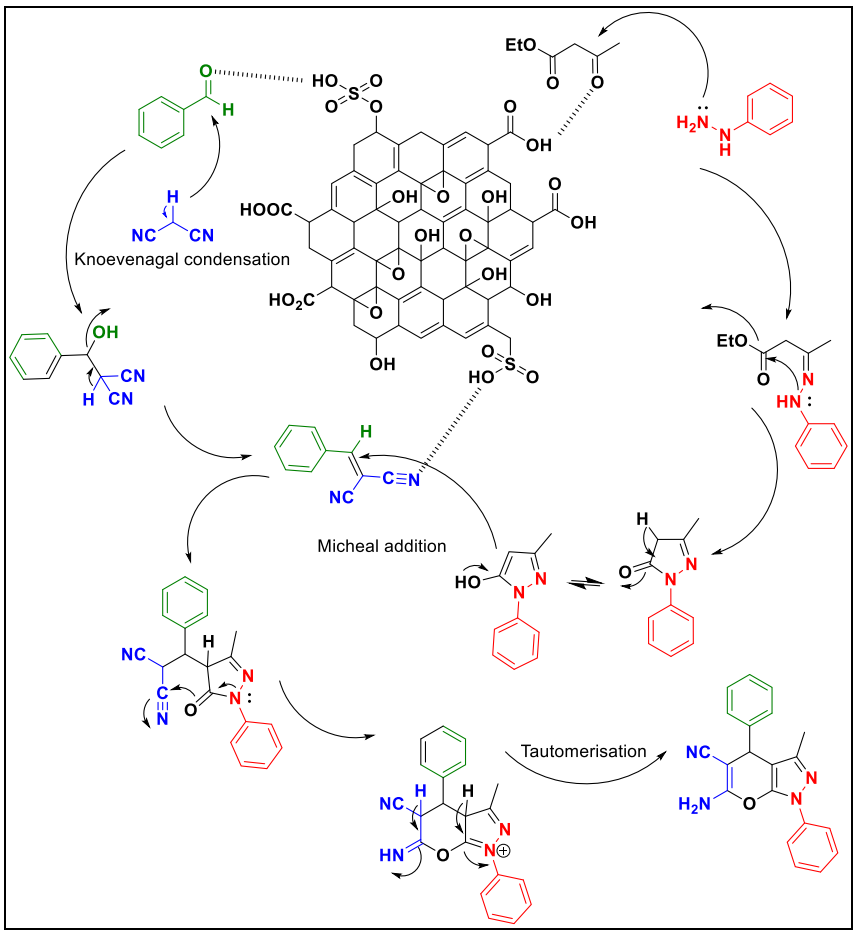

Scheme III.B.10. *A plausible route for the synthesis of 1,4-dihydropyrano[2,3-c]pyrazoles.*

A plausible mechanism for the synthesis of 1,4-dihydropyranopyrazoles using SGO was shown here (Scheme III.B.10). At first, 5-methyl-2-phenyl-2,4-dihydro-3*H*-pyrazole-3-one was formed by the condensation of phenylhydrazine and ethyl acetoacetate. Subsequently, knoevenagal condensation between

aromatic aldehyde and malononitrile exerted 2-benzylidenemalonitrile. Afterthat, pyrazolone and benzylidenemalononitrile participated in Micheal addition followed by cyclization. Finally, the desired 1,4-dihydropyranopyrazole was obtained through tautomerization in the last step of the reaction mechanism.

III.B.3.3. Conclusion

In conclusion, an efficient carbocatalyst SGO is employed for the synthesis of substituted pyranopyrazoles from commercially available aldehydes. Sulfonated graphene oxide (SGO) acts as heterogeneous acid catalyst and itself is capable to furnish the desired 6-Amino-3-methyl-4-phenyl-1,4-[2,3-c]pyrazole-5-carbonitriles with excellent yield. It can be envisioned that such a cheap and robust solid acid catalyst SGO holds great potential for a wide range of acid-catalysed reactions.

III.B.4. Experimental section

III.B.4.1. General information

The reactions were monitored by TLC [carried out on Merck silica gel (60 F254) by using UV light as visualizing agent]. NMR spectra of all the products were taken in $CDCl_3$/DMSO-d_6 (TMS as an internal standard) using a Bruker AV-300 spectrometer operating for ^{1}H at 300 MHz and for ^{13}C at 75 MHz. ^{1}H NMR spectroscopic data are represented as follows: chemical shift (ppm), multiplicity (s = singlet, d= doublet, t = triplet, dd = doublet of doublets, m = multiplet, brs = broad), integration, coupling constants in Hertz (Hz). ^{13}C NMR spectroscopic data are reported in ppm. Coupling constants were reported as J values in Hertz (Hz).The chemicals and reagents were purchased from Merck, Spectrochem, and Sigma-Aldrich.

III.B.4.2. General procedure for the preparation of the catalyst

SGO-1 and SGO-2 were prepared by the Tours method according to the literature. In brief, 9:1 mixture of concentrated H_2SO_4/H_3PO_4 (360:40 ml) was taken in a beaker, after that graphite powder (3.0 g) was added slowly to it taking the whole system in an ice bath to keep the temperature below 20 ^oC. $KMnO_4$ (9.0 g) was then added slowly in portions to the solutions. Afterward, the reaction mixture was heated to 50 ^oC and stirred for 12 h. After the reaction, the mixture was centrifuged (5000 rpm for 30 min), and the supernatant was decanted away. The remaining solid material was then washed with water successively, 30% HCl and ethanol to remove the remaining salt. The solid obtained was then dried to obtain the powdered graphene oxide [29]. In SGO-2 9.0 g of $KMnO_4$ is only replaced by 18 g.

III.B.4.3. General procedure for the synthesis of 6-Amino-3-methyl-4-phenyl-1,4-[2,3-c]pyrazole-5-carbonitriles

In a 25-mL round-bottomed flask phenyl hydrazine/hydrazine hydrate (1.5 mmol), ethyl acetoacetate (1 mmol), aromatic aldehyde (1 mmol), malononitrile (1 mmol), and SGO (0.03 g) were refluxed at water medium for appropriate period of time. The progress of the reaction was monitored by TLC and after completion of the reaction, the ice-cold water was added to the reaction mixture. Then, the precipitated organic product was decanted, washed with water and recrystallized from proper solvents to give pure products.After that, the catalyst was recovered by centrifugation and washed with ethanol and dried. All the products are known, and their melting point was found to be identical to those reported in the literature.

III.B.4.4. Spectral data of various pyranopyrazole derivatives

5a.6-Amino-3-methyl-1,4-diphenyl-1,4-dihydropyrano[2,3-c]pyrazole-5-carbonitrile (Table III.B.3, entry 1) [19]

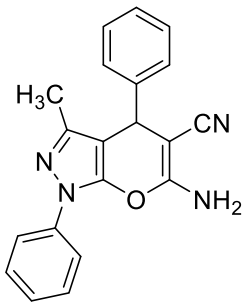

^{1}H NMR (400 MHz, DMSO-d_6) δ (ppm) 1.76 (s, 3H), 4.66 (s, 1H), 7.20-7.49 (m, 10H), 7.76-7.78 (d, 2H, *J*= 8Hz);

^{13}C NMR (100 MHz, DMSO-d_6) δ (ppm) 12.58, 36.74, 58.16, 98.65, 119.98, 126.19, 127.06, 127.79, 128.54, 129.35, 143.62, 143.88, 145.27, 159.43.

IR (KBr, cm^{-1}) bands 3469, 3332, 2197, 1654, 1514, 1384, 753.

5b.6-Amino-3-methyl-1-phenyl-4-(*p*-tolyl)-1,4-dihydropyrano[2,3c]pyrazole-5-carbonitrile (Table III.B.3, entry 2) [19]

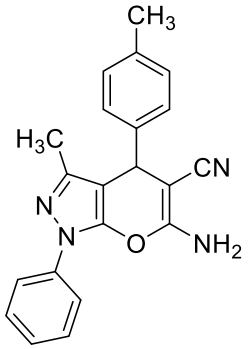

^{1}H NMR (400 MHz, DMSO-d_6) δ (ppm) 1.81 (s, 3H), 2.22 (s, 3H), 4.89 (s, 1H), 7.08-7.44 (m, 9H), 7.68-7.70 (d, 2H, *J*=8Hz);

^{13}C NMR (100 MHz, DMSO-d_6) δ (ppm) 12.17, 21.60, 60.33, 99.48, 121.05, 126.11, 127.66, 129.25, 129.39, 129.48, 135.39, 137.84, 139.68, 146.81, 160.05.

5c.6-amino-4-(4-methoxyphenyl)-3-methyl-1-phenyl-1,4-dihydropyrano[2,3-c]pyrazole-5-carbonitrile (Table III.B.3, entry 3)[19]

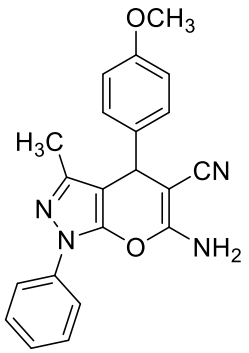

^{1}H NMR (400 MHz, DMSO-d_6) δ (ppm) 1.92 (s, 3H), 3.95 (s, 3H), 4.38 (s, 1H), 7.15-7.90 (m, 11H);

^{13}C NMR (100 MHz, DMSO-d_6) δ (ppm) 12.52, 58.16, 60.326, 98.65, 119.98, 126.19, 127.06, 127.79, 128.43, 129.35, 137.54, 143.62, 143.98, 145.27, 159.54.

5d.6-amino-4-(4-hydroxyphenyl)-3-methyl-1-phenyl-1,4-dihydropyrano[2,3-c]pyrazole-5-carbonitrile (Table III.B.3, entry 4) [19]

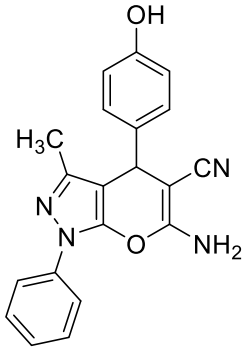

^{1}H NMR (400 MHz, DMSO-d_6) δ (ppm) 2.30 (s, 1H), 4.94 (s, 1H), 6.59-6.64 (t, 2H), 6.78 (s, 1H), 7.16-7.19 (t, 2H), 7.35-7.39 (t, 4H), 7.62-7.64 (d, 2H, *J*=8Hz);

^{13}C NMR (100 MHz, DMSO-d_6) δ (ppm) 12.19, 33.41, 56.21, 99.48, 112.41, 115.71, 120.18, 121.13, 126.10, 129.48, 133.85, 145.41, 146.73, 147.73, 159.27;

IR (KBr, cm^{-1}) bands 3527, 3314, 2178, 1724, 1589, 814, 753.

5e.6-amino-4-(4-bromophenyl)-3-methyl-1-phenyl-1,4-dihydropyrano[2,3-c]pyrazole-5-carbonitrile (Table III.B.3, entry 5)[19]

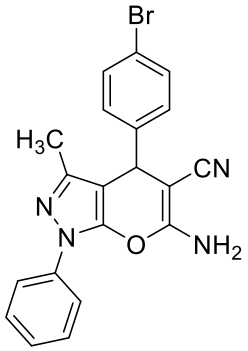

^{1}H NMR (400 MHz, DMSO-d_6) δ (ppm) 2.17 (s, 3H), 4.92 (s, 1H), 7.17-7.69 (m, 11 H);

^{13}C NMR (100 MHz, DMSO-d_6) δ (ppm) 12.11, 33.18, 58.16, 99.41, 119.59, 121.11, 126.20, 129.47, 130.10, 131.49, 131.65, 143.62, 143.88, 145.27, 159.43;

IR (KBr, cm^{-1}) bands 3320, 2919, 1598, 1503, 1293, 1157, 752.

5f.6-amino-4-(4-fluorophenyl)-3-methyl-1-phenyl-1,4-dihydropyrano[2,3-c]pyrazole-5-carbonitrile (Table III.B.3, entry 6) [19]

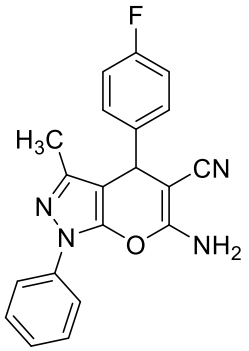

^{1}H NMR (400 MHz, DMSO-d_6) δ (ppm) 2.30 (s, 1H), 4.94 (s, 1H), 7.05-7.44 (m, 9H), 7.67-7.69 (d, 2H, *J*=8Hz);

^{13}C NMR (400 MHz, DMSO-d_6) δ (ppm) 12.50, 33.02, 58.16, 99.41, 115.17, 115.38, 121.11, 129.47, 129.61, 138.78, 145.19, 146.87, 148.34, 159.43;

IR(KBr, cm^{-1}) bands 3330, 2918, 1567, 1498, 1071, 751.

5g.6-amino-4-(3-nitrophenyl)-3-methyl-1-phenyl-1,4-dihydropyrano[2,3-c]pyrazole-5-carbonitrile (Table III.B.3, entry 7) [19]

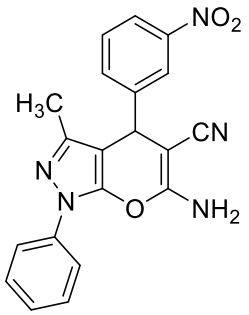

^{1}H NMR (400 MHz, DMSO-d_6) δ (ppm) 2.33 (s, 1H), 5.13 (s, 1H), 7.18-7.73 (m, 10H), 8.07 (s, 1H);

^{13}C NMR (100 MHz, DMSO-d_6) δ (ppm) 12.40, 33.42, 58.167, 98.31, 121.19, 121.75, 122.29, 126.28, 129.51, 130.25, 134.89, 145.19, 146.87, 148.34, 158.43.

5h. 6-amino-3-methyl-4-phenyl-1,4-dihydropyrano[2,3-c]pyrazole-5-carbonitrile (Table III.B.3, entry 8) [19]

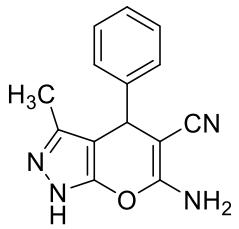

^{1}H NMR (400 MHz, DMSO-d_6) δ (ppm) 2.10 (s, 1H), 5.33 (s, 1H), 7.16-7.80 (m, 7H), 11.45 (brs, 1H);

^{13}C NMR (100 MHz, DMSO-d_6) δ (ppm) 11.81, 33.32, 58.167, 98.71, 121.10, 126.23, 129.47, 130.11, 131.49, 131.62, 143.65, 143.88, 159.43.

5i. 6-amino-3-methyl-4-(p-tolyl)-1,4-dihydropyrano[2,3-c]pyrazole-5-carbonitrile (Table III.B.3, entry 9) [19]

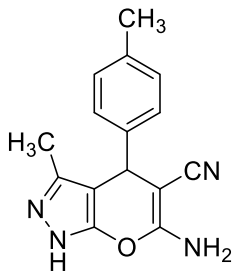

^{1}H NMR (400 MHz, DMSO-d_6) δ (ppm) 1.67 (s, 3H), 2.20 (s, 3H), 5.62 (s, 1H), 7.30-7.49 (m, 5H), 7.76-7.78 (d, 2H, *J*=7.6Hz), 11.45 (brs, 1H);

^{13}C NMR (100 MHz, DMSO-d_6) δ (ppm) 13.392, 21.234, 33.508, 58.301, 98.311, 117.990, 120.226, 124.864, 128.793, 134.764, 138.784, 148.202, 159.411.

III.B.4.4. Scanned copies of ^{1}H and ^{13}C NMR spectra of synthesised compounds

Figure III.B.2. *Scanned copy of ^{1}H and ^{13}C NMR spectra of 6-Amino-3-methyl-1,4-diphenyl-1,4-dihydropyrano[2,3c]pyrazole-5-carbonitrile*

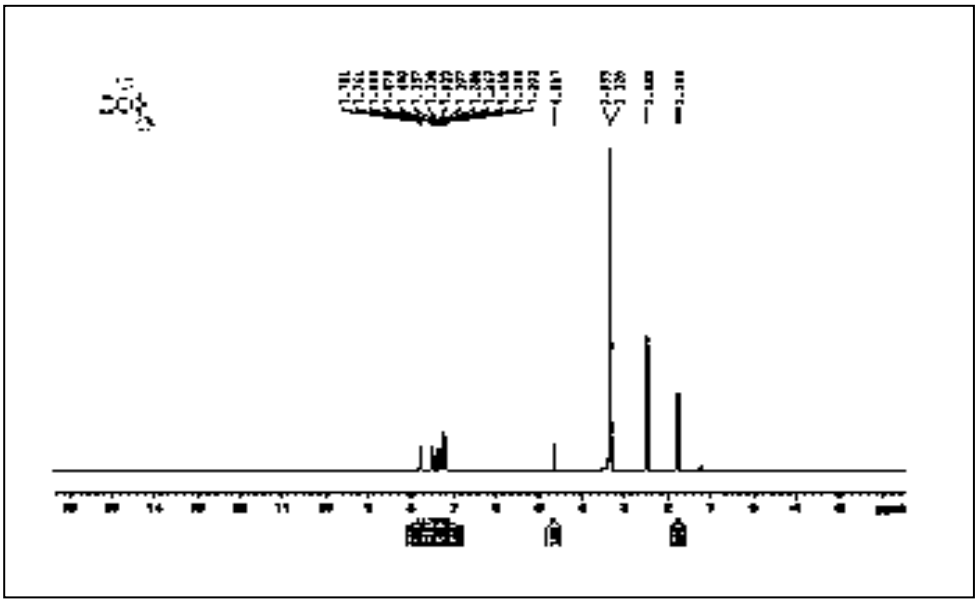

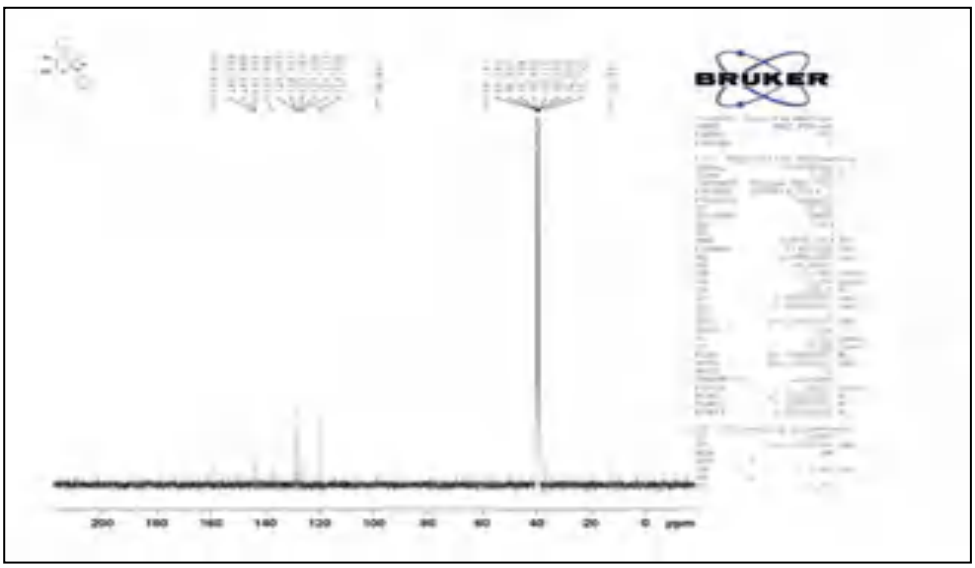

Figure III.B.3. *Scanned copy of ^{1}H and ^{13}C NMR spectra of 6-Amino-3-methyl-1-phenyl-4-(p-tolyl)-1,4-dihydropyrano[2,3c]pyrazole-5-carbonitrile*

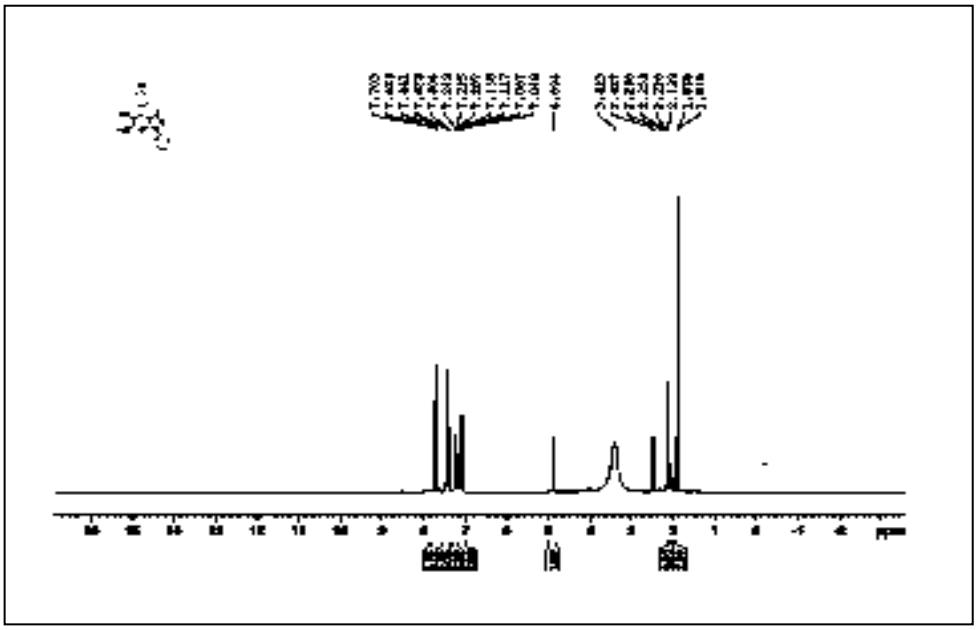

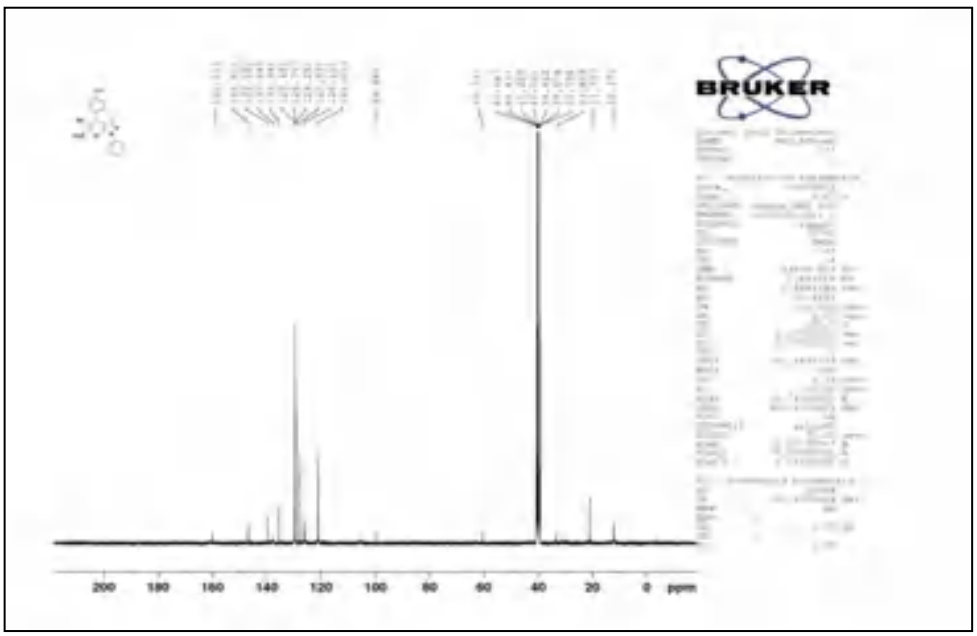

Figure III.B.4. *Scanned copy of ^{1}H and ^{13}C NMR spectra of 6-amino-4-(4-methoxyphenyl)-3-methyl-1-phenyl-1,4-dihydropyrano[2,3-c]pyrazole-5-carbonitrile*

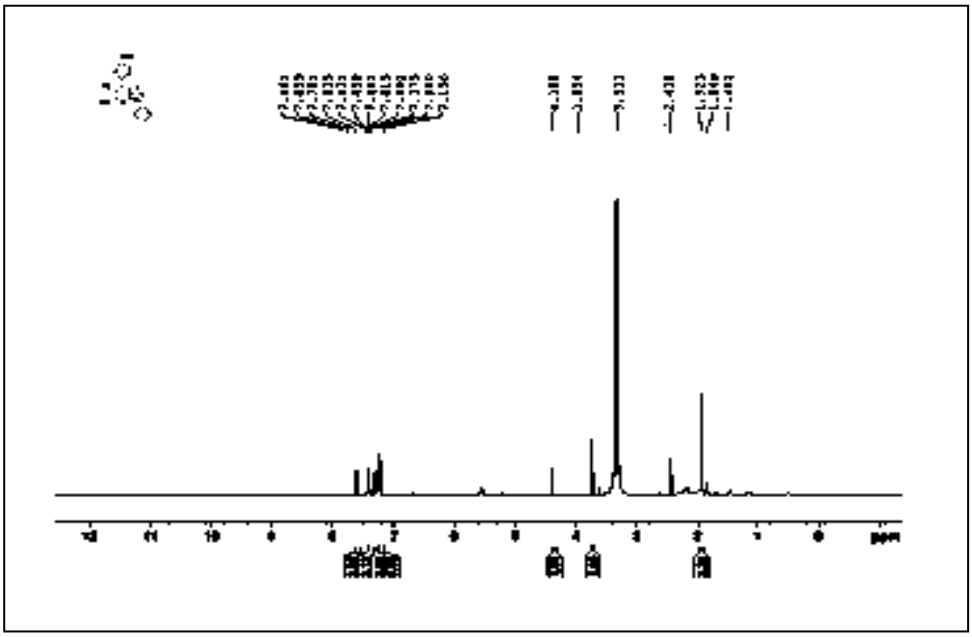

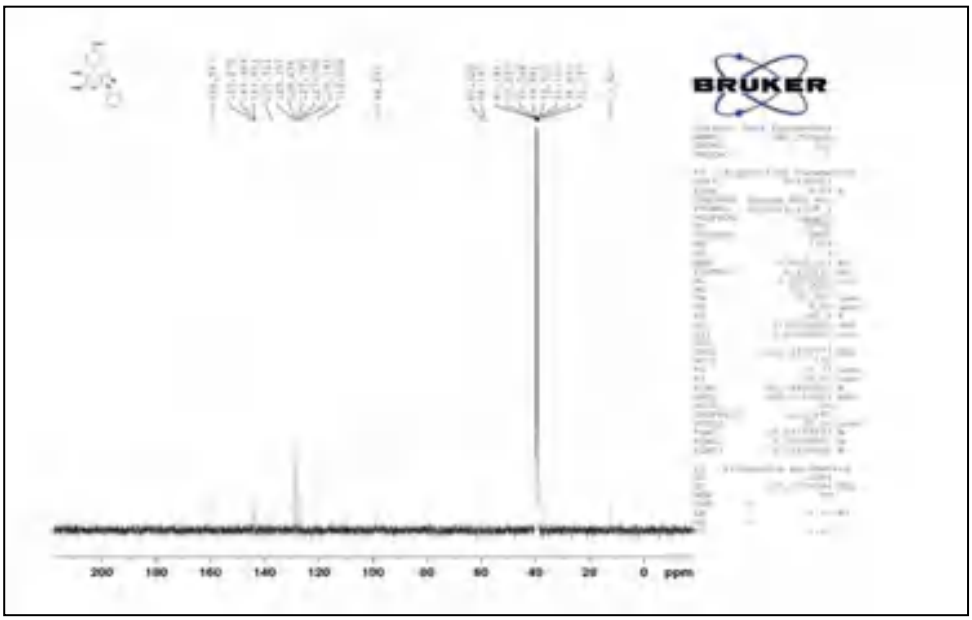

Figure III.B.5. *Scanned copy of ^{1}H and ^{13}C NMR spectra of 6-amino-4-(4-bromophenyl)-3-methyl-1-phenyl-1,4-dihydropyrano[2,3-c]pyrazole-5-carbonitrile*

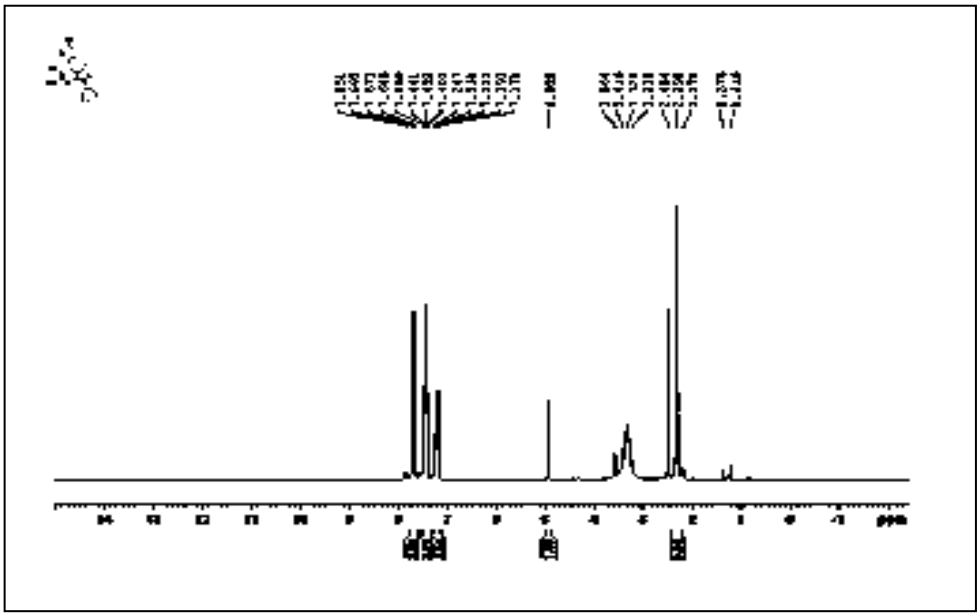

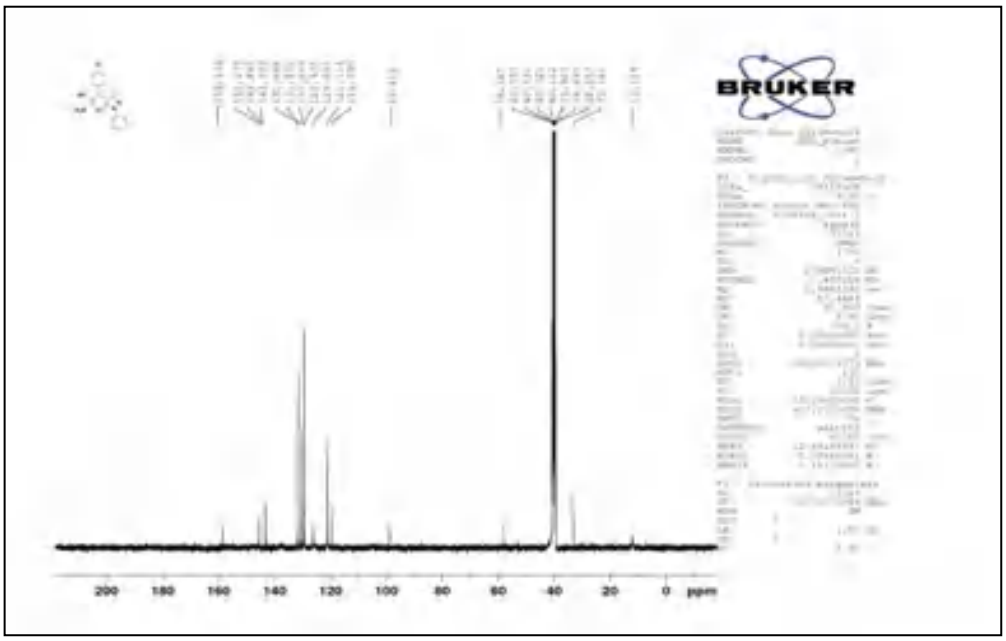

Figure III.B.6. *Scanned copy of ^{1}H and ^{13}C NMR spectra of 6-amino-4-(4-fluorophenyl)-3-methyl-1-phenyl-1,4-dihydropyrano[2,3-c]pyrazole-5-carbonitrile*

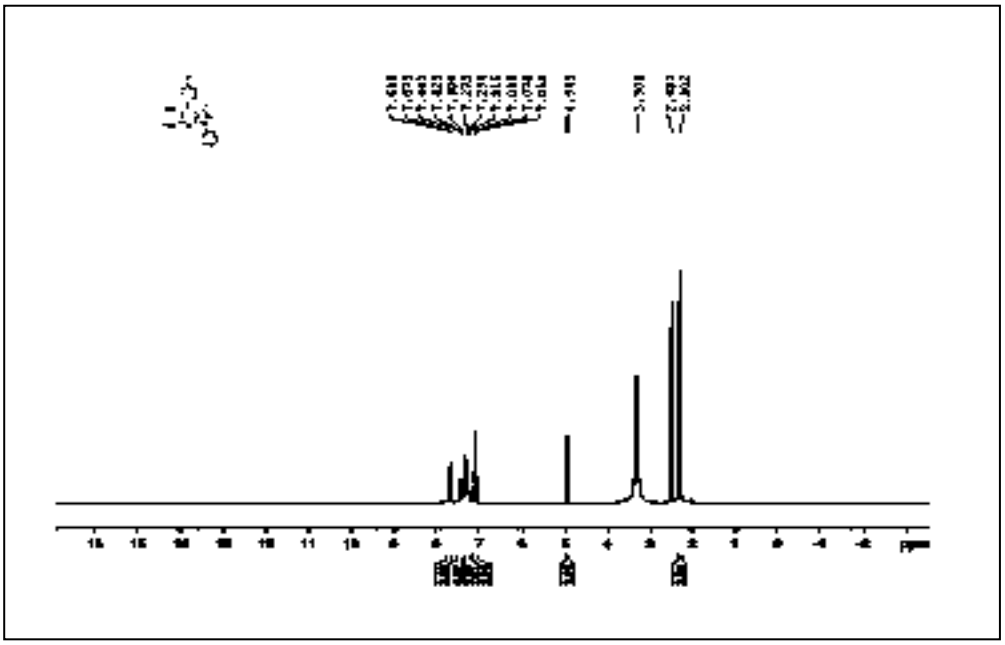

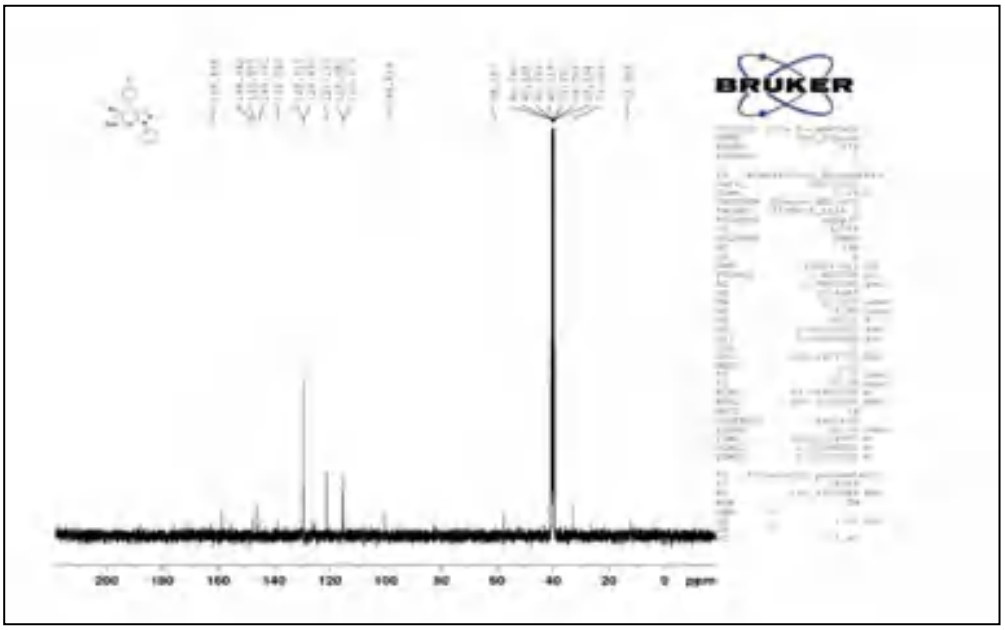

Figure III.B.7. *Scanned copy of ^{1}H and ^{13}C NMR spectra of 6-amino-4-(3-nitrophenyl)-3-methyl-1-phenyl-1,4-dihydropyrano[2,3-c]pyrazole-5-carbonitrile*

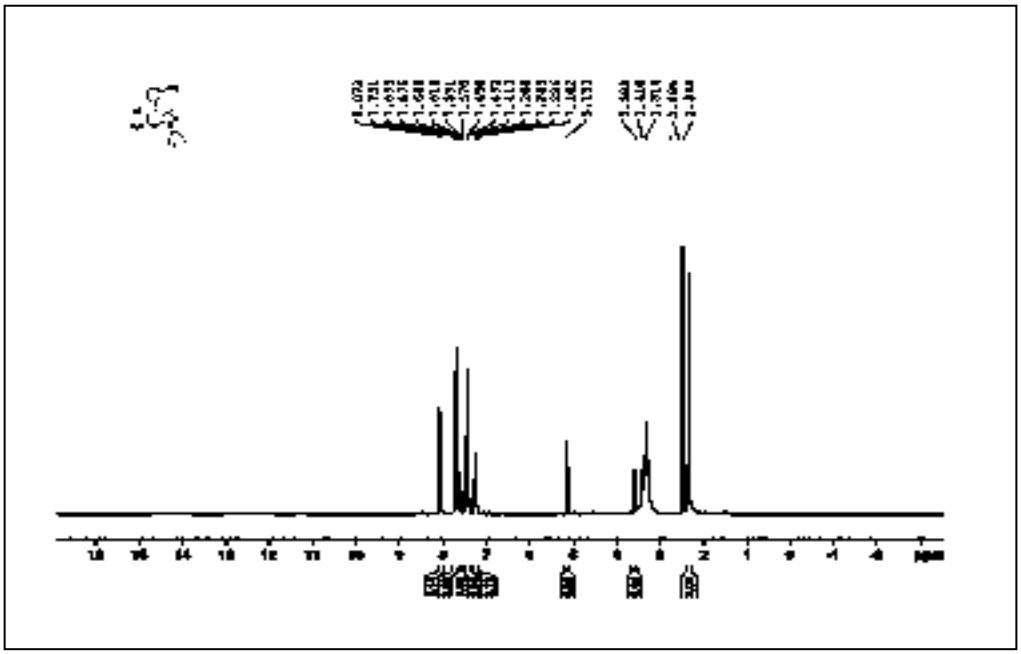

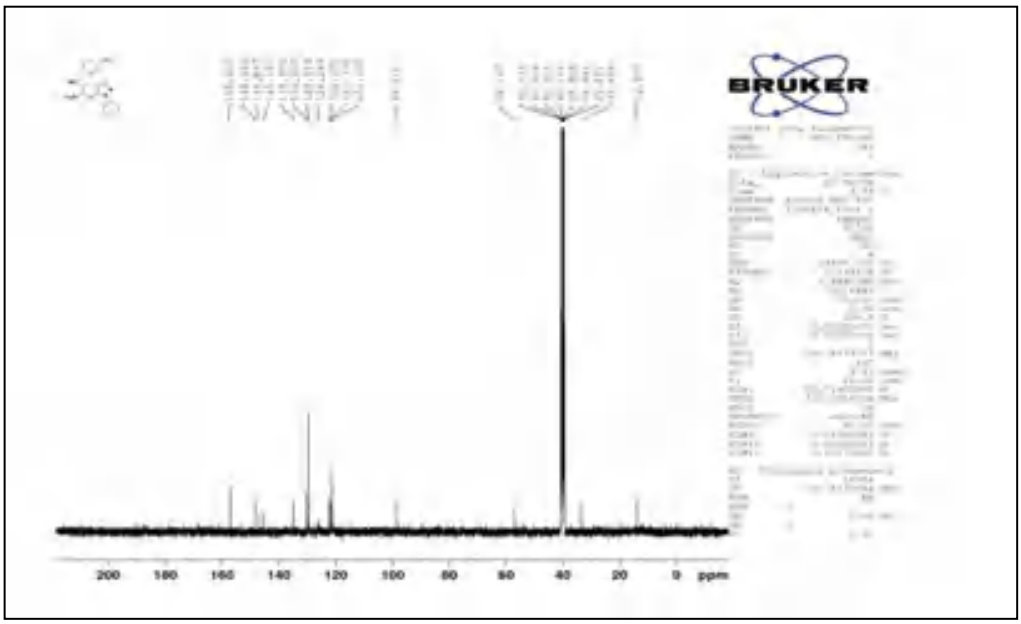

Figure III.B.8. *Scanned copy of ^{1}H and ^{13}C NMR spectra of 6-amino-3-methyl-4-phenyl-1,4-dihydropyrano[2,3-c]pyrazole-5-carbonitrile*

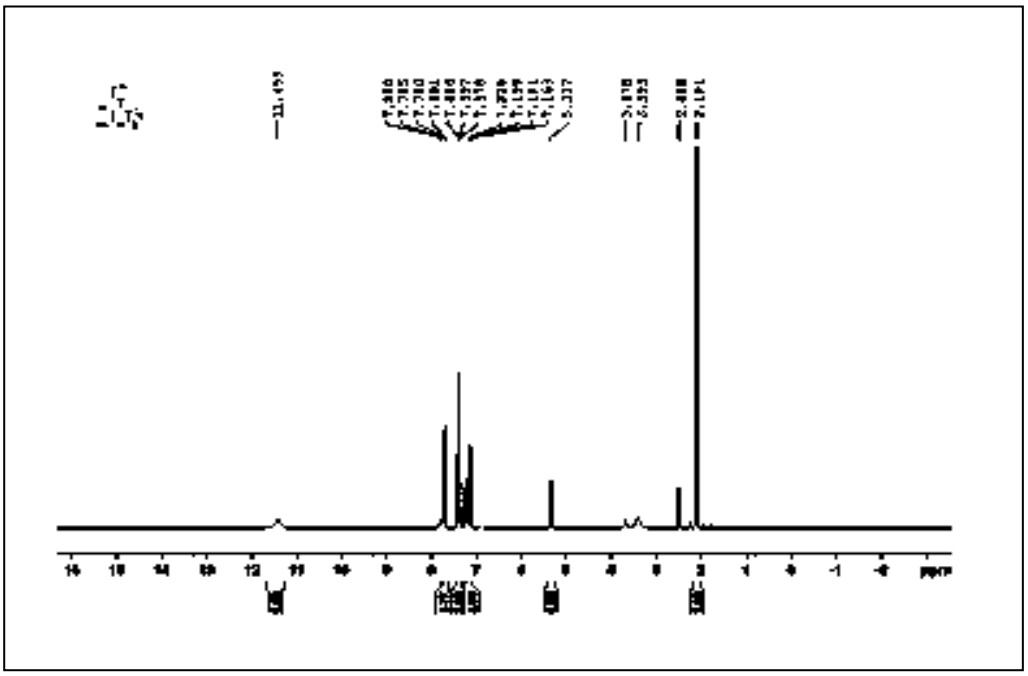

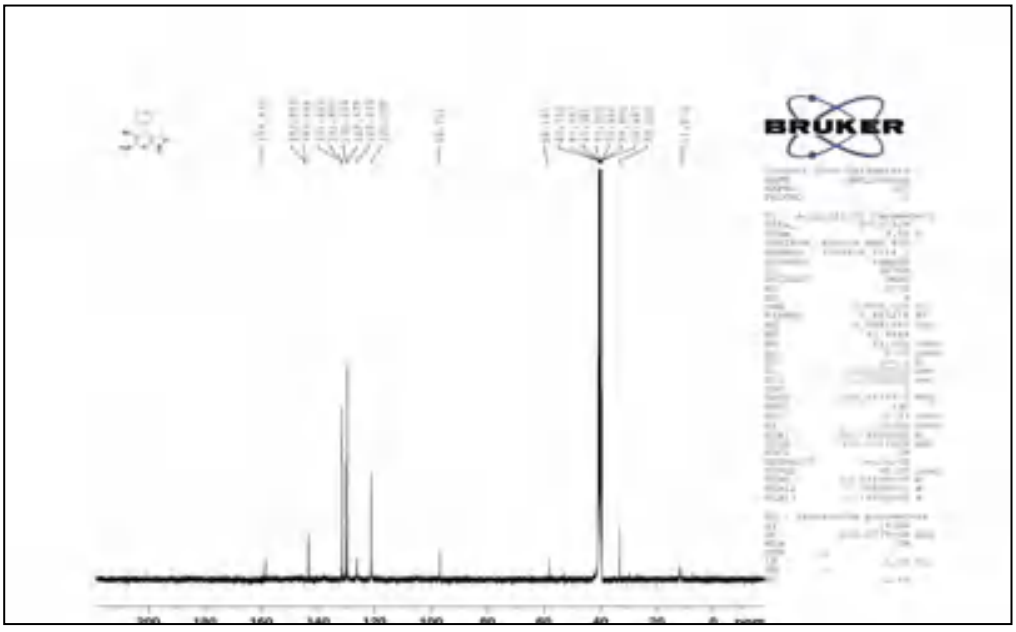

Figure III.B.9. *Scanned copy of ^{1}H and ^{13}C NMR spectra of 6-amino-3-methyl-4-(p-tolyl)-1,4-dihydropyrano[2,3-c]pyrazole-5-carbonitrile*

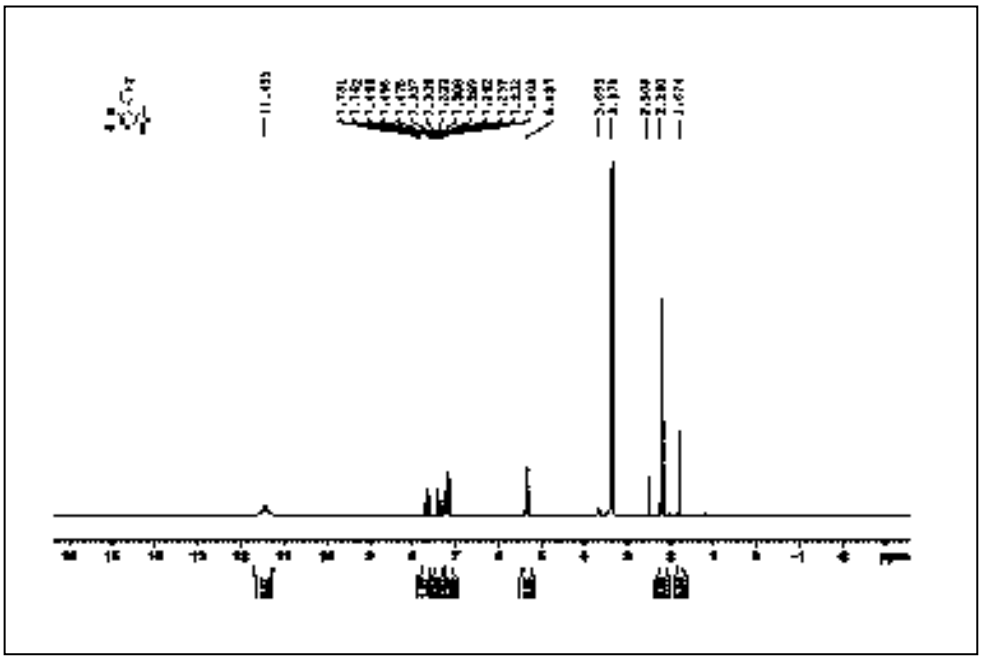

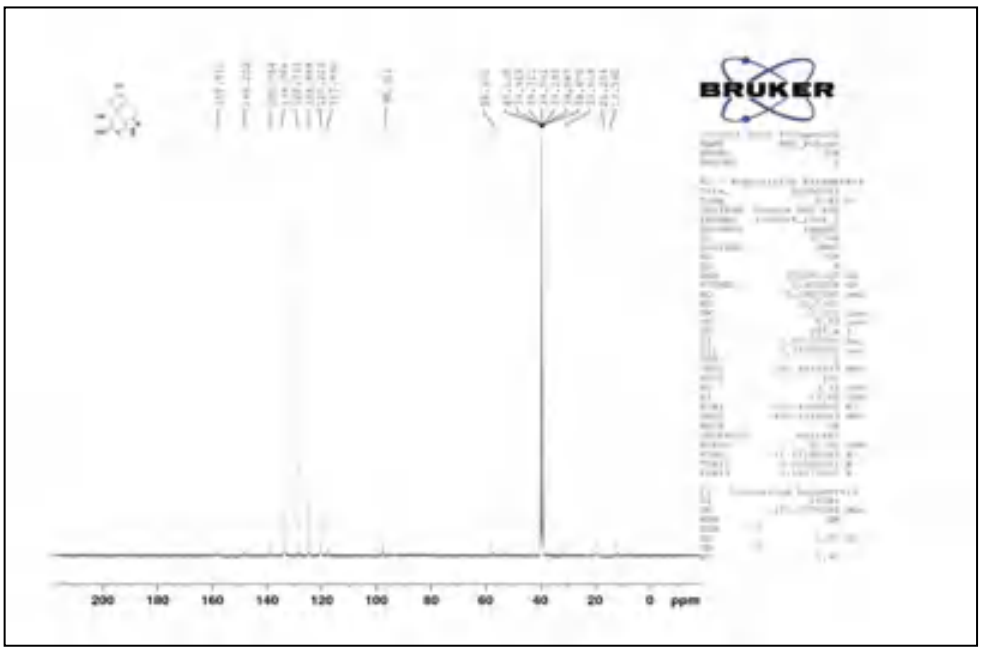

III.B.5. References

References are given in Bibliography under Chapter III, Section B

Bibliography

I.A.5. References

(1) K. S.Novoselov, A. K.Geim, S. V.Morozov, D.Jiang, Y.Zhang, S. V.Dubonos, I. V.Grigorieva and A. A. Firsov, *Science,* 2004, **306**, 666-669.

(2) C.Berger, Z.Song, X.Li, X.Wu, N.Brown, C.Naud, D.Mayou, T.Li, J.Hass, A. N.Marchenkov, E. H.Conrad, P. N.First and W. A. de Heer, *Science,*2006, **312**, 1191-1196.

(3) C. N. R.Rao, A. K.Sood, K. S.Subrahmanyam and A. Govindaraj, *Angew. Chem. Int. Ed.,* 2009, **48**, 7752-7777.

(4) K. P.Loh, Q. L.Bao, P. K.Ang and J. X. Yang, *J. Mater. Chem.*, 2010, **20**, 2277–2289

(5) V. Georgakilas, J. N. Tiwari, K. C. Kemp, J. A. Perman, A. B. Bourlinos, K. S. Kim and R. Zboril, *Chem. Rev.,* 2016, **116**, 5464–5519.

(6) V. Georgakilas, M. Otyepka, A. B. Bourlinos, V. Chandra, N. Kim, K. C. Kemp, P. Hobza, R. Zboril and K. S. Kim, *Chem. Rev.*, 2012, **112**, 6156–6214.

(7) M. Inagaki and F. Kang, *J. Mater. Chem. A.,* 2014,**2**, 13193-13206.

(8) L. Zhang, J. Liang, Y, Huang, Y. Ma, Y. Wang and Y. Chen, *Carbon,*2009, **47**, 3365-3368.

(9) A. Vul and A. T. Dideikin, *Front. Phys.,* 2018, **6**, 1-24.

(10) O. Mohammadi, M. Golestanzadeh and M.Abdouss, *New J. Chem.,* 2017,**41**, 11471-11497.

(11) J. H. Bitter, *J. Mater. Chem*., 2010, **20**, 7312-7321.

(12) D. S. Su, J. Zhang, B. Frank, A.Thomas, X. C.Wang, J.Paraknowitsch andR. Schlogl, *ChemSusChem.,* 2010, **3**, 169-180.

(13) B. Brodie, *Ann. Chim. Phys*., 1855, **45**, 351-353.

(14) D.Li and Kaner, R. B. *Science,* 2008, **320**, 1170-1171.

(15) L. Staudenmaier, *Ber. Dtsch. Chem. Ges*., 1898, **31**, 1481-1487.

(16) D. C.Marcano, D. V.Kosynkin, J. M.Berlin, A.Sinitskii, Z.Sun, A.Slesarev, L. B.Alemany, W.Luand J. M. Tour, *ACS Nano,* 2010, **8**, 4806-4814.

(17) A. M.Dimiev, L. B.Alemany andJ. M. Tour, *ACS Nano*, 2013, **7**, 576-588.

(18) C. Su andK. P.Loh,*Acc. Chem. Res.,* 2013,**46**, 2275-2285.

(19) S.Rana and S. B.Jonnalagadda, *Catal. Commun.,*2017, **92**, 31-34.

(20) H. Yang, C. Shan, F. Li, D. Han, Q. Zhang and L. Niu,*Chem. Commun.*, 2009, **26**, 3880–3882.

(21) W. Lee, J.U. Lee, B.M. Jung, B. J-Hyung, J.W. Yi, S.B. Lee and B.S.Kim,*Carbon,*2013, **65**, 296–304.

(22) E. Bekyarova, M.E. Itkis, P. Ramesh, C. Berger, M. Sprinkle, W.A. De Heer and R.C. Haddon, *J. Am. Chem. Soc.,* 2009, **131**, 1336-1337.

(23) A.C. Obreja, D. Cristea, R. Gavrila, V. Schiopu, A. Dinescu, M. Danila and F. Comanescu,*Science,* 2013, **276**, 458– 467.

(24) S. Rani, M. Kumar, R. Kumar, D. Kumar, S. Sharma and G. Singh, *Mater. Res. Bull.,* 2014, **60**, 143-149.

(25) A. Gholampour, M. V. Kiamahalleh, D. N. H. Tran, T. Ozbakkaloglu, and D. Losic, *ACS Appl. Mater. Interfaces.,*2017, 9, **49**, 43275–43286.

(26) R. Kumar, M. Kumar, A. Kumar, R. Singh, R. Kashyap, S. Rani and D. Kumar, *Mater Today: Proc.,*2019, **18**, 1556-1561.

(27) H. Tondro, H. Zilouei, K. Zargoosh and M. Bazarganipour, Bioresour. Technol., 2020, **306**, 123124-123159.

(28) V.Polshettiwar.,R. Luque.,A.Fihri.,H.Zhu.,M.Bouhrara andJ.-M. Basset, *Chem. Rev.,* 2011, **111**, 3036-3075.

(29) D. R.Dreyer, H. P. Jia and C. W. Bielawski, *Angew. Chem. Int. Ed.,* 2010, **49**, 6813-6816.

(30) D. R.Dreyer, H. P.Jia, A. D.Todd, G.Jeng and Bielawski, C. W. *Org. Biomol. Chem.,* 2011, **9**, 7292-7295.

(31) H.Huang, J.Huang, Y. M.Liu, H. Y.He, Y. Cao and K. N. Fan, *Green Chem.,* 2012, **14**, 930-934.

(32) Y. Gao, P.Tang, H.Zhou, W.Zhang, H.Yang, N.Yan, G. Hu, D.Mei, J. Wang and D. Ma, *Angew. Chem. Int. Ed.,* 2016, **55**, 3124-3128.

(33) K. B.Dhopte, R. S.Zambare, A. V.Patwardhan and P. R. Nemade, *RSC Adv.,* 2016, **6**, 8164-8172.

(34) S. Bhattacharya, P.Ghosh and B. Basu, *Tetrahedron Lett.,* 2018, **59**, 899-903.

(35) V. D. Ebajo Jr., C. R. L.Santos, G. V.Alea, Y. A.Lin and C.-H. Chen, *Sci Rep.,* 2019, **9**, 15579-15590.

(36) M. Karthik and P. Suresh, *ACS Sustainable Chem. Eng.,* 2019, **7**, 9028-9034.

(37) H.Wu, C.Qiu, Z.Zhang, B.Zhang, S.Zhang, Y.Xua, H.Zhou, C.Sua and K. P. Loh, *Adv. Synth. Catal.,* 2020, **362**, 789-794.

(38) F.Hu, M.Patel, F.Luo, C.Flach, R. Mendelsohn, E.Garfunkel, H. He andM. Szostak, *J. Am. Chem. Soc.,* 2015, **137**, 14473-14480.

(39) H. Yang, X.Cui, X.Dai, Y.Deng and F. Shi, *Nat. Commun*.,2015, **6**, 6478-6487.

(40) G. A. B.Gon alves,S. M. G. Pires,M. M. Q.Simoes,M. G. P. M. S.Neves and P. A. A. P. Marques,*Chem Commun.,*2014, **50**, 7673-7676.

(41) T. A. J. Siddiqui,B. G.Ghule,S.Shaikh,P. V. Shinde,K. C. Gunturu,P. K.Zubaidha,J. M. Yun,C. O'Dwyer,R. S.Mane,K. H.Kim,*RSC Adv.,* 2018, **8**, 17373-17379.

(42) G.Lv,H. Wang,Y.Yang,T.Deng,C.Chen,Y.Zhu and X. Hou,*ACS Catal.,* 2015, **5**, 5636-5646.

(43) C.Su, R.Tandiana, J.Balapanuru, W. Tang, K.Pareek, C. T.Nai, T.Hayashi and Loh, K. P. *J. Am. Chem. Soc*.,2015, **137**, 685-690.

(44) B.Majumdar, D.Sarma, T.Bhattacharya and T. K. Sarmsa, *ACS Sustainable Chem. Eng.,* 2017, **5**, 9286-9294.

(45) S. Bhattacharya, P. Ghosh and B. Basu, *Tetrahedron Lett.,* 2017, **58**, 926-931.

(46) P. Choudhury and B. Basu, *J. Flow Chem.,* 2020, **10**, 389-396.

(47) M.Atarod, M.Nasrollahzadeh and S.M. Sajadi, *J. Colloid Interface Sci*.,2016,**465**, 249-258.

(48) S.Naghdi, K. Y. Rhee and Jaleh, B. *Appl. Surf. Sci.,* 2016,**364**, 686-693.

(49) S. Lowa and Y.-S. Shon, *Adv Nano Res*., 2018, **6**, 357–375.

(50) D. R.Dreyer,S. Park,C. W.Bielawski and R. S. Ruoff,*Chem. Soc. Rev.,* 2010, **39**, 228-240.

(51) M. N. Groves, C. Malardier-Jugroot and M. Jugroot,*J. Phys. Chem. C*., 2012, **116**, 10548-10556.

(52) D.Astruc, F. Lu and J. R. Aranzaes, *Angew. Chem*. *Int. Ed*.,2005, **44**, 7852-7872.

(53) V.K.Gupta, A.Mittal, D.Jhare and J. Mittal, *RSC Adv.,* 2012,**2**, 8381-8389.

(54) R.Saravanan, E.Thirumal, V.K.Gupta, V. Narayanan and A. Stephen, *J. Mol. Liq*., 2013,**177**, 394-401.

(55) R.Saravanan, V.K.Gupta, E. Mosquera and F. Gracia, *J. Mol. Liq.,* 2014, **198**, 409-412.

(56) R.Saravanan, S.Joicy, V.K.Gupta, V. Narayanan and A. Stephen, *Mater. Sci. Eng. CMater. Biol. Appl.,* 2013,**33**, 4725-4731.

(57) R.Saravanan, S.Karthikeyan, V.K.Gupta, G.Sekaran, V. Narayanan and A. Stephen, *Mater. Sci. Eng. CMater. Biol. Appl.,* 2013,**33**, 91-98.

(58) R.Saravanan,V.K.Gupta, V. Narayanan and A. Stephen, *J. Taiwan Inst. Chem. Eng.* 2014,**45**, 1910-1917.

(59) T. A. Saleh and V.K. Gupta, *J. Colloid Interface Sci.,* 2011,**362**, 337-344.

(60) T. A. Saleh and V.K. Gupta, *J. Colloid Interface Sci*.,2012,**371**, 101-106.

(61) R.Saravanan, V.K.Gupta, V. Narayanan and A. Stephen, *J. Mol. Liq.,* 2013,**181**, 133-141.

(62) R.Saravanan, M. M. Khan, F.Gracia, J.Qin, V.K. Gupta and S. Arumainathan, *Sci. Rep.,* 2016,**6**, 31641-31652.

(63) M. Pe´rez-Lorenzo, *J. Phys. Chem. Lett.,* 2012, **3**, 167-174.

(64) P.Taladriz-Blanco, P. Herve´s and J. Pe´rez-Juste, *Top. Catal*., 2013, **56**, 1154-1170.

(65) Negishi, E.;deMeijere, A.; Handbook of Organopalladium Chemistry for Organic Synthesis, Wiley, **2003**.

(66) N.Miyaura, K.Yamada, A. Suzuki, *Tetrahedron Lett.,* 1979, **20**, 3437-3440.

(67) E.-I.Negishi and S.Baba, *J. Chem. Soc., Chem. Commun*., 1976, 596b-597b.

(68) D.Milstein andJ. K. Stille, *J. Am. Chem. Soc.,* 1978, **100**, 3636-3638.

(69) T. R. Kelly, Q.Li and V. Bhushan, *Tetrahedron Lett.*, 1990, **31**, 161–164

(70) K.Tamao, K.Sumitani and M. Kumada, *J. Am. Chem. Soc.,* 1972, **94**, 4374-4376.

(71) T. Hiyama, *J. Organomet. Chem.,* 2002, **653**, 58-61.

(72) K.Sonogashira, Y.Tohda and N. Hagihara, *Tetrahedron Lett.,* 1975, **16**, 4467-4470.

(73) R.Martin andS.L. Buchwald, *Acc. Chem. Res.,* 2008,**41**, 1461-1473.

(74) G.M.Scheuermann, L.Rumi, P.Steurer, W.Bannwarth and R. Mülhaupt, *J. Am. Chem. Soc.,* 2009,**131**, 8262-8270.

(75) L.Rumi, G.M.Scheuermann, R.Mülhaupt and W. Bannwarth, *Helv. Chim. Acta***.**,2011*,* **94**, 966-976.

(76) A. R.Siamaki, A-El-R. S.Khder, V. Abdelsayed, M. S. El-Shall and B. F.Gupton, *J. Catal*.,2011,**279**, 1-11.

(77) A. Khannanov, I. Il'yasov, A. Kiiamov, I. Vakhitov, A. Kirgizov, A. Lamberovb, A. M.Dimiev, *New J. Chem*.,2019,**43**, 19035-19043.

(78) M. Gómez-Martínez, E. Buxaderas, I. M. Pastor and D. A. Alonso, *J. Mol. Catal. A Chem.,* 2015,*1*, 404-405.

(79) N. Shang, C. Feng, H. Zhang, S. Gao, R. Tang, C. Wang and Z.Wang, *Catal. Commun*., 2013,**40**, 111-115.

(80) A. H.Al-Marri, M. Khan, M. R. Shaik, N. Mohri, S. F. Adil, M. Kuniyil, H. Z.Alkhathlan, A. Al-Warthan, W. Tremel, M. N. Tahir, M. Khan, M. R. H. Siddiqui, *Arab. J. Chem*., 2016, **9**, 835-845.

(81) K. S.Gayen, T. Sengupta, Y.Saima, A. Das, D. K.Maiti and A. Mitra, *Green Chem.*, 2012,**14**, 1589-1592.

(82) M. Meldal and C. W.Tornøe, *Chem. Rev*.,2008, **108**, 2952-3015.

(83) K. Zhou, J. Zhang, G. Qiu and J.Wu, *Org. Lett*., 2019, **21**, 275-278.

(84) N. Ichiishi, A. J.Canty, B. F. Yates and M. S. Sanford, *Organometallics,* 2014, **33**, 5525-5534.

(85) K. Zhang, J.M. Suh,T. H. Lee, C.J. Hwan, J. W. Choi, H. W. Jang and R. S.Varma, *Nano Converg.,* 2019,**6**, 1-7.

(86) V. S.Sadu, H.-R.Bin, D.-M.Lee, K.-I. Lee,*Sci. Rep*.,2017,**7**, 242-252.

(87) A.Mittal, S.; Kumari, Parmanand,D. Yadav and S. K.Sharma, *Appl. Organomet. Chem*., 2020, **34**, 5362-5374.

(88) M.Tobisu and N. Chatani,*Angew. Chem*.,2006, **118**, 1713-1715.

(89) Yu. M.Shafran, V. A.Bakulev and V. S. Mokrushin,*Russ. Chem. Rev*., 1989, **58**, 148-162.

(90) E. J.Martinez, E. J.Corey,*Org. Lett.,* 1999, **1**, 75-78.

(91) D. Verma, S. Verma, A. K.Sinha and S. L. Jain,*ChemPlusChem.,* 2013, **78**, 860-865.

(92) X.Tian, F.Su and X. S. Zhao,*Green Chem.,* 2008, **10**, 951-956.

(93) M.Kitano, K.Nakajima, J. N.Kondo, S.Hayashi and M. Hara,*J. Am. Chem. Soc.,* 2010, **132**, 6622-6623.

(94) H. I.Ryoo, L. Y.Hong, S. H.Jung and D.-P. Kim,*J. Mater. Chem*.,2010, **20**, 6419-6421.

(95) Y.Zhao, H.Wang, Y.Zhao and J. Shen,*Catal. Commun.,* 2010, **11**, 824-828.

(96) H.Xiao, Y.Guo, X.Liang and C. Qi *J. Solid State Chem.,* 2010, **183**, 1721-1725.

(97) H. T.Gomes, S. M.Miranda, M. J.Sampaio, A. M. T.Silva and J. L.Faria,*Catal. Today.,* 2010,**151**, 153-158.

(98) R.Fareghi-Alamdari, M.Golestanzadeh, F.Agend and N. Zekri,*C. R. Chim.,* 2013, **16**, 878-887.

(99) R.Fareghi-Alamdari, M.Golestanzadeh, F.Agend and N. Zekri,*Can. J. Chem*., 2013, **91**, 982-991.

(100) M.Toda, A.Takagaki, M.Okamura, J. N.Kondo, S.Hayashi, K.Domen and M. Hara,*Nature*, 2005, **438**, 178-178.

(101) S.Suganuma, K.Nakajima, M.Kitano, D.Yamaguchi, H.Kato and S.Hayashi,*J. Am. Chem. Soc*.,2008, **130**, 12787-12793.

(102) F.Liu, J. Sun, L.Zhu, X.Meng, C. Qi and F.-S. Xiao, *J. Mater. Chem*.,2012, **22**, 5495-5502.

(103) P. P.Upare, J.-W.Yoon, M. Y.Kim, H.-Y.Kang, D. W.Hwang, Y. K. Hwang, H. H. Kung and J.-S. Chang, *Green Chem*., 2013, **15**, 2935-2943.

(104) P. Gao, D. D. Sun and W. J. Ng, *RSC Adv*.,2013, **3**, 15202-15210.

(105) H. Naeimi and M. Golestanzadeh, *RSC Adv*.,2014, **4**, 56475-56488.

(106) E. Vessally, A. Hassanpour, R. Hosseinzadeh-Khanmiri, M. Babazadeh and J.Abolhasani, *Monatsh. Chem.,* 2017, **148**, 321-326.

(107) A. Sengupta, C. Su, C. Bao,C. T. Nai and K. P.Loh,*ChemCatChem.,*2014, **6**, 2507-2511.

(108) E. Lam, J.H.Chong, E. Majid, Y. Liu, S. Hrapovic, A. C. W. Leung and J. H. T. Luong,*Carbon,* 2012, **50**, 1033-1043.

(109) M.-S. Hosseini, M.Masteri-Farahani, *Tetrahedron,* 2021, **83**, 132083-132106.

(110) M. Mirza-Aghayana,N.Ganjbakhsh,M. M.Tavanaa and R. Boukherroub, *Ultrason.Sonochem.,*2016,**29**, 371-379.

(111) M. C. Nongbeab, T. Ekou, L. Ekou, K. B. Yao,E.L. Grogneca and F.-X. Felpin, *Renew. Energy.,* 2017,**106**, 135-140.

(112) M-S.Hosseini, M. M.Farahani and S.Shahsavarifar, *J. Taiwan Inst. Chem. Eng*., 2019, **102**, 34-40.

(113) Q. Hou, W.Li, M.Ju, L.Liu, Y.Chenand and Q. Yang, *RSC Adv*.,2016, **6**, 104016-104024.

(114) X.Zhao, J. Wang, C.Chen, Y.Huang, A.Wang and T. Zhang, *Chem. Commun.,* 2014, **50**, 3439-3442.

(115) E.Vessally, A.Hassanpour, R.Hosseinzadeh-Khanmiri, M.Babazadeh and Abolhasani, *J. Monatsh. Chem.,* 2017, **148**, 321-326.

(116) M.Brahmayya, S. A.Dai and S.-Y. Sue, *Sci. Rep.,* 2017, **7**, 4675-4688.

(117) M.Brahmayya, S.-Y. Suen and S. A. Dai, *J. Taiwan Inst. Chem. Eng.,* 2018, **83**, 174-183.

(118) P.Basak, S.Dey and P. Ghosh, *ChemistrySelect,* 2020, **5**, 626-636.

(119) M. M.Antunes, P. A.Russo, P. V.Wiper, J. M.Veiga, M. Pillinger, L. Mafra, D. V.Evtuguin, N. Pinna and A. A. Valente, *ChemSusChem,*2014, **7**, 804-812.

I.B.6. References

(1) M. Carbone, Y. Li, C.Irace, E.Mollo, F.Castelluccio, D. A. Pascale, G. Cimino, R. Santamaria, W. Y.Guo and M. Gavagnin, *Org. Lett*.,2011, **13**, 2516-2519.

(2) A. V.Gulevich, A. S. Dudnik, N.Chernyak, V. Gevorgyan, *Chem. Rev*.,2013, **113**, 3084-3213.

(3) R. J.Mathvink, A. M.Barritta, M. R.Candelore, M. A.Cascieri, L. Deng, L.Tota, C. D. Strader, M. J.Wyvratt, M. H. Fisher and A. E. Weber, *Bioorg. Med. Chem. Lett*.,1999, **9**, 1869-1874.

(4) G. D. Diana, D. L.Volkots, T. J. Nitz, T. R. Bailey, M. A. Long, N.Vescio, S. Aldous, D. C. Pevear and F. J. Dutko, *J. Med. Chem*.,1994, **37**, 2421-2436.

(5) H. Z. Zhang, S.Kasibhatla, J.Kuemmerle, W. Kemnitzer, K.OllisMason, L.Qiu, C.Crogan-Grundy, B. Tseng, J. Drewe and S. X. Cai, *J. Med. Chem*.,2005, **48**, 5215-5223.

(6) F. I. Carroll, J. L. Gray, P. Abrahm, M. A.Kuzemko, A. H. Lewin, J. W.Boja and M. J. Kuhar, *J. Med. Chem*.,1993, **36**, 2886-2890.

(7) L. J. Street,R. Baker,T. Book,A. J. Reeve,J. Saunders,T.Willson,R. S.Marwood, S. Patel and S. B. Freedman,*J. Med. Chem.*, 1992, **35**, 295–305.

(8) J. W. Clitherow, P. Beswick, W. J. Irving, D. I. C. Scopes, J. C. Barnes, J.Clapham, J. D. Brown, D. J. Evans and A. G. Hayes, *Bioorg. Med. Chem. Lett*., 1996, **6**, 833-838.

(9) C. B. Vu, E. G.Corpuz, T. J. Merry, S. G. Bartlett. C. Pradeepan, R. S. Bohacek, M. C.Botfield, C. J.Eyermann, B. A. Lynch, I. A. MacNeil and M. K. Ram, *J. Med. Chem*.,1999, **42**, 4088-4094.

(10) J. Matsumoto, T. Takahashi, M. Agata, H.Toyofuku and N. Sasada, *Jpn. J. Pharmacol*.,**1994**, **65**, 51-58.

(11) B. L.Mylari, T. A. Beyer, P. J. Scott, C. E.Aldinger, M. F. Dee. T. W. Siegel and W. J. Zembrowski, *J. Med. Chem.,*1992, **35**, 457-465.

(12) B. S.Orlek, F. E. Blaney, F. Brown, M. S. G. Clark, M. S. Hadley, J. Hatcher, G. J. Riley, H. E. Rosenberg, H. J. Wadsworth and P. Wyman, *J. Med. Chem*.,1991,**34**, 2726-2735.

(13) T. Nakamura, M. Asano, Y. Sekiguchi, Y. Mizuno, K. Tamaki, F. Nara, Y. Kawase, Y. Yabe, D.Nakai, E.Kamiyama, Y.Urasaki-Kaneno, T.Shimozato, H. Doi-Komuro, T.Kagari, W.Tomisato, R. Inoue, M. Nagasaki, H.Yuita, K.Oguchi-Oshima, R. Kaneko and T. Nishi, *Eur. J. Med. Chem*.,**2012**, *51*, 92-98.

(14) A. Domling, *Chem. Rev*.,2006, **106**, 17-89.

(15) D. Tejedor and F. Garcia-Tellado, *Chem. Soc. Rev*.,2007, **36**, 484-491.

(16) B.Kaboudin and L. Malekzadeh, *Tetrahedron Lett.,*2011, **52**, 6424-6426.

(17) J. K. Augustine, V.Akabote, S. G. Hegde and P. Alagarsamy, *J. Org. Chem*.,2009, **74**, 5640-5643.

(18) Srivastava, R. M.; Freire, M. V. S.; Chaves, A. S. S. C.; Beltrao, T. M. *J. Heterocycl. Chem.,***1987**, *24*, 101.

(19) Adib, M.; Jahromi, A. H.; Tavoosi, N.; Mahdavi, M.; Bijanzadeh, H. R. *Tetrahedron Lett.,***2006**, *47*, 2965.

(20) S.Kandre, P. R. Bhagat, R. Sharma and A. Gupte, *Tetrahedron Lett.*, 2013, **54**, 3526-3529.

(21) J. J. Lade, B. N. Patil, K. S. Vadagaonkar and A. C.Chaskar, *Tetrahedron Lett*.,2017, **58**, 2103-2108.

(22) Y. Wang, R. L. Miller, D. R. Sauer and S. Djuric, W. *Org. Lett*., 2005, **7**, 925-928.

(23) (a) R. F. P. Poulin, A. L.; Tartar and B. P. De´prez, *Tetrahedron Lett*.,2001, **42**, 1495-1498.

(b) R.Milcent and G. Barbier, *J. Heterocycl. Chem.,*1983, **20**, 77-80.

(24) F.Eloy and R. Lenaers, *Chem. Rev*.,1962, **62**, 155-183.

(25) B.Kaboudin and F. Saadati, *Tetrahedron Lett*., 2007, **48**, 2829-2832.

(26) W. Wang, H. Xu, Y. Xu, T. Ding, W. Zhang, Y. Ren and H. Chang, *Org. Biomol. Chem.,*2016, **14**, 9814-9822.

(27) M. R.Kuram, W. G. Kim, K.Myung and S. Y. Hong, *Eur. J. Org. Chem*.,**2016**, 438-442.

(28) K. B.Dhopte, R. S.Zambare, A. V. Patwardhan and P. R.Nemade, *RSC Adv.,* 2016, **6**, 8164-8172.

(29) D. C.Marcano, D. V.Kosynkin, J. M. Berlin, A.Sinitskii, Z. Sun, A.Slesarev, L. B.Alemany, W.Luand J. M. Tour, *ACS Nano,* 2010, **8**, 4806-4814.

(30) D. S.Bolotin, K. I.Kulish, N. A.Bokach, G. L.Starova, V. V.Gurzhiy and V. Y.Kukushkin, *Inorg. Chem.,* 2014, **53**, 10312-10324.

I.C.6. References

(1) A. R. Katritzky, C. W. Rees and E. F. V. Scriven, Comprehensive Heterocyclic Chemistry II, Oxford, London, 1996.

(2) B. Y. Kim, J. B. Ahn, H. W. Lee, S. K. Kang, J. H. Lee, J. S. Shin, S. K. Ahn, C. I. Hong and S. S. Yoon, *Eur. J. Med. Chem.,* 2004, **39**, 433-447.

(3) I. J. Enyedy, S. Sakmuri, W. A. Zaman, K. M. Johnson and S. Wang, *Bioorg. Med. Chem. Lett.*, 2004, **13**, 513-517.

(4) V. Klimesova', M. Svoboda, K. Waisser, M. Pour and J. Kaustova', *Framaco*, 1999, **54**, 666-672.

(5) E. Figgemeier, E. C. Constable, C. E. Housecroft and Y. C. Zimmermann, *Langmuir,* 2004, **20**, 9242-9248.

(6) E. C. Constable, C. E. Housecroft, M. Neuburger, D. Phillips, P. R. Raithby, E. Schofield, E. Sparr, D. A. Tocher, M. Zehnder, and Y. Zimmermann, *Dalton Trans.,* 2000, **13**, 2219-2228.

(7) R. W. Armstrong, A. P. Combs, P. A. Tempest, S. D. Brown and T. A. Keating, *Acc. Chem. Res.,* 1996, **29**, 123-131.

(8) F. Krohnke, *Angew. Chem. Int. Ed.,* 1963, **2**, 225-276.

(9) N. Montazeri and S. Mahjoob, *Chin. Chem. Lett.,* 2012, **23**, 419-422.

(10) M. M. Heravi, K. Bakhtiari, Z. Daroogheha and F. F. Bamoharram, *Catal. Commun.,* 2007, **8**, 1991-1994.

(11) L. Nagarapu, A. R. Peddiraju and S. Apuri, *Catal. Commun.,* 2007, **8**, 1973-1976.

(12) A. Davoodnia, M. Bakavoli, R. Moloudi, N. Tavakoli-Houseini and M. Khashi, *Monatsh Chem.,* 2010, **141**, 867-870.

(13) A. Maleki and R. Firouzi-Haji, *Sci Rep.,* 2018, **8**, 17303-17311.

(14) J. Safari, S. Gandomi-Ravandi and M. Borujeni, *Chem. Sci.,* 2013, 125, 1063-1070.

(15) M. Adib, H. Tahermansouri, S. A. Koloogani, B. Mohammadia and H. R. Bijanzadeh, *Tetrahedron Lett.,* 2006, **47**, 5957–5960.

(16) R. Nagase, J. Osada, H. Tamagaki and Y. Tanabe, *Adv. Synth. Catal.,* 2010, **352**, 1128-1134.

(17) T. Funatomi, K. Wakasugi T. Misaki and Y. Tanabe, *Green Chem.,* 2006, 8, 1022-1027.

(18) N. Montazeri, S. Khaksar, A. Nazari, S. S. Alavia, S, M. Vahdat and M. TajbakhshcJ, *Fluorine Chem.,* 2011, **132**, 450-452.

(19) C. W. Fairhurst, *Adv. Dent. Res.,* 1992, **6**, 78-81.

(20) L. Thomé, A. Gentils, J. Jagielski, F. Garrido and T. Thomé, *Vacuum*, 2007, **81**, 1264-1270.

(21) L. Koroleva, *Glass. Ceram.,* 2004, **61**, 299-302.

(22) A. E. Navaei, M. Rezaei, A. H. Navaei, H. Feyzallahzadeh and Z. F. Yan, *Chem. Eng. Commun.*, 2009, **196**, 1417-1424.

(23) E. Tabrizian, A. Amoozadeh, S. Rahmani, E. Imanifar, S. Azhari and M. Malmir, *Chin. Chem. Lett.,* 2015, **26**, 1278-1282.

(24) M. Ghaedi, S. Hajjatia, Z. Mahmudia, I. Tyagib, S. Agarwal, A. Maity and V. K. Gupta *Chem. Eng. J.*, 2015, **268**, 28-37.

(25) A. Maleki and T. Kari, *Catal. Lett.,* 2018, **148**, 2929-2934.

(26) A. Asfaram, M. Ghaedi, S. Agarwal, I. Tyagi and V. K. Gupta, *RSC Adv.,* 2015, **5**, 18438-18450.

(27) V. K. Gupta, N. Atar, M. L. Yola, Z. Üstündağ and L. Uzun, *Water Res.,* 2014, **48**, 210-2017.

(28) H. Wang, W. Zhao, J. Du, F. Wei, Q. Chen and X. Wang, *RSC Adv.,* 2019, **9**, 5158-5163.

II.A.5. References

(1) H.Kolbe,*Ann. Chem. Pharm*., 1849, **69**, 257-294.

(2) R.Breslow,*Acc. Chem. Res*., 1991, **24**, 159-164.

(3) C. J. Li, T. H.Chan, New York, John Wiley & Sons, 1997.

(4) M. Siskin,A. R.Katritzky,*Science*, 1991, **254**, 231-237.

(5) A.Wurtz,*Justus Liebigs Ann. Chem*., 1855, **96**, 364-375.

(6) R.Fittig,*Justus Liebigs Ann. Chem*., 1859, **110**, 23-45.

(7) C.Glaser,*Justus Liebigs Ann. Chem*., 1870, **154**, 137-171.

(8) F.Ullmann, J. Bielecki,*ChemischeBerichte,* 1901, **34**, 2174-2185.

(9) Cadiot P, Chodkiewicz W. In chemistry of acetylenes. Viehe HG, Dekker M. ed. New York, 1969, 597-647.

(10) R. D.Stephens, C. E.Castro,*J. Org. Chem*. 1963, **28**, 3313-3315.

(11) E. J.Corey, G. H.Posner,*J. Am. Chem. Soc.*, 1967, **89**, 3911-3912.

(12) K.Tamao,K. Sumitani,M.Kumada,*J. Am. Chem. Soc*., 1972, **94**, 4374-4376.

(13) R. F.Heck, *Org. React*., 1982, **27**, 345-390.

(14) K.Sonogashira,*J.Organomet. Chem*., 2002, **653**, 46-49.

(15) A. O.King, N. Okukado, E. Negishi,*J. C. S. Chem. Comm.*, 1977, **19**, 683-684.

(16) J. K.Stille,*Angew. Chem. Int. Ed*., 1986, **25**, 508-524.

(17) N.Miyaura, K.Yamada, A.Suzuki,*Tetrahedron Lett*., 1979, **20**, 3437-3440.

(18) S. Murahashi, M.Yamamura, K.Yanagisawa,N.Mita, K.Kondo, *J. Org. Chem*. 1979, **44**, 2408-2417.

(19) Y.Hatanaka,T.Hiyama,*J. Org. Chem*., 1988, **53**, 918-920.

(20) H.Tokuyama,S.Yokoshima, T.Yamashita, T.Fukuyama,*Tetrahedron Lett.*, 1998, **39**, 3189-3192.

(21) L. Liebeskind,J.Srogl,*J. Am. Chem. Soc*., 2000, **122**, 11260-11261.

(22) D.Astruc, F.Lu, J. R.Aranzaes,*Angew. Chem. Int. Ed*., 2005, **44**, 7852-7872.

(23) R.Saravanan, E.Thirumal, V. K.Gupta, V.Narayanan, A.Stephen,*J. Mol. Liq*., 2013, **177**, 394-401.

(24) R.Saravanan, V. K.Gupta, E.Mosquera, F.Gracia,*J. Mol. Liq*., 2014, **198**, 409-412.

(25) T. A.Saleh, V. K. Gupta,*J. Colloid. Interface. Sci*., 2011, **362**, 337-344.

(26) T. A.Saleh, V. K.Gupta,*J. Colloid. Interface. Sci*., 2012, **371**, 101-106.

(27) D.Astruc,*Inorg. Chem*., 2007, **46**, 1884-1894.

(28) J. Liu,*AcsCatal*., 2017, **7**, 34-59.

(29) D.Wang, D.Astruc,*Chem. Soc. Rev*., 2017, **46**, 816-854.

(30) N. B.Singh, S. Agarwal,*Emerg. Mater. Res*., 2016, **5**, 5-43.

(31) N.Miyaura, A. Suzuki,*Chem. Rev*., 1995, **95**, 2457-2483.

(32) S.Budagumpi, R. A.Haque, A. W.Salman,*Coord. Chem. Rev*., 2012, **256**, 1787-1830.

(33) E. A. B.Kantchev, C. J.O'Brien, M. G.Organ,*Angew. Chem. Int. Ed*., 2007, **46**, 2768-2813.

(34) A.de Meijere, F. E.Meyer,*Angew. Chem. Int. Ed. Engl*., 1994, **33**, 2379-2411.

(35) A. O.King, N. Yasuda,*Org. Process. Res. Dev*., 2005, **9**, 646-650.

(36) A. O.King, N.Yasuda,*Top Organomet. Chem*., 2004, **6**, 205-245.

(37) P.Veerakumar, P.Thanasekaran, K. L.Lu, K. C.Lin, S. Rajagopal,*ACS Sustain. Chem. Eng*., 2017, **5**, 8475-8490.

(38) N. T. S.Phan, M.Van Der Sluys, C. W.Jones,*Adv. Synth.Catal*. 2006, **348**, 609-679.

(39) V. P.Ananikov, I. P.Beletskaya,*Organometallics*, 2012, **31**, 1595-1604.

(40) F.Amoroso,S.Colussi, *Catal. Lett*. 2013, **143**, 547-554.

(41) S. R.Sanjaykumar,B. D.Mukri, S.Patil, G.Madras, M. S.Hegde.,*J. Chem. Sci.* 2011, **123**, 47-54.

(42) D.Khalili, A. R.Banazadeh, E.Etemadi-Davan,*Catal. Lett*., 2017, **147**, 2674-2687.

(43) I. B.Chorkendorff,J. W. Niemantsverdriet, WILEY-VCH Verlag GmbH & Co. KGaA: Weinheim, Germany, 2003, 1-22.

(44) A. V.Astakhov, O. V.Khazipov, A. Y.Chernenko, D. V.Pasyukov, A. S.Kashin, E. G.Gordeev, V. N.Khrustalev, V. M.Chernyshev, V. P.Ananikov,*Organometallics,* 2017, **36**, 1981-1992.

(45) F. X.Felpin, T.Ayad, S. Mitra,*Eur. J. Org. Chem*. 2006, **2006**, 2679-2690.

(46) F. X.Felpin,*Synlett*., 2014, **25**, 1055-1067.

(47) E. Cini, E. Petricci, M.Taddei,*Catalysts*, 2017, **7**, 89.

(48) Z. Wu, Y. Wang, L. Sun, Y. Mao, M. Wang and C. Lin, *J. Mater. Chem. A,* 2014, **2**, 8223-8229.

(49) G.Lu, R.Franzen, Q.Zhang, Y. Xu, *Tetrahedron Lett*., 2005, **46**, 4255-4259.

(50) M. Lysen and K.Kohler, *Synthesis*, 2006, **17**, 692-698.

(51) K. S. Novoselov,V. I.Fal′ko, L.Colombo, P. R.Gellert, M. G.Schwab, K.Kim,*Nature,* 2012, **490**,192-200.

(52) (a) G. M.Scheuermann, L.Rumi, P. Steurer, W. Bannwarth, R. Mülhaupt, *J. Am. Chem. Soc*., 2009, **131**, 8262-8270; (b) L.Rumi, G.

M.Scheuermann, R. Mülhaupt, W. Bannwarth,*Helv. Chim. Acta*., 2011, **94**, 966-976.

(53) (a) G.Xiang, J.He, T.Li, J.Zhuang, X. Wang,*Nanoscale*, 2011,**3**, 3737-3742; (b) S. J. Hoseini, M. Dehghani, H.Nasrabadi,*Catal. Sci. Technol*., 2014, **4**, 1078-1083.

(54) S.Moussa, A. R.Siamaki, B. F.Gupton, M. S.El-Shall,*ACS Catal.*, 2012, **2**, 145-154.

(55) J.Hu, Y.Wang, M.Han, Y.Zhou, X.Jiang, P.Sun,*Catal. Sci. Technol*. 2012,**2**, 2332-2340.

(56) N.Shang, S.Gao, C.Feng, H.Zhang, C.Wang, Z.Wang,*RSC Adv*., 2013,**3**, 21863-21868.

(57) N.Shang, C.Feng, H.Zhang, S.Gao, R.Tang, C.Wang, Z.Wang,*Catal. Commun*., 2013,**40**, 111-115.

(58) Y.Li, X.Fan, J.Qi, J.Ji, S.Wang, G.Zhang, F.Zhang,*Nano Res*., 2010, **3**, 429-437.

(59) S. S. Shendage, U. B.Patil, J. M.Nagarkar, *Tetrahedron Lett*., 2013,**54**, 3457-3461.

(60) J.Li, A.Corma, J.Yu,*Chem. Soc. Rev*., 2015, **44**, 7112-7127.

(61) S.Bhattacharyya, D.Samanta, S.Roy, V. P.Haveri Radhakantha, T. K.Maji,*ACS Appl. Mater. Interfaces*., 2019, **11**, 5455-5461.

(62) A. Kumbhar,*Top Curr. Chem*., 2017, **375**, No. 2.

(63) Y.Wang, J.Liao, Z. Xie, K.Zhang, Y.Wu, P. Zuo, W.Zhang, J.Li, *ACS Appl. Mater. Interfaces*., 2020, **12**, 11419-11427.

(64) M.Shamzhy, M.Opanasenko, P.Concepcion, A. Martínez,*Chem. Soc. Rev.*, 2019, **48**, 1095-1149.

(65) N.Wang, Q.Sun, R.Bai, X.Li, G.Guo, J.Yu,*J. Am. Chem. Soc*., 2016, **138**, 7484-7487.

(66) C. Baleizao, A. Corma, H. Garcia, A. Leyva, *Chem. Commun*., 2003, **85**, 606-607; (b) C. Baleizao, A. Corma, H. Garcia, A. Leyva, *J. Org. Chem*., 2004, **69**, 439-446.

(67) V. H.Pham, T. T.Dang, S. H.Hur, E. J.Kim, J. S.Chung,*ACS Appl. Mater. Interfaces*., 2012, **4**, 2630-2636.

(68) P.Cotugno, M.Casiello, A.Nacci, P.Mastrorilli, M. M.Dell'Anna, A.Monopoli,*J.Organomet. Chem.*, 2014, **752**, 1-5.

(69) J.Mondal, A.Modak, A. Bhaumik,*J. Mol.Catal. A Chem*., 2011, **350**, 40-48.

(70) Y. L.Zhang, S.Wei, F. J.Liu, Y. C.Du, S.Liu, Y. Y.Ji, T.Yokoi, T.Tatsumi, F. S. Xiao,*Nano Today*, 2009, **4**, 135-142.

(71) J. K.Cho, R. Najman, T. W.Dean, O.Ichihara, C.Muller, M.Bradley,*J. Am. Chem. Soc*., 2006, **128**, 6276-6277.

(72) Y.Lee, M. C.Hong, H.Ahn, J.Yu, H.Rhee,*J.Organomet. Chem*., 2014,**769**, 80-93.

(73) (a) Y.Hirokawa, T.Tanaka, E. S.Matsuo,*J. Chem. Phys*., 1984,**81**, 6379-6380; (b) K.Kubota, S. Fujishige, I.Ando,*J. Phys. Chem*. 1990, **94**, 5154-5158.

(74) M. Shibayama, Y. Suetoh, S.Nomura,*Macromolecules*, 1996,**29**, 6966-6968.

(75) D. E. Bergbreiter, B. L.Case, Y. S.Liu, J. W.Caraway,*Macromolecules*, 1998, **31**, 6053-6062.

(76) (a) Y.Mei, Y.Lu, F. Polzer, M. Ballauff, M.Drechsler,*Chem. Mater*., 2007, **19**, 1062-1069; (b) D. E. Bergbreiter, P. L. Osburn, A.Wilson, E. M.Sink,*J. Am. Chem. Soc*. 2000, **122**, 9058-9064.

(77) (a) H. I.Melendez-Ortiz, E. Bucio, G.Burillo,*Radiat. Phys. Chem*. 2009, **78**, 1-7; (b) H.Nur, V. T. Pinkrah, J. C.Mitchell, L. S. Benee, M. J.Snowden,*Adv. Colloid. Interface. Sci*., 2010, **158**, 15-20.

II.B.6. References

(1) (a) A. Suzuki, *In Modern Arene Chemistry,*ed. D. Astruc, Wiley-VCH, Weinheim, 1st edn, 2004, vol. 80, ch. 3, pp 53-106; (b) R. F. Heck, *Acc. Chem. Res*., 1979, **12**, 146-151.

(2) A. Fihri, M. Bouhrara, B. Nekoueishahraki, J. M. Basset and V. Polshettiwar, *Chem. Soc. Rev.,* 2011, **40**, 5181-5203.

(3) Z. Z. F. S. Zhou, D. S. Liu, Ch. Shen and L.Y. Tan, Luo, *Inorg. Chem. Commun*., 2011, **14**, 659-664.

(4) P. J. M. Hajduk, J. Bures, Prastgaard and S.W. Fesik, *J. Med. Chem*., 2000, **43**, 3443-3447.

(5) J. Hassan, M. Sévignon, C. Gozzi, E. Schulz and M. Lemaire, *Chem Rev*., 2002, **102**, 1359-1470.

(6) A. Fihri, M. Bouhrara, B. Nekoueishahraki, J. M. Basset and V. Polshettiwar, *Chem. Soc. Rev.,* 2011, **40**, 5181-5203.

(7) V. P. W. Bo¨hm and W. A. Herrmann, *Chem. Eur. J.,* 2000, **6**, 3679-3681.

(8) J. H. Park, F. Raza, S. J. Jeon, H. I. Kim, T. W. Kang, D. Yim and J.H. Kim, *Tetrahedron Lett.,* 2014, **55**, 3426-3430.

(9) S. Paul, Md. M. Islam and Sk. M. Islam, *RSC Adv*., 2015, *5*, 42193-42221.

(10) L. Yin and J. Liebscher, *Chem. Rev*. 2007, **107**, 133-173.

(11) Q. Sun, L. F. Zhu, Z. H. Sun, X. Ju. Meng and F. S. Xiao, *Sci. China Chem*., 2012, **55**, 2095-2103.

(12) C. Pan, M. Liu, L. Zhao, H. Wu, J. Ding and J. Cheng, *Catcom*., 2008, **9**, 1685-1687.

(13) R. B. Bedford, U. G. Singh, R. I. Walton, R. T. Williams and S. A. Davis, *Chem. Mater.,* 2005, **17**, 701-707.

(14) M. J. Jin, A. Taher, H. J. Kang, M. Choi and R. Ryoo, *Green Chem*., 2009, **11**, 309-313.

(15) X. Jin, J. Li and H. Li, *J. Exp. Nanosci*., 2018, **13**, 95-106.

(16) R. K. Ramchandani, B. S. Uphade, M. P. Vinod, R. D. Wakharkar, V. R. Choudhary and A. Sudalai, *Chem. Commun*., 1997, 2071-2072.

(17) Y. Wan, H. Wang, Q. Zhao, M. Klingstedt, O. Terasaki and D. Zhao, *J. Am. Chem. Soc*., 2009, **131**, 4541-4550.

(18) Y. L. Nong, N. Qiao, T.H. Deng, Z. Pan and Y. Liang, *Catal. Commun.,* 2017, **100**, 139-143.

(19) A. Wali, S. M.; Pillai, V. K. Kaushik and S. Satish, *Appl. Catal. A*., 1996, **135**, 83-93.

(20) W. K. Kundhikanjana, J. Lai, H. L. Wang, H. J. Dai, M. A. Kelly and Z. X. Shen, *Nano Lett*., 2009, **9**, 3762-3765.

(21) J. Wang, H. Hu, X. Wang, C. Xu, M. Zhang and X. Shang, *J. ApplPolm Sci*., 2011, **122**, 1866-1871.

(22) T. Kuila, S. Bose, P. Khanra, N. H. Kim and J. H. Lee, *Compos.-A:Appl.Sci. Manuf*., 2011, **42**, 1856-1861.

(23) J. Yang, X. Yan, M. Wu, F. Chen, Z. Fei and M. Zhong, *J Nanopart Res*., 2012, **14**, 717-726.

(24) J. Hass, W. A. Heer and E. H. Conrad, *J. Phys. Condens. Matter*., 2008, **20**, 1-27.

(25) S. S. Shendage, A. S. Singh and J. M. Nagarkar, *Tetrahedron Lett*., 2014, **55**, 857-860.

(26) M. G´omez-Mart´ınez, E. Buxaderas, M. I. Pastor and D. A. Alonso, *J. Mol. Catal. A. Chem.,* 2015, **404**, 1-7.

(27) G. M. Scheuermann, L. Rumi, P. Steurer, W. Bannwarth and R. Mu¨lhaupt, *J. Am. Chem. Soc.,* 2009, **131**, 8262-8270.

(28) S.-H. Kim, G. H. Jeong, D. Choi, S. Yoon, H. B. Jeon, S.-M. Lee and S.-W. Kim, *J. Colloid Interface Sci*., 2013, **389**,85-90.

(29) S. S. Shendage, U. B. Patil and J. M. Nagarkar, *Tetrahedron Lett*., 2013, **54**, 3457–3461.

(30) V.Sharavath and S. Ghosh, *RSC Adv*., 2014, **4**, 48322–48330

(31) C. Premi and N. Jain, *RSC Adv*., 2016, **6**, 74961-74967.

(32) J. R. Anasdass, P. Kannaiyan, R. Raghavachary, S. C. B. Gopinath and Y. Chen, *PLOS ONE*, 2018, **13**, 0193281-0193294.

(33) A. Zarnegaryan and D. Elhamifar, *Heliyon*, 2020, **6**, 03741-03749.

(34) J.Y. Jang, H. M. Jeong and B. K. Kim, *Macromol. Res*., 2009, **17**, 626-629.

(35) C. H. Chen, W. H. Yen, C. F. Kuan and C. L. Chiang, *Polym. Compos*., 2010, **31**, 18-24.

(36) J. R. Potts, S. H. Lee, T. M. Alam, J. An, M. D. Stoller and R. D. Piner, *Carbon,* 2011, **49**, 2615-2623.

(37) X. Zeng, J. Yang and W. Yuan, *Eur. Polym. J.,* 2012, **48**, 1674-1682.

(38) V. H. Pham, T. T. Dang, S. H. Hur, E. J. Kim and J. S. Chung, *ACS Appl. Mater. Interfaces*.,2012, **4**, 2630-2636.

(39) J. M. Thomassin, M. Trifkovic, W. Alkarmo, C. Detrembleur, C. J r me and C. Macosko, *Macromolecules,* 2014, **47**, 2149-2155.

(40) D. L.Trimm, ed. C. H. Bartholomew, *Elsevier*, Amsterdem, 1991, 68, 29-51.

(41) R. K. Gupta, Z. A. Alhamed and F. Yakuphanoglu, *Mater. Lett.,* 2013, **112**, 75-77.

(42) F. Chekin, *Bull. Mater. Sci*., 2015, **38**, 887-893.

(43) J. Xu, S. Gai, F. He, N. Niu, P. Gao, Y. Chen and P. Yang, *Dalton Trans*., 2014, **43**, 11667-11675.

(44) D. R. Anton and R. H. Crabtree, *Organometallics,* 1983, **2**, 855-859.

(45) B. Basu, K. Biswas, S. Kundu and S. Ghosh, *GreenChem*. 2010, **12**, 1734-1738.

(46) A. Mahanta, M. Mondal, A. J. Thakur and U. Bora, *Tetrahedron Lett*., 2016, **57**, 3091-3095.

(47) S. Bhattacharya, A. Srivastava and S. Sengupta, *Tetrahedron Lett*., 2005, **46**, 3557-3560.

(48) A. Ohtaka, T. Okagaki, G. Hamasaka, Y. Uozumi, T.Shinagawa, O. Shimomura and R. Nomura, *Catalysts*, 2015, **5**, 106-118.

(49) S. R. Sanjaykumar, B. D. Kumari, S. Patil, G. Madras and M. S. Hegde, *J. Chem. Sci*., 2011, **123**, 47-54.

(50) M. Bakherad, A. Keivanloo and S. Samangooei, *Tetrahedron Lett*., 2012, **53**, 5773–5776.

(51) V. Calo, A. Nacci, A. Monopoli, A. Fornaro, L. Sabbatini, N. Cioffi, N. Ditaranto, *Organometallics*, 2004, **23**, 5154-5158.

(52) l. Bin,W. J. Qing, G. D. Hua, L. X. Ming, C. X. Qin, P. Yue and G. H. Wei, *Sci China Chem*., 2014, **57**, 1310-1314.

III.A.6. References

(1) E. Vitaku, D. T. Smith and J. T. Njardarson, *J. Med. Chem*., 2014, **57**, 10257-10274.

(2) P. J. J. Martins, S. Santos, L. R. Raposo, C. Roma-Rodrigues, P. V. Baptista and A. R. Fernandes, *Molecules*, 2015, **20**, 16852-16891.

(3) T. Karabasanagouda, A. V. Adhikari and M. Girisha, *Indian J. Chem.,* 2009, **48**, 430-437.

(4) (a) Q. Liu and Y. N. Zhang, *Bull. Korean Chem. Soc*., 2011, **32**, 3559-3560, (b) A. Domling, *Curr. Opin. Chem. Biol*., 2002, **6**, 306-313, (c) C. O. Kappe, *Curr. Opin. Chem. Biol.,* 2002, **6**, 314-320.

(5) E. Rafiee and H. Jafari, *Bioorg. Med. Chem. Lett*., 2006, **16**, 2463-2466.

(6) G. Abbiati, E. M. Beccalli, G. Broggini and C. Zoni, *Tetrahedron*, 2003, **59**, 9887-9893.

(7) S. Batra, S. K. Rastogi, B. Kundu, A. Patra and A. P. Bhaduri, *Tetrahedron Lett.*, 2000, **41**, 5971-5974.

(8) A. Barria,V. Derkach and T. Soderling, *J. Biol. Chem*., 1997, **272**, 32727-32730.

(9) B. Kafle, N. G. Aher, D. Khadka, H. Park and H. Cho, *Chem. Asian J.,* 2011, **6**, 2073-2079.

(10) J. Han, H. Guo, X. G. Wang, M. L. Pang and J. B. Meng, *Chin. J. Chem.,* 2007, **25**, 129-131.

(11) M. Pinerio and T. M. Pinho-e-Melo, *Eur. J. Org. Chem.,* 2009, **31**, 5287-5307.

(12) O. H. Kan, I. Adachi, R. Kido and K. Hirose, *J. Med. Chem.,* 1967, **10**, 411-418.

(13) X. H. Zhang, Y. H. Zhan, D. Chen, F. Wang and L. Y. Wang, *Dyes Pigm.,* 2012, **93**, 1408-1415.

(14) (a) E. Aret, H. Meekes, E. Vlieg and G. Deroover, *Dyes Pigm.,* 2007, **72**, 339-344 (b) Y. K. Kang, K. J. Shin and K. H. Yoo, *Bioorg. Med. Chem. Lett.,* 2000, **10**, 95-99.

(15) (a) P. Conti, C. Dallanoce, M. D. Amici, C. D. Micheli and K. N. Klotz, *Bioorg. Med. Chem.,* 1998, **6**, 401-408; (b) M. G. Gordaliza, T. Faircloth, M. A. Castro, J. M. M. DelCorral, M. L. López-Vázquez and A. San Feliciano, *J. Med. Chem.,* 1996, **39**, 2865-2868.

(16) T. Ishioka, A. Kubo, Y. Koiso, K. Nagasawa, A. Itai and Y. Hashimoto, *Bioorg. Med. Chem.,* 2002, **10**, 1555-1566.

(17) I. Nakamura, M. Okamoto and M. Terada, Org Lett., 2010, **12**, 2453-2455.

(18) D. B. Lowe, S. Magnuson, N. Qi, et al. *Bioorg. Med. Chem. Lett.,* 2004, **14**, 3155-3159.

(19) D. Villemin, B. Martin and B. Garrigues, *Synth. Commun.,* 1993, **23**, 2251-2257.

(20) (a) Y. Q. Zhang and C. Wang, *Chin. J. Org. Chem.,* 2008, **28**, 141-144; (b) Q. Liu and R. T. Wu, *J. Chem. Res.,* 2011, **35**, 598-599.

(21) Y. Q. Zhang and C. Wang, *Chin. J. Org. Chem.,* 2008, **28**, 1267-1271.

(22) S. Tu, J. Zhang, R. Jia, B. Jiang, Y. Zhang and H. Jiang, *Org. Biomol. Chem.,* 2007, **5**, 1450-1453.

(23) K. Ablajan and H. Xiamuxi, *Synth. Commun.,* 2012, **42**, 1128-1136.

(24) F. Saikh, J. Das and S. Ghosh, *Tetrahedron Lett.,* 2013, **54**, 4679-4682.

(25) Q. Liu and X. Hou, *Phosphorus Sulfur Silicon Relat. Elem.,* 2012, **187**, 448-453.

(26) H. Kiyani and F. Ghorbani, *J. Chem. Soc.,* 2017, **21**, 112-119.

(27) M. S. Patil, C. Mudaliar and G. U. Chaturbhuj, *Tetrahedron Lett.,* 2017, **58**, 3256-3261.

(28) H. Kiyani and F. Ghorbani, *Res. Chem. Intermed.,* 2015, 41, 2653-2664.

(29) H. Kiyani, F. Ghorbani, *Elixir Org. Chem. A.,* 2013, **58**, 14948-14950.

(30) M. Ahmadzadeh, Z. Zarnegar and J. Safari, *Green Chem. Lett. Rev.,* 2018, 11, 78-85.

(31) Q. Liu, H. M. Ai, Z. Li, *Ultrason. Sonochem.,* 2011, **18**, 477-479.

(32) M. Mirzazadeh and G. Mahdavinia, *H. J. Chem.,* 2012, 9, 425-429.

(33) S. Tu, J. Zhang, R. Jia, B. Jiang, Y. Zhang and H. Jiang, *Org. Biomol. Chem*., 2007, **5**, 1450-1453.

(34) S. N. Maddila, S. Maddila, W. E. Zyl and S. B. Jonnalagadda, *Res. Chem. Intermed.,* 2016, **42**, 2553.

(35) H. Kiyani, A. Kanaani, D. Ajloo, F. Ghorbani and M. Vakili, *Res. Chem. Intermed.*, 2015, **41**, 7739-7773.

(36) G. Minunni and S. D'Urso, Cuss. chim. it&., 68, 485 (1928); c. A., 43, 1120 (1929)

(37) R. Schiff and M. Betti, *Ber.* 1897, **80**, 1885-1887.

(38) M. S. Patil, C. Mudaliar and G. U. Chaturbhuj, *Tetrahedron Lett.,* 2017, **58**, 3256-3261

(39) Q. Liu and X. Hou, *Phosphorus Sulfur Silicon Relat. Elem.,* 2012, **187**, 448-453.

(40) M. M. Heravi, K. Bakhtiari, S. Taheri and H. A. Oskooie, *J. Chin. Chem. Soc.,* 2007, **54**, 1557-1560.

(41) M. Fagnoni, D. Dondi, D. Ravelli and A. Albini, *Chem. Rev.,* 2007, **107**, 2725-2756.

(42) F. Saikh, J. Das and S. Ghosh, *Tetrahedron Lett.,* 2013, **54**, 4679-4682.

(43) H. Kiyani and F. Ghorbani, *J. Saudi Chem. Soc.,* 2017, **21**, 112-119.

(44) P. L. Salzberg and J.V. Supniewski, *In Organic Synthesis Collection,* John Wiley, New York, USA, 1995.

(45) B. Zwanenburg and A.S. Mwakaboko, *Bioorg. Med. Chem.,* 2011, **19**, 7394-7400.

(46) S. G. Stewart, D. Spagnolo, M. E. Polomska, M. Sin, M. Karimi and L. Abraham, *J. Bioorg. Med. Chem. Lett.,* 2007, **17**, 5819-5824.

(47) M. G. Dekamin and Z. Karimi, *J. Organomet. Chem.,* 2009, **694**, 1789-1794.

(48) D. R. Dreyer and C. W. Bielawski, *Chem. Sci.,* 2011, **2**, 1233-1240.

(49) F. Hu, M. Patel, F. Luo, C. Flach, R. Mendelsohn, E. Garfunkel, H. He and M. Szostak, *J. Am. Chem. Soc.,* 2015, **137**, 14473-14480.

(50) D. R. Dreyer, H.-P. Jia and C. W. Bielawski, *Angew. Chem. Int. Ed.,* 2010, **49**, 6813-6816.

(51) C. Su, R. Tandiana, J. Balapanuru, W. Tang, K. Pareek, C. T. Nai, T. Hayashi and K. P. Loh, *J. Am. Chem. Soc.,* 2015, **137**, 685-690.

(52) B. Majumdar, D. Sarma, T. Bhattacharya and T. K. Sarma, *ACS Sustainable Chem. Eng.,* 2017, **5**, 9286-9294.

(53) C. Su and K. P. Loh, *Acc. Chem. Res.,* 2013, 4**6**, 2275-2285.

(54) S. Navalon, A. Dhakshinamoorthy, M. Alvaro, H. Garcia, *Chem. Rev.,* 2014, **114**, 6179-6212.

(55) Q. Hou, W. Li, M. Ju, L. Liu, Y. Chen and Q. Yang, *RSC Adv.,* 2016, **6**, 104016-104024.

(56) M. Mirzazadeh and G. H. Mahdavinia, *J. Chem.,* 2012, **9**, 425-429.

III.B.5. References

(1) W. P Smith, L. S. Sollis, D. P. Howes, P. C. Cherry, I. D. Starkey, K. N. Cobley, H. Weston, J. Scicinski, A. Merritt and A. Whittington, et al. *J. Med. Chem.,* 1998, **41**, 787-797.

(2) J. L. Wang, D. Liu, Z. J. Zheng, S. Shan, X. Han, S. M. Srinivasula, C. M. Croce, E. S. Alnemri and Z. Huang, *Proc. Natl. Acad. Sci.,* 2000, **97**, 7124-7129.

(3) A. M. Grumezescu, E. Andronescu, A. Ficai, C. Bleotu, D. E. Mihaiescu and M. C. Chifiriuc, *Int. J. Pharm.,* 2012, **436**, 771-777.

(4) K. Mazaahir, S. Shilpi, R. K. Khalilur and S. T. Sharanjit, *Bioorg. Med. Chem. Lett.,* 2005, **15**, 4295-4298.

(5) C. K. Sheng, J. H. Li and N. J. Hideo, *Med. Chem.,* 1984, **27**, 539-544.

(6) M. Bihani, P. P. Bora, G. Bez and H. Askari, *ACS Sustainable. Chem. Eng.,* 2013, **1**, 440-447.

(7) M. Fatahpour, F. N. Sadeh, N. Hazeri, M. T. Maghsoodlou, Md. S. Hadavi and S. Mahnaei, *Jour. of Saudi Chem. Soc.,* 2017, **21**, 998-1006.

(8) S. C. Kuo, L. J. Huang and H. J. Nakamura, *Med. Chem.,* 1984, **27**, 539-544.

(9) H. Junek and H. Aigner, *Chem. Ber.,* 1973, **106**, 914-921.

(10) G. Tacconi, G. Gatti and G. J. Desimoni, *Prakt. Chem.,* 1980, **322**, 831-834.

(11) A. Sharanin, L.Yu, G. Sharanina and V. V. Zh. Puzanova, *Org. Khim.,* 1983, **19**, 2609.

(12) G. Kaupp, M. R. Naimi-Jamal and J. Schmeyers, *Tetrahedron*, 2003, **59**, 3753-3760.

(13) L. He, Z. Tang, L. F. Cun, A. Q. Mi, Y. Z. Jiang and L. Z. Gong, *Tetrahedron*, 2006, **62**, 346-351.

(14) S. R. Meghana, K. P. Mahesh, S. M. Swapnil and M. S. Manikrao, *J. Mol. Catal. A*, 2005, **235**, 267-270.

(15) S.-B. Guo, S.-X. Wang and J.-T. Li, *Synth. Commun.,* 2007, **37**, 2111-2120.

(16) B. List, *Tetrahedron*, 2002, **58**, 5573-5590.

(17) G. Vasuki and K. Kumaravel, *Tetrahedron Lett.,* 2008, **49**, 5636-5638.

(18) M. Babaie and H. Sheibani, *Arab. J. Chem.,* 2011, **4**, 159-162.

(19) M. Kangani, N. Hazeri, M. T. Mghsoodlou, S. M. Habibi-khorasani and S. Salahi, *Res. Chem. Intermed.,* 2015, **41**, 2513-2519.

(20) G. Nagendrappa, *Resonance,* 2002, **7**, 59-63.

(21) D. R. Park, H. Kim, J. C. Jung, S. H .Lee and I. K. Song, *Chem. Res. Intermed.,* 2008, **34**, 2-5.

(22) A. Vafaee, A. Davoodnia and M. Pordel, *Chem. Res. Intermed.,* 2015, **41**, 8343-8354.

(23) P. H. Li, B. L. Li, Z. M. An, L. P. Mo, Z. S. Cui and Z. H. Zhang, *Adv. Synth. Catal.,* 2013, **355**, 2952-2959.

(24) B. Maleki, H. Eshghi, M. Barghamadi, N. Nasiri, A. Khojastehnezhad, S. S. Ashrafi and O. Pourshiani, *Res. Chem. Intermed.,* 2016, **42**, 3071-3093.

(25) R. Konakanchi, R. Gondru, V. B. Nishtala and L. R. Kotha, *Synth. Commun.,* 2018, **48**, 1994-2001.

(26) A. Iskalieva, B. M. Yimmou, P. R. Gogate, M. Horvath, P. G. Horvath and L. Csoka, *Ultrason. Sonochem.,* 2012, **19**, 984-993.

(27) S. Zhu, J. Wang and W. Fan, *Catal. Sci. Technol.,* 2015, **5**, 3845-3858.

(28) Q. Hou, W. Li, M. Ju, L. Liu, Y. Chen and Q. Yang, *RSC Adv.,* 2016, **6**, 104016-104024.

(29) D. C. Marcano, D. V. Kosynkin, J. M. Berlin, A. Sinitskii, Z. Sun, A. Slesarev,L. B. Alemany, W. Lu and J. M. Tour, *ACS Nano*, 2010, **8**, 4806-4814.

Index

Reprints of Published Articles

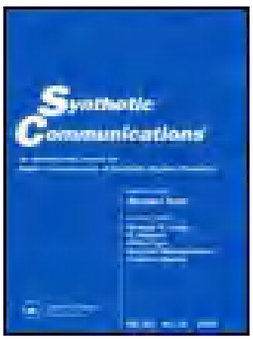

Synthetic Communications

An International Journal for Rapid Communication of Synthetic Organic Chemistry

ISSN: 0039-7911 (Print) 1532-2432 (Online) Journal homepage: http://www.tandfonline.com/loi/lsyc20

Poly (methyl methacrylate)-graphene oxide supported palladium catalyst: A ligand free protocol for Suzuki and Heck coupling reaction in water medium

Puja Basak & Pranab Ghosh

To cite this article: Puja Basak & Pranab Ghosh (2018): Poly (methyl methacrylate)-graphene oxide supported palladium catalyst: A ligand free protocol for Suzuki and Heck coupling reaction in water medium, Synthetic Communications, DOI: 10.1080/00397911.2018.1515365

To link to this article: https://doi.org/10.1080/00397911.2018.1515365

SYNTHETIC COMMUNICATIONS®
https://doi.org/10.1080/00397911.2018.1515365

Poly (methyl methacrylate)-graphene oxide supported palladium catalyst: A ligand free protocol for Suzuki and Heck coupling reaction in water medium

Puja Basak and Pranab Ghosh

Department of Chemistry, University of North Bengal, Darjeeling, West Bengal, India

ABSTRACT

A green and efficient approach for the ligand free Suzuki–Miyaura and Mizoroki–Heck C–C cross coupling reaction using low palladium loaded Graphene oxide-polymer composite catalyst has been described. High yields, easy work-up, easy availability and handling, eco-friendly and reusability of the catalysts are the main aspects of the present method. The simplicity of the entire sequence has made the protocol meritorious as a reasonable contribution to the existing methods in the field of substituted biphenyls and olefins. The supported heterogeneous catalyst was characterized using HRTEM, ICP-AES, PXRD, XPS, TGA, and FT-IR spectroscopy.

GRAPHICAL ABSTRACT

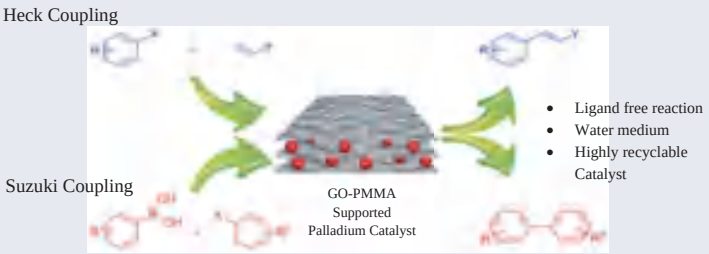

ARTICLE HISTORY
Received 9 May 2018

KEYWORDS
Aqueous medium; GO-PMMA-Pd catalyst; Heck reaction; ligand free; Suzuki–Miyaura coupling

Introduction

Heterogeneous palladium catalyzed C–C cross coupling reactions have attracted much attention over past two decades. As a representative of this class of reaction, Suzuki and Heck coupling are most significant because biaryl moieties and substituted olefins are present in pharmaceuticals,[1–4] wide range of natural products such as alkaloids and many agrochemicals and biologically active compounds.[2,5] Although homogeneous catalyst offers excellent result, they have some drawbacks because of difficult separation procedure that often contaminates the products. However, most of them employ different types of ligands such as sterically hindered trialkyl phosphines, triarylphosphines,[6] *N*-heterocyclic carbenes,[7] based Pd (II) complexes. Use of these ligands is unenviable

CONTACT Pranab Ghosh pizy12@yahoo.com Department of Chemistry, University of North Bengal, Darjeeling, West Bengal, India.
Color versions of one or more of the figures in the article can be found online at www.tandfonline.com/lsyc.
Supplemental data for this article can be accessed on the publisher's website.

because they are toxic and moisture sensitive. However, with growing interest towards greener reactions, ligand free solid supported heterogeneous catalysts are in demand. They have the advantage of enhanced synthetic efficiency and operational simplicity.[8–11] Previous reports include the immobilization of Pd on activated carbon,[12] polymers,[13,14] zeolites,[15] mesoporous carbon,[16] silica, alumina or titania.[17,18]

In the recent years, graphene oxide (GO) has attracted much attention owing to its wide range of application in different fields such as fuel cells,[19] nanocomposite materials,[20–23] and electronic devices.[24] GO has two dimensional layered sheets with several oxygen containing functional groups like epoxy, hydroxy, carbonyl, carboxyl, etc. Palladium nanoparticles supported on graphene and graphene derivatives enlarge the surface area of the composite,[25] increasing the distance between the sheets. Utilising this phenomenon, catalytic activity of GO-Pd/SGO-Pd,[25,26] Pd NPs supported on single layer-GO[27] and polyamine modified GO-Pd[28] have been successfully tested in Suzuki–Miyaura coupling. Reports regarding GO–supported palladium catalyst using ethanol at refluxed condition,[29] and GO-supported NHC-Palladium catalyst using aqueous-organic mixed solvents[7] are very scanty. In some cases, it is reported that,[7,29] the activity of GO-supported palladium catalyst reduces gradually due to the agglomeration and leaching of metal nanoparticles (NPs). In view of that and to overcome the drawbacks of the previously reported protocols, we have developed a new GO-based heterogeneous catalyst and employed it in Suzuki–Miyaura and Mizoroki–Heck reaction. The reaction conditions are mild and the catalyst can be recycled for five runs without significant loss in its catalytic activity.

Preliminary studies on polymer supported GO has revealed significant increase in mechanical and thermal properties of the composite.[30–33] Driven by this fact, the idea of a new solid support, which allows better stability, easy recovery of products and simple separation procedure is hypothesized. Poly (methyl methacrylate) [PMMA] is a non-conductive polymer and its composite with GO enhances the thermal stability of the material. Based on the above perspective, our present explorative work involves the deposition of Pd NPs on GO-PMMA composite through in situ polymerization of MMA. Wielded by the environmental concerns, water is selected as solvent instead of hazardous solvents such as DMF, DMA, NMP, etc. Utility of GO enhances the thermal stability of poly (methyl methacrylate)[34,35] and Pd NPs are strongly immobilized in between the layers of graphene oxide–PMMA composite.[24,29] To the best of our knowledge, GO-PMMA supported Pd catalyst has not been employed in Suzuki and Heck coupling reactions. Simpler reaction conditions, ligand free protocol, low Pd content and tolerance to wide range of functional groups are the salient features of our work.

Results and discussion

The morphology of the catalyst (GO-PMMA-Pd) was analyzed by transmission electron microscope (TEM). The micrograph and particle size distribution curve of *in situ* prepared GO-PMMA-Pd catalyst is represented in Figure 1. The TEM images show the mono dispersed palladium without agglomeration on the GO-PMMA-sheet during *in situ* polymerization of MMA. The average size of the Pd NPs has been determined from the TEM images and was found to be around 4.8 nm.

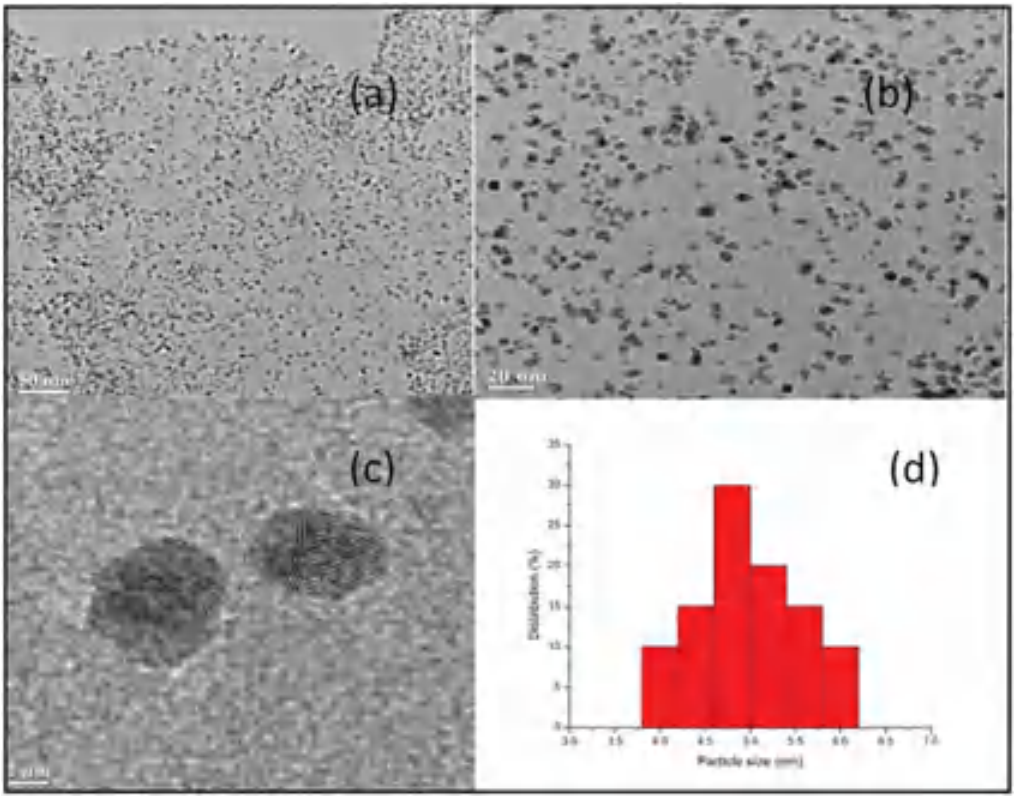

Figure 1. TEM image of GO-PMMA-Pd composite catalyst (a) at 50 nm (b) at 20 nm (c) at 2 nm (d) Particle size distribution curve of GO-PMMA-Pd catalyst.

The catalyst life is a factor that can control the economic viability of industrial processes and as a consequence high thermal resistance of a catalyst support is found to be suitable for different kinds of thermal reaction.[36]

Thermogravimetric Analysis (TGA) of the solid support has been analyzed for several samples with different *wt* % of GO loading as shown in Figure 2. It is very interesting to observe that composite with the lowest *wt* % of GO exhibited maximum thermal stability (Fig. 2).

The catalyst was subjected to powder X-ray diffraction (XRD) for composition analysis (Fig. 3). Three sharp peaks at around $2\theta = 40.1°$, 46.6° and 68.9° represents the crystalline planes (111), (200) and (220), respectively, in fcc structure of Pd.[29] However the intensity of (111) plane is higher than (200) and (220) plane. The absence of strong GO peak at $2\theta = 10.63°$[37] and the appearance of characteristic broad PMMA peak at $2\theta = 14.8°$ indicated the formation of GO-polymer composite. The FTIR spectrum of GO has a peak at 1735 cm^{-1} which is assigned to the carbonyl stretching frequency. The FT-IR peak of PMMA at 1148 cm^{-1} is associated with the stretching vibration of the C–O bond in the C–O–C moiety, whereas the peak at 1731 cm^{-1} is due to the acrylate carbonyl groups. FT-IR spectrum (Fig. 4) revealed that the resultant GO-PMMA-Pd composite catalyst contained several functional groups like –OH (3454 cm^{-1}) and C=O (1731 cm^{-1}). Therefore, it has a strong tendency to readily

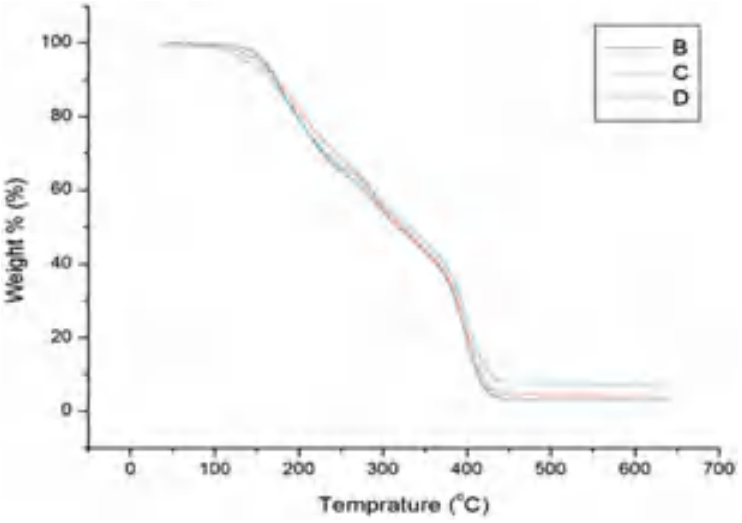

Figure 2. TGA results of (B) 2 *wt*% (C) 5 *wt*% (D) 10 *wt*% GO in PMMA.

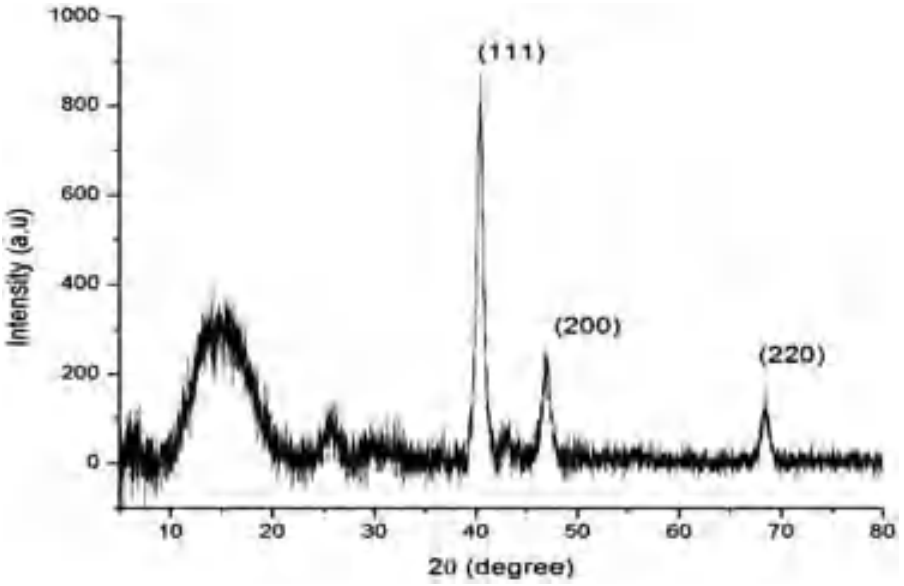

Figure 3. XRD pattern of GO-PMMA-Pd composite catalyst.

interact with metal ions by hydroxyl and carboxyl group. It is considered that the bond between Pd and GO-PMMA can be formed through some physical/chemical interactions such as Vander Waals force, H-bonding and other bonds.[38] The shift of other stretching frequencies also points towards the association of PMMA with GO (Fig. 4). Furthermore, a hump obtained at around $2\theta = 23°$ suggests the presence of reduced graphene oxide (RGO).[39] Hence, it can be concluded that a small amount of GO has been converted into RGO when HCOOH was employed. GO-PMMA-Pd catalyst was further characterized by XPS, as shown in Figure 5. High-resolution XPS spectrum was corrected with reference to the carbon 1 s peak at 284.8 eV shown in Figure 5(b).

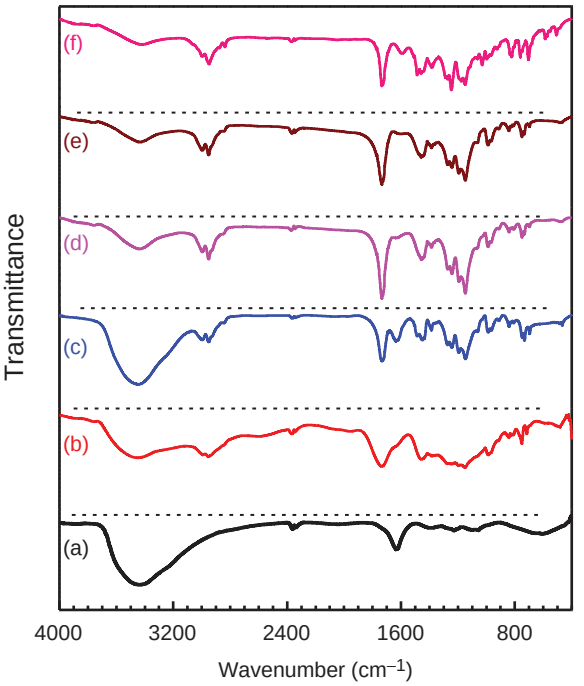

Figure 4. Comparison of FT-IR spectra of (a) GO (b) GO-PMMA (c) GO-PMMA-Pd (d) PMMA-Pd (e) PMMA and (f) recycled catalyst after fifth run.

The binding energies of Pd 3d at 335.87 and 341.2 eV for GO-PMMA-Pd corresponded to the Pd^0 Pd $3d_{5/2}$ and Pd $3d_{3/2}$, respectively. Thus, the presence of metallic Pd in the composite is confirmed (Fig. 5(c)).

Leaching of metal from the heterogeneous GO-PMMA support was examined by hot filtration test as described in the literature.[40] After 1 h completion of reaction, the reaction mixture was filtered to separate out the catalyst and HPLC was carried out with the obtained filtrate (38% conversion). The ICP-AES analysis of the filtrate showed the absence of any palladium. The filtrate was then heated for another 4 h at 90 °C without the addition of catalyst and the corresponding HPLC pattern (Fig. 6) did not show any noticeable conversion which implied that metals are not getting leached from the solid GO-PMMA support during first 1 h of the reaction.

The Pd content was found to be 5.559 *wt*% in this heterogeneous catalyst. The recyclability of the catalyst was tested for Suzuki coupling reaction and the catalyst was recyclable for five consecutive runs without significant drop in activity. The sudden drop in Pd content (Fig. 7) after the fifth run may be attributed to the leaching of Pd from the catalyst. The development of recoverable catalyst is one of the indispensable principles of the green synthetic organic chemistry and the key purpose of this study was to place a recyclable catalyst for Suzuki and Heck reaction in aqueous medium. Initially, for screening the reaction, phenylboronic acid and 4-iodo anisole has been chosen as the model substrates in presence of GO-PMMA-Pd catalyst. The favorable condition of the reaction was achieved by varying the parameters such as catalyst loading, solvent, time, base and temperature. Finally the protocol was optimized by using water as solvent, K_2CO_3 as base and catalyst loading (0.3 mol % Pd) in 6 mg of

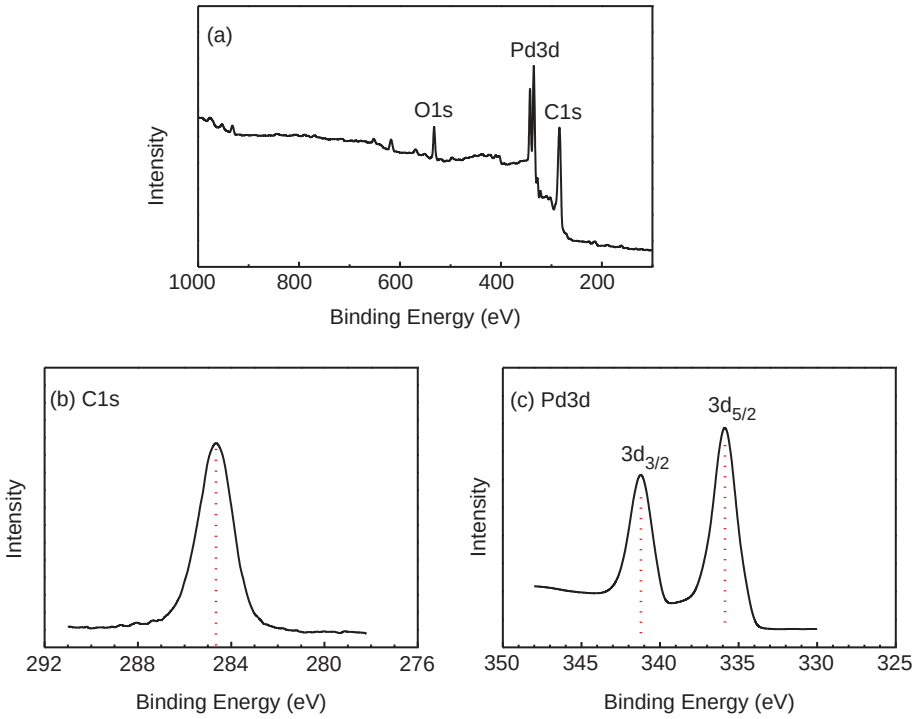

Figure 5. (a) Full-range XPS spectrum of GO-PMMA-Pd catalyst. C 1s peak at 284.8 eV shown in (b). In (c) the binding energies of Pd 3d at 335.87 and 341.2 eV for GO-PMMA-Pd corresponded to the Pd^0 Pd $3d_{5/2}$ and Pd $3d_{3/2}$, respectively.

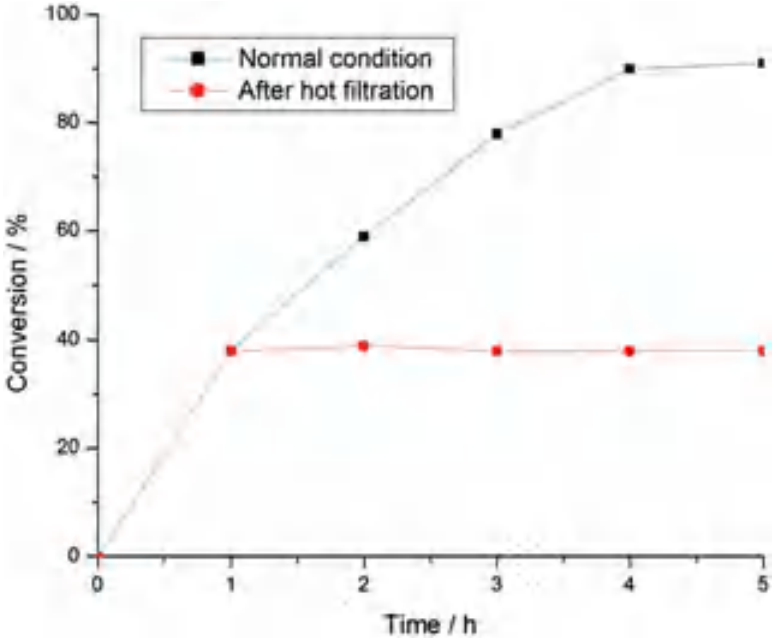

Figure 6. Comparison of normal time profile with hot filtration test. Conversions (±2%) at different time intervals for each plot were measured by HPLC.

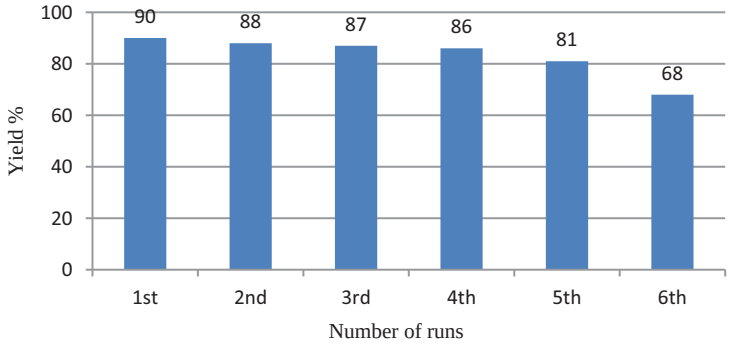

Figure 7. Recycling efficiencies of GO-PMMA-Pd catalyst for Suzuki coupling reaction.

Table 1. Optimization of reaction parameters for Suzuki reaction based on the result of the following combination in the protocol[a].

Entry	Solvent	Base	Pd loading (mol%)	Additive	Time (h)	Yield[b] (%)
1	DMF	K_2CO_3	0.1	Bu_4NBr	1	42
2	DMSO	K_2CO_3	0.1	Bu_4NBr	2	29
3	Water	K_2CO_3	0.2	Bu_4NBr	3	63
4	Ethanol	K_2CO_3	0.2	Bu_4NBr	3	58
5	Water	K_2CO_3	0.3	SDS	4	72
6	Water	K_2CO_3	0.3	Bu_4NBr	4	90
7	Water	Na_2CO_3	0.3	Bu_4NBr	6	76
8	Water	Cs_2CO_3	0.3	Bu_4NBr	6	75
9	Water	Et_3N	0.3	Bu_4NBr	6	78
10	Water	KOH	0.3	Bu_4NBr	4	62
11	Water	K_2CO_3	0.3	CTAB	6	72
12	Water	K_2CO_3	0.3	TMAI	4	52
13	Water	K_2CO_3	0.3	Bu_4NBr	24	25[c]
14	Water	K_2CO_3	0.5	Bu_4NBr	12	86[d]

[a]Reaction of 4-Iodo anisole (1 mmol), Phenyl boronic acid (1.5 mmol), Pd loading (0.3 mol%), K_2CO_3 (1 mmol), TBAB (10 mol%), water (2 mL) at 90 °C;
[b]Isolated yields.
[c]Room temperature reaction;
[d]Temp of the reaction 100 °C.

GO-PMMA-Pd catalyst at 90 °C (Table 1). In order to enhance the yield of 4-methoxy-1,1′ biphenyl in water, different surfactants were employed in the study (Table 1). It is established that the yield of the product can be improved by increasing the reaction time. We started increasing the reaction time by keeping all parameters similar and found that the best yield is achieved in 4 h of reaction (Table 1, entry 6). However, *ortho*-substituted compounds require longer reaction time.

The synthetic efficacy of this catalyst in water mediated Suzuki coupling reaction was conducted with a number of different aryl halides and arylboronic acids under optimized condition (Table 2, entries 1–16). The electron withdrawing aryl iodides and bromides gave excellent yields of corresponding products (entries 3, 6 and 8). Although relatively longer reaction time was required for electron donating aryl iodides and bromides but each of them offered an excellent yield of products (entries 1–2 and 4–5). The aryl chlorides gave only trace amount of the corresponding product even after 24 h of exertion of reaction. The arylboronic acids with methoxy, methyl, nitro groups were rapidly converted to their corresponding products at high to moderate yield at 90 °C as shown in Table 2 (entries 9, 15 and 16).

Table 2. GO-PMMA-Pd catalyzed Suzuki reaction of different aryl halides with phenyl boronic acid[a].

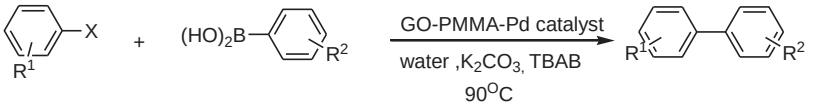

Entry	Aryl halide	Boronic acid	Products	Time (h)	Yield[b] (%)
1.	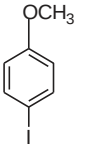	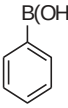	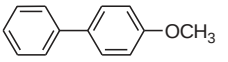	4	90
2.	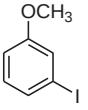	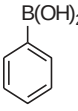	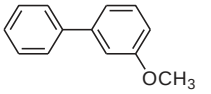	4	88
3.	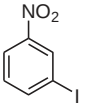	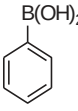	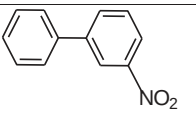	2	92
4.	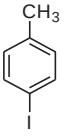	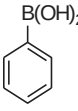	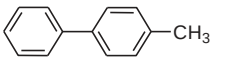	6	86
5.	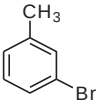	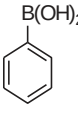	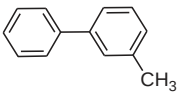	6	84
6.	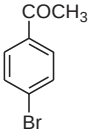	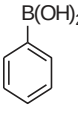	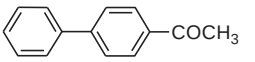	1.5	93
7.	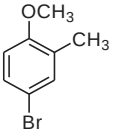	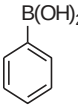	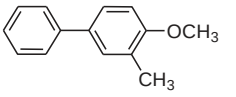	4	85
8.	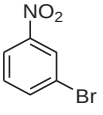	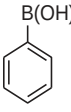	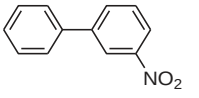	3	89

continued

Table 2. Continued.

9.	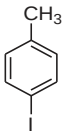	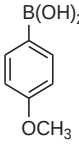	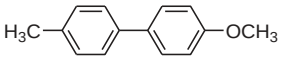	4	86
10.		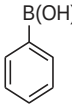	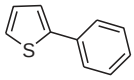	6	58
11.	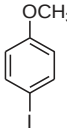	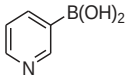	No reaction	–	Nil
12.	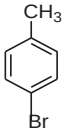	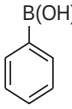	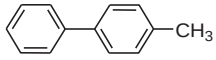	6	79
13.	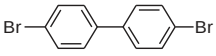	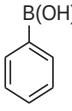	No reaction	–	Nil
14.	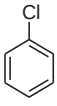	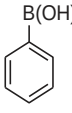	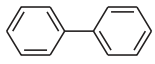	24	35[c]
15.	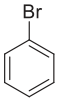	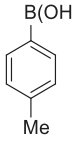	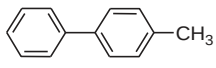	4	88
16.	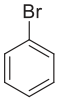	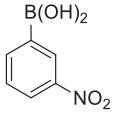	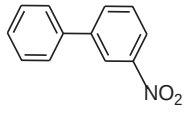	4	71

[a]Reaction of aryl halide (1 mmol), Phenyl boronic acid (1.5 mmol), palladium loading (0.3 mol%), K_2CO_3 (1 mmol), TBAB (10 mol%), water (2 mL) at 90 °C.
[b]Isolated yields.
[c]Reaction temperature 120 °C.

The above success in Suzuki coupling reaction prompted us to look for such expectancy in Heck coupling reaction too. The Heck reaction was optimized by varying the reaction parameters temperature, solvent, base, catalyst loading (Table 3). In that instance, 4-iodo anisole was successfully coupled with methyl acrylate in presence of TBAB and 0.2 mol% Pd in GO-PMMA-Pd catalyst at 100 °C. All types of aryl halides

Table 3. Optimization of reaction parameters of Heck reaction[a].

Entry	Solvent	Base	Temp (°C)	Pd-loading (mol%)	Time (h)	Yield (%)[b]
1	DMF	K_2CO_3	120	0.1	4	75[c]
2	Water	K_2CO_3	100	0.1	5	72
3	Water	Et_3N[d]	100	0.2	5	80
4	Water	K_2CO_3	100	0.2	4	85
5	Water	K_2CO_3	80	0.3	5	78
6	Water	K_2CO_3	Rt	0.3	24	25[e]

[a]Reaction of 4-Iodo anisole(1 mmol), methyl acrylate (2 mmol), Pd loading (0.2 mol%), K_2CO_3 (1 mmol), TBAB (10 mol%), water 3 mL.
[b]Isolated yields.
[c]solvent was DMF.
[d]triethyl amine was used as base.
[e]room temperature.

gave good to excellent yield, which indicates the high efficiency of this heterogeneous catalyst (Table 4) in Heck coupling too.

Figure 7 represents the recyclability of the GO-PMMA-Pd catalyst for Suzuki coupling reaction upto the sixth run. The reduction of yield after fifth run could be due to the leaching of Pd NPs from GO-PMMA surface. The palladium content after fifth run was confirmed by ICP-AES and it was found to be 1.357 *wt*%. However, when the reaction was performed with only PMMA-Pd^0, a drastic change in yield was observed from 88% to 56% in second run. This observation clearly indicated that presence of GO in the composite plays a vital role to improve the catalytic ability of GO-PMMA-Pd system.

Experimental

Materials and physical measurements

Palladium (II) acetate 99.98% was purchased from Sigma Aldrich. Graphite powder, H_2O_2 (solution 30%), 98.5% pure methyl methacrylate were purchased from commercial supplier. The morphology of the catalyst (GO-PMMA-Pd) was analyzed by TEM, (Model: JEM-2100, accelerating voltages 60–200 KV in 50 V steps; resolution: 1.9 Å to 1.4 Å). Inductively coupled plasma spectroscopy (ICP) was analyzed on ARCOS, Simultaneous ICP spectrometer (SPECTRO analytical instruments GmbH, Germany). Powder XRD data and X-ray photoelectron spectroscopy (XPS) was obtained from Bruker D8 Advanced X-ray Powder Diffractometer (Cu Kα radiation, $\lambda = 1.54$ Å) and an XPS instrument (Omicron: Serial no. 0571) respectively. NMR spectra were taken in $CDCl_3$ using a Bruker AV–300 spectrometer operating for ^1H at 300 MHz and for ^{13}C at 75 MHz. Splitting patterns of protons were described as s (singlet), d (doublet), t (triplet), br (broad) and m (multiplet). Chemical shifts were reported in parts per million (ppm) relative to TMS as internal standard.

General procedure for preparation of GO-PMMA-supported Pd catalyst

Initially for the preparation of catalyst 20 mg of GO was suspended in 20 mL of toluene. The slurry was then dispersed through ultrasonication for 60 min. After ultrasonication methyl methacrylate was injected to a well dispersed solution of GO. Benzoyl peroxide

Table 4. Reaction of aryl halides with different vinyl compounds[a].

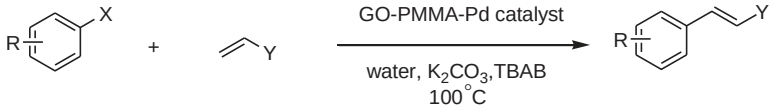

Entry	Aryl halides	Olefins	Product	Time (h)	Yield[b] (%)
1	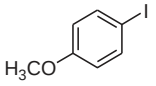	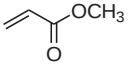	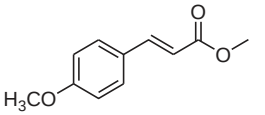	4	85
2	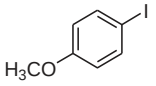	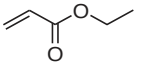	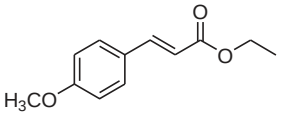	4	83
3	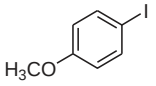	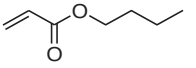	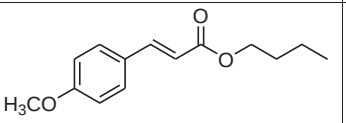	6	84
4	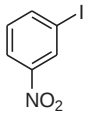	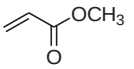	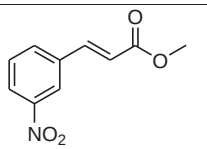	4	88
5		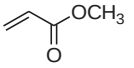	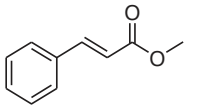	5	90
6	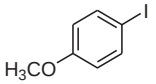	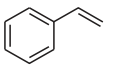	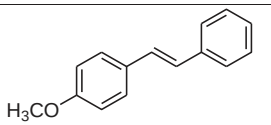	5	79
7		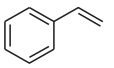	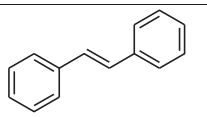	4	80
8	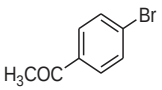	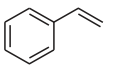	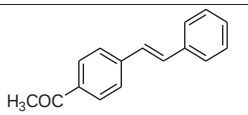	4	84

[a]Reaction of aryl halide (1 mmol), vinyl compound (2 mmol), GO-PMMA-Pd catalyst (0.2 mol%), K_2CO_3 (1 mmol), TBAB (10 mol%), water 3 mL.
[b]Isolated yields.

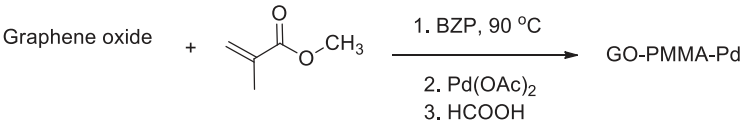

Scheme 1. Preparation of GO-PMMA-Pd catalyst.

(BZP, 0.1 mol%) was added to initiate the polymerization of methyl methacrylate (MMA). The resulting mixture was then stirred well at 90 °C for 4 h. The temp of the solution was maintained at 90 °C. Stirring was continued for another 3 h followed by the addition of 40 mg $Pd(OAc)_2$ and 100 mg of HCOOH as shown in Scheme 1. The dark brown precipitate instantly turned into black after the addition of HCOOH. The obtained residue was washed several times with water and residual solvent was shuffled off by rotary evaporator, and dried at 60 °C.

Procedure for cross coupling of 4-iodo anisole and phenyl boronic acid using GO-PMMA-Pd catalyst

A 25 mL RB was charged with 4-iodo anisole (1.0 mmol), phenylboronic acid (1.5 mmol), GO-PMMA-Pd catalyst (0.3 mol % Pd), K_2CO_3 (1 mmol), TBAB (10 mol %) and 2 mL water. The mixture was allowed to stir at 90 °C for an appropriate time (Table 1) and the extent of the reaction was monitored by thin layer chromatography (TLC). After the completion of the reaction, the reaction mixture was extracted by ethyl acetate (2 × 25 ml) and washed with water repeatedly. The catalyst was filtered off and washed several times with ether and water (1:1) until no significant product was obtained in the wash. The recovered catalyst was reused for the next coupling experiment. The reaction mixture was dried over anhydrous Na_2SO_4, concentrated in vacuum and purified by column chromatography on silica gel 60–120 mesh using petroleum ether as eluent to obtain pure product. The catalyst recovered after fifth run was subjected to ICP-AES for Pd content analysis. The isolated products were analyzed by ^1H NMR and ^{13}C NMR spectroscopy.

4-methoxy-1,1′ biphenyl[41]: ^1H NMR ($CDCl_3$, 300 MHz) δ 3.85 (s, 3H), 6.98 (d, 2 H, $J = 6.9$ Hz), 7.238–7.319 (1 H, m), 7.397 (d, 2 H, $J = 7.8$ Hz), 7.511–7.564 (m, 4 H, $J = 8.7$ Hz); ^{13}C NMR δ 55.37, 114.22, 126.68, 126.76, 128.18, 128.75, 133.80, 140.85,159.16.

General procedures for the heck coupling reactions

A mixture of 4-iodo anisole (1 mmol), methyl acrylate (2 mmol), GO-PMMA-Pd catalyst (0.2 mol % Pd), K_2CO_3 (1 mmol), TBAB (10 mol %) and 3 ml water was stirred under 100 °C. The reaction took significant time for completion (Table 3) and the progress of the reaction was monitored by TLC. After completion, the reaction mixture was extracted with ethyl acetate and washed with water repeatedly. The combined organic mixture was dried over anhydrous $NaSO_4$ and purified by column chromatography using petroleum ether/ethyl acetate as eluent to afford pure product. The catalyst was separated and washed for several times with ether and water. The recovered catalyst was

used in next cycles and the isolated products were characterized by ^{1}H and ^{13}C NMR spectroscopy.

(E)-methyl 3-(4-methoxyphenyl) acrylate[42]: ^{13}C NMR δ 51.27, 55.29, 114.33, 115.03, 126.57, 130.13, 144.31, 161.11, 166.91.

Conclusion

A greener protocol using ligand free GO-PMMA-Pd catalyst is proposed. The prepared catalyst was characterized by different spectroscopic and microscopic techniques. The newly made catalyst effectively generates different C–C cross coupled product even at a very low Pd content in high yields at optimal condition. The simple operational procedure, easy removal of catalyst, reusability of the catalyst and environmentally benign process are the most significant and outwit factors of our proposed scheme in comparison to the existing protocols.

Acknowledgments

The authors thank IIT Bombay for ICP-AES analysis, IACS Kolkata for PXRD analysis and XPS analysis, NEHU (SAIF) for TEM analysis.

Funding

One of the authors (PB) is thankful to council of scientific and industrial research (CSIR), NEW DELHI, INDIA, New Delhi for financial support.

References

[1] (a) Suzuki, A. The Suzuki Reaction with Arylboron Compounds in Arene Chemistry. In *Modern Arene Chemistry*, 1st ed.; Wiley-VCH: Weinheim, **2004**.; pp 53–106; b) Heck, R. F. Palladium-Catalyzed Reactions of Organic Halides with Olefins. *Acc. Chem. Res.* **1979**, *12*, 146. DOI: 10.1002/chin.197937153. c) Yahiaoui, S.; Fardost, A.; Trejos, A.; Larhed, M. Chelation-Mediated Palladium(II)-Catalyzed Domino Heck−Mizoroki/Suzuki−Miyaura Reactions Using Arylboronic Acids: Increasing Scope and Mechanistic Understanding. *J. Org. Chem.* **2011**, *76*, 2433–2438.

[2] Fihri, A.; Bouhrara, M.; Nekoueishahraki, B.; Basset, J. M.; Polshettiwar, V. Nanocatalysts for Suzuki Cross-Coupling Reactions. *Chem. Soc. Rev.* **2011**, *40*, 5181–5203. DOI: 10.1039/c1cs15079k.

[3] Zhou, Z. Z.; Liu, F. S.; Shen, D. S.; Tan, C.; Luo, L. Y. Efficient Palladium-Catalyzed Suzuki Cross-Coupling Reaction with β-Ketoamine Ligands. *Inorg. Chem. Commun.* **2011**, *14*, 659–662. DOI: 10.1016/j.inoche.2011.01.044.

[4] Hajduk, P. J.; Bures, M.; Praestgaard, J.; Fesik, S. W. Privileged Molecules for Protein Binding Identified from NMR-Based Screening. *J. Med. Chem.* **2000**, *43*, 3443–3447. DOI: 10.1021/jm000164q.

[5] Hassan, J.; Sévignon, M.; Gozzi, C.; Schulz, E.; Lemaire, M. Aryl-Aryl Bond Formation One Century after the Discovery of the Ullmann Reaction. *Chem. Rev.* **2002**, *102*, 1359–1470. DOI: 10.1021/cr000664r.

[6] Böhm, V. P. W.; Herrmann, W. A. Nonaqueous Ionic Liquids: superior Reaction Media for the Catalytic Heck-Vinylation of Chloroarenes. *Chemistry* **2000**, *6*, 1017–1025. DOI: 10.1002/(SICI)1521-3765(20000317)6:6<1017::AID-CHEM1017>3.0.CO;2-8.

[7] Park, J. H.; Raza, F.; Jeon, S. J.; Kim, H. I.; Kang, T. W.; Yim, D.; Kim, J. H. Recyclable N-Heterocyclic Carbene/Palladium Catalyst on Graphene Oxide for the Aqueous-Phase Suzuki Reaction. *Tetrahed. Lett.* **2014**, *55*, 3426–3430. DOI: 10.1016/j.tetlet.2014.04.078.

[8] Paul, S.; Islam, M. M.; Islam, S. M. Suzuki–Miyaura Reaction by Heterogeneously Supported Pd in Water: Recent Studies. *RSC Adv.* **2015**, *5*, 42193–42221. DOI: 10.1039/C4RA17308B.

[9] Yin, L.; Liebscher, J. Carbon-Carbon Coupling Reactions Catalyzed by Heterogeneous Palladium Catalysts. *Chem. Rev.* **2007**, *107*, 133–173. DOI: 10.1021/cr0505674.

[10] Sun, Q.; Zhu, L. F.; Sun, Z. H.; Meng, X. J.; Xiao, F. S. Porous Polymer Supported Palladium Catalyst for Cross Coupling Reactions with High Activity and Recyclability. *Sci. China Chem.* **2012**, *55*, 2095–2103. DOI: 10.1007/s11426-011-4491-8.

[11] Pan, C.; Liu, M.; Zhao, L.; Wu, H.; Ding, J.; Cheng, J. Palladium Chloride Catalyzed Hiyama Cross-Coupling Reaction Using Phenyltrimethoxysilane. *Catcom.* **2008**, *9*, 1685–1687.

[12] Bedford, R. B.; Singh, U. G.; Walton, R. I.; Williams, R. T.; Davis, S. A. Nanoparticulate Palladium Supported by Covalently Modified Silicas: Synthesis, Characterization, and Application as Catalysts for the Suzuki Coupling of Aryl Halides. *Chem. Mater.* **2005**, *17*, 701–707. DOI: 10.1021/cm048860s.

[13] Jin, M. J.; Taher, A.; Kang, H. J.; Choi, M.; Ryoo, R. Palladium Acetate Immobilized in a Hierarchical MFI Zeolite-Supported Ionic Liquid: A Highly Active and Recyclable Catalyst for Suzuki Reaction in Water. *Green Chem.* **2009**, *11*, 309–313. DOI: 10.1039/b817855k.

[14] Jin, X.; Li, J.; Li, H. An Efficient Poly(Amic Acid) Salt-Stabilised Palladium Nanocatalyst with Excellent Recyclable Performance for Suzuki–Miyaura Coupling Reactions under Mild Conditions. *J. Exper. Nanosci.* **2018**, *13*, 95–106. DOI: 10.1080/17458080.2017.1413600.

[15] Ramchandani, R. K.; Uphade, B. S.; Vinod, M. P.; Wakharkar, R. D.; Choudhary, V. R.; Sudalai, A. Pd–Cu–Exchanged Montmorillonite K10 Clay: an Efficient and Reusable Heterogeneous Catalyst for Vinylation of Aryl Halides. *Chem. Commun.* **1997**, *21*, 2071–2072. DOI: 10.1039/a705870e.

[16] Wan, Y.; Wang, H.; Zhao, Q.; Klingstedt, M.; Terasaki, O.; Zhao, D. Ordered Mesoporous Pd/Silica-Carbon as a Highly Active Heterogeneous Catalyst for Coupling Reaction of Chlorobenzene in Aqueous Media. *J. Am. Chem. Soc.* **2009**, *131*, 4541–4550. DOI: 10.1021/ja808481g.

[17] Nong, Y. L.; Qiao, N.; Deng, T. H.; Pan, Z.; Liang, Y. Solid Sheet of Anodic Aluminium Oxide Supported Palladium Catalyst for Suzuki Coupling Reactions. *Catalys. Commun.* **2017**, *100*, 139–143. DOI: 10.1016/j.catcom.2017.06.032.

[18] Wali, A.; Pillai, S. M.; Kaushik, V. K.; Satish, S. Arylation of Acrylonitrile with Iodobenzene over Pd/MgO Catalyst. *Appl. Catal. A.* **1996**, *135*, 83. DOI: 10.1016/0926-860X(95)00190-5.

[19] Kundhikanjana, W. K.; Lai, J.; Wang, H. L.; Dai, H. J.; Kelly, M. A.; Shen, Z. X. Hierarchy of Electronic Properties of Chemically Derived and Pristine Graphene Probed by Microwave Imaging. *Nano Lett.* **2009**, *9*, 3762–3765. DOI: 10.1021/nl901949z.

[20] Wang, J.; Hu, H.; Wang, X.; Xu, C.; Zhang, M.; Shang, X. Preparation and Mechanical and Electrical Properties of Graphene Nanosheets-Poly(Methyl Methacrylate) Nanocomposites via in Situ Suspension Polymerization. *J. Appl. Polym. Sci.* **2011**, *122*, 1866–1871. DOI: 10.1002/app.34284.

[21] Kuila, T.; Bose, S.; Khanra, P.; Kim, N. H.; Rhee, K. Y.; Lee, J. H. Characterization and Properties of in Situ Emulsion Polymerized Poly(Methyl Methacrylate)/Graphene Nanocomposites. *Compos A. APPL Sci Manuf.* **2011**, *42*, 1856–1861. DOI: 10.1016/j.compositesa.2011.08.014.

[22] Yang, J.; Yan, X.; Wu, M.; Chen, F.; Fei, Z.; Zhong, M. Self-Assembly between Graphene Sheets and Cationic Poly(Methyl Methacrylate) (PMMA) Particles: preparation and Characterization of PMMA/Graphene Composites. *J. Nanopart. Res.* **2012**, *14*, 717–724. DOI: 10.1007/s11051-011-0717-0.

[23] Hass, J.; Heer, W. A.; Conrad, E. H. The Growth and Morphology of Epitaxial Multilayer Graphene. *J. Phys: Condens. Matter*. **2008**, *20*, 323202. DOI: 10.1088/0953-8984/20/32/323202.
[24] Shendage, S. S.; Singh, A. S.; Nagarkar, J. M. Facile Approach to the Electrochemical Synthesis of Palladium-Reduced Graphene Oxide and Its Application for Suzuki Coupling Reaction. *Tetrahedron Lett*. **2014**, *55*, 857–860. DOI: 10.1016/j.tetlet.2013.12.022.
[25] Omez-Mart, G.; Inez, M.; Buxaderas, E.; Pastor, M. I.; Alonso, D. A. Palladium Nanoparticles Supported on Graphene and Reduced Graphene Oxide as Efficient Recyclable Catalyst for the Suzuki–Miyaura Reaction of Potassium Aryltrifluoroborates. *J. Mol. Catal. A: Chem*. **2015**, *404–405*, 1–7. DOI: 10.1016/j.molcata.2015.03.022.
[26] Scheuermann, G. M.; Rumi, L.; Steurer, P.; Bannwarth, W.; Mülhaupt, R. Palladium Nanoparticles on Graphite Oxide and Its Functionalized Graphene Derivatives as Highly Active Catalysts for the Suzuki-Miyaura Coupling Reaction. *J. Am. Chem. Soc*. **2009**, *131*, 8262–8270. DOI: 10.1021/ja901105a.
[27] Yamamoto, S-i.; Kinoshitab, H.; Hashimoto, H.; Nishina, Y. *Nanoscale* **2012**, *00*, 1–3.
[28] Shang, N.; Feng, C.; Zhang, H.; Gao, S.; Tang, R.; Wang, C.; Wang, Z. Suzuki–Miyaura Reaction Catalyzed by Graphene Oxide Supported Palladium Nanoparticles. *Catal. Commun*. **2013**, *40*, 111–115. DOI: 10.1016/j.catcom.2013.06.006.
[29] Shendage, S.; Patil, B. U.; Nagarkar, J. M. Electrochemical Synthesis and Characterization of Palladium Nanoparticles on Nafion–Graphene Support and Its Application for Suzuki Coupling Reaction. *Tetrahedron Lett*. **2013**, *54*, 3457–3461. DOI: 10.1016/j.tetlet.2013.04.092.
[30] Jang, J. Y.; Jeong, H. M.; Kim, B. K. Compatibilizing Effect of Graphite Oxide in Graphene/PMMA Nanocomposites. *Macromol. Res*. **2009**, *17*, 626–635. DOI: 10.1007/BF03218920.
[31] Chen, C. H.; Yen, W. H.; Kuan, C. F.; Chiang, C. L. *Polym. Compos*. **2010**, *31*, 18–24.
[32] Potts, J. R.; Lee, S. H.; Alam, T. M.; An, J.; Stoller, M. D.; Piner, R. D.; Ruoff, R. S. Thermomechanical Properties of Chemically Modified Graphene/Poly(Methyl Methacrylate) Composites Made by in Situ Polymerization. *Carbon* **2011**, *49*, 2615–2623. DOI: 10.1016/j.carbon.2011.02.023.
[33] Zeng, X.; Yang, J.; Yuan, W. Preparation of a Poly(Methyl Methacrylate)-Reduced Graphene Oxide Composite with Enhanced Properties by a Solution Blending Method. *European Polm. J*. **2012**, *48*, 1674–1682. DOI: 10.1016/j.eurpolymj.2012.07.011.
[34] Pham, V. H.; Dang, T. T.; Hur, S. H.; Kim, E. J.; Chung, J. S. Highly Conductive Poly(Methyl Methacrylate) (PMMA)-Reduced Graphene Oxide Composite Prepared by Self-Assembly of PMMA Latex and Graphene Oxide through Electrostatic Interaction. *Acs. Mater. Interfaces Appl. Mater. Interfaces* **2012**, *4*, 2630–2636. — DOI: 10.1021/am300297j.
[35] Thomassin, J.-M.; Trifkovic, M.; Alkarmo, W.; Detrembleur, C.; Jérôme, C.; Macosko, C. Poly(Methyl Methacrylate)/Graphene Oxide Nanocomposites by a Precipitation Polymerization Process and Their Dielectric and Rheological Characterization. *Macromol*. **2014**, *47*, 2149–2155. DOI: 10.1021/ma500164s.
[36] Trimm, D. L. Thermal stability of catalyst support In *Catalyst Deactivation*; , Ed.; Elsevier Science Publishers, **1991**.; pp 29–51.
[37] Gupta, R. K.; Alahmed, Z. A.; Yakuphanoglu, F. Graphene Oxide Based Low Cost Battery. *Mater. Lett*. **2013**, *112*, 75–77. DOI: 10.1016/j.matlet.2013.09.011.
[38] Chekin, F. Sol–Gel Synthesis of Palladium Nanoparticles Supported on Reduced Graphene Oxide: An Active Electrocatalyst for Hydrogen Evolution Reaction. *Bull. Mater. Sci*. **2015**, *38*, 887–893. DOI: 10.1007/s12034-015-0954-4.
[39] Xu, J.; Gai, S.; He, F.; Niu, N.; Gao, P.; Chen, Y.; Yang, P. Reduced Graphene Oxide/Ni(1-x)Co(x)Al-Layered Double Hydroxide Composites: Preparation and High Supercapacitor Performance. *Dalton Trans*. **2014**, *43*, 11667–11675. DOI: 10.1039/C4DT00686K.

[40] Anton, D. R.; Crabtree, R. H. Dibenzo[a,e]Cyclooctatetraene in a Proposed Test for Heterogeneity in Catalysts Formed from Soluble Platinum-Group Metal Complexes. *Organometallics* **1983**, *2*, 855–859. DOI: 10.1021/om50001a013.

[41] Mahanta, A.; Mondal, M.; Thakur, A. J.; Bora, U. An Improved Suzuki–Miyaura Cross-Coupling Reaction with the Aid of in Situ Generated PdNPs: Evidence for Enhancing Effect with Biphasic System. *Tetrahedron Lett.* **2016**, *57*, 3091–3095. DOI: 10.1016/j.tetlet.2016.05.098.

[42] Sanjaykumar, S. R.; Mukri, B. D.; Patil, S.; Madras, G.; Hegde, M. S. Ce0·98Pd0·02O2-δ: Recyclable, Ligand Free Palladium(II) Catalyst for Heck Reaction. *J. Chem. Sci.* **2011**, *123*, 47–54. DOI: 10.1007/s12039-011-0103-6.

ChemPubSoc Europe

DOI: 10.1002/slct.201904164

Chemistry SELECT Full Papers

Catalysis

Sulfonated Graphene-Oxide as Metal-Free Efficient Carbocatalyst for the Synthesis of 3-Methyl-4-(hetero) arylmethylene isoxazole-5(4*H*)-ones and Substituted Pyrazole

Puja Basak, Sourav Dey, and Pranab Ghosh*[a]

A straightforward, simple and unprecedented transformative protocol has been accomplished towards furnishing a wide variety of pharmaceutically promising functionalised 3-methyl-4-(hetero)arylmethylene isoxazole-5(4*H*)-ones and 6-Amino-3-methyl-4-phenyl-1,4-[2,3-c]pyrazole-5-carbonitriles. Sulfonated graphene oxide (SGO), a new class of heterogeneous carbocatalyst, was found to be efficient for thisone pot rapid conversion of isoxazoles and pyranopyrazoles from aldehyde. The prepared SGO was characterised by FEG-SEM, HR-TEM, FTIR and was recyclable up to 5th run without a significant drop in its catalytic activity. Metal free synthesis, good to excellent yield, high atom economy, usage of readily available starting material, operational simplicity, easy workup, and recyclable catalyst are the fundamental features of this protocol.

Introduction

In recent times, multicomponent reactions(MCR) are emerging as ecologically sustainable processes in pharmaceutical chemistry, drug designing, and fine chemical synthesis. Due to the increasing demand in green chemistry, MCRs have been paid much attention to achieve high yield, high selectivity and synthetic simplicity in various research fields, such as the discovery of lead compounds in medicinal chemistry or combinatorial chemistry.

Substituted isoxazoles display beneficial biological properties such as antitumor,[1] antifungal,[2] cytotoxic, anti-inflammatory,[3] antibacterial and anti-HIV activities.[4–6] Furthermore, compounds belonging to this class have been employed as versatile building blocks of a variety of natural products,[7] synthetic drug molecules,[8(a,b)] fungicides and insecticides.[8] In particular, isoxazoles are privileged scaffolds in various organic synthesis,[9] liquid crystalline material,[10] optical storage as well as nonlinear optical research[11] and filter dyes in photographic films[12(a–d)] (Figure 1). A series of androgen antagonists with isoxazole motifs are found to have medicinal utility[13(a–c)] and some of them also exhibit full antagonistic activity towards human prostate tumor cells and human metastatic breast cancer cells (Figure 1).[14]

As a consequence of the above, a number of researchers have set their goal to synthesize isoxazole derivatives. The most common approaches to 3-methyl-4-(hetero)arylmethylene isoxazole-5(4*H*)-ones are the multistep condensation of ethyl acetoacetate with hydroxylamine hydrochloride followed by Knoevenagel type reaction with aromatic aldehydes.[15] The convenient methodologies demand solid state heating, solid-state grinding,[16] ultrasonic irradiation,[17] microwave heating,[18] application of visible light in the presence of sodium acetate in ethanol.[19] Nevertheless, different moisture sensitive reagents are also employed for the synthesis of isoxazole derivatives like phthalimide-N-oxyl salts,[20] sodium sulphide,[21] boric acid,[22] sulphated polyborate,[23] sodium azide,[24] potassium sorbate,[25] SnII-montmorillonite,[26] etc.[27–33] Most of the conditions, however, suffer from drawbacks such as harsh reaction conditions, high temperature, strongly acidic/basic condition, prolonged reaction time, use of homogeneous catalyst, low yield and suffer from rapid loss of catalytic activity. Although, the acceptable yield of isoxazole has been reported in most of the

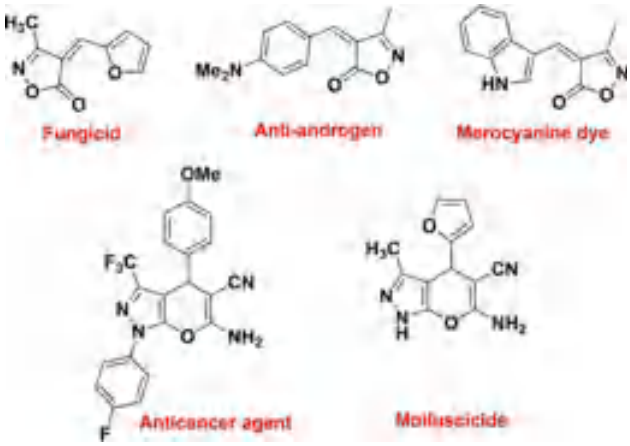

Figure 1. Some example of compounds containing isoxazole and pyranopyrazole moiety.

[a] *P. Basak, S. Dey, P. Ghosh*
Department of Chemistry, University of North Bengal, Dist-Darjeeling, West Bengal, India
Tel.: +91 (0353) 2776381
fax: +91 (0353) 2699001
E-mail: pizy12@yahoo.com

Supporting information for this article is available on the WWW under https://doi.org/10.1002/slct.201904164

protocols where either toxic metal catalyst and costly reagents were used,[23,24] or people had to suffer handling tedious reaction conditions and work up process.[19,24, 26] To avoid these drawbacks it is imperative to develop a high yielding greener, radiation and metal-free efficient method for its synthesis with a broad range of substrate applicability.

Another organic moiety pyranopyrazoles, ubiquitous in many biologically active heterocyclic compounds, have attracted much consideration because of its wide range of activity like antimicrobial,[34] antitumor,[35] anticancer,[36] anticoagulant,[37] diuretic, anti-inflammatory and so on.[38,39] Some important Pharmaceutical agents and drug molecules containing dihydropyrano[2,3-c]pyrazole ring in their core structure were shown in (Figure 1). Due to 'broad spectrum of biological activity, several methods have emerged to synthesize these promising drug molecules. Most of the conventional method for the preparation of dihydropyrano[2,3-c]pyrazole involves four-component reaction using various catalytic system such as tungstate sulphuric acid,[40] Cesium carbonate supported on hydroxyapatite coated $Ni_{0.5}Zn_{0.5}Fe_2O_4$ magnetic nanoparticles,[41] nano MgO,[42] glycerol,[43] silica coated magnetic $NiFe_2O_4$ nanoparticles supported $H_3PW_{12}O_{40}$ (NFSPWA),[44] maltose,[45] trichloroacetic acid,[46] γ-Fe_2O_3@Cu_3Al-LDH,[47] NaF.[48] However, considering ecological issues avoidance of the use of hazardous homogeneous catalyst[46] and toxic metal catalyst[40–44] is essential to prevent environmental pollution. Based on this conception,it was felt to explore a one pot four-component, environmentally benign, high yielding MCR route of pyranopyrazoles.

As a part of our ongoing efforts, presently we have employed a well documented environmentally benign nanomaterial to synthesize substituted isoxazoles and pyranopyrazoles. As an alternative of nonmetal for important organic transformation, carbonaceous nanomaterials have received considerable attention owing to their sustainability and affordability.[49] Graphene oxide (GO), a two dimensional unique nanomaterial, upon exhaustive oxidation during preparation, contains a variety of oxygen containing functionalities (e.g. alcohols, epoxides, carboxylates, sulphate groups), these extrinsic functional groups provides moderate acidic properties (pH = 4.2) and makes GO an excellent heterogeneous acidic catalyst for various synthetic transformation reactions. Compared with other conventional solid acid catalysts, GO and its derivatives are interesting due to the presence of high surface area and abundant functional group inactive sites. Previously, GO and its derivative sulfonated graphene oxide (SGO) has been used as an efficient carbocatalyst in hydration, oxidation, Aza-Michael addition, condensation, hydrolysis of cellulose and hydration of alkynes.[50–59] However, synthesis of SGO requires complicated post functionalization process with fuming H_2SO_4 or Chlorosulfonic acid[57] and to avoid these harsh processes we have reportedherein a one pot synthesis of SGO.[58,59] Among metal free catalysts, sulfonated graphene oxide (SGO) is a highly air-stable, environmentally friendly acid catalyst for use in various chemical reactions.

Considering all these aspects, it was felt to explore the ingenious role of SGOfor the synthesis of 3-methyl-4-(hetero) arylmethylene isoxazole-5(4*H*)-ones and 6-Amino-3-methyl-4-phenyl-1,4-[2,3-c]pyrazole-5-carbonitriles. Our results indeed show that SGO alone is capable of achieving different types of isoxazoles and pyranopyrazoles with diverse functional groups of pharmaceutical interest.

Morphological studies and recyclability experiment of the catalyst SGO has also been carried out. To reduce the environmental hazards and the shortcomings of the previously reported methods a metal free cyclisation pathway has been established in our present work. A possible route of the reaction is also established which implies the profound effect of SGO in governing the reaction.

Result and discussion

We have assessed the catalytic activity of SGO as an acid catalyst in promotion of isoxazole and pyranopyrazole synthesis. SGO was synthesised by the Tours method shown in scheme 1 and was extensively purified to remove any metal impurity.

Fourier-transform infrared spectroscopy (FTIR) studies

The presence of various oxygen containing functional groups, namely hydroxyl, epoxide, carbonyl, sulfonic and carboxylic acid in the synthesised SGO was confirmed by FTIR spectra. FTIR spectra of SGO-1 show significant bands at 1393, 1057 and 857 cm^{-1} which are accounted for the O=S=O stretching, -SO_3 symmetrical stretching and S-OH stretching vibration respectively. Another vibration modes in SGO comprises of hydroxyls (between 3100–3800 cm^{-1}), carboxyls (1640-1760 cm^{-1}), C-OH

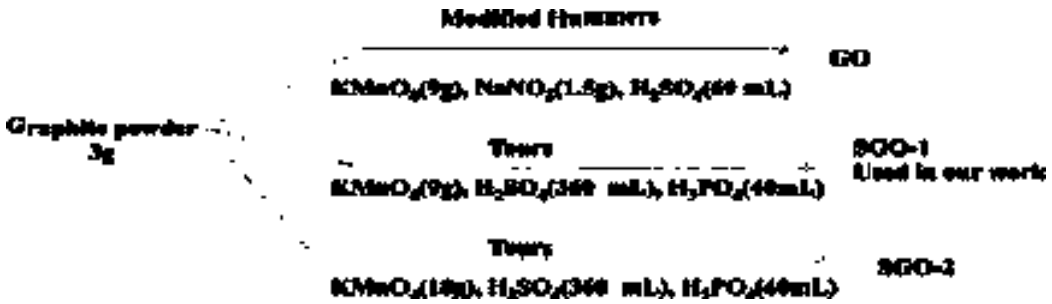

Scheme 1. Preparation of GO, SGO-1, and SGO-2 by different approaches.

vibration (between 3000–3600 cm^{-1}), epoxides (C–O-C at 840 and 1220–1340 cm^{-1}), etc (Figure 7).[55,59]

Evaluation of catalytic activity of SGO through the synthesis of substituted isoxazoles and pyranopyrazoles

As a first instance, we focused our study on the synthesis of 3-methyl-4-arylmethyleneisoxazole-5(4*H*)-ones. For screening the reaction condition, benzaldehyde, ethyl acetoacetate and hydroxylamine hydrochloride were selected for the model reaction. The effects of the reaction parameters such as solvent, temperature, amount of the catalyst are discussed briefly in Table 1. It was noticed that except toluene other solvents produced the desired product in moderate to good yield. Further investigation revealed that solvent free stirring yielded the corresponding products with an excellent yield at room temperature (Table 1). Inspired by this expectancy, we altered the amount of the catalyst SGO under solvent free condition to achieve the optimal condition of the reaction. Depending upon the time, yield and temperature, 25 mg SGO-1 displayed the best result (entry 8, Table 1) and was opted asoptimum quantity for the promotion of the reaction (Table 1). In order to show catalytic efficiency, SGO-1 was also compared with GO and SGO-2 (entry 9, 10 Table 1) and results revealed that SGO-1 exerted the desired product with high yield.

In order to test the water tolerance of the catalyst, we have also carried out the reaction in an aqueous medium (entry 2, Table 1). Upto 82% yield of the entry suggested that there is no chance of poisoning the catalyst by water. To reconfirm the anticipation, after the 1st run the recovered catalyst was dried in a rotary evaporator at 50 °C and reused under the identical condition and in each case, we observed almost identical yield upto 3rd run.

After achieving the optimised condition, we used some substituted aromatic aldehydes in order to get different substituted 3-methyl-4-(hetero)arylmethylene isoxazole-5(4*H*)-ones. The study also indicated that various aromatic aldehydes afforded the corresponding products with high yield (except 2-nitro and 4-nitrobenzaldehyde). Aldehydes with electron donating groups considerably increase the nucleophilicity on carbonyl oxygen, thereby efficiently yielding the desired product with excellent yield (Table 2, entries 2, 4, 8, 13, 18 and 22), whereas, the aldehydes with electron withdrawing groups affording relatively poor yield of the product. 2-Napthaldehyde (Table 2, entry 9) gave moderate yield whereas 1-Naphthaldehyde (Table 2, entry 10) did not respond to reaction and the reason may be due to the hindrance offered by steric factor. Again, we examined the reaction in the case of aliphatic aldehyde also (Table 2, entry 20) which gave a trace amount of product. The generality of the reaction was further extended in case of heterocyclic and α,βunsaturated aldehydes which also afforded the corresponding product with good yield (Table 2, entries 7, 11 and 17, 19). The versatility of the reaction was further tested by using methyl acetoacetate instead of ethyl acetoacetate. As expected we get the same product and with almost identical yield (Table 2, entry 21, 22, 23).

Mechanism

A probable mechanism for the synthesis of 3-methyl-4-arylmethylene isoxazole-5(4*H*)-ones by SGO is depicted below (Scheme 2). It is suggested that acid catalysed oxime (I) formation actually initiated the reaction. The oxime so formed

Table 1. Optimization of reaction parameters for the synthesis of 3-methyl-4-(hetero)arylmethylene isoxazole-5(4*H*)-ones based on the result of the following combination inthe protocol.[a]

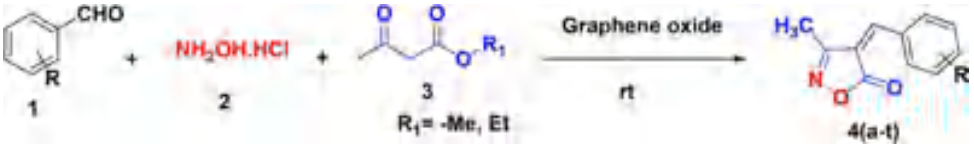

Entry	Catalyst (SGO-1) mg	Solvent	Temperature° C	Time(h)	Yield (%)[b]
1.	None[c]	Water	Rt	8	Trace
2.	50	Water	Rt	2	82%
3.	50[d]	Water	100	1	84%
4.	50	Ethanol	Rt	2	74%
5.	50	MeCN	Rt	2	52%
6.	50	Neat	Rt	2	91%
7.	50	Toluene	Rt	2	NR
8.	**25**	**Neat**	**Rt**	**1**	**90%**
9.	25 (GO)	Neat	Rt	1	84%[e]
10	25 (SGO-2)	Neat	Rt	1	87%[f]
11.	25	Neat	Rt	12	86%
12.	15	Neat	Rt	4	60%
13.14.	10	Neat	rt	12	49%
	100 [g]	Neat	rt	4	81%

[a] Reaction of benzaldehyde (1 mmol), ethyl acetoacetate (2 mmol), hydroxylamine hydrochloride (2.5 mmol) at room temperature (rt). [b] Isolated yield after purification through column chromatography on silica gel. [c] No sulfonated graphene oxide (SGO) was added. [d] Temperature of the reaction 100 °C.[e] GO was used as catalyst, [f] SGO-2 was used as catalyst. [g] The reactants are used 5 mmol each.

Table 2. SGO catalysed synthesis of different substituted 3-methyl-4-(hetero)arylmethylene isoxazole-5(4*H*)-ones.[a]

Entry	Aldehyde	R	Product	Time	Yield(%)[b]	Mp (°C) Found	Reported
1.	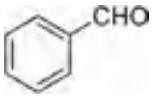	Et	4a	1	90	141-142	141-143
2.	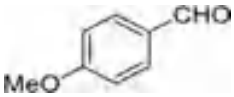	Et	4b	1.5	89	176-178	174-176
3.	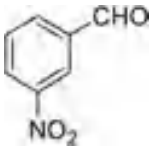	Et	4c	1.5	80	141-143	142-144
4.	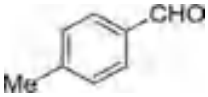	Et	4d	1.5	87	135-136	135-136
5.	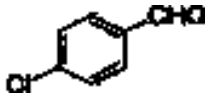	Et	4e	2	84	119-121	118-120
6.	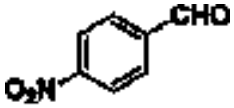	Et	4f	4	Trace	-	-
7.	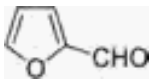	Et	4 g	1.5	91	237-239	238-241
8.	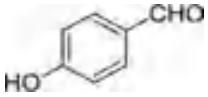	Et	4 h	1.5	84	215-216	214-216
9.	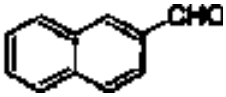	Et	4i	3	64	165-166	-
10.	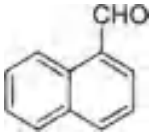	Et	4j	8	NR	-	-
11.	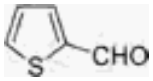	Et	4k	1.5	90	144-146	146-147
12.	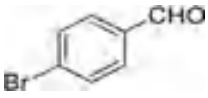	Et	4 l	2.5	82	122-125	120-122
13.	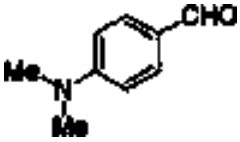	Et	4 m	1	93	225-227	227-228
14.	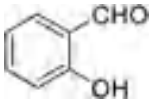	Et	4n	2	82	200-202	198-201
15.	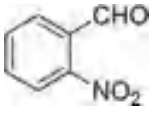	Et	4o	8	Trace	-	-

Table 2. continued

Entry	Aldehyde	R	Product	Time	Yield(%)[b]	Mp (°C) Found	Reported
16.	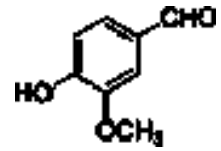	Et	4p	2.5	90	214-216	211-214
17.	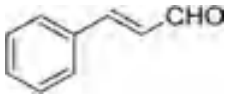	Et	4q	2	84	172-174	171-173
18.	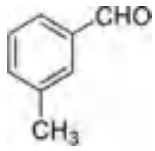	Et	4r	2.5	87	108-110	-
19.		Et	4 s	2.5	86	239-240	240-242
20.		Et	4 t	8	Trace	-	-
21.	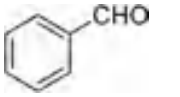	Me	4a	2	84	141-142	141-143
22.	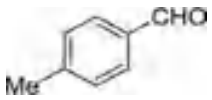	Me	4d	2	86	135-136	135-136
23.	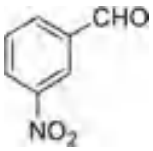	Me	4c	2	78	141-143	142-144

[a] Reaction of aldehyde (1 mmol), ethyl acetoacetate (2 mmol), hydroxylamine hydrochloride (2.5 mmol), SGO (25 mg) at room temperature.
[b] Isolated yield after purification through column chromatography on silica gel.

subsequently guided the Knoevenegal condensation between aromatic aldehyde and intermediate (I). This will be followed by successive cyclisation along with the elimination of ethanol to yield the desired product.

The versatility and the catalytic performance of the prepared catalyst SGO were also observed in one pot-four component synthesis of 1,4-dihydropyrano[2,3-c]pyrazoles using hydrazine hydrate/phenylhydrazine, aromatic aldehyde, malononitrile, ethyl acetoacetate, and the results are summarised below.

To examine the feasibility of the reaction and to optimize the reaction parameters, a model reaction was carried out using phenylhydrazine, ethyl acetoacetate, malononitrile and 4-bromo benzaldehyde as the starting components. Different solvents EtOH, DMF, DCM, CH_3CN, THF (Table 3. Entry 2–6) were implemented to get the desired product in high yield, but H_2O, the green solvent was proved to be more appropriate for this reaction (Table 3 entry 8). However, temperature has a considerable effect on the reaction, as can be seen from (Table 3. entry 11) that room temperature reaction exerted less than 40% yield.

Investigating the catalytic efficiency of synthesized SGO-1, it was compared with GO and SGO-2, but SGO-1 afforded the desired product with high yield. Other Lewis acids were also employed to get the desired product. The results indeed showed that high yield was only achieved in the presence of SGO-1 (Table 4. Entry 3)

After optimizing the reaction parameters, the versatility of the reaction was examined by varying different aromatic aldehydes and the results were summarized in Table 5. Aldehydes with electron withdrawing groups, however, exerted the desired product with high yield and quicken the entire process (Table 5. entry 5, 6, 7, 10). As an extension of our present work we have replaced phenylhydrazine with hydrazine hydrate and the results were satisfactory as shown in (Table 5. entry 8–10).

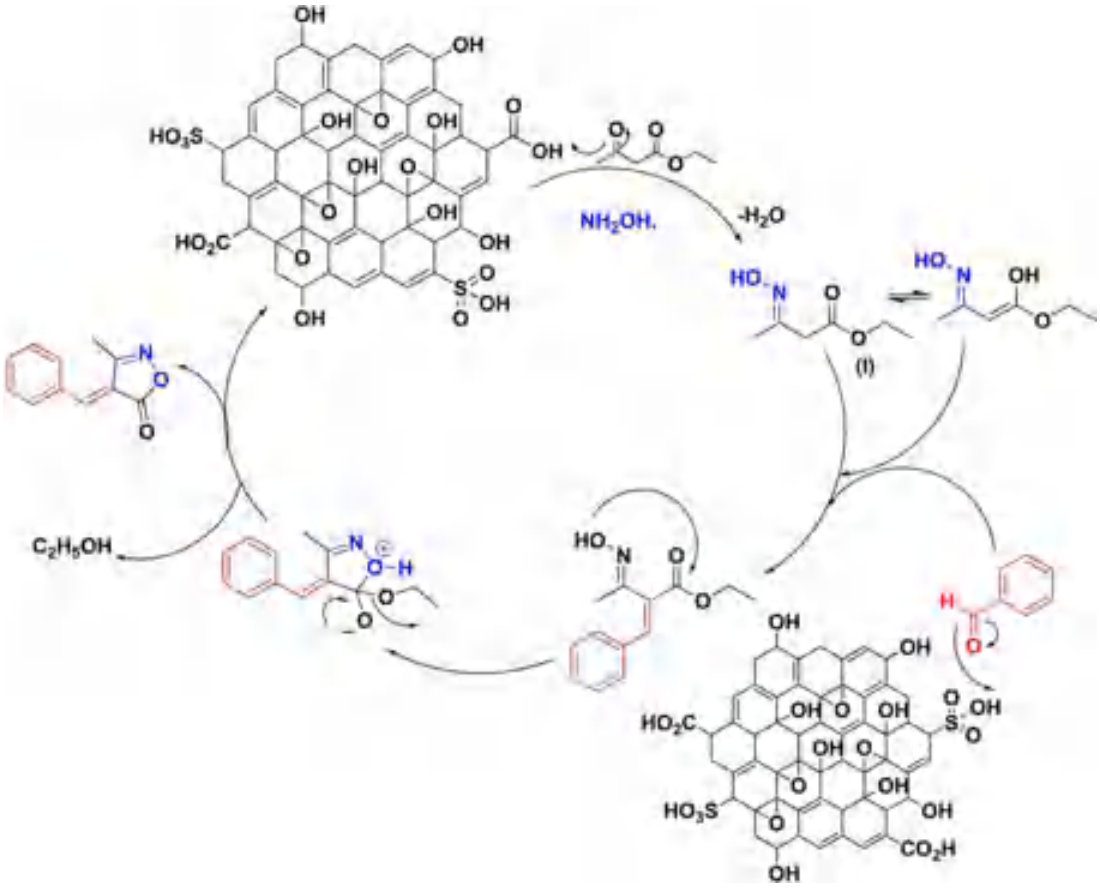

Scheme 2. A possible route for SGO catalysed synthesis of 3-methyl-4-(hetero) arylmethylene isoxazole-5(4*H*)-ones.

Table 3. Optimization of reaction condition for the synthesis of 1,4-dihydropyrano[2,3-c]pyrazoles.[a]

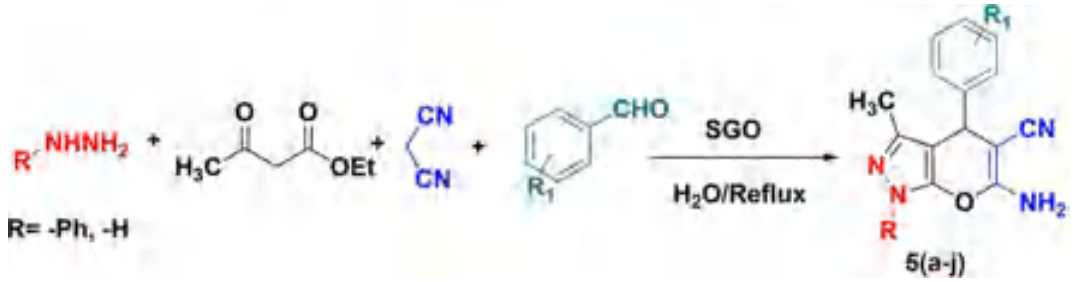

Entry	Time (min)	solvent	Catalyst amount(mg)	Yield(%)
1	120	No solvent	20	< 50
2	60	EtOH /Reflux	20	55
3	60	DMF/Reflux	20	45
4	60	CH_3CN/Reflux	20	40
5	120	DCM/Reflux	20	< 40
6	120	THF/Reflux	20	< 30
7	60	H_2O/Reflux	20	65
8	**60**	**H_2O/Reflux**	**30**	**91**
9	60	H_2O/Reflux	50	94
10	60	H_2O/Reflux	10	< 50
11	120	H_2O/r.t	40	< 40[b]

[a] Reaction of phenylhydrazine (1.5 mmol), ethyl acetoacetate (1 mmol), malononitrile (1 mmol), 4-bromo benzaldehyde (1 mmol) and SGO-1 with varying amount at refluxed condition. [b] Room temperature reaction.

Table 4. Comparison of the efficiency of the present catalyst with a different catalytic system.

Entry	Condition	Catalyst	Yield(%)
1	No solvent	-	<30
2	H_2O/Reflux	GO	78[b]
3	H_2O/**Reflux**	**SGO-1**	**91**[c]
3	H_2O/Reflux	SGO-2	85
4	H_2O/Reflux	Al_2O_3	<40
5	H_2O/Reflux	$FeCl_3$	70
6	H_2O/Reflux	$ZnCl_2$	<50

[a] Reaction of phenylhydrazine (1.5 mmol), ethyl acetoacetate (1 mmol), malononitrile (1 mmol), 4-bromo benzaldehyde (1 mmol), catalyst 30 mg at refluxed condition in water. [b] GO was prepared by Modified hummers method. [c] SGO-1 by Tours method.

Mechanism

A plausible mechanism for the synthesis of 1,4-dihydropyrano [2,3-c]pyrazoles using SGO was shown here (Scheme 3). At first, 5-methyl-2-phenyl-2,4-dihydro-3*H*-pyrazole-3-one was formed by the condensation of phenylhydrazine and ethyl acetoacetate. Subsequently, knoevenagal condensation between aromatic aldehyde and malononitrile exerted 2-benzylidenemalononitrile. Afterthat, pyrazolone and benzylidenemalononitrile participated in Micheal addition followed by cyclisation. Finally, the desired 1,4-dihydropyrano[2,3-c]pyrazole was obtained through tautomerisation in the last step of the reaction mechanism.

Table 5. Synthesis of different substituted 1,4-dihydropyrano[2,3-c]pyrazoles.[a]

Entry	Product	R	Aldehyde	Time	Yield	Mp (°C) Found	Reported
1	5a	-Ph	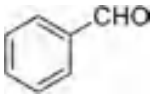	60	80	169-170	170-172
2	5b	-Ph	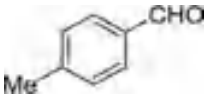	60	82	180-182	180-182
3	5c	-Ph	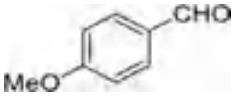	60	84	175-176	177-179
4	5d	-Ph	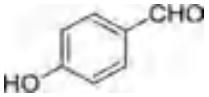	60	83	197-198	195-197
5	5e	-Ph	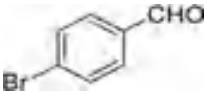	50	89	180-182	180-182
6	5f	-Ph	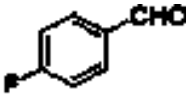	50	91	177-178	174-177
7	5 g	-Ph	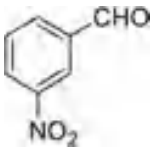	60	88	188-190	190-191
8	5 h	-H	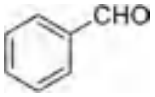	50	77	240-241	240-242
9	5i	-H	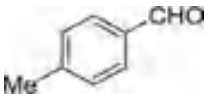	50	80	203-205	205-207
10	5j	-H	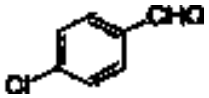	50	88	231-232	231-233

[a] Reaction of R-$NHNH_2$(1.5 mmol), ethyl acetoacetate (1 mmol), malononitrile (1 mmol), aromatic benzaldehyde (1 mmol), 30 mg of SGO at refluxed condition in H_2O.

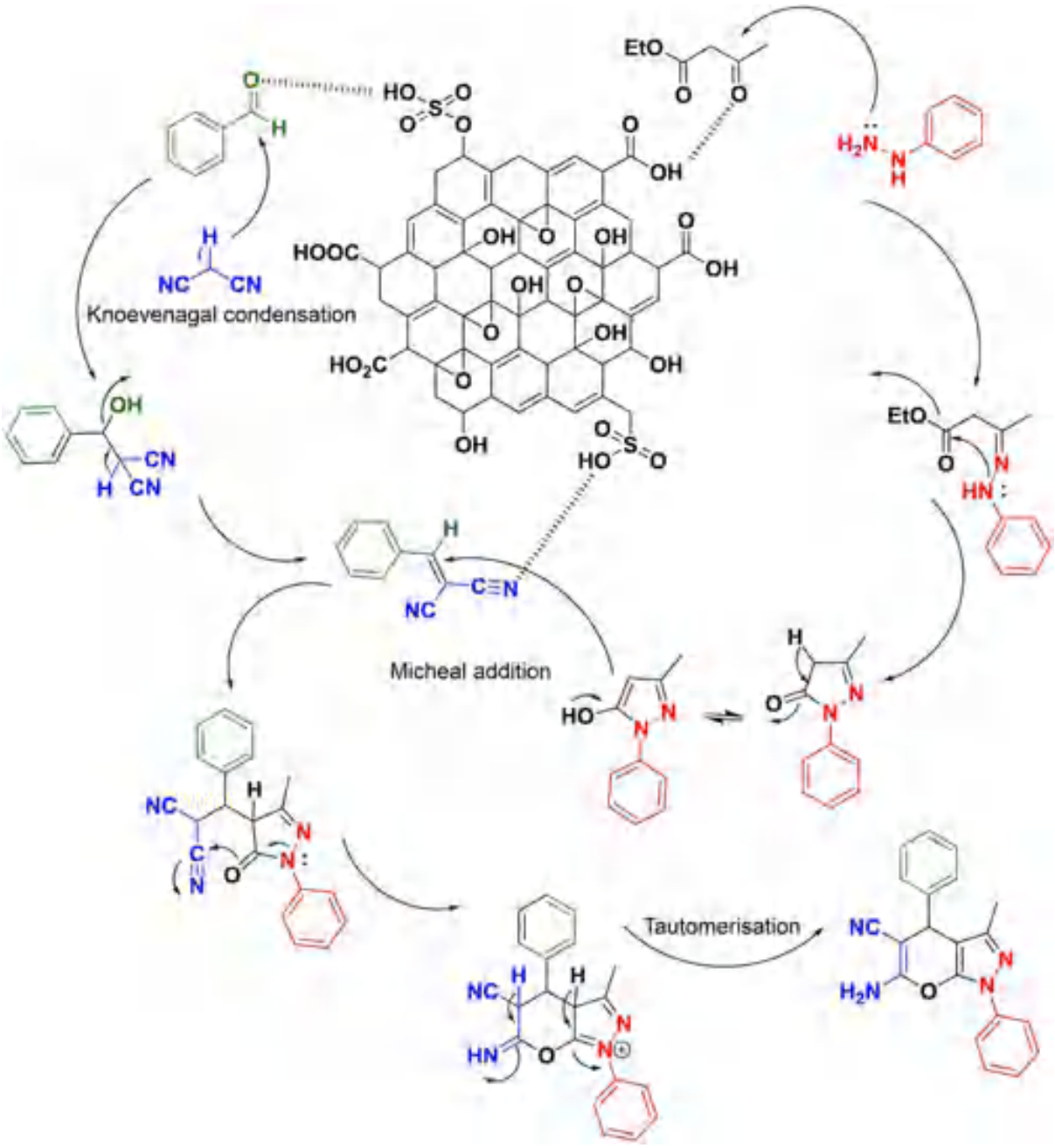

Scheme 3. A plausible route for the synthesis of 1,4-dihydropyrano[2,3-c]pyrazoles.

HR-TEM and SEM analysis

Morphological study of graphene oxide (SGO) and SGO after 5th run was carried out by HR-TEM microscopy to investigate the disintegration of SGO sheets due to the reactions (Figure 2). After reuseSGO sheets appear to have disintegrated along with slight aggregation. The possible explanation may be put forward that, after catalysis, its reduction to rGO leads disintegration into smaller sheets. Furthermore, the morphological study (SEM images) confirms the formation of multiple

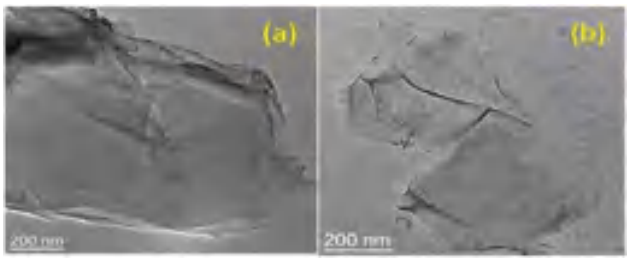

Figure 2. HR-TEM images of (a) SGO and (b) SGO after 5th run.

SGO sheets (Figure 3). Thus, from the above, it may be included that SGO has really taken part in the reaction.

The S content in fresh SGO and the residue left after 5th run was 3.12 and 0.68 wt% respectively (Figure 4). The decreased percentage of S in SGO after 5th run reveals that the functional groups containing sulfur have had participated in the reaction.

For structural studies, XRD spectra of the synthesized catalyst SGO, and that of it after 5th run are shown in Figure 5. A comparison indicates a reduction in intensity of the first peak ($2\Theta = 9.98$) which is a characteristic peak of sulfonated graphene oxide. After 5th cycle, a new peak appears at $2\Theta =$ 24.64, which indicates the partial formation of rGO. These results show proportional reduction of the content of functional groups on SGO during the reaction.

The Raman spectra of both SGO and used SGO after 5th run showed a characteristic D peak at 1346 cm^{-1} and G peak at 1582 cm^{-1} (Figure 6). The ratio of intensities of D and G band (I_D/I_G) of SGO and used SGO after 5th run displayed 0.91 and 0.93 respectively. However, the slight increased (I_D/I_G) ratio suggested that during successive runs partial formation of rGO has occurred through the restoration of some C=C bonds.

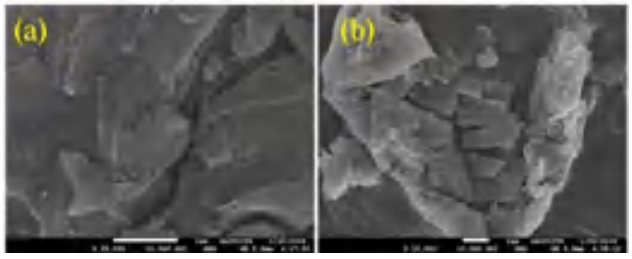

Figure 3. SEM images of (a) SGO and (b) SGO after 5th run.

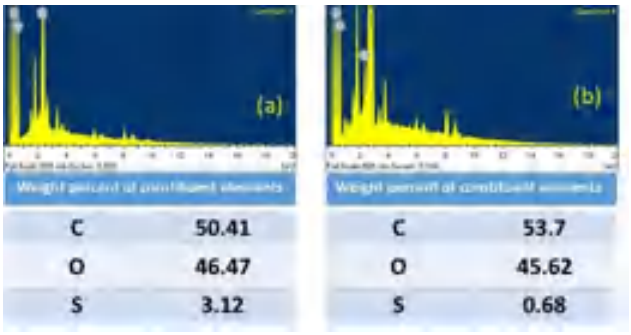

Figure 4. EDX spectra of (a) SGO and (b) SGO after 5th run.

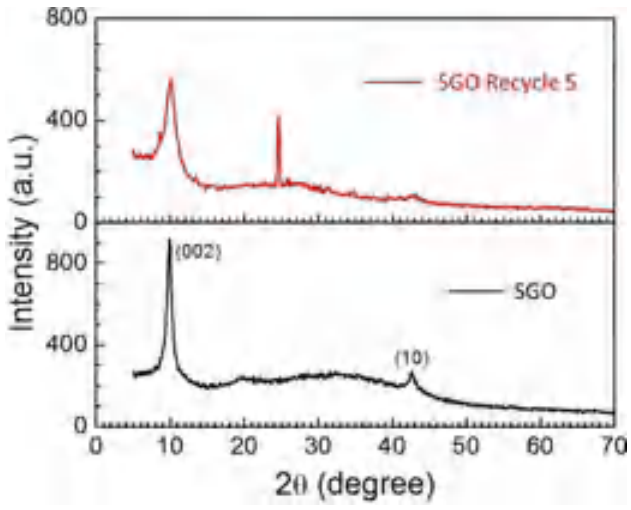

Figure 5. XRD spectra of synthesized SGO and SGO catalyst after 5th recycle.

Recyclability experiment

To check the recyclability of the catalyst SGO, a model reaction between benzaldehyde, ethylacetoacetate and hydroxylamine hydrochloride in presence of 100 mg of SGO was carried out. After the completion of the reaction, ethyl acetate (20 ml) was added into the reaction mixture and centrifuged at 4000 rpm for 5 minutes. The supernatant liquidcontaining the product was decanted off and the process was repeated thrice.The recovered catalyst was then washed with water and acetone repeatedly to obtain dry SGO. The SGO catalyst could easily be separated from the reaction mixture by simple centrifugation and was found to retain its acidic property, even after 5 runs (Figure 8). This was further supported by comparing the FTIR data of fresh SGO and recovered catalyst (Figure 7). This may be attributed that the involvement of the nucleophilic oxo groups in SGO during the reaction may reduce the catalytic activity of SGO after 5th run.

Conclusion

In conclusion, a green and efficient methodology for the synthesis of a variety of isoxazoles and pyranopyrazoles from commercially available aldehydes has been established. We have unfolded a new role of sulfonated graphene oxide as an efficient and heterogeneous carbocatalyst. SGO, itself is capable of furnishing the desired 3-methyl-4-(hetero)arylmethylene isoxazole-5(4*H*)-ones and 6-Amino-3-methyl-4-phenyl-1,4-[2,3-c]

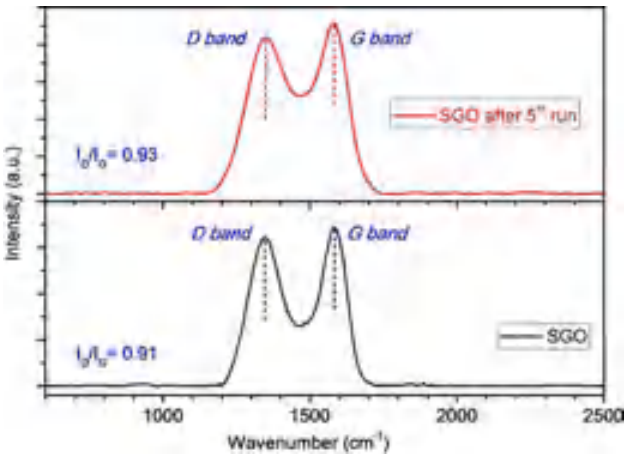

Figure 6. Raman spectra of SGO and SGO after 5th run.

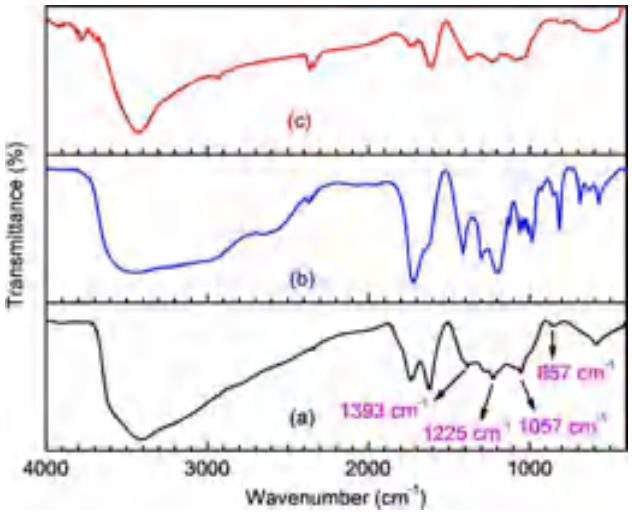

Figure 7. FTIR spectra of SGO (a) fresh (b) after 2nd run (c) after 5th run.

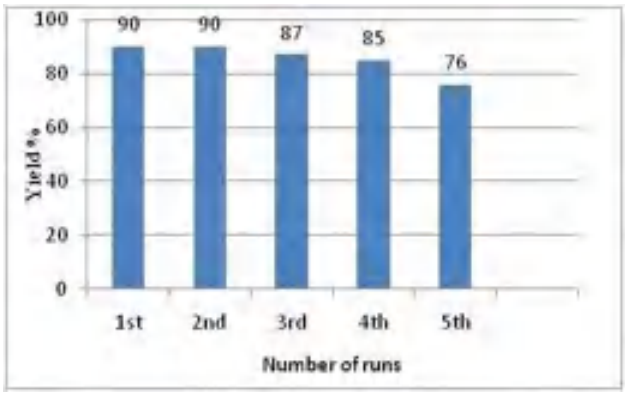

Figure 8. Recyclability experiment of catalyst SGO.

pyrazole-5-carbonitriles with excellent yield. It can be envisioned that such a cheap and robust solid acid catalyst SGO holds great potential for a wide range of acid-catalysed reactions.

Supporting Information Summary

Supplementary data include experimental details, ^{1}H NMR,^{13}C NMR spectra and IR data of all the synthesized compounds (4a-4s, 5a-5j). HRMS of few compounds have also been presented.

Acknowledgment

One of the authors (P.B) is thankful to CSIR, New Delhi for financial support and IACS (Kolkata) for HR-TEM, SEM and XRD analysis.

Keywords: Aldehyde · Carbocatalyst · Ethyl acetoacetate · Isoxazole · Pyranopyrazole · Sulfonated graphene oxide.

[1] E. Vitaku, D. T. Smith, J. T. Njardarson, *J. Med. Chem.* **2014**, *57*, 10257–10274.
[2] P. Martins, J. Jesus, S. Santos, L. R. Raposo, C. Roma-Rodrigues, P. V. Baptista, A. R. Fernandes, *Molecules* **2015**, *20*, 16852–16891.
[3] T. Karabasanagouda, A. V. Adhikari, M. Girisha, *Indian J. Chem.* **2009**, *48*, 430–437.
[4] a) Q. Liu, Y. N. Zhang , *Bull. Korean Chem. Soc.* **2011**, *32*, 3559–3560; b) A. Domling, *Curr. Opin. Chem. Biol.* **2002**, *6*, 306–308; c) C. O. Kappe, *Curr. Opin. Chem. Biol.* **2002**, *6*, 314–320.
[5] a) E. Rafiee, H. Jafari, Bioorg, *Med. Chem. Lett.* **2006**, *16*, 2463–2466; b) M. S. Patil, C. Mudaliar, G. U. Chaturbhuj, *Tetrahedron Lett.* **2017**, *58*, 3256–3261.
[6] G. Abbiati, E. M. Beccalli, G. Broggini, C. Zoni, *Tetrahedron* **2003**, *59*, 9887–9893.
[7] J. Han, H. Guo, X. G. Wang, M. L. Pang, J. B. Meng, *Chin. J. Chem.* **2007**, *25*, 129–131.
[8] a) X. H. Zhang, Y. H. Zhan, D. Chen, F. Wang, L. Y. Wang, *Dyes Pigm.* **2012**, *93*, 1408–1415; b) B. Kafle, N. G. Aher, D. Khadka, H. Park, H. Cho, *Chem. Asian J.* **2011**, *6*, 2073–2079.
[9] M. Pinerio, T. M. Pinho-e-Melo, *Eur. J. Org. Chem.* **2009**, *31*, 5287–5307.
[10] a) B. Kafle, N. G. Aher, D. Khadka, H. Park, H. Cho, *Chem. Asian J.* **2011**, *6*, 2073–2079; b) O. H. Kan, I. Adachi, R. Kido, K. Hirose, *J. Med. Chem.* **1967**, *10*, 411–418; c) T. Karabasanagouda, A. V. Adhikari, M. Girisha, *Indian J. Chem.* **2009**, *48*, 430–437; d) M. M. Santos, N. Faria, J. Iley, *Bioorg. Med. Chem. Lett.* **2010**, *20*, 193–195; e) A. Kamal, E. V. Bharathi, J. S. Reddy, *Eur. J. Med. Chem.* **2011**, *46*, 691–703.
[11] a) X. H. Zhang, Y. H. Zhan, D. Chen, F. Wang, L. Y. Wang, *Dyes Pigm.* **2012**, *93*, 1408–1415; b) P. Diana, A. Carbone, P. Barraja, G. Kelter, H. H. Fiebig, G. Cirrincione, *Bioorg. Med. Chem.* **2010**, *18*, 4524–4529; c) T. Kwon, A. S. Heiman, E. T. Oriaku, K. Yoon, H. Lee, *J. Med. Chem.* **1995**, *38*, 1048–1051.
[12] a) E. Aret, H. Meekes, E. Vlieg, G. Deroover, *Dyes Pigm.* **2007**, *72*, 339–344; b) Y. K. Kang, K. J. Shin, K. H. Yoo, *Bioorg. Med. Chem. Lett.* **2000**, *10*, 95–99; c) X. H. Zhang, Y. H. Zhan, D. Chen, F. Wang, L. Y. Wang, *Dyes Pigm.* **2012**, *93*, 1408–1415.
[13] a) P. Conti, C. Dallanoce, M. D. Amici, C. D. Micheli, K. N. Klotz, *Bioorg. Med. Chem.* **1998**, *6*, 401–409; b) M. G. Gordaliza, T. Faircloth, M. A. Castro, J. M. M. Del Corral, M. L. López-Vázquez, A. San Feliciano, *J. Med. Chem.* **1996**, *39*, 2865–2868; c) T. Kwon, A. S. Heimann, E. T. Oriaku, K. Yoon, *J. Med. Chem.* **1995**, *38*, 1048–1051.
[14] T. Ishioka, A. Kubo, Y. Koiso, K. Nagasawa, A. Itai, Y. Hashimoto, *Bioorg. Med. Chem.* **2002**, *10*, 1555–1566.
[15] a) Y. Q. Zhang, C. Wang, *Chin. J. Org. Chem.* **2008**, *28*, 141–144; b) Q. Liu, R. T. Wu, *J. Chem. Res.* **2011**, *35*, 598–599.
[16] Y. Q. Zhang, C. Wang, *Chin. J. Org. Chem.* **2008**, *28*,1267-1271.
[17] K. Ablajan, H. Xiamuxi, *Synth. Commun.* **2012**, *42*, 1128–1136.
[18] S. Tu, J. Zhang, R. Jia, B. Jiang, Y. Zhang, H. Jiang, *Org. Biomol. Chem.* **2007**, *5*, 1450–1453.
[19] F. Saikh, J. Das, S. Ghosh, *Tetrahedron Lett.* **2013**, *54*, 4679–4682.
[20] H. Kiyani, F. Ghorbani, *J. Chem. Soc.* **2017**, *21*, 112–119.
[21] Q. Liu, X. Hou, *Phosphorus Sulfur Silicon Relat. Elem.* **2012**, *187*, 448–453.
[22] H. Kiyani, F. Ghorbani, *Res. Chem. Intermed.* **2015**, *41*, 2653–2664.
[23] M. S. Patil, C. Mudaliar, G. U. Chaturbhuj, *Tetrahedron Lett.* **2017**, *58*, 3256–3261.
[24] H. Kiyani, F. Ghorbani, *Elixir Org. Chem. A.* **2013**, *58*, 14948–14950.
[25] Q. Liu, H. M. Ai, Z. Li, *Ultrason. Sonochem.* **2011**, *18*, 477–479.
[26] M. Ahmadzadeh, Z. Zarnegar, J. Safari, *Green Chem. Lett. Rev.* **2018**, *11*, 78–85.
[27] a) Q. Liu, Y. N. Zhang, *Bull. Korean Chem. Soc.* **2011**, *32*, 3559–3560; b) C. M. Moorhoff, D. F. Schneider, *Monatsh. Chem.* **1998**, *129*, 409–417.
[28] M. Mirzazadeh, G. H. Mahdavinia, *J. Chem.* **2012**, *9*, 425–429.
[29] S. Tu, J. Zhang, R. Jia, B. Jiang, Y. Zhang, H. Jiang, *Org. Biomol. Chem.* **2007**, *5*, 1450–1453.
[30] S. N. Maddila, S. Maddila, W. E. Zyl, S. B. Jonnalagadda, *Res. Chem. Intermed.* **2016**, *42*, 2553–2566.
[31] H. Kiyani, A. Kanaani, D. Ajloo, F. Ghorbani, M. Vakili, *Res. Chem. Intermed.* **2015**, *41*, 7739–7773.

[32] D. Setamdideh, *J. Mex. Chem. Soc.* **2015**, *59*, 191–197.
[33] A. U. Khandebharad, C. H. Gill, B. R. Agrawal, *Res. J. Chem. Sci.* **2015**, *5*, 27–32.
[34] W. P. Smith, L. S. Sollis, D. P. Howes, P. C. Cherry, I. D. Starkey, K. N. Cobley, H. Weston, J. Scicinski, A. Merritt, A. Whittington, P. Wyatt, N. Taylor, D. Green, R. Bethell, S. Madar, R. J. Fenton, P. J. Morley, T. Pateman, A. Beresford, *J. Med. Chem.* **1998**, *41*, 787–797.
[35] J. L. Wang, D. Liu, Z. J. Zheng, S. Shan, X. Han, S. M. Srinivasula, C. M. Croce, E. S. Alnemri, Z. Huang, *Proc. Mont. Acad. Sci.* **2000**, *97*, 7124–7129.
[36] A. M. Grumezescu, E. Andronescu, A. Ficai, C. Bleotu, D. E. Mihaiescu, M. C. Chifiriuc, *Int. J. Pharm.* **2012**, *436*, 771–777.
[37] K. Mazaahir, S. Shilpi, R. K. Khalilur, S. T. Sharanjit, *Bioorg. Med. Chem. Lett.* **2005**, *15*, 4295–4298.
[38] C. K. Sheng, J. H. Li, N. Hideo, *J. Med. Chem.* **1984**, *27*, 539–544.
[39] M. Bihani, P. P. Bora, G. Bez, H. Askari, *ACS Sustainable Chem. Eng.* **2013**, *1*, 440–447.
[40] M. Farahi, B. Karami, I. Sedighimehr, H. M. Tanuraghaj, *Chin. Chem. Lett.* **2014**, *25*, 1580–1582.
[41] F. Moeinpour, A. Khojastehnezhad, *Chin. Chem. Lett.* **2015**, *26*, 575–579.
[42] M. Babaie, H. Sheibani, *Arabian J. Chem.* **2011**, *4*, 159–162.
[43] H. S. Sohal, A. Goyal, R. Sharma, R. Khare, S. Kumar, *Eur. J. Chem.* **2013**, *4*, 450–453.
[44] B. Maleki, H. Eshghi, M. Barghamadi, N. Nasiri, A. Khojastehnezhad, S. Sedigh Ashrafi, O. Pourshiani, *Res. Chem. Intermed.* **2016**, *42*, 3071–3093.
[45] M. Kangani, N. Hazeri, M. T. Mghsoodlou, S. M. Habibi-khorasani, S. Salahi, *Res. Chem. Intermed.* **2015**, *41*, 2513–2519.
[46] Z. Karimi-Jaberi, M. M. ReyazoShams, *Heterocycl. Commun.* **2011**, *17*, 177–179.
[47] D. Azarifar, M. Tadayoni, M. Ghaemi, *Appl. Organomet. Chem.* **2018**, *32*, 4293.
[48] R. Konakanchi, R. Gondru, V. B. Nishtala, L. R. Kotha, *Synth. Commun.* **2018**, *48*, 1994–2001.
[49] D. R. Dreyer, C. W. Bielawski, *Chem. Sci.* **2011**, *2*, 1233–1240.
[50] C. Su, K. P. Loh, *Acc. Chem. Res.* **2013**, *46*, 2275–2280.
[51] S. Navalon, A. Dhakshinamoorthy, M. Alvaro, H. Garcia, *Chem. Rev.* **2014**, *114*, 6179–6212.
[52] F. Hu, M. Patel, F. Luo, C. Flach, R. Mendelsohn, E. Garfunkel, H. He, M. Szostak, *J. Am. Chem. Soc.* **2015**, *137*, 14473–14480.
[53] D. R. Dreyer, H.-P. Jia, C. W. Bielawski, *Angew. Chem. Int. Ed.* **2010**, *49*, 6813–6816; *Angew. Chem.* **2010**, *122*, 6965–6968.
[54] C. Su, R. Tandiana, J. Balapanuru, W. Tang, K. Pareek, C. T. Nai, T. Hayashi, K. P. Loh, *J. Am. Chem. Soc.* **2015**, *137*, 685–690.
[55] B. Majumdar, D. Sarma, T. Bhattacharya, T. K. Sarmsa, *ACS Sustainable Chem. Eng.* **2017**, *5*, 9286–9294.
[56] Z. Wei, Y. Yang, Y. Hou, Y. Liu, X. He, S. Deng, *ChemCatChem.* **2014**, *6*, 2354–2363.
[57] S. Zhu, J. Wang, W. Fan, *Catal. Sci. Technol.* **2015**, *5*, 3845–3858.
[58] D. C. Marcano, D. V. Kosynkin, J. M. Berlin, A. Sinitskii, Z. Sun, A. Slesarev, L. B. Alemany, W. Lu, J. M. Tour, *ACS Nano* **2010**, *8*, 4806–4814.
[59] Q. Hou, W. Li, M. Ju, L. Liu, Y. Chen, Q. Yang, *RSC Adv.* **2016**, *6*, 104016–104024.

Submitted: November 1, 2019
Accepted: December 27, 2019

RSC Advances

PAPER

View Article Online
View Journal | View Issue

Cite this: *RSC Adv.*, 2021, **11**, 32106

Convenient one-pot synthesis of 1,2,4-oxadiazoles and 2,4,6-triarylpyridines using graphene oxide (GO) as a metal-free catalyst: importance of dual catalytic activity†

Puja Basak, Sourav Dey and Pranab Ghosh *

A convenient and efficient process for the synthesis of 3,5-disubstituted 1,2,4-oxadiazoles and 2,4,6-triarylpyridines has been described using an inexpensive, environmentally benign, metal-free heterogeneous carbocatalyst, graphene oxide (GO). GO plays a dual role of an oxidizing agent and solid acid catalyst for synthesizing 1,2,4-oxadiazoles and triarylpyridines. This dual catalytic activity of GO is due to the presence of oxygenated functional groups which are distributed on the nanosheets of graphene oxide. A broad scope of substrate applicability and good sustainability is offered in this developed protocol. The results of a few control experiments reveal a plausible mechanism and the role of GO as a catalyst was confirmed by FTIR, XRD, SEM, and HR-TEM analysis.

Received 21st August 2021
Accepted 16th September 2021

DOI: 10.1039/d1ra06331f

rsc.li/rsc-advances

Introduction

Nitrogen-containing heterocyclic compounds are valuable due to their potential application as a key intermediate in the synthesis of numerous drugs.[1] 3,5-Disubstituted 1,2,4-oxadiazoles are a remarkably important class of nitrogen-containing heterocyclic scaffold as they are widely used as pharmacophores, bioactive molecules, and functional materials.[1,2] Among the oxadiazole derivatives, the 1,2,4-oxadiazole motif has received interest due to its application as a stable bioisostere in place of an amide, ester, or urea functionality.[3] These compounds when selectively functionalized, have performed as various muscarinic agonists,[4] benzodiazepine receptor partial agonists,[5] serotonergic (5-HT3) antagonists,[6] dopamine transporters,[7] antischistosomal drugs,[8] G-quadruplex ligands for probing DNA superstructure in antitumor research.[9,10] Another nitrogen-containing heterocycle, pyridines are ubiquitous and have attracted much attention due to their unique biological, medicinal, and pharmaceutical properties.[11–13] 2,4,6-Triarylpyridines are frequently used as a synthon in supramolecular chemistry owing to their π-stacking ability.[14] In addition, pyridines have received a growing interest as monomeric building blocks in thin films and organometallic polymers.[15]

It is noteworthy that, in the last decade many efficient protocols have been developed to synthesize these significant heterocyclic moieties. Among the known synthetic strategies of 1,2,4-oxadiazoles, the most conventional approach involves the use of amidoximes as starting materials or intermediates. Other common approaches involve *O*-acylation of amidoximes by an activated carboxylic acid derivative, followed by cyclodehydration,[16] the 1,3-dipolar cycloaddition of nitrile oxide to nitriles, and intermolecular cyclodehydration reaction of amidoximes with aldehydes followed by oxidative dehydrogenation.[17,18] Besides this, base-mediated one-pot synthesis, MnO_2/GO based synthesis, microwave-assisted efficient synthesis of oxadiazoles using PTSA and $ZnCl_2$ have also been reported.[17,19–21] On the other hand, efficient protocols for the synthesis of another important heterocycle 2,4,6-triarylpyridines involve condensation reaction between benzaldehydes, acetophenones, and ammonium acetate in presence of different acid catalysts[22–24] *e.g.* pentafluorophenylammonium triflate,[23] heteropolyacid,[25] $HClO_4$–SiO_2,[26] Brønsted-acidic ionic liquid,[27] and nano-metal catalyst.[23,28,29] Nevertheless, most of the traditional synthetic method requires harsh reaction condition, prolonged heating, and use of toxic transition metal catalyst. However, only a few protocols have shown greener context and high atom economy. Multicomponent reaction (MCR) is considered to be an effective and straightforward approach for the synthesis of heterocycles in an atom economical way. Considering the efficiency of MCRs and the aspects of green chemistry,[30–33] there is a need for new methods which involve metal-free, environmentally friendly catalytic protocol to synthesize 1,2,4-oxadiazoles and 2,4,6-triarylpyridines.

Recently, carbonaceous nanomaterials have gained considerable attention in green chemistry, especially in the development of metal-free sustainable heterogeneous catalysts.[34–36] Among the carbonaceous nanomaterials, graphene oxide (GO)

Department of Chemistry, University of North Bengal, Darjeeling, West Bengal, India. E-mail: pizy12@yahoo.com; Fax: +91-353-2699001; Tel: +91-353-2776381

† Electronic supplementary information (ESI) available: The scanned copies of ^1H and ^{13}C NMR are included in this section. See DOI: 10.1039/d1ra06331f

Table 1 Optimization of reaction condition for the synthesis of amidoxime (intermediate)[a]

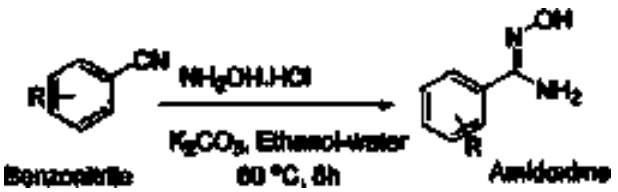

Entry	Solvent	Temp (°C)	Base	Yield[b] (%)
1	Water	100	K_2CO_3	68
2	Water	100	Cs_2CO_3	72
3	Ethanol	80	K_2CO_3	66
4	Ethanol	80	TEA	70
5	Ethanol–water	80	TEA	80
6	Ethanol–water	80	—	<50[c]
7	Ethanol–water	**80**	**K_2CO_3**	**91**
8	Ethanol–water	80	K_2CO_3	94[d]
9	Ethanol–water	80	Cs_2CO_3	93
10	THF	120	K_2CO_3	54
11	Toluene	110	K_2CO_3	<50
12	CH_3CN	82	K_2CO_3	68
13	DMF	120	K_2CO_3	76

[a] Reaction condition: benzonitrile (1.5 mmol), hydroxylamine hydrochloride (1.5 mmol), base (1.5 mmol) and solvent (5 mL). [b] Isolated yield. [c] No base was added. [d] The reaction was carried out for 24 h.

has been reported to accelerate several organic transformation reactions replacing different hazardous chemical reagents. GO, a thin two-dimensional unique nanomaterial contains different oxygen functionalities like carbonyl (–C=O), carboxyl (–COOH), epoxy (–O–), and hydroxyl (–OH) on its edges and basal plane.[37–39] On account of the presence of large surface area, and diverse oxygen functionalities, GO has been identified as a heterogeneous solid acid catalyst (pH 4.5 at 0.1 mg mL^{-1}) as well as a benign oxidizing agent.[40–42] Its abundance from low-cost natural carbon sources, low toxicity, reusability, and metal-free catalytic activity makes this heterogeneous carbon material (GO) as a promising carbocatalyst. Due to the inherent acidic and oxidation property of GO, it is explored as a catalyst in different organic transformations like C–H oxidations,[43] oxidative coupling of amines[44] to the imines, oxidation of thioanisole,[45] glutaraldehyde to glutaric acid,[46] 5-hydroxymethylfurfural,[47] benzylpyrazolyl coumarins,[48] Fisher esterification,[49] and transamidation.[50–54] The versatility and sustainability of GO as a catalyst leads us to employ GO as a metal-free catalyst for the synthesis of substituted 1,2,4-oxadiazoles and 2,4,6-triarylpyridines to overcome the drawbacks of the reported protocols and reduce environmental hazards. Our present study explores the role of GO as an acid catalyst as well as an oxidizing agent using the surface-bound oxygen-containing functional groups. To unleash the dual catalytic activity of GO, a plausible oxidative cyclization pathway to the

Table 2 Optimization of reaction condition for the synthesis of 3,5-disubstituted 1,2,4-oxadiazole from amidoxime[a]

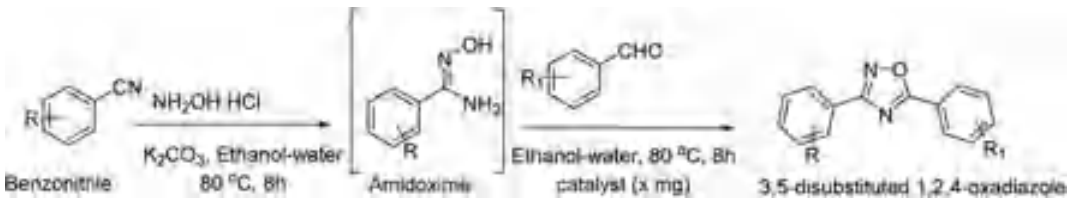

Entry	Catalyst (mg)	Solvent	Temperature	Time (h)	Yield%
1	—	Ethanol	80	12	Trace
2	15 (GO)	Ethanol	80	12	73
3	15 (GO)	Water	100	12	77
4	15 (GO)	DMF	100	12	60
5	15 (GO)	Ethanol–water	80	12	79
6	15 (GO)	Ethanol–water	80	24	83
7	25 (GO)	Ethanol–water	80	12	89
8	**25 (GO)**	**Ethanol–water**	**80**	**8**	**88**
9	25 (GO)	Ethanol–water	RT	12	52
10	25 (graphite)	Ethanol–water	80	8	40[b]
11	25 (rGO)	Ethanol–water	80	8	45[c]
12	25 (GO)/oxidant	Ethanol–water	80	8	67[d]
13	Oxidant	Ethanol–water	80	8	<40[e]
14	25 (GO)	Neat	80	8	69
15	25 (GO)	Ethanol–water	80	8	85[f]
16	—	Ethanol–water	80	8	Nil[f]

[a] Reaction condition: benzaldehyde (1 mmol), amidoxime (1 mmol) and ethanol–water(5 mL), pristine GO (25 mg). [b] Graphite powder was used. [c] Reduced graphene oxide (rGO). [d] GO and extra oxidant 30% H_2O_2 (1 mmol) were used. [e] Only H_2O_2 was used. [f] Under inert atmospheric condition.

Table 3 Synthesis of diversely functionalised 3,5-disubstituted 1,2,4-oxadiazole[a]

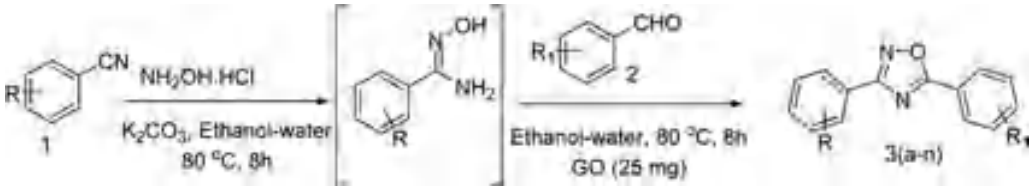

Entry	R	R_1	Product	Yield[b] (%)
1	4-H	4-H	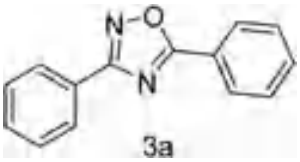 3a	83
2	4-H	4-CH_3	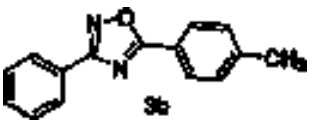 3b	81
3	4-H	4-OCH_3	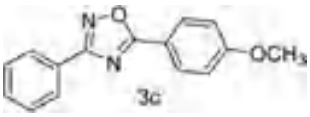 3c	80
4	4-H	4-F	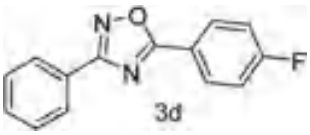 3d	78
5	4-H	3-NO_2	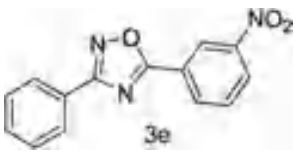 3e	75
6[c]	4-H	4-$N(CH_3)_2$	No 1,2,4-oxadiazole, only imine formation	—
7	4-H	1-Napthaldehyde	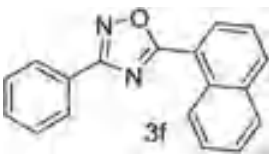 3f	62
8	4-H	Furan-2-carbaldehyde	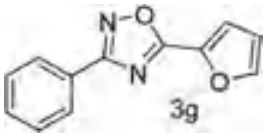 3g	72
9	4-H	Thiophene-2-carbaldehyde	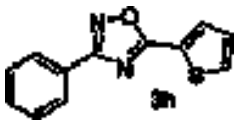 3h	70
10	4-CH_3	4-H	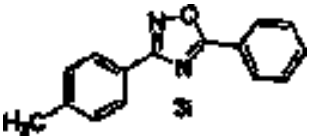 3i	80

Table 3 (*Contd.*)

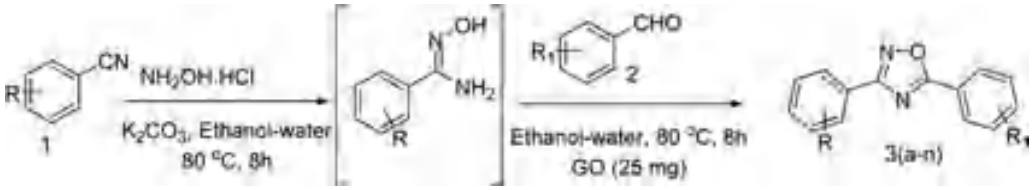

Entry	R	R_1	Product	Yield[b] (%)
11	4-OCH_3	4-H	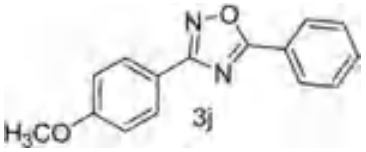 3j	78
12	4-OCH_3	4Cl	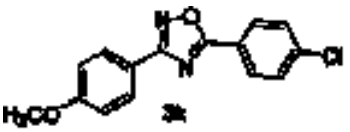 3k	82
13	4-Pyridinecarbonitrile	4-H	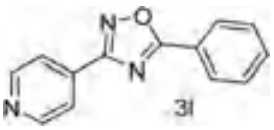 3l	68
14	4-H	CH_3CHO	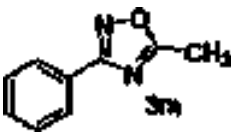 3m	75
15[d]	4-H	Heptaldehyde	NR	—
16[e]	CH_3CN	4-H	NR	—

[a] In the first step, benzonitrile (1 mmol), hydroxylamine hydrochloride (1.5 mmol), K_2CO_3 (1.5 mmol), and ethanol–water (5 mL) were stirred for 8 h and in the 2nd step benzaldehyde (1 mmol) and GO (*x* mg) were added and stirred for another 8 h. [b] Isolated yield after purification through column chromatography. [c] 4-(Dimethylamino)benzaldehyde (1 mmol) was used. [d] Heptaldehyde was used. [e] Acetonitrile (1 mmol) was used.

synthesis of oxadiazoles and triarylpyridines under benign conditions has also been established.

Results and discussion

For screening the reaction parameter benzonitrile (1.5 mmol), hydroxylamine hydrochloride (1.5 mmol), and base (1.5 mmol) were taken as model substrates to find out suitable conditions for the synthesis of amidoxime (intermediate). To satisfy our curiosity, the reaction was performed in different solvents *e.g.* polar protic, polar aprotic, and nonpolar. However, in absence of a base, a low yield was obtained (Table 1, entry 6). Gratifyingly, the reaction results showed (Table 1) the formation of amidoxime is highly favored in mixed solvent ethanol–water (1 : 3) using K_2CO_3 as a base. To control the reaction conditions, after completion of the reaction, the solvent was removed by a rotary evaporator to separate the intermediate. While monitoring the TLC, only one spot was observed other than the reactant. After workup and purification by column chromatography, 91% yield of the intermediate (amidoxime) was obtained (Table 1, entry 7). Although other bases were also employed (Table 1, entries 2, 5 and 9), K_2CO_3 exerted the best result in an ethanol–water solvent. The synthesized amidoxime was characterized by NMR (300 MHz) and the spectral data was shown in ESI.†

In the second step of the reaction, benzaldehyde (1 mmol) and the catalyst were added to the reaction mixture to prioritize the synthesis of 3,5-disubstituted 1,2,4-oxadiazole. In presence of a small amount of GO, 73% yield of the product was obtained at 80 °C temperature (entry 2). Further increase in the amount of GO, proved to be favorable in the formation of 1,2,4-oxadiazole. No product was obtained when the reaction was carried out in absence of GO (Table 2, entry 1). High yield of the product was observed in aqueous ethanolic solution with a ratio ethanol–water (1 : 3). The outstanding catalytic activity of GO in ethanol–water (1 : 3) is revealed due to its better dispersibility. To establish the catalytic activity of GO, few controlled experiments were carried out using various catalysts. Other

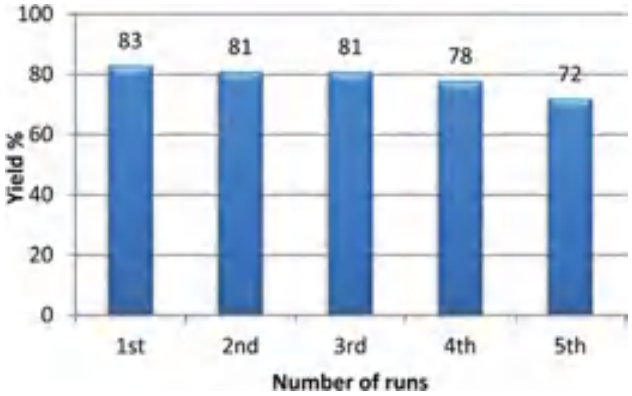

Fig. 1 Recyclability study of GO for the synthesis of 3,5-disubstituted 1,2,4-oxadiazole.

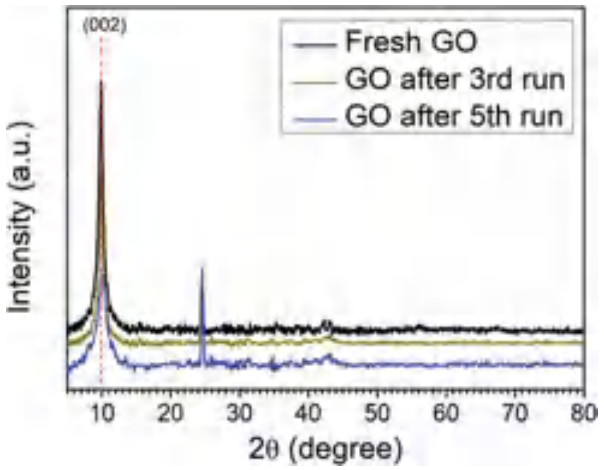

Fig. 2 XRD spectra of fresh GO, after 3rd run and 5th run.

carbonaceous nanomaterials *e.g.* powdered graphite, reduced graphene oxide (rGO) showed less catalytic activity than GO because they do not contain as many hydroxyl and carboxylic groups, indicating oxygen-containing functional groups in graphene oxide have a profound effect in catalyzing the synthesis of 3,5-disubstituted 1,2,4-oxadiazole. The reaction was also carried out in presence of GO and an oxidant H_2O_2, the reason for the low yield may be due to the oxidation of benzaldehyde to benzoic acid in presence of H_2O_2 (Table 2, entry 12). The yield was not improved when only an H_2O_2 oxidant was used (entry 13). These control experiments infer the significant catalytic role of GO in the reaction.

The scope and the substrate applicability of the reaction were also examined and results were summarized in Table 3.

With the optimized condition in hand, we have extended the substrate scope in organic transformations and a series of diversely substituted aldehydes and benzonitriles are subjected to the synthesis of 3,5-disubstituted 1,2,4-oxadiazole (Table 3). Both the electron-donating (Table 3, entries 2, 3, 10 and 11) and electron-withdrawing groups (entries 4 and 5) in the substituents afforded the corresponding product in good to excellent

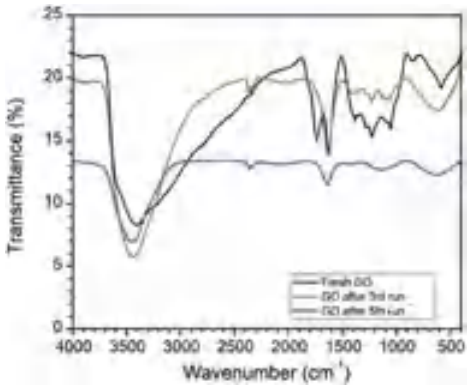

Fig. 3 Comparative FTIR of fresh GO, after 3rd run and 5th run.

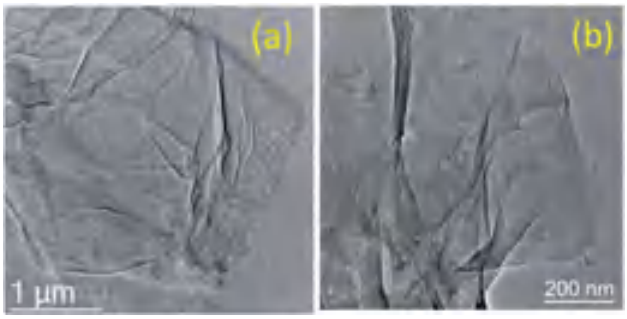

Fig. 4 HR-TEM images of (a) GO and (b) GO after the 5th run.

yield which indicates that the electronic nature of the substituents is not much influential to determine the yield of the reaction. 1-Napthaldehyde offered the product with low yield and the reason may be due to steric hindrance (Table 3, entry 7). In the case of 4-*N*,*N*-(dimethylamino) benzaldehyde, the reaction was stopped at amidoxime, no desired oxadiazole is obtained (Table 3, entry 6). The present catalytic condition showed a wide tolerance to heterocyclic aldehydes (Table 3 entries 8, 9) and they were found to be highly effective to afford the corresponding product. The generality of the reaction was examined in the case of aliphatic aldehydes also. Interestingly, acetaldehyde was equally effective to yield the product with excellent quantity (entry 14). However, no product was found with increasing the side chain of aliphatic aldehydes (entry 15). It was disappointing that acetonitrile did not exert the corresponding product (entry 16). Due to the heterogeneous nature

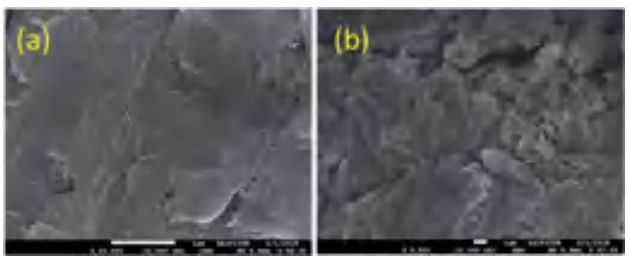

Fig. 5 SEM images of (a) GO and (b) GO after the 5th run.

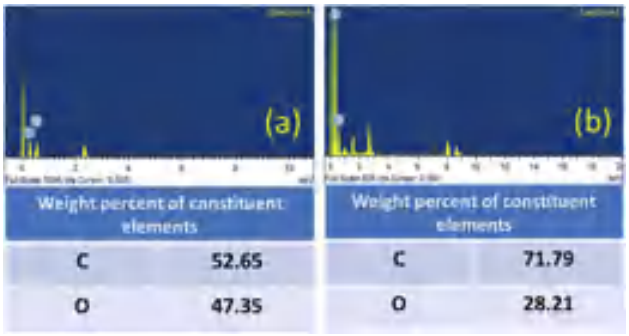

Fig. 6 EDX spectra of (a) GO and (b) GO after the 5th run.

of GO, it can be easily isolated from the reaction mixture and reused. The catalytic activity of GO was examined for five consecutive cycles for the synthesis of 3,5-disubstituted 1,2,4-oxadiazole from benzaldehyde and amidoxime under reflux conditions for 8 h to ascertain the recyclability potential of graphene oxide. The catalyst was separated after each recycles and washed thoroughly with ethanol and reused. A marginal decrease in the yield of oxadiazole is observed after each cycle which indicates a slight loss of catalytic activity of GO with recycling (Fig. 1).

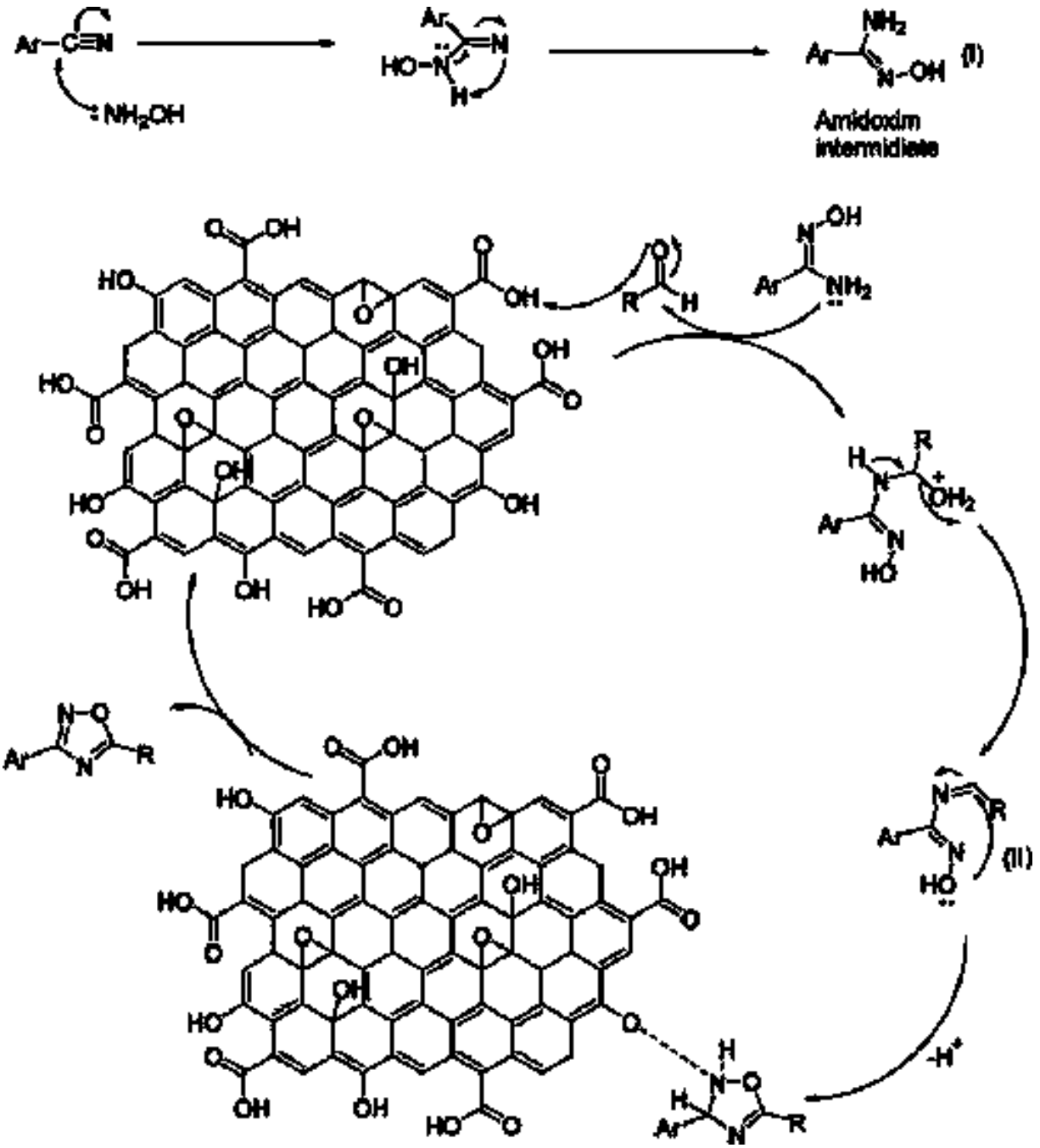

Scheme 1 A plausible route to the synthesis of 3,5-disubstituted 1,2,4-oxadiazole.

The catalytic activity arises some structural changes in GO which were analyzed by FTIR, XRD, SEM, HR-TEM, and EDX analysis. The XRD spectra of fresh GO and recycled catalyst (GO after 3rd run and 5th run) are shown in Fig. 2. A comparison of spectra indicates the reduction in the intensity of the first characteristic peak of GO ($2\theta = 10.01$) and the appearance of a new peak at ($2\theta = 24.62$) due to the formation of partially reduced GO/reduced graphene oxide upon reuse. These results confirm the reduction of the functional groups of GO during the reaction.

The comparison of the FTIR spectra revealed that the peak at 1720 cm^{-1} in fresh GO has completely disappeared after reuse. In addition to this, the peak intensity of the hydroxyl group at 3400 cm^{-1} decreases after reuse. FTIR data strongly support the reduction of GO to rGO in this oxidative cyclization reaction (Fig. 3).

A morphological study of GO and GO after the 5th run was carried out using SEM and HR-TEM to investigate the disintegration of graphene oxide sheets after the reaction. In HR-TEM, the graphene oxide sheets are disintegrated into smaller sheets with slight aggregation after recycle (Fig. 4).

Moreover, the SEM images (Fig. 5) also reveal the formation of multiple small GO sheets after reuse. As GO catalyzes the reaction, its reduction to reduced graphene oxide possibly leads to its disintegration into smaller sheets.

The contribution of oxygen-containing functionalities during the reaction was further confirmed by the EDX analysis (Fig. 6). The carbon content was increased from 52.65% (fresh GO) to 71.79% (GO after 5th run) and the oxygen content was decreased from 47.35% (fresh GO) to 28.21% (GO after 5th run). The decrease in the oxygen content, therefore, indicates the role of GO in this cyclization reaction as an oxidizing agent. The universality and the dual catalytic activity of GO were established by a plausible mechanism (Scheme 1).

Mechanism

A plausible mechanism of GO catalyzed synthesis of 3,5-disubstituted 1,2,4-oxadiazole has been proposed (Scheme 1) based on literature reports[55] and our controlled experiments (Table 2). Now, we propose the formation of amidoxime intermediate (I) from benzonitrile and hydroxylamine hydrochloride. However, in the first step, a base is required to neutralize hydroxylamine hydrochloride. In the 2nd step protonation of aldehyde, oxygen occurs and subsequently, a nucleophilic attack by amidoxime occurs at the electrophilic center of aldehyde. After that, the intermediate (II) undergoes an oxidative cyclization in presence of GO to produce 1,2,4-oxadiazoles. This mechanism is in good agreement with the control experiments as described in Table 2. However, in presence of only H_2O_2 oxidant the yield of the reaction was diminished (Table 2, entry 11). The role of GO as an acid catalyst and an oxidant was confirmed as its absence did not lead to the oxadiazole product. The oxygen containing functional groups of GO are consumed during the reaction and the activity of GO gradually decreases. The activity of recycled GO is lower than that of the pristine GO. Good yield of the product was obtained even under an inert atmosphere which strongly establish (Table 2, entry 15), the prime role of GO in absence of atmospheric oxygen.

In connection to our previous work, the catalytic activity of synthesized GO was investigated in the case of 2,4,6-triarylpyridine synthesis. To find out the optimized condition of the reaction, acetophenone (2 mmol), benzaldehyde (1 mmol), and ammonium acetate (2 mmol) were selected as model substrates and the results were summarized in Table 4. As can be seen from Table 4 that neither polar nor non-polar solvents were found suitable for the reaction. The best result was obtained under neat or solvent-free conditions (Table 4, entry 11). The effect of temperature and the amount of catalyst was also examined to find out the optimized condition. Studies reveal

Table 4 Optimization of reaction condition for the reaction of 2,4,6-triarylpyridine[a]

Entry	Temp (°C)	Solvent	Catalyst GO (mg)	Ammonia source	Yield[b] (%)
1	100	H_2O	15	NH_4OAc	65
2	80	Ethanol	15	NH_4OAc	55
3	100	DMF	15	NH_4OAc	53
4	100	DMSO	15	NH_4OAc	45
5	100	Toluene	15	NH_4OAc	50
6	80	CH_3CN	15	NH_4OAc	30
7	100	Ethylene glycol	15	NH_4OAc	60
8	100	Neat	15	NH_4OAc	83
9	120	Neat	30	NH_4OAc	90
10	150	Neat	30	NH_4OAc	86
11	**100**	**Neat**	**30**	**NH_4OAc**	**92**
12	80	Neat	30	NH_4OAc	80
13	100	Neat	—	NH_4OAc	Trace
14	100	Neat	30	$(NH_4)_2CO_3$	48
15	100	Neat	30	$(NH_4)_2SO_4$	Trace
16	RT	Neat	30	NH_4OAc	<20

[a] Reaction condition: acetophenone (2 mmol), benzaldehyde (1 mmol), ammonium acetate (2 mmol), reaction time: 2 h [b] Isolated yields.

Table 5 Synthesis of 2,4,6-triarylpyridine derivatives in presence of GO[a]

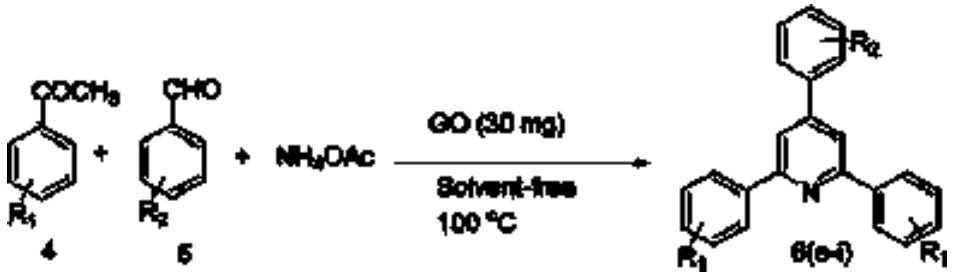

Entry	R_1	R_2	Product	Time (h)	Yield[b] (%)
1	4-H	4-H	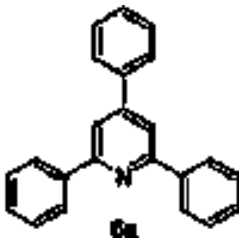	2 h	92
2	4-H	4-Me	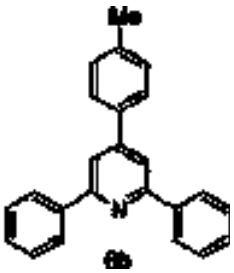	2 h	86
3	4-H	4-Cl	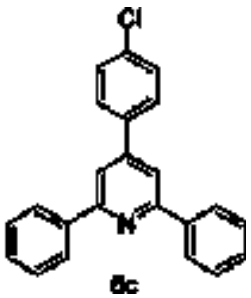	1 h	93
4	4-H	4-NO_2	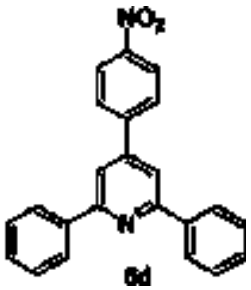	1 h	88

Table 5 (*Contd.*)

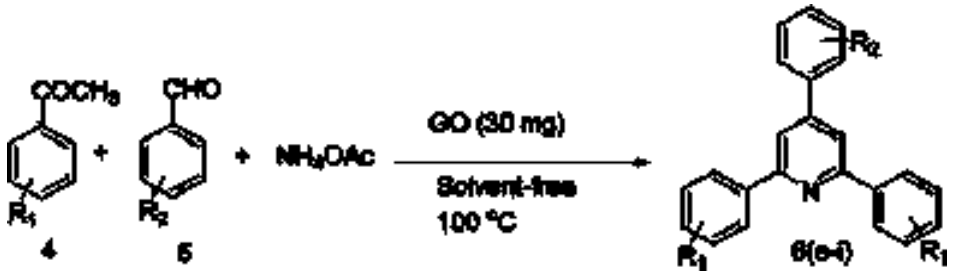

Entry	R_1	R_2	Product	Time (h)	Yield[b] (%)
5	4-H	4-OMe	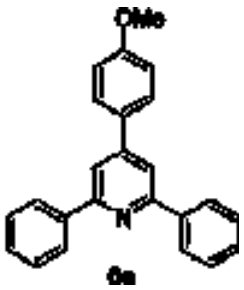	2 h	83
6	4-H	Furan-2-carbaldehyde	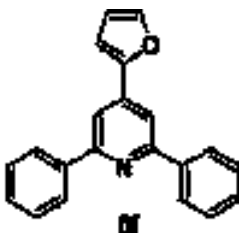	2 h	78
7	4-Me	4-H	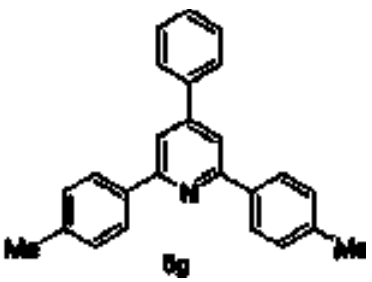	2 h	87
8	4-Br	4-H	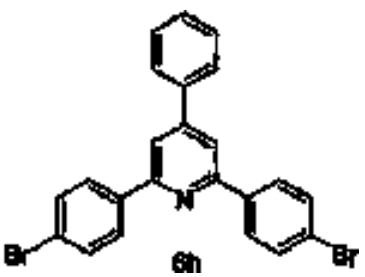	1 h	90

Table 5 (*Contd.*)

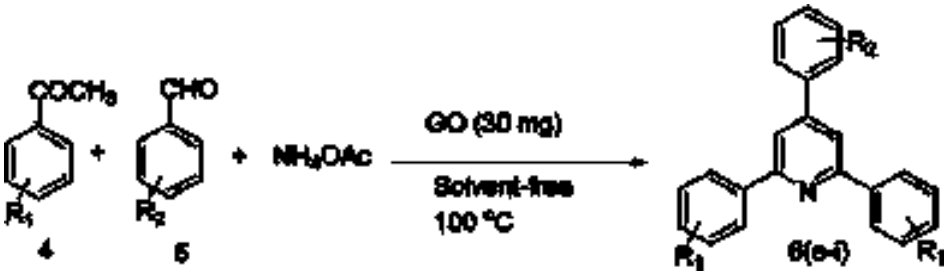

Entry	R_1	R_2	Product	Time (h)	Yield[b] (%)
9	4-Br	4-Cl	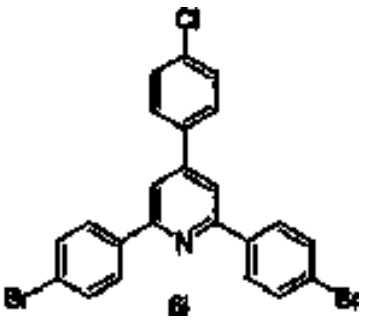	1 h	94

[a] Reaction condition: acetophenone (2 mmol), benzaldehyde (1 mmol), ammonium acetate (2 mmol) and GO (30 mg). [b] Isolated yields after purification through column chromatography on silica gel.

that the yield increases with increasing temperature. Room-temperature reaction afforded only 20% of the product which strongly indicates the vital role of temperature in governing the reaction (entry 16). However, after 120 °C the yield decreases with a further increase in temperature (Table 4, entry 10). To ascertain the catalytic function of GO, the reaction was performed in absence of catalyst and only a trace amount of product was obtained. The amount of the catalyst was also altered and optimum condition offered a neat reaction with 30 mg of GO at 100 °C temperature. Ammonia sources other than ammonium acetate produced the corresponding product with a low yield (Table 4, entries 14 and 15).

To explore the catalytic activity of GO, a wide variety of aromatic aldehydes and substituted acetophenones were subjected to synthesize 2,4,6-triarylpyridines. Based on the above-optimized results, GO catalyzed reaction was carried out at 100 °C temperature under solvent-free condition and the results are summarized in Table 5. First, the compatibility of the substituents in the phenyl ring of acetophenone and benzaldehyde was examined. All the electron-donating and electron-withdrawing substituents on the aromatic ring are equally capable of producing the corresponding product with a good yield. However, aldehydes with electron-withdrawing groups (Table 5, entries 3, 4 and 9) exerted excellent yield and reacted faster than the aromatic aldehydes with electron-donating groups (Table 5, entries 2, 5, 7). In the case of heterocyclic aldehydes, the reaction has smoothly proceeded as can be seen from entry 6.

The probable mechanism for the synthesis of 2,4,6-triarypyridines using GO is described in Scheme 2. At the very first step, aldol condensation occurs between acetophenone and aromatic aldehyde. Acetophenone is activated by the acidic group of GO and the nucleophilic attack occurs at the carbonyl carbon of aromatic aldehyde. After that, an acetophenone molecule is reacted with an ammonia source to form enamine (II). In the third stage, Michael's addition between enamine (II) and the aldol condensation product (I) occurs. GO protonates the condensation product (I), thereby facilitating the Michael addition by enamine (II). The intermediate (III) is formed by Michael's addition and undergoes cyclization to form dihydropyridine (V). At the last step, oxidation to dihydropyridine occurs and gives the ultimate product 2,4,6-triarylpyridine (VI).

The main advantage of heterogeneous catalysts is their reusability in organic transformation. For this purpose, acetophenone, benzaldehyde, and ammonium acetate were taken in a reaction vial in presence of 120 mg of GO. The model reaction was carried out for an adequate time and after completion of the reaction, ethyl acetate (30 mL) was added into the reaction vial and centrifuged for four times. The supernatant liquid after centrifugation was decanted off and the residual catalyst was washed repeatedly with water and acetone. The dry GO was then collected and reused for the 2nd run. It was observed that GO

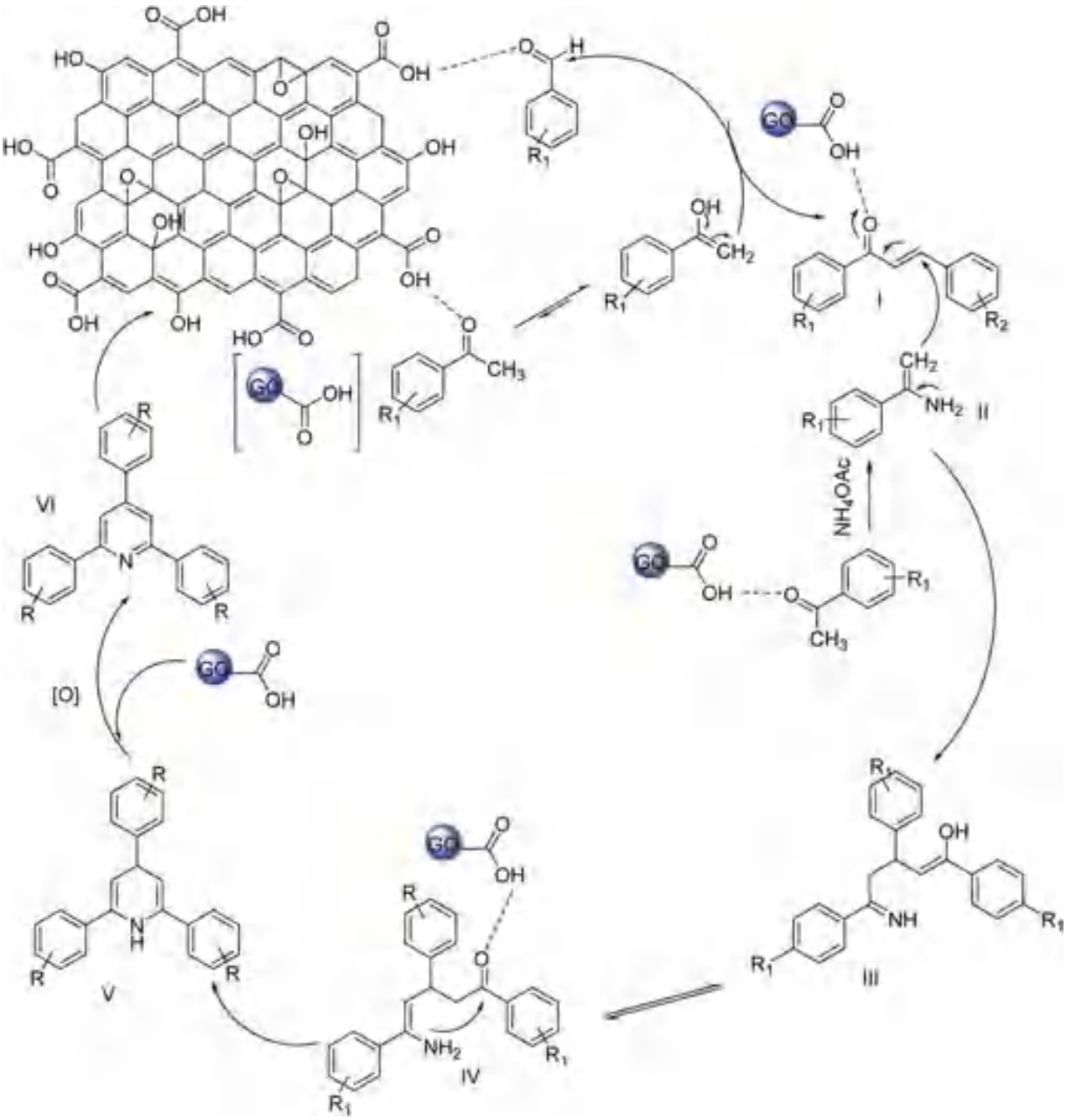

Scheme 2 A possible route of GO catalyzed synthesis of 2,4,6-triarylpyridine.

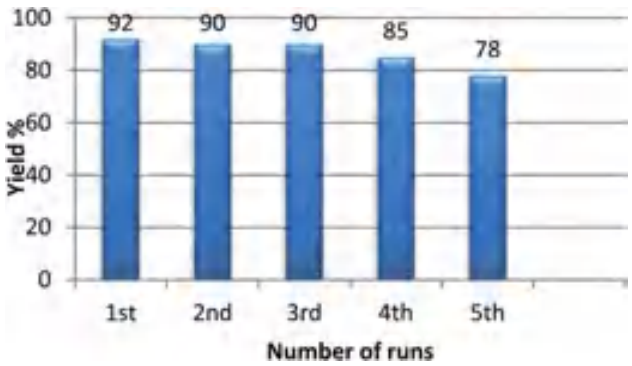

Fig. 7 Recyclability experiment of catalyst GO for the synthesis of 2,4,6-triarylpyridines.

could easily retain its acidic property without significant loss in its catalytic activity even after 5 successive runs (Fig. 7). Although there may be loss of some oxygenated groups due to subsequent runs, the recovered catalyst shows almost equal efficiency with the fresh GO.

Conclusion

In conclusion, carbocatalyst based metal-free catalytic pathway for the synthesis of 3,5-disubstituted 1,2,4-oxadiazoles and 2,4,6-triarylpyridines has been established. The solid acid catalyst, GO facilitates the synthesis of oxadiazoles and triarylpyridines with good yield, easy recovery, and under mild

reaction conditions. The dual catalytic activity of GO has been demonstrated without any undesired by-product under benign conditions. The present protocol gives a clean strategy to provide a wide variety of substituted oxadiazoles and pyridines.

Conflicts of interest

The authors declare no competing financial interest.

Acknowledgements

PB is thankful to CSIR-New Delhi, India for the CSIR-Senior Research Fellowship [File no: 09/285(0072)/2016-EMR-I].

References

1 M. Carbone, Y. Li, C. Irace, E. Mollo, F. Castelluccio, D. A. Pascale, G. Cimino, R. Santamaria, W. Y. Guo and M. Gavagnin, *Org. Lett.*, 2011, **13**, 2516–2519.
2 A. V. Gulevich, A. S. Dudnik, N. Chernyak and V. Gevorgyan, *Chem. Rev.*, 2013, **113**, 3084–3213.
3 R. J. Mathvink, A. M. Barritta, M. R. Candelore, M. A. Cascieri, L. Deng, L. Tota, C. D. Strader, M. J. Wyvratt, M. H. Fisher and A. E. Weber, *Bioorg. Med. Chem. Lett.*, 1999, **9**, 1869–1874.
4 F. I. Carroll, J. L. Gray, P. Abrahm, M. A. Kuzemko, A. H. Lewin, J. W. Boja and M. J. Kuhar, *J. Med. Chem.*, 1993, **36**, 2886–2890.
5 J. W. Clitherow, P. Beswick, W. J. Irving, D. I. C. Scopes, J. C. Barnes, J. Clapham, J. D. Brown, D. J. Evans and A. G. Hayes, *Bioorg. Med. Chem. Lett.*, 1996, **6**, 833–838.
6 C. B. Vu, E. G. Corpuz, T. J. Merry, S. G. Pradeepan, C. Bartlett, R. S. Bohacek, M. C. Botfield, C. J. Eyermann, B. A. Lynch, I. A. MacNeil and M. K. Ram, *J. Med. Chem.*, 1999, **42**, 4088–4098.
7 J. Matsumoto, T. Takahashi, M. Agata, H. Toyofuku and N. Sasada, *Jpn. J. Pharmacol.*, 1994, **65**, 51–57.
8 B. L. Mylari, T. A. Beyer, P. J. Scott, C. E. Aldinger, M. F. Dee, T. W. Siegel and W. J. Zembrowski, *J. Med. Chem.*, 1992, **35**, 457–465.
9 B. S. Orlek, F. E. Blaney, F. Brown, M. S. G. Clark, M. S. Hadley, J. Hatcher, G. J. Riley, H. E. Rosenberg, H. J. Wadsworth and P. Wyman, *J. Med. Chem.*, 1991, **34**, 2726–2735.
10 T. Nakamura, M. Asano, Y. Sekiguchi, Y. Mizuno, K. Tamaki, F. Nara, Y. Kawase, Y. Yabe, D. Nakai, E. Kamiyama, Y. Urasaki-Kaneno, T. Shimozato, H. Doi-Komuro, T. Kagari, W. Tomisato, R. Inoue, M. Nagasaki, H. Yuita, K. Oguchi-Oshima, R. Kaneko and T. Nishi, *Eur. J. Med. Chem.*, 2012, **51**, 92–98.
11 B. Y. Kim, J. BokAhn, H. W. Lee, S. K. Kang, J. H. Lee, J. S. Shin, S. K. Ahn, C. Hong and S. S. Yoon, *Eur. J. Med. Chem.*, 2004, **39**, 433–447.
12 L. Tian, J. Song, J. Wang and B. Liu, *Chin. Chem. Lett.*, 2009, **20**, 288–291.
13 R. D. Allen and G. A. R Johnston, *Med. Res. Rev.*, 1983, **3**, 91–118.
14 E. C. Constable, C. E. Housecroft, M. Neuburger, D. Phillips, P. R. Raithby, E. Schofield, E. Sparr, D. A. Tocher, M. Zehnder and Y. Zimmermann, *Dalton Trans.*, 2000, **13**, 2219–2228.
15 E. Figgemeier, E. C. Constable, C. E. Housecroft and Y. C. Zimmermann, *Langmuir*, 2004, **20**, 9242–9248.
16 (*a*) Y. Wang, R. L. Miller, D. R. Sauer and S. W. Djuric, *Org. Lett.*, 2005, **7**, 925–928; (*b*) S. Kandre, P. R. Bhagat, R. Sharma and A. Gupte, *Tetrahedron Lett.*, 2013, **54**, 3526–3529; (*c*) B. Kaboudin and L. Malekzadeh, *Tetrahedron Lett.*, 2011, **52**, 6424–6426; (*d*) B. Kaboudin and F. Saadati, *Tetrahedron Lett.*, 2007, **48**, 2829–2832.
17 J. K. Augustine, V. Akabote, S. G. Hegde and P. Alagarsamy, *J. Org. Chem.*, 2009, **74**, 5640–5643.
18 D. S. Bolotin, K. I. Kulish, N. A. Bokach, G. L. Starova, V. V. Gurzhiy and V. Y. Kukushkin, *Inorg. Chem.*, 2014, **53**, 10312–10324.
19 (*a*) M. Okimoto and Y. Takahashi, *Bull. Chem. Soc. Jpn.*, 2003, **76**, 427–428; (*b*) D. B. Repke, H. P. Albrecht and J. G. Moffat, *J. Org. Chem.*, 1975, **40**, 2481–2487.
20 W. Wang, H. Xu, Y. Xu, T. Ding, W. Zhang, Y. Ren and H. Chang, *Org. Biomol. Chem.*, 2016, **14**, 9814–9822.
21 F. Saadati, B. Kaboudin, R. Hasanloei, Z. Namazifar, X. Marset and G. Guillena, *Appl. Organomet. Chem.*, 2020, **34**, 5838–5849.
22 M. Adib, A. H. Jahromi, N. Tavoosi, M. Mahdavi and H. R. Bijanzadeh, *Tetrahedron Lett.*, 2006, **47**, 2965–2967.
23 N. Montazeri and S. Mahjoob, *Chin. Chem. Lett.*, 2012, **23**, 419–422.
24 J. Safari, S. Gandomi-Ravandi and M. Borujeni, *Chem. Sci.*, 2013, **125**, 1063–1070.
25 M. M. Heravi, K. Bakhtiari, Z. Daroogheha and F. F. Bamoharram, *Catal. Commun.*, 2007, **8**, 1991–1994.
26 L. Nagarapu, A. R. Peddiraju and S. Apuri, *Catal. Commun.*, 2007, **8**, 1973–1976.
27 A. Davoodnia, M. Bakavoli, R. Moloudi, N. Tavakoli-Houseini and M. Khashi, *Monatsh. Chem.*, 2010, **141**, 867–870.
28 A. Maleki and R. Firouzi-Haji, *Sci. Rep.*, 2018, **8**, 17303–17311.
29 E. Tabrizian, A. Amoozadeh, S. Rahmani, E. Imanifar, S. Azhari and M. Malmir, *Chin. Chem. Lett.*, 2015, **26**, 1278–1282.
30 G.-L. Wu and Q.-P. Wu, *Adv. Synth. Catal.*, 2018, **360**, 1949–1953.
31 R. Mishra, A. Jana, A. K. Panday and L. H. Choudhury, *Org. Biomol. Chem.*, 2018, **16**, 3289–3302.
32 C.-Y. Chen, W.-P. Hu, P.-C. Yan, G. C. Senadi and J.-J. Wang, *Org. Lett.*, 2013, **15**, 6116–6119.
33 C. C. Răzvan, R. Eelco and V. A. O. Romano, *Green Chem.*, 2014, **16**, 2958–2975.
34 D. S. Su, S. Perathoner and G. Centi, *Chem. Rev.*, 2013, **113**, 5782–5816.
35 O. Mohammadi, M. Golestanzadeh and M. Abdouss, *New J. Chem.*, 2017, **41**, 11471–11497.
36 N. Oger, Y. F. Lin, E. L. Grognec, F. Rataboul and F. X. Felpin, *Green Chem.*, 2016, **18**, 1531–1537.

37 D. R. Dreyer and C. W. Bielawski, *Chem. Sci.*, 2011, **2**, 1233–1240.
38 S. Navalon, A. Dhakshinamoorthy, M. Alvaro and H. Garcia, *Chem. Rev.*, 2014, **114**, 6179–6212.
39 S. Zhu, J. Wang and W. Fan, *Catal.: Sci. Technol.*, 2015, **5**, 3845–3858.
40 C. Su and K. P. Loh, *Acc. Chem. Res.*, 2013, **46**, 2275–2285.
41 (*a*) D. R. Dreyer, H. P. Jia and C. W. Bielawski, *Angew. Chem., Int. Ed.*, 2010, **49**, 6813–6816; (*b*) D. R. Dreyer, H. P. Jia, A. D. Todd, G. Jeng and C. W. Bielawski, *Org. Biomol. Chem.*, 2011, **9**, 7292–7295.
42 T. Szabo, E. Tombacz, E. Illes and I. Dekany, *Carbon*, 2006, **44**, 537–545.
43 H. P. Jia, D. R. Dreyer and C. W. Bielawski, *Tetrahedron*, 2011, **67**, 4431–4434.
44 H. Huang, J. Huang, Y. M. Liu, H. Y. He, Y. Cao and K. N. Fan, *Green Chem*, 2012, **14**, 930–934.
45 G. A. B. Gonçalves, S. M. G. Pires, M. M. Q. Simoes, M. G. P. M. S. Neves and P. A. A. P. Marques, *Chem. Commun.*, 2014, **50**, 7673–7676.
46 X. Chu, Q. Zhu, W.-L. Dai and K. Fan, *RSC Adv.*, 2012, **2**, 7135–7139.
47 G. Lv, H. Wang, Y. Yang, T. Deng, C. Chen, Y. Zhu and X. Hou, *ACS Catal.*, 2015, **5**, 5636–5646.
48 T. A. J. Siddiqui, B. G. Ghule, S. Shaikh, P. V. Shinde, K. C. Gunturu, P. K. Zubaidha, J. M. Yun, C. O. Dwyer, R. S. Mane and K. H. Kim, *RSC Adv.*, 2018, **8**, 17373–17379.
49 B. Roy, D. Sengupta and B. Basu, *Tetrahedron Lett.*, 2014, **55**, 6596–6600.
50 R. Wang, Z. Wu, Z. Qin, C. Chen, H. Zhu, J. Wu, G. Chen, W. Fan and J. Wang, *Catal.: Sci. Technol.*, 2016, **6**, 993–997.
51 S. Bhattacharya, P. Ghosh and B. Basu, *Tetrahedron Lett.*, 2018, **59**, 899–903.
52 Z. Chen, Y. Wen, Y. Fu, H. Chen, M. Ye and G. Luo, *Synlett*, 2017, **28**, 981–985.
53 J. Porwal, N. Karanwal, S. Kaul and S. L. Jain, *New J. Chem.*, 2016, **40**, 1547–1553.
54 H. P. Mungse, N. Bhakuni, D. Tripathi, O. P. Sharma, B. Sain and O. P. Khatri, *J. Phys. Org. Chem.*, 2014, **27**, 944–951.
55 K. B. Dhopte, R. S. Zambare, A. V. Patwardhan and P. R. Nemade, *RSC Adv.*, 2016, **6**, 8164–8172.